THE SHEAR STRENGTH OF UNSATURATED SOILS

by

CHUNG KWONG WONG, B.Sc.(Hon.)

A Thesis submitted for the Degree of

Doctor of Philosophy

Department of Civil Engineering

University of Glasgow

December,1984.

To my dear wife, Sue Fong.

ABBREVIATED TABLE OF CONTENTS

DETAILED TABLE OF CONTENTS

ACKNOWLEDGEMENTS

The research project described herein was carried out at the Department of Civil Engineering, University of Glasgow.

The author wishes to express his thanks to Professor H.B. Sutherland, S.M.,F.I.C.E.,F.I.Struct.E.,F.R.S.E., Cormack Professor of Civil Engineering, for suggestion this research topic and for his continued interest in the progress of the work.

The author is deeply indebted to Mr. W.Stewart for his valuable help and suggestions throughout his work and especially during the preparation of the author's thesis.

The author is grateful to Mr. T.Finlay for his valuable advice on various aspects of the experimental work.

Special gratitude is extended to Mr. W.Henderson, the chief technician, for his generous assistance in the design and assembly of the apparatus. Thanks also due to Mr. I.Todd for helping to set up the electronic equipment, and the computing staff for their assistance and discussion.

The author also wishes to thank The Croucher Foundation for providing financial assistance during the period of this research without which this research would not have been possible.

Finally, I would like to express my sincerest thanks to my wife for her continuous encouagement and optimism throughout my research.

SUMMARY

This thesis is concerned with various aspects of the shear strength of unsaturated soils. Early attempts by previous investigators to describe the behaviour of unsaturated soils used the principle of effective stress, modified to suit unsaturated soils. This line of reasoning has been superseded by an approach, developed from the principle of continuum mechanics, which describes the shear strength of unsaturated soils in terms of two independent stress state variables(Fredlund,1973). The author has based his work on this approach, and in particular investigated unverified assumption made by Fredlund regarding a planar form of failure surface.

The influence of soil suction, which is a stress state variable of unsaturated soils, is discussed with respect to effective stress and shear strength. Detailed reviews of both these aspects of unsaturated soil are presented in Chapters 4 and 5.

Apparatus was constructed to carry out triaxial tests on unsaturated samples of Grangemouth clay. The unsaturated samples were obtained from saturated samples by applying a desaturation and consolidation process. The standard triaxial set-up was modified to allow for the measurement and control of the pore air and pore water pressures during testing. Other modifications included the use of a double-walled cell, a diffused air volume indicator and an automatic volume change logging system. A series of tests was carried out specifically to establish suitable strain rates which would allow the proper dissipation

and equalization of pore pressures during testing. This resulted in a strain rate of 0.003 mm/min. being adopted for drained tests and 0.0041 mm/min. for all other test types used.

The main test programme consisted of two series, which were distinguished by the initial stress state applied to the sample. In series I, drained, constant water-content and unconfined tests were carried out. Series II consisted of drained tests only. Four truly undrained tests were also carried out.

The results of these tests and those of nine previous investigations were analysed using three methods. The first two of these, the numerical method and the 2-dimensional graphical method, are based on the theory of Fredlund et al(1978). This theory assumes that, when triaxial test results are recorded in terms of stress state variables and plotted in terms of three orthogonal axes, the resulting failure surface will be a plane. For the angle $\emptyset^b$ used in the shear strength equation, the numerical and 2-dimensional graphical methods gave very similar results. However, due to the nature of the methods, the value of cohesion C′, that they produced varied considerably. In general, the numerical method produced a more conservative(i.e. lower) value for C′.

The value of the correlation coefficient obtained from the numerical or 2-dimensional graphical method was an indication of how well the results compared to a straight line sloping at an angle $\emptyset^b$ to the matrix suction axis. A high correlation coefficient for angle $\emptyset^b$ does not necessarily imply that the failure surface is planar. Similarly, a low correlation coefficient does not necessarily imply that the failure surface

is not planar. Therefore, neither method could be used to confirm that the failure surface was planar.

The author used a third method whereby the form of the failure surface was obtained by using a 3-dimensional graphical program called GINOPLOT. In all but a few cases, the 3-dimensional plot in verification of Fredlund assumption was essentially planar, irrespective of the combination of stress state variables used to describe it. Therefore, to verify that the shear strength equation for unsaturated soils proposed by Fredlund et al represents a planar failure surface, and to obtain the shear strength parameters for use in the equation, the numerical method and the 3-dimensional graphical method must be used together.

The effect of test type on C' and $\emptyset^b$ is clearly demonstrated and so, in practical terms, the choice of parameters for use in the shear strength equation remains difficult. When dealing with unsaturated soils it is extremely important to assess how the degree of saturation will vary in the field and reproduce, as far as possible, the same conditions in the test set-up. For a soil in which the degree of saturation decreases after loading, a drained test should be used, whereas if the degree of saturation increases, a constant water-content test should be used.

CHAPTER 1: INTRODUCTION

Chapter 1 INTRODUCTION

The last three or four decades have witnessed a considerable increase in our knowledge of the behaviour of saturated soils. Problems encountered by practicing engineers however, are not always in soils which are fully saturated. The construction of earthfill dams, highways and airport runways all use compacted soils which are unsaturated. Also, large portions of the earth's land surface are subjected to desiccating influences that leave the upper portion of the profile cracked and unsaturated.

The concentration on fully saturated soil is not difficult to understand; the theoretical formulations are straightforward and the shear strength parameters can be obtained from triaxial tests with comparative ease. In many cases the initially unsaturated soil may be expected to become fully saturated during the lifetime of the soil structure and, a design involving unsaturated soils based on soil strength parameters obtained under fully saturated conditions is likely to be conservative. The strength of a partially saturated specimen usually lies somewhere between the drained and the undrained strength of the same specimen when fully saturated, and therefore the drained and undrained strengths of fully saturated specimens represent extremes (Poulos, 1981). If the partially saturated undrained strength is higher than the fully saturated undrained strength, then the specimen is contractive. In that case the fully saturated undrained strength should be used,

unless it can be shown with certainty that the soil will never become fully saturated in-situ. If the partially saturated undrained strength is lower than the fully saturated undrained strength then the specimen is dilative, and in this case the partially saturated condition should be used because it yields a lower strength. However, the drained strength may be more critical, in which case the partially saturated condition need not be considered.

The transition from testing dry soils to testing fully saturated soils involves a number of problems in the design of the apparatus and the interpretation of the results. The problems involved in coping with two separate pore fluids (air and water) are considerable and there has been an understandable reluctance on the part of research workers to enter this tricky field.

Numerical modelling of the behaviour of fully saturated soils has not yet reached a stage where, even for one soil, the behaviour of that soil can be accurately predicted over the complete range of possible stress and strain paths. For partially saturated soils, the problems involved are even more complex and it is not surprising that numerical analysts have tackled first the simpler case of fully saturated soils.

When the mechanical aspects of any multi-phase system are being investigated, one of three basic approaches can be made i.e. the continuum mechanics approach, the particulate mechanics approach or the empirical approach (D.Y.F. Ho, 1981).

Based on continuum mechanics, any representative element of a system can be considered as a free body and its stress state can be analysed by the concept of force equilibrium. Once the stress state variables are identified, the mechanical behaviour of the system can be related to the material properties in the form of constitutive equations.

Assuming that the behaviour of a saturated soil is dependent on a number of factors such as applied stress (σ), pore pressure (u), void ratio (e), particle orientation, stress or strain history, etc. (not all of which are necessarily independent) and using the fact that experimentally equal changes in applied stress (σ) and pore pressure (u) produce no effect on the response of the soil, we can conclude that only the applied stress and pore pressure enter into the description of the soil response as their difference, which can be defined as the effective stress ($\sigma' = \sigma - u$). It then becomes instructive to attempt to study and model the behaviour of saturated soil in terms of variations of effective stress. To some, this approach has been regarded as the philosophical approach (D.M. Wood, 1979).

The particulate mechanics approach is basically a mechanics approach at a microscopic level. The stress state of the constituent particles in a system is examined. Forces and stresses acting at particle contacts and adjacent phases are considered and the mechanical behaviour of the system is then evaluated through constitutive equations of the particulate stress variables and material properties. In the past, this

method has been called the mechanistic approach. It was typified by Bishop (1959) who strived to show, from considerations of the forces and pressures acting at particle contacts and in the pore fluid, that the stress controlling volume change due to deformation of the soil structure was (6 - u), whatever the area of contact between soil particles.

Theoretical mechanics or fundamental physics is ignored, in general, in the empirical approach. The mechanical behaviour of a system is simply related to its material properties through empirical or observed evidence. This approach has also been favoured by some researchers in describing the shear behaviour of unsaturated soils. Yong (1979) proposed an empirical three-dimensional relationship between water potential (i.e. soil suction), dry density and shear strength for unsaturated soils. The empirical nature of this approach severely limits its general applicability.

The difference between the first two approaches becomes more important for unsaturated soils than for saturated soils. Although substitute effective stress equations have been produced for unsaturated soils using the particulate mechanics approach ,the nature of the interparticle forces considered is more complex than for saturated soils, and the description of the response indicates a much more elaborate dependence on the extra variables that have to be introduced. For this reason, the particulate mechanics approach to partly saturated soils has met with only limited success(Lambe,1960).

Past research workers have directed their attention to the behaviour of partially saturated soils, and the initial attempts to describe their behaviour used the principle of effective stress, modified to suit partially saturated soils. This line of reasoning has been largely superseded by an approach, developed from the principle of continuum mechanics, which describes the behaviour of partially saturated soils in terms of two independent stress state variables and the author has based his own theoretical work on this approach (Fredlund,1973). Stress state variables are described in Chapter 4.

An unsaturated soil may be considered as a four phase system: solid, air, water and air-water interface (contractile skin). It was considered however that, before describing the present investigation into the behaviour of unsaturated soils, a brief exposition of some of the more fundamental physical properties of the air and water phases and the combined air-water system was necessary and this is presented in Chapter 2.

CHAPTER 2

THE NATURE OF UNSATURATED SOIL

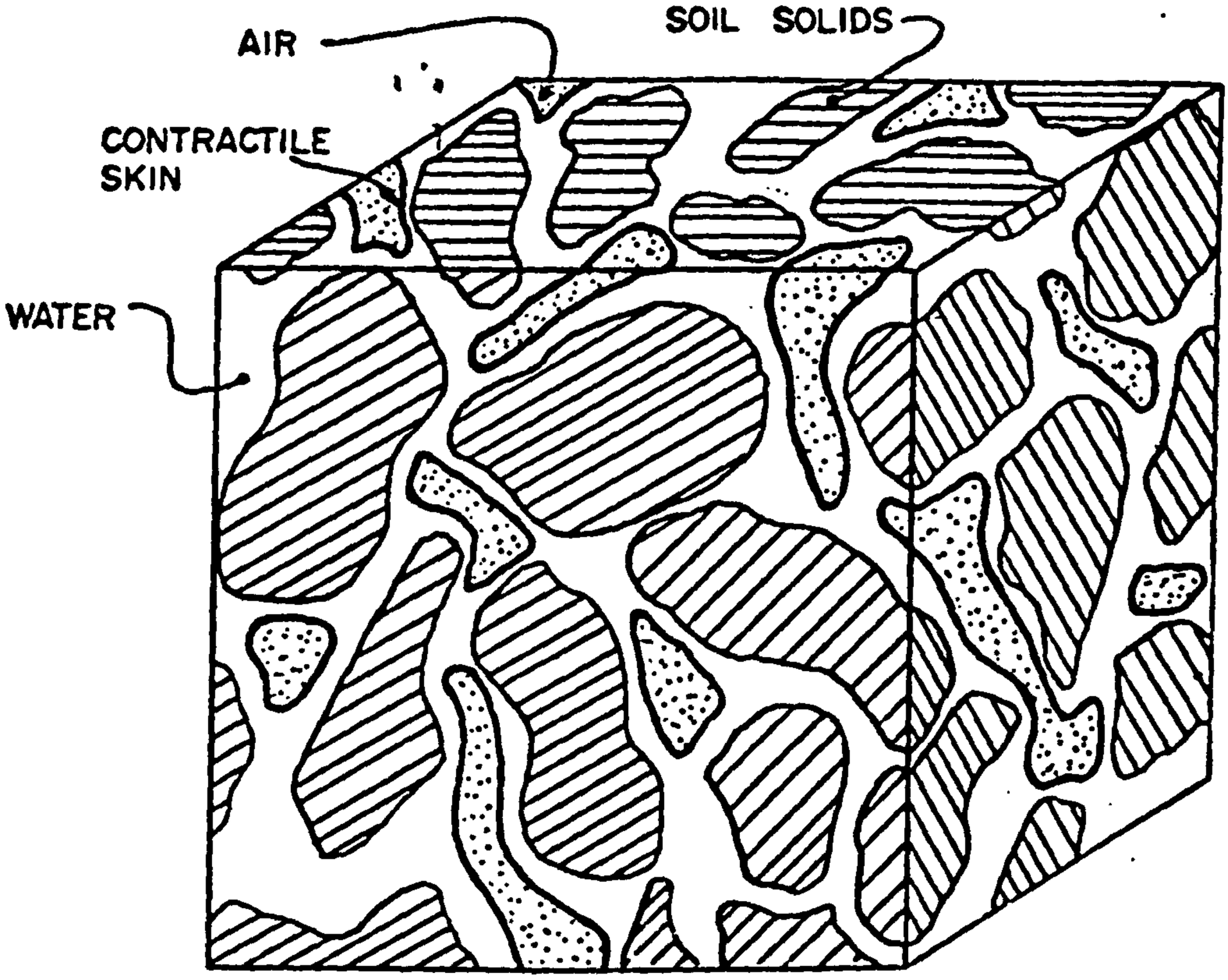

Figure 2.1: Element of an unsaturated soil
(after Fredlund,D.G.,1973)

with two phases that come to equilibrium under applied stress gradients (i.e soil particles and contractile skin) and two phases that flow under applied stress gradient (i.e. air and water). From the standpoint of the volume-weight conditions of an unsaturated soil, it is possible to consider the soil as a three-phase system, since the volume of the contractile skin is small and its weight can be considered as part of the weight of water.

When air is mixed with water it is immiscible, except for approximately 2% (by volume) that dissolves in the water. Since there is no chemical reaction, the resulting solution is a simple mixture. In the presence of a foreign solid, such as soil particles, the air and water pressures can differ and change at different rates during consolidation and shear processes.

2.2 The state of air and water phases in partially saturated soils

If a soil is completely dry then only air pressures will occur within its pores. If the soil is completely saturated only water pressures can occur. Obviously the effects of the water and air phases in a soil depend upon the degree of saturation.

Aitchison (1956) attempted to classify various categories of unsaturation in soils, and contributed some rather interesting definitions in terms of what he considered to be the 'parameters of unsaturation'.

These parameters were:

$p^{\bullet}$ = pressure deficiency in the pore water.

P_g = pressure in adsorbed gas or occluded air bubbles.

Sr = degree of pore space water saturation.

Δw = soil moisture deficit.

n_f = relative compressibility of the pore fluid;

n_f = Cf/Cw where Cf = the coefficient of compressibility of the pore fluid ; Cw = the compressibility of air free water.

Aitchison outlined four categories of unsaturation:

(1) Saturated

(2) Quasi-saturated.

(3) Partially saturated.

(4) Unsaturated.

The definitions were as follows:

(1) Saturated soil

$Sr = 100\%$; $\Delta w = 0$; $n_f = 1$; $p^* < 0$

Pg does not exist

(2) Quasi-saturated soil

A quasi-saturated soil was one in which all pores were filled with water and in which a pressure deficiency existed in the pore water. A finite value of soil moisture deficit occurred in the quasi-saturated state.

Thus $Sr = 100\%$; $\Delta w = 0$; $0 < p^* < p^*_d$

$n_f = 1$ and Pg does not exist

p^*_d is the critical pressure deficiency in the soil water at which the largest pore will drain.

(3) Partially saturated soil

$Sr < 100\%$; $\Delta w = 0$; $p^* < 0$; $n_f > 1$; $P_g > 0$

A partially saturated soil has some adsorbed or occluded air but will not absorb any water.

(4) Unsaturated soil

$Sr < 100\%$; $p^{\bullet} > 0$; $\Delta w > 0$; $n_f > 1$

These definitions covered all possibilities but they did not gain international acceptance.

Sparks (1963) followed the same line of reasoning as Aitchison (1956) and classified the categories of the unsaturated state as follows:

(i) quasi-unsaturated

(ii) critically unsaturated

(iii) unsaturated

(iv) partially undersaturated

He introduced another 'parameter of unsaturation' the soil moisture deficit, $\Delta\Omega_p$, which was the amount of water added to the existing natural value of Ω, where Ω was defined as the volume of pure water divided by the volume of soil grains (both at atmospheric pressure). The complexity of these categories discouraged their usage and they received little attention from research workers.

In 1965, Barden discussed how moisture affects clays and how the two phases of air and water existed in various states. As a guide for comparison, Barden used Bishop's effective stress equation for unsaturated soil (i.e. $\sigma' = (\sigma - Ua) + X(Ua - Uw)$ and assumed that optimum moisture content gave a

degree of saturation(Sr) of 90%, but pointed out that, in reality, the value of Sr optimum varied with the type of soil. Five states of partial saturation were given. These are listed below:

(i) Extremely dry. Sr ≤ 5%

The air phase is continuous throughout the soil mass and the water is in the form of highly viscous adsorbed water firmly attached to the skeleton by capillary forces. As Sr is so small, the parameter X in Bishop's effective stress equation is also small, and the equation becomes $\sigma' = \sigma - Ua$, where σ = total applied stress and Ua = pore-air pressure. Water pressures cannot be measured and the suction term (Ua - Uw) is very high. (Uw = pore-water pressure). Bishop's effective stress equation for unsaturated soils is discussed in Chapter 4.

(ii) Dry of optimum. 5% ≤ Sr ≤ 20%

As more water is added to a soil, there is a gradual transition from adsorbed to free water. The water tends to redistribute itself until the curvature of the air-water menisci are equal throughout the soil. At this stage both air and water pressures can be measured. The suction term (Ua - Uw) can still be large and Uw will rarely exceed zero.

(iii) At optimum. Sr ≡ 20%

This seems to be a changeover point from a continuous air system to a discontinuous air system.

(iv) Wet of optimum. 20% ≤ Sr ≤ 25%

Air no longer exists in a free state and is said to be occluded. There is no way of measuring Ua and the air exists

in the form of bubbles which can cause the pore fluid to be highly compressible but has little or no effect on the pressure of the pore fluid, which is now equal to Uw so that the effective stress equation is now $\sigma' = \sigma - U_w$.

(v) Very wet Sr ≥ 95%

It can be assumed that the small amount of air still present in the soil is trapped by the skeleton. Although the pore fluid will still tend to be highly compressible, any fluid that flows from the soil will be fairly incompressible.

Gulhati (1978) tried to narrow the ranges of saturation such that in each range partially saturated soil behaved in a similar fashion, differing only in degree of saturation. Table 2.1 identifies these narrower ranges as five states of partial saturation.

Table 2.1

States of partial saturation (after Gulbati, 1978)

Serial No. of State	Degree of Saturation	Description of State	Anticipated behaviour
1	Very high	air in the form of occluded bubbles in the pore water. No continuity in air phase	similar to saturated soil with a more compressible fluid than water
2	High	Transition-H	Complex
3	Medium	Water exists in inter-connected lenses around particle contacts. Air exists in inter-connected channels. Both air and liquid phase continuous	A function of two stress state variables (i.e.(σ - Ua) and (Ua - Uw).
4	Low	Transition-L	Complex
5	Very low	No continuity in liquid phase	Similar to dry soil

The second and fourth states of Table 2.1 are transition states from the first to the third state and from the third to the fifth state respectively. These transition states, are highly complex and much beyond the realm of current understanding.

It is the third state of partial saturation that is often implied when engineers talk of partially saturated soil. In this state continuity exists both in the water and in the air phase. Research in recent years has been focussed on this state.

The research described in this thesis is concerned with the third state of partial saturation and the terms partly saturated, partially and unsaturated are considered as interchangeable, applying to all soils in which the degree of saturation is less than 100% and greater than 0%.

2.3 The dimensions and physical condition of the air phase in an unsaturated soil

Air can exist in two distinct conditions within the voids of an unsaturated soil.

(i) as occluded air bubbles

and (ii) as a continuous air phase open to the atmosphere.

Air filled voids can arise in a number of ways. For convenience, in this instance, it is useful to think of the water as saturated with air in solution and under a fairly high pressure. The first way considered is by the reduction of the pore water pressure (If back pressure is used to increase the degree of saturation of a specimen to 100% and then the back pressure is released, air will come out of solution). This air may appear in the form of many bubbles of varying size, depending on the local concentration of air in the pore water (Figure 2.2(b)). Equilibrium will be established between pore-water pressure, surface tension, bubble radii, and air pressure inside the bubble. These occluded bubbles will be attracted differently by different soil particles, possibly resulting in shapes other than spherical. It is assumed that they will also be separated from the soil particles by films of water, (Jennings, 1960). If the pressure in the water in Fig.2.2(b) is

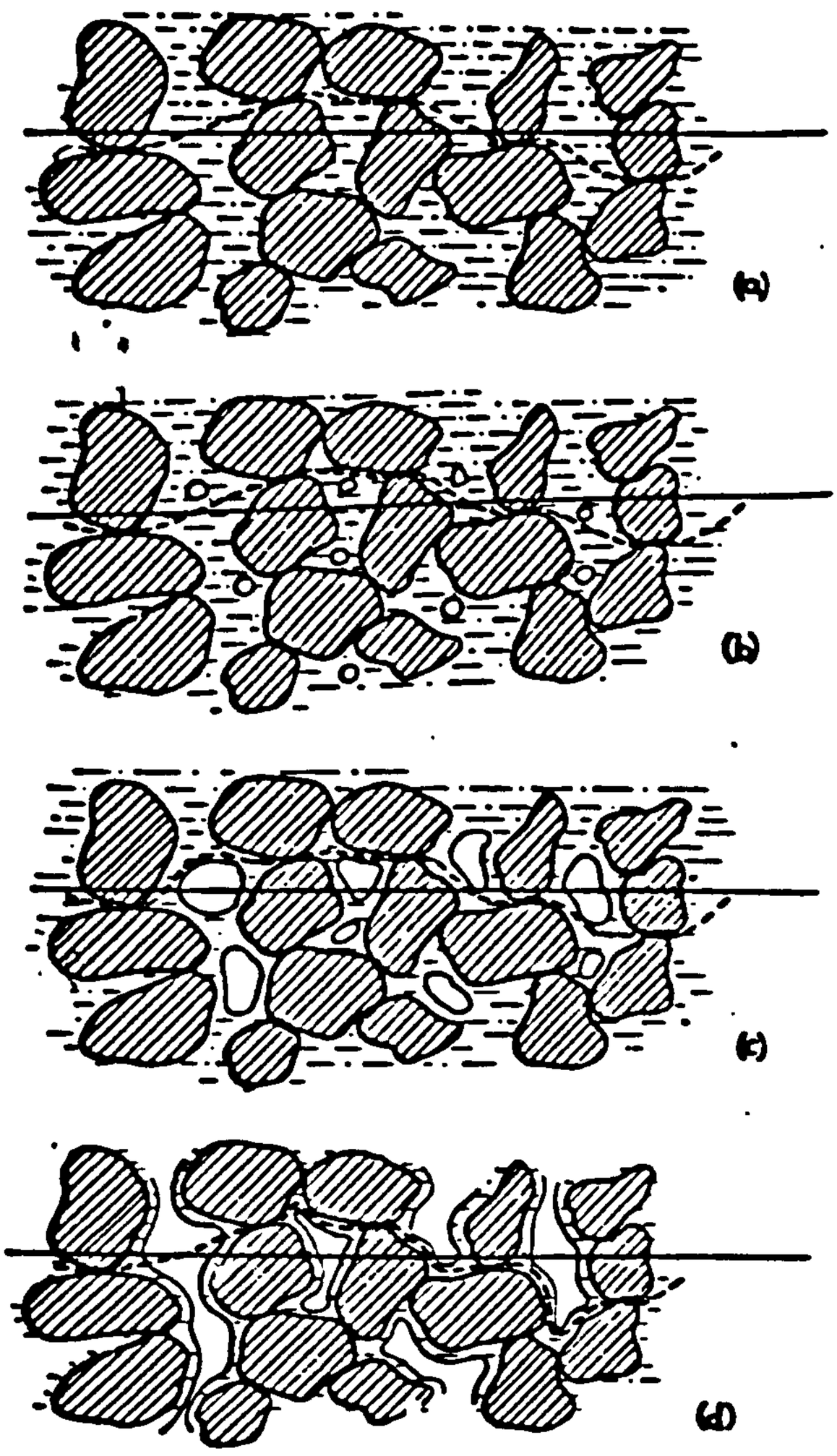

Figure 2.2: States of water-air in a soil (after Jennings,J.E. 1960)

(a) Pore fluid is water only; pore-water pressure positive
(b) Pore fluid is water with occluded air bubbles; pore-water pressure is positive
(c) Pore fluid is water with occluded air bubbles; pore-water pressure is negative
(d) Pore fluid is water with some occluded air bubbles and some air-voids connected directly to the atmosphere; pore-water pressure is negative

now further reduced, perhaps even to a negative value, the air bubbles will grow until a stage is reached as shown in Fig.2.2(c) where some of the voids are almost fully occupied with air. The bubbles may still be viewed as occluded and separated by films of water from the grains. If the pore water pressure is now still further reduced, some of the air bubbles will become continuous voids, some of which will contact with the atmosphere as shown in Fig. 2.2(d). The pressure in the water of the water films will now almost always be negative and the gas pressures in the continuous voids will be atmospheric. The second way considered is by the entrapment of air during compaction. Lastly, occluded air bubbles can form as a result of wetting up of the soil either due to an external supply of water or due to reduction in the volume of voids during compression (Burland, 1961).

There is no doubt that air can exist in the above two conditions. The question is whether air can exist in occluded form for an indefinite period or whether such a condition is unstable. Hilf (1956) deduced that bubbles are inherently unstable in water from his consideration of the stability of a single bubble in relation to the physics of solution of air in water. Blight (1961) observed under a microscope the stability of a single bubble in air-saturated water. He found in every case that the bubble radius decreased with time until the bubble finally vanished. Poulos (1964) concluded that the pressure difference between all bubbles of different size caused diffusion of air through the water from the smaller bubbles to the larger bubbles. Diffusion would continue until either (i)

all bubbles reached the same size, or (ii), until the large bubbles expanded and formed air spaces. At equilibrium, the pressure in all such air spaces must be equal, so that the radius of curvature of all menisci also must be equal. The possibility that the air would achieve state (i) above is extremely unlikely, since such a condition could only develop if all bubbles achieve the same diameter simultaneously. Thus, it appears likely that the air in a partially saturated soil exists in the form of many connected or unconnected air spaces.

2.4 The stability of air bubbles in a soil

Air is dissolved in water by a dynamic process in which it diffuses through the soil water from contact with air of higher pressure towards contact with the soil and air of low pressure. The soil air pressure, Ua is always greater than the pressure of neighbouring water, Uw. This difference is due to the surface tension of water and depends on the curvature of the air-water contact, which is determined by the dimensions of the soil pores. (i.e. $Ua - Uw = 2T/r$, one form of Kelvin's equation where T=surface tension and r=radius of soil pore).

Therefore, for a bubble in a given pore the minimum air pressure is reached when the bubble has a spherical form (b_2 in Figure 2.3) touching the neighbouring soil particles. Considering a soil which is in contact with air at atmospheric pressure, the following conditions will apply:-

(1) For a spherical air bubble in a soil Ua > Uatm (Uatm = the atmospheric pressure), air will migrate from the bubble to the surrounding water. As the bubble loses

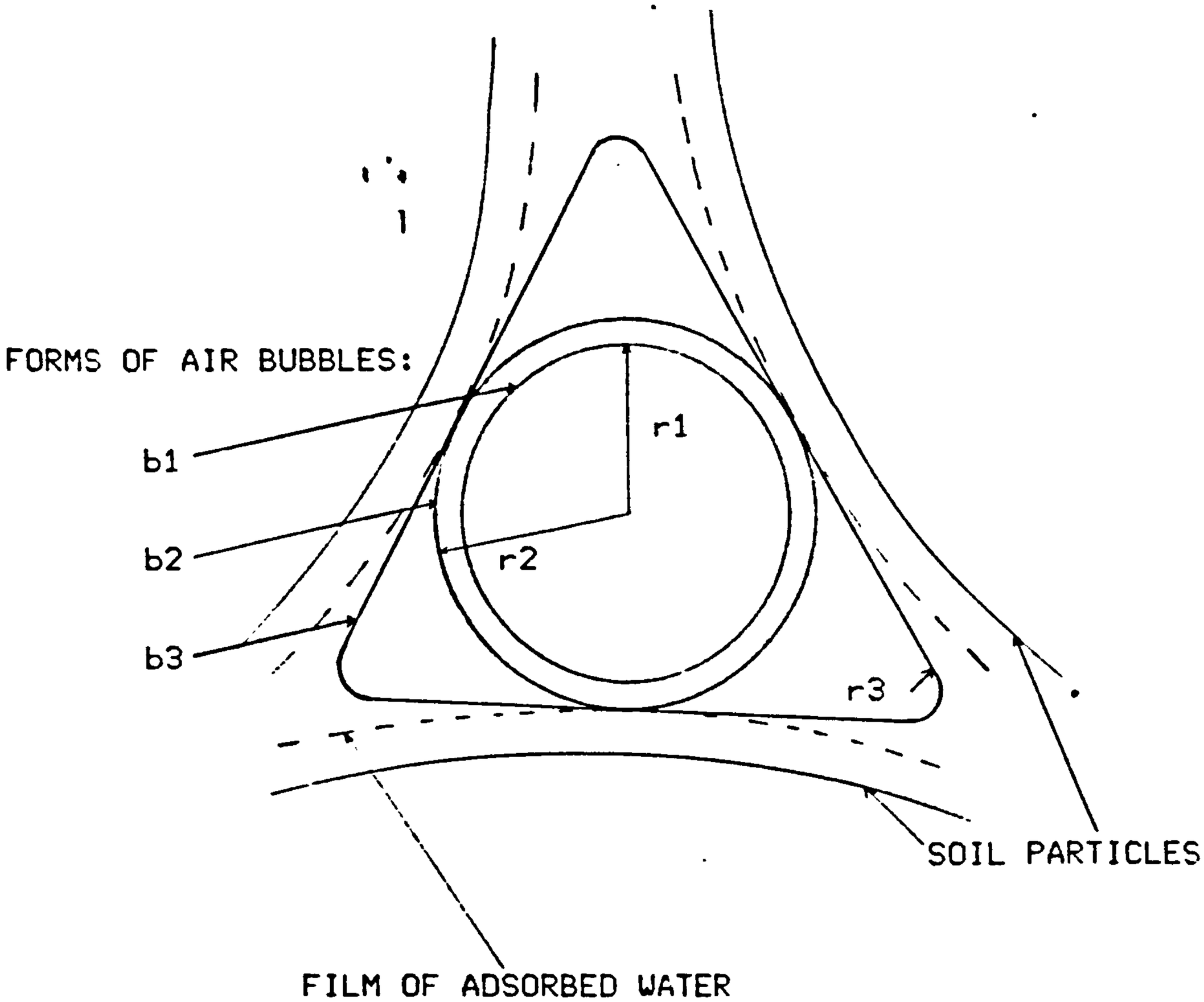

Figure 2.3: Forms of air bubbles in soils

air to the water it becomes smaller, i.e. r decreases, the bubble will dissolve in water and the soil air pressure, Ua will increase until the bubble disappears (i.e. Ua = Uw + 2T/r).

(2) For a spherical bubble Ua < Uatm, the dissolved air will separate out of the water and enter the bubble, which becomes larger. The ultimate size of the bubble will be controlled by the size of the pore in the soil. Therefore, the air pressure in the bubble must decrease until ~~it~~ *the bubble* attains the form b_3 (figure 2.3).

(3) For a spherical bubble Ua = Uatm, there will be no tendency for air to migrate into or out of the bubble and the bubble size will not change. However, the system is in unstable equilibrium and the slightest fluctuation in atmospheric pressure or temperature will cause the bubble to become unstable.

(4) For a bubble of the star form (b_3 in Fig.2.3) Ua > Uatm, the air dissolves and Ua decreases until it reaches Uatm.

(5) For the same case as (4) when Ua < Uatm, Ua will increase until it reaches Uatm.

The theoretical discussion presented above indicates that, enclosed air bubbles in a soil are unstable and always either decreasing or increasing in size. The bubble of the form b_3 in fig. 2.3 is stable when Ua = Uatm.

2.5 Density and compressibility characteristics of an air-water mixture.

2.5.1 The density of an air-water mixture.

The density and compressibility of an air-water mixture are formulated on the basis of conservation of mass. The density of gas depends on three variables : pressure, temperature and the kind of gas under consideration. Boyle's Law[1] deals with the compressibility of free air and Henry's Law[2] deals with the solubility of air in water.

Fredlund (1976) considered a cubic element with impervious sides containing an air-water mixture. All sides are fixed with the exception of the top which is in the form of a sealed, frictionless piston. Taking the volume of water as Vw and the volume of free air as Va', and applying the principle of conservation of mass to the element gives

$$\gamma_m \; V = \gamma_w \; V_w + \gamma_a \; V_a'$$

or

$$\gamma_m = \frac{\gamma_w \; V_w + \gamma_a \; V_a'}{V_w + V_a'} \qquad \ldots\ldots (2.1)$$

where V = total volume of the element (i.e. free air, Va' and water, Vw)

γ_m = density of the air water mixture

γ_w = density of water

and γ_a = density of air

[1] Boyle's Law: If the temperature of a given kind of gas is held constant, its density is proportional to the absolute pressure.

2

Henry's Law: The weight of gas dissolved in a fixed quantity of a liquid at constant temperature, is directly proportional to the pressure of gas above the solution.

If the force on the piston is increased then, applying Boyle's Law to the free air and dissolved air and assuming that the volume of water and the total mass of air (i.e. free and dissolved air) remain constant gives:

$$(Uai + dUa)\ (Va + dVa) = Uai\ Va$$

i.e. $$Uai\ Va + Uai\ dVa + Va\ dUa + dUa\ dVa = Uai\ Va$$

i.e. $$dVa\ (Uai + dUa) = -\ Va\ dUa$$

i.e. $$dVa = \frac{-V\ dUa}{Uai + dUa} \quad \ldots\ldots\ (2.2)$$

where Uai = initial air pressure

dUa = change in air pressure

Va = volume of free and dissolved air

dVa = change in air volume

Since Va = Vai' + Vdi'

where Vai' = initial volume of free air

Vdi = initial volume of dissolved air

and the final air pressure, Ua = Uai + dUa.

Therefore, equation (2.2) can be rewritten as:

$$dVa = \frac{-(Vai' + Vdi)\ dUa}{Ua} \quad \ldots\ldots\ (2.3)$$

In addition, dVa = dVa' + dVd

where dVa' = change in free air volume

dVd = change in dissolved air volume

But, the volume of gas dissolved in a given volume of liquid is independent of pressure i.e. dVd = 0

$$\text{so that } dVa = dVa' = \frac{-(Vai' + Vdi)dUa}{Ua} \quad \ldots\ldots (2.3a)$$

The new volume of free air, Va′ corresponding to a pressure Ua, is :

$$Va' = Vai' + dVa = Vai' - \frac{(Vai' + Vdi)dUa}{Ua}$$

$$\text{or} \quad Va' = Vai' - (Vai' + Vdi)\left(1 - \frac{Uai}{Ua}\right) \ldots\ldots (2.4)$$

Substituting (2.4) into (2.1), writing the volumes of air and water in terms of the initial degree of saturation and omitting the weight of air terms, gives:

$$\gamma_m = \frac{\gamma_w S}{S + (1-S)\frac{Uai}{Ua} + S.H\frac{Uai}{Ua}} \quad \ldots\ldots(2.5)$$

where S = initial degree of saturation =Vw/V

and H = Henry′s volumetric coefficient of solubility
= (Va-Va′)/Vw

For the case where the air has not had time to dissolve in the water, the S.H. (Uai/Ua) term can be omitted. It should be noted that the difference between the air and water pressures does not appear in the derivation.

2.5.2 The compressibility of an air-water mixture

the general definition for volume compressibility C is:

$$C = \frac{-1}{V}\,\frac{dV}{dU} \qquad \ldots\ldots (2.6)$$

in which V is the instantaneous volume, which is dependent on pressure U.

Bishop and Eldin (1950) and Skempton and Bishop (1954) based their approximate calculation of the compressibility of the air-water mixture on Boyle's Law and Henry's Law of solubility and derived the average compressibility of the air-water mixture for a change in pore pressure from Po to P (absolute) as

$$Cm = (1 - S + S.H)\,\frac{Po}{2P} \qquad \ldots\ldots (2.7)$$

where Cm = compressibility of air-water mixture

The surface tension and therefore the difference between the air and water pressures was disregarded.

Koning (1963) calculated the compressibility of an air-water mixture using Boyle's Law. He only partly accounted for the influence of surface tension between air and water, and for practical purposes, where small pressure changes occur, his formulae is sufficient. The modulus of compressibility of an air-water mixture was given as:

$$\frac{1}{Kw} = \frac{Kwo}{(1 - \frac{Va}{V}) + \frac{Va}{V}\,x\,\frac{Kwo}{Ka}} \qquad \ldots\ldots (2.8)$$

where Kw = modulus of compressibility of an air-water mixture.

Kwo= modulus of compressibility of water without air bubbles (assumed to be 20,000 kg/cm^2)

Ka = modulus of compressibility of air bubbles (Ka values of from 1 to 5 kg/cm^2 have been introduced).

Va = volume of air

V = total volume (= volume of water + volume of air)

Boyle's Law, Henry's Law of solubility and surface tension between air and water greatly influence the air-water mixture compressibility. One of the first attempts to take into account the influence of all these factors was made by Schuurman (1964). In 1966, Schuurman, enlarged and corrected his 1964 paper using surface tension and the above laws to obtain a relationship between air and water pressures. The compressibility of an air-water mixture was given as:

$$Cm = \frac{1}{Va' + Vw}\left[\frac{(Vai' + Vd)Uai}{(Va' + Vd)^2} - \frac{2Ts}{3ro}\times\frac{1}{Va'}\times\left(\frac{Vai'}{Va'}\right)^{1/3}\right]^{-1} \quad \ldots\ldots (2.9)$$

where Ts = surface tension (= 74 x 10^{-6} kgf/cm)

ro = initial radius of air bubbles

His theory was correct only if the degree of saturation was in excess of 85%, when the air was assumed to be present in the form of bubbles. To account for surface tension effects, it was necessary to assume the number and size of air bubbles

and apply the Kelvin's equation (i.e. $U_a - U_w = 2T/r$).

The final equation was unusable from an engineering standpoint.

Fredlund (1976) derived the compressibility of an air-water mixture, Cm, using a direct proportioning of the air and water and in accordance with the compressibility definition (Eqn. 2.6)

$$C_m = \frac{1}{V_w + V_a'}\left(\frac{dV_w}{dU} + \frac{dV_a'}{dU}\right) \quad \ldots\ldots (2.10)$$

Note that the volume of dissolved air is within the volume of water, and U is a reference pressure for the mixture.

Either the air or water pressure can be used as a reference pressure. By applying the chain rule of differentiation,

$$C_m = \frac{1}{V_w + V_a'}\left(\frac{dV_w}{dU_w}\frac{dU_w}{dU} + \frac{dV_a'}{dU_a}\frac{dU_a}{dU}\right) \quad \ldots\ldots (2.11)$$

$$\text{Fredlund defined } B_{aw} = \frac{dU_a}{dU_w} \quad \text{and} \quad B_{wa} = \frac{dU_w}{dU_a}$$

The pore pressure parameters Baw and Bwa can also be written as the ratio of the Ba and Bw pore-pressure parameters proposed by Bishop and Henkel (1962).

$$B_a = \frac{\Delta U_a}{\Delta 63} \; ; \quad B_w = \frac{\Delta U_w}{\Delta 63}$$

$\Delta 63$ = an equal all-round stress increment in the undrained test

$$\text{Therefore, } B_{aw} = \frac{B_a}{B_w} \quad \text{and} \quad B_{wa} = \frac{B_w}{B_a}$$

The Baw pore pressure parameter should always be less than 1.0 for undrained loading, becoming equal to 1.0 at saturation.

The Bwa pore pressure parameter should always be greater than 1.0, for undrained loading, becoming equal to 1.0 at saturation.

Using the water pressure as a reference pressure,

$$Cm = \frac{-1}{Vw + Va'}\left(\frac{dVw}{dUw} + \frac{dVa'}{dUa} \times Baw\right)$$

Substituting equation (2.3a) in the above equation and since the compressibility of water $Cw = \frac{-1}{Vw} \times \frac{dVw}{dUw}$

and also writing the volumes of air and water in terms of the initial degree of saturation , S, we have

$$Cm = SCw + Baw\frac{(1 - S)}{Ua} + Baw\frac{S.H}{Ua} \quad \ldots\ldots \quad (2.12)$$

where H = Henry's volumetric coefficient of solubility

Fredlund recommended that an experimentally measured pore pressure parameter Baw or Bwa should be used to take account of surface tension effects.

It should be noted that when the degree of saturation is above 85%, the air is in the form of bubbles, so that the air pressure, Ua, cannot be measured but must be predicted. In other words, equations (2.5) and (2.12) are only suitable when the air phase can be considered as a continuous phase.

2.6 Anomalies in the behaviour of unsaturated soil.

Olson and Langfelder (1965) suggested three very interesting anomalies associated with unsaturated soil.

(1) If water cavitates at a pressure of approximately -1 atmosphere (gauge) then how can pore water pressures of -100 psi (or -7 bar) and lower be possible in unsaturated soils where the water films have ready access to air?

(2) If the tensile strength of perfectly deaired water is approximately 2,800 psi (or 193 bar) (R.B. Green, 1951), then how is it possible to have tensile stresses greater than 100,000 psi (or 6897 bar) as suggested by theoretical calculations based on measurement of vapour pressure?

(3) The third anomaly is suggested by the simple model shown in Fig.2.4. In this model, it is assumed that the entire surface of each particle is hydrated. Capillary theory indicates that the pressure is always greater in fluid (gaseous or liquid) on the concave side of an interface between two immiscible fluids. Referring to Fig. 2.4 and taking the ambient air pressure as zero (gauge), the pore water pressure is negative at A, positive at B and zero at C. The obvious question is : how is it possible for a continuous water film to have different pressures at different locations without undergoing flow? Or, more importantly, what pore water pressure is actually measured with the usual pore water pressure measuring equipment?

To help explain these anomalies, Olson and Langfelder

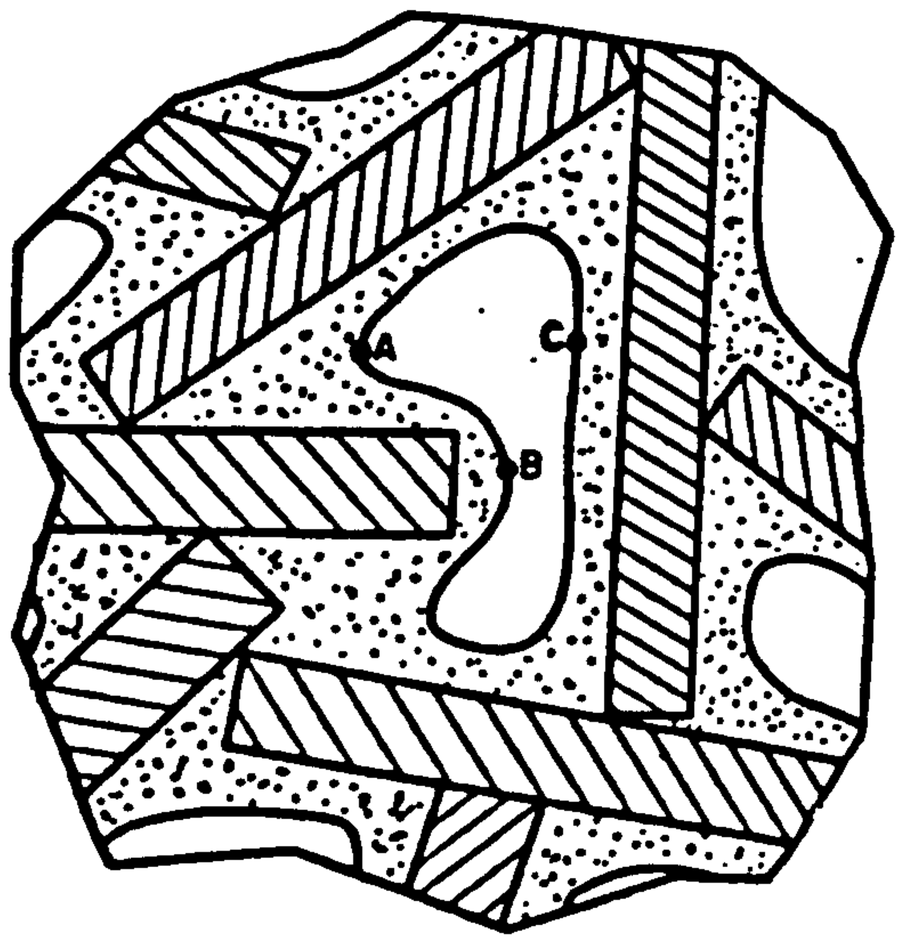

Figure 2.4: Idealized section through an unsaturated cohesive soil

presented an equation for the total head in the pore water as follows:

$$h = \frac{u}{\gamma_w g} + w + a + z$$

in which $u/\gamma_w g$ = the pressure head

w = the osmotic head

a = the adsorptive head

and z = the position head

The explanations of the anomalies are as follows:

Observations that water in free contact with air cavitates at a pressure of approximately -1 atmosphere probably apply to the pore water in an unsaturated soil i.e. the actual limiting negative pore water pressure in the soil is approximately -1 atmosphere. If a probe records lower pressures (using the axis translation technique, see appendix 1) the water films are so thin that all the water is within the range of influence of osmotic and adsorptive fields. Thus the pore water at some point in the soil may have a pressure of -1 atmosphere, but the total head at that point is further lowered by the presence of osmotic and adsorptive effects. A pressure lower (more negative) than -1 atmosphere must be applied to the water in the probe to reduce the total head of the water in the probe to the total head of water at the point under consideration in the soil.

Similarly, calculated negative pore water pressures of lower than -100,000 psi (or 6897 bar) for nearly dry soils mean that such a negative pore water pressure would have to be

applied to the water in a probe in order to reduce the total head of the water in the probe to the total head of the water. The actual pressure in the water tightly adsorbed against the surface of the clay is likely to be positive, not negative,and therefore the anomaly of water having an actual tensile strength of only 2,800 psi (or 193 bar), whereas vapour pressure calculation suggest much more negative pore water pressures, is also resolved.

The third anomaly is resolved by noting that in an unsaturated soil where the probe records a negative pore water pressure, the actual pore water pressure in the soil may be negative, zero or positive, depending on location. It does not make any difference where the probe is located in the soil because the probe does not measure the pore water pressure, but records the water pressure in the probe, which is the pressure that must be applied to that water to reduce its total head to the total head of the water in the soil. The axis-translation technique operates by raising the total head of the water in the soil rather than by lowering the total head of the water in the probe, but the end result is the same.

Because the pore water pressure measured with a probe is not equal to the actual pore water pressure in the soil, except at certain locations, it would be more expressive to refer to the pore water pressure in the probe as the 'equivalent pore water pressure'.

Fredlund (1976) pointed out another air-water mixture anomaly. Consider a sample of unsaturated soil contained in a sealed piston and cylinder arrangement. As the load on the

piston is increased (i.e. total stress), the free air is compressed in accordance with Boyle's Law (Fig.2.5) under the new increased air pressure, air goes into solution in accordance with Henry's Law. This results in a further decrease in the size of the free air bubbles. At high degrees of saturation, this volume decrease may be a significant percentage of the total volume of free air.

If the radius of curvature is decreasing during the decrease in free air volume, Kelvin's equation given by Ua - Uw = 2Ts/r indicates that the difference between the air and water pressures must increase. Since a positive total stress was initially applied, it is logical to assume that the water pressure has undergone a positive increase. Therefore the air phase must have undergone a positive increase. In fact, the air phase must have undergone a larger increase to satisfy Kelvin's equation. This increase in air pressure (due to surface tension) would result in a further decrease in volume in accordance with Henry's Law. Once again, Kelvin's equation must be satisfied and the air bubble moves faster and faster towards self destruction as the air pressure goes to infinity.

The above description is the result of strictly applying Boyle's Law, Henry's Law and Kelvin's equation. It certainly does not appear feasible and compatible with observed behaviour. The above apparent anomaly is partly overcome by assuming that, although the free air volume is decreasing, the radius of curvature is increasing, as shown in zone 1 of Fig. 2.5.

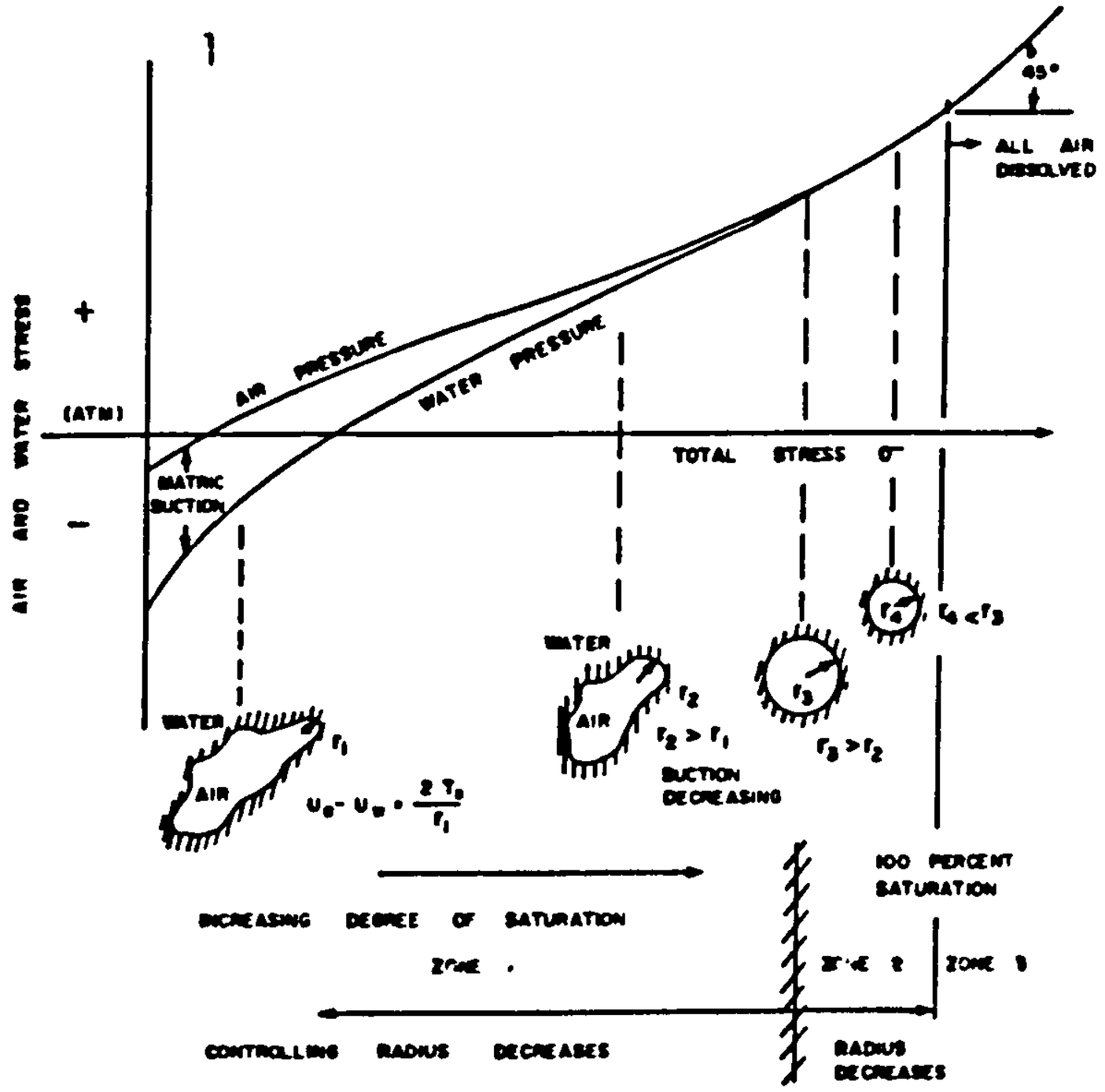

Figure 2.5: Pore air and pore water responses to a change in total pressure in a closed system
(after Fredlund,D.G.,1976)

However, increased compression of the sample will eventually result in the air bubbles being occluded (zone 2). At this time the self destruction mechanism takes over.

2.7 The flow of water in an unsaturated soil.

Fredlund (1981) pointed out some of the misconceptions concerned with the flow of water in an unsaturated soil.

Firstly, water does not flow from a point of high water content to a point of low water content. Even in a homogeneous soil a difference in water content does not mean that a water content gradient exists, since there is the possibility of different stress history effects. Secondly, water does not flow as a result of a suction gradient ; flow occurs independently in the water and air phases due to gradients in each phase. Thirdly, the salts in a soil, as reflected by the osmotic or solute suction, affect flow in an unsaturated soil in the same manner as in a saturated soil. Suction in unsaturated soils will be discussed in detail in Chapter 3.

Fredlund defined 'fundamental driving potentials' to describe the flow of air and water in unsaturated soils. Under the influence of these driving potentials, fluid will always flow from a region of higher potential to a region of lower potential. The two main driving potentials are:

(i) The driving potential for the water phase of an unsaturated soil (which is the same as a saturated soil). If the velocity head is neglected, the driving potential is a hydraulic head.

$$hw = \beta + \frac{Uw}{\rho \gamma_w} \quad \text{.....(2.14)}$$

where hw = total head in the water phase

β = elevation head from an arbitrary datum

Uw = pore water pressure

γ_w = density of water, and

g = acceleration due to gravity

The driving potential is the same whether the degree of saturation is 100 percent or less. It is the same whether the pore water pressure is positive or negative.

(ii) The driving potential for the air phase of an unsaturated soil is similar to the water phase except that the elevation head is neglected.

$$ha = \frac{Ua}{g \gamma_a}$$

where ha = total head in the air phase

Ua = pore-air pressure, and

γ_a = density of air

The flow of the air phase is actually in response to independent gradients in each of the components constituting air. However, in general, the driving potential can simply be used as the pore-air pressure, Ua.

Another important driving potential is the thermal gradient as reflected by a change in temperature with space and time. Changes in temperature can significantly affect the pore-air phase and cause flow in the air phase. A change in temperature produces a less significant effect on the water

phase in an unsaturated soil. However, the change in pore-air pressure produces a change in the pore-water pressure in accordance with the Baw pore-pressure parameter of the soil (Fredlund, 1976). Fredlund also indentified three secondary driving potentials which may have some influence on flow.

(a) Diffusion of air through the water phase and the solution of air in-water. These mechanisms are in response to the pore-air pressure.

(b) A chemical gradient which could cause flow from a region of high concentration to a region of lower concentration, independent of other gradients.

(c) An electrical gradient which could cause a flow of water from a point of high voltage to a point of lower voltage.

Saturated soils are a special case of unsaturated soils. The analysis of the latter is complex and involves idealisation of the soils as three or four phase systems which are decisively influenced by the degree of saturation. The interaction of the air and water phases is not well understood and calculation of basic properties such as the density and the compressibility of air-water mixtures is extremely tentative. As mentioned earlier, soil suction is a very important parameter in unsaturated soils and the next chapter will deal with this parameter in detail.

CHAPTER 3

SOIL SUCTION

Chapter 3

Soil Suction

3.1 Introduction

The first group to recognize the important role played by the soil fluid in the behaviour of soils was probably Croney et al at the Road Research Laboratory in London (1948). They borrowed their terminology from soil science and observed the effect of soil moisture deficiency (soil suction) on soil behaviour.

When pore water pressures are positive, there is no conceptual difficulty in understanding the presence of water in soil. However, when the pore water pressures become negative i.e. below atmospheric pressure, such as in soil above a water table, the problem of understanding the mechanisms becomes more difficult. In soil science, this problem is now treated thermodynamically, where the mechanisms of soil water retention need not be considered in developing a rational understanding of and theory for the behaviour. When an unsaturated soil comes in contact with a pool of free water, it absorbs water; the soil exerts a suction on the free water. (Fig. 3.1)

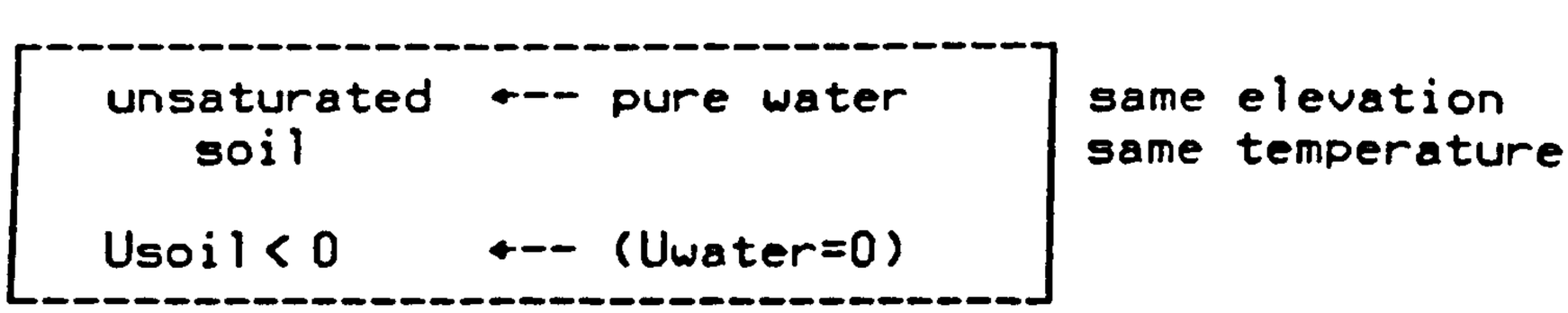

Fig. 3.1. Diagrammatic representation of soil suction

Negative pore-water pressure is a term commonly used to refer to the suction in a soil sample. This is particularly true in a partly-saturated soil in which the pore spaces contain both air and water. Even at equilibrium (i.e. no flow), the pressures in each phase are different, the air pressure always being higher because of surface tension effects. The difference in the pressures is expressed algebraically as (Ua-Uw) and this term is called the suction or pressure deficiency.

In soil physics, the suction is represented by an equivalent column of water in a simple capillary tube, that is,

$$h = \frac{(Ua - Uw)}{\gamma_w^g} = \frac{2Ts}{r\,\gamma_w^g} \quad \ldots\ldots (3.1)$$

where Ts is the surface tension of water (gm/cm)

r is the radius of capillary tube (cm)

γ_w^g is the unit weight of water (dynes/cm^3)

For large value of suction, h becomes very large and for convenience Schofield (1935) expressed h (in cm) in terms of pF where $pF = \log_{10} h$ ..... (3.2)

Aitchison (1960) defined suction for a soil-water-air system as the pressure deficiency in the water phase of the pore fluid with respect to the soil air pressure under defined conditions of external stress and temperature for a specific soil.

Croney and Coleman (1960) reserved the term suction to indicate the pressure deficiency in the specific case of a test specimen free from external stress. The term negative pore-water pressure was used for any pressure deficiency measured in

situ or in the laboratory with the soil subjected to a particular stress system.

In these definitions, it is implied that suction is a function of inter alia water content and pore space saturation. Hence at a low degree of saturation, very high suction values are possible; the suction may exceed hundreds and even thousands of atmospheres which infers that the pore water must be capable of withstanding absolute tensions. This property of water has been discussed by Bolt and Miller (1958) and Marshall (1959), and they support the supposition that water can take absolute tensions. Blight (1961) and Donald (1961) succeeded in obtaining an absolute tension of 40 p.s.i. in tap water with a simple laboratory experiment. Aitchison (1960) reported that absolute tensions in water were possible, but he thought it unlikely that the soil water was ever subjected to absolute tensions exceeding 200 atms. He also postulated that the soil water could not exist in a state of tension in any soil pore if

(a) the tension was sufficient to drain the pore or,
(b) the tension or pressure deficiency in the soil water did not exceed the pressure of the soil air or,
(c) the pore was of such small dimensions that the attraction of the water molecules to the soil surface produced a pressure which was greater than the pressure deficiency in the soil water.

Conversely, the soil water in any pore might be considered to be in a state of tension if

(d) the pressure deficiency in the soil water exceeded the

pressure of the soil air, or

(e) some of the water in the pore was sufficiently remote from the soil-water interface to be substantially free of attractive forces or,

(f) an increase of suction or moisture tension caused the pore to drain in accordance with capillary laws.

3.2 Matrix, osmotic and total suctions

The suction present in a soil sample is made up of two main components which act together to produce the total suction.

The review panel for the soil mechanics symposium, 'Moisture Equilibria and moisture changes in soils' (Aitchison et al,1965) adopted the subdivision of soil suction and the definitions quoted by the International Society of Soil Science.

(a) Matrix or capillary suction (hm) where hm=(Ua - Uw)

The negative gauge pressure relative to the external gas pressure on the soil water, to which a solution identical in composition with the soil water must be subjected in order to be in equilibrium, through a porous permeable wall, with the soil water. Note that this parameter may be identified with the definition of matrix or capillary potential given in section 3.3.

(b) Osmotic and solute suction (hs)

The negative gauge pressure to which a pool of pure water must be subjected in order to be in equilibrium through a

semi-permeable (i.e. permeable to water molecules only) membrane, with a pool of water containing a solution identical in composition with the soil water. Note that this parameter may be identified with the definition of osmotic potential given in section 3.3.

(c) Total suction (h)

The negative gauge pressure relative to the external gas pressure on the soil water to which a pool of pure water must be subjected in order to be in equilibrium, through a semi-permeable membrane, with the soil water. Total suction is thus equal to the sum of matrix or soil water suction and osmotic suction. (This relationship has been experimentally verified by Krahn and Fredlund (1972)). Total suction may also be derived from the measurement of the partial pressure of water vapour in equilibrium with the soil water. Note that this parameter may be identified with the definition of total potential given in section 3.3, when gravitational and external gas pressure potentials can be neglected.

$$h = (U_a - U_w) + h_s \quad \ldots\ldots (3.3)$$

Since the changes in the osmotic component with water content are relatively small (Krahn and Fredlund ,1972), it is possible to use matrix suction as a substitute for the total suction variable. In this case either the changes in osmotic suction must be assumed to be small or else simulated between the field and the laboratory.

It is difficult to measure matrix suction in the field due to cavitation of the measuring system at pore-water stresses approaching 100 KPa (1 atm.) negative. In the laboratory these difficulties are circumvented by using the axis-translation technique (Hilf, 1956) (see appendix 1).

3.3 Soil water potential

Soil suction can also be determined by the more flexible thermodynamic variable of potential, or in this particular case soil water potential. According to the International Society of Soil Science, soil water potential (Q) is defined as the work done per unit quantity of pure water in order to transport reversibly and isothermally an infinitesimal quantity of water from a pool of pure water outside the adsorptive force fields at a specified elevation and at atmospheric pressure to the soil water (at the point under consideration).

The components of soil water potential are:

(a) matrix or capillary potential(Qm) - This results from the interaction of water with the adsorptive force fields emanating from solid surfaces. The equivalent soil suction component is the matrix suction (hm).

(b) Osmotic or solute potential (Qs) - This results from the interaction of water with force fields emanating from dissolved substances. The equivalent soil suction component is the solute suction (hs).

(c) Pressure potential (Qp) - This results from the difference in potential energy of water caused by an

external pressure other than that applied to the reference water.

(d) Gravitational potential (Qz) - This results from the potential energy water has due to its position in gravitational field relative to that of the reference water. There is no equivalent soil suction component.

1

Bolt and Miller (1958) considered total suction as being the intersection of a number of components of suction including osmotic potential, adsorption potential,pressure potential and gravitational potential. Marshall (1959) subdivided total suction into only two components, matrix suction and solute suction and considered the matrix suction as the moisture stress measurable by tensiometer, pressure membrane or suction plate while total suction was the moisture stress measurable in terms of vapour pressure. Aitchison (1960) pointed out that the difference between matrix suction and total suction was not significant within the range of moisture stresses commonly considered, and supported this argument with experimental evidence.

Schofield (1960) found that with a swollen sodium montmorillonitic clay the hydrostatic pressure mid-way between the surfaces of two platelets was about 1 atmosphere greater than that of pure water in equilibrium through a pressure membrane. This observation therefore contradicted the assumption that matrix suction was equivalent to total suction but Schofield reasoned that the pressure measured through the

pressure membrane was the only pressure that interested the engineer and therefore this value could be used in problems of effective stress.

Gardner (1960) also regarded the matrix potential (capillary potential) as being the suction measured through a pressure membrane.

Krahn and Fredlund (1972) experimentally verified that the sum of matrix and osmotic suction was equal to total suction, and concluded that the matrix and total suction were dependent on the moulding water content but essentially independent of the dry density for remoulded, compacted soils.

Soil suction has been given many different names during past investigations; soil pressure deficiency, soil moisture deficiency, negative pore water pressure, capillary suction, matrix suction, capillary potential, negative potential, pore water suction, pore water tension, soil moisture tension, etc.

In this thesis, the term matrix suction will generally be adopted to represent the total suction, since the difference between total suction and matrix suction is very small and can be neglected.

3.4 Mechanisms of soil-water retention

Soil suction is dependent on, *inter alia*, the moisture content of a soil. The water present in a soil is retained by a combination of effects but mainly by surface tension, adsorption and osmotic imbibition. These mechanisms of soil-water retention will be described briefly in this section.

(a) Surface tension

The phenomenon of surface tension is due to the existence of molecular forces. In a suspended drop of water, for example, the particles in the interior of the liquid are attracted equally in all directions by other molecules of the liquid. The resultant attraction on any molecule in the interior is, therefore, zero. A molecule on the surface of the drop of water, on the contrary, is not attracted equally on all sides, since the molecules of the gas surrounding the drop exert less attraction upon the water molecule than is exerted by the other water molecules. The resultant attraction is, therefore, inward along a line perpendicular to the surface of the liquid at that point. It has been found that the behaviour of a drop of water under the action of these forces is identical to the behaviour of a simulated drop which is enclosed in a watertight membrane of a uniform tension. The tension that this watertight membrane would have to possess in order to produce the observed phenomena is defined as surface tension.

(b) Adsorption of water on clay minerals

In most natural soils and particularly in expansive clays, the soil particles consist of a significant fraction of clay mineral particles, which cannot be considered as inert. The clay particles have negatively charged surfaces which attract water, called adsorbed water which can form in the following ways:

(i) Hydrogen bonding - The same bonds which form with the water can also form between the hydrogen ion (H+) and the

oxygen (O--) or . the hydroxyl (OH-) ions which normally compose the surface of clay minerals.

(ii) Polar adsorption - Since water molecules are not symmetrical this results in polarized charges and the positive side of water molecules can therefore be attracted and aligned towards the surface of the clay particles.

(iii) Cation adsorption - The positively charged cations, e.g. Na+, Ca+, which also adsorb water around them, are themselves attracted to the negatively charged clay particles.

(c) Osmotic imbibition:

As mentioned above, cations are adsorbed onto clay particles and the adsorbed ions and water constitute the diffuse double layer. This adsorption of cations with the double layer can establish a solute concentration difference between the soil water beyond the double layer and that in the double layer. Therefore, the potential or soil suction of the water beyond the double layer must be such that this water is in equilibrium with the water within the double layer.

It may be stated, in general, that two types of forces account for the soil-water retention in soils:

(a) Surface tension (capillary) forces.
(b) The attraction of soil particle surfaces for water molecules (adsorption).

It appears that water held in a fairly coarse porous medium, in excess of a very thin adsorbed layer (about two molecules thick), is governed by capillary forces (Foster,

1948). The moisture contents of partly saturated soils encountered in practice are definitely in the capillary range (i.e. as high as 10,000 KN/sq.m).

3.5 Relationship between the soil suction and moisture content.

The quantity of water held in a soil at a given suction and the quantity that will be transferred by a given change of suction can be determined from a knowledge of the relationship between soil suction and moisture content.

Although the suction of soil increases with decreasing moisture content, the relationshp for any material is not in general unique. A single method cannot be used for exploring the variation of suction with moisture content over the moisture range from saturation to oven-dryness, and in practice at least three methods have to be employed. Originally the suction-plate, centrifuge and vacuum-desiccator methods were used. (Croney and Coleman,1960). The relationship is a function of the grading of the soil, its compressibility, its density and the mineral nature of the soil particles (see Fig. 3.2).

Croney and Coleman (1954) noted that complete shearing in soil produced a suction condition that was found to depend solely on the moisture content of the soil and was independent of the initial suction prior to disturbance. Thus for each soil a unique relationship without hysteresis was found connecting suction in the fully sheared condition with the moisture content.

Water content, for a given soil suction, is highly sensitive to soil material variability such as variations in

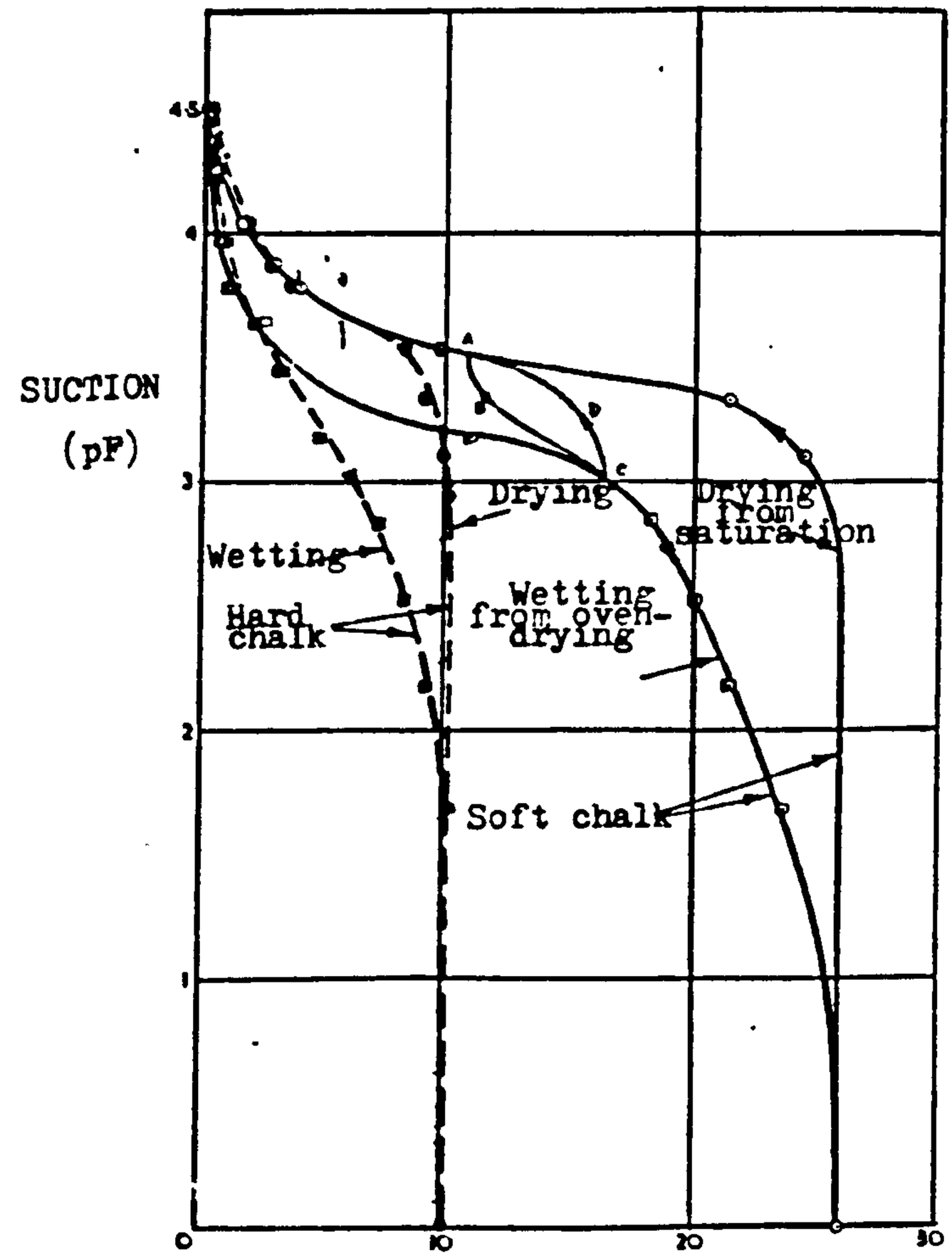

Figure 3.2: Relationships between suction and moisture content for samples of hard and soft chalk (after Croney,D.,1952)

soil type, clay content, density, soil structure, etc.. For example, typical non-seasonal variations in water contents in clay soils occurring over only a few centimetres at depth can be as much as 20%(Richards,1974). A good example of the comparison between soil suction and water content measurements in a practical situation is shown in Figure 3.3.

Aitchison [1] and Richards (1965) determined the relationship between clay content and water content at constant soil suction in the B-horizon of a Red-brown Earth. This soil was described as a moderately active clay with

Liquid limit	70 - 80%
-2μ fraction	50 - 65%

The results for three soil suctions controlled in a pressure membrane apparatus are shown in Figure 3.4.. Included on this figure are best-fit correlations, resulting from statistical analyses.

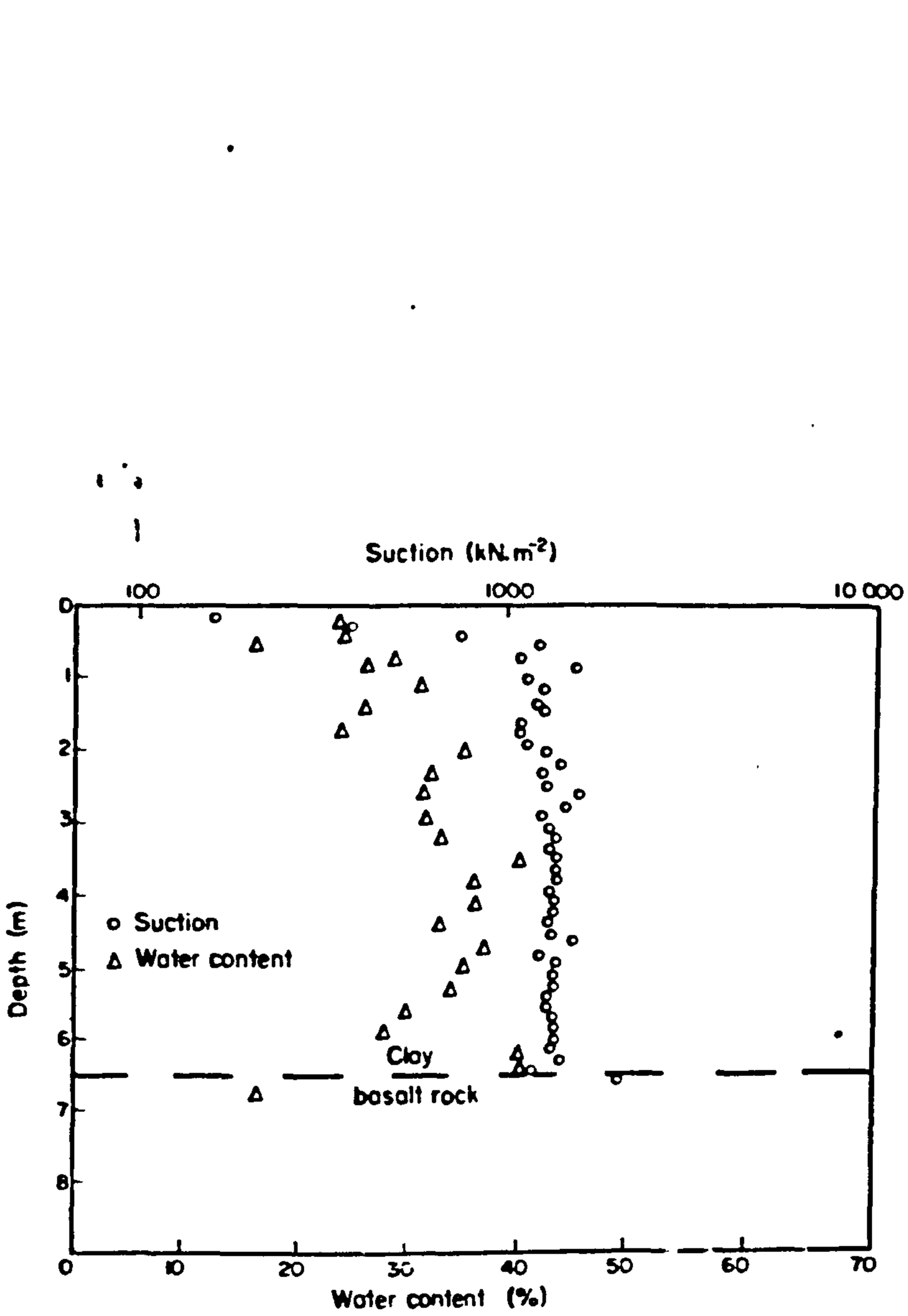

Figure 3.3: Water content and soil suction profiles in a basaltic clay (after Richards,B.G.,1974)

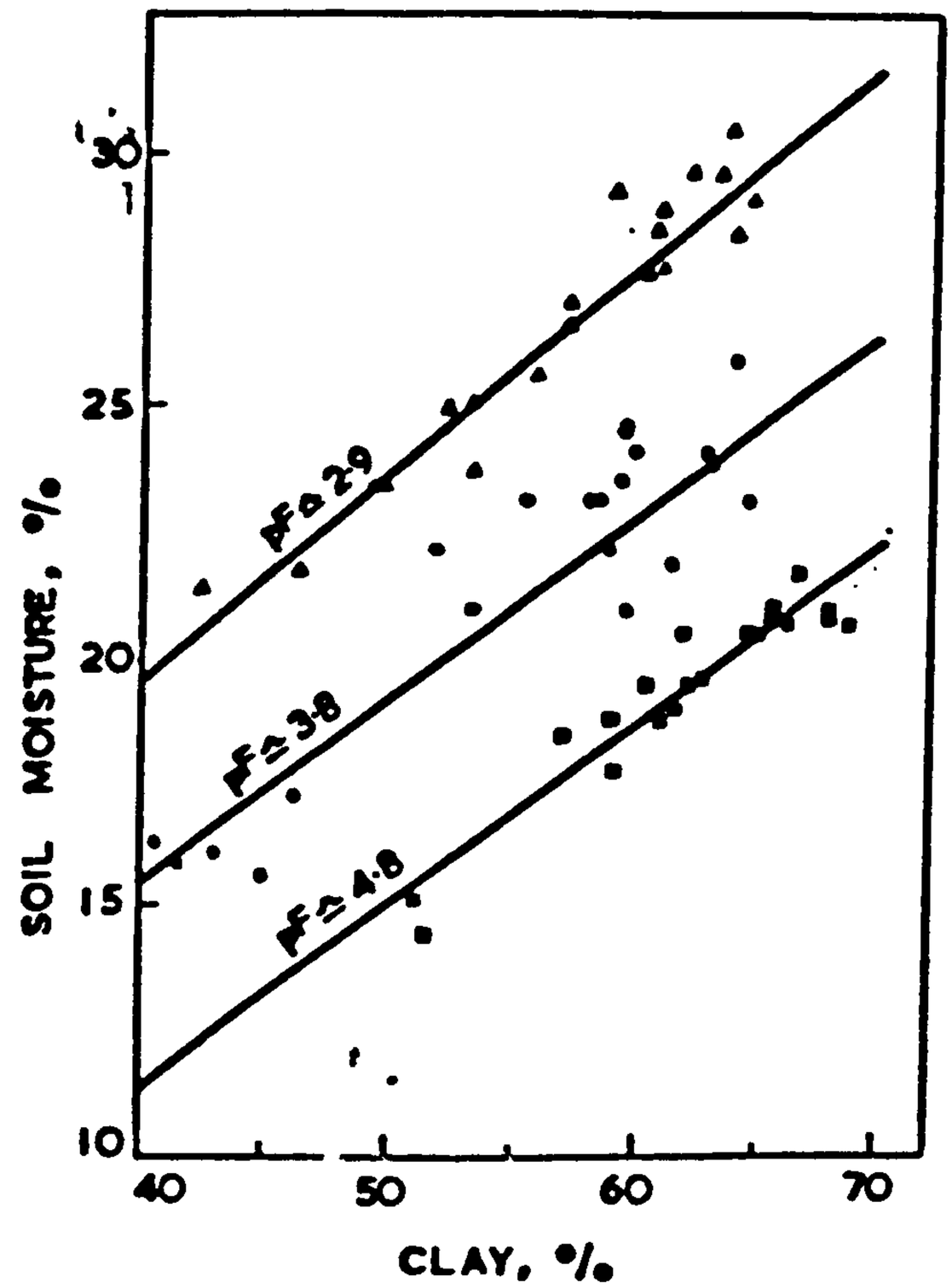

Figure 3.4: Relation between clay content and water content at constant moisture tension in the B horizon of a soil at the Waite Institute,S.A. (after Aichison,G.D. and Richards,B.G.,1965)

3.6 Hysteresis

Yong and Warkentin (1975) explained the hysteresis that occurred due to drying and wetting, in the relationship between suction and moisture content.

When a soil made up of uniform spheres dries the water exists as rings around the points of contact of the spheres. On wetting, the rings increase in size until they touch to form connecting wedges of water. With further increases in water content, water fills the voids and excludes the air. This occurs when the pressure within the pores is low, i.e. a matrix suction of approximately zero. The final filling is very rapid and there is a large change in moisture content/matrix suction curve. On drying, emptying of the interconnecting voids does not occur until the pressure is high enough to overcome the surface tension forces in the pore with the smallest diameter. Therefore, for the same matrix suction a drying soil has a higher water content than a wetting soil. Muir-Wood (1979) reported Haines' (1930) conclusion that during exit (i.e. drying) fine pore spaces dominate, on entry(i.e. wetting), wider sections are more important. The effect is hysteresis--- the system is influenced by its previous history.

Hysteresis in real soils and particularly in clays is more difficult to explain. After wetting, the first drying curve can be greatly different from the initial wetting curve and may not achieve the original moisture content at zero pore suction. If the soil is re-wet or dried from a new position on the retention curve a new path is followed which is called a

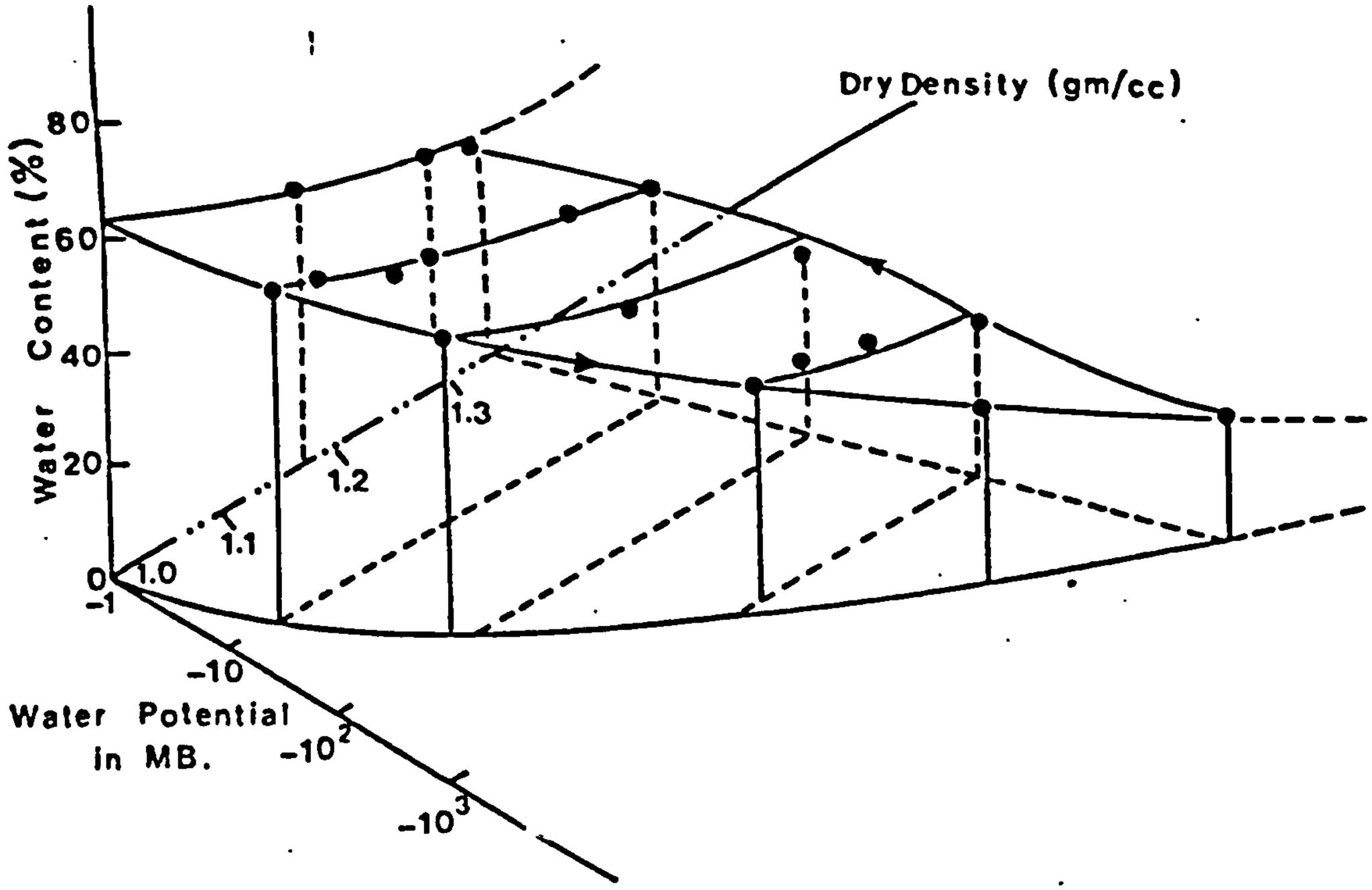

Figure 3.5: Soil-water potential surface for Sainte Rosalie clay (Yong, Japp and How,1971). For a given soil type there exists a singular surface showing the interdependence between water content, dry density, and soil-water potential.

scanning curve (see Fig. 3.5). These scanning curves define the water content/matrix suction changes as the soil dries due to evaporation and moistens due to irregularly spaced rain. Any calculations of water redistribution must use the scanning curves and this leads to considerable practical difficulties.

Chapter 3 indicated that soil suction was an extremely influencial parameter in the behaviour of unsaturated soils, and this has been followed by a detailed description of the nature of suction in unsaturated soils, which highlighted the relationship between moisture content and suction, and the hysteresis phenomenon. Other fundamental soil properties which are effected by soil suction are effective stress and hence shear strength. The next two chapters describe how these two properties have evolved to take account of the suction present in unsaturated soils.

CHAPTER 4

A REVIEW OF THE PRINCIPLE OF EFFECTIVE STRESS AND STRESS STATE VARIABLES

Chapter 4

A review of the principle of effective stress and stress state variables

4.1. General

This chapter presents a review of effective stress in saturated and partially saturated soils. It discusses the development of numerous so called 'effective stress' equations and the difficulties in applying them to practical problems. Common to all these equations is the incorporation of a parameter which is dependent on the soil behaviour. This means that the equations are constitutive relationships rather than descriptions of the stress state. This soil parameter has been proven essentially impossible to evaluate uniquely. More recently, there has been an increased tendency to uncouple the effective stress equations and use two independent stress state variables to describe the shear strength and volume change behaviour of unsaturated soils.

4.2 Stress state variables

Using the continuum mechanics approach, the mechanical process associated with engineering problems in soils is governed by:

(i) the conservation of mass ; and

(ii) the equations of motion.

The variables associated with these fundamental equations are defined as 'state variables'. They are required for the fundamental characterization of the continuum and are

independent of the type of material involved.

The procedure advocated by Fredlund (1974) for the prediction of 'stress state variables' is based on the equations of motion, (or indirectly the conservation of energy) and utilizes the principle of superposition of coincident equilibrium stress fields from which 'stress state variables' can be extracted. It is assumed that each phase has an independent continuous stress field associated with it. Therefore, the number of independent equations is equal to the cartesian coordinate directions multiplied by the number of phases in the continuum. An additional overall or total stress field can be written for the assembled element since the equilibrium equations associated with each phase are linear.

Although equilibrium equations can be readily written for any number of phases, the extracted 'stress state variables' will be meaningful only if they are measurable quantities and the 'stress state variables' are established in order to analyse the behaviour of a multiphase system. How stress state variables were first used to describe the behaviour of partly saturated soils will be discussed in section 4.5.

4.3 The principle of effective stress : INTRODUCTION.

The success of the effective stress equation in describing the behaviour of saturated soils has led research workers into a search for a similar statement for unsaturated soils. During the last two decades there have been numerous equations proposed in the literature ; however, none have proven satisfactory in practice.

Before discussing effective stresses in soils it is advisable to have a clear understanding of what is meant by the effective stress principle. It is also of vital importance to appreciate why the effective stress concept is so useful in the study of the mechanical properties of soils.

4.4. The principle of effective stress (or effective stress law)

4.4.1 Saturated soils.

The discovery of the principle of effective stress and the realization of its basic importance in Soil Mechanics was due to Terzaghi (1923).

Terzaghi states that all mechanical aspects of a saturated soil are governed by the difference between the total and pore water pressures. From a physical standpoint it refers to the equilibrium of the soil structure of a saturated soil but says nothing of a constitutive nature. Terzaghi's statement on effective stress is consistent with the definition of a stress state variable as used in continuum mechanics.

The validity of the principle of effective stress for saturated soils has been adequately verified by the work of Rendulic (1936), Bishop and Eldin (1950),Henkel (1959 and 1960) and Skempton (1960).

However, the general expression for effective stress in porous materials, even for saturated porous materials, has been shown to be more complex (Skempton, 1960), and Terzaghi's equation can be considered as a special case applicable to saturated soils only.

The development of a more general expression for effective stress began with Bishop and Eldin (1950), who suggested treating volume change and shear strength separately with respect to effective stress. They argued that the shear strength of a soil in compression was dependent on the area of contact between soil particles whereas the volume change was independence of the contact area. Skempton (1960) reinforced Bishop's and Eldin's statement and derived two separate expressions to predict the behaviour of saturated porous materials, one with respect to shear strength and one with respect to volume change.

For shear strength

$$\sigma' = \sigma - \left(1 - \frac{a \tan \psi}{\tan \phi'}\right) Uw \qquad . \quad (4.1)$$

where σ', σ = effective and total applied stress

ψ = angle of internal friction

ϕ' = angle of shearing resistance

a = As/A = contact area ratio

As = contact area between two particles on a statistical plane.

A = gross area in a plane parallel to the contact.

Uw = pore water pressure

For volume change

$$\sigma' = \sigma - (1 - Cs/C)Uw \qquad (4.2)$$

where Cs = compressibility of the soil particles

C = compressibility of the soil structure

In general, the above two equations can be written as

$$\sigma' = \sigma - ku \qquad (4.3)$$

The values of k for shear strength and volume change differ from each other and from unity, though in uncemented soils in the range of stress usually encountered in engineering practice this difference is too small to be observed experimentally (as, for example, in tests by Rendulic, 1937; Taylor, 1944 and Bishop and Eldin, 1950).

Jennings and Burland (1962) gave an interpretation of effective stress in saturated soils in the 'form of two propositions':

(a) All measurable effects of a change of stress, such as compression, distortion and a change of shearing resistance of a soil are exclusively due to changes in effective stress.

(b) the effective stress, σ', is defined as the excess of the total applied stress over the pore pressure, u

$$\text{i.e. } \sigma' = \sigma - u \qquad (4.4)$$

These propositions are completely consistent with Terzaghi's proposition and allow the effective stress to be viewed as a stress state variable.

Bishop and Blight (1963) reviewed Skempton's treatment of volume change and shear strength. They concluded that '...the effective stress is, by definition, that function of total stress and pore pressure which controls the mechanical effects

of a change in stress, such as volume change and a change in shear strength. The principle of effective stress is the assertion that such a function exists, with determinant factors under a given set of conditions. They also stated that the principle of effective stress can only be applied to saturated soils if account is taken of the effective stress path.

Their definition has a subtle difference from Terzaghi's original statement. The incorporation of the word 'function' in two places significantly changes the interpretation of effective stress, allowing the use of soil parameters to describe the state of stress. This effective stress statement is therefore a constitutive relationship, especially since it can only be applied when account is taken of the effective stress path.

Matyas and Radharishna (1968) stated the principle of effective stress as follows:

(a) the changes in volume and shear strength of a soil element caused by a change in its stress state are entirely due to the change in effective stress; in other words shear strength and void ratio are unique functions of effective stresses.

(b) the effective stress which is responsible for the mechanical effects in soil element is uniquely determined by the total and pore pressure.

The words 'unique function' refer to a constitutive relationship.

The research literature appears to reveal a progressive deviation from Terzaghi's original concept of effective stress. Originally, Terzaghi proposed that the difference between the total and pore pressure was a stress state variable that governed all deviations from equilibrium conditions. Other definitions have allowed for the incorporation of soil parameters to describe the state of stress, thus becoming constitutive relationship.

4.4.2 Unsaturated soils.

In general the effective stress, σ', in unsaturated soil can be expressed as the following function:

$$\sigma' = f(\sigma, Ua, Uw) \qquad (4.5)$$

where Ua = the pore air pressure

Uw = the pore water pressure

σ = the total stress

Any form of the effective stress equation should satisfy the following requirements:

(a) the boundary cases for full saturation and for a completely dry state.

(b) the behaviour (volume change and shear strength) of a soil element exposed to a change in stress should be predictable in terms of effective stresses and should be independent of the manner in which the total stresses and the pore pressure change.

(c) the correctness of the form of such an effective stress equation should be verified experimentally.

In partially saturated soils it is practically impossible to satisfy all three requirements and therefore the use of any equation for the effective stress is necessarily limited to those cases which can be verified experimentally.

In a lecture given by Bishop in Oslo in 1955, he discussed various aspects of the applicability of the principle of effective stress to partly saturated soils. He proposed a tentative generalised expression for the effective stress in which a parameter, X, is introduced to account for the degree of saturation (published in 1959 in Teknisk Ukeblad, Oslo 39).

$$\sigma' = (\sigma - U_a) + X (U_a - U_w) \qquad (4.6)$$

where σ' = generalised effective stress

σ = total stress

U_a = pore air pressure

U_w = pore water pressure

X = a parameter which equals unity for saturated soils and decreases with decreasing degree of saturation.

A number of research workers have attempted to extend the principle of effective stress to the case of partly saturated soils. Aitchison and Donald (1956) have shown that provided the soil remains fully saturated, the soil moisture suction or pressure deficiency, p^*, in the soil water contributes directly to the effective stress in the soil and equation (4.4) becomes:

$$\sigma' = \sigma + p^* \qquad (4.7)$$

As soon as air enters the pore space the pressure in the pore-water no longer acts over the whole cross-sectional area and equation (4.4) no longer applies.

On the basis of a study of orderly packed uniform spheres, Aitchison (1956) developed a method of determining the contribution of the pore water tension to the intergranular stress. The transformation of negative pore water pressure to intergranular stress $\overline{\sigma'}$ (i.e. $\overline{\sigma'} = (\sigma - Ua) + Aw(Ua - Uw)$ where Aw = the area of water per unit interparticle area), requires the multiplication of the former by the factor X given by the expression:

$$X = \overline{\sigma'}/\overline{Uc} = Sr + (0.31/Uc)\sum_{0}^{Uc} \overline{Uc}\,\Delta Sr \qquad (4.8)$$

where Uc is (Ua - Uw) at which X and $\overline{\sigma'}$ are being computed.

Sr is the degree of saturation.

$\overline{Uc}$ is the average value of (Ua - Uw) during which the degree of saturation changes by ΔSr.

X is thus larger than the degree of saturation for all degrees of saturation except 100% when its value is 1.0.

Jennings (1957), Croney et al (1958), Bishop (1959) and Aitchison (1960) all proposed modified forms of effective stress equation to account for the two-phase nature of the pore fluid in an unsaturated soil.

$$\sigma' = \sigma + B\ p^{\bullet} \text{ (Jennings, 1957)} \qquad (4.9)$$

where p' is the negative pressure in the pore water and

B is a statistical factor based on the contact area and must be measured experimentally in each case.

$$\sigma' = \sigma - B' U_w \quad \text{(Croney, Coleman and Black, 1958)} \quad (4.10)$$

where $-U_w$ = soil moisture suction

and B' = the holding or bonding factor which is a measure of the number of bonds under tension effective in contributing to the shear strength of the soil

Aitchison (1960) gave:

$$\sigma' = \sigma + \chi p^{\bullet} \quad (4.11)$$

where $p^{\bullet}$ denotes pressure deficiency in pore water

$= (-U_w)$

$\chi = \sigma^{\bullet}/p^{\bullet}$ has values between 0 and 1

and $\sigma^{\bullet}$ is the component of effective stress due to the pressure deficiency ($p^{\bullet}$) in the pore water

The gaseous phase was assumed to be at atmospheric pressure ($U_a = 0$). However, all the equations are equivalent when the pore air pressure is atmospheric. Under these conditions $\chi = B = B' = X$.

Discussion at the Conference on Pore Pressure and Suction in soils (1960) showed that there was a substantial

measure of agreement between the various expressions defining effective stress in partially saturated soils and that the one proposed by Bishop was the most general since it included a term for the pressure in the gas phase. In a written discussion to the conference, Aitchison and Bishop proposed that the effective stress equation, for a partly saturated soil should take the form:

$$\sigma' = (\sigma - U_a) + X(U_a - U_w) \qquad (4.12)$$

$$= \sigma - U_a + Xp^*$$

Equation (4.12) can be re-written in the form:

$$\sigma' = \sigma - (XU_w + (1 - X)\, U_a) \qquad (4.13)$$

$$= \sigma - U^*$$

The quantity $(XU_w + (1 - X)\, U_a)$ may be considered as an equivalent pore pressure, U^*, i.e. that portion of the effective stress in a soil resulting from fluid pressures in the pores. This retains the present understanding of the effective stress law in which the effective stress is considered as being made up of two components - one resulting from total normal pressure and the other from pressures exerted by the fluid in the pores. If the soil is saturated $X = 1$ and the equation reduces to Terzaghi's expression.

In 1960, Bishop et al restated equation (4.12) and attempted to prove its validity by comparing the results of triaxial tests performed on saturated and unsaturated samples.

Lambe (1960a) defined effective stress in terms of internal stresses in a particular soil system and related the force system at the micro level to the behaviour at the macro level.

Lambe showed that a new effective stress equation could be formed by considering:

(i) forces at mineral to mineral contact

(ii) forces at air-mineral contact

(iii) forces at water-mineral or water-water contact

(iv) electrical forces

This leads to a generalised equation of the form:

$$\sigma = \bar{\bar{\sigma}} A_m + U_a A_a + U_w A_w + R - A \quad (4.14)$$

where $\bar{\bar{\sigma}}$ = mineral to mineral contact stress

A_m = fraction of the total interparticle area that is mineral to mineral contact

U_a = mineral-air contact stress

A_a = fraction of total interparticle area that is mineral-air contact.

A_w = fraction of total interparticle area that is mineral-water or water-water contact.

R = total interparticle electrical repulsion divided by total interparticle area.

A = total interparticle electrical attraction divided by total interparticle area.

Although the expression is reasonable, there is no way of obtaining quantitatively individual parameters such as $\bar{\bar{\sigma}}$, A_m, R and A for natural soil systems.

Lambe (1960b) suggested that the parameter X used by Bishop included structural effects (i.e. fabric) which would greatly limit the use of measured X value. X was certainly not

a soil property dependent only on the degree of saturation, and he further compared his own equation with that of Bishop (equation 4.12) and stated that

$$\sigma = \bar{\bar{\sigma}} Am + Ua (1 - X) + Uw X + R - A$$

$$\text{or} \quad \sigma' = \bar{\bar{\sigma}} Am + \bar{U} + (R - A) \qquad (4.15)$$

where $\bar{U}$ = the equivalent pore pressure

$$(4.12) = (4.15) \text{ if } \sigma' = \bar{\bar{\sigma}} Am + (R - A) \qquad (4.16)$$

Lambe's equation was regarded by Sridharan (1968) as the most general and fundamental one. Such an approach, using parameters that cannot be directly measured would be valuable if it actually led to simple correlations. Unfortunately this does not seem to be the case.

Bishop and Donald (1961) performed a triaxial test on a partly saturated silt in order to verify equation (4.12). In this test the cell pressure σ_3, the pore-water pressure Uw, and the pore-air pressure Ua were varied during the shearing process, in such a way that both (σ_3 - Ua) and (Ua - Uw) remained constant throughout the test. It was found that these variations had no effect on the strength or stress/strain behaviour (Figure 4.1). However, a change in (σ_3 - Ua) or (Ua - Uw) alone had a marked effect on the shape of the stress/strain curve. It was therefore concluded that the form of equation (4.12) was correct and that the behaviour of the soil was independent of the absolute values σ, Uw and Ua.

An extension of Terzaghi's effective stress expression to unsaturated soils was suggested by Skempton (1960). The

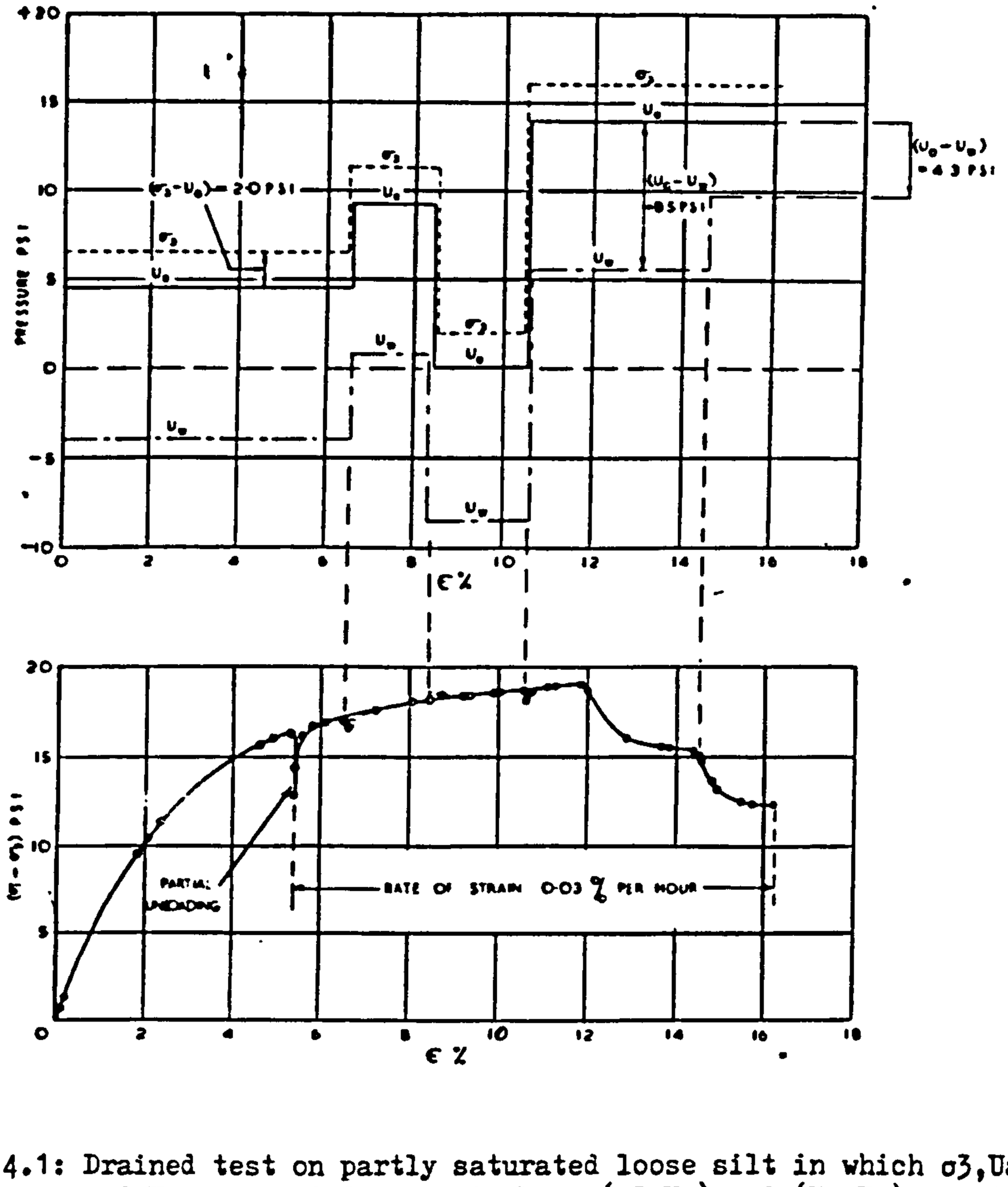

Fig.4.1: Drained test on partly saturated loose silt in which σ3,Ua and Uw are varied so as to keep (σ3-Ua) and (Ua-Uw) constant. (after Bishop and Donald,1961)

specific equation proposed for describing the shear behaviour of unsaturated soils was as follows:

$$\sigma' = \sigma - (1 - a \tan\psi/\tan\phi') \, Sr \, Uw \qquad (4.17)$$

where a = particle contact area

ψ = angle of intrinsic friction

ϕ' = angle of shearing resistance

Sr = degree of saturation

$$Sr = 1 + (1 - X)\left(\frac{Ua - Uw}{Uw}\right) \qquad (4.18)$$

Jennings and Burland (1962) were apparently the first research workers to seriously question the validity of Bishop's equation. They stated that it was necessary to show that the soil behaviour was unaffected by changes in (σ - Ua) and X (Ua - Uw) such that their sum, σ', was constant, in order to demonstrate the validity of the principle of effective stress. On the basis of tests on a number of soils, they argued that Bishop's equation did not uniquely define the relationship between void ratio and effective stress for most soils below a critical degree of saturation (Fig. 4.2). For silts and sands, the critical value of Sr was estimated as 20% and as high as 85 to 90% for clays. Jennings and Burland as well as Coleman (1962) stated that the first step in the analysis of triaxial tests on unsaturated soils was to reduce the stress with the pore air pressure as the base pressure. The axial stress was therefore (σ1 - Ua), the lateral stress, (σ3 - Ua) and the pore

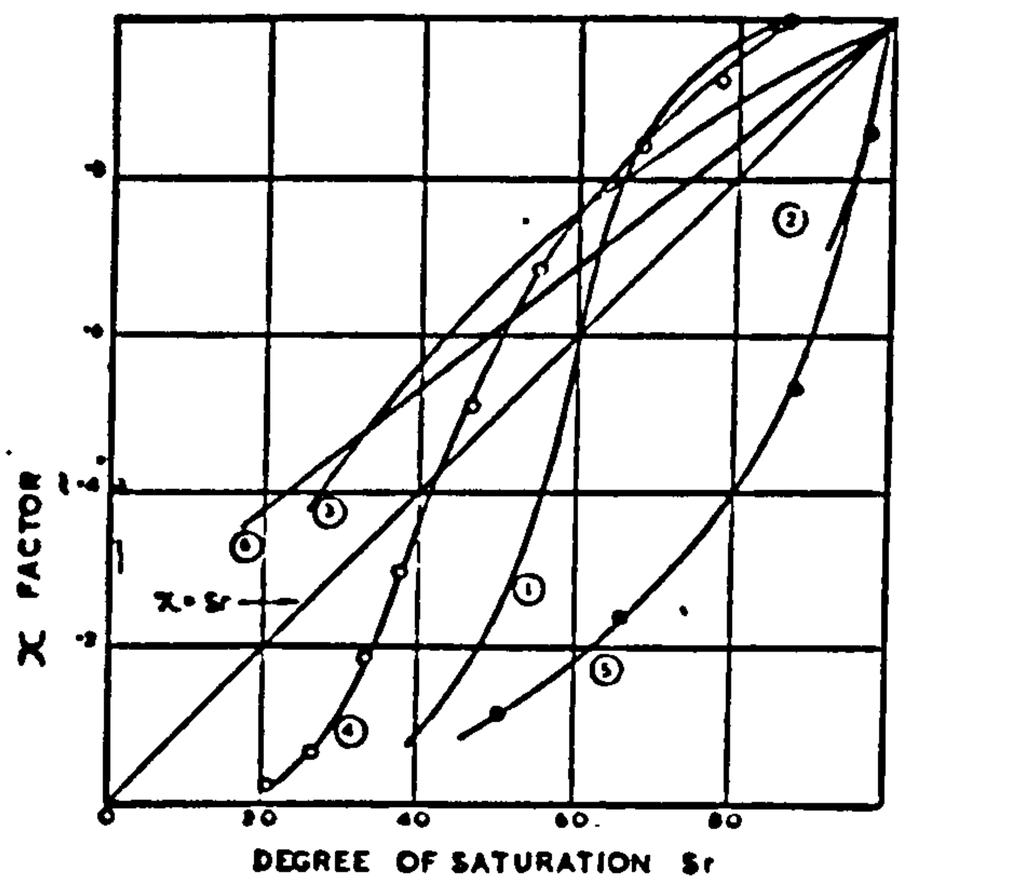

Fig. 4.2 Curves of parameter χ against degree of saturation for various soils

(after Jennings and Burland, 1962)

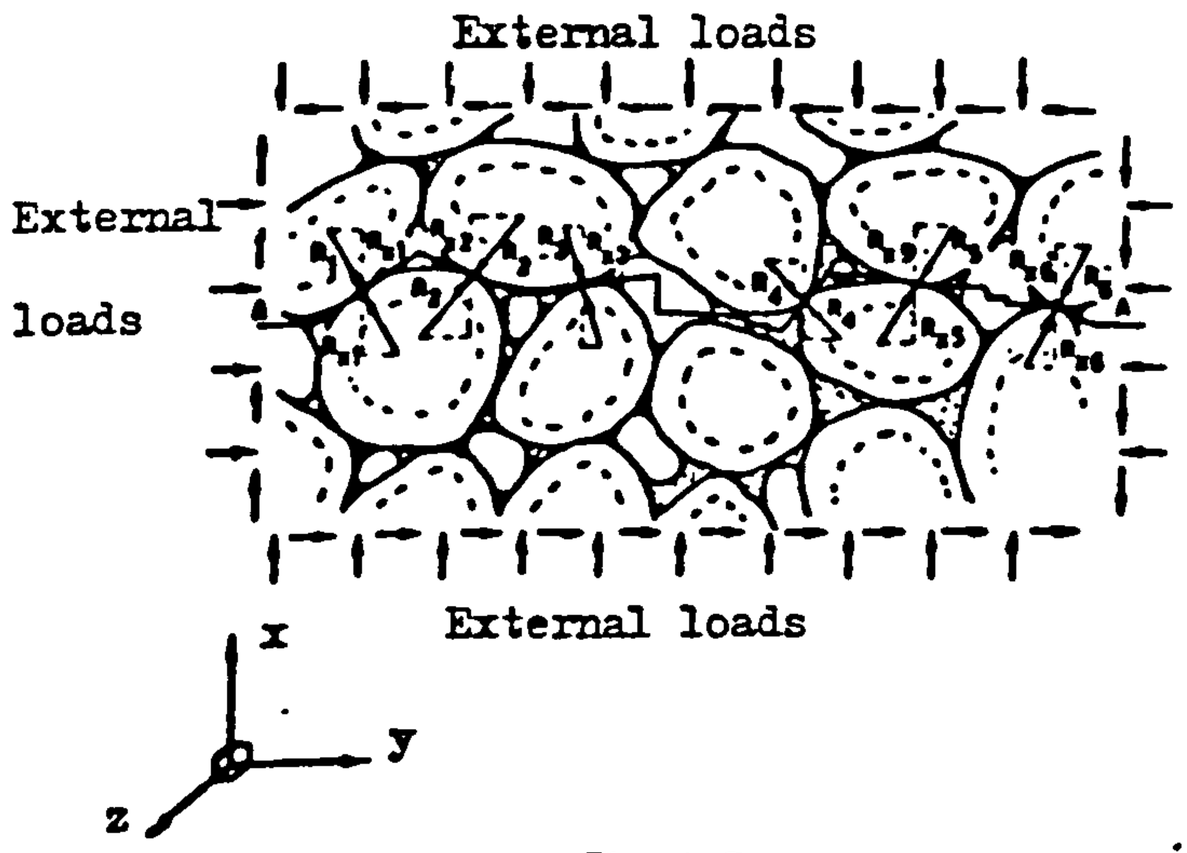

Fig. 4.3

Wavy plane through particle contacts considered by Sparks (1963). The plane AA cuts air-water interfaces as well as passing through particle contacts. Forces are resolved and summed in the x direction for a portion of the plane AA having unit projected area on the yz plane.

water stress (Uw - Ua).. Coleman went on to use these relative pressures as independent stress variables describing volumetric deformation i.e. in general, for a small change in some soil property Ei and for small changes of the stress parameters then,

$$dEi = C_{i1}\,(dUw-dUa)+C_{i2}\,(dp-dUa)+C_{i3}\,(d\sigma 1-d\sigma 3) \qquad (4.19)$$

where $p = (\sigma 1 + \sigma 2 + \sigma 3)/3$

and C_{i1}, C_{i2}, C_{i3} may be expected to be themselves dependent on degree of saturation, previous history, etc., and will not be definite soil properties.

Sparks (1963) suggested that the derivation of equation (4./2) was incorrect because the effect of surface tension was ignored. Sparks considered the x-section through soil shown in Fig.4.3., and noted that any section AA could cut interfaces between air and water on which surface tension forces acted. By summing interparticle forces, including repulsive forces (e.g.electrical) and attractive forces (e.g. Van der Waals) between particles,pore pressure forces and surface tension effects, he produced an equation for the effective normal stress (on the yz plane) as follows:

$$\sigma'x = \sigma x - dUa - BUw + \gamma T \qquad (4.20)$$

where T was the surface tension at the air water interface. If the pores were filled with water $\alpha = \gamma = 0$, and if filled with air $B = \gamma = 0$. As an alternative form, Sparks gave

$$\sigma'x = \sigma x + n\,(Ua - Uw) - Ua\,(1 - a) \qquad (4.21)$$

$$\text{where } n = B + T\gamma/(Ua - Uw) \qquad (4.22)$$

and he showed that $\alpha + B = 1 - a$ (4.23)

where a = the proportional projection of the particle contact areas to the yz plane.

Donald (1963) introduced the surface tension into the X parameter, defining $X = Sr + f(Sr)/(Ua - Uw)$ (4.24)

where Sr is the degree of saturation of the pores, and f(Sr) incorporates the surface tension effects.

In 1963, Bishop and Blight re-evaluated the effective stress equation for unsaturated soils. They noted that variation in the suction term (Ua - Uw) caused problems because it did not result in a direct change in effective stress. This was attributed to the fact that the surface tension in the pore water acted over only a part of the surface area of the soil particles. They expressed the law for unsaturated soils in a more general form, i.e.

$$\sigma' = (\sigma - Ua) + f(Ua - Uw) \qquad (4.25)$$

They also noted that the stress paths of each of the two components (i.e. $(\sigma - Ua)$ and $(Ua - Uw)$ must be considered in stress-volume change predictions. They suggested that shear strength was less sensitive to the stress path. Matyas (1963) and M.I.T. (1963) also have shown that the parameter X is largely stress path dependent and that anomalous values of X are frequently obtained.

Blight (1965) pointed out that the X parameter was dependent on the type of process to which the soil was subjected

and observed the collapse phenomenon as constituting a limitation to the effective stress equation. Burland (1965) further questioned Bishop's effective stress equation. He separated the forces on the soil particle in terms of internally applied water stress and externally applied loads (Fig.4.4). The water stress always acts isotropically whereas the externally applied loads produce shear. He explained the collapse phenomenon in terms of shear due to a decrease in the normal stress (i.e. suction).

During 1965, the Review Panel for the Symposium entitled 'Moisture Equilibria and Moisture changes in soils' adopted the subdivision of soil suction and the definitions quoted by the International Society of Soil Science. Total suction was acknowledged to be composed of two components, the matrix suction and osmotic suction (Aitchison et al,1965). Suction in soils was discussed in detail in Chapter 3.

With the consideration of the components of total suction, more effective stress expressions for unsaturated soils were proposed (Newland, 1965) (Richard, 1966) (Sridharan, 1968). However, like Bishop's and the other proposals, soil properties like the X factor were involved in these expressions.

Newland (1965) categorised stresses in unsaturated soils as endogenic and exogenic. Endogenic stresses were defined as stress components originating internally whereas exogenic stresses were resultants of externally applied stresses. An effective stress equation for unsaturated soils was proposed as follows:

$$\sigma' = \sigma i + X(Ua - Uw) + (\sigma - Ua) \qquad (4.26)$$

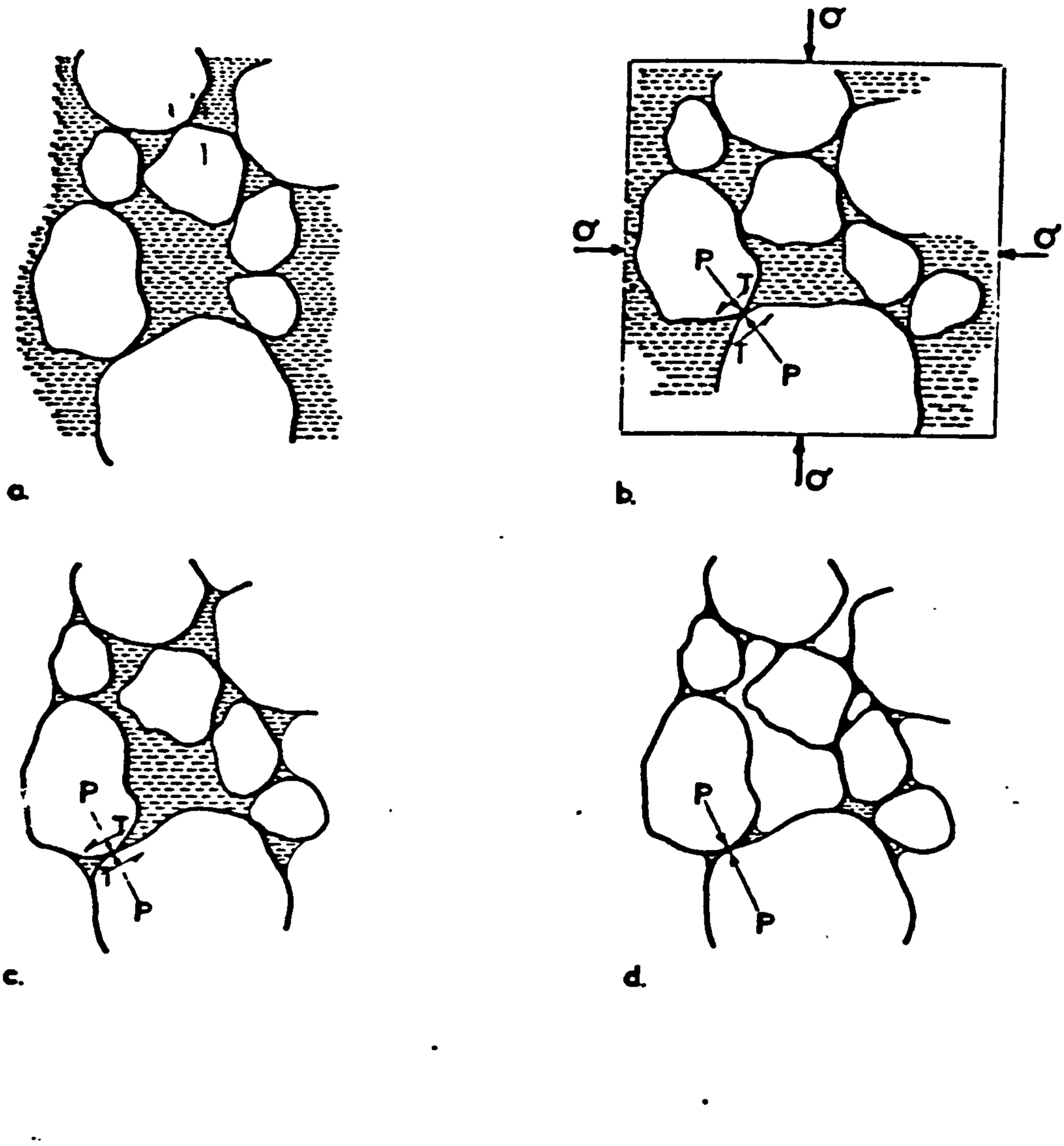

Fig.4.4: Model of a fine silt (a) initially loose and fully saturated; (b) grain slip due to large increment in isotropic applied stress: $T/P \rightarrow \mu$ (coefficient of friction at intergranular contact) ; (c) small grain slip due to menisci at soil boundary: $T/P \rightarrow \mu$; (d) menisci at grain contacts, no further slip: $T/P \rightarrow 0$. (Burland 1965). With menisci at soil boundary effect of increase in negative pore pressure will be identical to that of an applied isotropic external pressure - both shear and normal forces at contacts will increase, some slip will occur, and average ratio T/P is likely to be close to μ. Menisci at grain contacts produce essentially normal forces only. (after Burland, 1965)

where σ_i and $(U_a - U_w)$ = endogenic stress

$(\sigma - U_a)$ = exogenic stress

σ_i = intrinsic stress arising from interparticle forces (originating from electrical, osmotic and Van der Waals effects)

Richard [1] (1966) considered solute suction (osmotic suction) as playing an important role in the physical behaviour of unsaturated soil and postulated a further effective stress equation.

$$\sigma' = \sigma - U_a + X_m (h_m + U_a) + X_s (h_s + U_a) \quad (4.27)$$

where X_m = effective stress parameter for matrix suction

h_m = matrix suction.

X_s = effective stress parameter for solute suction.

h_s = solute suction

Unfortunately, he did not present data to substantiate the equation.

A further complicating factor was noted by Blight (1966) for desiccated clays. Desiccation produces a significant and irreversible increase in shear strength. For the Orange Free State clay (a montmorillonite clay) and for Scott clay (a kaolinite clay), the variation of X was very dependent on the method of calculation (from shear strength data or from shrinkage tests) as well as stress history. (Fig. 4.5).

The physical interpretation of the measured soil

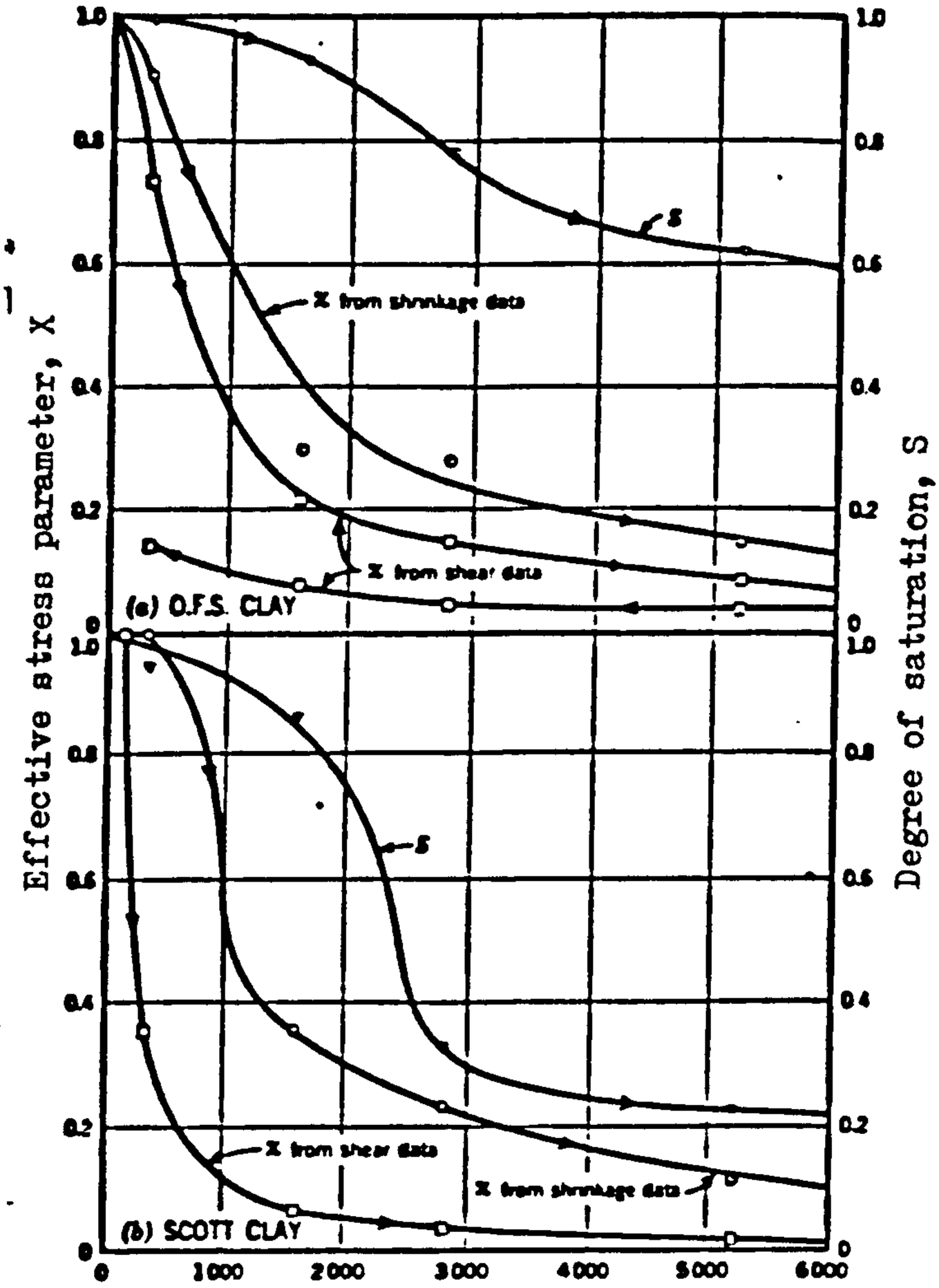

Fig. 4.5 Variation of effective stress parameter χ with suction determined from shrinkage data and shear data for Orange Free State clay and Scott clay (Blight, 1966).

suction (Ua - Uw) was questioned by Blight (1967). In his previous article (Blight, 1966) he published suction values of tens of thousands of pounds per square inch measured by relative humidity methods, and concluded '... moisture tensions of this magnitude are incompatible with existing measurements of the tensile strength of water and for this reason, suction, as measured, must be considered merely a convenient index of the affinity of the soil for free water'.

Prior to this time the X parameter had been evaluated by comparing the strength of saturated soils with the same soil when it was not saturated. Blight (1967) suggested that X could be more reliably evaluated by comparing the shearing strength of two unsaturated samples in 'two closely similar conditions', thus eliminating the need for saturating the soils. He also presented calculations for determining the X parameter in a unit cube composed of single sized spheres. This was accomplished by summing forces across a plane through the contact points as shown in Fig. (4.6) and with p expressed in terms of the geometry of the pores and the surface tension T, the expression reduces to

$$X = a_w + c_w.T/p \qquad (4.28)$$

According to the above expression, when $\theta = 45^{o}$ (i.e. the menisci of any two spheres in contact merge with the menisci of adjacent spheres), the value of X will be:

$$X = 0.27 + 1.30 = 1.57$$

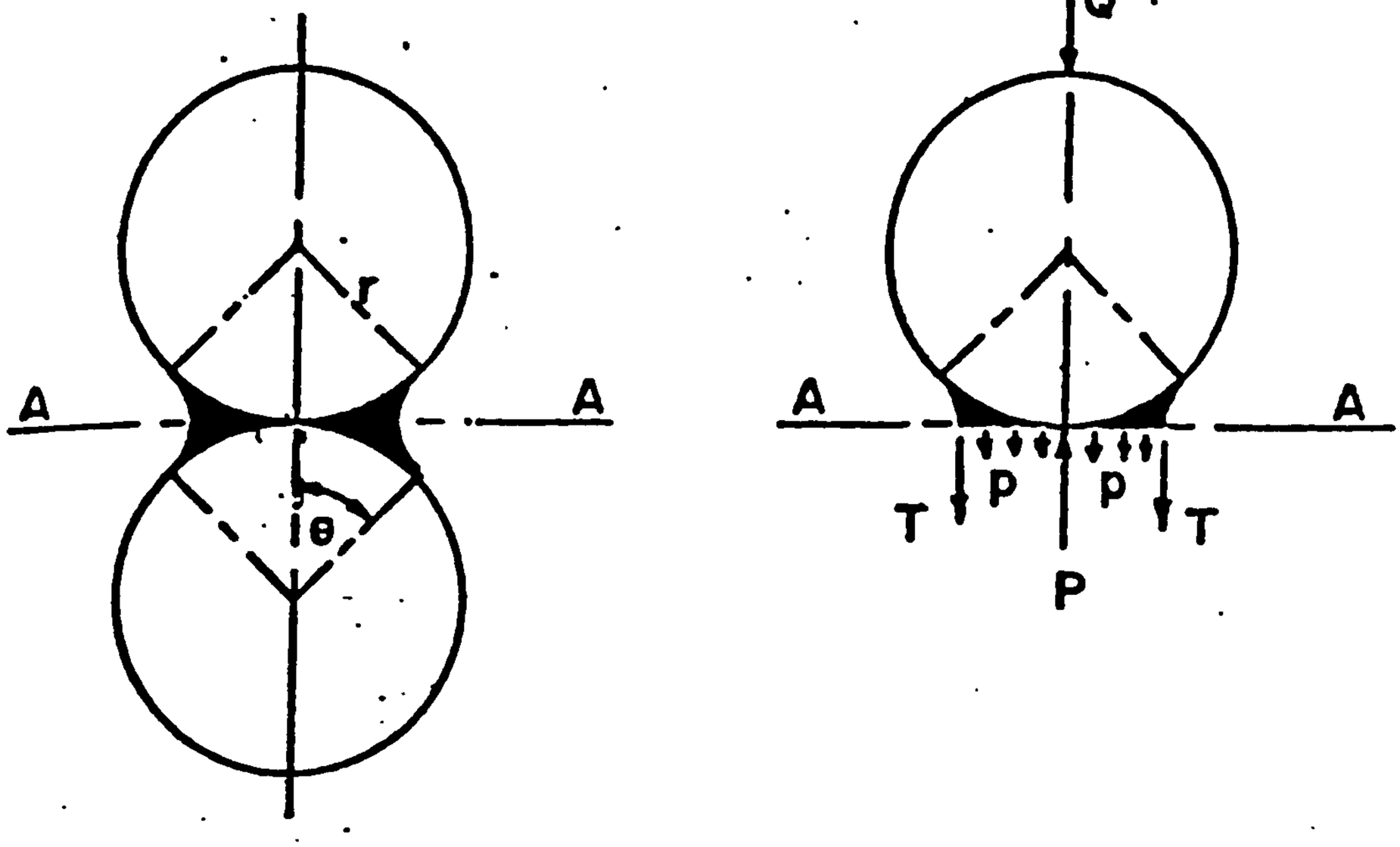

Figure 4.6

Assume pore air pressure=0

$Q = P - p \cdot aw - T \cdot cw$

where Q = total stress

P = contact stress

p = pore water pressure

T = surface tension constant

aw = Aw/A = water area ratio; and A = total area

cw = Cw/A where Cw = circumference of water

cw has units of in/in^2

Then if Q = 0 and P = σ'

(effective stress or more literally intergranular stress.)

$$P = p \cdot aw + cw \cdot T$$

But $P = X \cdot p$

Therefore, $X = aw + cw.T/p$

The parameter X is (or at least was) usually considered to be approximately equal to aw (Skempton 1960) which in this case would give X = 0.27. These calculations lend some credibility to experimental work which produced values of X greater than one (M.I.T., 1963).

Blight(1967) performed various tests and presented excellent data that clearly pointed to the inadmissibility of the X parameter as a valid concept in the effective shear equation. His apparent refusal to recognize this fact is rather astonishing with his conclusion expressing considerable optimism that the behaviour of unsaturated soils could be predicted by the use of a single effective stress equation.

In 1967, Aitchison expressed serious misgivings with regard to the separate rigorous evaluation of the X parameter and soil suction. He pointed out the complexity of X was such that a specific value may only relate to a single combination of σ and (Ua - Uw) and a particular stress path. His thinking appears to mark a new direction in the consideration of unsaturated soils. A direct quote of his reasoning states 'Its individuality (i.e. X) in relation to the other components of the equation means one thing only - that the effective stress law is no longer valid as a law, but is merely a statement of principle. In practice, this involves a second conclusion - that each parameter of effective stress σ and (Ua - Uw), must be treated separately and made to follow the correct stress path if the correct value of X (which may not be known) is to function within a statement (as in $\sigma' = (\sigma - Ua) + X (Ua - Uw)$), or, to

put the point another way : because of the complexity of the X term we may be forced to accept the fact that we can only achieve a proper value of effective stress in the soil if we follow a unique stress path for each of the terms σ and (Ua - Uw) ; having achieved it (i.e. a proper value of effective stress) by this means, we in fact no longer need to attempt to quantify the X term. Thus the complexity of the X term ceases to signify as soon as we uncouple the two parameters in unsaturated soils". Aitchison (1969) presented constitutive relationship data consistent with the above concepts. The tests were performed on a conventional but modified oedometer such that the air (chamber) pressure could be controlled.

Further evidence in support of Aitchison's reasoning was given by Matyas and Radhakrishna (1968). They confirmed the findings of Jennings and Burland (1962) that the principle of effective stress was inadequate to explain the volumetric behaviour of partially saturated soils subjected to different stress paths. The use of an effective stress equation for both compression and wetting processes gave rise to anomalous values of the parameter X. This confirmed that X was highly path dependent, a fact which was now well established (M.I.T. (1963), Bishop and Blight (1963)).

4.5. Stress state variables approach

The first research workers to seriously consider stress state variables were Matyas and Radhakrishna (1968). They used the concept of 'state' and 'state parameters' to express functional relationships between stress and deformation

gradient history. The equations used to express a unique relationship between different state parameters were termed 'state functions', and a physical quantity such as σ, associated with an element of material, was uniquely determined by the state of the element and given a unique function such as

$$\sigma \doteq f(J1, J2, J3, S1, S2, \ldots) \qquad (4.29)$$

where J1, J2, etc.[1] were stress parameters and S1, S2, etc. were other state parameters. The quantity σ was then defined as a 'state point function'.

They suggested that void ratio (e) and degree of saturation (Sr) could be expressed as stress dependent quantities. For a soil sample subjected to triaxial loading, void ratio and degree of saturation could be expressed by the equations:

$$e = F(Pa, q, Uc, eo, Sro, \lambda) \qquad (4.30)$$

$$Sr = \phi(Pa, q, Uc, eo, Sro, \lambda) \qquad (4.31)$$

where $Pa = [(\sigma 1 + 2\,\sigma 3)/3 - Ua)$

= mean normal stress

$q = \sigma 1 - \sigma 3$

= major principal stress difference

$Uc = Ua - Uw$ = suction

eo = initial void ratio

Sro = initial degree of saturation

λ = parameter describing fabric or structure

If the variability of the soil structure was reduced,

as in carefully prepared laboratory samples, then the parameter λ could be omitted.

Thus the state of the soil could be represented by a point in three dimensional space whose axes represented the state parameters. Such a point was called a 'state point' and the path followed by this point as the element changed was called a 'state path'. Thus, the 'state history' could be represented by the three state parameters e, (σ - Ua), (Ua - Uw). If the void ratio was truly a state point function, as suggested by e = F(Pa,q, Uc, eo, Sro), then movement of the state point would generate a state surface as shown in Fig. (4.7).

Point A(eo, Sro) in Fig.4.7 represents the initial state of an element of soil. Line A'B'C' lies in the (e, σ - Ua) plane (i.e. saturated soil). AA', BB' and CC' are wetting paths for different constant (σ - Ua) conditions. Starting at initial state point A (eo. Sro), it is possible to generate a surface as shown in the figure 4.7, by following different state paths.

There are obviously non-unique aspects of such a surface. Consider two paths:

(i) Desaturation at constant applied stress (σ - Ua).

(2) Decreasing applied stress at constant suction.

These paths cannot lie on the surface shown in figure 4.7. Both paths will fall below this surface. (See Chapter 3 section 3.6). Thus, such a surface is limited by two conditions.

(1) The degree of saturation does not decrease.

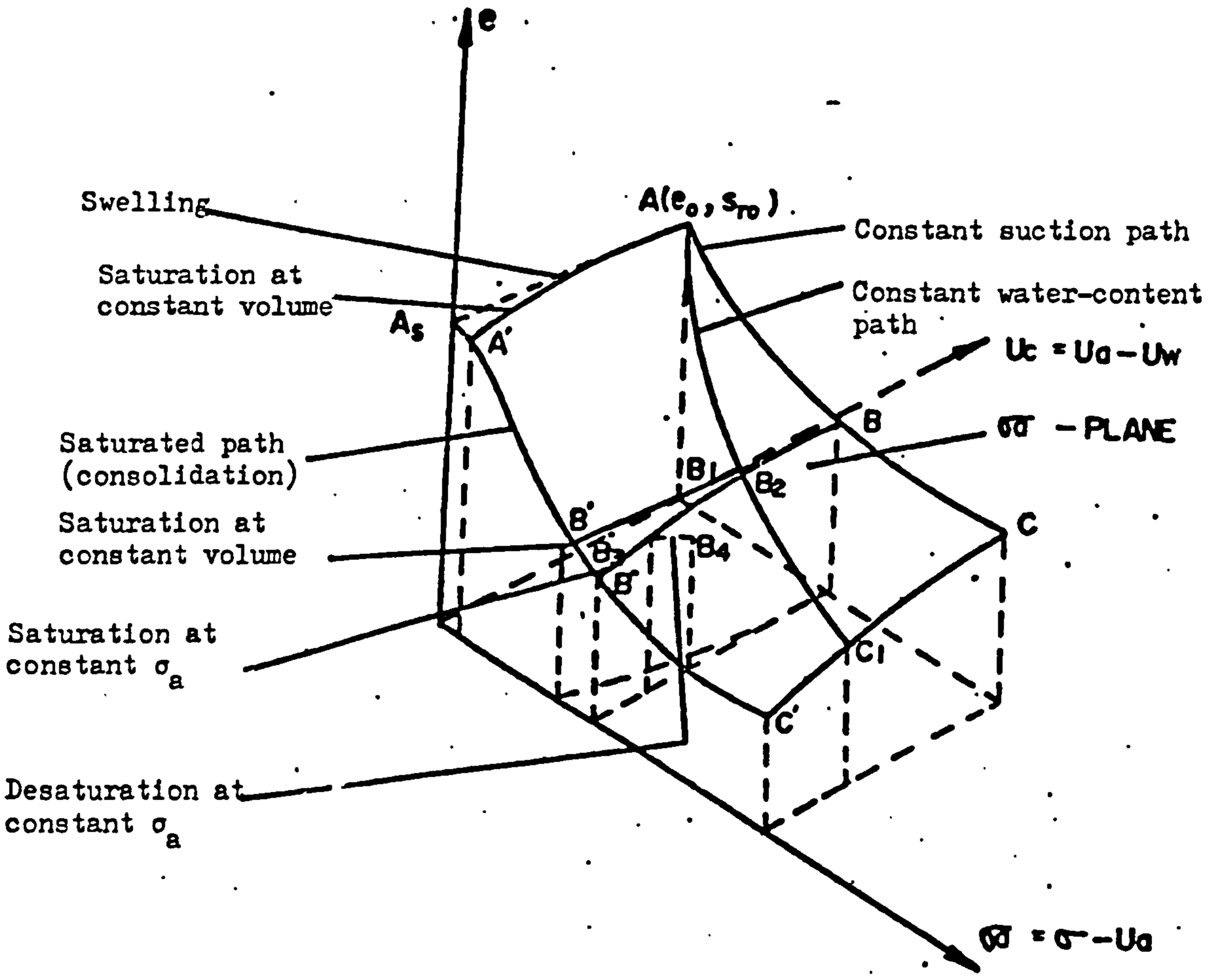

Fig.4.7: The variation of void ratio in (e, σa, Uc) space.
(after Matyas and Radhakrishna,1968)

(2) No positive volume changes (swelling) are permitted.

It might therefore be possible to predict strains for a given stress path (subject to the above conditions) by deriving a theoretical expression for void ratio (e) as a state point function or by plotting void ratio contours on a (Pa, Uc) plane and superimposing a given stress path. An illustration of this procedure is shown in Figure 4.8.

Matyas's and Radhakrishna's testing program consisted of two series of tests:

(1) Test Series A - isotropic compression.

(2) Test Series B - Ko compression.

They concluded that the behaviour of unsaturated soils must be expressed as a function of two components (applied stress and suction). Such behaviour could not however be explained or predicted by any single equation without reference to the changing state of the soil.

Barden, Madedor and Sides (1969) advocated the separate control of the components (σ - Ua) and (Ua - Uw) when predicting volume change in unsaturated soils. They used a modified Rowe consolidometer to obtain constitutive relationship data, and concluded that the compression behaviour was best treated in terms of the separate components of applied stress and suction pressure, rather than as a combined function (Fig. 4.9).

The equation that they used was

$$dV/V = C_1\, d(\sigma - Ua) + C_2\, d(Ua - Uw) \qquad (4.32)$$

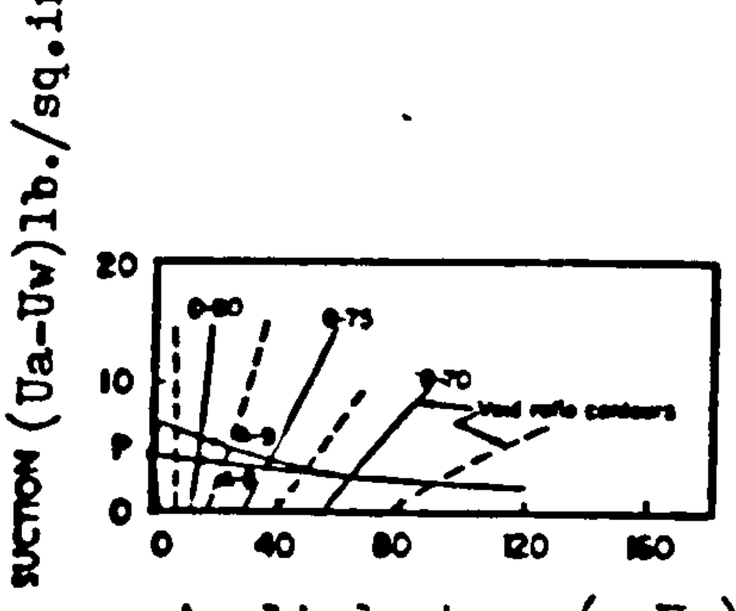

Fig.4.8a:Void ratio contours in stress space (series A)

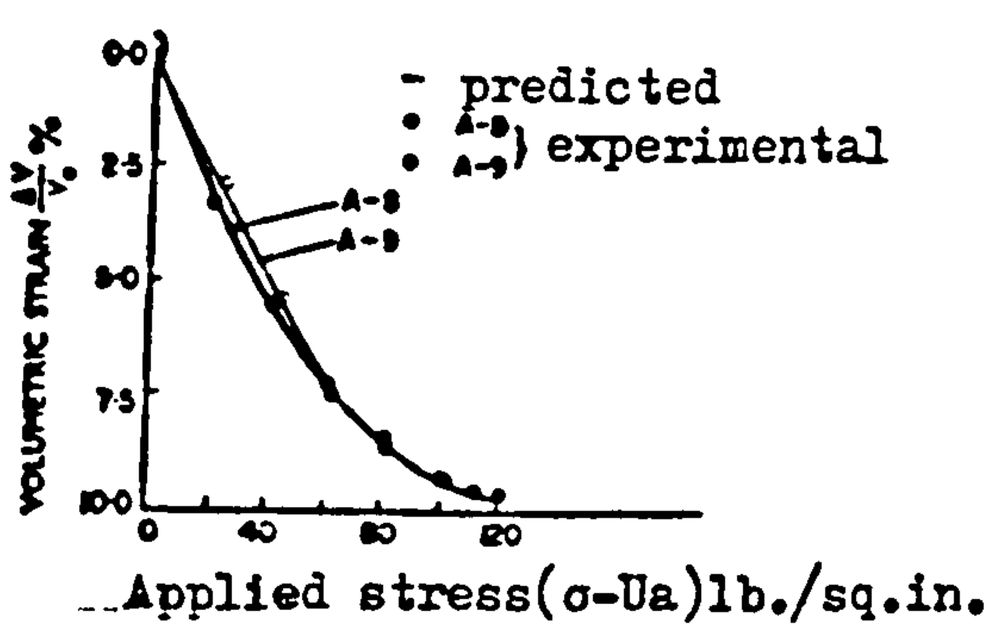

Fig.4.8b:Comparison of predicted and measured volumetric strains (test A-8 and A-9)

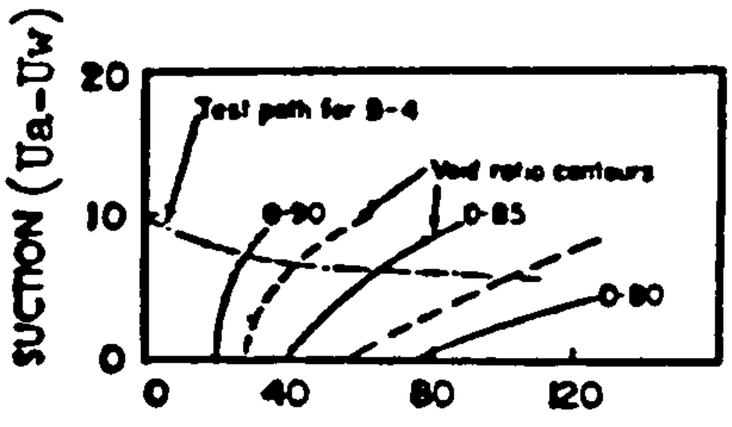

Fig.4.8c:Void ratio contours in stress space (series B)

(after Matyas and Radhakrishna,1968)

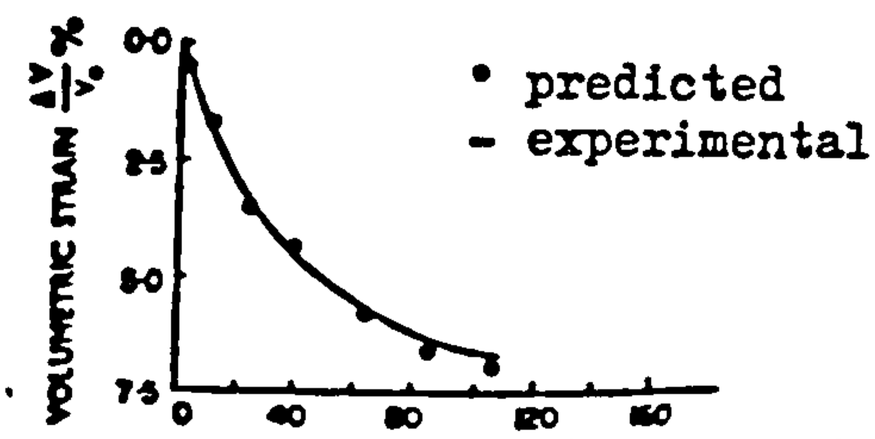

Fig.4.8d:Comparison of predicted and measured volumetric strains (test B-4)

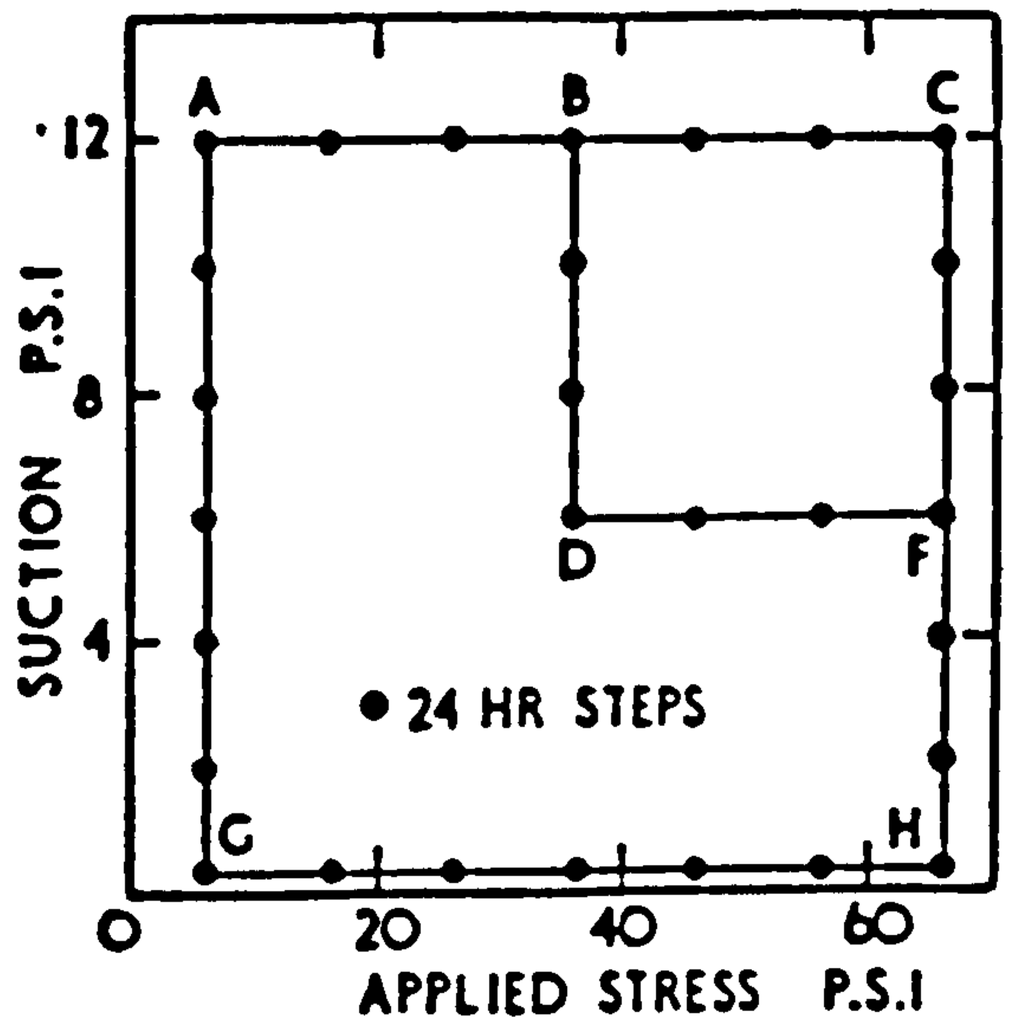

Fig.4.9 (a): Group 1 (preliminary tests): paths ACH , AGH, ABDFH. Samples with closely similar initial water contents gave similar volume changes A to H independent of stress path. The moulding water content was found to be extremely important in determining the initial structure of the soil.

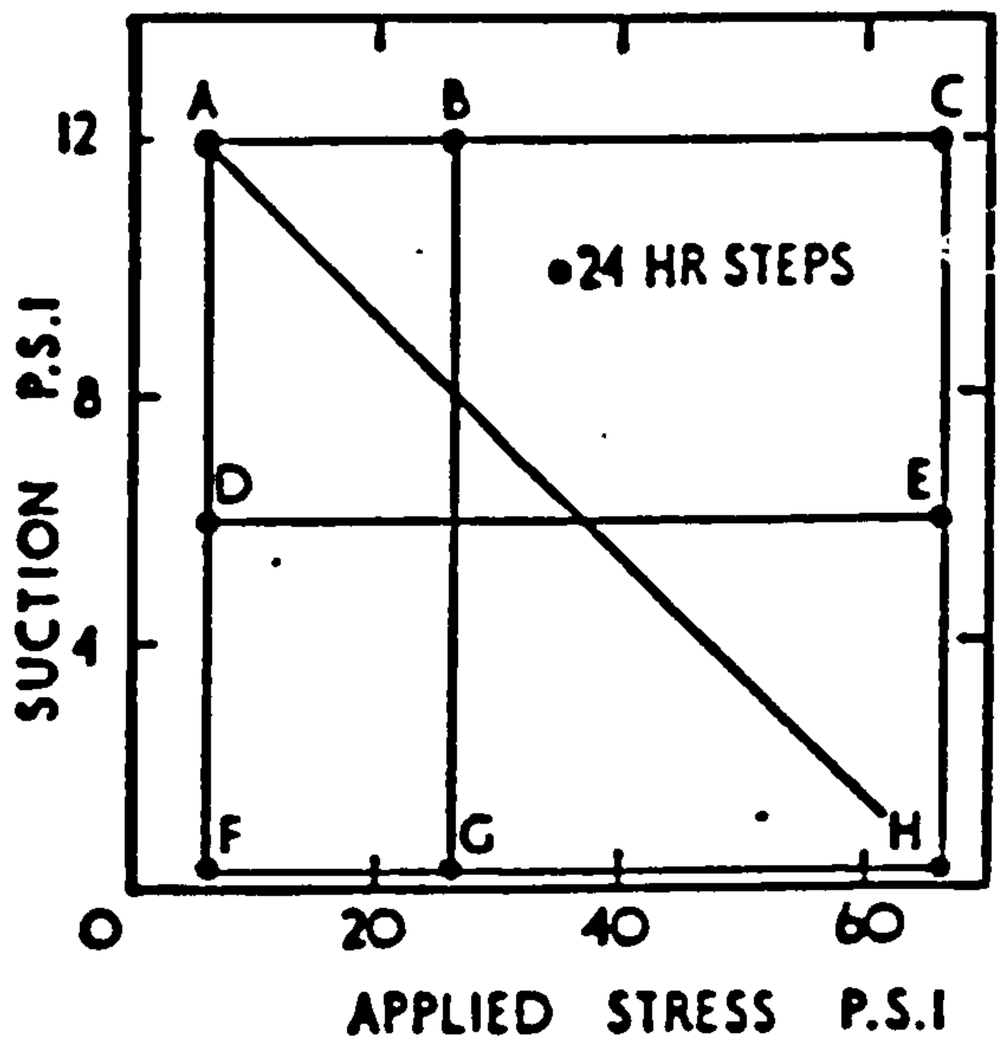

Fig.4.9 (b): Groups 2 to 11.(Samples with ten different initial water contents): paths ACH, ABGH, ADEH, AFGH, AH, AFH. Paths ACH, ABGH, ADEH, AFGH, were found to give similar volumetric strains A to H indicating an essential stress path independence. Significantly larger strains were found on paths AH and AFH apparently due to the extremely large increments of applied stress along these paths.(Barden, Madedor and Sides,1969)

as suggested by Coleman (1962), where dV = volumetric strain and C_1 and C_2 = compressibilities.

Their testing program was rather extensive and some of their conclusions were as follows:

(1) Structure is important and is influenced by moulding water content and method of compaction.

(2) Compression behaviour must be treated in terms of the separate components of applied stress and suction.

(3) Stress-strain relations for one-dimensional consolidation can be stated by equation 4.32 where C_1 and C_2 are primarily functions of current stresses (within certain limitation - i.e. collapse).

(4) The main cause of stress path dependency appears to be a reversal in direction of wetting or drying possibly caused by hysteresis between the saturating and desaturating processes.

Aitchison (1969) described a modified oedometer in which each component (б - Ua), (Ua - Uw) governing effective stress was separately controlled. Such procedures were designed to simulate the field conditions as near as possible. Any variety of stress change could be imposed on the sample. Typical laboratory test data were supplied, which largely supported the conclusions made in the previous two papers.

Brackley (1971) used two independent stress variables (i.e (б - Ua) and (Ua - Uw)) in his study of partial collapse of unsaturated expansive clays. Difficulties were encountered in attempts to apply Bishop's effective equation. Subsequently,

the description of volume change behaviour was proposed as a function of the two independent stress variables.

Fredlund (1973) and Fredlund and Morgenstern (1976) proposed two constitutive relations which describe the volume change behaviour of an unsaturated soil.

For the soil of volume V, the volumetric strain is:

$$\varepsilon = \frac{\Delta V}{V} = \frac{1}{v}\frac{\partial v}{\partial(\sigma-U_a)}\,d(\sigma-U_a) + \frac{1}{v}\frac{\partial v}{\partial(U_a-U_w)}\,d(U_a-U_w) \qquad (4.33)$$

For the change in volume of water in the element, ΔV_w

$$\theta_w = \frac{\Delta V_w}{V} = \frac{1}{v}\frac{\partial V_w}{\partial(\sigma-U_a)}\,d(\sigma-U_a) + \frac{1}{v}\frac{\partial V_w}{\partial(U_a-U_w)}\,d(U_a-U_w) \qquad (4.34)$$

where v = unit volume

V_w = volume of water in the element

$\frac{1}{v}\frac{\partial v}{\partial(\sigma-U_a)}$ = compressibility of the soil structure when $d(U_a - U_w)$ is zero

$\frac{1}{v}\frac{\partial v}{\partial(U_a-U_w)}$ = compressibility of the soil structure when $d(\sigma - U_a)$ is zero

$\frac{1}{v}\frac{\partial V_w}{\partial(\sigma-U_a)}$ = slope of the water volume vs. $(\sigma - U_a)$ plot when $d(U_a - U_w)$ is zero.

$\frac{1}{v}\frac{\partial V_w}{\partial(U_a-U_w)}$ = slope of the water volume vs. $(U_a - U_w)$ plot when $d(\sigma - U_a)$ is zero.

Each equation can be viewed as a three-dimensional surface with two independent stress state variables forming the abscissas (i.e. $(\sigma - U_a)$ and $(U_a - U_w)$).

The above equations can be written using other combination of stress state variables ; (б - Uw) and (Ua - Uw) or (б - Ua) and (б - Uw).

Fredlund and Morgenstern (1977) described the stress state of an unsaturated soil within the context of multiphase continuum mechanics, constructing equilibrium equations for each phase of an unsaturated soil in terms of measurable variables. Special consideration was paid to the air-water interface (contractile skin) such that an unsaturated soil was viewed as a four-phase system.

The stress state variables governing the behaviour of an unsaturated soil were extracted from the equilibrium equations to form independent stress tensors(see fig.4.10), i.e.

$$\begin{bmatrix} б_x - U_w & \tau_{yx} & \tau_{zx} \\ \tau_{xy} & б_y - U_w & \tau_{zy} \\ \tau_{xz} & \tau_{yz} & б_z - U_w \end{bmatrix}$$

and

$$\begin{bmatrix} U_a - U_w & 0 & 0 \\ 0 & U_a - U_w & 0 \\ 0 & 0 & U_a - U_w \end{bmatrix}$$

The analysis revealed that two of the three stress state variables could be chosen since any combination could, by mere algebraic manipulation, be converted to the other combination. The possible combinations are:

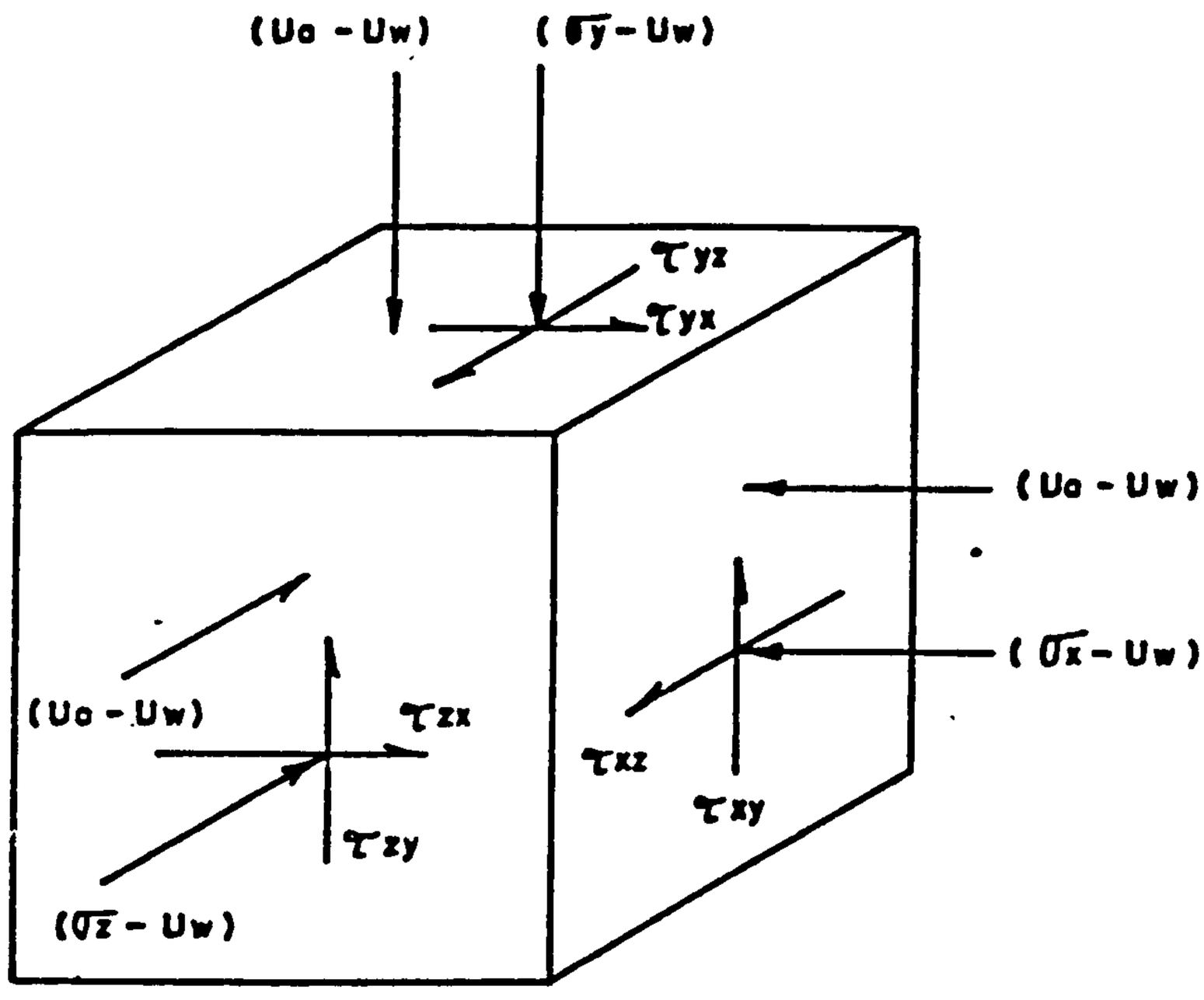

Fig.4.10: Stresses in the soil structure at a point.

(1) $(\sigma - U_a)$ and $(U_a - U_w)$

(2) $(\sigma - U_w)$ and $(U_a - U_w)$

(3) $(\sigma - U_a)$ and $(\sigma - U_w)$

Null tests were performed to experimentally test the proposed stress-state variables. (i.e. The test could be stated as $\Delta\sigma x = \Delta\sigma y = \Delta\sigma z = \Delta U_w = \Delta U_a$. If the change in overall volume was zero and the change in degree of saturation was zero, equilibrium of the soil particles and contractile skin had been maintained).

Fredlund,Morgenstern and Widger (1978) proposed that the shear strength of an unsaturated soil could be written in terms of two independent stress state variables.

One form of the shear strength equation was:

$$\tau = C' + (\sigma - U_w) \tan \phi' + (U_a - U_w) \tan \phi^{\bullet} \quad (4.35)$$

A second form of the shear strength equation was

$$\tau = C' + (\sigma - U_a) \tan \phi' + (U_a - U_w) \tan \phi^{b} \quad (4.36)$$

where C' = effective cohesion parameter

ϕ' = the effective friction angle with respect to changes in $(\sigma - U_w)$ when $(U_a - U_w)$ held constant

or the effective friction angle with respect to changes in $(\sigma - U_a)$ when $(U_a - U_w)$ held constant

$\phi^{\bullet}$ = friction angle with respect to changes in $(U_a - U_w)$ when $(\sigma - U_w)$ held constant

ϕ^b = friction angle with respect to changes in (Ua - Uw) when (σ - Ua) held constant

The stress circle corresponding to the failure conditions in the case of an unsaturated soil must be plotted on a three-dimensional diagram. The axes in the horizontal plane are the stress state variables and the ordinate is the shear strength. The three-dimensional diagram is reduced to a two-dimensional plot of effective normal stress versus shear strength for a saturated soil.

Fredlund (1979) confirmed that two state variables were required to describe the stress state of an unsaturated soil (e.g. (σ - Ua) and (Ua - Uw). There was a smooth transition from the unsaturated case to the saturated case as the pore-air pressure became equal to the pore-water pressure and the degree of saturation approached 100%. Therefore, the matrix suction (i.e. (Ua -Uw)) reduced to zero and the pore-water pressure could be substituted for the pore-air pressure (i.e. (σ - Uw)).

Lloret and Alonso (1980), following the line of reasoning of Matyas and Radhakrishna (1968), used state surfaces with two independent stress state variables (σ - Ua) and (Ua - Uw) to describe the consolidation and swelling behaviour of an unsaturated soil (i.e. void ratio and degree of saturation). Spline functions were used to approximate the three-dimensional constitutive surfaces.

4.6 Summary

The following table summarises all the effective stress equations for unsaturated soils.

Equation	Proposed by
$\sigma' = (\sigma - Ua) + X\,(Ua - Uw)$	Bishop (1955)
$\sigma' = \sigma + B\,p^{\bullet}$	Jennings (1957)
$\sigma' = \sigma - B'\,Uw$	Croney, Coleman and Black (1958)
$\sigma' = \sigma + \psi p^{\bullet}$	Aitchison (1960)
$\sigma' = (\sigma - Ua) + Aw(Ua - Uw)$	Lambe (1960a)
$\sigma' = \sigma - (1 - \frac{a \tan\psi}{\tan\phi'})\,Sr\,Uw$ (for shear strength)	Skempton (1960)
$\sigma x' = \sigma x + n(Ua - Uw) - Ua(1 - a)$	Sparks (1963)
$\sigma' = (\sigma - Ua) + f(Ua - Uw)$	Bishop and Blight (1963)
$\sigma' = \sigma i + X(Ua - Uw) + (\sigma - Ua)$	Newland (1965)
$\sigma' = \sigma - Ua + Xm(hm + Ua) + Xs\,(hs + Ua)$	Richards (1966)

4.7 Conclusion

The approach of using two independent stress state variables (i.e. $(\sigma - U_a)$ and $(U_a - U_w)$) marked the beginning of a new era. It was obviously time for engineers to stop pitting their wits, ingenuity and imagination against that highly controversial and elusive X parameter and to embark on the development of equipment and testing procedures that would allow evaluation of volume changes and shear strength in unsaturated soils.

Great promise exists for using two independent stress state variables in solving foundation problems on expansive unsaturated soils. Unfortunately, field data is not yet available for comparison with laboratory results. It may be some time before these methods are proven to be of merit.

In chapter 5, an examination of the validity of the principle of effective stress as applied to the shear strength of unsaturated soils has been carried out, making use of previous research workers' results.

CHAPTER 5: SHEAR STRENGTH

CHAPTER 5: SHEAR STRENGTH

5.1 The shear strength of saturated soils

The shear strength of a soil is its maximum resistance to shearing stresses. When this resistance is exceeded failure occurs, usually taking the form of surfaces of slip.Shear strength is usually assumed to be made up of:

(i) Internal friction, or the resistance due to interlocking of the particles

(ii)Cohesion, or the resistance due to the forces tending to hold the particles together in a solid mass

Generally speaking, coarse-grained soils such as sands derive their shear strength almost entirely from intergranular friction, but with other soils the strength is a combination of both forms of resistance.

In 1776, Coulomb suggested that the shear strength characteristics of a soil could be represented by the expression: $\tau = C + \sigma \tan\phi$----------(5.1)

where τ denotes shear strength
C denotes apparent cohesion
σ denotes total pressure normal to shear plane
ϕ denotes angle of shearing resistance

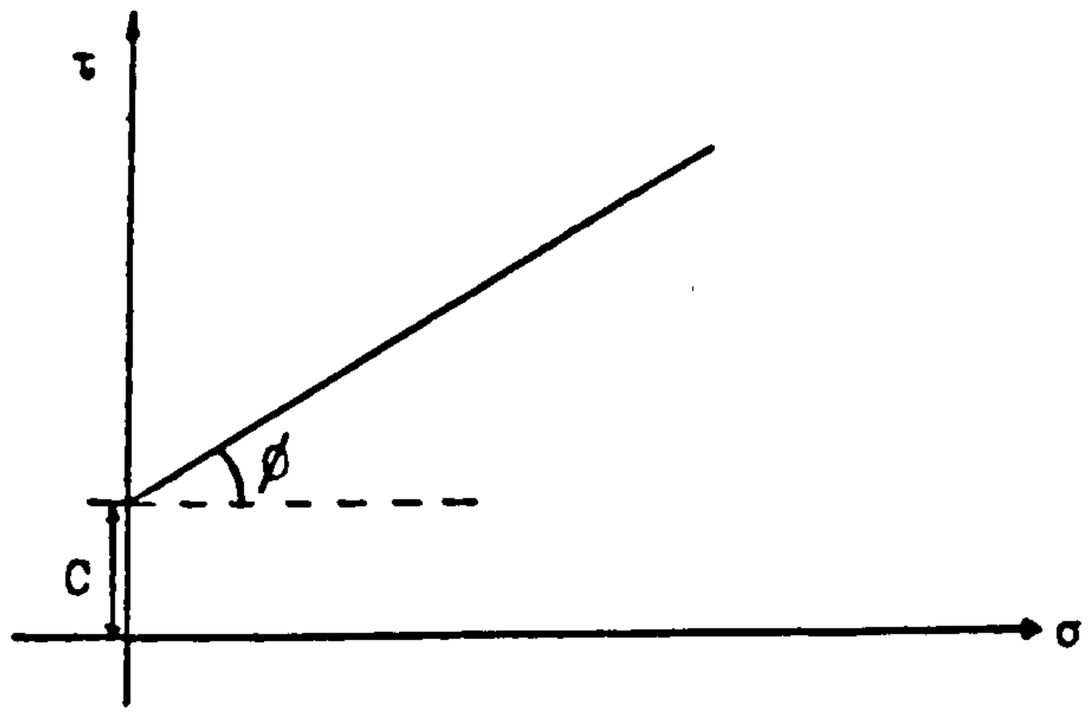

Figure 5.1: The Coulomb relationship

In a more fundamental form, first put forward by Hvorslev in 1937, Coulomb's equation was rewritten as:

$$\tau = Ce + (\sigma - Uw)\tan\phi e \text{----------(5.2)}$$

where Ce denotes true cohesion
ϕe denotes true angle of internal friction
Uw denotes the pore water pressure

The cohesion and internal friction will, in general, depend upon the void ratio of the soil at the instant of shear failure.

Taylor(1948) introduced an idealised form of Coulomb's equation, i.e. $\tau = \sigma \tan\phi$----------(5.3)
where again ϕ is the angle of shearing resistance under the special conditions appertaining to a drained shear test.

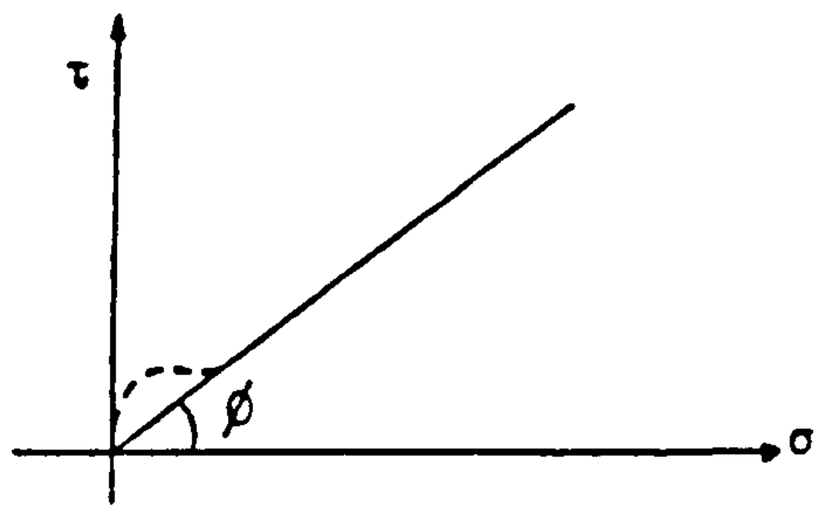

Figure 5.2: The Taylor relationship

It is necessary, in considering these forms of the shear strength law, to emphasise the implicit assumptions involved in the selection of the cohesion and friction parameters. In the first place, the C and ϕ of the Coulomb equation are merely empirical constants, determined experimentally, which depend on the stress conditions imposed on the soil element, and in particular, whether or not the soil is allowed to drain during the shearing process.

Hvorslev, in his attempt to define shear strength in terms of fundamental cohesion and friction properties introduced the principle of effective stress. The development of this principle

was discussed in detail in Chapter 4 and, for saturated soils, there are ample grounds for its acceptance in the theories of shear strength behaviour. In general terms, however, Ce and Øe are not specific fundamental soil properties, but will depend on the void ratio of the soil at failure. They are therefore dependent on both the past history of the soil and the stress conditions which exist during the shearing process. This may be summarised in the statement that both the Hvorslev and the original Coulomb equation are applicable only to the over-consolidated region of the soil behaviour in shear. On the other hand, a similar analysis of what has been termed the Taylor equation(equation 5.3) leads to the conclusion that the angle of shearing resistance, Ø, includes both cohesion and friction effects and that the equation holds over the normally consolidated range.

It is evident therefore that for each of these shear strength relationships it is necessary to specific the past history of the sample, which in turn involves an a priori assumption, with respect to effective stresses. Hence the cohesion and friction parameters which are involved in the three expressions quoted above cannot be accurately described as fundamental soil characteristics.

When dealing with shear strength equations, it is customary to designate extreme soil types as those when one of the components of shear strength tends to zero.

In the case of coarse-grained soils such as sands and gravels, it has been well established(Bishop and Eldin,1950) that the cohesion component is essentially zero and that the

shear strength is given by $\tau = (\sigma - U_w)\tan\phi_e$, where ϕ_e is mainly dependent on the initial density(void ratio) of the soil.

For purely cohesive clays, $\phi_e = 0$ and the shear strength depends on the cohesion component only, which in turn will be determined by the maximum consolidation pressure(p), so that the shear strength becomes a function of the cohesion term,i.e. $\tau = F(Ce)$.

Intermediate soil types which can be called sand-clay soils involve both cohesion and friction. The shear strength in this case is represented by the general equation:

$$\tau = F_1(Ce) + F_2(\phi e) \text{----------(5.4)}$$

5.2 The shear strength of unsaturated soils

Previous studies of the shearing strength of partially saturated clays have dealt with the examination and/or modification of the effective stress equations as described in Chapter 4. This approach was considered promising because of the demonstrated success of the fundamental effective stress equation for fully saturated clays. However, the problems associated with the measurement of the pore air pressure, necessary for the modification of the effective stress equation for the case of partially saturated clays, are in most cases complex and thus render this approach difficult. Lewis and Ross(1955) investigated the relationship between the shear strength of remoulded clays and soil suction(soil-water potential). While the results of the studies showed that there was no simple relationship between the shear strength of

remoulded cohesive soils and soil suction, it was demonstrated that the shear strength of such soils was a function of soil type, dry density, and soil moisture suction. Along the same lines, Croney and Coleman(1960) showed that the unconfined compressive strength of clay soils varied linearly with the soil suction. This is supported in part by the work of Towner(1961) who showed that the shear strength of clay soils could be considered to vary linearly with initial suction, despite the fact that the values obtained showed some scatter. This was acceptable because of the difficult in duplicating the initial fabric of the samples.

With these points in mind and with the understanding that the integrity and stability of a remoulded soil sample can be determined in terms of the soil water energy relationship(see Chapter 3), it would appear therefore that a relationship exists between the interacting internal energy components of the soil and the resultant shearing strength. Yong, Japp and How(1971) recognized that interactions occurred between soil particles through associated water layers, and experimentally observed shear strengths were examined in terms of intrinsic soil water energy relationships. The usefulness of such an approach is in assessing the influence of environmental moisture content changes on the shear strength of partially saturated clays. The theory shows that shear strength is dependent on the energy status of the material---all other test constraints remaining constant.

Part of chapter 4 reviewed the development of independent

stress state variables to describe the behaviour of unsaturated soils. This approach has been used mainly to describe the volume change behaviour of unsaturated soils, but several investigations have also been made to apply it to the shear strength characterization of unsaturated soils(Bishop et al,1960; Massachusetts Institution of Technology (MIT),1963 ; Sridharan, 1968; Maranha das Neves,1971;Gulhati,1975); however, none has proven completely successful.

Fredlund and Morgenstern(1977) showed from a stress field analysis that any two of three possible stress variables could be used to define the stress state in an unsaturated soil. Possible combinations were:

(1) (σ - Ua) and (Ua - Uw),
(2) (σ - Uw) and (Ua - Uw),
(3) (σ - Ua) and (σ - Uw)

where σ = total normal stress
Ua = pore-air pressure
Uw = pore-water pressure

Null experiments (i.e. $\Delta\sigma=\Delta Ua=\Delta Uw$) supported the proposed theoretical stress state variables(Fredlund et al,1977).

In 1978, Fredlund, Morgenstern and Widger proposed equations for the shear strength of an unsaturated soil in terms of two independent stress state variables. One form of the shear strength equation is:

$$\tau = C' + (\sigma-Uw)\tan\phi' + (Ua-Uw)\tan\phi^{b}\text{----------(5.5)}$$

where C′ = effective cohesion parameter
ϕ' = the friction angle with respect to changes in (σ-Uw) when (Ua-Uw) is held constant,
and ϕ^{b} = friction angle with respect to changes in (Ua-Uw) when (σ-Uw) is held constant

The transition from an unsaturated soil to a saturated soil (i.e. Ua=Uw) is obvious. A second form of the shearing equation

is:

$$\tau = C^{*} + (\sigma - U_a)\tan\phi^{a} + (U_a - U_w)\tan\phi^{b} \text{ --------(5.6)}$$

where C^{*} = cohesion intercept when the two stress variables are zero;

ϕ^{a} = the friction angle with respect to changes in $(\sigma - U_a)$ when $(U_a - U_w)$ is held constant;

ϕ^{b} = friction angle with respect to changes in $(U_a - U_w)$ when $(\sigma - U_a)$ is held constant

The stress state variables used in Eq.5.5 are $(\sigma - U_w)$ and $(U_a - U_w)$. The advantage of this combination of variables is that it provides a readily visualized transition from the unsaturated to the saturated case. The disadvantage arises in that, when the pore-water pressure is changed, two stress state variables are being affected. The relative significance of each variable must be borne in mind when considering the shear strength(This is also the disadvantage associated with utilizing the $(\sigma - U_a)$ and $(\sigma - U_w)$ combination of stress state variables).

The combination of stress state variables used in Eq.5.6 is $(\sigma - U_a)$ and $(U_a - U_w)$. The advantage of this combination is that only one stress variable is affected when the pore-water pressure is changed. Regardless of the combination of stress variables used to define the shear strength, the value of shear strength obtained for a particular soil with certain values of σ, U_a and U_w must be the same.

Examining equation 5.6 when the matrix suction $(U_a - U_w)$ is zero, the $(\sigma - U_a)$ plane will have the same friction angle parameter as the $(\sigma - U_w)$ plane when using the first combination

of stress state variables(i.e.(σ-Uw) and (Ua-Uw)). Therefore, ϕ^a is the same as ϕ'. Also C' is the same as C'. The shear strength equation is now:

$$\tau = C' + (\sigma - Ua)\tan\phi' + (Ua-Uw)\tan\phi^b \text{ ----------(5.7)}$$

Since equation 5.5 or 5.7 will give the same value for shear strength, it is possible to equate them and obtain the relationship between the various angles of friction, viz:

$$\tan\phi' = \tan\phi^b - \tan\phi^a \text{ ----------(5.8)}$$

Fredlund, Morgenstern and Widger suggested that the second form (i.e.Eq.5.7) would prove to be the most useful in engineering practice.

Graphically, the equation can be visualised on a three-dimensional plot (i.e.a modified Mohr-Coulomb envelope) using the stress state variable as abscissas(Fig.5.3a). The equation can also be visualised as a two-dimensional graph with matrix suction contoured as the third variable(Fig.5.3b). The ordinate intercepts of the various matrix suction contours can be plotted versus matrix suction to give the friction angle, ϕ^b (Fig.5.4). A procedure for using these graphs to obtain values of ϕ^b is discussed in chapter 9. The form of the equation assumes that the failure surface is a plane, an assumption discussed in chapter 10.

It should be noted that there is a smooth transition from the unsaturated to the saturated soil condition. As saturation is approach, the pore-air pressure, Ua, becomes equal to the pore-water pressure, Uw. At this condition, the shear strength equation reverts back to the conventional equation for a saturated soil,i.e. $\tau = C' + (\sigma - Uw)\tan\phi'$

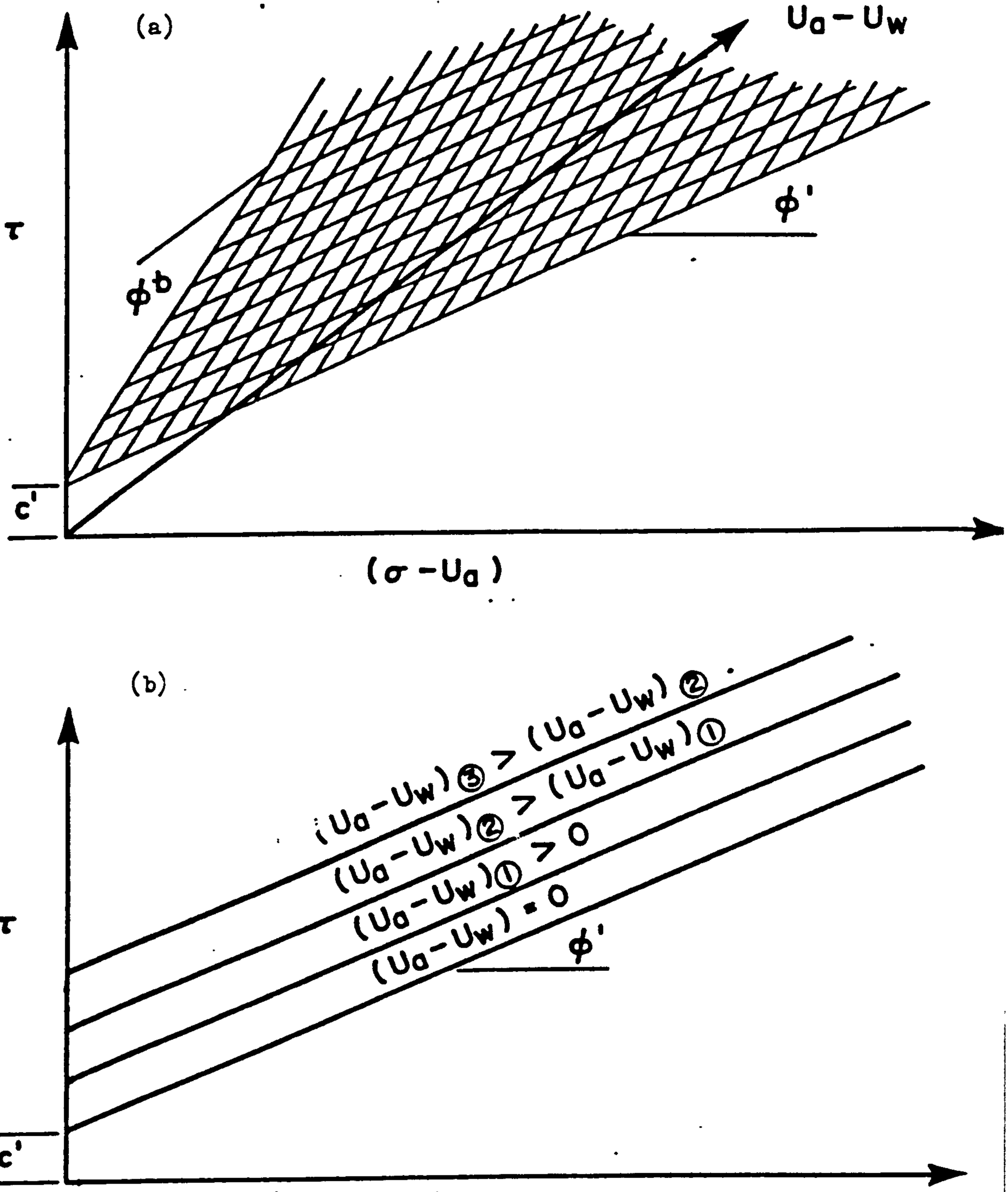

Fig.5.3: Graphical representations of the shear strength of an unsaturated soil. (after Fredlund, 1980)

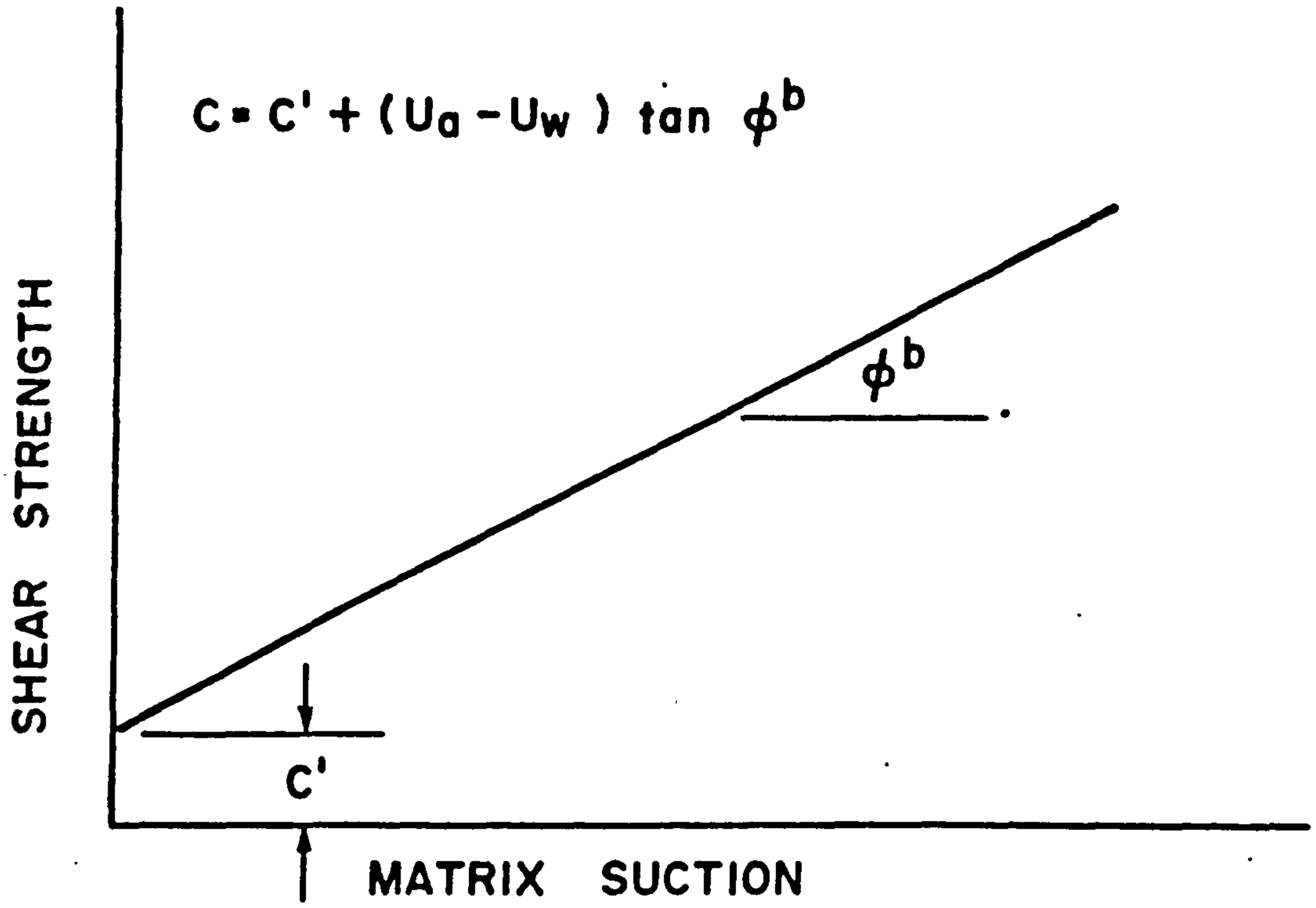

Fig.5.4: Graphical representation of the increase in shear strength with matrix suction. (after Fredlund , 1980)

A three-dimensional plot of the stress state variables versus shear strength is difficult to analyse, and so a procedure was outlined by Ho(1981) to assist in obtaining the desired shear strength parameters. For convenience in handling the strength data from triaxial tests, the stress point at the top of each stress circle can be used, i.e.((б1 +б3)/2-Uw) and (Ua-Uw). the equation for the plane through the stress points is:

$$(б1 - б3)/2 = d' + ((б1+б3)/2-Uw)\tan\phi' + (Ua-Uw)\tan\phi^{b} \text{----(5.9)}$$

where d' = the intercept when the two stress points are zero,

ϕ' = the angle between the stress point plane and the ((б1 +б3)/2-Uw) axis when (Ua-Uw) is held constant,

ϕ^{b} = the angle between the stress point plane and the (Ua-Uw) axis when ((б1+б3)/2-Uw) is held constant

The relationship between a plane through the stress points and the failure surface is discussed in Chapter 9, along with the corresponding soil parameters. It is necessary to plot the data in a special manner in order to obtain the ϕ^{b} friction parameters.

Satija(1978), Gulhati and Satija(1981) followed the same lines as Fredlund, and used two independent stress state variables (i.e.(б-Ua) and (Ua-Uw)) to describe the shear strength of partially saturated soils. They found that the strength generated by (б-Ua) was both greater and more stable than that contributed by (Ua-Uw), and the relationship between shear strength and the stress state variables, (б-Ua)f and (Ua-Uw)f, could be written in the form:

$$(б1-б3)f/2 = a + (б3-Ua)f\cdot\tan\alpha + (Ua-Uw)f\cdot\tan\beta \text{ ---(5.10)}$$

where a denotes an intercept on the shear stress axis;
α denotes a coefficient associated with the stress state variable ($\bar{\sigma}$ -Ua) which represents externally applied stress;

and β denotes a coefficient associated with the other stress state variable (Ua-Uw) which represents the internally generated stress

As for Fredlund, the strength of partially saturated soil is related to the stress state variables in such a way that the surface depicting the failure condition on a three-dimensional stress plot is a planar surface(see Figure 5.5).

Gulhati and Satija conclude that α is both greater in magnitude than β and more stable than β. In other words, the stresses originating internally are not as 'effective' as those applied externally in generating shear strength in partially saturated soil. Gulhati(1980) suggests there is no evidence to assume that C′ and Ø′, which are parameters that express the behaviour of saturated soil, continue to remain relevant for soil in the partially saturated state.

Ho and Fredlund(1982) suggested a multistage triaxial testing procedure for unsaturated soils, which could obtain the maximum amount of information from a limited number of tests and which would help to eliminate the effects of variability in the soil from one test to the next. The testing procedure involved the control of the air and water pressures during the entire test rather than their measurement in a closed system. Suction in the sample was maintained constant during the application of the deviator stress. Maintaining the pore-air and pore-water pressure was similar to performing a 'slow' or drained test on a saturated soil. The axis-translation technique was used to

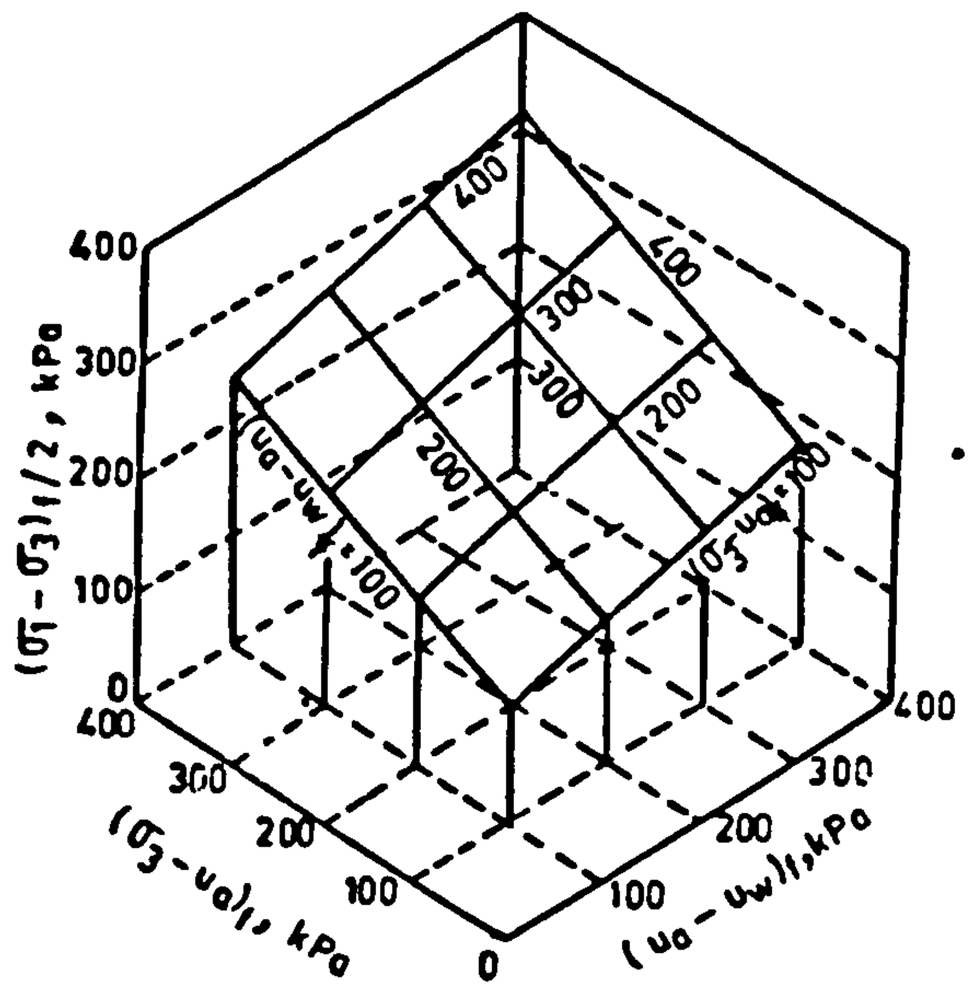

Fig.5.5: Three dimensional plot between

$\frac{(\sigma 1-\sigma 3)f}{2}$ vs. $(\sigma 3-Ua)f$ and $(Ua-Uw)f$

for A-samples.

(after Gulhati and Satija,1981)

impose suctions greater than 100 KPa(1 atm.) (See appendix 1).

The analysis of the multi-stage test results was based on Fredlund et al(1978) shear strength equation. The multistage triaxial testing procedure was used to evaluate the friction angle, ϕ^b from a single test(see chapter 9).

The matrix suction term in the shear strength equation for an unsaturated soil can be considered as contributing to the cohesion of the soil:

$$C = C' + (Ua - Uw)\tan\phi^b \text{ ----------(5.11)}$$

where C is the total or apparent cohesion of the soil
The relationship between cohesion due to suction, matrix suction and friction angle ϕ^b is shown in Figure 5.6, which illustrates that the suction in an unsaturated soil increases the cohesion of an unsaturated soil. In this way, conventional saturated soil shear strength concepts can be applied to practical problems involving unsaturated soils.

In the lecture---'The shear strength of unsaturated soils and its relationship to slope stability problems in Hong Kong' delivered by Fredlund(1980) to the Hong Kong Geotechnical Society. He mentioned that unsaturated soils have not been commonly associated with slope stability problems since the negative pore-water pressure(or matrix suction) increases the soil's strength. This is mainly because there is reservation regarding the long-term reliability of matrix suction. As a result, limited laboratory shear strength testing has been performed on unsaturated soils and little attempt has been made to utilize the results for the computation of a factor of safety.

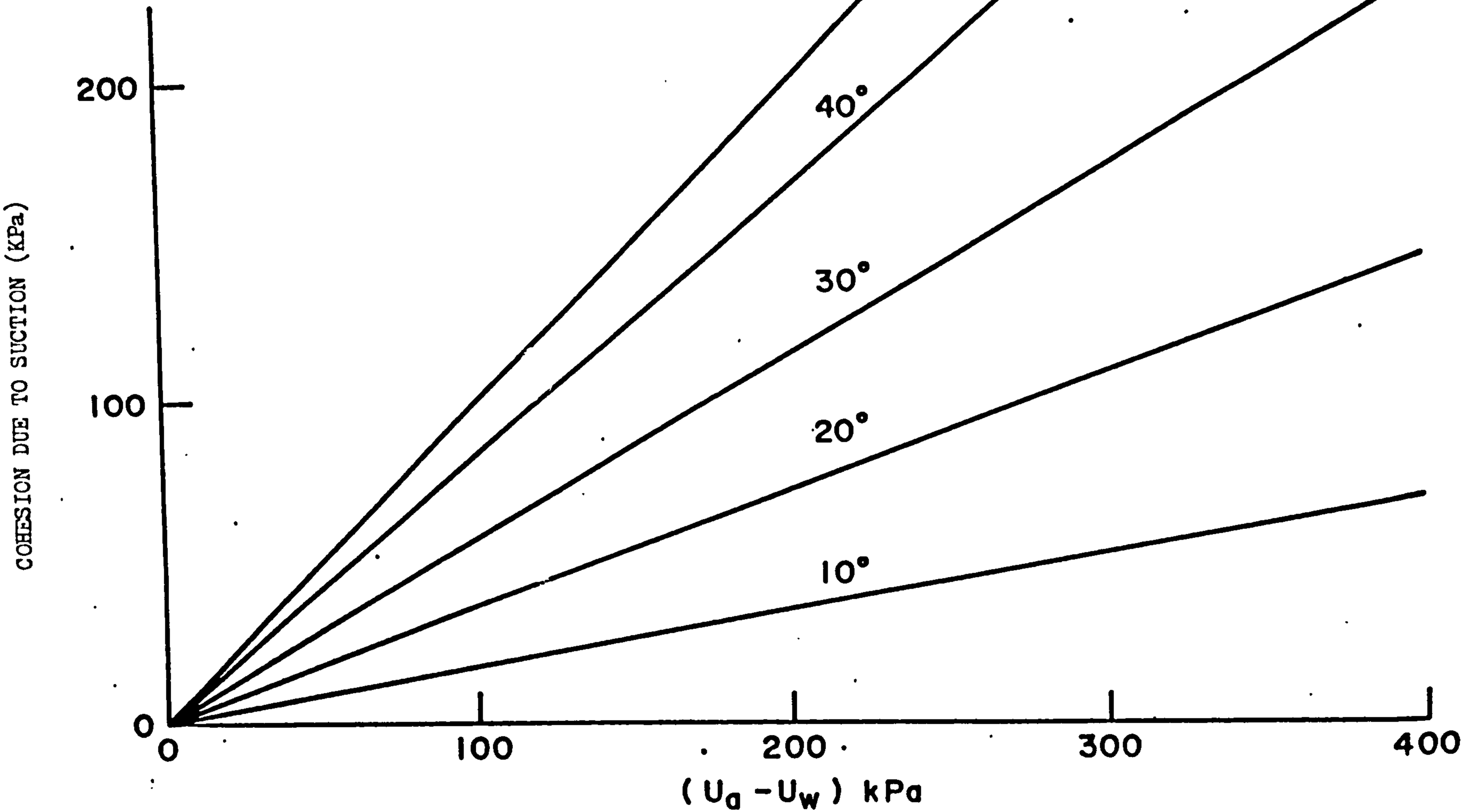

Fig.5.6: Relationship between cohesion, matrix suction and the friction angle ϕ^b. (after Fredlund, 1980)

Slope stability analyses are commonly performed on slopes in Hong Kong. Generally, the Janbu simplified method is used and effective shear strength parameters are used in the analysis(i.e. effective cohesion,C′,and effective angle of friction,Ø′). The computed factor of safety often gives values that are below one(e.g.0.9) even for slopes showing no sign of distress. The stability of the slope is commonly attributed to the effects of soil suction. He addressed the following question---'Could different limit equilibrium methods of slices yield different computed factors of safety ?'. The study of various methods of analysis demonstrated that the factor of safety computed by different methods is of secondary significance. However, an increase in cohesion significantly increases the computed factor of safety(see figure 5.7). This may justify the matrix suction increase in the cohesion of the soil.

i.e. $C = C' + (Ua-Uw)\tan\emptyset^b$

5.3 Discussion of shear strength concepts for unsaturated soils

Shear strength concepts proposed for unsaturated soil, can be classified into three groups; namely, the particulate mechanics approach, the empirical approach and continuum mechanics approach.

In an attempt to follow Terzaghi′s postulation of describing the shear behaviour of saturated soils by using effective stress,Bishop et al(1960), Skempton(1960), Newland(1965), Richard(1966) and Sridharan(1968) obtained expressions for the effective stress in unsaturated soils which were similar in form

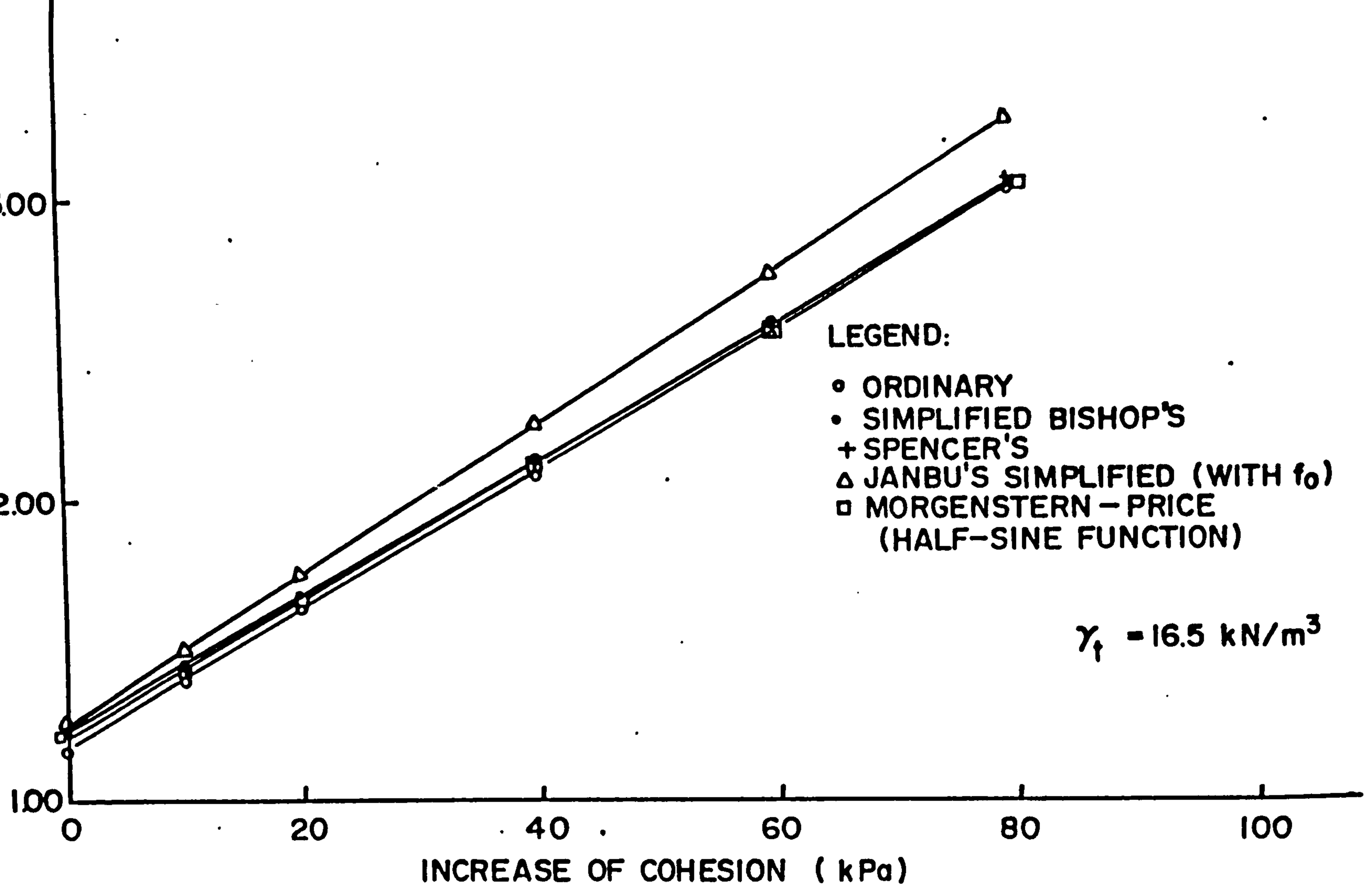

Fig.5.7: Increase in factor of safety for an increase in cohesion for example slope.
(after Fredlund,1980)

to that derived for saturated soils. However, these expressions did not satisfy force equilibrium conditions as applied to an element of unsaturated soil. They all included at least one parameter which was dependent on the properties of the soil, and so the expressions became constitutive relationships. The particulate mechanics approach used to develop these expressions lead to questions regarding their credibility. Basically, the effective stress theories for unsaturated soils of Skempton(1960), Newland(1965) and Richards(1966) can all be viewed as variation of the Bishop et al(1960) X factor concept. Although Bishop et al, Bishop and Donald(1961), and Bishop and Blight(1963) claimed to have demonstrated the validity of an effective stress equation for unsaturated soils, and the uniqueness of the X-factor concept, the scatter in the research results which are in support of Bishop's effective stress theory for unsaturated soils cast doubt on the validity of the claims (see figure 5.8). Also convincingly presented counter arguments (Jennings and Burland,1962)(M.I.T.,1963)(Gulhati,1975)(Satija, 1978) have been reported.

The work of Jennings and Burland highlighted the shortcomings in Bishop's effective stress equation as well as the method suggested for determining X. The method was based on the assumption that soils in saturated and partially saturated states have the same value of a certain engineering property such as shear strength or void ratio and X was solved by comparison. Implicit in such a determination of X is the assumption that the strength parameter or the compressibility of

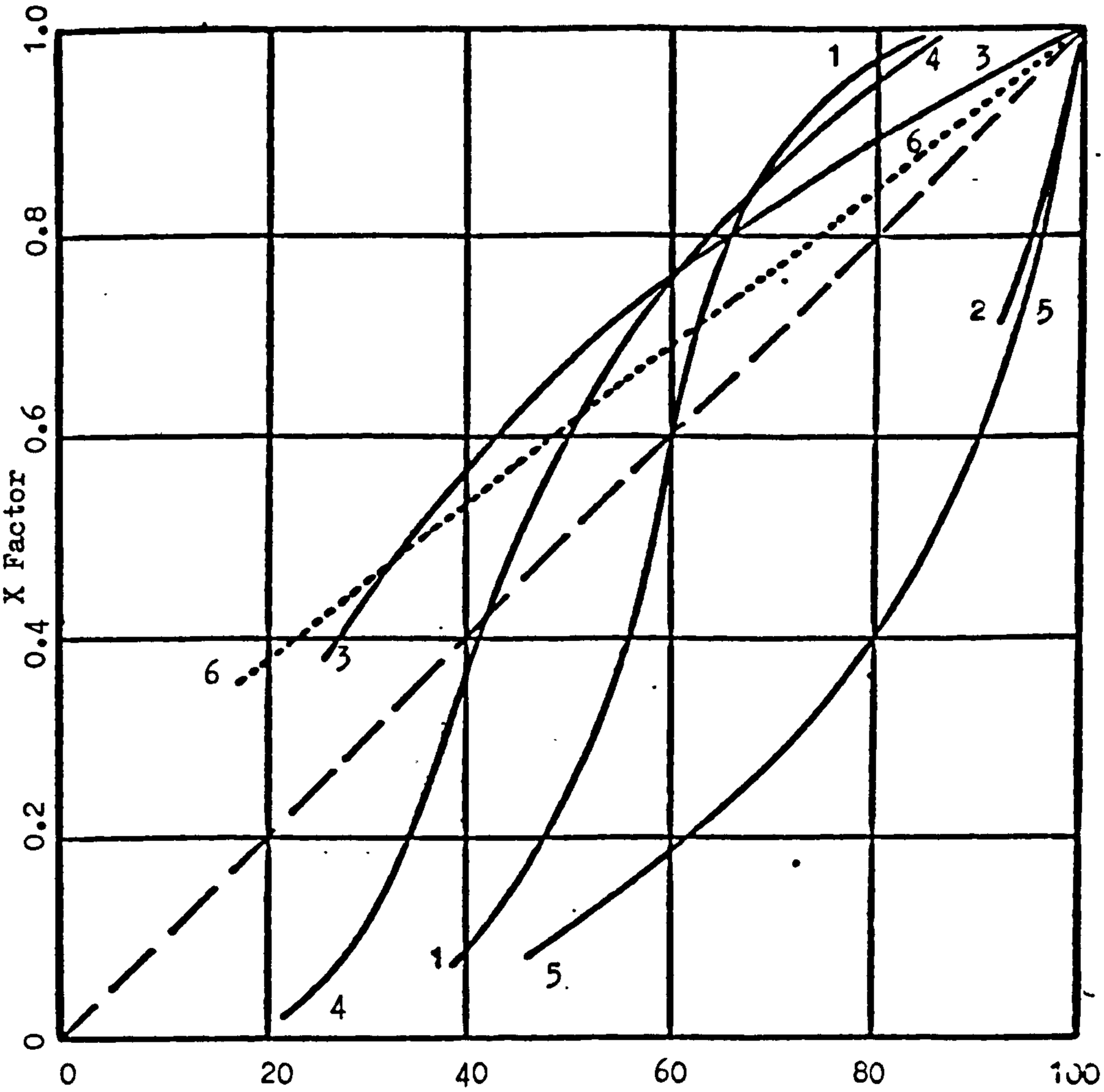

1.Compacted Boulder clay (4% -2μ)) Bishop et al,1960
2.Compacted Shale (22% -2μ)

3.Breahead silt: Bishop and Donald,1961

4.Silt (3% -2μ)
5.Silty clay (23% -2μ)) Burland,1961

6.Theorectical: Donald,1960

Fig.5.8: Variation of X factor with degree of saturation.
(after Jennings and Burland, 1962)

the soil are not functions of the degree of saturation. In other words, whenever two samples of a soil have the same strength or void ratio they must have the same effective stress. The two soil samples under consideration had, however, different degrees of saturation and consequently different stress histories. This method of determination of the X-factor is thus burdened with an untenable assumption.

Gulhati(1975) also commented on the shortcomings of Bishop's effective stress equation and the manner of determining X, as follows. An increase in effective confining stress is known to increase the strength of saturated soil. An increase in (σ-Ua) also increases the strength of partially saturated soil. This strength increase in partially saturated soil, however, appears to be not as much as in the saturated soil, possibly on account of the different response of the soil skeleton of partially saturated soil in relation to the response of the soil skeleton of saturated soil. This difference originates because the skeleton of the former is more rigid, due to the existence of tension in its pore water. This difference in response is ignored when X is computed by equating:

$$\sigma' = \sigma - U_w = (\sigma - U_a) + X(U_a - U_w) \text{----------(5.12)}$$

Since (σ-Ua) does not in fact generate as much strength as a similar change in effective confining stress in saturated soil, (σ-Ua) is not fully 'effective', but mathematically it is assumed to be fully 'effective' and, therefore, the term X(Ua-Uw) is forced to become smaller in order to satisfy the mathematical equality of the above equation; this occurs by an artificial reduction in the value of X. Therefore as saturation

increased, Gulhati found that X decreased and argued that this was because X was not only a function of saturation and in the equality X was being mathematically forced to manifest the phenomenon of different responses of saturated and partially saturated soil.

Gulhati summarised the limitations in evaluating the magnitude of X in tabular form and it is reproduced as Table 5.1. He suggested that Blight's(1967) method of evaluating X(see figure 5.9) seemed more promising than Bishop et al(see figure 5.10) because it was not burdened with the assumption that C' and $\emptyset'$ of saturated and partially saturated soils are the same. It merely assumed that C' was negligible and the value of $\emptyset'$ for samples with very slightly different degrees of satyration was the same. However, the values of X determined by Gulhati(1972) using Blight's method were in fact less accurate than the values obtained using the method proposed by Bishop et al. He explained this was because Blight's method involved the explicit use of the assumption that X was a function of the degree of saturation only.

There are also shortcomings in the effective stress concept for unsaturated soils suggested by Sridharan(1968). The involvement of interparticle stresses in the proposed effective stress equation constituted a flaw; mixing continuum mechanics with particulate mechanics is not acceptable to fundamental physics. In addition, the ratio of area of water-mineral and water-water contact to the total area of the 'wavy-plane',aw, which is required in the proposed equation, makes the concept

(Gulhati,1975) Table 5.1 : The factor X

Researchers	Concept of X	Techniques suggested to evaluate magnitude of X
1.AITCHISON(1956)	A factor that transforms tension in pore water to its contribution to intergranular stress which is believed to be effective stress.	On the basis of idealized models using relation between (Ua-Uw) and degree of saturation S.
2.LAMBE(1960)	A factor that represents proportion of water to water contact per unit area of a "wavy plane" through soil.	None
3.SRIDHARAN(1968)	Do	On the basis of knowledge of soi type, surface area, pore size distribution, and water content.
4.BISHOP(1959)	A function of degree of saturation S. for S = 0; X = 0 S = 100 %; X = 1 0 < S < 1; 0 < X < 1	None.
5.BISHOP ET AL(1960)	Do	By equating $\bar{\sigma}$ of saturated and partially saturated soil samples having the same magnitude of an engineering property.
6.BLIGHT(1967)	Do	By equating ratios of $\bar{\sigma}$ in two partially saturated soils with slightly different degrees of saturation to the ratio of their observed strengths.

Run shear tests on

Partially saturated sample at S = S1 (measure strength, σ, Ua, Uw)

Partially saturated sample at S = S2 (measure strength, σ, Ua, Uw)

S1 ≒ S2

ratio of strength = ratio of $\bar{\sigma}_f$

$$\frac{\text{Strength at S1}}{\text{Strength at S2}} = \frac{((\sigma-Ua) + X1(Ua-Uw))_f \text{ at S1}}{((\sigma-Ua) + X2(Ua-Uw))_f \text{ at S2}} \quad \ldots\ldots(*)$$

Since X = f(S) only and S1 ≒ S2

then X1 = X2 so let X1 = X2 = X in Eqn.(*)

Solve for X

Assumptions in such a determination of X

Explicit:

(i) $\bar{\sigma}$ = (σ-Ua) +X(Ua-Uw) for partially saturated soil is correct.

(ii) ϕ' for samples at slightly different degrees of saturation is same and c' is negligible.

(iii) X is a function of degree of saturation only.

Since determination of X requires explicit use of assumption (iii), values so obtained do not lend themselves to interpretation.

Fig.5.9: Blight's(1967) X-factor. (Gulhati,1975)

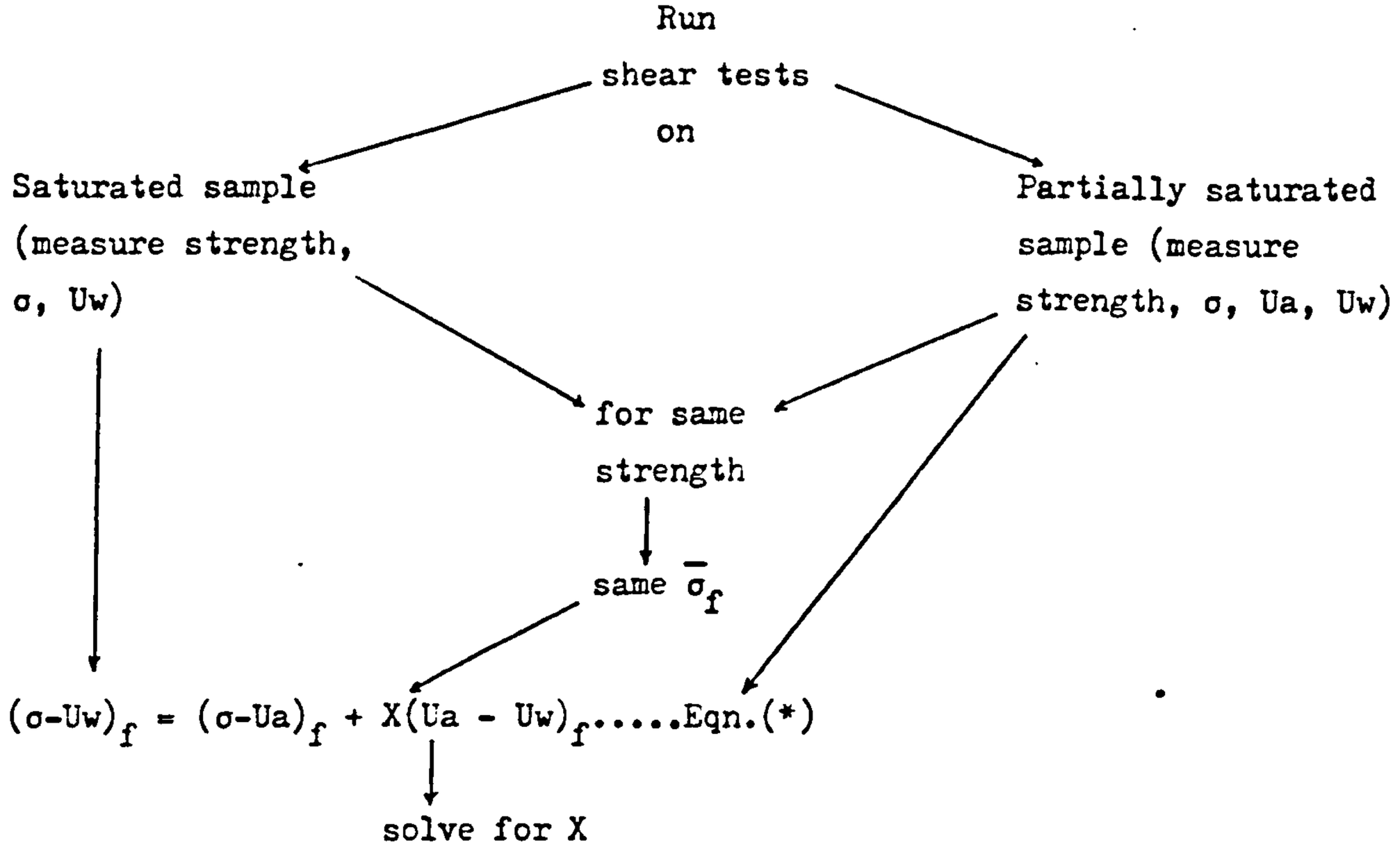

Assumptions in such a determination of X

Explicit:

(i) $\bar{\sigma} = (\sigma - Ua) + X(Ua - Uw)$ for partially saturated soil is correct.

(ii) c' and Ø' for saturated and partially saturated soils are same.

Implicit:

(iii) X = f(S) only.

Since these assumptions are not necessarily valid X only empirical. It reflects influence of degree of saturation as well as of incorrectness of assumptions (i) and (ii). X lends itself to interpretation since left hand side of Eqn.(*) is correct.

Fig.5.10: Bishop et al's (1960) X-factor. (Gulhati,1975)

experimentally impractical.

The empirical nature of the approach by Yong et al(1971) in describing the shear behaviour of unsaturated soils by a three-dimensional relationship between water potential, dry density and shear strength(see figure 5.11) leads to a problem-specific approach which cannot be applied in general.

Although it was recognized that there might have been more than one stress state variable governing the behaviour of unsaturated soils as early as 1962(Jennings and Burland,1962) (Coleman,1962), there was no attempt to demonstrate these stress state variables theoretically or experimentally until the early 1970's. Up to this time, the use of force equilibrium to study stress state variables, as in continuum mechanics, had been neglected.

In 1978, shear strength equations for unsaturated soils were proposed by Fredlund et al and Satija based on independent stress state variables. These two equations were founded on the same postulation that ($\bar{\sigma}$-Ua),($\bar{\sigma}$-Uw) and (Ua-Uw) were the only independent stress state variables governing the mechanical behaviour of unsaturated soils and that any two of these stress state variables could be used to define the stress state in an unsaturated soil. Nevertheless, these two proposed shear strength equations for unsaturated soils were derived and used in different ways by Fredlund et al(1978) and Satija(1978).

Terzaghi's saturated soil shear strength theory stated that a stress circle corresponding to failure conditions could be plotted on a two-dimensional plot of ($\bar{\sigma}$-Uw) versus shear

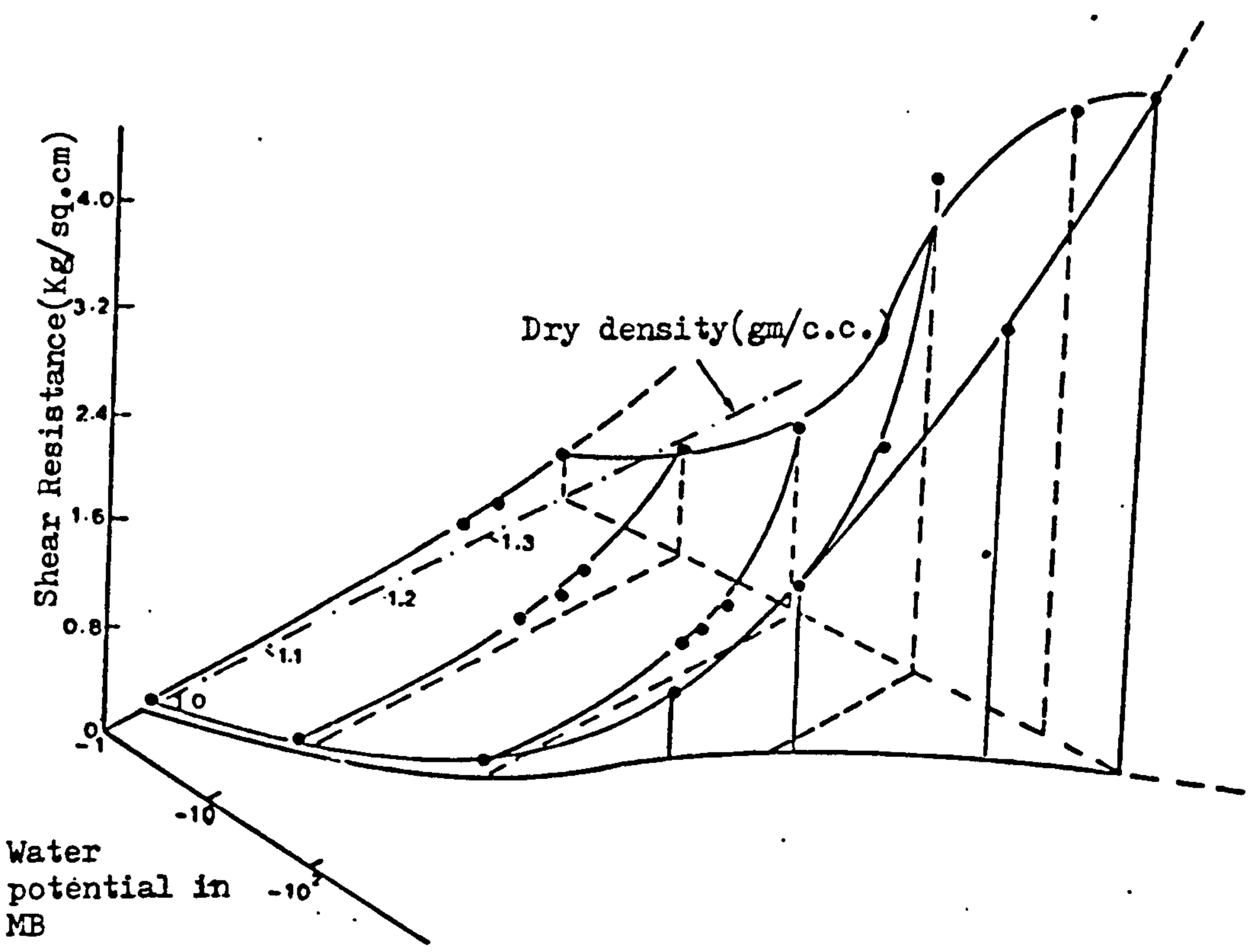

Fig.5.11: Soil-water potential: shear strength surface for Sainte Rosalie clay (Yong, Japp and How, 1971). This form of plotting incorporates the fabric or dry density component of soil structure which is seen to be influential in the development of shear strength.

strength. Fredlund et al(1978) suggested that for unsaturated soils, the stress circle corresponding to the failure conditions could be plotted on a three-dimensional diagram with two stress state variables as the horizontal axes and the shear strength as the ordinate. Shear strength equations for unsaturated soils in terms of possible combinations of stress variables were then established. The original published equations were in terms of (б-Uw) and (Ua-Uw)(Fredlund et al,1978), but subsequently the combination (б-Ua) and (Ua-Uw) has been used(Ho,1981). If (б-Ua) and (Ua-Uw) are used, the proposed shear strength equations are as follows:

$$\tau = C' + (б-Ua)\tan\phi^{a} + (Ua-Uw)\tan\phi^{b} \text{ --------(5.13)}$$

(see figure 5.12)

or in stress point form,

$$(б1-б3)/2 = d^{*}+((б1+б3)/2-Ua))\tan\psi^{a}+(Ua-Uw)\tan\psi^{b} \text{ -----(5.14)}$$

(see figure 5.13)

where C' and ϕ^{a} $(=\phi')$ are parameters for the soil in the saturated state which can be determined in the conventional manner, and ϕ^{b} can be determined from test data in which the two stress state variables have been varied by controlling the magnitude of б, Ua and Uw.

In an attempt to assess whether the shear strength of an unsaturated soil was a function of some combination of the stress state variables (i.e.(б-Ua),(б-Uw) and (Ua-Uw)), Satija(1978) performed statistical studies on experimental data from unsaturated soil shear tests. Three combinations of stress state variables and three stages of shear were considered(Table 5.2). First, a graphical method was used to isolate the trends

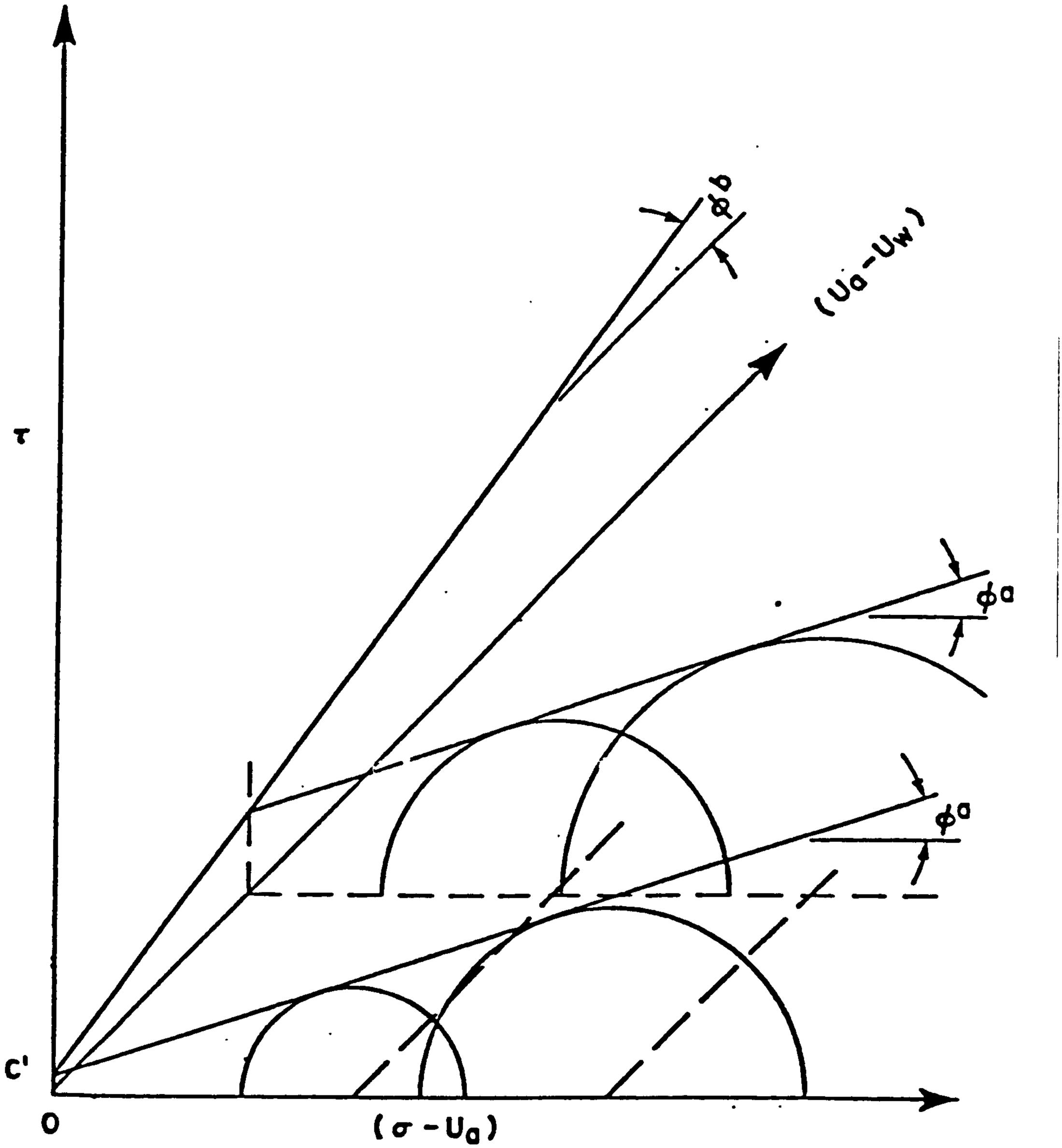

Fig.5.12: Three-dimensional failure surface using stress variables (σ-Ua) and (Ua-Uw). (after Ho,1981)

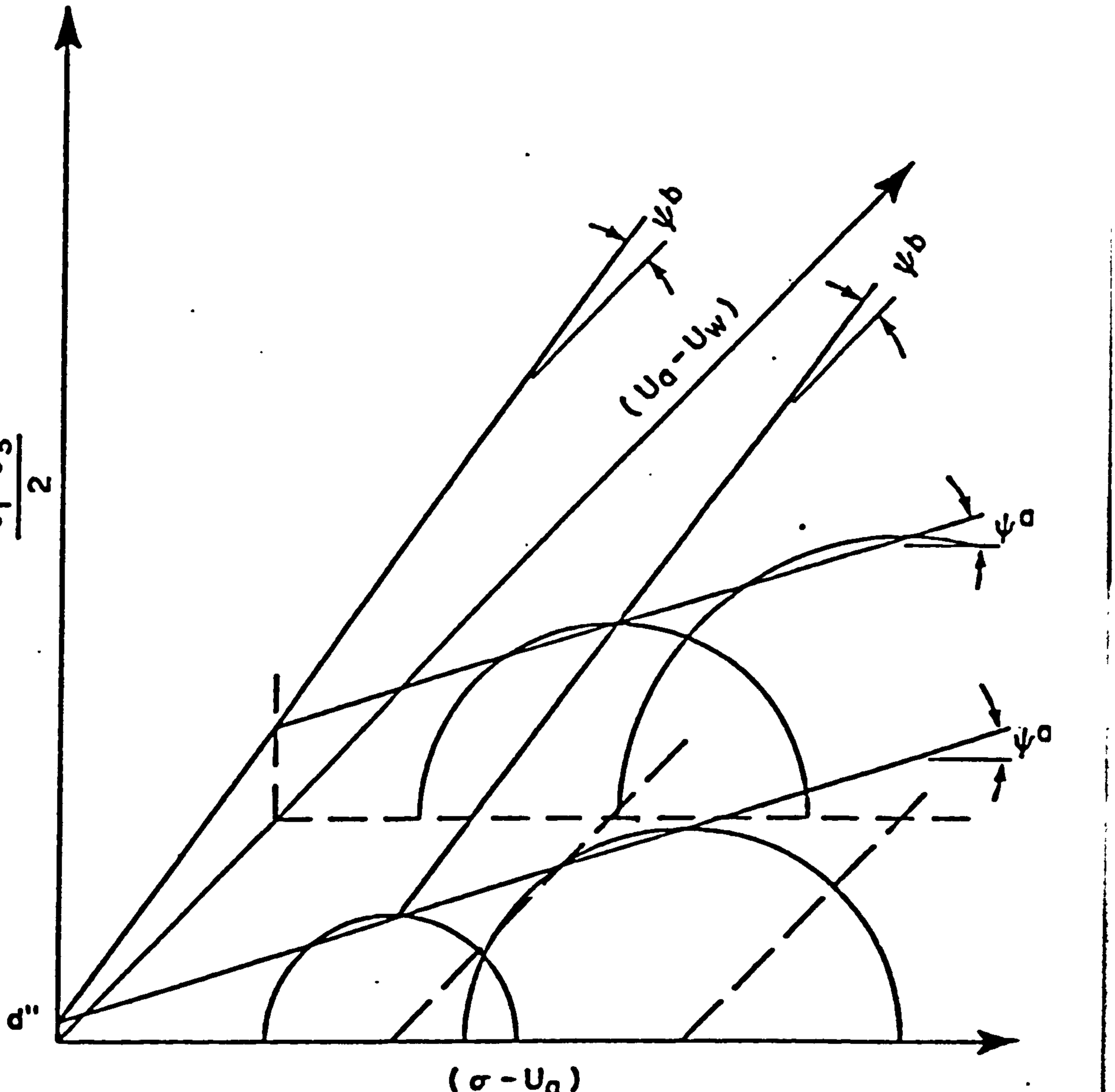

Fig.5.13: Fredlund et al (1978) three-dimensional failure surface using stress variables (σ-Ua) and (Ua-Uw) in stress point form. (after Ho,1981)

Table:5.2 Combinations of stress state variables and stages of shear used (Satija,1978).

Combination	Stress state variables (a) and (b)
A	$(\sigma - Ua)$ and $(Ua - Uw)$
B	$(\sigma - Ua)$ and $(\sigma - Uw)$
C	$(\sigma - Uw)$ and $(Ua - Uw)$

Stage	Plane of which normal stress is considered	Normal stress
Pre-shear	Any	--
At failure	Minor principal plane	$\sigma 3$
At failure	Plane of maximum shear	$\frac{\sigma 1+\sigma 3}{2}$

between shear strength and the chosen variables; then, the experimental data was subjected to linear regression analysis in 54 paths(Table5.3). It was established that the relations between shear strength and the three combinations of stress state variables were all linear. Through algebraic manipulation, inter-relationships amongst the parameters of the linear relations between shear strength and the three combinations of stress state variables were also demonstrated. Not only the data of Satija(1978) but also the data of Donald(1961), Blight(1961), Gulhati(1972) and Kawakami and Abe(1975) satisfied the hypothesis that the shear strength was a function of (6-Ua) and (Ua-Uw), acting independently (see Table 5.4 and 5.5). As a result, a statistically valid shear strength equation for unsaturated soils was proposed as follows:

$$(\sigma_1-\sigma_3)f/2 = a + (\bar{\sigma}_3-U_a)f\cdot\tan\alpha + (U_a-U_w)f\cdot\tan\beta \quad \text{----(5.15)}$$

This equation represents a planar surface in three-dimensional space with ($\bar{\sigma}$ -Ua) and (Ua-Uw) as abscissas and (σ_1-σ_3)f/2 as ordinate(see figure 5.14), similar to the surface proposed by Fredlund et al(1978). Satija's shear strength equation for unsaturated soil is presented in such a way that it is neither in accordance with the Mohr-Coulomb failure hypothesis nor the stress point method. Moreover, there is no smooth transition from Satija's shear strength equation for unsaturated soils to Terzaghi's shear strength equation for saturated soils. When saturation is approached(i.e. Ua=Uw), Satija's equation for saturated soils does not conform to either

Table 5.3: Paths used in the linear regression analyses (Satija,1978).

Combination of stress state variables	Stage/plane	Data from different types of test	Manner of treating stress state variables
A: a=(σ-Ua), b=(Ua-Uw)	I.Pre-shear/ any plane	1. $\overline{CW}$	(i)with stress state variable designated(b) in the 1st column as variable and that designated (a) as a constant.
B: a=(σ-Ua), b=(σ-Uw)	II. At failure/ minor principal plane	2. CD	
C: a=(σ-Uw), b=(Ua-Uw)	III.At failure/ plane of maximum shear	3. $\overline{CW}$ & CD	(ii)with stress state variable designated(a) as variable and that designated (b) as constant.

Table 5.4: Satija's (1978) results

Sample designation & Type of test	Intercept KPa	Arc tan of coeff. assoc. with $(\sigma 3-Ua)_f$	Arc tan of coeff. assoc. with $(Ua-Uw)_f$	Corr. coeff.
	a	α	β	r
A $\overline{CW}$	41	41.5°	32°	1.00
A CD	57	42.5°	26°	1.00
A $\overline{CW}$ & A CD	58	42°	27°	1.00
B $\overline{CW}$	26	43°	25.5°	1.00
B CD	29	44°	21°	0.99
B $\overline{CW}$ & B CD	34	43°	21.5°	1.00

Table 5.5: Results of Multiple Linear Regression Analysis on Published Data

Type of test	No. of tests	a KPa	α	β	Correlation coefficient, r
Donald, 1961: Braehead silt					
Sample prepared by desaturation from a slurry					
$\overline{CW}$	10	16	49.5°	27.5°	1.00
$\overline{CW}$ & CD	26	21	49.5°	21.8°	0.99
Blight, 1961: Compacted Talybont clay					
$\overline{CW}$	23	78	54°	6°	1.00
Blight, 1961: Compacted Mangla Shale					
$\overline{CW}$	10	2	20°	3°	1.00
$\overline{CW}$	9	35	37.5°	36.5°	1.00
$\overline{CW}$	27	36	33°	23°	0.99
Blight, 1961: Compacted Selset clay					
$\overline{CW}$	11	85	32°	14.5°	0.99
Gulhati, 1972: Compacted Dhanauri clay					
$\overline{CW}$	6	23	35°	16.5°	1.00
CD	5	20	36°	16°	0.99
$\overline{CW}$ &	11	30	36°	13.5°	0.99
Kawakami and Abe, 1975: Compacted Sandy Silt					
$\overline{CW}$	5	-14	52.7°	31.5°	1.00

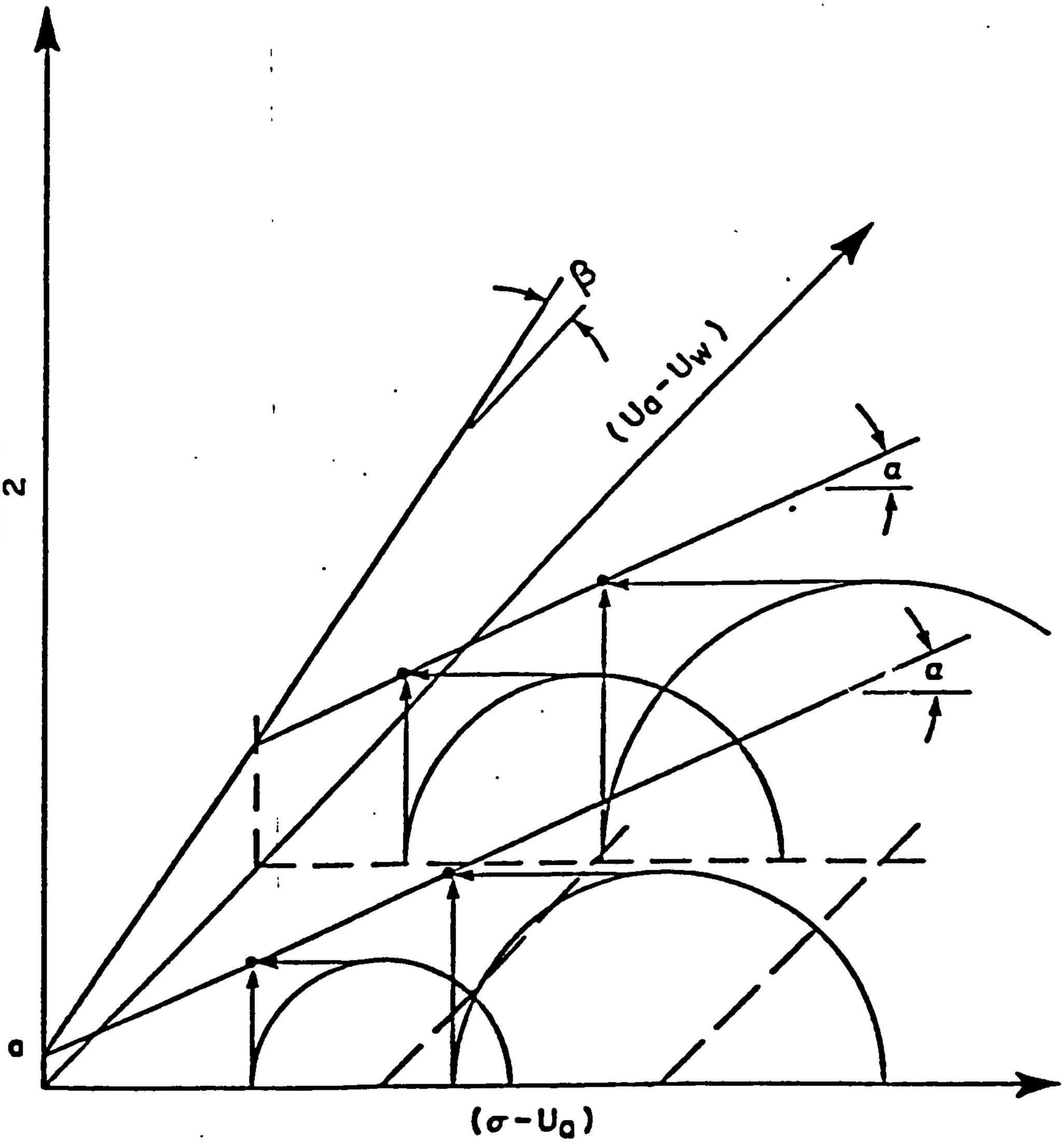

Fig.5.14: Satija's (1978) shear strength equation in three-dimensional plot. (after Ho,1981)

the conventional or stress point equation.

By comparing the equation of Fredlund et al and Satija, it can be demonstrated that Satija's equation predicts a higher value for shear strength(figure 5.15). It should be noted that the over-estimation of shear strength by Satija's equation will result in an over-estimation of the factor of safety in slope stability analyses involving unsaturated soils. Taking this together with the inability of the equation to be reduced to the conventional form when a soil is saturated means that Satija's shear strength equation for unsaturated soils should not be regarded as a satisfactory form of equation and therefore the equation proposed by Fredlund et al(1978) will be used for the interpretation of data in this thesis.

5.4 Conclusion

Among the three possible sets of stress state variables, there are preferences in choosing which set to use in the shear strength equation for unsaturated soils(Ho,1981).

The set, ($\bar{\sigma}$-Ua) and ($\bar{\sigma}$-Uw) can be regarded as the most undesirable of all. The disadvantages are two-fold. Firstly, the effect of (Ua-Uw) cannot be visualized if this combination of stress variables is used. Secondly, when the total normal stress, $\bar{\sigma}$ is changed, both stress variables are affected and consequently, the relative sigificance of each variable must be borne in mind when considering the shear strength. As a result, this combination will not be considered in setting up the shear strength equations for unsaturated soils.

The combination, ($\bar{\sigma}$-Uw) and (Ua-Uw) also has the disadvantage

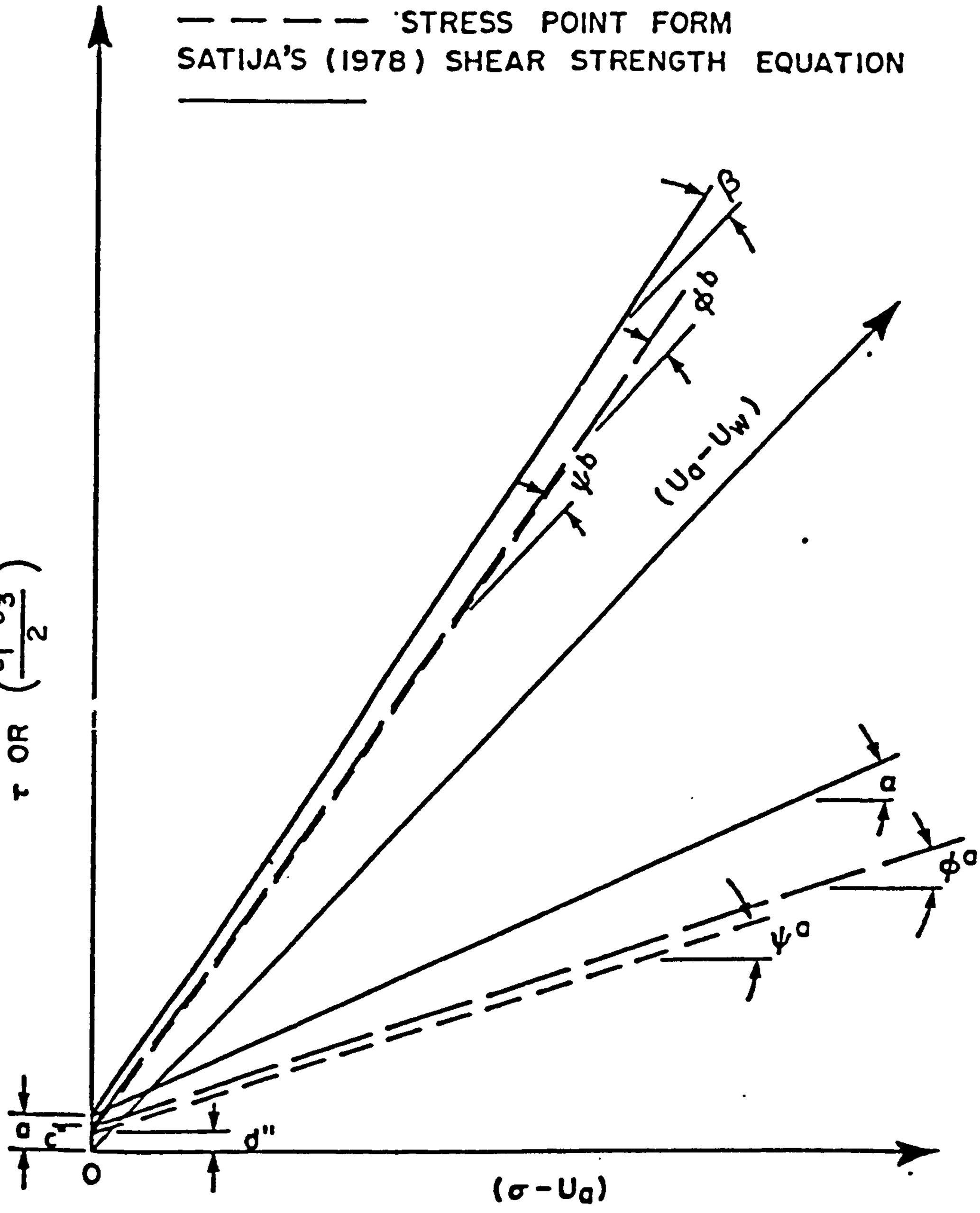

Fig.5.15: Comparison between unsaturated soil shear strength equations proposed by Fredlund et al (1978) and Satija (1978). (after Ho,1981)

that when the pore water pressure, Uw is changed, two stress state variables are affected. However, this combination does have a marked advantage in providing a readily visualized transition from the unsaturated to the saturated case. Similarly, this is the advantage associated with using the (6-Ua) and (Ua-Uw) combination of stress state variables. Moreover, in the (6-Ua) and (Ua-Uw) combination, only one stress variable is affected when the pore water pressure is changed.

It is evident that both the (6-Uw), (Ua-Uw) and (6-Ua),(Ua-Uw) combinations are acceptable in setting up the unsaturated soil shear strength equations. In addition, the individual effect of each stress variable on the shear strength of an unsaturated soil can be easily visualized when these two shear strength equations are evaluated together.

In general, under natural field conditions, the pore air pressure, Ua remains virtually constant. It is the change in the pore water pressure,Uw due to moisture infiltration or evaporation that alters the stress state of an unsaturated soil. As a result, it will be most desirable if the relative shear strength contributions of the total stress,6 and the pore water pressure,Uw can be readily inspected from the established shear strength equation. Therefore, the (6-Ua) and (Ua-Uw) combination of stress state variables is considered to be the best combination used to analyse data obtained from unsaturated soil testings.

CHAPTER 6

TEST EQUIPMENT AND TECHNIQUES

Chapter 6

Test equipment and techniques

6.1 General

Commercially available soil testing equipment is not sufficiently sophisticated to be used for the complete evaluation of unsaturated soil behaviour. The techniques used for testing partially saturated soils differ from those used for testing saturated soils principally because of the need to measure(and differentiate between) the pore air pressure and the pore water pressure. This chapter discusses some of the problems encountered when testing partially saturated soils and describes the equipment used by the author in his tests.

6.2 Testing techniques for partially saturated soils

Since both air and water are fluids some means must be found to separately measure them. Porous discs with various pore sizes are commonly used for this purpose(Bishop and Henkel,1962)

A porous stone(disc) with small pores(i.e. high air entry value) allows the slow passage of water but resists air flow. As long as the difference between the air and water pressure does not exceed the air entry value of the porous disc, there is a continuous column of water from the sample to the pressure transducer below the porous disc and the pressure measured is that of the water phase. Although the fine porous disc does not leak air, dissolved air diffuses through the water in the disc and collects at the base of the disc in the form of free air bubbles. The net result is a gradual increase in the measured

water pressure until it approaches the air pressure. For long term(i.e.duration > 1 day), undrained tests, this is a major problem that has not yet been completely overcome.

The pore water in an unsaturated soil can exist in a highly negative state relative to atmospheric pressure conditions. However, it is impossible to measure directly absolute pressure less than one atmosphere below atmospheric because the water cavitates. Hilf(1956) employed an axis-translation technique whereby the air pressure surrounding the sample was elevated by an amount such that the water pressure became positive relative to atmospheric pressure. The axis-translation technique is acceptable since the equilibrium of the air-water menisci are solely dependent upon the difference between the air and water pressure, regardless of the absolute pressure values.

Olson and Langfelder(1965) experimentally verified the axis-translation technique. They obtained a 1/1.018 ratio between the air and water pressure during translation (see appendix 1).

A porous disc with relatively large pores will readily allow passage of air and thereby form a continuous column of air between the air in the sample and the air measuring system. In an undrained system, the air pressure can be measured using a transducer. The volume of air in the pressure measuring system must be kept to a minimum due to the compressive nature of air. Thin coarse porous discs or glass fibre cloth have proven to be a satisfactory air reservoir at the end of a sample. At higher degrees of saturation, when the air appears to be discontinuous and (Ua-Uw) is small, water tends to enter the air pressure measuring system.

The separation and measurement of the air and water pressures can be achieved only if two conditions are satified:

(i) that the pressure does not drop below -1 atmosphere(or in practice, about -13 psi at sea level in long term tests), as cavitation then occurs in the measuring system and allows water to be drawn from it through the porous disc into the sample;

(ii) that the value of the initial negative pore-water pressure does not exceed the air entry value of the saturated porous element, since air entering the porous element replaces water which is then drawn into the sample.

If the above balance is not achieved, not only are the initial pore pressure readings missed or incorrectly recorded, but subsequent readings at higher cell pressures may be incorrect or subject to serious time lag, due to the wetting up of the sample near the porous element and to the air drawn into the system.

The first condition places a lower limit on the values of pore-water pressure which can be directly measured; beyond this limit values can only be inferred from indirect tests(for example, Croney, Coleman and Bridge,1952; Hilf,1956). The second condition can readily be satisfied within this limit since porous ceramics having an air entry of 20-30 psi and adequate mechanical strength are available.

Except for unjacketed, unconfined samples in which time has been allowed for equilibrium to be established, the air pressure in the pore space is not, in general, atmospheric. A third condition for a balance to be achieved is then that the

difference between air and water pressure in the sample (Ua-Uw) shall not exceed the air entry value of the saturated porous element. In undrained tests this difference does not usually exceed the value of the initial negative pore pressure, except during shear in a very dilatant soil, and this condition is thus readily satisfied.

A final point concerns the rate of testing and diffusion of air. Partially saturated soil is generally less permeable than saturated soil and therefore when testing the former type of soil, very low shear rates must be used. If an undrained test is to last for more than a few hours, air will diffuse from the soil sample, through the rubber membrane and into the water within the triaxial cell. This problem can be overcome by surrounding the sample with mercury. This is explained in detail in the following section.

6.3 Equipment

Table 6.1 summarises the types of equipment used by previous research workers for testing unsaturated soils. The most significant shortcoming has been the inability to measure accurately the volume changes of the air and water phases. For example, it is not sufficient to simply measure water volume change without correcting for the volume of diffused air.

The equipment used in this research is described under the following headings:

(1) Constant pressure system

(2) Design of the cell

(3) Base plate design

TABLE 6.1. SUMMARY OF TEST EQUIPMENT (UNSATURATED SOIL TESTING)

Reference	One-Dimensional	Three-Dimensional	Controlled* or Measured Stresses			Displacements or Volume Changes			Monitored Diffused Air	Remarks
			Total	Water	Air	Total** Volume	Water	Air		
Conventional Consolidometer	√		√	X	X	√	X	X	X	
Conventional Suction Apparatus		√	X	X	√	X	√	X	X	Pressure plate device
Hilf (1956)		√	√	√	X	√	X	X	X	Modified concrete air meter
Bishop and Donald (1961)		√	√	√	√	√	√	X	√	Used for strength testing
M.I.T. (1963)	√	√	√	√	√	√	√	X	√	
Dunn (1964)		√	√	√	√	√	X	X	X	No test results reported
Matyas and Radhakrishna(1968)	√	√	√	√	√	√	√	√	X	Essentially same as Bishop and Donald (1961).
Barden, Madedor and Sides (1969)	√		√	√	√	√	√	X	X	Modified Rowe and Barden consolidometer
Aitchison (1969)	√		√	X	√	√	X	X	X	Modified conventional consolidometer
Escario (1969)	√		√	X	√	√	X	X	X	Capable of high suctions
Pufahl (1970)	√		√	X	√	√	X	X	X	Modified anteus consolidometer
Compton (1970)	√		√	√	√	√	√	X	X	Modified Bishop consolidometer
Neves (1971)		√	√	√	√	√	X	X	X	National laboratory of Civil Engineering, Lisbon, Portugal
Fredlund (1973)	√	√	√	√	√	√	√	X	√	University of Alberta, Canada.

* The stress can be manipulated to various levels and held constant.
** For one-dimensional testing, total volume decreases for suction increase, cannot be measured.

(4) Measurement of total, air and water pressures

(5) Measurement of total volume change

(6) Measurement of water volume change

(7) Measurement of diffused air volume change

(8) Layout of plumbing

A considerable amount of time and effort was spent on the development of the equipment and the testing procedures required to attain consistent and reliable results. A short test programme called 'Null test' was used to determine the reliability of the equipment(see appendix 3).

(1) Constant pressure system

The pressures were maintained constant by means of Norgren compressed air precision controllers(11-818-110). The manufacturers maintain that the accuracy of the regulator is within 0.005 bar(0.07 psi). Repeatability is claimed within 0.00125 bar(0.02 psi) for change in air flow; 0.00315 bar(0.05 psi) when turning supply on and off. Temperature compensation is designed to limit the change in pressure to 0.00315 bar(0.05 psi) for a 5.5 ^{o}C(10 ^{o}F) change in temperature. However, variations may be significantly larger due to variations in atmospheric pressure (The regulator operates as a differential pressure regulator with respect to atmospheric pressure).

The pressure transducers used were made by Bell & Howell Ltd. and measured pressures with an accuracy of $\pm$ 0.02 bar ($\pm$ 0.3 p.s.i.).

Since the same type of regulator was used to control all pressures(i.e. total, water and air), fluctuations in atmospheric pressure did not affect the difference between any two pressures in the system.

(2) Design of the cell

Figure 6.1 shows the modified triaxial cell, as designed, for testing unsaturated soils. The main feature of the cell(for 1 1/2inch diameter samples) was the addition of an inner lucite (or perspex) cylinder to contain mercury (internal diameter=2 5/8inches) seated on a round perspex cushion which in turn was held down onto the pedestal at the cell base by screws. The O-ring on the outside surface of the perspex cushion formed a good seal for the inner lucite cylinder. In order to avoid the metal part of the pedestal coming into contact with mercury, the top face of the cushion and upper part of the pedestal were covered with latex. The zone between the inner lucite cylinder and the soil sample was occupied by mercury which prevented the diffusion of air through the rubber membrane(0.01" thick) to the surrounding water, so that a truly undrained condition could be achieved. It was intended that fluctuations in the level of mercury and the position of the loading cap would be measured by cathetometer,so that the sample volume change could be calculated. However, this method was not used by the author due to the inconsistent measurements achieved when using the cathetometer and its unsuitability for automatic data logging.

Because of the high density of mercury, account must be taken of the difference between the lateral pressures at the top and bottom of the sample in tests in the low effective stress range. This is normally achieved by using the average lateral pressure. The air pressure was led from the cell base to the top cap through a 1/8 inch nylon tube and the low air entry disc was

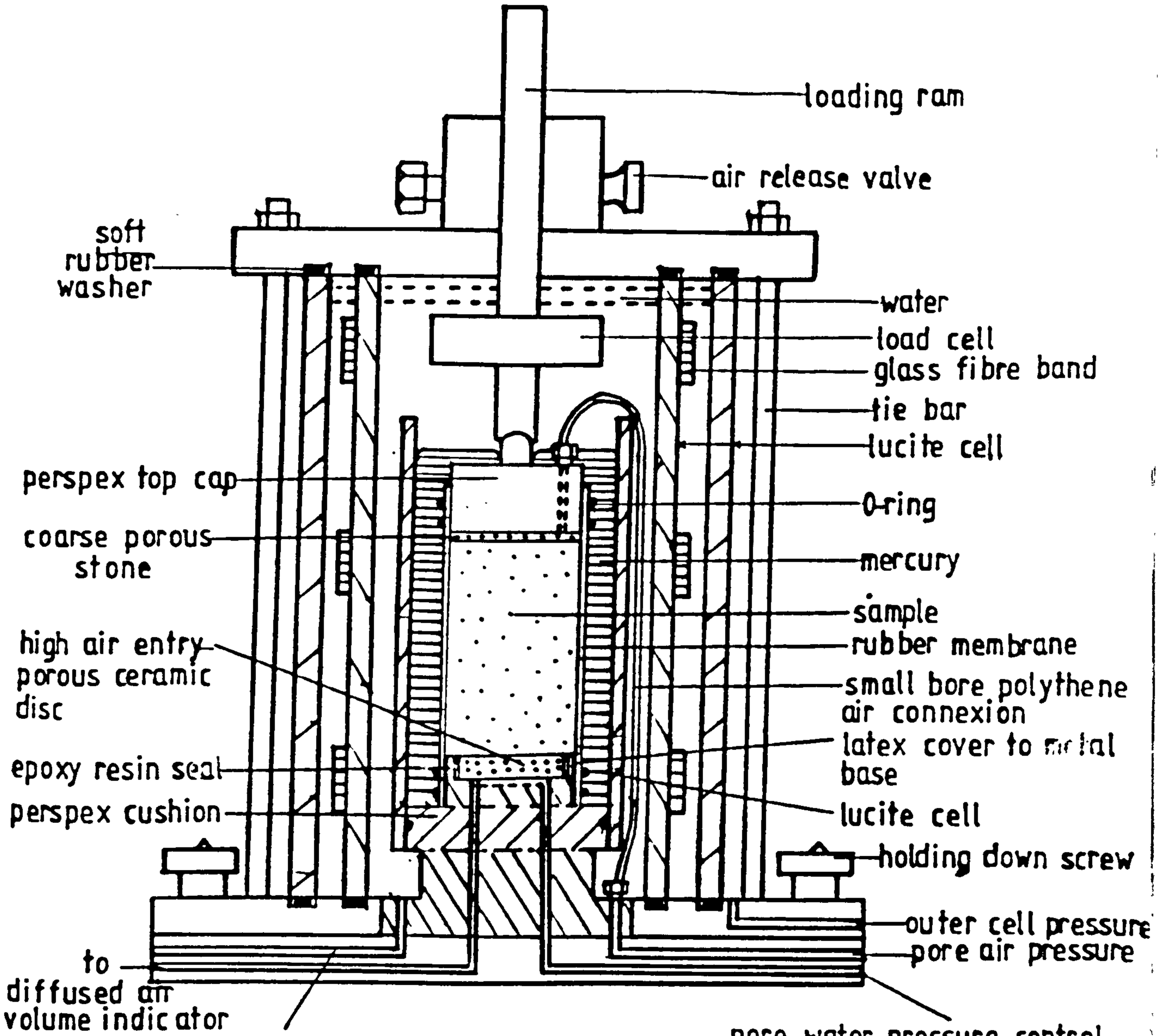

FIG.6.1 MODIFIED TRIAXIAL CELL FOR TESTING UNSATURATED SOILS

a 3/16 inch thick coarse corundum stone placed below the top cap.

Another modification to the triaxial cell was the addition of an outer cell. This modification was based on the principle that, if the pressure on both sides of a container is the same, the container itself will remain unstressed, and therefore should not change in volume. If the soil sample is placed in the internal cell which has a completely separate liquid circuit from that in the outer cell, and the same pressure is maintained in the two circuits, then any volume change measured on the internal circuit should be due only to the volume change of the sample. This behaviour will be independent of all effects in the external circuit(except pressure changes) including any variability due to the sealing torques(see appendix 4).

(3) Base plate design

The base was modified to accommodate the outer and inner perspex cylinders. For the 1 1/2inch diameter sample, a 1 3/16inch diameter high air entry disc of 3/8inch thickness was bonded directly into the top of the pedestal with an epoxy resin'Twin-bond', as this arrangement gave the maximum contact area with the sample. A circular perspex cushion with a soft O-ring on the outside circle was seated on the pedestal, to give support to the inner cell. Another inlet hole was made at the cell base to lead a completely separate pressure system to the outer cell.

(4) Measurement of total, air and water pressures

The total, air and water pressures were measured both by the transducers and pressure gauge. One pressure gauge was used to

measure all three pressures, the advantage being that any error or uncertainty occurring with the gauge readings would cancel out when the pressures were subtracted. The range of the transducers was 0 to 7 bar(0-100 psi) and the digital voltmeter displayed the pressure to within 0.005 bar.

Since de-aired water was used throughout the experiments, some means had to be used to separate the de-aired water and the air pressure supply which was used to control total and water pressures. Two pots, half-filled with mercury were employed for that purpose, since air has a negligible solubility in mercury.

(5) Measurement of total volume change

The total volume change of the soil sample was calculated by measuring the volume of water entering or leaving the cell to compensate for changes in sample volume.

Bishop and Henkel(1957) pointed out that there were three principal methods which could be used to measure the volume changes which occurred in a triaxial test sample. These were based on the measurement of:

(a) the volume of water entering or leaving the cell to compensate for changes in sample volume

(b) the volume of fluid entering or leaving the pore space of the sample

(c) the linear changes in the principal dimensions of the sample

Each of these methods has its associated advantages, disadvantages and practical problems; method(a) is relevant to the author's tests.

To use method(a), it was necessary to calibrate the cell, as this was itself subject to volume change with changes of cell

pressure. The importance of entrapped air and the torque used in tightening the sealing nuts of the cell for the validity of the calibration correction was also emphasized. Hysteresis effects were due mainly to the elasto-plastic deformation of the plastic cylinder of the triaxial cell. To overcome the problem of cell calibration the double cell construction described in section(2) was adopted. The volume change was measured by a volume change indicator(paraffin-water type) and an automatic volume change logging device(after Darley,1972). The calibration of the paraffin-water volume gauge was not pressure dependent, provided that the base of the graduated tube was always connected to the triaxial cell and not to the pressure supply. The automatic volume change logging device was based on the Bishop self-compensating mercury constant-pressure unit and incorporated a linear displacement transducer. Four T-pieces were required to reverse the flow and reset the system(see appendix 5).

(6) Measurement of water volume change

The water leaving and entering the sample was also measured by a paraffin-water volume change indicator and an automatic volume change logging device which were the same type as used in the total volume change measurement. To measure the water volume change, the diffused air volume must be subtracted from the total water volume change. In order to measure the diffused air volume, a side nylon tube was used to by-pass the automatic volume change logging device, so that its operation was unaffected by the flushing procedure.

(7) Measurement of diffused air volume change

The diffused air volume was generally measured once a day by flushing water through the base plate and recovering the air bubbles in a burette inside the diffused air volume indicator(after Fredlund,1973)(see appendix 6).

(8) Layout of plumbing

A board of plumbing was required to support the operation of the triaxial cell(figure 6.2). The total and water pressures were controlled through air-mercury-water pots but the air pressure was regulated directly to the sample. Transducers measured the pore air, pore water and cell pressures and the pressure applied to the diffused air volume indicator.

An automatic data logging system was used to collect the data accumulated during testing. All the equipment was in the same temperature-controlled room and the temperature and relative humidity were continuously recorded on a strip chart recorder(thermohydrograph).

6.4 Preparation of equipment

Before the tests were performed, the equipment was checked to ensure that it was functioning properly.

(a) De-airing of the fine porous disc

The reliability of the pore pressure measurements depend, in the first place, on the properties of the fine-grained porous disc, sealed into the modified cell base. The reliability also depends on the disc being thoroughly de-aired and saturated.

Since the properties of the disc have to be tested when it is saturated, the procedure for reaching saturation will be

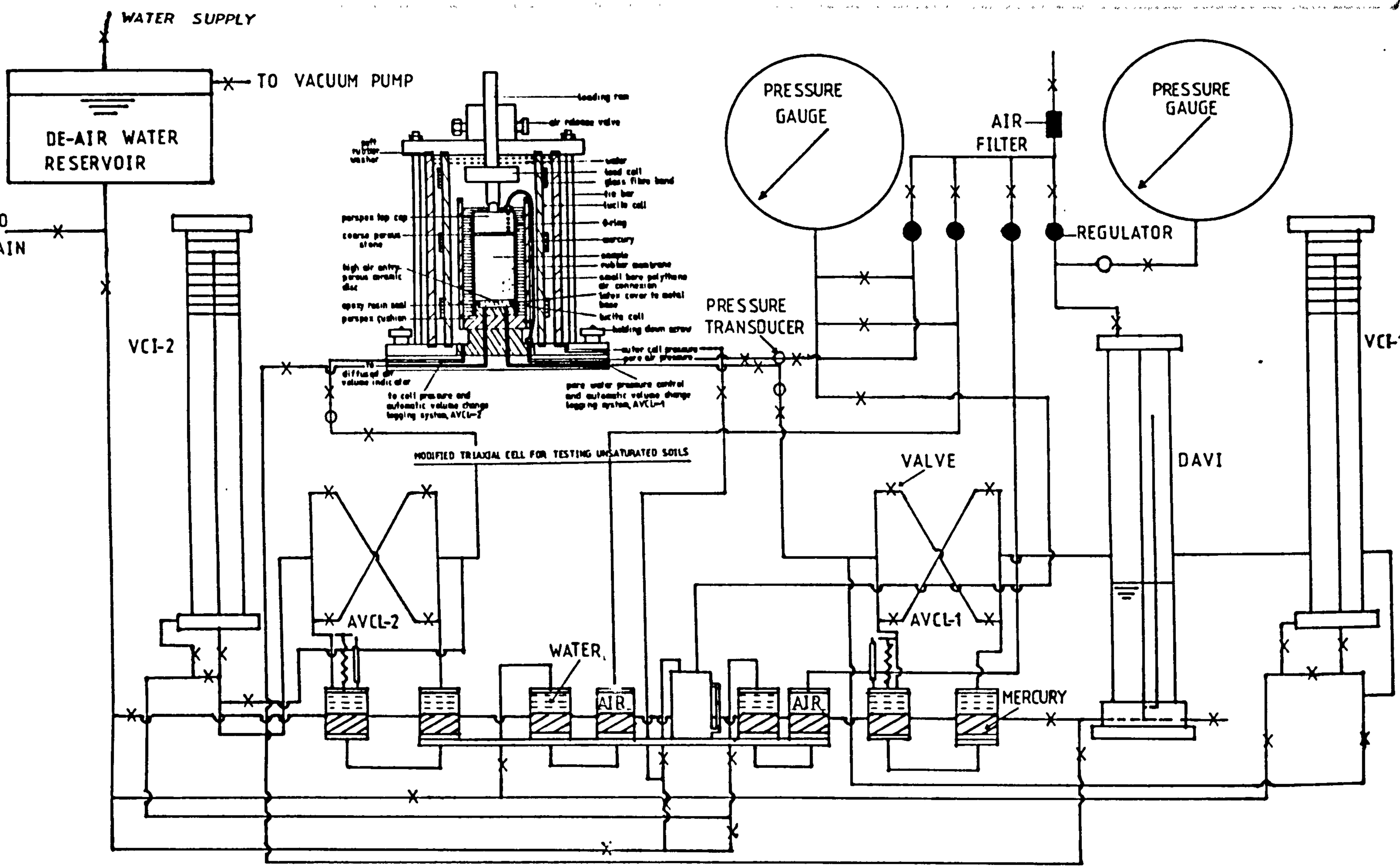

FIG.6.2 DIAGRAMMATIC LAYOUT OF APPARATUS FOR TESTING UNSATURATED SOILS

discussed first.

Several alternative techniques for de-airing are available. The detachable mounting may be de-aired and saturated under a vacuum before fixing(under water) to the pedestal. Alternatively, the cell can be assembled and filled with de-aired water at a pressure of about seven bar(100 psi). If the valves connecting the cell to the measuring system are closed, this pressure will build up in the disc and connecting passage beneath. After several hours have been allowed for the air bubbles to dissolve in this water, the valve is opened to flush this water through. For a new disc, the process may need to be repeated several times in order to ensure full saturation. The latter method was used by the author.

To be at all suitable for its purpose, the porous disc should have a high retention capacity for water. The quantitative evaluation of this property is based on the concept of 'air entry value'. By definition, the air entry value of a porous material, fully saturated by a wetting phase(water), is that pressure at which a non-wetting phase(air), in contact with the material, starts to displace the wetting phase, thus initiating the process of desaturation.

The base plate must not be boiled in water since the differing thermal properties of the materials composing the base plate can result in a fine crack around the circumference of the high air entry disc. The disc performed satisfactorily without using the boiling technique.

(b) Permeability test

The permeability of the porous disc was calculated by

measuring the de-aired water volume seeping through the disc during the saturation process. The results of a subsequent test would reveal the presence of cracks in the porous disc since the permeability of a particular disc measured at a particular time should have a similar value at a later date.

(c) Air entry check

It was not necessary to check on the actual air entry value of the disc, but only to ensure that the disc could withstand air pressures greater than those encountered during a test. For example, a disc with an air entry value of 15 bar was used to measure suctions up to 7 bar.

The highest pressure was applied to the porous disc for at least one day. During this time, the water volume change indicator showed a slow movement of diffused air out of the base plate. The base was periodically flushed and the diffused air measured, and the measured volume was essentially equal to that registered on the water volume change indicator.

A rapid increase in the amount of air collecting below the base means that either there is a leak in the high air entry disc or past the O-ring sealing off the base plate. However, a properly designed O-ring seal rarely allows leakage to occur.

(d) System leaks

Each section of the apparatus associated with the measurement of water pressure and water volume change was highly susceptible to leakage. An attempt was made to eliminate leakage in all parts of the system, since the water measuring section must be very precise. This section of the equipment consisted of the

water volume change indicator or automatic logging system and the base plate.

(i) Water volume change indicator

A Bishop paraffin-water volume change indicator performs well when testing high water content soils over a short period of time. When testing low water content soils over long periods of time(one month or more) minute leaks accumulate to produce unacceptable errors in the analysis of the data. Table 6.2 shows the order of magnitude of leakage associated with the conventional water volume change indicator measured during proving tests.

Table 6.2 : Leakage from Wykeham Farrance water volume change indicator with standard valves

VCI No.	Applied pressure (bar)	Elapsed time (min.)	leakage	Comments
1	5	1260	0.30 c.c. or 2.381×10^{-4} c.c./min.	Including tubing to AVCI (17-8-1982)
2	5	728	0.15 c.c. or 2.060×10^{-4} c.c./min.	just itself (13-8-1982)
2	5	999	0.55 c.c. or 5.506×10^{-4} c.c./min.	including tubing to triaxial cell (17-8-1982)
3	5	5018	0.20 c.c. or 3.986×10^{-5} c.c./min.	itself and short nylon tube from pressure supply (13-8-1982)

where VCI = volume change indicator
AVCL = automatic volume change logging system

The nylon lines on the volume change indicator and the line to the base plate contributed some leakage in response to a pressure gradient. The amount of leakage was generally insignificant and was reduced by using copper tubing rather than nylon tubing.

Most of the leakage was contributed by the valves, but this could overcome by tightening the valve packings.

In addition, air in the volume change indicator undergoes a volume change when the back pressure is changed or when the temperature is changed. The water between the burette and the outer lucite tube can also slowly diffuse through the outer lucite. All of these are registered on the same burette. It should be noted that the pyrex glass burette did not allow the diffusion of water.

To ensure the proper functioning of the water volume change indicator, it was subjected to a back pressure of 5 bar for several days. The observed volume change over a two days period did not exceed 0.1 c.c..

(ii) Base plate

There are three possible sources of leakage from the base plate: through the ceramic disc; past the O-ring seal between the base plate and the bottom of the chamber; through or around the valves connected to the base. Although water seeps through the high air entry disc, it must not allow the passage of free air at pressures below the air entry value. Air may diffuse through the water in the ceramic disc but this should not be considered as leakage; it is important to differentiate between

air diffusion and air leakage.

If free air is passing through the disc as a result of a rupture in the air-water meniscus, the rate of air flow increases by several orders of magnitude. The rupture may be due to fine cracks in the ceramic disc. Diffusivity of air through water in a ceramic disc should always be less than 2×10^{-5} sq.cm/sec. This is the diffusivity for pure water and the value when the water is in the high air entry ceramic disc should be approximately one order of magnitude less(i.e. 2×10^{-6} sq.cm/sec).

Leakage through a valve on the base plate can be observed by placing a high water pressure above the ceramic disc and a somewhat lower back pressure below. A closed valve on the base is connected to the water volume change indicator. Water leakage from the closed valve is registered as a volume of water moving out from the chamber.

(e) The permeability of rubber and lucite

Summary of the rate of water seepage through rubber(after D.G. Fredlund,1973)

Description	rate of flow(c.c./day)	permeability (cm/sec)
Water vapour below the rubber membrane(water at bottom of disc)	0.093	5.84×10^{-11}
Water in contact with the membrane	0.113	7.10×10^{-11}
Water in contact with membrane(vacuum grease seal)	0.094	5.90×10^{-11}

The rubber membrane in all three Fredlund tests was 0.040 cm thick. The values of permeability are approximately one order of magnitude lower than those presented by Poulos(1974) who showed 'thin' latex membrane(0.005 cm) to have a permeability constant of 3.6×10^{-10} cm/sec. It should be noted that latex rubber deteriorates with time when subjected to water or water vapour on one side and air on the other.

The lucite appears to impede the loss of water; however it does not stop it, so lucite cannot be considered as impermeable to water transmission and this must be kept in mind during equipment design.

The international critical tables document three cases of measured transmission of moisture through Nitrocellulose ('Pyroxylin') plastics.

case No	Description	Thickness (cm)	Flow rate (cc/sq.cm/day)	Permeability** (cm/sec)
1a	one surface dried by $CaCl_2$ and the other	0.0762	0.000288	8.29×10^{-11} *
b	exposed to the summer atmosphere			1.38×10^{-10} *
2	Air dried by $CaCl_2$ on one side and saturated air on the other	0.160	0.00062	5.81×10^{-11}
3	same as 2	0.0117	0.0117	3.08×10^{-11}

* Assumed a relative humidity of 100% for 1a and 25% for 1b

** A temperature of 63 ^{o}F was assumed in all cases in order to compute the differential vapour pressure.

In the very long term, both the permeability of the rubber membrane and the permeability of the lucite could have an effect on volume change measurements. However, for the tests carried out in this research, the rubber membrane and the lucite were considered to be impermeable.

Test equipment used for unsaturated soils has been developed from the basic triaxial testing rig through modifications by various researchers. The author considers the follow three modifications as essential for accurate testing:

(i) Double-walled cell

Reduces the variability of the calibration factor and thus increases confidence in the volume change measurements. It also reduces the amount of time spent on calibration and simplifies the problem of studying creep effects in the perspex.

(ii) Diffused air volume indicator

The diffusion of air through saturated high air entry discs can be a major source of error in volume change measurements. The use of a diffused air volume indicator allows corrections to be made to the volume change measurements.

(iii) Mercury layer

The mercury layer prevents diffusion of air through the rubber membrane and is necessary if truly undrained test conditions are required.

A further modification incorporated in the present tests was the use of an automatic volume change logging system. This automatically recorded, at suitable intervals, the total and water volume change of a soil sample during a triaxial test. The

system was checked by using paraffin-water volume change indicators in parallel. The main attraction of the system was its suitability for automatic data logging and subsequent manipulation of the data by computer programmes.

The following photographs illustrate the apparatus used by the author for testing unsaturated soils. Each photograph is accompanied by a brief description of the particular piece of apparatus shown.

Before going on to describe the test program and test procedure, the next chapter, which is essentially self-contained, considers the effect of strain rate on pore water pressure dissipation and equalization during testing. This is an extremely important aspect of testing unsaturated soils and is discussed in some detail, together with the author's choice of strain rate for his own tests.

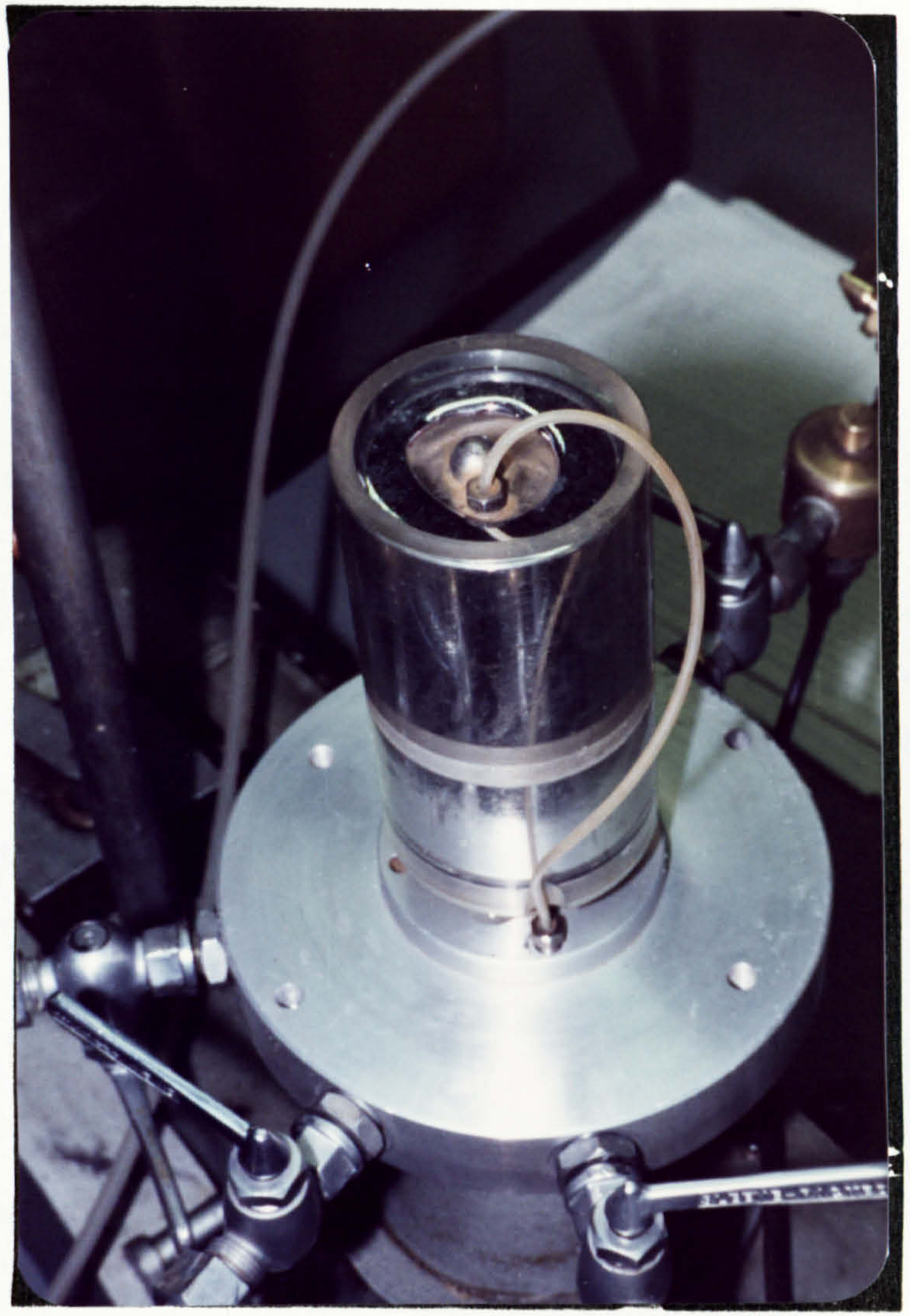

Fig.6.3: Mercury jacket around the soil sample showing the pore air pressure measurement through the top cap.

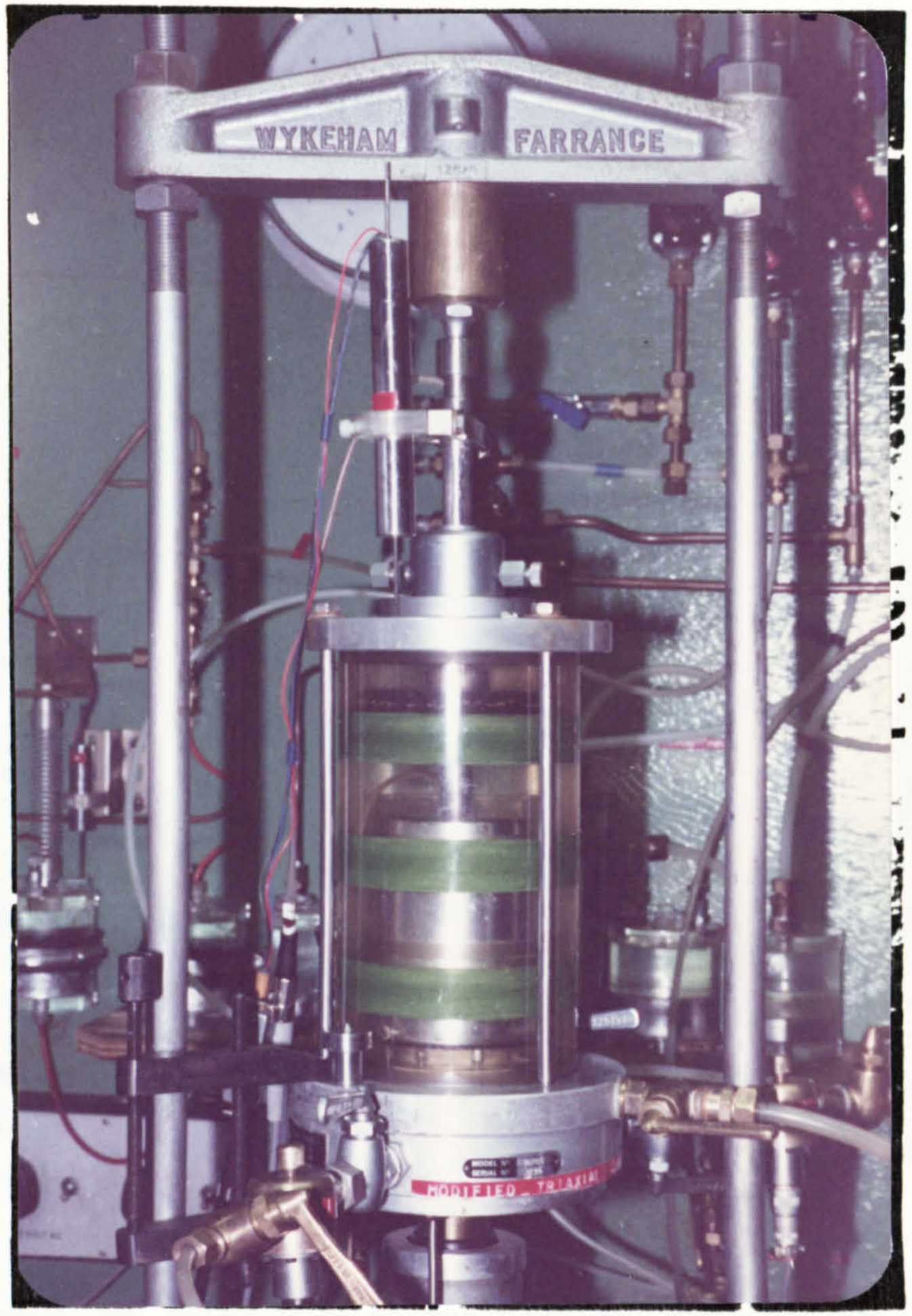

Fig.6.4: Typical setup of the modified triaxial cell for testing unsaturated soils under undrained conditions, with mercury surrounding the soil sample.

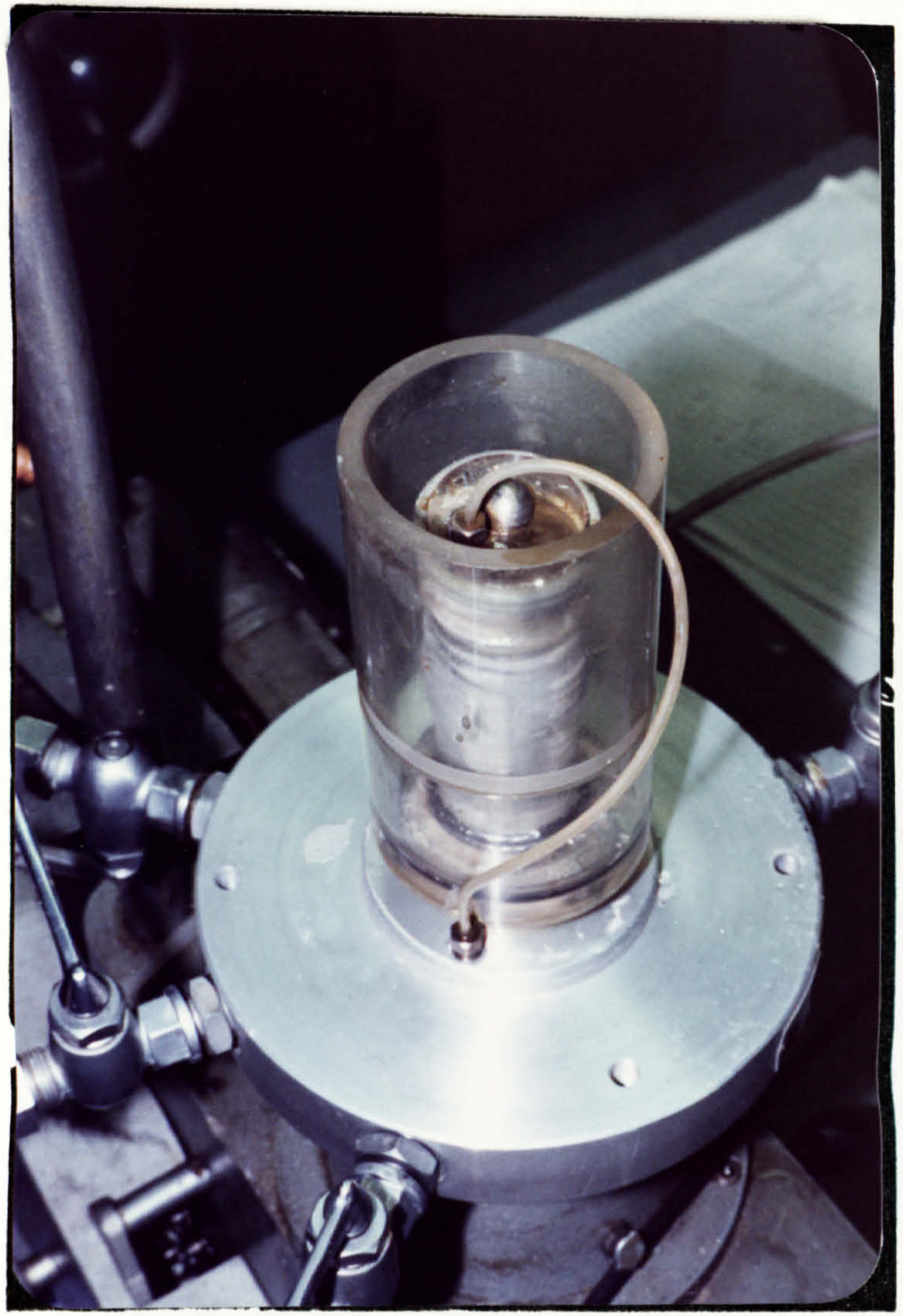

Fig.6.5: Soil sample after drainage of mercury. Note residual mercury at the pedestal and the coating formed by the mercury on the surface of the rubber membrane.

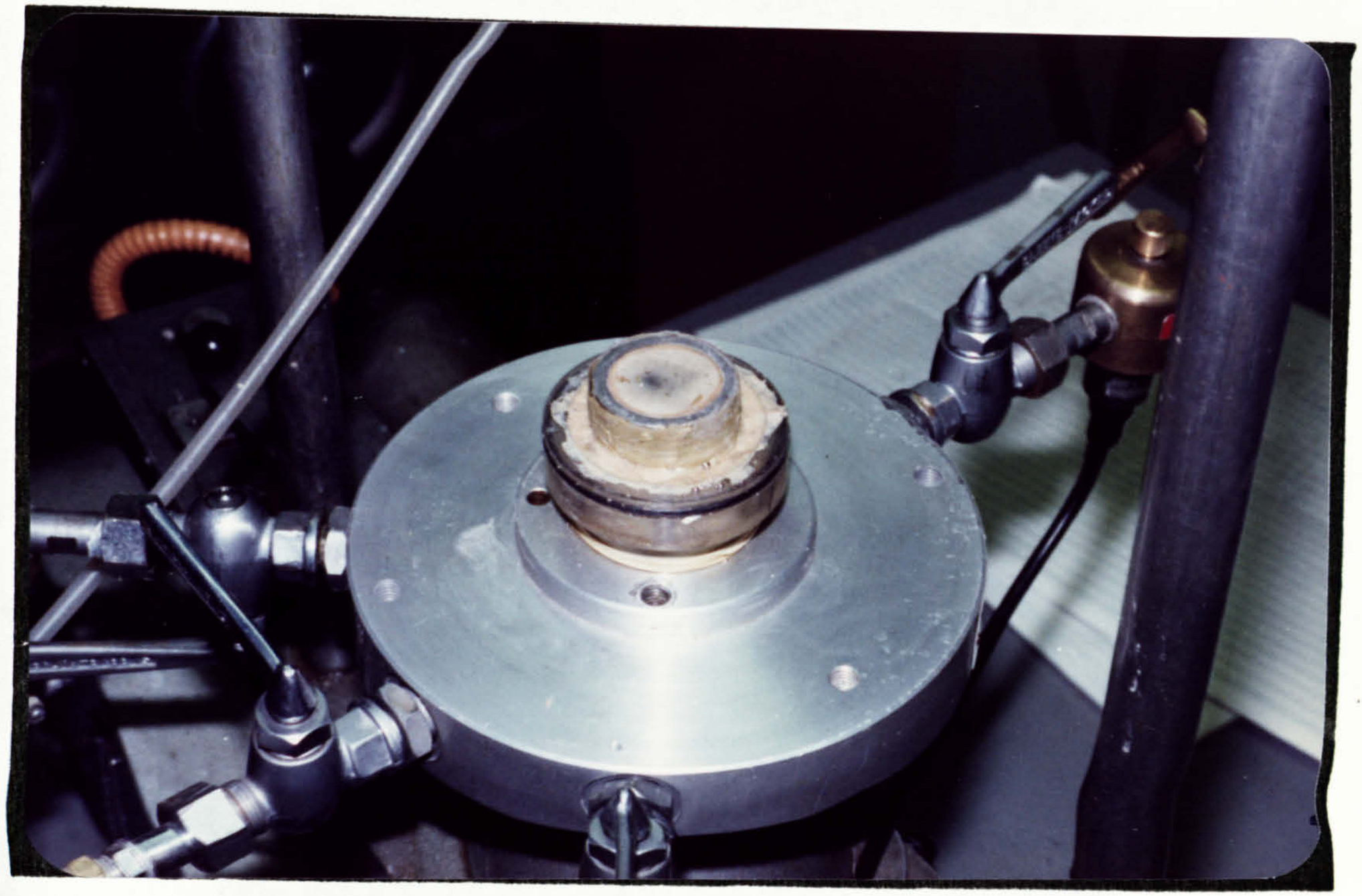

Fig.6.6: The modified pedestal with a high air entry disc on the top. The 'O' ring forms a seal against the inner surface of the inner lucite cell, which contains the mercury. In order to avoid the metal part of the pedestal coming into contact with mercury, the top and upper part of the pedestal were covered with latex.

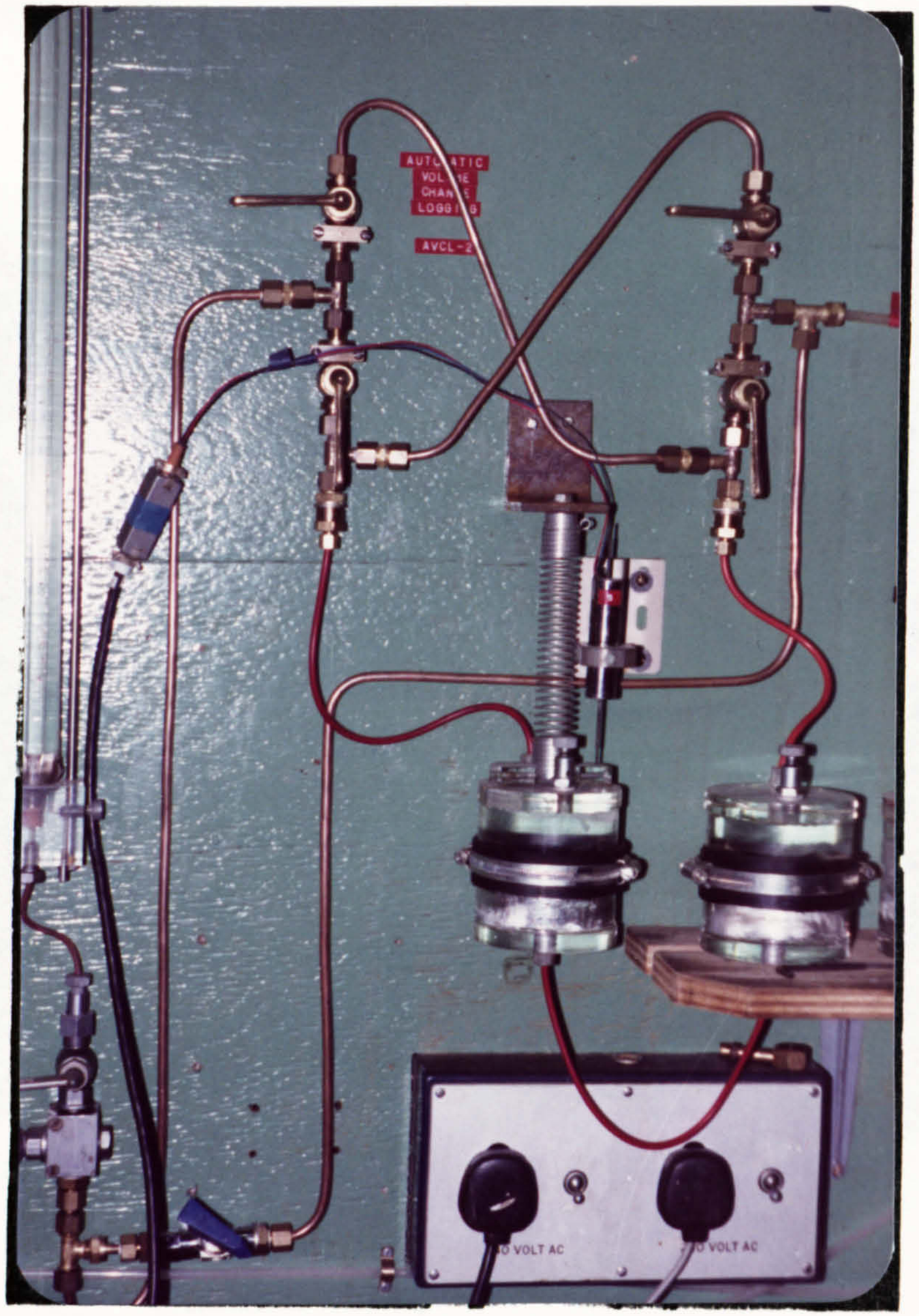

Fig.6.7: Automatic volume change logging system to measure total volume changes (AVCL-2).

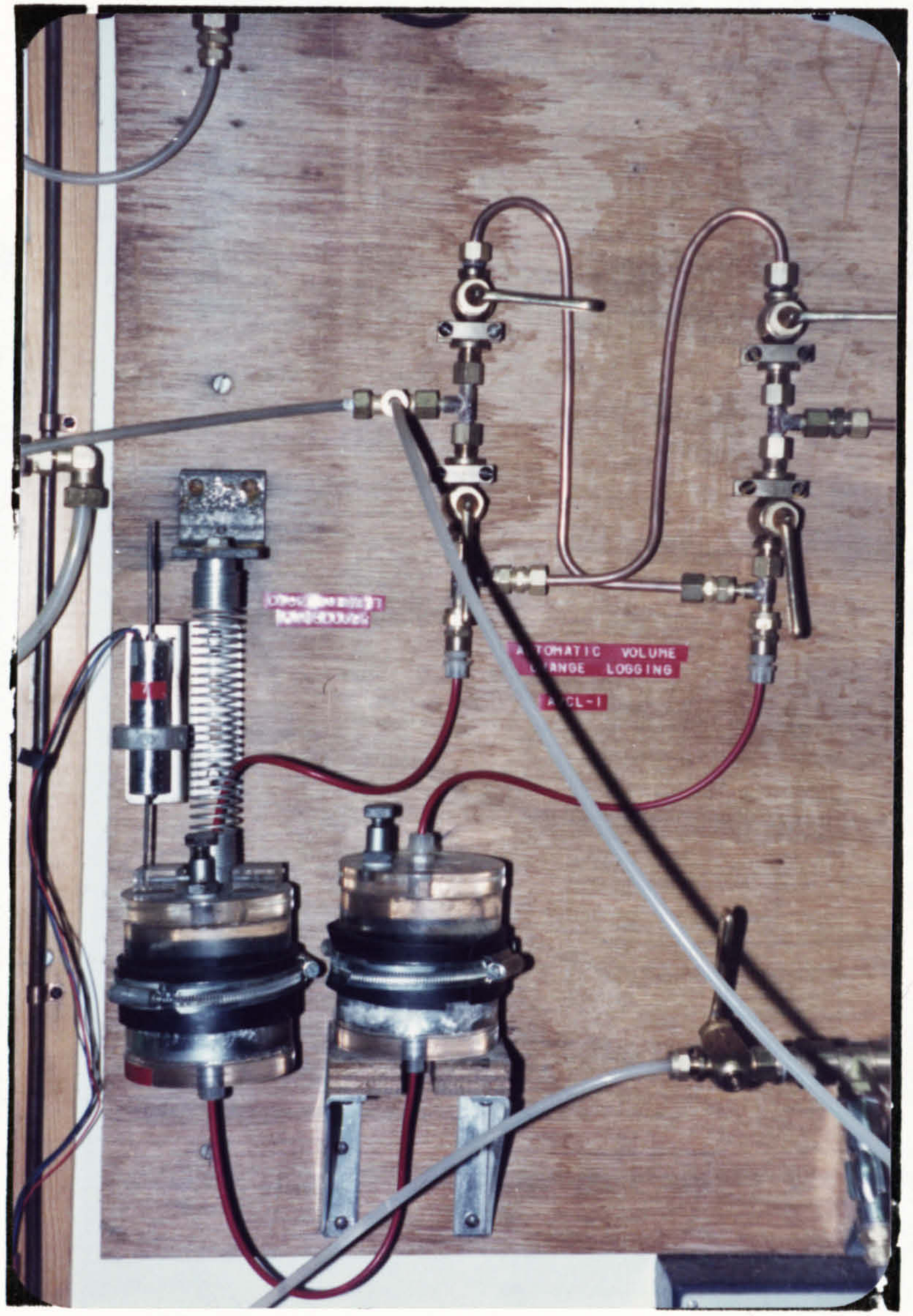

Fig.6.8: Automatic volume change logging system to measure water volume changes (AVCL-1).

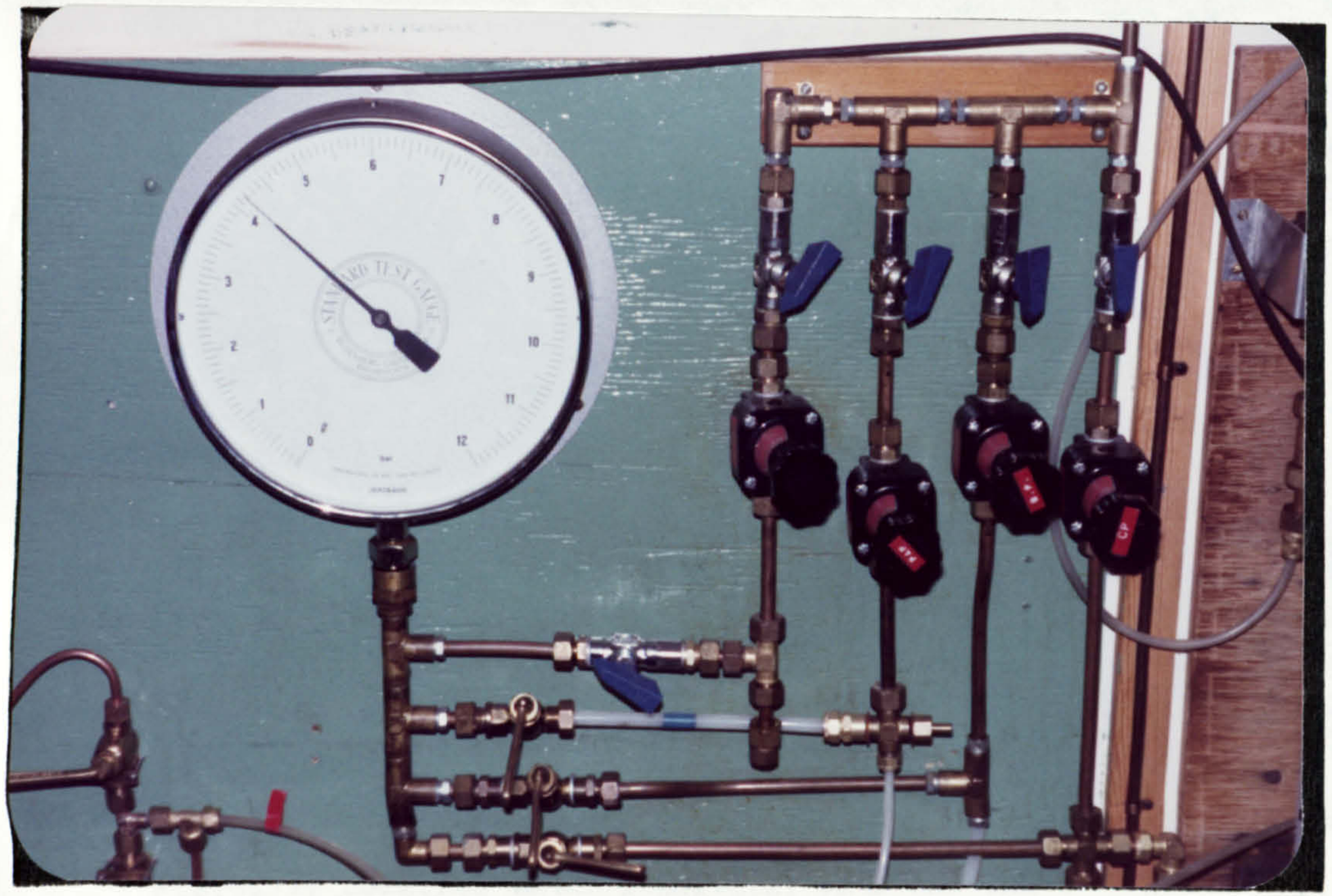

Fig.6.9: One pressure gauge was used to measure total(cell), air and water pressures. This ensured that any error or uncertainty in the gauge readings was cancelled out when the pressures were subtracted.

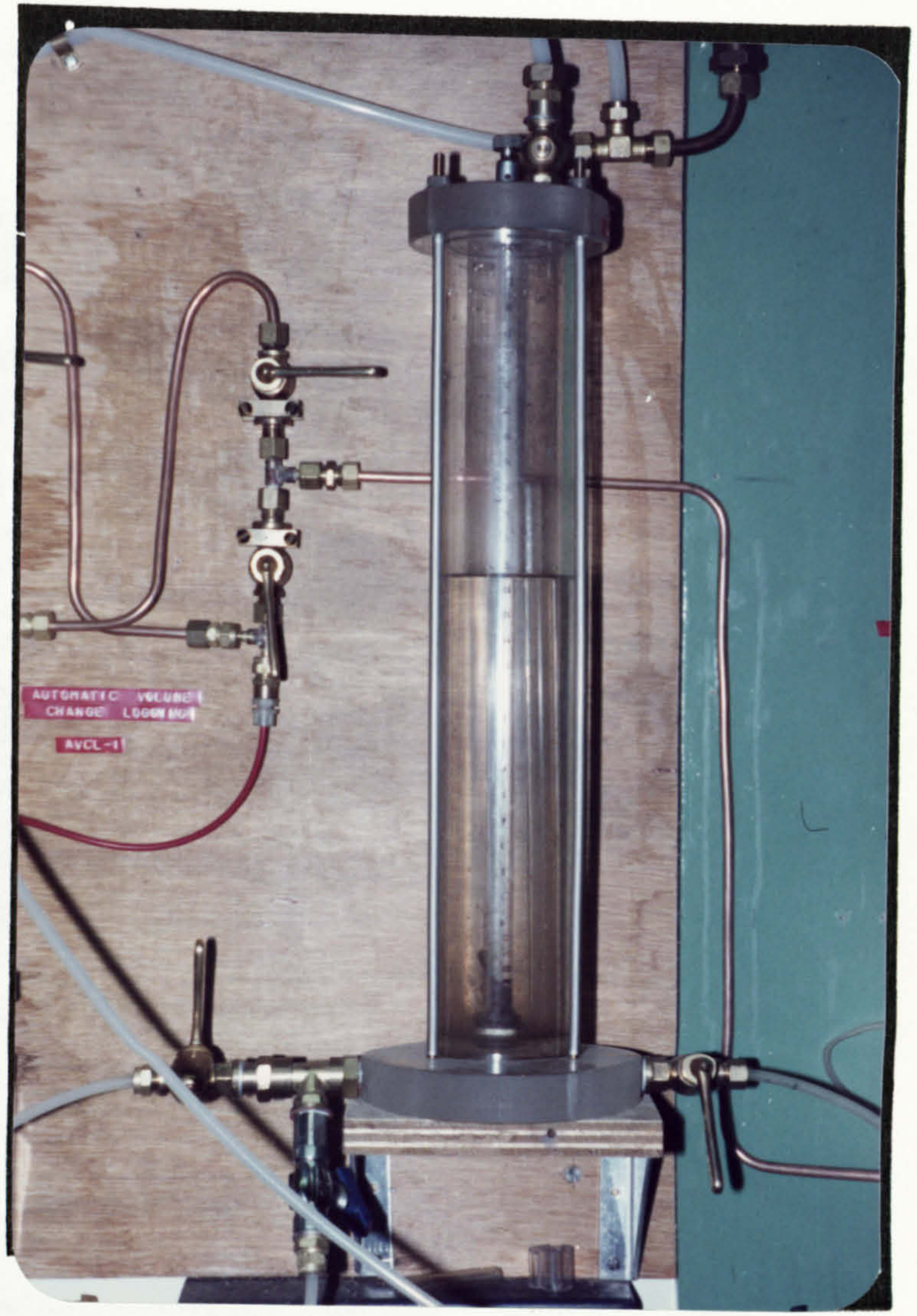

Fig.6.10: The diffused air volume indicator used to flush and measure the diffused air which collected at the bottom of the pedestal during a drained test.

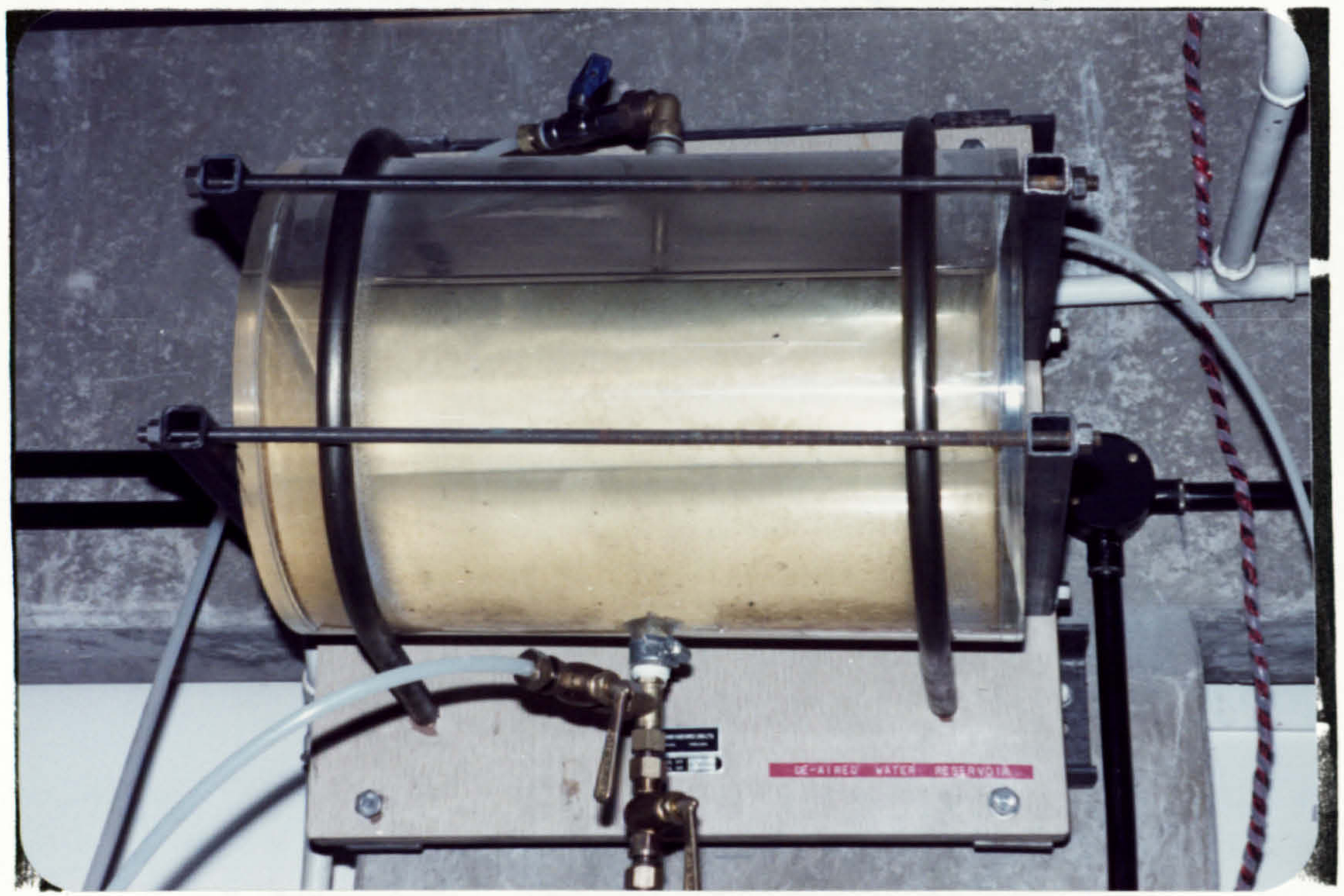

Fig.6.11: De-aired water reservoir, with one end connected to ordinary tap water and the other end to a vacuum pump.

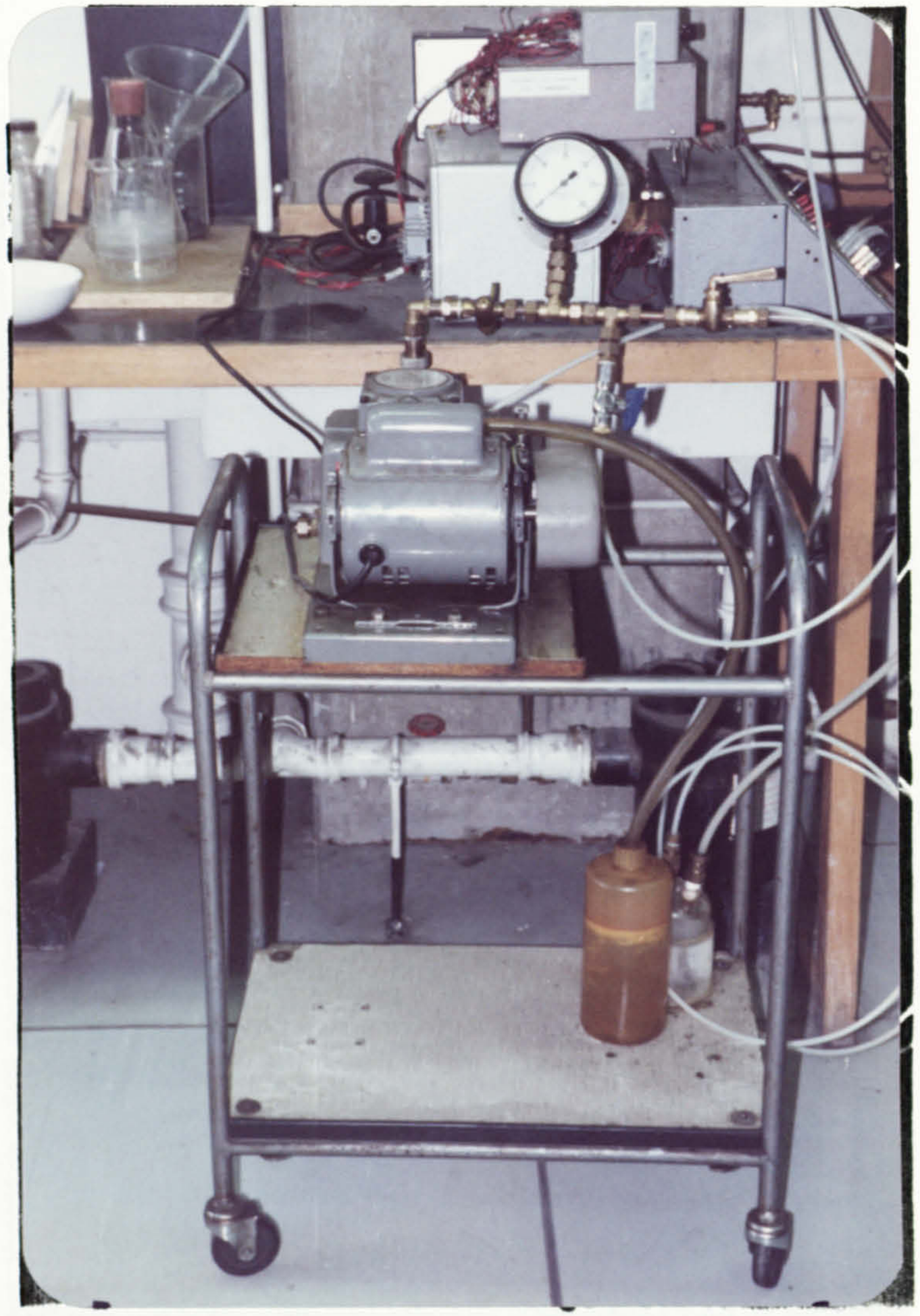

Fig.6.12: The vacuum pump used to de-air the tap water.

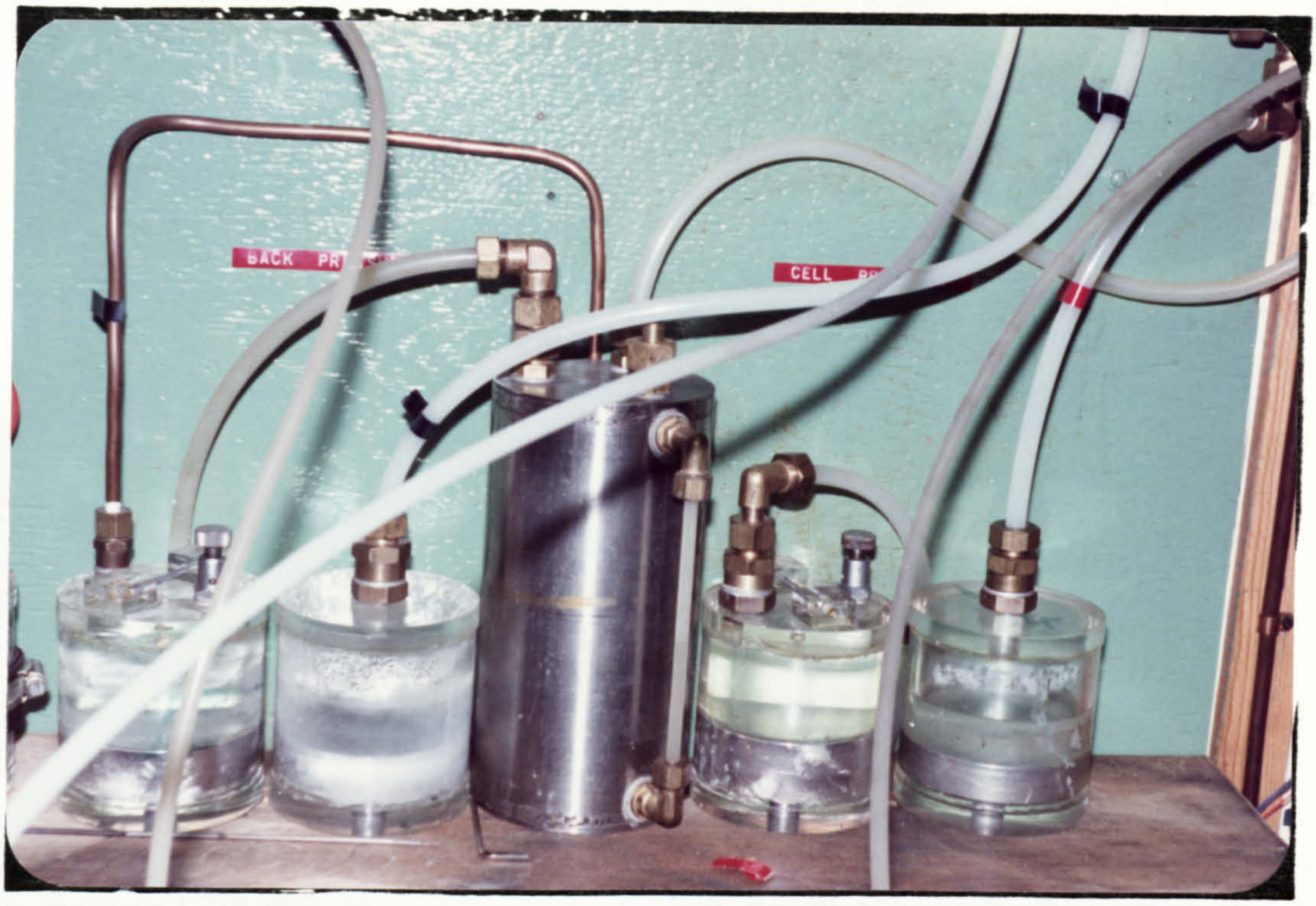

Fig.6.13: Compressed air/water/mercury/de-aired water cylinders; used to separate the de-aired water from the compressed air pressure.

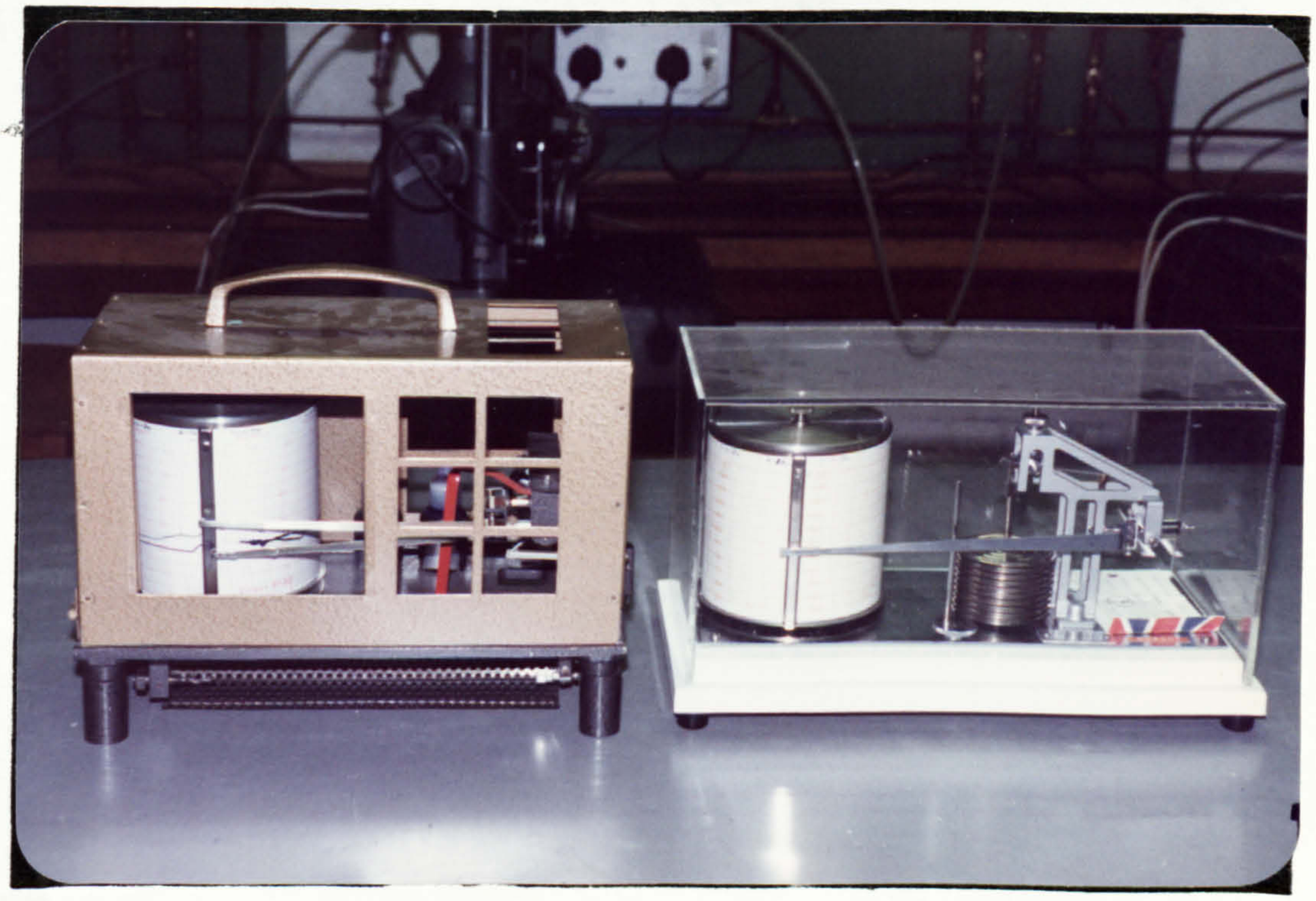

Fig.6.14: The temperature, relative humidity and atmospheric pressure were continuously recorded by the thermohydrograph and barometer recorders.

Fig.6.15: The data logging equipment used to collect all the data from the unsaturated soil tests.

CHAPTER 7

SELECTION OF TEST DURATION

Chapter 7 Selection of test duration

7.1 General

Pore pressure dissipation or equilization is an extremely important property in triaxial testing. This chapter considers some of the factors which affect that property in saturated and unsaturated soil tests, including the influence of high air entry discs, and describes how the required strain rates for triaxial tests on unsaturated Grangemouth clay specimens were determined.

7.2 The effect of strain rate on saturated soil shear tests

For saturated soils, the presence of errors in the experimentally determined shear strength parameters due to an inappropriate choice of strain rate has long been recognised (Gibson and Henkel, 1954) (Bishop and Henkel, 1957 & 1962) (Crawford, 1960) (Blight, 1963).

Two main types of laboratory tests are used to determine deformation and strength characteristics of saturated soils: the fully drained test, in which any excess pore-water pressure is supposed to be dissipated, and the undrained test, in which no volume change of the sample is permitted and no dissipation of excess pore water pressure is permitted. The conditions that obtain in an undrained test are not difficult to satisfy. Theory indicates, however, that the conditions of a fully drained test are strictly satisfied only if the rate of loading is infinitely slow, and in practice, a certain amount of pore water pressure is always left undissipated at the time

failure occurs. Consequently, the stresses applied to the sample are prevented from becoming fully effective and the measured strength differs from the fully drained strength by an amount dependent upon the magnitude of the undissipated pore-water pressure. The principal factors which control the pore-water pressure, and therefore the measured strength, in a drained test are: the permeability and compressibility of the soil, the location of the drainage surfaces around the sample, and the rate of testing. Therefore, prior to carrying out drained tests on a particular soil, a suitable rate of testing must be selected so that the effect of the undissipated pore-water pressure is negligible. A satisfactory rate of testing may be selected from a series of trials, by measuring the strength of samples which are free to drain in the same way but are tested at different rates. Alternatively a theoretical estimate may be made.

Based on the general theory of consolidation developed by Biot (1941), Gibson and Henkel (1954) derived an expression for estimating the test duration necessary to ensure a certain closeness of approximation to fully drained condition.

The expression may be written in the form:

$$t_f = \frac{2h^2}{nC_v\,(1 - \overline{U}_f)} \quad \text{(for drained test)} \quad \ldots\ldots(7.1)$$

where t_f = failure time

$2h$ = height of cylindrical sample

C_v = consolidation coefficient = K/C

K = coefficient of permeability

C = compressibility parameter

$\overline{Uf}$ = average degree of consolidation

n = a numerical factor which depends upon the extent and location of the drainage surfaces which are assumed to be fully efficient

The consolidation coefficient, Cv, depends not only on the permeability and deformation characteristics of the sample but also on the type of test carried out. If radial flow is permitted, no standard method is available for the determination of Cv but expressions have been derived, and numerical results plotted, by Silveira (1953), and Gibson and Lumb (1953) relating the average degree of consolidation $\overline{Uf}$ to the time factor, $T = Cvt / a^2$ for radial flow only, and for radial plus end drainage, where a = radius of the sample. These curves may be used to determine Cv, the consolidation coefficient.

Generally, strain rates are chosen in such a way as to avoid any non-uniformity in pore pressure distribution within a sample. In undrained tests, axial strain rates are selected to ensure at least 95 percent equalization of the induced pore pressure. In drained tests, 95 percent dissipation of the induced pore pressure produces a negligible error in the measured strength (Bishop and Henkel, 1957).

Bishop and Henkel (1957) developed standard procedures for determining strain rates for triaxial testing on saturated soils. The requisite time to failure for a drained test may be

written as $t_f = \frac{h^2}{nCv0.05} = \frac{20h^2}{nCv}$ ..... (7.2)

The consolidation stage of the test, may be used to find the coefficient of consolidation Cv. To calculate Cv, the initial straight line portion of the plot of volume change against $\sqrt{t}$ is produced to cut the line representing 100% consolidation. The time intercept of this point (t_{100}) may be obtained for various drainage conditions. Using these values for t_{100}, Cv may be readily calculated.

For undrained shear tests, the rate of testing has a marked influence on the pore pressures observed during the test. This arises from three causes:

(a) time lag in the pore pressure measuring device.

(b) progressive equalization of non-uniformity in pore pressure resulting from end restraint or from a natural tendency to zone failure.

(c) a modification in the behaviour of the soil structure as the rate of shear is reduced.

In choosing a rate of testing it is necessary to determine the relative influence of these three factors on the observed values of pore pressure, so that the results obtained will lead to a true measure of the physical properties of the soil. Factor (a) is negligible provided the pore pressure measuring apparatus is well designed. For details refer to 'The measurement of soil properties in the triaxial test' by

Bishop and Henkel(1962).

Blight (1963) investigated the relationship between the equalization of pore pressure and the test duration for drained and undrained triaxial compression tests. He stated that the principal source of inaccuracy in the undrained triaxial test arose from differences in pore pressure between the central failure zone and the ends of the specimen. In the drained test, one of the main sources of error in measuring shear strength parameters in terms of effective stress, is the estimation of the minor principal effective stress, since it is assumed that it is equal to the difference between the triaxial cell pressure and the controlled drainage pressure. The simplest way to avoid errors due to pore pressure differences is to use a rate of strain which will allow the pore pressure to equalize by internal redistribution of moisture. Experimental and theoretical work by Blight (1961) indicated that, for most soils the pore pressure set up at the ends of a specimen exceeded that produced in the failure zone. It was only in tests on sedimented normally consolidated clays and sensitive clays that the reverse could apply. Also, the pore pressures which developed along the central axis of the specimen were greater than those at the perimeter (Blight, 1963). Therefore, undrained tests with pore pressure measurement should be conducted at a slow enough rate to allow the pore pressures to equalise throughout the specimen. If this is not done, the pore pressure measured at the base of the specimen may not be equal to the pore pressure in the zone of failure (Bishop and Henkel, 1962 ; Barden, 1965, Blight, 1963). Blight (1965)

concluded that the times proposed by Gibson and Henkel (1954) for pore pressure equalization in drained tests were considerably longer than those actually required to achieve a given degree of drainage. The equations used to calculate the test duration, t_f corresponding to a degree of drainage or pore equalization of 95 percent were as follows:

For tests without drains

$$t_f = 1.6 \frac{h^2}{C_v} \quad \ldots\ldots (7.3)$$

For tests with all-round drains

$$t_f = 0.07 \frac{h^2}{C_v} \quad \ldots\ldots (7.4)$$

The meaning of the term 'test duration' depend on the object of the test. If the object is only to measure the shear strength parameters of a soil, the test duration of the test may be taken as the time to failure. If complete information on the stress path is required, the duration will be the period between the start of the test and the first significant stress measurement.

Bishop and Gibson (1963) investigated the influence of boundary drainage on strength and consolidation characteristics of soils measured in the triaxial apparatus. They suggested that, in a drained test and after a certain time interval, the coefficient of consolidation and the degree of dissipation of pore pressure depended upon the relative permeabilities and dimensions of the specimen and of the drainage elements in

contact with it. Therefore, tests which use filter paper strips are not generally recommended as a way of determining the actual coefficient of consolidation. However, the apparent value of consolidation coefficient obtained provides an accurate and relevant basis for determining the duration of a subsequent drained shearing stage of the triaxial compression test. The use of even rather inefficient filter-paper drains greatly reduces the duration of testing.

Bishop and Gibson also suggested that the requisite time to failure, t_f, for a given degree of dissipation at failure could be expressed in a convenient form as follows:

$$t_f = \frac{h^2}{nC_v(1 - \overline{U_f})} \quad \text{(drained test)} \quad \ldots\ldots (7.5)$$

where $n = \frac{0.75}{(1 + 3/\lambda)}$ (if drainage is from one end only) .....(7.6)

or $n = \frac{3}{(1 + 3/\lambda)}$ (if drainage is from both ends) .....(7.7)

$$\lambda = \frac{KD \times HS}{KS \times HD} \quad \ldots\ldots (7.8)$$

where KD = permeability of the drainage element to water

KS = KW, the coefficient of permeability of the soil sample with respect to the water phase

HS = length of drainage path

HD = thickness of the drainage element

λ = impedance factor

h = half of the actual length of the specimen

$\overline{U_f}$ = average degree of dissipation of the induced pore-water pressure at failure

When the drains are completely effective, $\lambda = \infty$, n = 0.75 or 3, and t_f is identical to that given earlier by Gibson and Henkel for 95% dissipation (equation 7.2).

7.3 The effect of strain rate on unsaturated soil shear tests

To date, little has been published regarding the choice of strain rates for unsaturated soil testing. Before the 1960's, conventional shear tests were conducted on unsaturated soils in the same way as saturated soils. No provision was made with respect to the choice of strain rate (Bishop and Henkel, 1957). In the early 1960's, with the increasing amount of publications on unsaturated soils research, understanding of the nature of unsaturated soils was broadened. A process of tailoring conventional shear testing apparatus to the nature of unsaturated soils was in progress.

The first and most important modification was designed to prevent water from being introduced into the sample as a result of air entry into the porous stones. This resulted in a high air-entry ceramic disc being used as an intermediary between the sample and the pore-water pressure monitoring system. With this modification, unsaturated soil samples could be tested in the conventional way (Bishop et al, 1960) (Lumb, 1966), (Ruddock, 1966). Several empirical procedures for determining strain rates to be used in the modified shear test were proposed.

In the discussion session of the 1960 ASCE research conference on shear strength of cohesive soils, Bishop et al suggested that the standard procedures for selecting strain

rates for saturated soil shear tests could be used for the modified unsaturated soil tests with some adjustments. It was recommended that the coefficient of consolidation (Cv) should be determined from a dissipation test using a fine ceramic disc and the strain rate so determined should be halved for samples with low degrees of saturation. Based on the assumption that failure to achieve full equalization of pore-water pressure in the sample in a modified undrained test on unsaturated soil would cause an increase in the measured cohesion without changing the angle of shearing resistance, Ruddock (1966) produced an empirical method for determining the strain rate for testing unsaturated soils under undrained conditions. From modified undrained tests on residual soils, it was reported that strain rates which resulted in full equalization of pore-water pressure during shearing also produced an insignificant value of measured cohesion. It was proposed therefore that a strain rate which produced a failure envelope without a cohesion intercept should be selected for testing unsaturated soils. Through a series of modified drained tests on unsaturated residual soils, Lumb (1966) reported that there was justification for choosing a strain rate for unsaturated soil shear tests using related theories for fully saturated soils (Bishop and Henkel, 1957). Experimentally determined shear strength parameters for a residual soil tested at various strain rates were presented to show that when the strain rate was equal to or smaller than that indicated by the theory for saturated soils, the measured shear strength parameters would be

relatively unaffected (Lumb, 1966 and 1968) (Table 7.1).

Table 7.1: Shear strength parameters for different failure times obtained from two or three stage tests on four undisturbed decomposed granite specimens* (Lumb,1966)

Theoretical pore pressure dissipation(%)	45	86	97	99
Failure time(min.) (based on the above degree of dissipation)	6.5	25	125	340
Drained cohesion (lb./sq.ft.)	1720	800	330	460
Drained angle of shearing resistance(degrees)	33.6	34.7	37.2	36.2

* The mean voids ratio was 0.53 and the mean degree of saturation was 64%. The graph of volume change against square root of time during the consolidation stages gave a theoretical time for 95% dissipation of pore pressure of 70 minutes, for 3 inch long specimens drained from both ends. Apart from the first two specimens, there was no great difference between the strength results, giving confirmation that a strain-rate corresponding to about 95% dissipation of pore pressure was normally sufficiently slow.

While the modified conventional tests were favoured by some in the 1960's, new techniques for testing unsaturated soils were gaining popularity. Shear tests with independent measurement and/or control of pore-water and pore-air pressures were accepted for testing unsaturated soils (Bishop et al 1960) (Bishop and Donald, 1961) (Donald, 1961) (M.I.T. 1963) (Gulhati, 1972) (Kawakami et al,1975) (Satija, 1978) (Escario, 1980). To some, these shear tests were regarded as modern tests for unsaturated soils (Satija, 1978).

It was realized that strain rates for the modern tests would have to be very slow in order to ensure equalization or dissipation of the induced pore-water and pore-air pressures (Donald, 1961) (Satija, 1978). However, no theoretical basis has so far been presented to determine appropriate strain rates when considering pore-air pressure dissipation. Using the effect of strain rate on deviator stress as a criterion, Donald (1961) suggested an empirical method to obtain an approximate strain rate for tests on unsaturated soils. Donald suggested that the coefficient of consolidation (Cv) be determined from tests on samples of approximately 50% saturation, by measuring the volume of water drained from the sample when it is subjected to an increase in suction. The consolidation curve obtained is compared with theoretical consolidation curves of saturated soil at 35, 50, 65 and 80 percent consolidation and therefore different Cv values are determined. Various times to failure can then be calculated and hence strain rates determined. Triaxial tests conducted using the strain rates resulted in a plot of maximum deviator stress against strain rate. The maximum deviator stress remained constant as the strain rate increased up to a certain value, after which the maximum deviator stress began to decrease. It was suggested that the strain rate at which this decrease began should be taken as appropriate for testing. In 1978, another empirical method was proposed by Satija. From the results of a series of constant water content and consolidated drained tests on compacted soil samples, it was concluded that the deviator stress was a relatively insensitive parameter to assess the influence of

strain rate (Fig. 7.1) . Instead, it was suggested by Satija that the changes in (Ua - Uw) for constant water content tests (Fig. 7.2 & 7.3) and the changes in water content for the consolidated drained tests (Fig. 7.4) would be more illustrative for this purpose. Consequently, marked changes in the above indicators with respect to changes in strain rates were used as the criteria for selecting appropriate strain rates for modern tests. It was concluded that a rate of strain of 0.04% per minute would be adequate for constant water content tests whereas a strain rate of 1/5 this value (i.e. 0.008% per minute) would be necessary for consolidated drained tests (Satija, 1978) (Satija and Gulhati, 1979). It was also recognized that the appropriate rate of strain would be different for samples at different degrees of saturation. For an experimental determination of the appropriate strain rate for any soil, it was recommended that samples at the relevant degree of saturation should be used.

Ho (1981) recommended that the unsaturated soil consolidation theory (Hasan and Fredlund, 1977) (Fredlund and Hasan, 1979) should be used in solving the strain rate problem for unsaturated soil testing. This theory proposed that the consolidation equation for the water phase in an unsaturated soil could be written as:

$$\frac{\partial Uw}{\partial t} = -Cw\left(\frac{\partial Ua}{\partial t}\right) + Cv\left(\frac{\partial^2 Uw}{\partial y^2}\right) \qquad \text{.....(7.9)}$$

where Cw = the interactive constant associated with the water phase equation

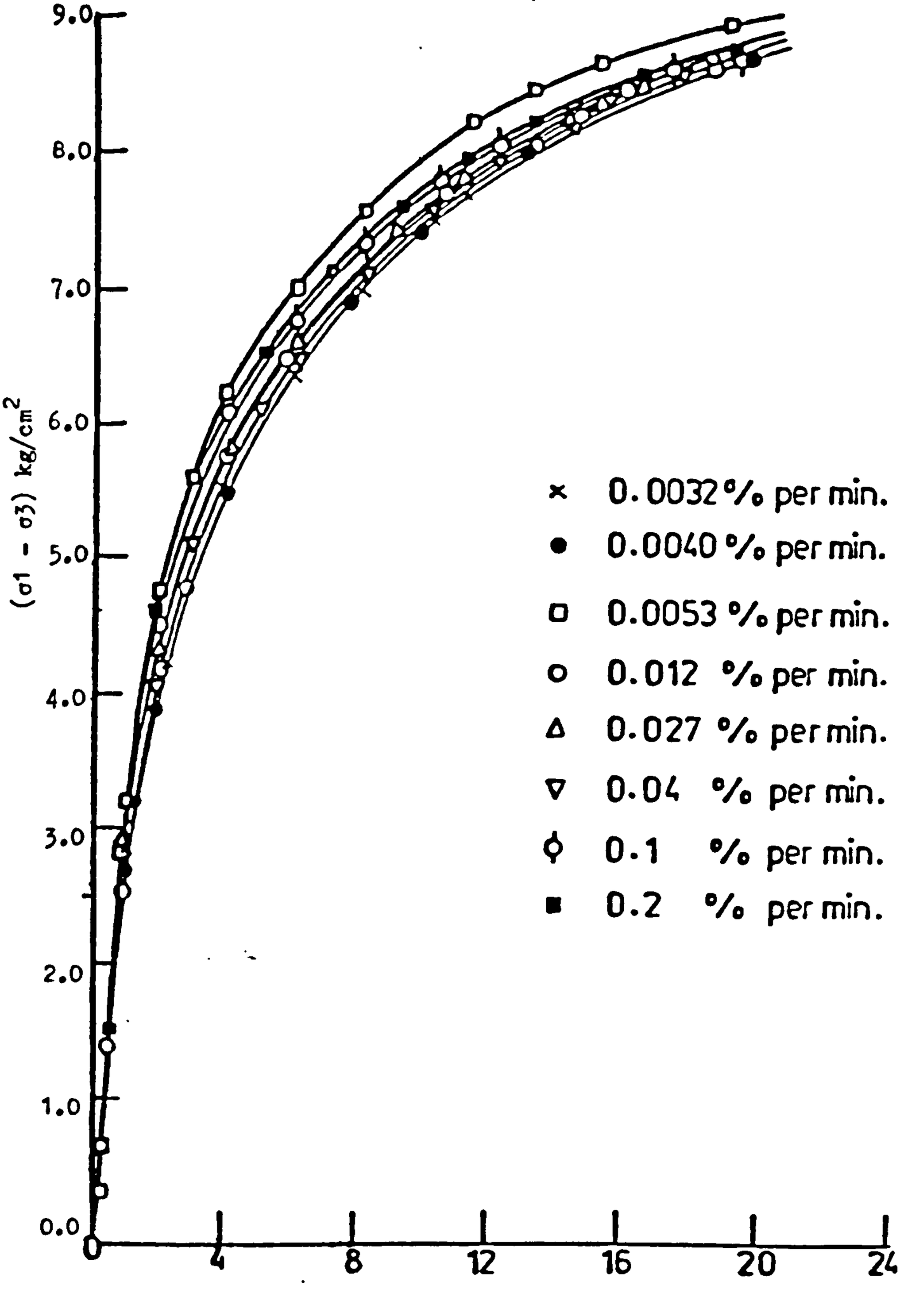

FIG.7.1: EFFECT OF RATE OF AXIAL DEFORMATION ON STRESS-STRAIN CHARACTERISTICS OF IDENTICAL SAMPLES SHEARED UNDER $\overline{CW}$ CONDITIONS (SATIJA, 1978).

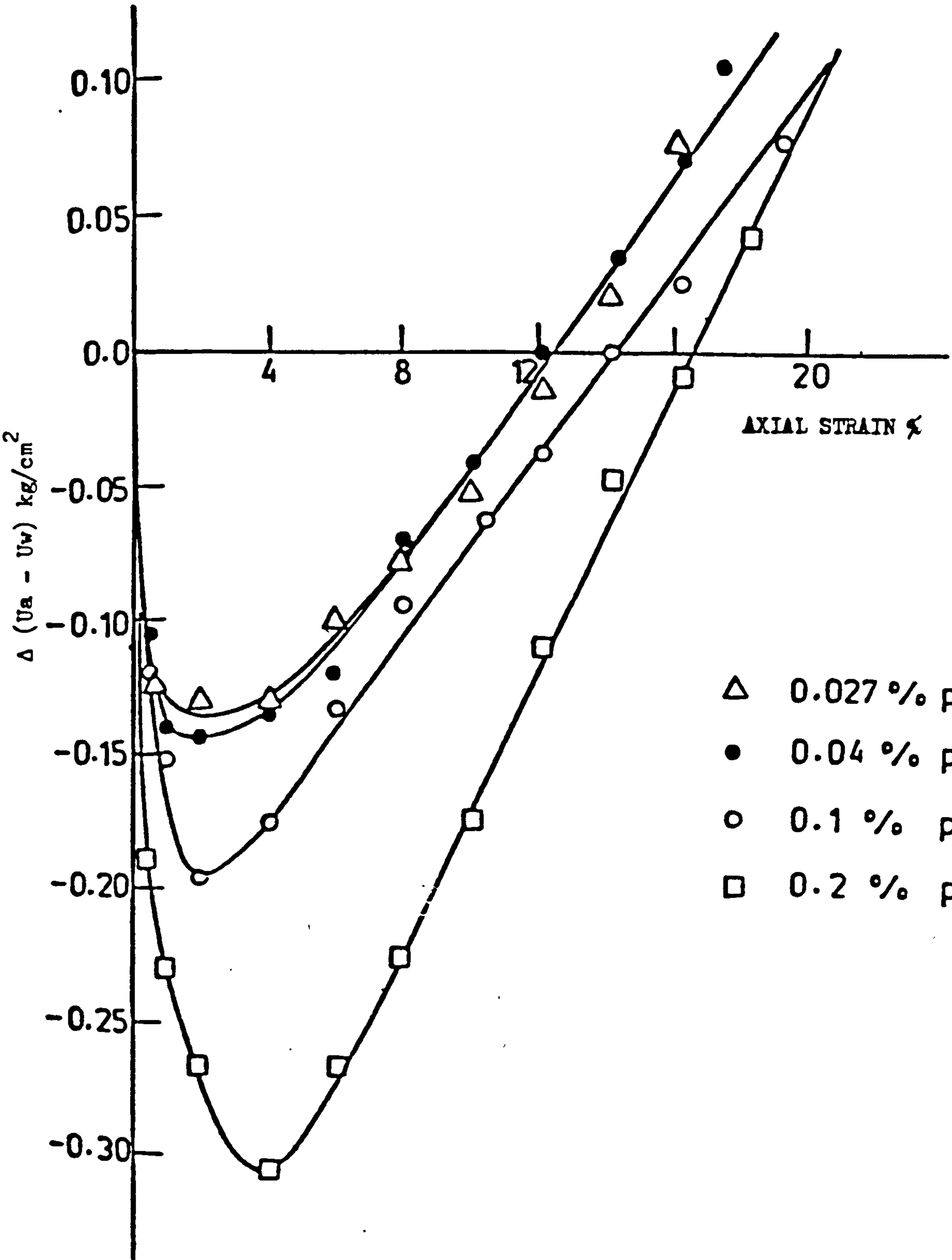

FIG.7.2: EFFECT OF RATE OF AXIAL DEFORMATION ON INDUCED (Ua - Uw) VERSUS AXIAL STRAIN FOR INDENTICAL SAMPLES SHEARED UNDER $\overline{CW}$ CONDITIONS (SATIJA, 1978) (HIGH STRAIN RATE).

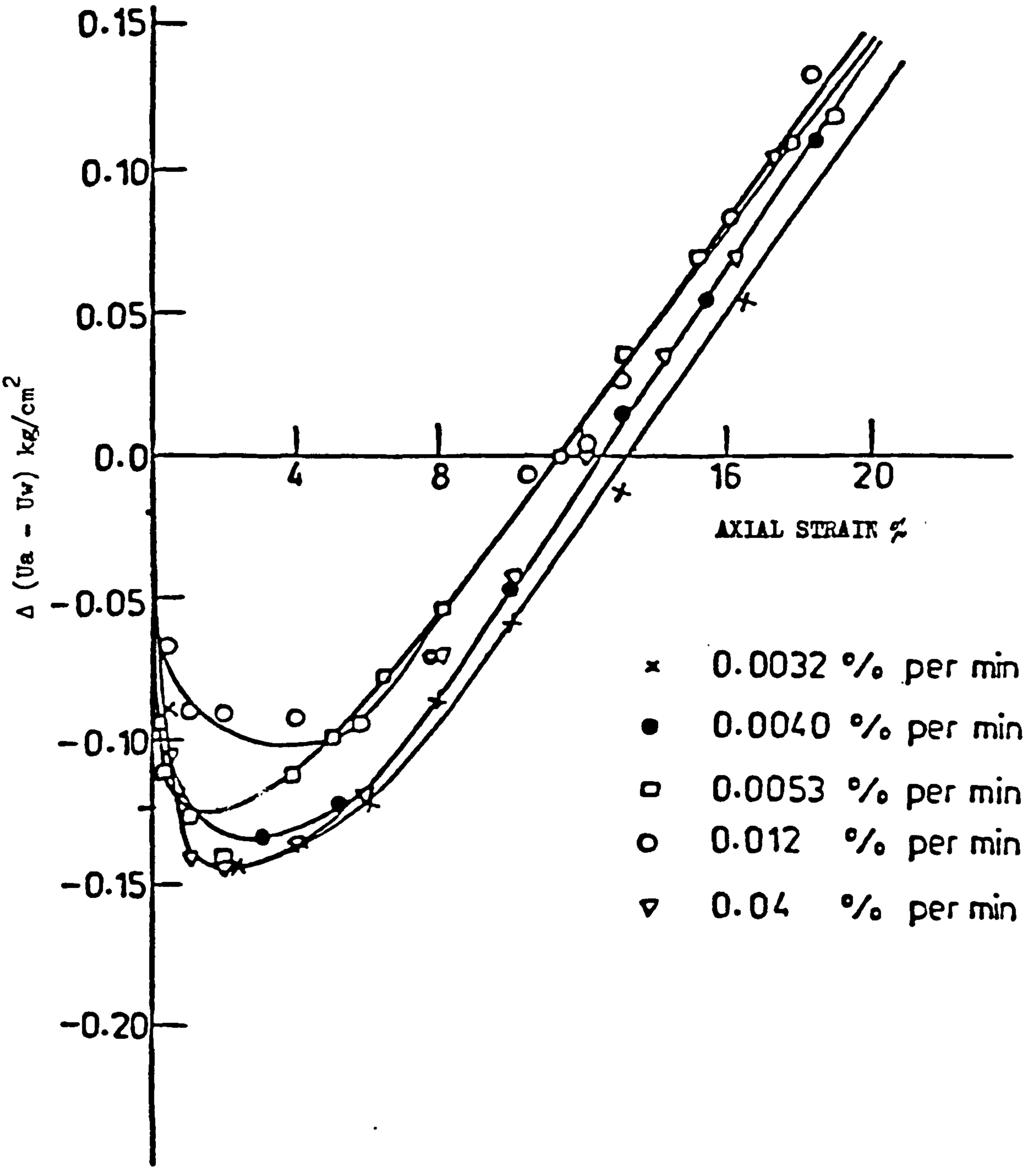

FIG.7.3: EFFECT OF RATE OF AXIAL DEFORMATION ON INDUCED (Ua - Uw) VERSUS AXIAL STRAIN FOR IDENTICAL SAMPLES SHEAR UNDER $\overline{CW}$ CONDITIONS (SATIJA , 1978) (LOW STRAIN RATE).

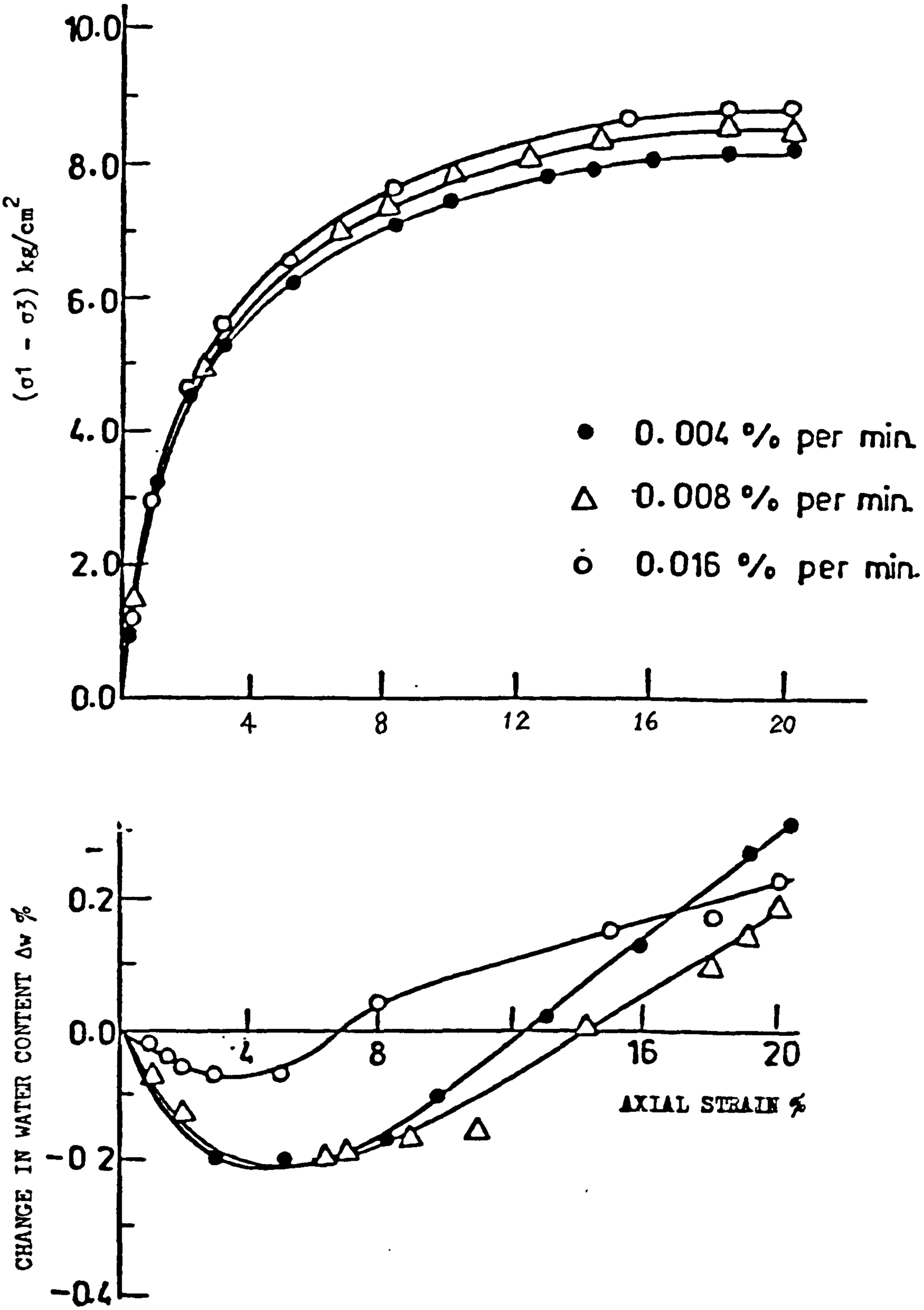

FIG.7.4: EFFECT OF RATE OF AXIAL DEFORMATION ON STRESS-STRAIN CHARACTERISTICS OF IDENTICAL SAMPLES SHEARED UNDER DRAINED CONDITIONS (SATIJA, 1978).

$C_v^w = \dfrac{KW}{\gamma_{wg} M_2^w}$, the coefficient of consolidation with respect to the water phase

KW = coefficient of permeability of the soil with respect to the water phase

γ_w = density of water

M_2^w = slope of the (Ua - Uw) plot when d($\bar{\sigma}$ - Ua) is zero

Generally, the pore-air pressure parameter of an unsaturated soil is smaller than the pore-water pressure parameter (Hasan and Fredlund, 1980). Under most conditions, the coefficient of permeability of the soil with respect to the water phase will be considerably smaller than the coefficient of permeability of the soil with respect to the air phase. Therefore it is justifiable to assume that the pressure gradient in the air phase in the above equation is negligible. As a result, the consolidation equation for the water phase in an unsaturated soil can be simplified to

$$\frac{\partial Uw}{\partial t} = Cv^w \left(\frac{\partial^2 Uw}{\partial y^2}\right) \quad \ldots\ldots(7.10)$$

which is similar in form to the conventional consolidation equation for saturated soils (Terzaghi and Frohlich, 1936).

The strain rate problem for drained shear tests on unsaturated soils can be subsequently solved by combining the simplified unsaturated soil consolidation theory with Bishop and

Gibson's postulation (1963) for determining failure time required in drained triaxial compression tests for saturated soils. Ho replaced the conventional consolidation equation (Terzaghi and Frohlich, 1936) with equation (7.10), and used Bishop and Gibson's formula to calculate the required time for a desired degree of dissipation of the induced pore-water pressure at failure as:

$$t_f = \frac{h^2}{nC_v^w (1-\overline{Uf})}$$, the required failure time for drained tests ..... (7.11)

where $n = \frac{0.75}{(1 + 3/\lambda)}$ if drainage is from one end only

or $= \frac{3}{(1 + 3/\lambda)}$ if drainage is from both ends

$$\lambda = \frac{KDx(HS)}{KSx(HD)} \qquad C_v^w = \frac{KS}{\gamma_{wgM}^w} \quad \text{..... (7.12)}$$

h = half of the actual length of the specimen, whether drainage is from one or both ends

λ = impedance factor

KD = permeability of the drainage element to water

KS = KW , the coefficient of permeability of the soil sample with respect to the water phase

HS = length of drainage path

HD = thickness of the drainage element

$\overline{Uf}$ = average degree of dissipation of the induced pore-water pressure at failure

The only modification of the original formula is the replacement of the saturated coefficient of consolidation by the coefficient of consolidation with respect to the water phase. With the presence of the impedance factor, eqn. (7.11) can also be used to find the required time for full dissipation of the induced pore pressures within the sample when the internal drainage problem is the governing factor.

Theoretically , equation (7.11) is applicable to undrained tests as well. As an interval drainage problem, the equalization process should take less time than that required for the dissipation process. Consequently, the time required for full dissipation of the induced pore pressures within a sample under drained conditions should be a çonservative estimate of the time required for full equalization of the induced pore pressures in a sample under undrained conditions. Accordingly, by setting the n value corresponding to a two end perfect drainage condition and a 95% degree of dissipation, eqn. (7.11) can be used to estimate the required time for a 95% pore pressure equalization in a sample under undrained conditions.

Once the required failure time is determined and the peak strain chosen, an appropriate axial strain rate corresponding to either 95% of dissipation or equalization of the induced pore pressures can be calculated for any unsaturated soil shear test with independent pore-air and pore-water pressure measurements.

To evaluate the permeability coefficient of an unsaturated soil with respect to the water phase, Corey's (1957)

theory can be applied (Fig. 7.5). It was stated as :

$$KS = K \left[\frac{S - Sr}{1 - Sr}\right]^4 \quad \ldots\ldots (7.13)$$

where K = the water permeability of the soil at saturation
S = degree of saturation of the soil
Sr = the residual degree of saturation which is the degree of saturation at which the relative air permeability becomes 100%

7.4 Discussion

Basically, the strain rate problem is one of pore-pressure dissipation or equalization in the sample and the measuring system. The problem can be divided into two parts, internal and external. The internal problem is the question of dissipating or equalizing excess pore pressures within the soil sample whereas the external problem is the assurance of dissipating or equalizing excess pore pressures across or within the drainage elements in contact with the sample. In other words, the strain rate problem hinges on the ability of the sample and the measuring system to dissipate or equalize excess pore pressures.

For conventional tests on saturated soils, highly permeable coarse porous stones or ceramic discs are used as drainage elements, thus creating boundary conditions which can be regarded as free drains. As a result, the internal drainage problem becomes the governing factor in the choice of strain rate, and consolidation theory can be used to estimate the amount of time that a sample needs to dissipate or equalize the induced excess pore pressure. Standard procedures for

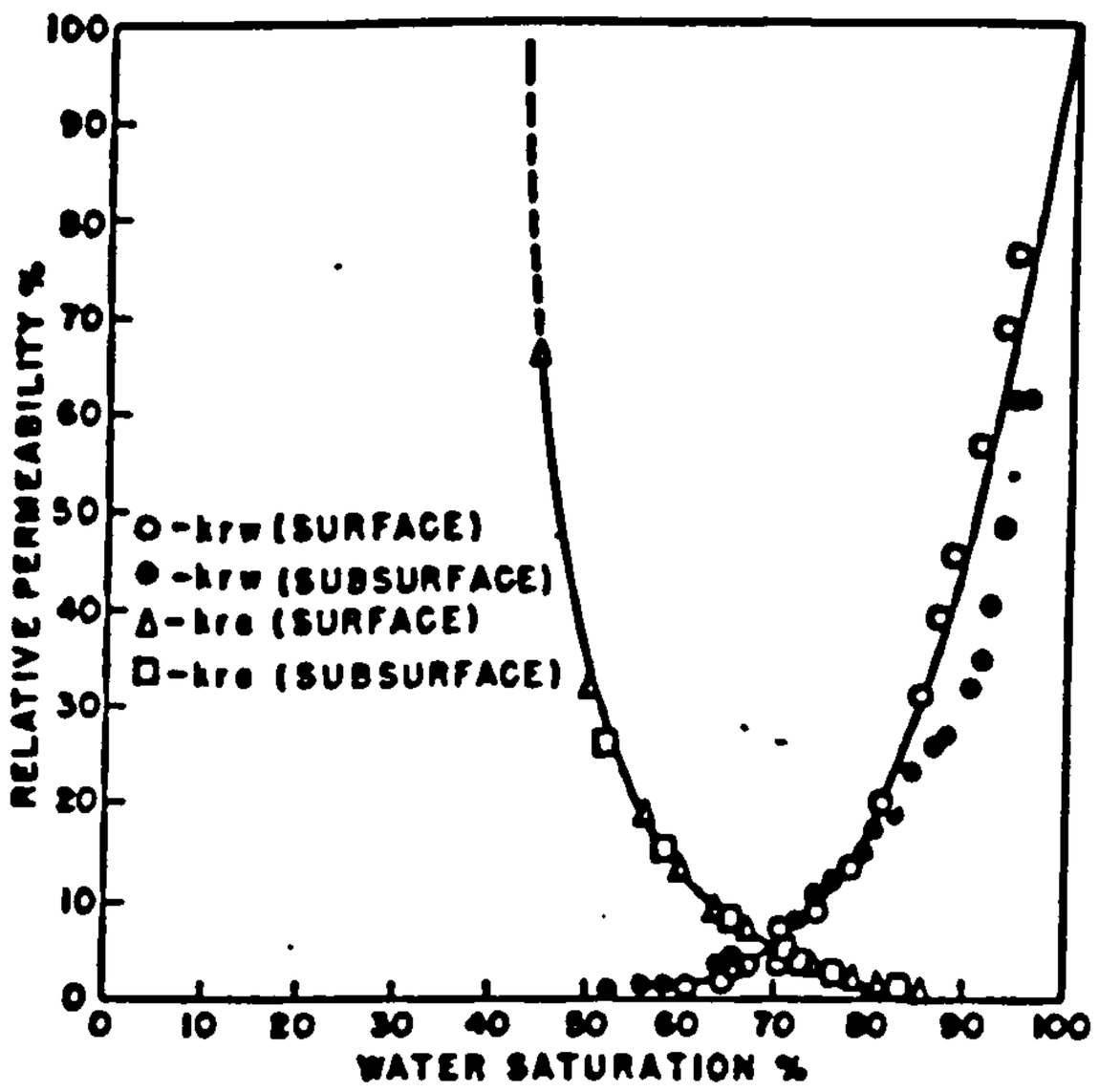

FIG.7.5: RELATIVE PERMEABILITY AS A FUNCTION OF SATURATION (COREY,1957).

determining strain rates for conventional tests on saturated soils are now established.

As far as shear tests for unsaturated soils are concerned, the nature of the strain rate problem is similar to that in saturated soils. In this case, it has to be determined whether the neutralization of excess pore pressures in the soil sample or the measuring system is the governing mechanism, i.e. the one that requires more time to dissipate or equalize the induced excess pore pressures. For all shear strength tests on unsaturated soils, high air entry discs which are impermeable to air are used as end drainage elements for water, whereas coarse porous discs which have no hindrance to air passing are used as end drainage elements for air. Thus,as far as the measuring system is concerned, the neutralization of excess pore-water pressure should dominate. Under normal circumstances, an unsaturated soil sample is more permeable to air than to water, and therefore the neutralization of the excess pore-water pressure should dominate the internal drainage problem as well. Unless the soil sample is much less permeable to water than the high air entry disc, the strain rate problem is an impeded drainage problem for drained shear tests on unsaturated soils.

Ho (1981) concluded that the impeded drainage due to the presence of the high air entry disc is the governing factor in determining the required failure time in unsaturated soil shear testing, and since soil properties like KS and M_2^w cannot be controlled, the choice of a high air entry disc for use in unsaturated soil shear testing is the only means of regulating

the strain rate. He presented a general plot for choosing strain rates for testing any type of unsaturated soil (Figure 7.6). The use of unsaturated soil properties (i.e. KS, M_w^2 and Cv) is essential when using this graph. Otherwise, unsafe strain rates will result if saturated soil properties are used.

In the author's tests, the effect of shear strain rate on unsaturated Grangemouth clay was studied both theoretically and experimentally.

Theoretically, a method similar to that described by Ho (1981) was used. Instead of using Corey's theory to evaluate the permeability coefficient of an unsaturated soil with respect to the water phase, Darcy's law was used because the residual degree of saturation, which is the degree of saturation at which the relative air permeability becomes 100%, was difficult to measure. The water permeability of unsaturated soils was obtained in the following way:

$$KS = \frac{\text{volume of water out of sample(c.c.)} \times \text{average drainage path (m)}}{\text{average area of sample (sq.cm)} \times \text{head difference (cm)} \times \text{time (sec.)}} \quad \text{m/sec}$$

where average drainage path
=(initial length + length after desaturation)/2
average area of sample
=(initial area + area after desaturation)/2
the head difference across the sample was assumed to be the applied matrix suction (Ua-Uw) across the sample

The effect of the effective confining pressure (63-Ua) on the permeability of unsaturated soils was not studied. It was kept constant and equal to 150 KN/sq.m in each permeability test.

The results of the permeability tests are summarized in

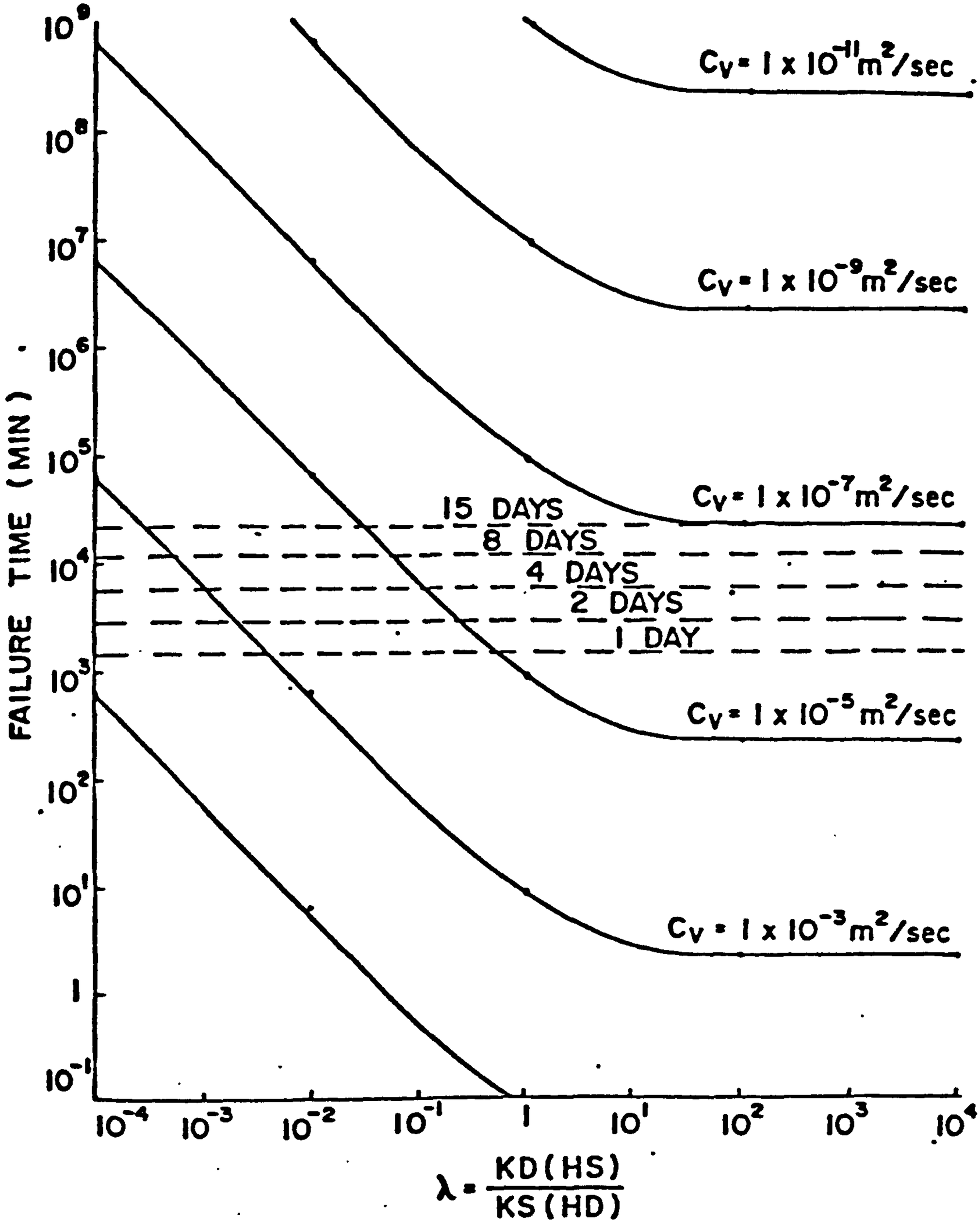

FIG. 7.6: FAILURE TIME REQUIRED IN SHEAR TESTING UNSATURATED SOILS WITH SAMPLE HEIGHTS EQUAL TO 5.5 INCHES (AFTER HO,1981).

the following table and plotted in figure 7.7.

Table 7.2: Summary of the permeability coefficients(KS) of unsaturated Grangemouth clay with respect to the water phase

Test No.	average degree of saturation(Sr) %	KS m/sec.
P1	69.24	1.72×10^{-10}
P2	73.91	1.49×10^{-10}
P3	79.73	1.72×10^{-10}
P4	80.59	2.05×10^{-10}
P5	84.03	3.06×10^{-10}
P6	88.52	2.42×10^{-10}
P7	92.98	6.40×10^{-9}
P8	96.05	1.87×10^{-9}
P9	100.00	2.85×10^{-9}

From the curve in figure 7.7, the water permeabilities of unsaturated Grangemouth clay specimens were interpolated as follows:

average degree of saturation(Sr) %	KS m/sec.
65	8.0×10^{-11}
70	1.0×10^{-10}
75	1.2×10^{-10}
80	2.0×10^{-10}
85	3.4×10^{-10}
90	6.8×10^{-9}
95	1.34×10^{-9}
100	2.85×10^{-9}

FIG.7.7: CHANGE OF WATER PERMEABILITY WITH DEGREE OF SATURATION(%)

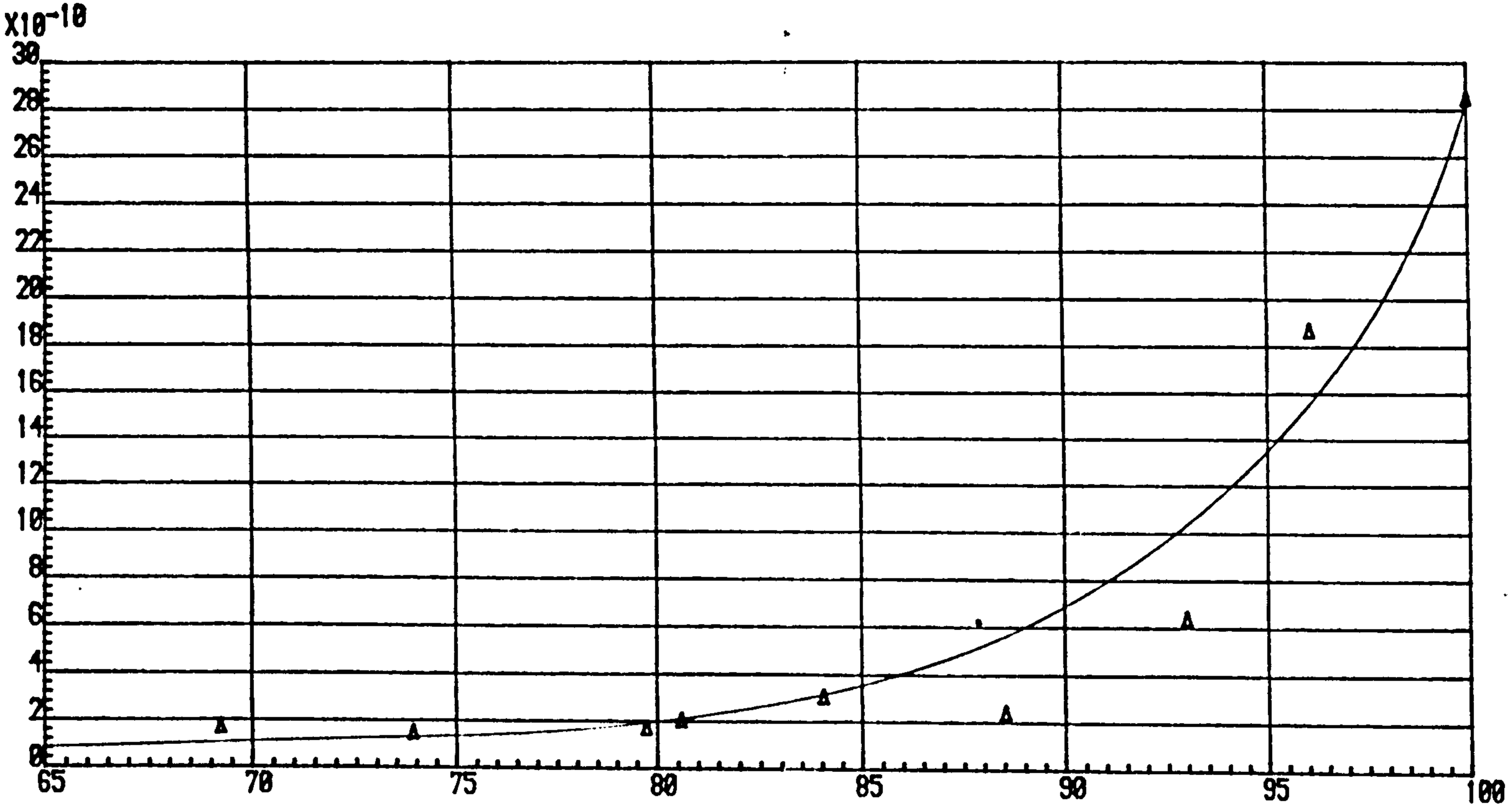

Before an appropriate testing time could be found the value of M^w_2 had to be evaluated. In order to obtain M^w_2, isotropic consolidation tests under applied suction (Ua-Uw) with (σ - Ua) set to zero (i.e. unconfined test with air as cell pressure $\sigma 3$=Ua) were run in the modified triaxial cell. Four different matrix suctions were applied to the same specimen in sequential order 150.00 KN/sq.m, 300.00 KN/sq.m, 450.00 KN/sq.m and 578.37 KN/sq.m. The corresponding volumetric water changes were measured and are shown in figure 7.8.

applied matrix suction KN/sq.m	volumetric water drainage
150.00	0.0441
300.00	0.0557
450.00	0.0712
578.37	0.0809

By linear regression, the slope M^w_2 of the (Ua-Uw) plot (for $d(\sigma - Ua)$ equal to zero) was calculated to be 8.78×10^{-5} m^2/KN. Knowing the thickness and permeability properties of the high air entry ceramic disc, the corresponding failure time for each degree of saturation of an unsaturated soil sample could be calculated.

Assuming a maximum axial strain value of 20%, the strain rate corresponding to each degree of saturation is shown in Table 7.3.

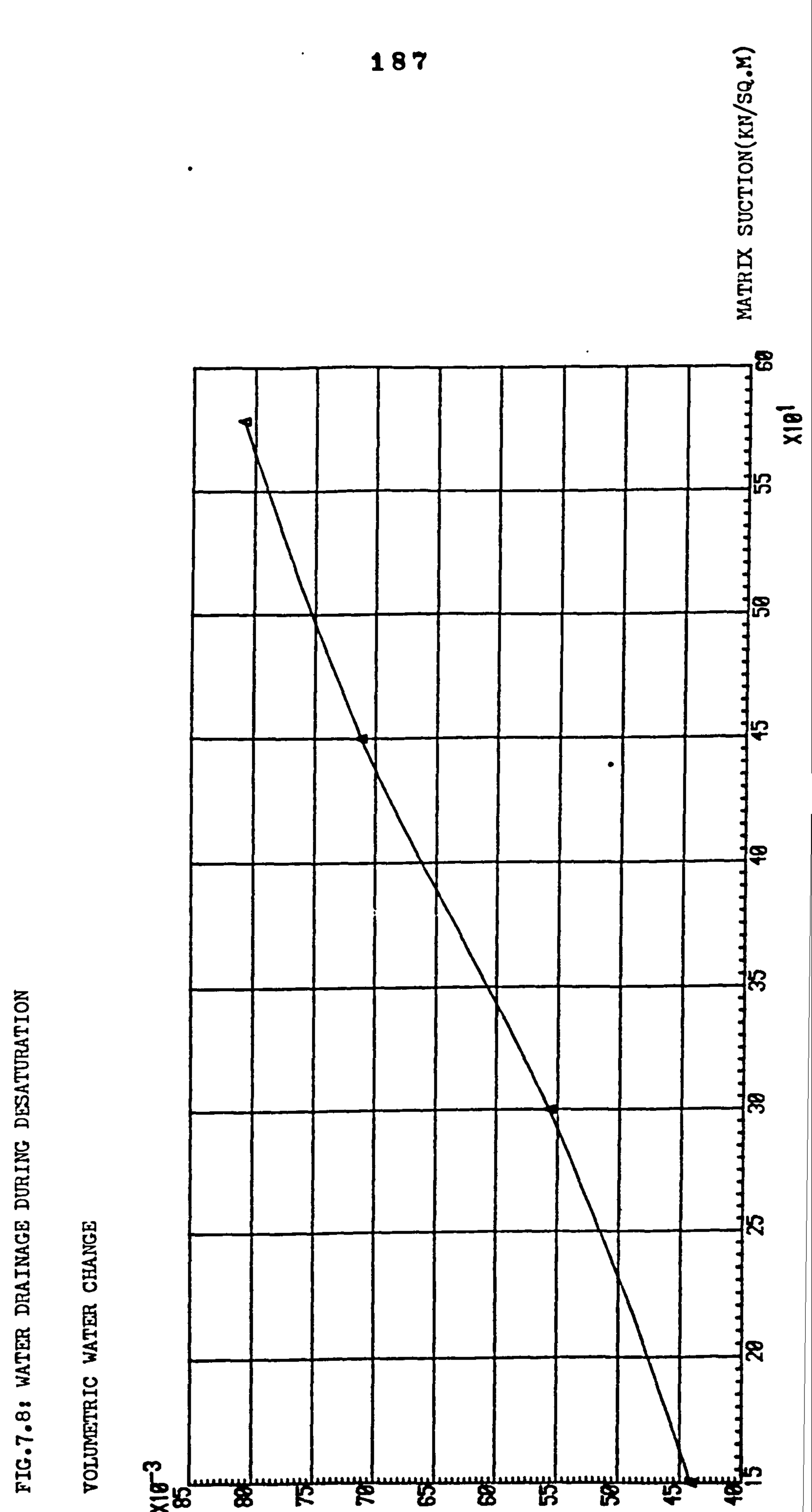

FIG.7.8: WATER DRAINAGE DURING DESATURATION

Table 7.3: Variation of time to failure and strain rate with degree of saturation for 5 bar and 15 bar high air entry ceramic discs

average Sr %	time to failure(mins.) 5 bar	15 bar	strain rate (mm/min.) 5 bar	15 bar
65	7055	7074	0.0022	0.0021
70	5638	5658	0.0027	0.0027
75	4698	4720	0.0032	0.0032
80	2827	2844	0.0054	0.0053
85	1667	1686	0.0091	0.0090
90	840	855	0.0181	0.0178
95	431	447	0.0352	0.0340
100	209	225	0.0727	0.0676

The difference in strain rates when 5 bar and 15 bar high air entry ceramic discs were used was small and therefore could be ignored. Figures 7.9 to 7.12 were used to select the appropriate strain rate in this investigation. A different strain rate could be chosen for each degree of saturation, but it was considered more practical to select one strain rate for all tests rather than alter the strain rate for each individual test. The degree of saturation of all unsaturated Grangemouth clay samples used in this research was greater than 75%, and therefore a strain rate of 0.003mm/min was adopted as an appropriate value for all drained tests.

Experimentally, a series of constant-water content (CW) and unconfined (U) tests were conducted to determine the effect of different strain rates on the testing of Grangemouth clay. All the unsaturated soil specimens were prepared using the desaturation and consolidation process described in section 8.5(a). The initial stress conditions for CW tests were identical, with cell pressure(σ_3)= 350 KN/sq.m; pore air

FIG.7.9: TIME TO FAILURE IN MINS. AGAINST DEGREE OF SATURATION (5 BAR DISC)

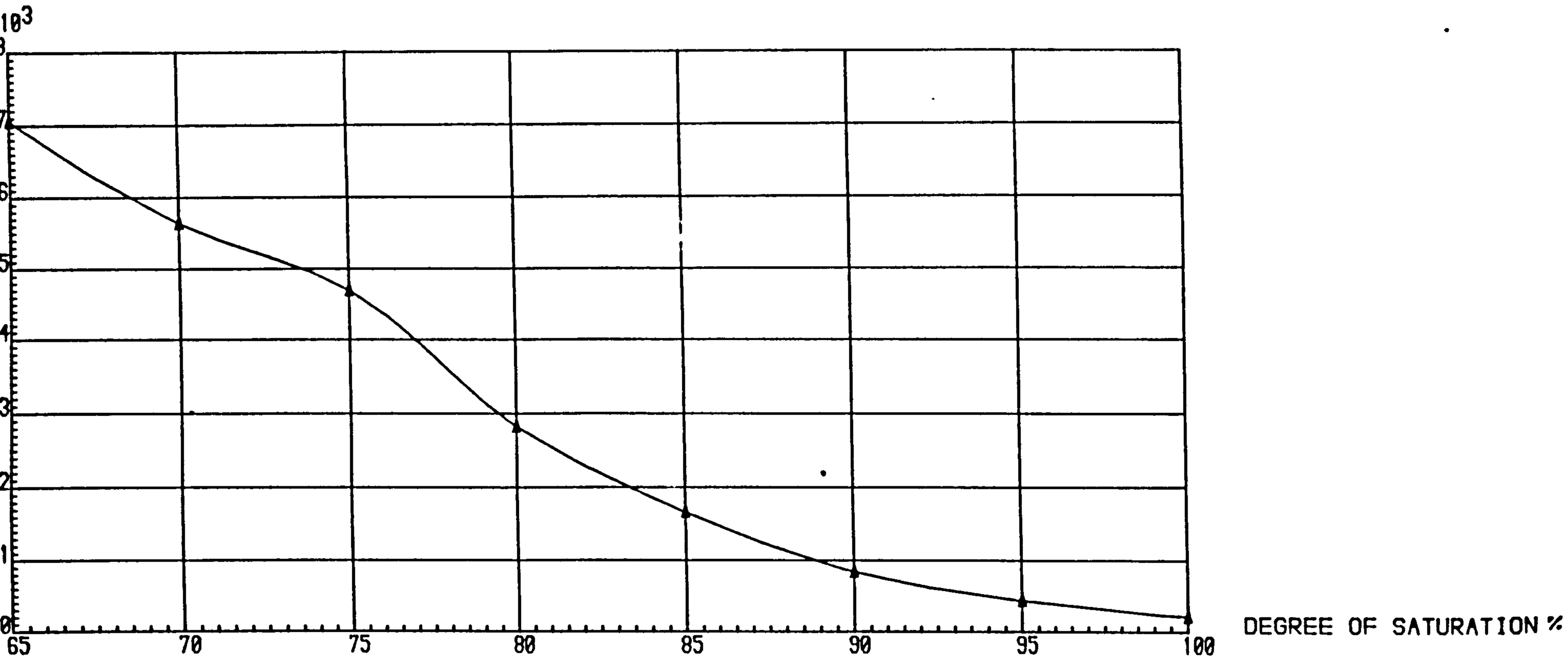

FIG.7.10: TIME TO FAILURE IN MINS. AGAINST DEGREE OF SATURATION (15 BAR DISC)

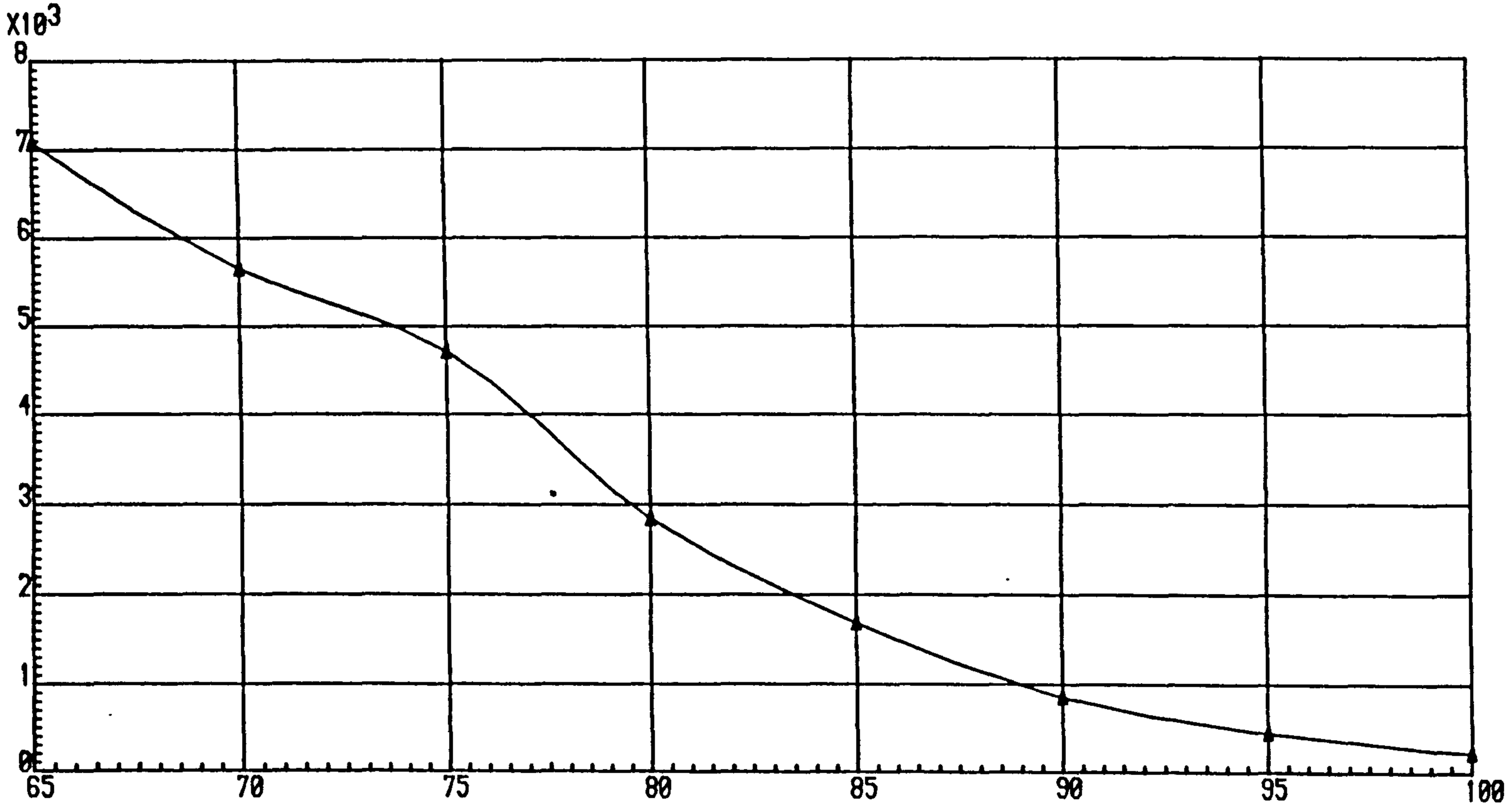

FIG.7.11: STRAIN RATE AGAINST DEGREE OF SATURATION (5 BAR HIGH AIR ENTRY DISC)

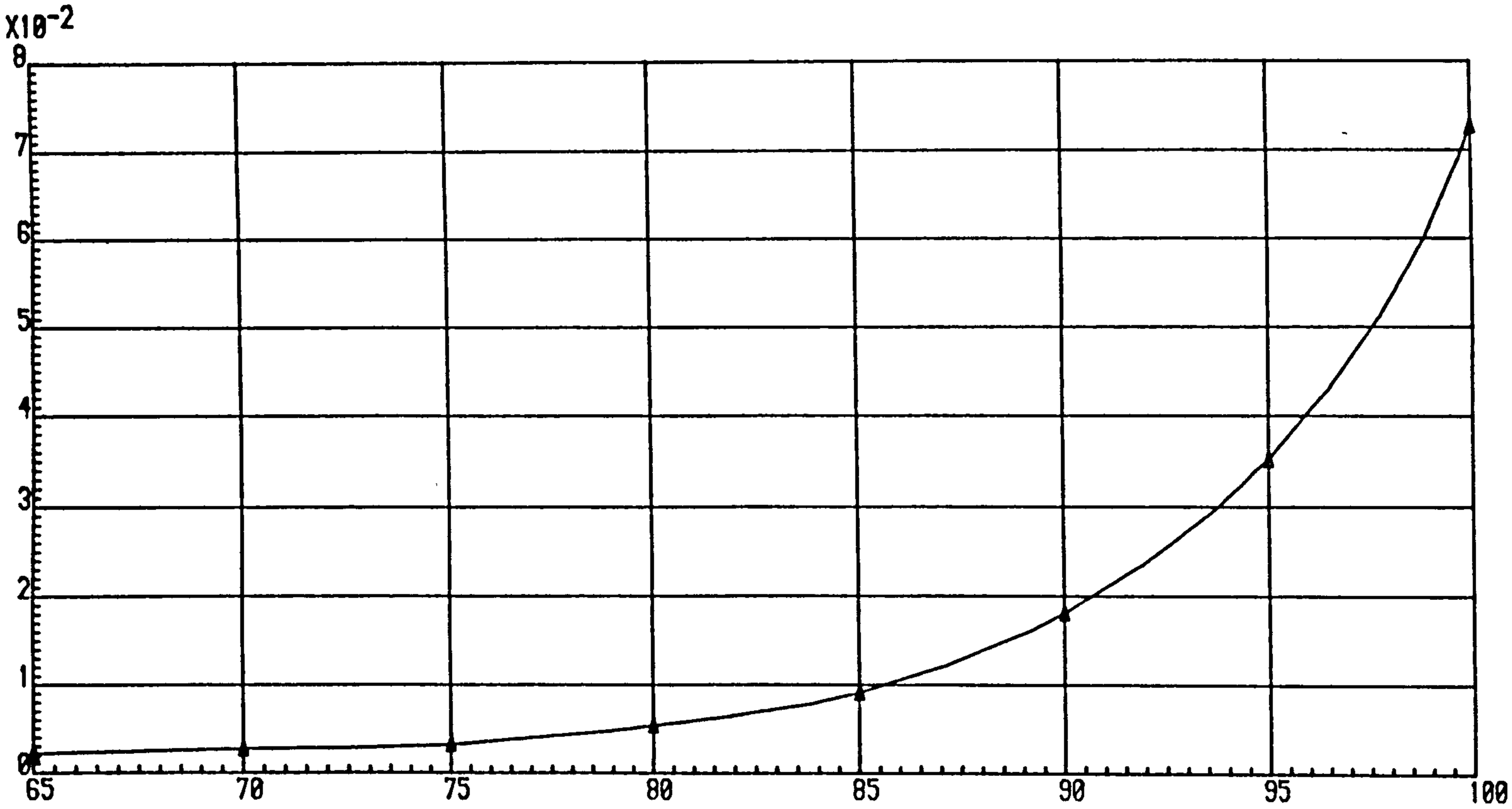

FIG.7.12: STRAIN RATE AGAINST DEGREE OF SATURATION (15 BAR HIGH AIR ENTRY DISC)

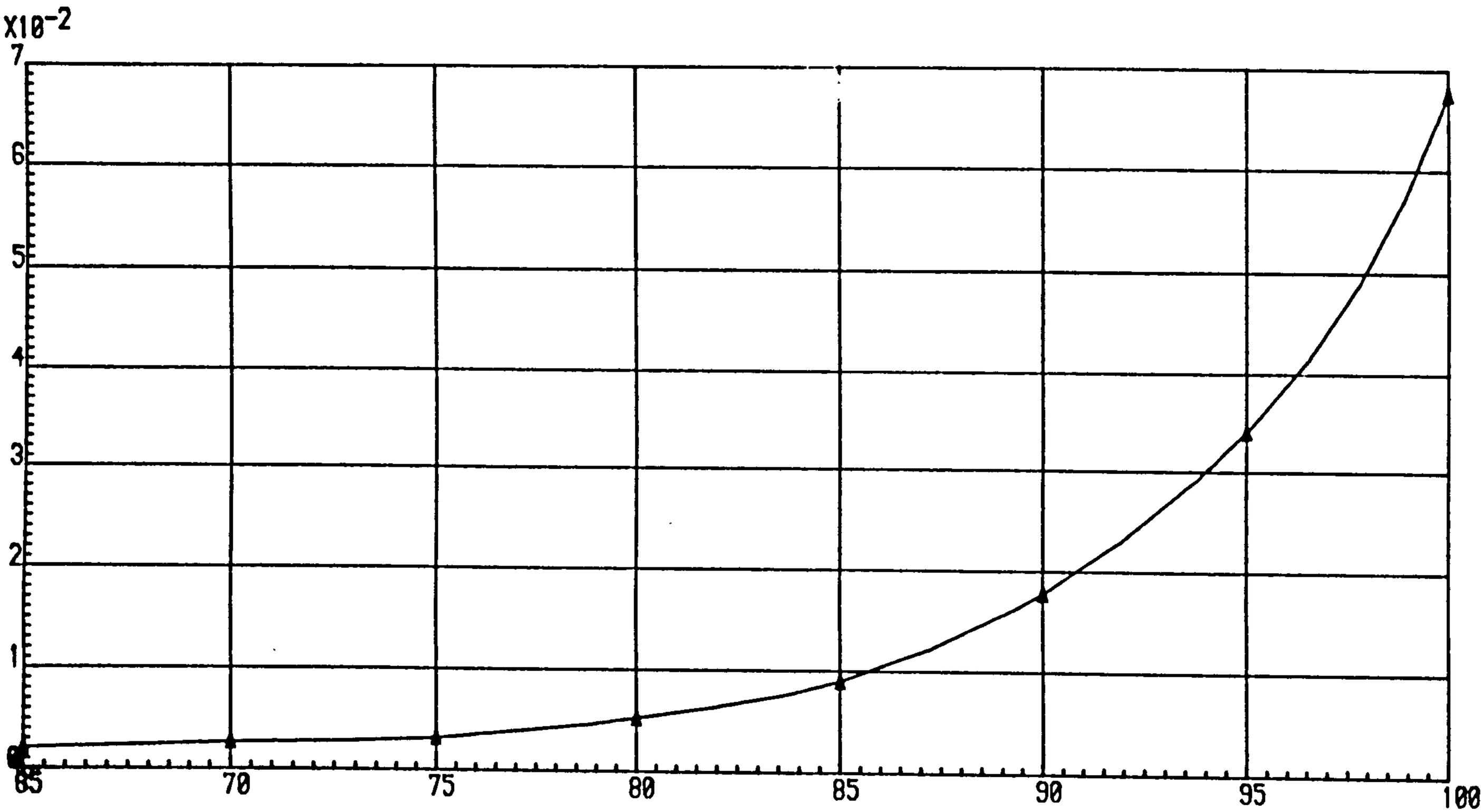

pressure(Ua)= 200 KN/sq.m and pore water pressure (Uw)= 50 KN/sq.m, so that the associated stress state variables were (σ3-Ua)=150 KN/sq.m and (Ua-Uw)= 150 KN/sq.m. Following Satija's approach, the change in matrix suction (Ua-Uw) was used as the parameter to study the effect of changing the shear strain rate, since changes in (Ua-Uw) were more sensitive than the deviator stress to the strain rate during shear.

A total of 16 constant water-content tests, made up of three groups, were conducted on specimens of unsaturated Grangemouth clay. Figures 7.13, 7.14 and 7.15 show plots of change in suction (Ua-Uw) against axial strain for the strain rates used in these tests. For each group of tests there was, in general, a plateau region which incorporated the majority of the strain rates. This plateau region was reached at an axial strain value between 5% and 10%. At the beginning of the tests, the tangents to the curves have a general relationship to the strain rate, i.e. the steeper the tangent, the slower the strain rate. Therefore, for the slowest strain rates, the matrix suction had more time to establish equalization and did so at a lower value of axial strain.

Considering the results from these tests, a strain rate of 0.0041 mm/min was selected as the most suitable value from both the practical position and from considerations of pore-water pressure dissipation and equalization.

Finally, five unconfined (U) tests conducted had a range of time to failure, t_f, from 0.5 hour to 312 hours (20% strain) (i.e. strain rate from 0.50 mm/min. to 0.00081 mm/min.). The initial stress conditions were identical with cell (air)

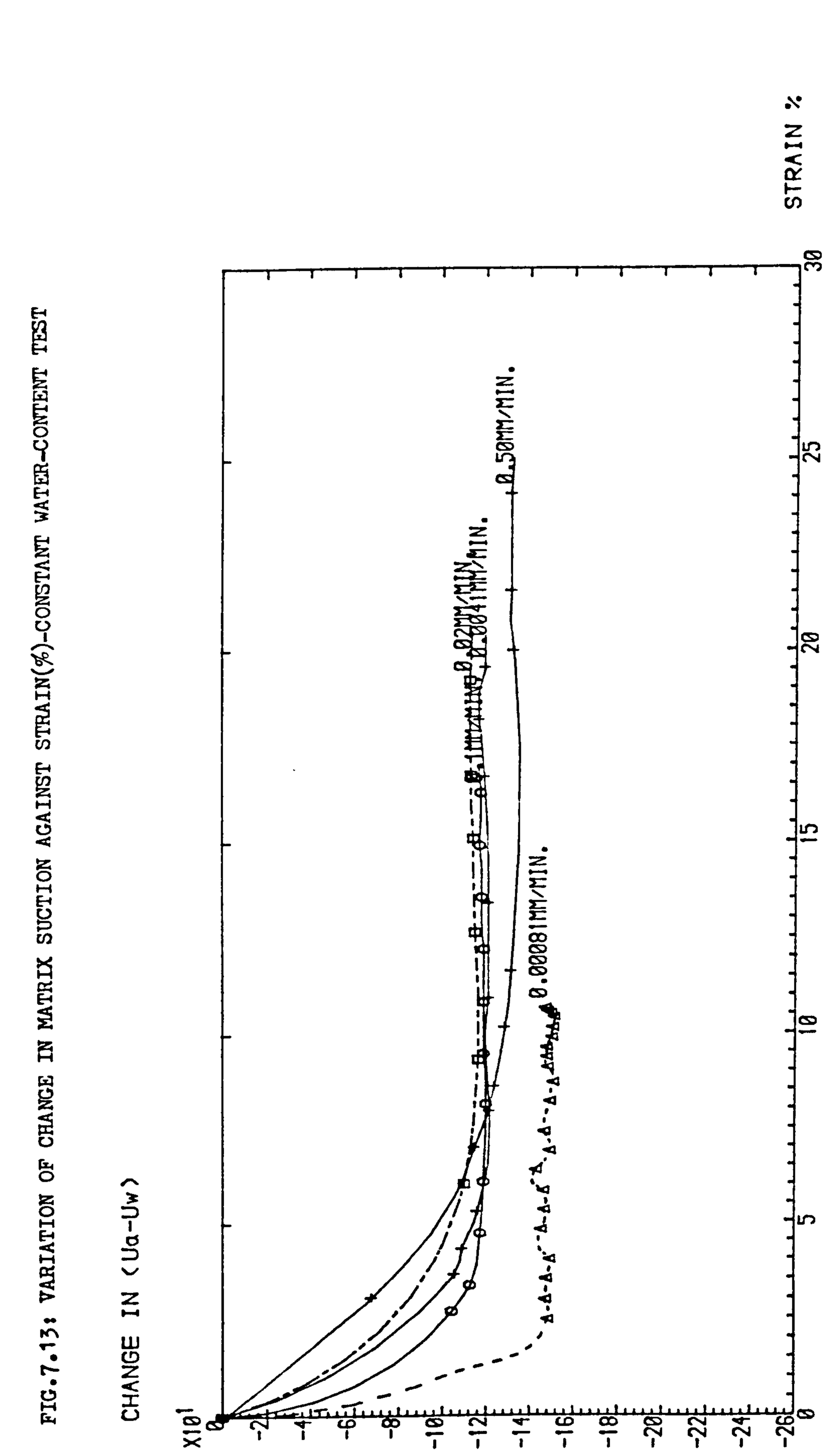

FIG.7.13: VARIATION OF CHANGE IN MATRIX SUCTION AGAINST STRAIN(%)-CONSTANT WATER-CONTENT TEST

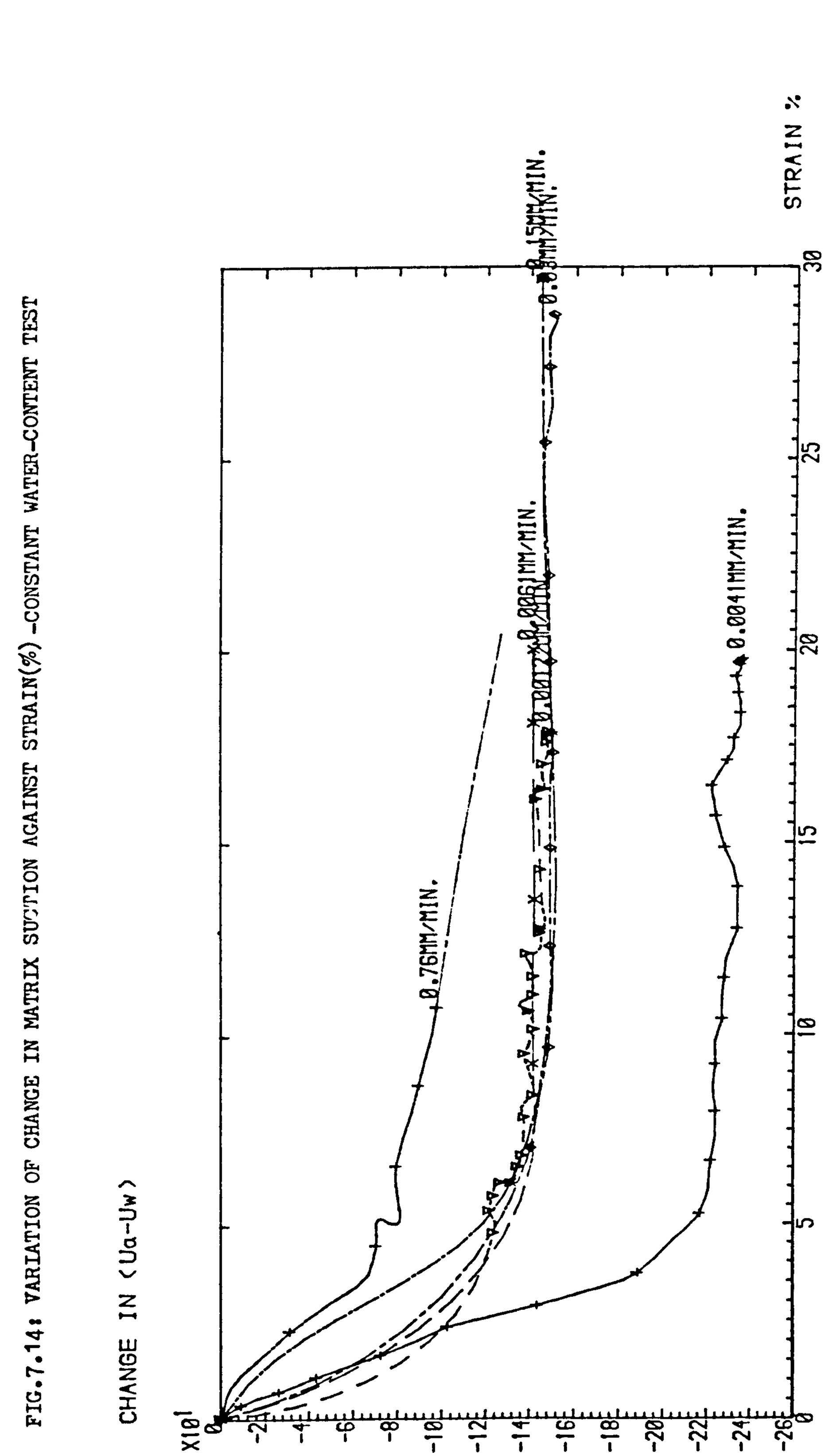

FIG.7.14: VARIATION OF CHANGE IN MATRIX SUCTION AGAINST STRAIN(%) -CONSTANT WATER-CONTENT TEST

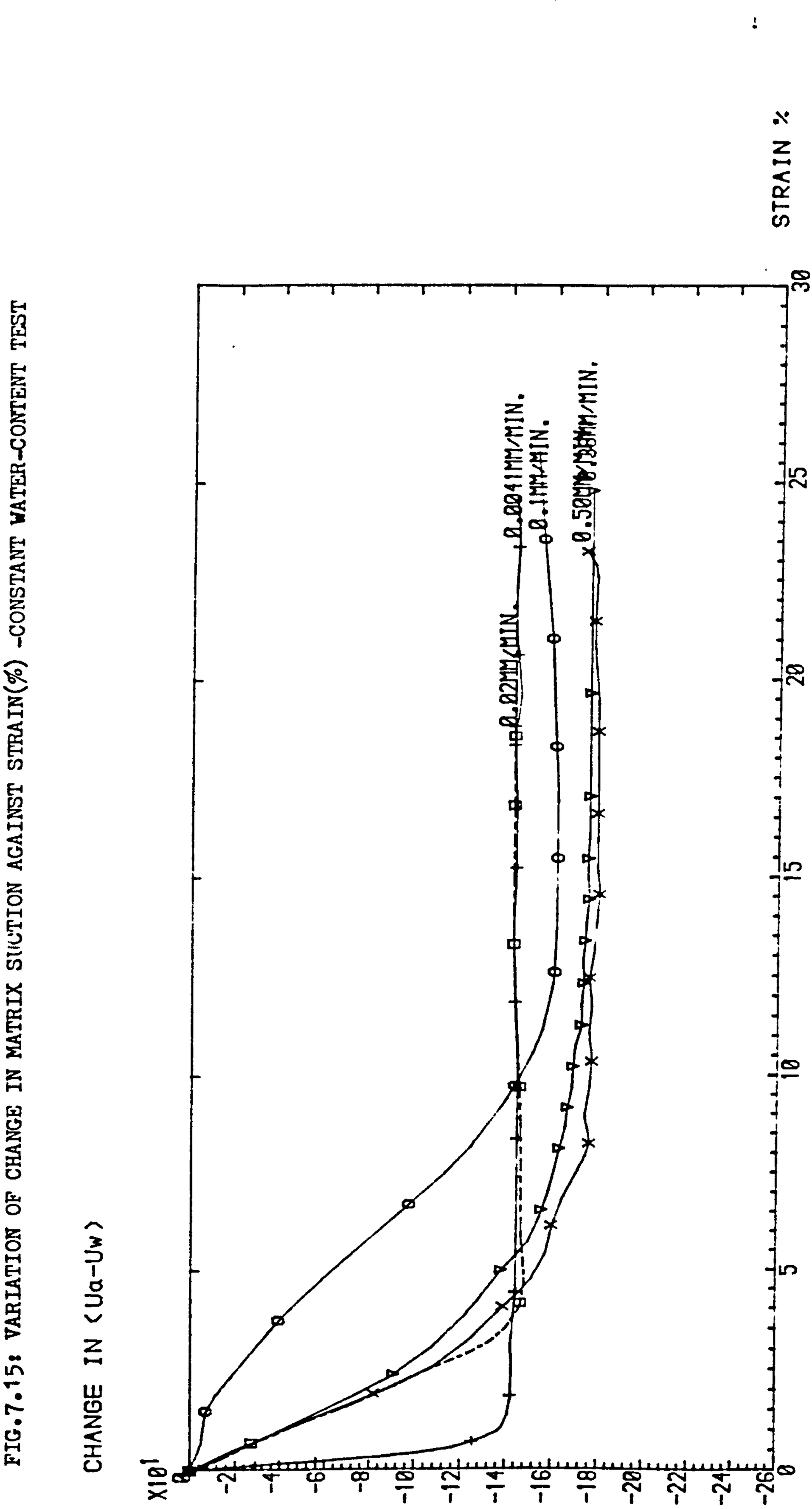

FIG.7.15: VARIATION OF CHANGE IN MATRIX SUCTION AGAINST STRAIN(%) -CONSTANT WATER-CONTENT TEST

pressure = 200 KN/sq.m and pore water pressure = 50 KN/sq.m, so that the associated stress state variables were (63-Ua) = 0 and (Ua-Uw) = 150 KN/sq.m. These tests were particular cases of constant water-content tests with effective confining pressure on the sample equal to zero, therefore any change in matrix suction under this investigation with different strain rates was excluding the effect of effective confining pressure(Fig.7.16).

7.5 Conclusion

It is still difficult to assess accurately all the soil properties required to estimate the strain rate for testing unsaturated soils, but parameters such as soil compressibility, permeability and the test drainage conditions are certainly important. This chapter described a theoretical and an experimental method for estimating the time required to shear an unsaturated soil under different drainage conditions. In using Ho's theoretical method to obtain an approximate strain rate for drained tests, the author incorporated Darcy's law instead of Corey's theory to evaluate the permeability coefficient of an unsaturated soil with respect to the water phase. This was because the residual degree of saturation used in Corey's theory was difficult to measure. Experimentally, constant water-content tests and unconfined tests were carried out based on Satija's suggestion of monitoring the changes in (Ua - Uw) for various strain rates. The results of these tests indicated appropriate strain rates for testing unsaturated Grangemouth clay specimens.

For triaxial tests on samples of unsaturated

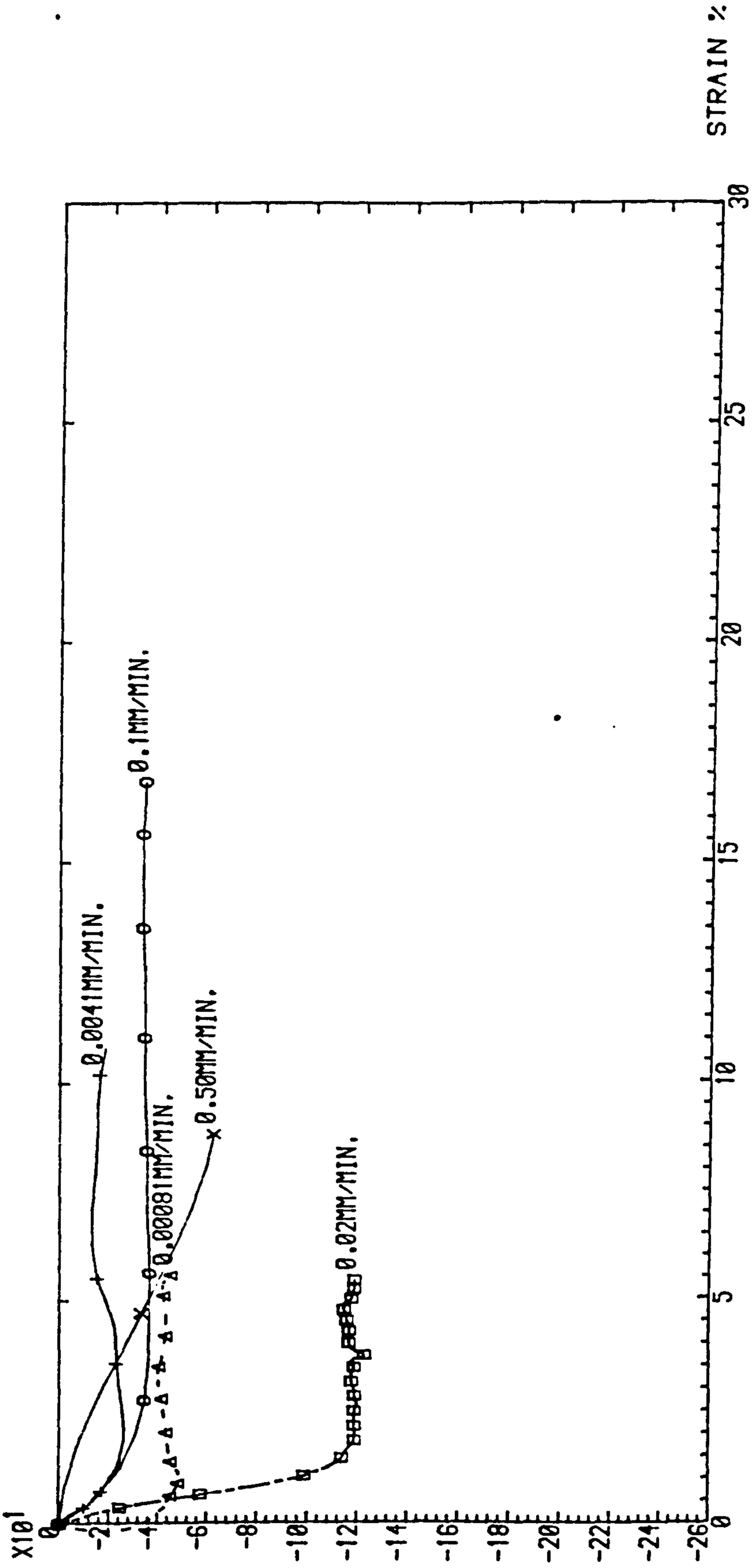

FIG.7.16: VARIATION OF CHANGE IN MATRIX SUCTION AGAINST STRAIN(%) -UNCONFINED TEST

CHANGE IN (Uq-Uw)

Grangemouth clay, the theoretical analysis indicated that a strain rate of 0.003 mm/min. would be suitable for drained tests. Using the experimental technique, a series of constant water-content and unconfined tests indicated that a strain rate of 0.0041mm/min would be suitable for undrained tests. The appropriate strain rate was used by the author in his triaxial testing programme.

CHAPTER 8

TEST PROGRAM, PROCEDURE AND DATA REDUCTION

CHAPTER 8 TEST PROGRAM, PROCEDURE AND DATA REDUCTION

8.1 General

The main purpose of the experimental programme was to collect more test data in order to investigate further the shear strength theory of unsaturated soil as proposed by Fredlund et al (1978) and to quantify the significance of soil suction in the shear strength of unsaturated soils. It was considered that the existing experimental verification of the theory, primarily undertaken by Satija(1978) and Ho(1981), was inadequate. Satija conducted two series of constant water-content tests and two series of drained tests on compacted samples of Dhanauri clay. Ho carried out an investigation of the shear strength of two unsaturated Hong Kong soils, decomposed granite and decomposed rhyolite. Ho used undisturbed samples but only drained multi-stage tests were carried out. It was the aim of the author's experimental programme to provide additional test data for use in Fredlund et al's theory, based on a wider variation of test parameters and using undisturbed soil samples. Within this programme, the effect of test type on the shear strength parameters and the effect of initial stress state on the stress conditions at failure have been investigated. The results of other investigations prior to 1978 have also been used and these are presented in chapter 9.

In order to carry out the triaxial shear tests, considerable modifications were made to standard triaxial shear equipment, and these modifications were described at length in Chapter 6.

Two further aspects of testing unsaturated soil were investigated:

(i) the influence of strain rate on the dissipation and equalization of pore water pressure (discussed in chapter 7).

(ii) the variation of pore air and pore water pressures during isotropic compression.

Investigation of the latter involved the use of truly undrained tests, which will be described in sections 8.3 and 8.5. Unfortunately, the results from an initial series of four such tests were extremely poor, revealing substantial inconsistencies with established theory. No convincing reasons for these inconsistencies have yet been advanced to the author's satisfaction, but it is considered likely that the method used to obtain unsaturated samples was at least partly to blame. The unsaturated samples were formed from saturated samples using a desaturation and consolidation procedure which maintained certain values of pore air and pore water pressures within the sample. In order to perform an undrained test at the end of the desaturation process, the air and water pressure valves had to be closed. It may be that this simple step destabilised the equilibrium condition within the sample, resulting in erroneous results. In any event, no further investigation of the variation of pore air and pore water pressures took place, and the results of the four tests carried out have been omitted from the thesis.

8.2 The soil

The soil samples used in this research were taken from block samples of a late glacial marine clay from Grangemouth. Detailed information on these undisturbed block samples is given in the thesis " A study of layered clay from Grangemouth " by B.M.A. OMER,1978.

The block samples have been properly treated and stored since being taken, and therefore it was assumed that the information on soil properties given in Omer's thesis was still applicable to the present investigation. The soil properties of the block sample used were as follows:

Soil type	%clay	%silt	%sand	S.G.	L.L.	P.L.	P.I.
Grangemouth clay	15	65	20	2.73	29	15	14

The clay is normally consolidated and has low undrained shear strength and high compressibility in its undisturbed state*. From Omer's investigations, the average shear strength parameters for such samples taken from 10.7m depth were:

effective cohesion (C') = 6.7 KN/sq.m

effective angle of shearing resistance (ϕ') = 34.2°

8.3 Types of shear strength test

It was pointed out in Chapter 4 that the stress state in an unsaturated soil depended primarily on two factors:

(i) the "effective" confining pressure, ($\bar{\sigma}3$ - Ua) and

(ii) the matrix suction, (Ua - Uw)

The shear strength of unsaturated soil can thus be investigated from two points of view:

(i) maintain the 'effective' confining pressure (б3 - Ua) constant and investigate the effect of varying the matrix suction (Ua - Uw).

(ii)maintain the matrix suction (Ua - Uw) constant and investigate the effect of varying the effective confining pressure (б3 - Ua).

It is also possible to compare a series of tests at one (Ua-Uw) value (varying (б3-Ua)) with another such series at a second (Ua-Uw) value. The same can be done with two series of tests at different constant values of (б3-Ua) and varying (Ua-Uw).

There are basically six types of tests which can be performed on unsaturated soils:

(a) true undrained tests with elevated pore-air pressure

(b) constant water content, varying (б3-Ua)

(c) constant water content, constant (б3-Ua)

(d) constant water content, (б3-Ua) = 0

i.e. unconfined tests with б3 = Ua

(e) drained tests, constant (б3-Ua) and (Ua-Uw)

(f) 'overdrained' tests

(a) True undrained tests with elevated pore air pressure (IU)

A true undrained test on an unsaturated soil is defined as one in which the masses of air and water contained by the soil remain constant throughout the test and changes occur in

both pore air pressure and pore water pressure.

This test has several limitations. The measurement of pore water pressure below one atmosphere over long periods leads to cavitation of the water in the measuring device. Since the equilibrium air pressure in the unstressed sample is in general also slightly negative, undrained tests can only be carried out on samples where the initial difference between pore air and water pressure is less than about 10 p.s.i.. This restriction can be overcome by using an elevated air pressure during the desaturation and consolidation stages.

In addition, it is difficult to maintain a strictly 'undrained' state when using a rubber membrane, since the air in the sample diffuses through the membrane into the water in the cell. This results in a significant reduction in the pore air pressure(see Table 8.1) and hence in the pore water pressure, so giving a misleading impression of the change in 'undrained' strength with time. Tests in which the rubber jacketed sample is surrounded by mercury in an intermediate cell are now used for unsaturated soil where strictly undrained conditions are necessary. This type of test has been successfully performed by Donald (1961) and the improvement in pore air pressure readings can be seen in Table 8.1.

(b) Constant water content, varying (σ_3 - u_a) tests

This type of test is really a 'partially undrained' test. An ordinary latex rubber membrane is used to enclose the sample and the cell fluid is water (without the intermediate mercury cell). After setting up the sample, the cell

TABLE 8.1

(after Bishop and Henkel, 1962)

Effect on pore-air pressure of diffusion through the rubber membrane

(Sample: Holiow ceramic cylinder $\frac{\text{air volume}}{\text{total volume}} = 77\%$)

Test condition	*Initial cell pressure (absolute)* lb/sq. in.	*Initial air pressure (absolute)* lb/sq. in.	*Pressure drop after*									
			2 *hours*		12 *hours*		24 *hours*		7 *days*		14 *days*	
			lb/sq. in.	%	lb/sq. in.	%	lb/sq. in.	%	lb/sq. in.	%	lb/sq. in.	%
Rubber membrane surrounded by de-aired water .	52·7	43·1	0·4	0·9	2·2	5·1	4·05	9·4	12·4	28·8	13·8	32·0
Rubber membrane surrounded by mercury . .	39·7	29·7	0·1	0·3	0·1	0·3	0·1	0·3	0·35	1·2	–	–

pressure is applied and the pore pressures in the sample are allowed to come to equilibrium. The cell fluid dissolves as much of the pore air as it requires.

Once equilibrium has been reached, axial loading is commenced. Changes in both pore air and pore water pressures then take place. As the cell fluid is now saturated at its pressure with dissolved air, little further loss of pore air occurs during the test.

(c) Constant water content, constant ($\bar{\sigma}_3$ = Ua) tests (CW)

This type of test is similar to the test described under (b), except that the air pressure in the pore space is controlled independently. It is either allowed to equilize with atmospheric pressure or is maintained at a suitably elevated value in order to raise the pore water pressure. This necessitates the use of a saturated porous disc to measure the pore water pressure, which has an air entry value greater than (Ua-Uw). The sample is sheared with the pore air pressure maintained at a constant value, so only changes in pore water pressure, Uw, take place.

This type of test is simpler to perform than types (a) and (b) since only changes in pore water pressure need be measured. The cell fluid is free to take up as much diffused air as it requires, without affecting the pore air pressure.

It is also a suitable test for soils which have a low water content and high clay fraction, where the difference between air and water pressures in the sample is of major importance.

(d) Unconfined tests with $\bar{\sigma}_3 \equiv U_a$ (U)

This is a special case of the test (c); it is an unconfined test in which the pore air pressure (Ua) is made to equal the cell pressure ($\bar{\sigma}_3$).

(e) Drained tests, constant ($\bar{\sigma}_3$-Ua) and (Ua-Uw) tests (D)

This type of test involves the control or maintenance of the air and water pressures during the test rather than their measurement in a closed system. The suction (Ua-Uw) is maintained constant throughout the shearing process. The process is comparable to performing a 'slow' or drained test on a saturated soil. The axis-translation technique is used to impose suctions greater than 100 KPa(1 atm.).

(f) 'Overdrained' tests

These tests are used to investigate the effect of drying-wetting hysteresis. The term 'overdrained' is similar to 'overconsolidated' but it is applied to the soil suction rather than to the confining pressure. When the desaturation of the test is virtually complete, the soil suction (Ua-Uw) is decreased to its test value, keeping $\bar{\sigma}_3$ and Ua at their initial values, and water is allowed to re-enter the sample until equilibrium is reached. This generally takes 3-4 days. The remainder of the test is performed as for test (e). The values of (Ua-Uw) are chosen to give roughly equal spacing to the degree of saturation at failure.

In the current test programme, four of these test types were

used, viz, true undrained test (TU), constant water-content, constant ($\bar{\sigma}3$-Ua) test (CW), unconfined test (U), and drained test (D).

The sample drainage conditions were altered by using the CW and D tests. In the CW tests with varying ($\bar{\sigma}3$-Ua), air could diffuse from the sample and thus the measured air pressure was subject to error. Theoretically, when the cell water was saturated with dissolved air, little further loss of pore air should take place. It was not possible to judge when this situation had been established. This problem was overcome by using an elevated air pressure maintained independently, as in test (c).

The test procedure was simplified by using the unconfined test (U), a special case of the CW test. The true undrained test was used when measuring variations in pore air and pore water pressures during isotropic compression. The overdrained test was not used. Details of the test programme will be given in the following section.

8.4 Test programme

The main programme of triaxial shear tests consisted of two series which were distinguished by the initial stress state applied to the sample.

For series (I),

$$(Ua - Uw) \geqslant (\bar{\sigma}3 - Ua) = \text{Constant}$$

For series (II),

$$(\bar{\sigma}3 - Ua) > (Ua - Uw) = \text{Constant}$$

The particular values of Ua, Uw, (63 - Ua) and (Ua - Uw) used in each series are shown in Table 8.2. For each initial stress state, different drainage conditions could be applied to the sample.

Test type	Description	Strain rate*
D	Drained test under constant confining, pore air and pore water pressures, with measurement of total and water volume changes.	0.003mm/min.
CW	Constant water-content test under constant pore air pressure, with measurement of pore water pressure and sample volume changes.	0.0041mm/min
U	Unconfined tests (63 = Ua), with measurement of pore water pressure changes.	0.0041mm/min

* From chapter 7

During the main testing programme, 38 tests were carried out. These consisted of 29 tests from series I (10 constant water-content, 12 drained and 7 unconfined) and 9 tests from series II, all drained. Details of the results are given in Appendix 8, ' Computations, Data Reduction and Results'.

Table 8.2: Initial stress conditions for test series I and II

Series I: $(Ua - Uw) \geqslant (\sigma 3 - Ua)$

Initial stress state	$\sigma 3$ KN/m^2	Ua KN/m^2	Uw KN/m^2	$(\sigma 3 - Ua)$ KN/m^2	$(Ua - Uw)$ KN/m^2
1	150	100	50	50	50
2	200	150	50	50	100
3	250	200	50	50	150
4	300	250	50	50	200
5	350	300	50	50	250
5a	350	200	50	150	150
6	400	350	50	50	300
6a	400	250	50	150	200
7	450	400	50	50	350
8	500	450	50	50	400
8a	500	350	50	150	300
9	550	500	50	50	450
10	600	550	50	50	500
10a	600	450	50	150	400
11	650	600	50	50	550
11a	650	350	50	300	300
12	700	650	50	50	600

Series II: $(\sigma 3 - Ua) > (Ua - Uw)$

Initial stress state	$\sigma 3$ KN/m^2	Ua KN/m^2	Uw KN/m^2	$(\sigma 3 - Ua)$ KN/m^2	$(Ua - Uw)$ KN/m^2
13	150	100	50	50	50(NOT USED)
14	200	100	50	100	50
15	250	100	50	150	50
16	300	100	50	200	50
17	350	100	50	250	50(NOT USED)
18	400	100	50	300	50
19	450	100	50	350	50
20	500	100	50	400	50
21	550	100	50	450	50
22	600	100	50	500	50
23	650	100	50	550	50
24	700	100	50	600	50(NOT USED)

8.5 Test procedure

The test procedure was basically the same for each type of test, with obvious modifications to suit the particular test being undertaken. The procedure detailed here was carried out for a true undrained test with elevated pore air pressure. The modifications to suit the other types of tests were in accordance with the description of tests (c), (d) and (e) given in section 8.3.

After thoroughly de-airing the pore water pressure measuring system in the manner described in section 7.4, the cell was emptied of water and removed. A pool of water was left lying on the surface of the ceramic disc to prevent it from drying out. The rest of the water was mopped up and cleared from the air pressure measuring lead.

Before each test was started, all the pressure transducers were checked. If necessary, a slight adjustment was made to the digital voltmeter in order to read 0.00 mV at 0.0 bar. The initial readings of the automatic volume change logging systems (AVCL), and the paraffin-water volume change indicators (VCI) were adjusted to suitable values, so that the volume changes occurring during a test could be recorded without changing the direction of flow. For the automatic volume change logging systems, a value of about -500 was set on the digital voltmeter, and for the paraffin-water volume change indicators, a value of about 1 c.c. was found to be convenient.

The sample was prepared from an undisturbed block of Grangemouth clay, which had been coated with paraffin wax directly after extraction and stored in a dampened room at

constant humidity and temperature until the time of testing.

A small block approximately 3"x3"x6" (i.e. 76.2x76.2x152.4mm) was cut to provide sufficient material for one 3"(i.e.76.2mm) high by 1 1/2"(i.e.38.1mm) diameter sample and enough trimmings for moisture content determination.

In a trimming frame the final cylindrical shape of the sample was obtained by alternately rotating the block and shaving the extra soil off with a wire saw, finally smoothing the sides by using a sharp straight edge. This method, followed with care, was found to minimise disturbance during preparation and yielded satisfactory cylindrical samples 3" high and 1 1/2" diameter (76.2 mm high and 38.1 mm diameter) for triaxial compression testing.

After trimming, the sample was weighed to the nearest 0.1 g and the initial dimensions of the sample were measured using a vernier scale. The moisture content determined from the soil trimmings was used in conjunction with the weight and overall dimensions of the sample to calculate the initial soil properties (e.g. degree of saturation, void ratio, etc.).

Filter paper drains were used in all tests to accelerate consolidation and pore water pressure dissipation or equilization. The drains made from Whatman's No. 54 filter paper, covered the entire vertical surface of the specimen. Vertical slits were cut at 1/4" intervals to prevent the development of tensile stresses in the paper. This configuration was recommended by Bishop and Gibson(1963).

A circular piece of filter paper was soaked in water

and placed on the surface of the high entry ceramic disc. After wiping off the excess water, the sample was lightly placed in position on the ceramic disc. Extreme care was exercised when placing the sample to ensure that intimate contact was obtained with the ceramic disc, and that the sample was located axially in such a way as to avoid tilting. Soaked side filter paper drains were then carefully pressed onto the sides of the sample. A weighed dry coarse porous disc was put on top of the sample with a dry piece of circular filter paper lying between them.

A rubber membrane was now placed over the sample using a membrane stretcher. Before sealing the membrane to the sample, the top end cap with an air pressure lead was placed on the coarse porous disc. The membrane was then sealed to the pedestal and top end cap with two rubber O-rings at each end. It was important to ensure that no air was trapped between the membrane and the sample and that the sample was in close contact with the end caps.

The inner perspex cylinder was seated on the round lucite cushion at the pedestal. The top face of the cushion and the upper part of the pedestal were covered with latex to prevent mercury from coming into contact with the metal of the pedestal. The air pressure lead was then connected through the base to the air pressure supply. The zone between the inner lucite cylinder and the soil sample was filled with mercury to a level just above the top of the rubber membrane surrounding the sample.

The triaxial cell chamber was placed over the specimen and clamped to the base, making certain that the base sealing

ring was in position. The cell pressure valve was opened to allow de-aired water into the cell. When the water level was about 1/2" below the top of the cell, the flow was decreased and the loading ram moved up and down in order to reduce, as much as possible, the volume of entrapped air inside the cell. The outer-cell pressure line was then connected to the pressure supply, and the cell was sealed with the ram in the raised position. At this time, all valves were closed.

After the desired cell pressure, pore air and pore water pressures were set, the initial readings on the volume change indicators (i.e. AVCL or VCI) were taken. The cell pressure and outer-cell pressure were applied first then the pore air pressure and lastly the pore water pressure. Readings, including the temperature, were taken at one minute intervals until the total volume change of the sample calculated from two successive readings was less than or equal to the water volume change. This procedure usually took about half an hour, at which time the readings were taken at 30 minute intervals. The ambient temperature was recorded because its value affected the readings taken from the AVCL systems. This temperature effect is presented in appendix 6.

For a fully saturated soil, it was not possible for the total volume change to be larger than the water volume change. Any discrepancy between these two volumes was probably due to cell deformation (on application of cell pressure) and entrapped air bubbles still present in the cell (for details see appendix 5). An unsaturated soil sample was formed from a saturated

sample by applying a desaturation and consolidation process*. By using this process, which was usually completed in 2 or 3 days, errors in volume change measurement were minimised. Volume change readings were taken at regular intervals(every 30 minutes) by a computer controlled data logger, until equilibrium was reached. In order to obtain an accurate measurement of the water volume change, it was necessary to flush out and measure the volume of diffused air which had accumulated at the base of the ceramic disc. Flushing was performed once a day and the appropriate correction applied to the measured water volume change.

When the sample pore pressures were in equilibrium, the air and water valves were closed and the loading stage of the undrained test could begin. The loading ram, incorporating the load cell, was brought into contact with the top cap. Care was taken to ensure that no load was applied to the sample at this point. The loading frame gears were set for an appropriate rate of strain (see Chapter 7). The strain LVDT rested on top of the triaxial cell and the initial load cell, strain LVDT, AVCL and pressures readings were noted. The motor was started and testing commenced.

Throughout the test, the values of load, strain, temperature, cell pressure, pore air and pore water pressures were recorded every 30 minutes by a data logger. Failure was usually indicated by a progressive reduction in the magnitude of the axial load but, if no definite failure was obvious, the test was continued until the specimen had reached 20% strain. The loading stage of each undrained compression test took 2 to 3

days to complete.

When dismantling the triaxial cell, the cell and outer-cell pressures were shut off and the water in the triaxial chamber allowed to drain. The outer-cell pressure line was disconnected and the triaxial cell chamber was removed from the base. A screw at the bottom surface of the inner cell was released and mercury was collected, via a funnel, into a beaker. When no more mercury could be collected from the funnel, the whole assembly(inner cylinder, sample, perspex cushion and pedestal) was dismantled from the cell base, and separated in a tray where the remaining mercury droplets could be collected.

After the rubber membrane was removed, the specimen and coarse porous stone were weighed. The difference in weight between the coarse porous stone before and after the test was used as a correction to the weight of specimen at the end of the test. The specimen was then placed in a drying oven and reweighed when dry, for moisture content determination. Finally, the pedestal was immersed in water to prevent the high air entry ceramic from drying out.

8.6 Failure criteria for saturated and unsaturated soils

The failure criteria suggested by Blight(1961) were used in this research. They are:

(1) Maximum (б1-б3)/(б3-Uw) gives the maximum values of the shear strength parameters.

(2) Maximum (б1-б3) corresponds to the maximum shear stress in the soil.

(3) A limiting axial strain (i.e. 20 %) in cases where a maximum deviator stress is not reached.

All three criteria must be equally valid for both saturated and unsaturated soils.

In drained tests no difficulty arises, since (σ3-Uw) is constant, the only variable is (σ1-σ3) and a maximum value of (σ1-σ3) denotes failure. In undrained tests, both (σ3-Uw) and (σ1-σ3) vary and the soil can be considered to have failed when maximum values of either (σ1-σ3)/(σ3-Uw) or (σ1-σ3) are reached.

In saturated soils, shear strength along any plane can be expressed as follows (see Chapter 5):

$$\tau = C' + (\sigma - U_w)\tan\phi'$$

Skempton and Bishop(1954) presented the above equation in terms of principal stresses, where it becomes:

$$\frac{1}{2}(\sigma_1 - \sigma_3) = \frac{C'\cos\phi' + (\sigma_3 - U_w)\sin\phi'}{1 - \sin\phi'}$$

If $C' = 0$, the above equation reduces to

$$\frac{\sigma_1 - \sigma_3}{\sigma_3 - U_w} = \frac{2\sin\phi'}{1 - \sin\phi'}$$

From this it follows that a maximum value of (σ1-σ3)/(σ3-Uw) will correspond to a maximum value of φ'.

In an unsaturated soil, the application of criterion (2) above presents no difficulty since (σ1-σ3) is a direct measure of true effective stress. Considering Bishop's

effective stress equation, viz: $\sigma_3' = (\sigma_3 - U_a) + X(U_a - U_w)$, criterion (1) becomes:

$$\frac{\sigma_1 - \sigma_3}{\sigma_3'} = \frac{\sigma_1 - \sigma_3}{(\sigma_3 - U_a) + X(U_a - U_w)}$$

which cannot be calculated without knowledge of the value of X.

The expression can be rewritten as:

$$\frac{\sigma_1 - \sigma_3}{\sigma_3'} = \frac{\sigma_1 - \sigma_3}{(\sigma_3 - XU_w) - U_a(1-X)}$$

As Ua usually does not vary as much as Uw, the approximate substitute for the failure criterion is therefore $(\sigma_1-\sigma_3)/(\sigma_3-U_w)$. This is analogous to the expression for a saturated soil. The third criterion can be applied to any test as a definition of failure.

Appendix 8 entitled 'Computations, Data Reduction and Results' gives the details of the computations which were carried out on the triaxial test results; including strain, volume change, cross-sectional area during testing, etc.. Data reduction (and computation) was accomplished using simple computer programs which are listed in the Appendix 8, together with the test results, summarised in tabular form.

Chapter 9 brings together triaxial test results from ten investigations, including the author's, and subjects them to numerical and graphical analyses based on the theory developed by Fredlund et al(1978) for the shear strength of unsaturated soils. The results of these analyses, and the author's test results themselves, are discussed in chapter 10.

CHAPTER 9

TEST RESULTS

Chapter 9 Test Results

9.1 Introduction

The objective of this research is to demonstrate, using test results from this and other investigations, the general applicability of the shear strength equation for unsaturated soils suggested by Fredlund et al(1978). The shear strength equation stated in terms of stress state variables is:

$$\tau = C' + (\sigma - U_a) \tan\phi' + (U_a - U_w) \tan\phi^b$$

where C' = cohesion intercept when the two stress state variables are zero.

ϕ' = the friction angle with respect to changes in $(\sigma - U_a)$ when $(U_a - U_w)$ is held constant.

ϕ^b = the friction angle with respect to changes in $(U_a - U_w)$ when $(\sigma - U_a)$ is held constant.

Conceptually, the equation can be visualized as a 3-dimensional plot with matrix suction plotted on the third axis. The validity and credibility of the form of this equation are based on the assumption that the Mohr-Coulomb failure envelope of an unsaturated soil is a planar failure surface in a 3-dimensional plot between two stress state variables and shear strength. For the particular form of the equation given above, as the soil approaches 100% saturation, Ua approaches Uw and the matrix suction component becomes 0. The remainder of the equation represents the shear strength of a saturated soil. In other words, the shear strength equation for saturated soils is a particular case of the more general shear strength equation for unsaturated soils.

Test results from various investigations, including the

author's, are analysed on a common basis using a numerical method and a 2-dimensional graphical method. Both of these methods were presented by Ho(1981) as a means of evaluating the friction angle with respect to matrix suction, ϕ^b. They do not confirm that the failure surface is planar. In order to investigate the form of the failure surface, the same test results are used in a 3-dimensional graphics program which plots stress state variables as abscissas against shear strength as ordinate. The resulting plots give an immediate visual impression of the failure surface and assess the validity of Fredlund's suggestion of a planar failure surface. At present, it is not possible to evaluate the angle ϕ^b using the 3-dimensional graphical method.

This chapter presents a brief description of the three methods used to analyse the results and lists each of the investigations in turn. Discussion of all the results presented follows in Chapter 10.

9.2 Methods of analysis

(i) The numerical method(after Fredlund et al.1978;Ho.1981)

The numerical method is basically a geometrical interpretation of the three-dimensional plot between the shear strength and the stress state variables. The advantage of this method is that the entire numerical manipulation can be easily done through computer programming.

In the following discussion, only the stress state variables [1/2(σ1+σ3)-Ua] and (Ua-Uw) will be used as discussed in Chapter

5. The other combinations could be considered with a similar outcome. The corresponding equation for the plane through the stress points is:

$$1/2(\sigma 1-\sigma 3) = d'+[1/2(\sigma 1+\sigma 3)-Ua]\tan\nu' + (Ua-Uw)\tan\nu^{b} \qquad (9.1)$$

where d' = the intercept when the two stress points are zero
ν' = the angle between the stress point plane and the [1/2(σ1+σ3)-Ua] axis when (Ua-Uw) is held constant

ν^{b} = the angle between the stress point plane and the (Ua-Uw) axis when [1/2(σ1+σ3)-Ua] is held constant

The shear strength equation defining the Mohr-Coulomb planar failure surface using the stress state variables (σ - Ua) and (Ua-Uw) is:

$$\tau = C' + (\sigma - Ua)\tan\phi' + (Ua-Uw)\tan\phi^{b} \qquad (9.2)$$

Figure 9.1 views the strength data parallel to the (Ua-Uw) axis. The conversions for the zero matrix suction plane (Bishop et al,1960) are:

$$\sin\phi' = \tan\nu' \qquad (9.3)$$

and $$C' = d'/\cos\phi' \qquad (9.4)$$

From the definitions of ϕ^{b} and ν^{b}

$$\tan\phi^{b} = \Delta\tau c/\Delta(Ua-Uw) \qquad (9.5)$$

and $$\tan\nu^{b} = \Delta\tau d/\Delta(Ua-Uw) \qquad (9.6)$$

where $\Delta\tau c$ = change in shear strength between the saturated soil failure envelope and the failure envelope corresponding to a particular (Ua-Uw) value
$\Delta\tau d$ = change in shear strength between the saturated soil failure envelope through the stress points and the failure envelope through the stress points at a particular (Ua-Uw) value

Combining equations 9.5 and 9.6 gives:

$$\tan\phi^{b}/\Delta\tau c = \tan\nu^{b}/\Delta\tau d \qquad (9.7)$$

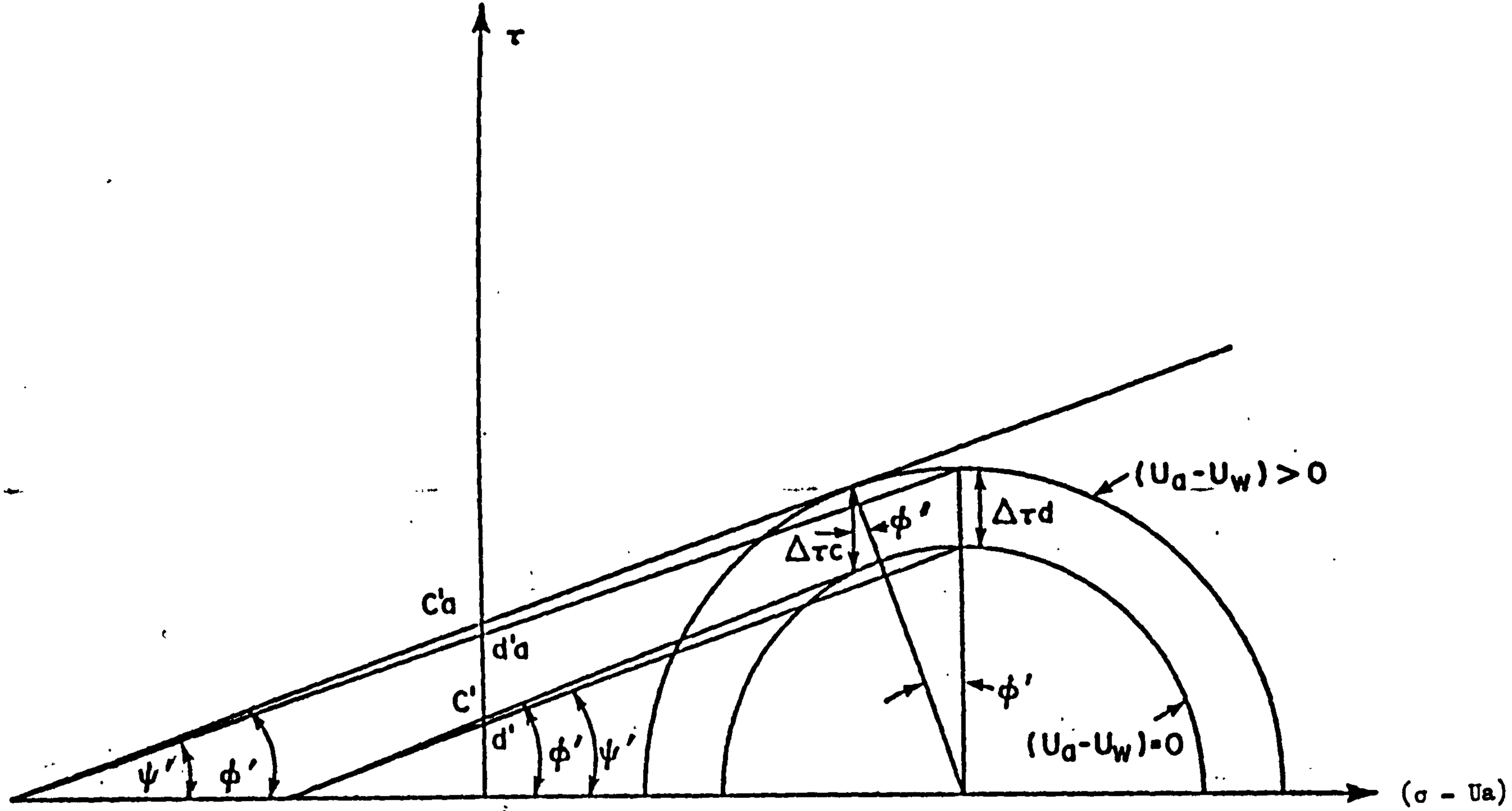

Fig.9.1: Failure circles looking parallel to (Ua - Uw) axis to compare failure envelopes.

Considering the shear strength axis in figure 9.1, gives:

$$\Delta\tau_c = C_a' - C' \qquad (9.8)$$

$$\Delta\tau_d = d_a' - d' \qquad (9.9)$$

where C_a' = the cohesion intercept of the failure envelope at a matrix suction (Ua-Uw)
d_a' = the cohesion intercept at a matrix suction (Ua-Uw) using the stress point method

Since ϕ' is constant for all matrix suction values.

$$\Delta\tau_d = (C_a' - C')\cos\phi' \qquad (9.10)$$

Substituting equations (9.8) and (9.10) into (9.7), gives:

$$\tan\phi^b = \tan\psi^b/\cos\phi' \qquad (9.11)$$

In order to compute ϕ^b, it is evident that ψ^b has to be obtained first. Viewing along the saturated soil failure envelope(figure 9.2,plane ABEF), if the matrix suction variable does not contribute to the shear strength, the three-dimensional failure surface viewed along the (Ua-Uw) axis should appear as a line. However, the existence of (Ua-Uw) does increase the shear strength by $\Delta\tau_d$, though [1/2(61+63)-Ua] remains the same (figure 9.2). From figures 9.2 and 9.3, it can be seen that ψ^b can be related to ψ' mathematically by using the angle d_a as a medium. By geometry, the right angle triangle BCD in figure 9.3 gives:

$$CB = \Delta\tau_d \cos\psi' \qquad (9.12)$$

Similarly, the right angle triangle ABC provides

$$\tan d_a = CB/\Delta(Ua-Uw) \qquad (9.13)$$

Combining equations (9.12) and (9.13) yields

$$\tan d_a = \Delta\tau_d \cos\psi'/\Delta(Ua-Uw) \qquad (9.14)$$

Substituting equation (9.6) into (9.14) gives

$$\tan\psi^b = \tan d_a/\cos\psi' \qquad (9.15)$$

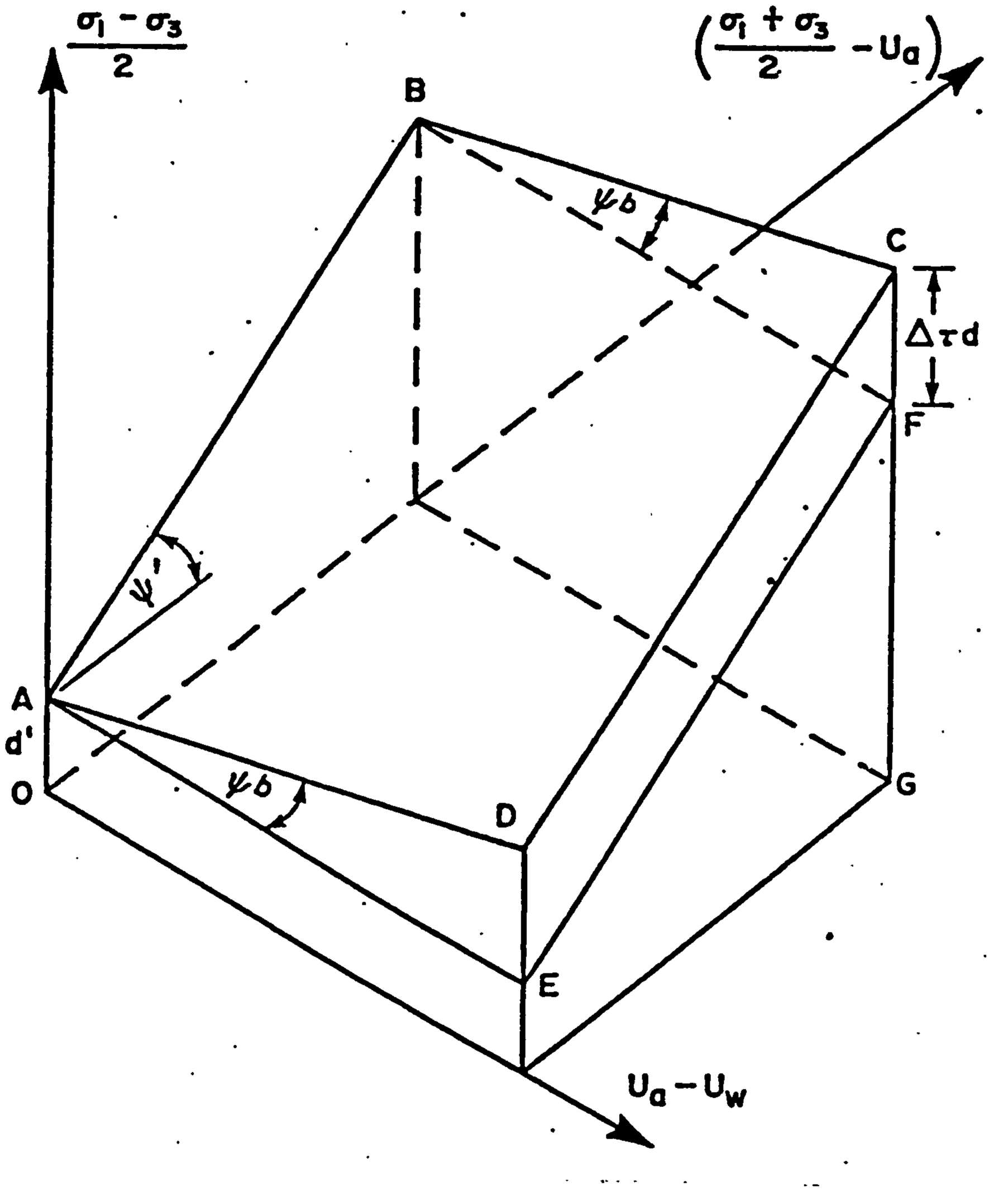

Fig.9.2: Three-dimensional failure surface using the stress point method (after Ho,1981).

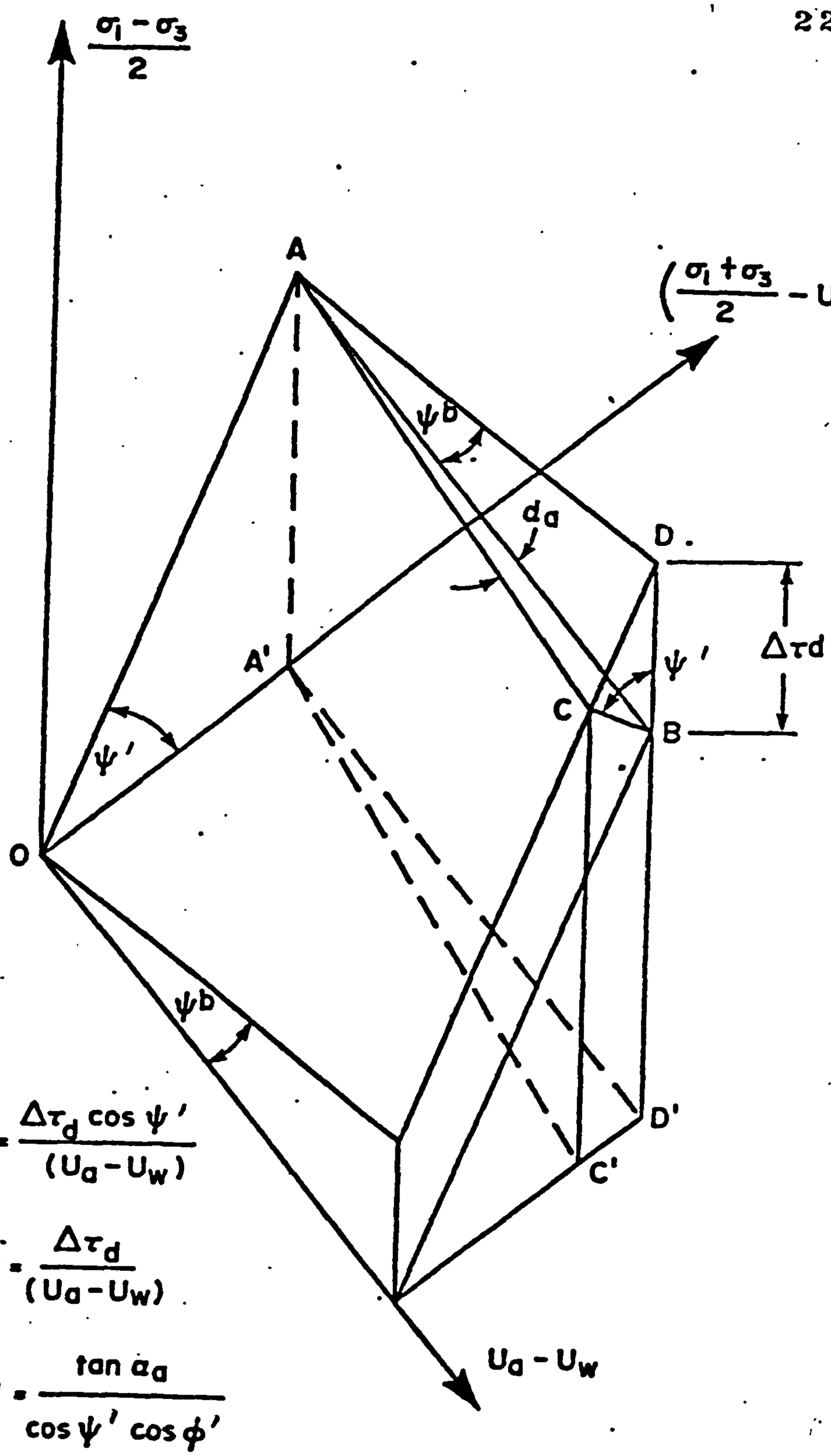

$$\tan d_a = \frac{\Delta\tau_d \cos\psi'}{(U_a - U_w)}$$

$$\tan \psi^b = \frac{\Delta\tau_d}{(U_a - U_w)}$$

$$\tan \phi^b = \frac{\tan \alpha_a}{\cos\psi' \cos\phi'}$$

Fig.9.3: Failure surface showing projection of shear strength onto the saturated strength plane (after Ho,1981).

Substituting equation (9.11) into (9.15) gives

$$\tan \phi^{b} = \tan \alpha_a / (\cos \psi' \cos \phi') \qquad (9.16)$$

The saturated soil shear strength parameters, C′ and ϕ' can be readily obtained from conventional triaxial test data. With equations (9.3) and (9.4), the corresponding ψ' and d′ can be obtained. The values of $\bar{\sigma}1$, $\bar{\sigma}3$, Ua and Uw of an unsaturated soil sample at shear failure can also be found by running an appropriate test. Consequently, 1/2($\bar{\sigma}1$-$\bar{\sigma}3$), [1/2($\bar{\sigma}1$+$\bar{\sigma}3$)-Ua] and (Ua-Uw) at failure can all be calculated. From equation 9.1, the projected shear strength, 1/2($\bar{\sigma}1$-$\bar{\sigma}3$) at the saturation plane can be obtained. Subtracting the projected shear strength from 1/2($\bar{\sigma}1$-$\bar{\sigma}3$) at failure gives $\Delta\bar{\tau}d$. With several sets of triaxial test data, a plot between $\Delta\bar{\tau}d\cos\psi'$ and (Ua-Uw) can be made. From the plot, the angle α_a can be obtained. Finally, with equations (9.16) and (5.8), the remaining shear strength parameters, ϕ^{b} and $\phi^{\bullet}$ can be calculated.

According to Fredlund, the $\Delta\bar{\tau}d\cos\psi'$ versus matrix suction plot should be a positively sloping straight line passing through the origin. When there is no matrix suction, a soil should not exhibit any extra shear resistance only that governed by Terzaghi's shear strength theory for saturated soils. Consequently, the $\Delta\bar{\tau}d\cos\psi'$ intercept which appears in the $\Delta\bar{\tau}d\cos\psi'$ versus matrix suction plot can be used as a refinement to the input of effective cohesion C′ obtained from saturated soil testing.

A short computer program, 'ANGLE' has been written for the numerical manipulations. The program listing is given in appendix 8.

(ii) The 2-dimensional graphical method(after Ho,1981)

The 2-dimensional graphical method which was mentioned in chapter 5, section 2, is an alternative to the numerical method and, in the absence of any computer facility, this method as described by Ho is recommended as a graphical alternative to the numerical method.

When (σ - Ua) and (Ua-Uw) are used, the shear strength equation is as follows:

$$\tau = C' + (\sigma - Ua)\tan\phi' + (Ua-Uw)\tan\phi^b \qquad (9.17)$$

Graphically, the equation can be visualized as a planar failure envelope on a three-dimensional plot using the stress state variables, (σ - Ua) and (Ua-Uw) as abscissas (see figure 5.3(a)). By viewing along the matrix suction axis, the equation can also be visualized as a two-dimensional graph with matrix suction contoured as the third variable (see figure 5.3(b)). Consequently, the ordinate intercepts of the various matrix suction contours can be plotted versus matrix suction to give the friction angle ϕ^b (see figure 5.4).

From conventional triaxial tests on saturated soil samples, the saturated soil shear strength parameters, C' and ϕ' can be readily obtained. With the values of σ_1, σ_3, Ua and Uw at failure from triaxial tests on unsaturated soil samples, Mohr circles corresponding to various matrix suction values can be drawn on a (σ - Ua) versus shear strength plot(figure 9.4). With the known angle of friction ϕ', the ordinate intercepts of the various matrix suction contours can then be found. Either by plotting or by linear regression analysis on the ordinate

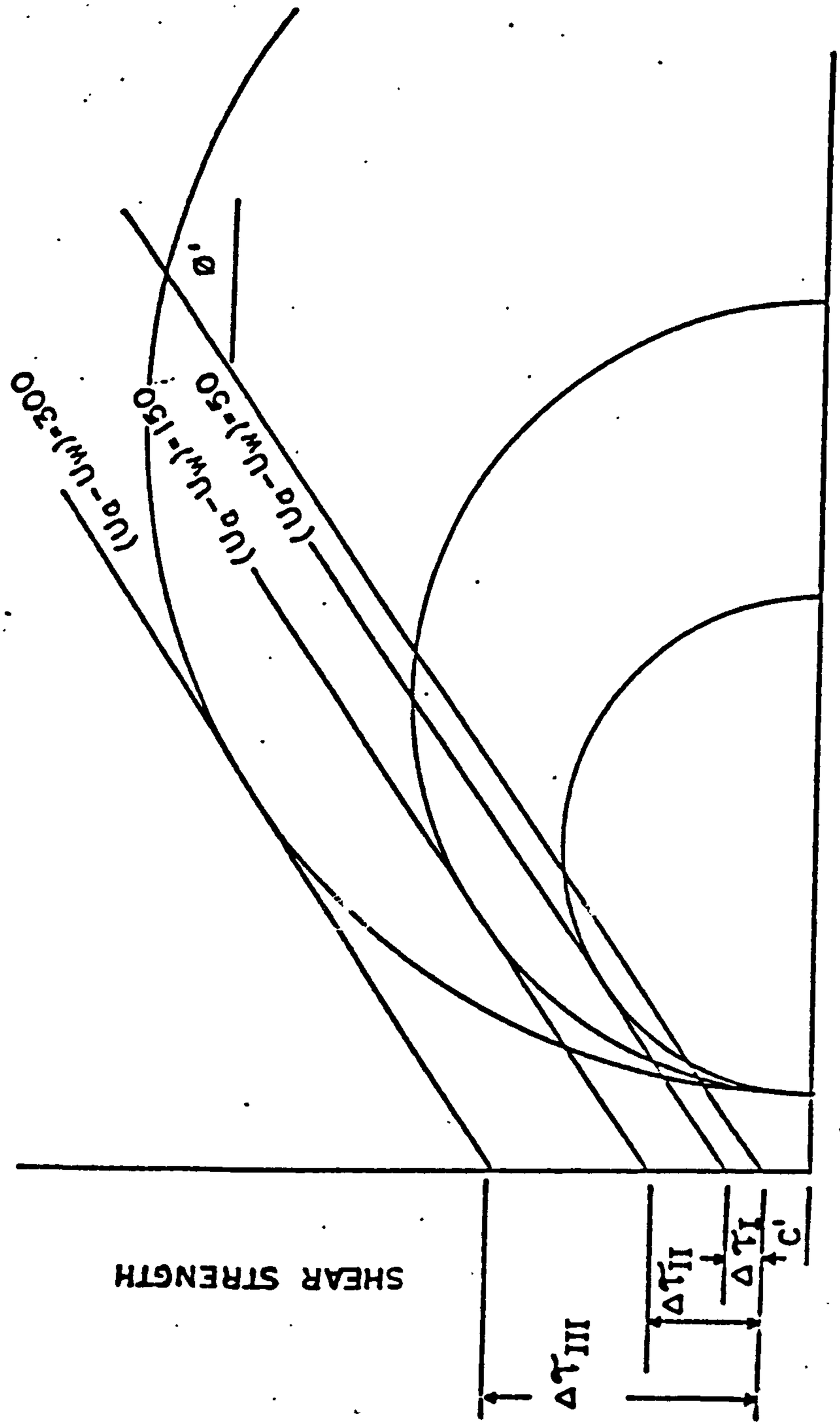

Fig.9.4: Interpretation of a multi-stage triaxial test to get the angle of friction with respect to matrix suction (after Ho,1981).

intercepts versus matrix suction data, the friction angle ϕ^b of the unsaturated soil in question can be obtained(figure 9.5). The resulting cohesion intercept in the ordinate intercept versus matrix suction plot can also be regarded as a correcting factor to the known cohesion intercept obtained from conventional tests on saturated samples. If ϕ' is required, equation 5.8 can be used to find the remaining unsaturated soil shear strength parameters.

(iii) The 3-dimensional graphical method

Since the independent published research data on unsaturated soils are usually random and scattered, it is impossible to identify positively any warping of the three-dimensional plane by means of the two-dimensional analysis mentioned above.

Recently, subroutine packages have been developed for drawing 3-dimensional sufaces defined randomly in the (X,Y) plane (i.e. Z=f(x,y)). The GINOSURF subroutine can generate a regular rectangular grid of surface heights from random surface heights. It also interpolates from a set of random surface heights to produce a regular rectangular grid of surface heights over an area of the (X,Y) plane(for details, see appendix 2).

All the test results available to the author have been used with this subroutine to produce three-dimensional plots of the failure surface. Fredlund et al (1978) stated that any combination of stress state variables as abscissas with the shear strength as ordinate should result in a planar failure surface. In order to test this hypothesis, the three-dimensional

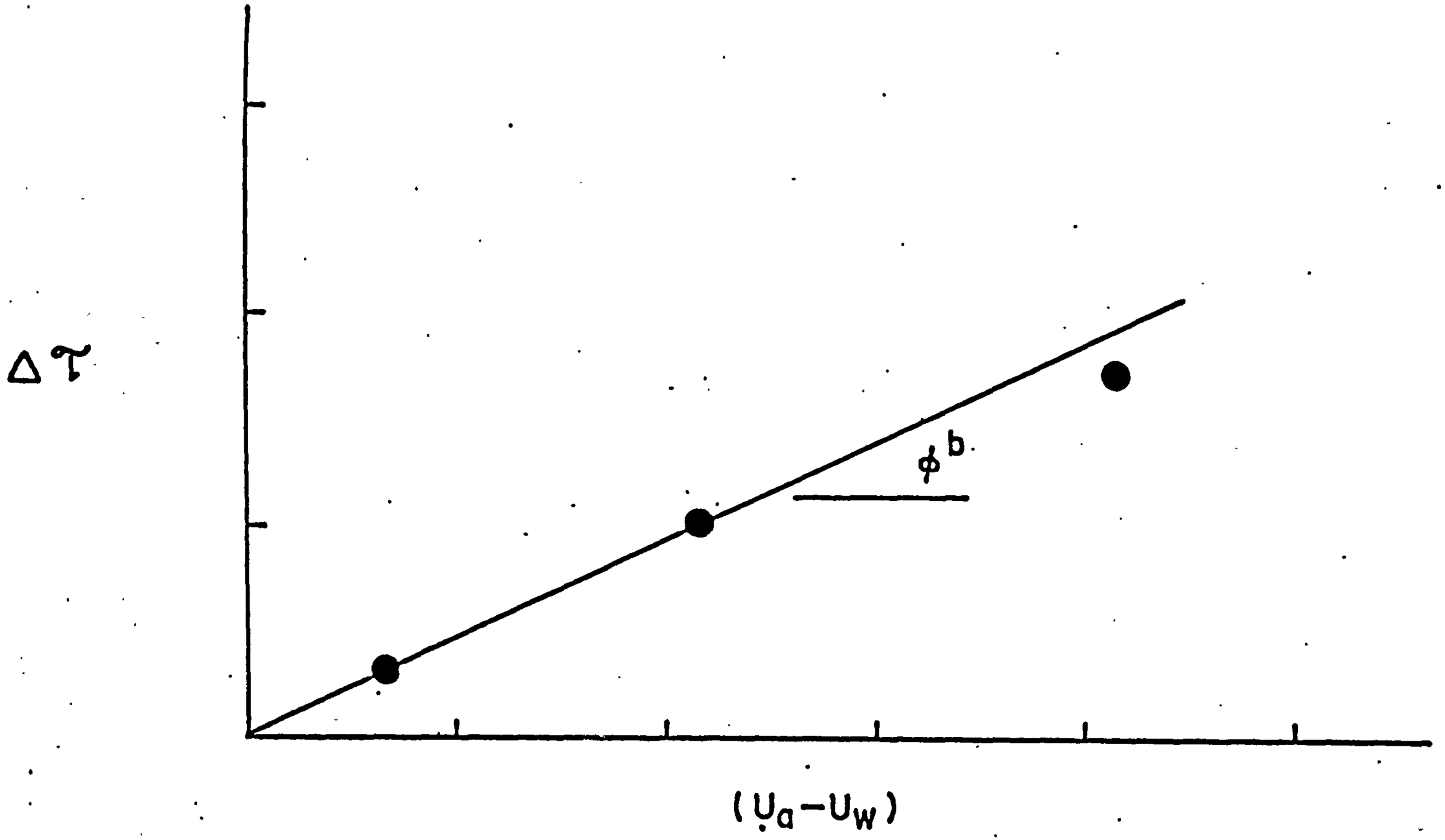

Fig.9.5: Determination of the angle of friction with respect to matrix suction, ϕ^b (after Ho,1981).

plots are presented as follows(figure 9.6):

Top plot: x-axis = (Ua - Uw)f

y-axis = [(σ1+σ3)/2 - Ua]f

z-axis = (σ1 - σ3)f/2

Middle plot: x-axis = (Ua - Uw)f

y-axis = [(σ1+σ3)/2 - Uw]f

z-axis = (σ1 - σ3)f/2

Bottom plot: x-axis = [(σ1+σ3)/2 - Ua]f

y-axis = [(σ1+σ3)/2 - Uw]f

z-axis = (σ1 - σ3)f/2

Figure 9.6 shows the axes used in the three-dimensional plots and the angles subtended by an ideally planar failure surface. To make comparisons easier, all three plots of test results for a particular soil are shown on the same page. Figure 9.7 shows a typical set of 3-dimensional plots obtained using the subroutine. The number of grid lines is directly proportional to the number of data input points. Areas of insufficient data are associated with sharp peaks and troughs in the 3-dimensional plots. If no scale multiplier is shown for the X, Y or Z axes then it can be taken as unity. The units are shown on each set of plots.

9.3 Experimental results

This section presents, where available, details of the soil type(s) and the type of test(s) used in ten investigations, including the author's. The results of applying the numerical

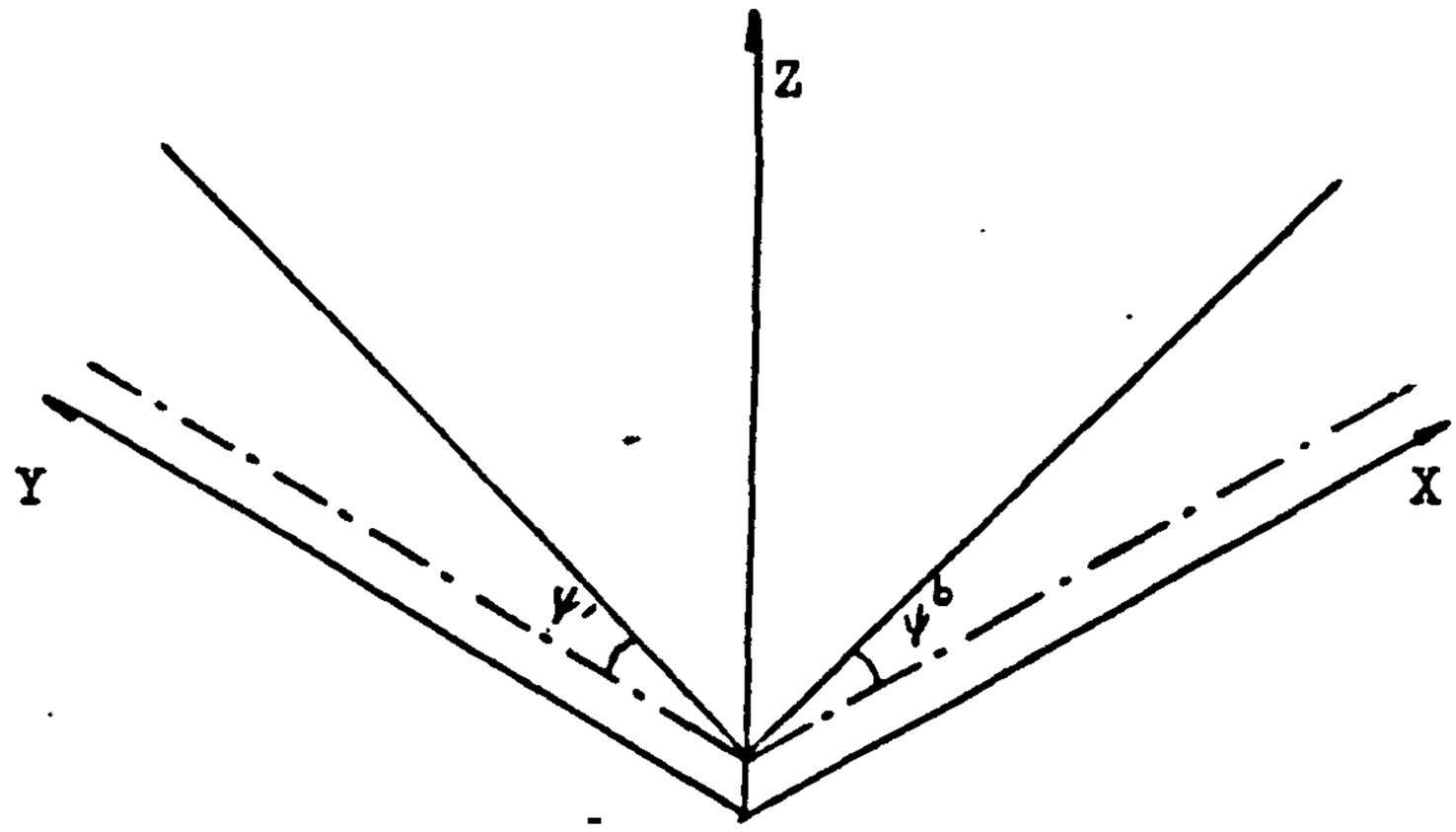

(a) Plot 1

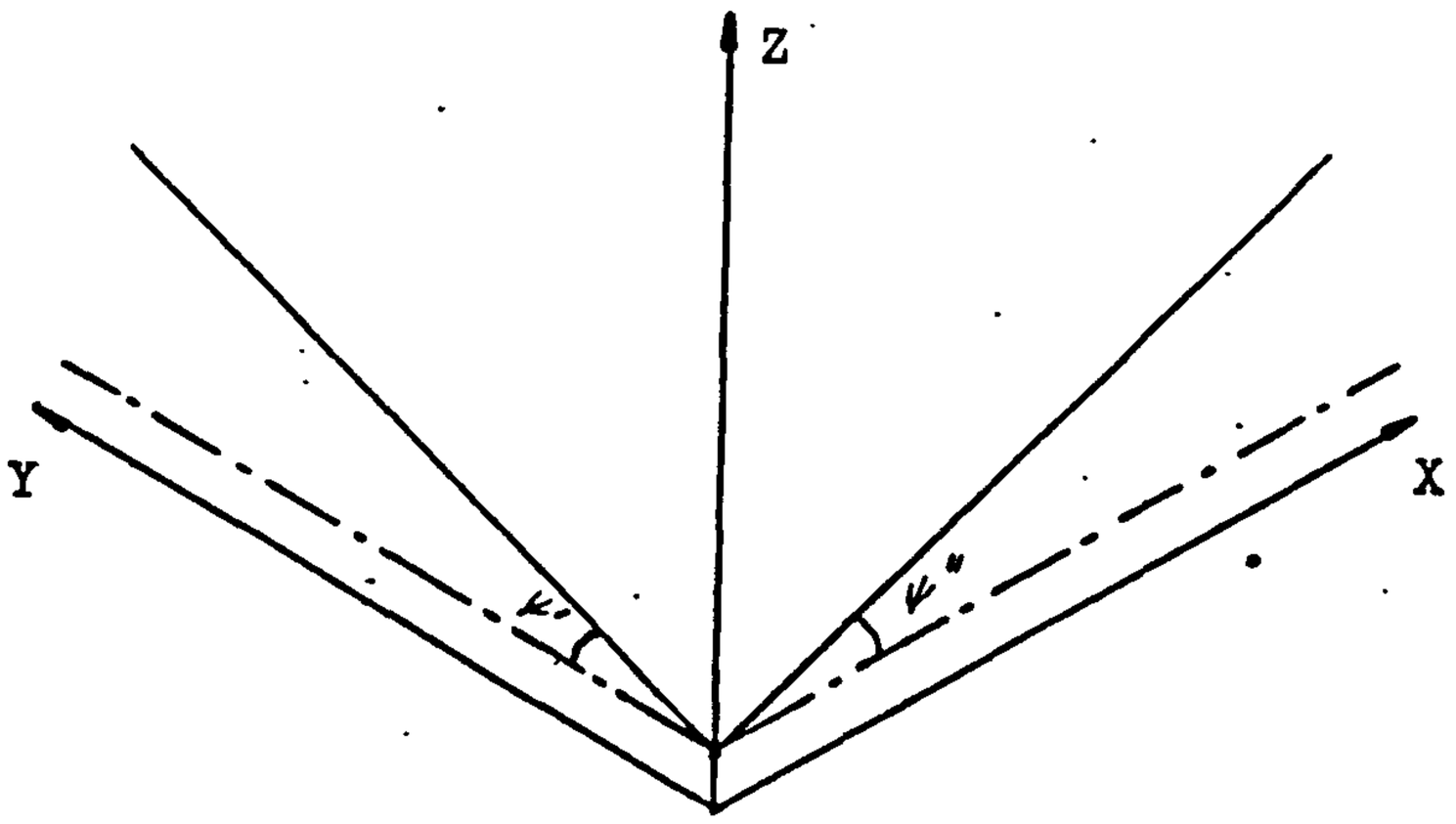

(b) Plot 2

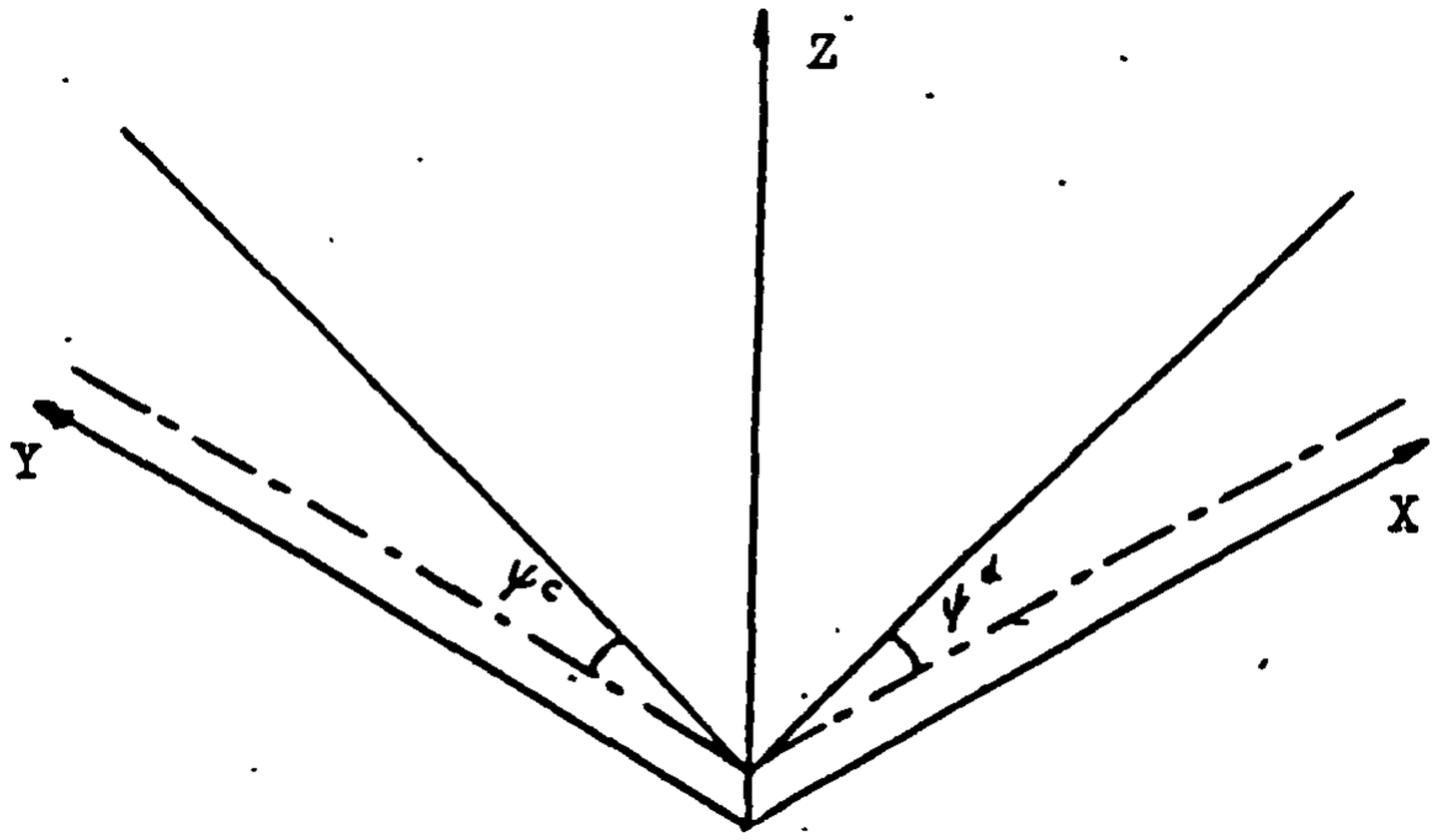

(c) Plot 3

Fig.9.6: Three-dimensional plots and the angles subtended by an ideally planar failure surface.

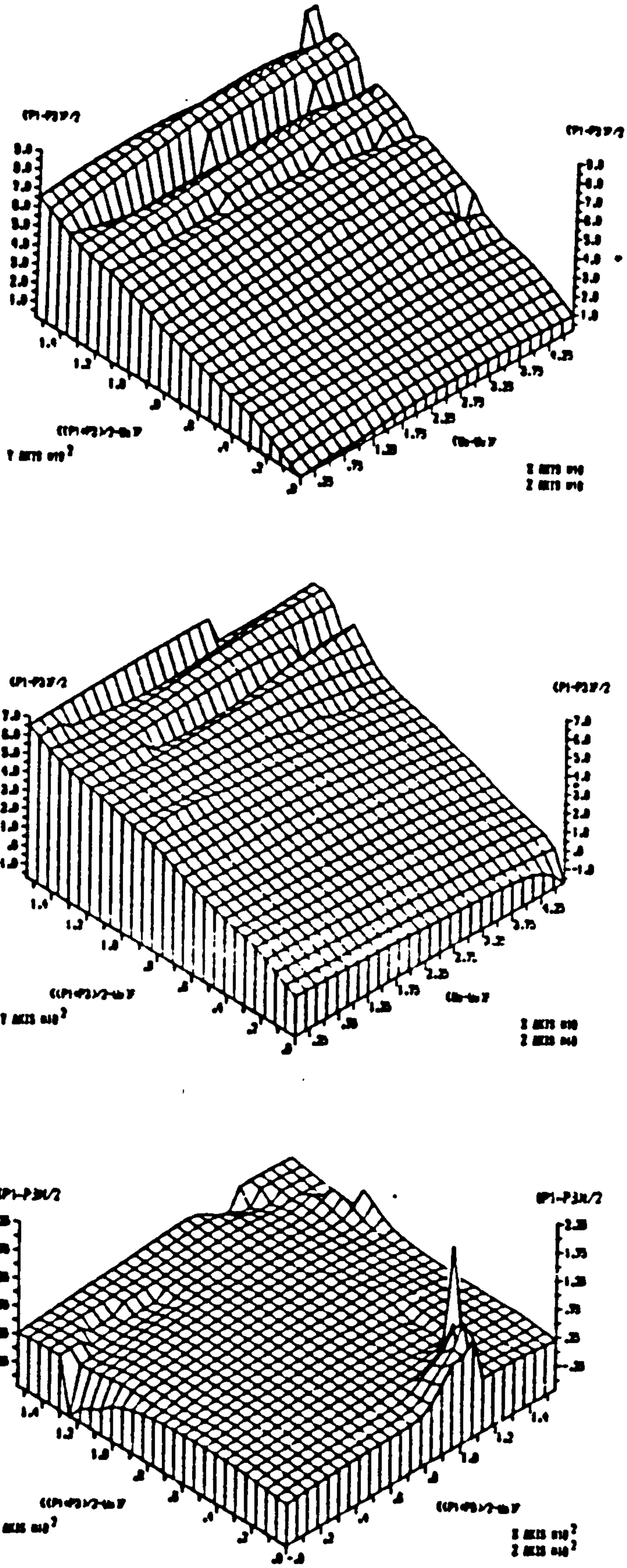

(UNITS IN POUNDS PER SQ. INCHES)

FIG.9.7: SHEAR STRENGTH DATA FOR MANGLA SHALE UNDER CW CONDITION (BLIGHT,1961)(FAILURE CRITERION: MAX. STRESS RATIO i.e. $(\sigma_1-\sigma_3)/(\sigma_3-U_w)$).

method, the 2-dimensional graphical method and the 3-dimensional graphical method to the triaxial test results obtained in these investigations are presented in Appendix 8, beginning from page A133. Subsequently, frequent reference will be made to the results presented in Appendix 8. Where specific points require clarification, brief comments are made at this stage on the results of some of the investigations, but the bulk of the discussion is presented in the next Chapter.

The first two methods (i.e. numerical and 2-dimensional) are very similar, so for most of the investigations only the results obtained using the numerical method are presented. In this method, the saturated soil parameters C′ and Ø′ were used as input data and their values are shown first for each set of numerical method results(e.g. on page A133). Linear regression was used to obtain the angle $Ø^{b}$ from data points which included the value of C′ for a fully saturated soil. From the resulting best straight line the new intercept(corrected C′) and the correlation coefficient, r, of the data could be found. The angle Ø° was also obtained, for use with an alternative set of stress state variables to that used in equation 9.2.

When the 2-dimensional graphical method was used, the results follow directly after those obtained using the numerical method. Lastly, the 3-dimensional plots are presented and, where available, the results of tests on saturated soil samples have been included in the plots.

Table 9.1 at the end of this Chapter summarises all the results obtained using the numerical and 2-dimensional graphical methods.

9.3.1 Bishop et al(1960)

Bishop et al(1960) performed triaxial tests on compacted shale and Boulder clay. The soil properties were as follows:

soils	type of shear test	compacted water content	clay content	*C′ KPa	*Ø′
shale	constant-water content	18.6 %	22 %	15.8	24.8
Boulder clay	constant-water content	11.6 %	18 %	9.6	27.3

* obtained from saturated soil specimens

The numerical method and the two-dimensional graphical method were applied to the results of Bishop et al. It is clear that both methods give very similar results for angle $\emptyset_b$.

Compacted shale: $\emptyset_b = 18.6^o$ (numerical); 18.1^o (graphical)

Boulder clay: $\emptyset_b = 22.2^o$ (numerical); 21.7^o (graphical)

The numerical method results, the 2-dimensional graphical method results and the 3-dimensional plots are shown on page A133-A140. For this investigation, the graphs associated with the 2-dimensional graphical method have been presented.

9.3.2 Donald(1961)

In 1961, Donald studied the mechanical properties of saturated and partly-saturated soils with special reference to the influence of negative pore water pressure. Truly undrained tests, constant water-content tests, drained tests and overdrained tests were carried out. The soil properties were as

follows:

soil	liquid limit	plastic limit	S.G.	*C′ KPa	*Ø′
London clay	66%	27%	2.75	0	20.3
Braehead silt	29%	23%	2.76	0	33.4

*obtained from saturated soil specimens

The numerical method results and 3-dimensional plots are shown on page A141-A145.

9.3.3 Blight(1961)

In 1961, Blight presented several sets of triaxial test data for unsaturated soils from his study on strength and consolidation characteristics of compacted soils.

The properties of the soils were as follows:

soils	S.G.	L.L. %	P.L. %	clay fraction %	compacted water content %	*C′ psi	*Ø′
Mangla shale (silty clay)	2.79	38.2	21.6	21	16 to 18.5	1.5	24.1
Talybont clay (sandy silt)	2.69	--	--	4	6.7 to 7.67	0	36.3
selset clay	2.70	33.1	16.6	20	11.5	0	26.4
Vaich moraine	2.65	--	--	--	1.9 to 8.0	0	38

*obtained from saturated soil specimens

Two types of tests were performed on the saturated specimens: consolidated undrained and consolidated drained.

All the tests on partly saturated soils were carried out at constant moisture content. The samples, at their compaction moisture contents, were allowed to come to equilibrium under the required confining pressure (63-Ua). They were then sheared with measured pore air and pore water pressures. Two different failure criteria were used by Blight; max. stress ratio and max. deviator stress. The numerical method results and the 3-dimensional plots are shown for both failure conditions on page A146-A155.

9.3.4 Matyas(1963)

In 1963, Matyas studied the compressibility and shear strength of compacted soils using Selset Boulder clay and Red Sasumua clay under constant water-content conditions.

The properties of the soils were as follows:

Compacted specimens	L.L.	P.L.	P.I.	S.G.	*C'psi	*Ø'
Selset Boulder clay	35%	17%	18%	2.71	1.3	24.7
Red Sasumua clay(1958)	93%	67%	26%	2.90	3.6	34.0
Red Sasumua clay(1962)	107%	70%	37%	2.94	3.9	32.6

*obtained from saturated soil specimens.

For the red Sasumua clay, the three-dimensional program was unable to execute the first two plots when the results from tests on saturated samples were included. This may have been due to a numerical problem related to the distribution of the results. For the unsaturated samples tested by Matyas, there was little variation in the value of matrix suction at failure, and

for the saturated samples the matrix suction was zero. Hence two 'lines' of results would be plotted in the Z-Y plane with very few data points between them. This may have caused problems for the program. Due to the change in variables, the third plot was not affected by this problem.

The numerical method results and 3-dimensional plots are shown on page A156-A160.

9.3.5 M.I.T.(1963)

A series of triaxial tests was run at M.I.T. in 1963 on an artificial mixture (by weight) of 80 % Potters flint and 20 % Peerless clay. The samples were compacted at a water content of 17.5 %, 3 % dry of optimum. The dry density was 1.6 Mg/m^3. The specimens were tested at a constant water content. The saturated specimens gave an effective angle of internal friction, $\emptyset' = 35.6$ and an effective cohesion $C' = 0.0$ KPa.

The numerical method results and 3-dimensional plots are shown on pages A161 and A162.

9.3.6 Gulbati(1972)

In 1972, Gulhati investigated the shear behaviour of compacted soils in the saturated and partially saturated states using three naturally occurring soils ranging from clayey silt to silty clay. The soils were Delhi silt, Ghagger clay and Dhanauri clay, which were tested under constant water-content and drained conditions. Classification data are tabulated below:

	Delhi silt A	Delhi silt B	Ghagger clay	Dhanauri clay
L.L. %	32	33	50	51
P.L. %	22	23	25	30
P.I. %	10	10	25	21
Sand size content%	15	29	4	1
Silt size content%	70	57	58	64
Clay size content%	15	14	38	35
Activity	0.67	0.71	0.66	0.60
S.G. of soils	2.67	2.67	2.77	2.81
*C′ (KN/sq.m)	0	0	--	11
*Ø′ (degrees)	38.4	38.4	--	29.1

*obtained from saturated soil specimens.

The numerical method results and 3-dimensional plots are shown on page A163-A169.

No results were presented for tests on Ghagger clay and the Delhi silt results did not distinguish between silt A and silt B. The three-dimensional plots for Delhi silt are shown twice, the second incorporating a sample area correction factor. The correction factor has little effect on the nature of the failure surface.

9.3.7 Satija(1978)

Satija conducted four series of constant water content and consolidated drained tests on compacted Dhanauri clay. The samples were divided into two types of high and low as-compacted densities. Both the constant water content and

consolidated drained tests were performed at each of the compaction conditions. Although the samples for a particular series of tests were compacted at the same density and water content, they were subjected to various initial stress states before being sheared. In an attempt to observe any warping of the failure surface, the initial stress states of the samples were set to form an equally spaced grid.

The properties of the Dhanauri clay were as follows:

L.L.=48.5%; P.L.=25%; sand=5%; silt=70%; clay=25%

The saturated soil shear strength parameters were:

For dry density = 14.5 KN/cu.m,

$C' = 20$ KN/sq.m and $\emptyset' = 29^{o}$ (drained tests)

$C' = 11$ KN/sq.m and $\emptyset' = 29^{o}$ (constant water-content)

For dry density = 15.5 KN/cu.m,

$C' = 37$ KN/sq.m and $\emptyset' = 28.5^{o}$ (drained tests)

$C' = 16$ KN/sq.m and $\emptyset' = 28.5^{o}$ (constant water-content)

The numerical method results, the 2-dimensional graphical method results and 3-dimensional plots are shown on page A170-A176.

9.3.8 Escario(1980)

Escario(1980) presented the results of a series of direct shear tests performed on compacted samples of Madrid Gray clay. For these results, only the two-dimensional graphical method was applied, see page A177-A179. It was not possible to use the numerical method because the original test data was not available. The soil had a L.L. of 81% and P.L. of 38%. The

initial compaction conditions consisted of a dry unit weight of $13.1\ KN/m^3$ and a water content of 29%. The direct shear box was enclosed and had a high air entry disc sealed in the base to maintain a constant matrix suction during shear.

The saturated soil shear strength parameters were:

$C' = 0\ KN/sq.m$ and $\emptyset' = 22.5^{o}$

9.3.9 Ho(1981)

Ho carried out an investigation on the shear strength of two unsaturated Hong Kong soils, namely, decomposed granite and rhyolite. The mineral compositions of these two residual soils are essentially the same, including quartz, orthoclase, plagioclase and biotite. The main difference between the two soils is their grain size distribution. In general, the decomposed granite has a sand size texture, whereas the decomposed rhyolite has a medium to fine silt size texture. Both residual soils are brittle and highly variable. Undisturbed samples were obtained from test drilling or open cuts at various sites on the Hong Kong island.

The saturated soil shear strength parameters were:

For decomposed granite:

$C' = 28.9\ KN/sq.m$ and $\emptyset' = 33.4^{o}$

For decomposed rhyolite:

$C' = 7.35\ KN/sq.m$ and $\emptyset' = 35.3^{o}$

In order to obtain the maximum amount of information from a limited number of tests and eliminate the effect of

variability in residual soils, a drained multi-stage test procedure was used.

The numerical method results and 3-dimensional plots are shown on page A180-A188. In Appendix 8, the numerical method was applied to the results of each individual sample and then to the results from all the samples of each soil type. The 3-dimensional plots are based on the results from all the samples.

9.3.10 Author's results

The properties of the Grangemouth clay used by the author were given in section 8.2 of chapter 8. The saturated soil shear strength parameters were:

$$C' = 6.7 \text{ KN/sq.m and } \emptyset' = 34.2^{o}$$

Three types of tests were conducted: constant water-content tests, drained tests and unconfined tests. The test programme was described in detail in chapter 8. Tables A8.1 and A8.2 on pages A194 and A195, list the stress conditions at failure for series I and series II tests, respectively.

The numerical method results and 3-dimensional plots are shown on page A189-A193.

9.4 Summary

The following table is a summary of all the results obtained from applying the numerical method and the two-dimensional graphical method. The column headings are explained below:

clay content/PI = clay content and/or plastic index of soil

Input C′ = effective cohesion obtained from tests on saturated soil specimens

Input Ø′ = effective angle of internal friction obtained from tests on saturated specimens

corrected C′ = value of intercept on shear strength axis obtained from linear regression in numerical method or 2-dimensional graphical method

$\emptyset^b$ = friction angle with respect to changes in (Ua-Uw) when (б-Ua) is held constant

$\emptyset^*$ = friction angle with respect to changes in (Ua-Uw) when (б-Uw) is held constant

r = correlation coefficient with respect to the computation of $\emptyset^b$ (i.e. refers to the best-fit line for $\emptyset^b$)

All the results were obtained using numerical method. If the 2-dimensional graphical method was used, the results are shown in brackets.

Table 9.1 : SUMMARY OF ALL RESULTS OBTAINED FROM NUMERICAL METHOD AND TWO DIMENSIONAL GRAPHICAL METHOD

Investigator (s)	soils	clay content	PI	No. of tests	Input c' kN/m^2	Input ϕ' °	corrected c' kN/m^2	ϕ^b	ϕ''	r	comments
Bishop et al (1960)	compacted shale	22%	—	8	15.8	24.8°	4.99 (23.2)	18.61 (18.1°)	-7.15° (-7.70°)	0.98 (0.97)	CW tests
	compacted Boulder clay	18%	—	8	9.6	27.3°	3.29 (14.3)	22.19° (21.7°)	-6.18° (-6.74°)	0.97 (0.97)	CW tests
Donald (1961)	Remoulded London clay	55%	39%	42	0	20.3°	16.34	10.44°	-10.52°	0.71	Undrained tests
	Remoulded Braehead silt	53%	6%	9	0	33.4°	8.55	8.72	-26.84	0.64	CW tests
				21	0	33.4°	3.38	16.93	-19.55	0.92	D tests
				3	0	33.4°	4.41	18.58	-17.92	0.99	overdrained tests
Blight (1961)	Talybont	4%	—	30	0	36.3°	14.62	5.98°	-32.2°	0.61	failure condition : max. stress ratio
				30	0	36.3°	20.34	4.23°	-33.45°	0.48	failure condition : max. deviator stress CW tests
	Mangla	21%	16.6 %	27	10.34	24.1°	21.17	14.89°	-10.28°	0.92	max. stress ratio
				27	10.34	24.1°	16.83	16.27°	- 8.84°	0.93	max. deviator stress CW tests
	Selset clay	20%	16.5 %	15	0	26.4°	10.28	20.54°	- 6.94°	0.96	max. stress ratio
				15	0	26.4°	5.10	21.15°	- 6.25°	0.97	max. deviator stress CW tests
	Vaich Moraine	0%	—	8	0	38°	9.17	1.17°	-37.26°	0.73	max. deviator stress CW tests

Investigator	soils	clay content	PI	No. of tests	Input c' kN/m^2	Input ϕ'	corrected c' kN/m^2	ϕ^b	ϕ"	r	comments
Escario (1980)	Madrid gray clay	30%	43%		0	22.5°	(0)	(16.1°)	(- 7.16°)	0.99	Shear box D tests
* Ho (1981)	Decomposed granite	—	—	3	28.9	33.4°	24.4 (31.20)	12.59° (12.40°)	-23.56° (-23.73°)	0.99	sample No.5
		—	—	3			20.46 (27.35)	36.77° (36.33)	5.03° (-8.09°)	0.95	sample No.6
		—	—	3			78.33 (102.70)	15.77° (14.63°)	-20.65° (-21.72°)	1.00	sample No.8
		—	4.3%	3			30.89 (44.00)	15.37° (16.18°)	-21.03° (-20.27°)	0.99	sample No.10
		4.5%	3.8%	3			43.63 (49.50)	12.74° (12.50°)	-23.43° (-23.60°)	0.98	sample No.20
		4.5%	—	3			43.8 (51.25)	12.74° (12.60°)	-23.42° (-23.60)	0.99	sample No.21
		14.0%	17.5%	3			22.05 (19.50)	22.45° (22.50)	-13.83° (-13.80°)	1.00	sample No.22
		3.0%	—	3			108.07 (138.00)	7.98° (8.00°)	-27.44 (-27.40°)	0.99	sample No.23
	Decomposed Rhyolite	6.5%	—	3	7.35	35.3°	21.5 (33.00)	11.65° (11.74)	-26.65° (-26.58°)	1.00	sample No.11A
		7.5%	—	3			46.82 (65.30)	9.88° (10.90)	-28.1° (-27.27)	0.96	sample No.11B
		12.0%	—	3			28.37 (36.00)	14.84° (15.90)	-23.9° (-22.94°)	0.99	sample No.11C
		5.0%	—	3			38.47 (56.00)	16.41° (15.41)	-22.47° (-23.38°)	1.00	sample No.11D
		10.0%	6.54%	3			9.63 (10.30)	13.02° (13.30)	-25.49° (-25.25)	0.96	sample No.12
		11.5%	9.26%	3			14.81 (16.70)	11.4° (11.74)	-26.86° (-26.58°)	0.95	sample No.14
		10.0%	6.39%	3			10.45 (12.00)	17.72° (17.70)	-21.24° (-21.25°)	0.94	sample No.15

Investigator	soils	clay content	PI	No. of tests	Input c' kN/m^2	Input ϕ'	corrected c' kN/m^2	ϕ^b	ϕ''	r	comments
Ho (1981)	Decomposed granite	No average value	—	24	28.9	33.4°	55.15	12.67°	-23.49°	0.51	all samples
	Decomposed Rhyolite	No average value	—	21	7.35	35.3°	24.29	13.59°	-25°	0.72	all samples
Wong (1984)	Grangemouth clay	15%	14%	10	6.7	34.2°	6.42	22.49°	-14.87	0.69	Series I : CW tests
				12	6.7	34.2°	18.69	5.88°	-29.97	0.53	Series I : D tests
				7	6.7	34.2°	14.89	12.05°	-24.99	0.99	Series I : U tests
				9	6.7	34.2°	-545.05	86.16	85.97	0.50	** Series II : D tests

CW tests = constant water-content tests
D tests = Drained tests
U tests = Unconfined tests
γ_d = dry density
w = moisture content
P I = Plastic index

All the results were obtained using numerical method.

* (Results of 2-dimensional graphical method were obtained from Ho (1981)'s thesis).

** *These values are not sensible. See page 271.*

If the 2-dimensional graphical method was used, the results are shown in brackets.

The next chapter presents a discussion of the results shown in appendix 8, with particular reference to Fredlund's theory and the hypothesis that the failure of an unsaturated soil can be represented on a three-dimensional plot, using stress state variables at failure, as a planar failure surface.

CHAPTER 10 DISCUSSION

Chapter 10 Discussion

10.1 General

The discussion of the results is broken down into various parts. First, for the author's tests, the values of parameters such as total and water volumes, deviator stress and matrix suction, degree of saturation and void ratio during testing are presented and discussed. Next, some general observations are made about the results of previous investigators and those of the author, particularly with respect to the numerical analysis and the 3-dimensional plots. This is followed by a more detailed discussion of particular aspects of all the test results. These include the significance of the correlation coefficient for angle $\emptyset^b$, the influence of percentage clay fraction on angle $\emptyset^b$ and the effect of test type on the test results.

10.2 Discussion of the author's tests

The following pages contain typical graphs which illustrate a number of characteristics of the tests conducted by the author. Fig.10.1 to 10.9 refer to series I tests and fig.10.10 to 10.13 refer to series II tests.

The first four figures are for drained tests. Fig.10.1 shows the change in total volume and water volume with respect to time, during the desaturation and consolidation stage. By definition, this stage must lead to a greater water volume change than total volume change. For the water volume change, the diffused air volume correction is indicated. In drained tests the suction should be maintained constant and Fig.10.2

Fig.10.1: THE CHANGE OF TOTAL & WATER VOLUMES DURING DESATURATION & CONSOLIDATION VS. SQR(TIME) (SERIES I:DRAINED TEST)

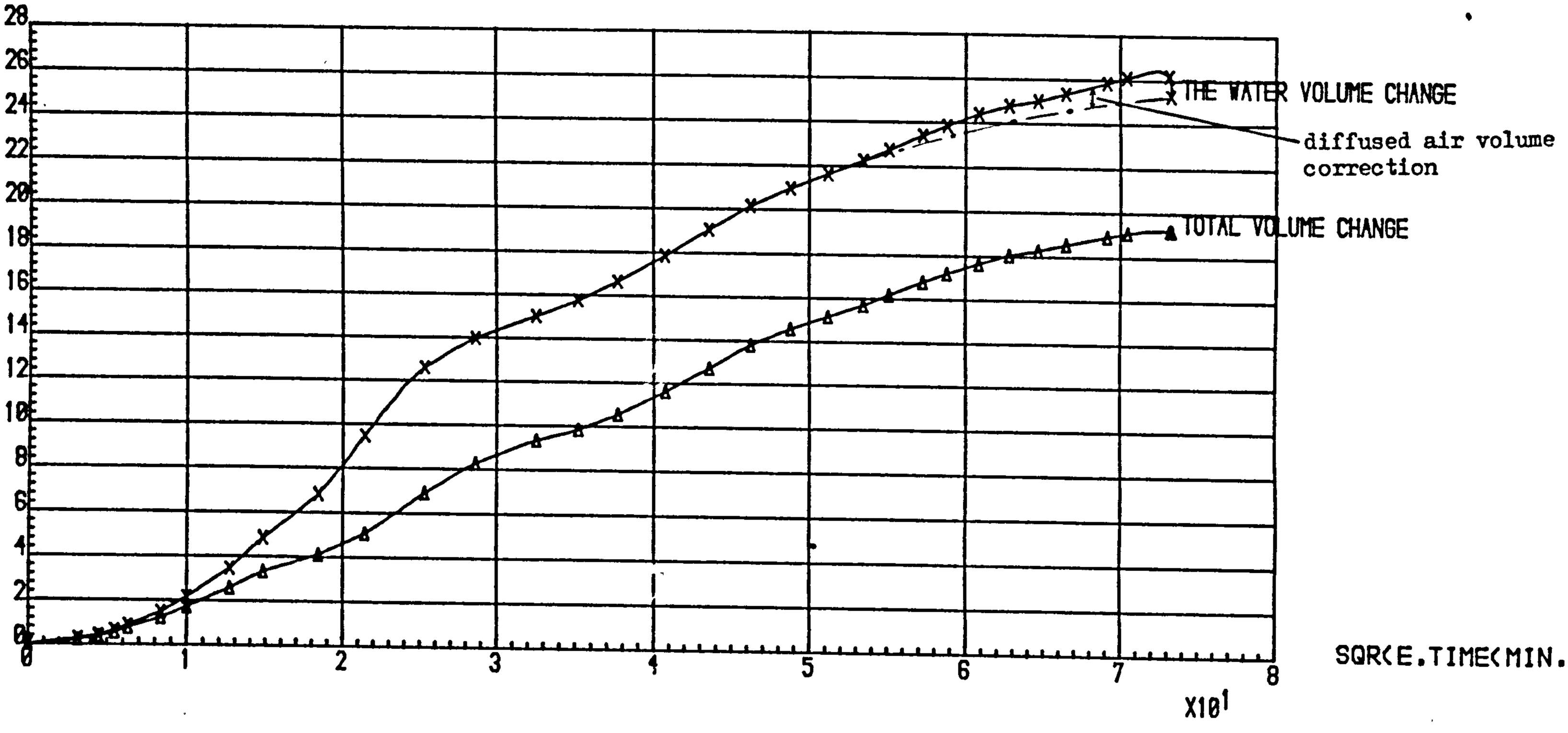

Fig.10.2: *THE CHANGE OF DEV.STRESS & M.SUCTION VS. STRAIN(%)* (SERIES I: DRAINED TEST)

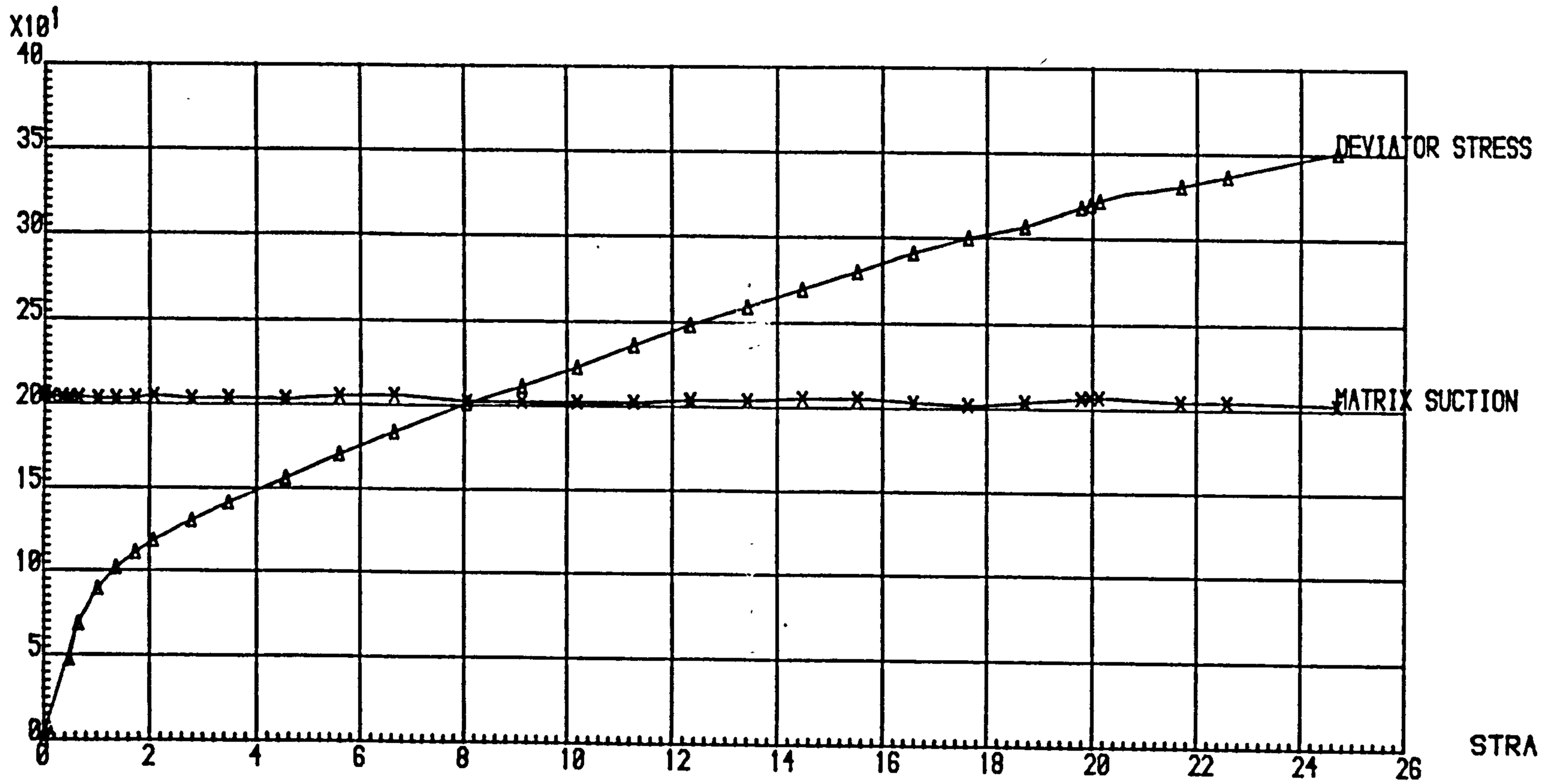

Fig.10.3: *THE DEGREE OF SATURATION(%) AGAINST STRAIN(%) DURING SHEAR* (SERIES I: DRAINED TEST)

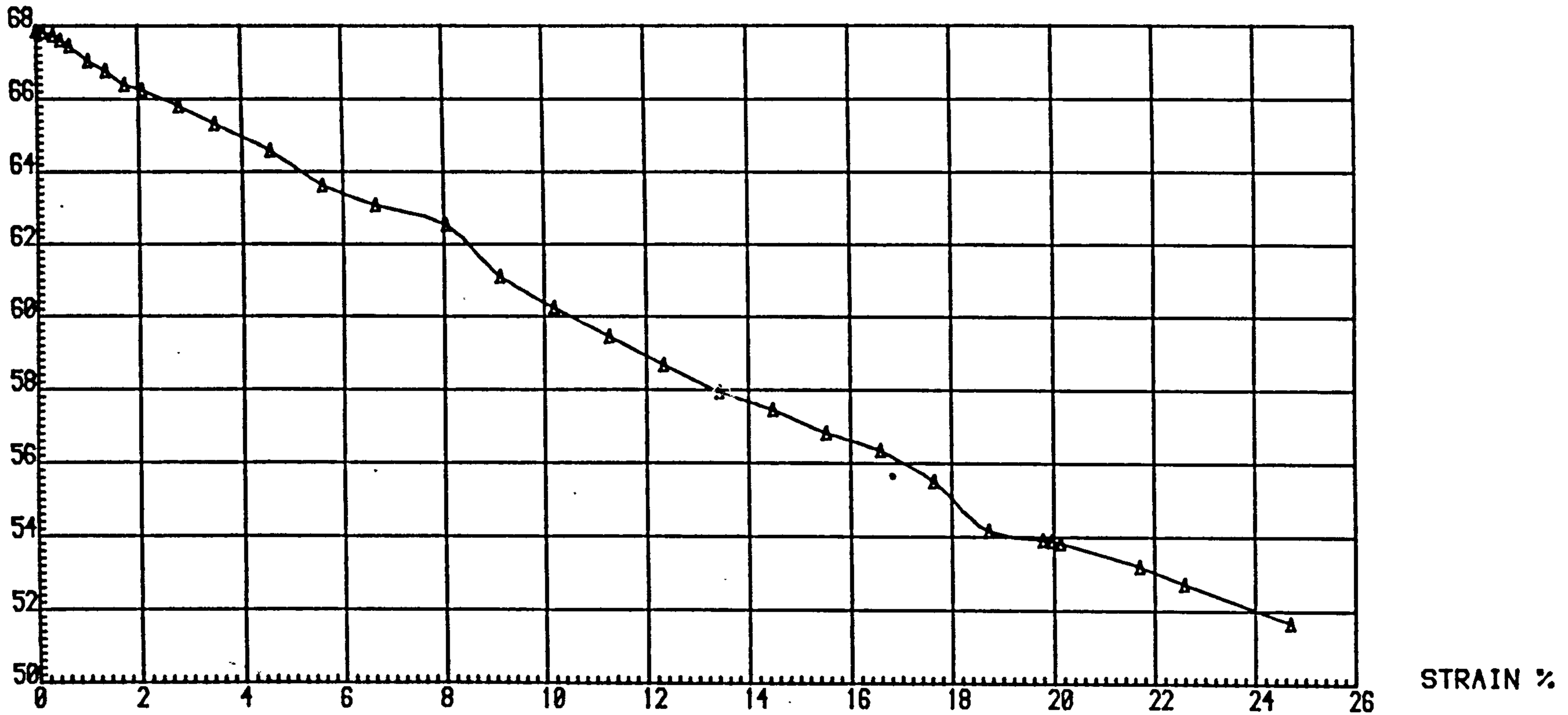

Fig.10.3: *THE DEGREE OF SATURATION(%) AGAINST STRAIN(%) DURING SHEAR* (SERIES I: DRAINED TEST)

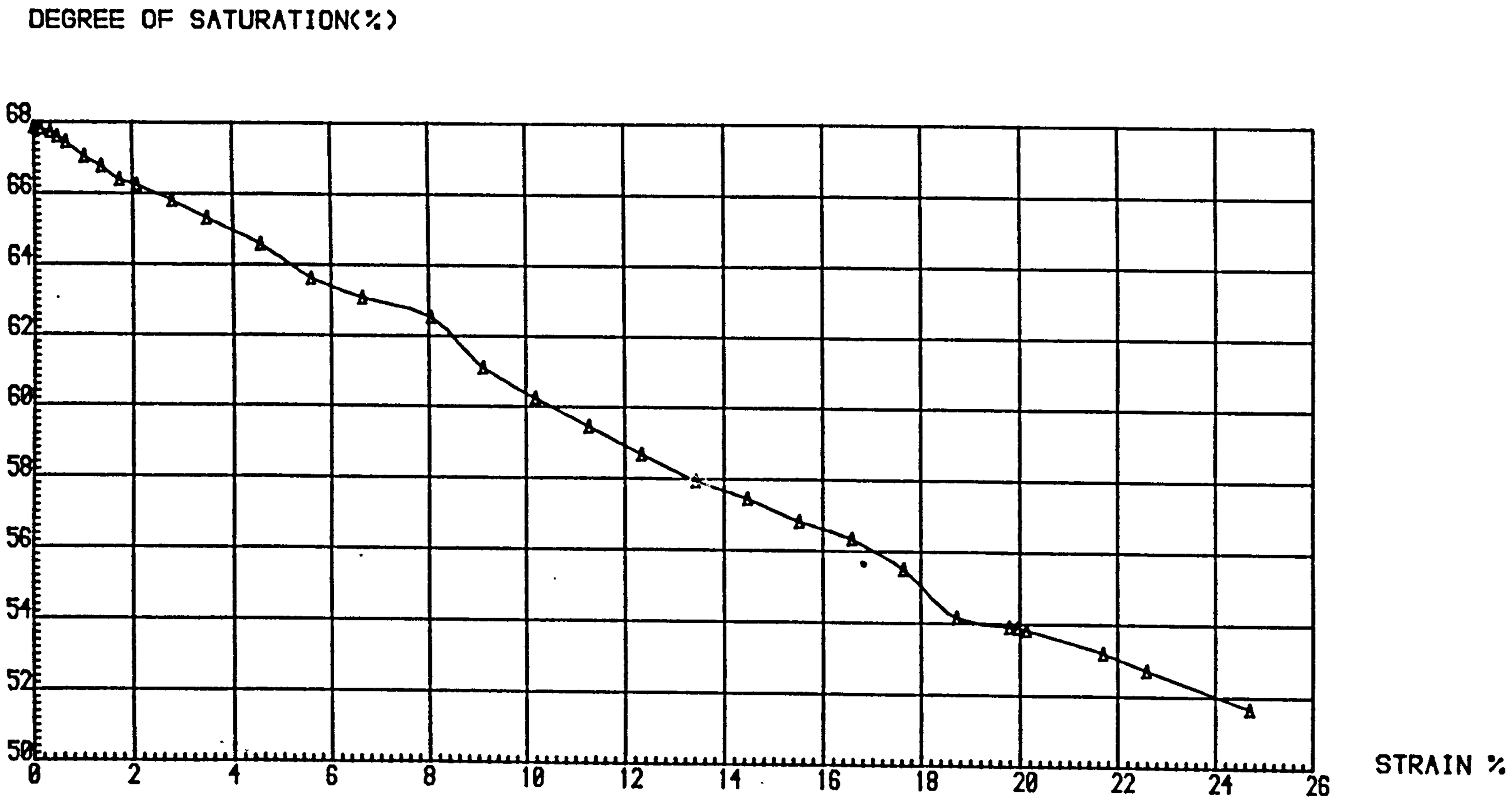

Fig.10.4: *THE VOID RATIO(%) AGAINST STRAIN(%) DURING SHEAR* (SERIES I: DRAINED TEST)

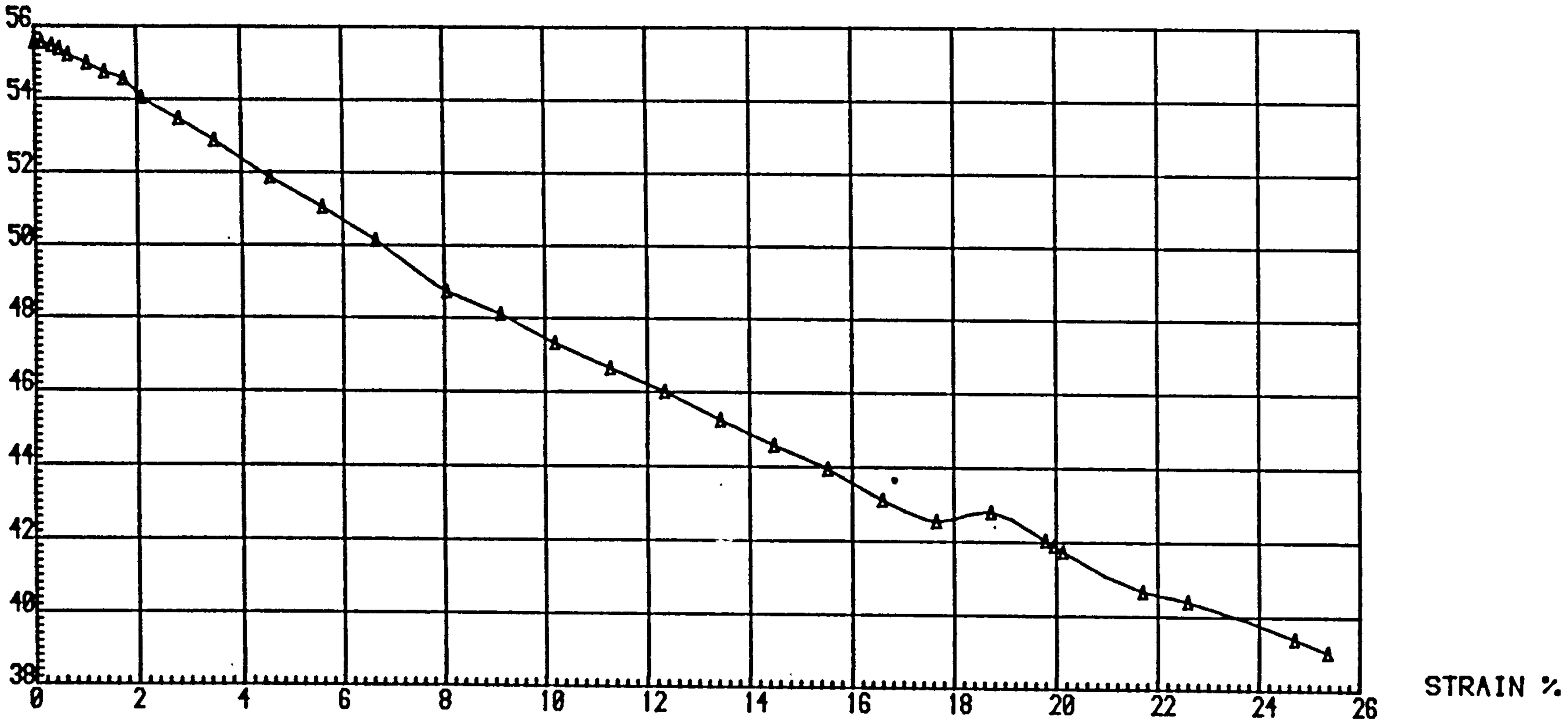

Fig.10.6: *THE CHANGE OF PWP, DEVIATOR STRESS & MATRIX SUCTION AGAINST STRAIN(%)-G211C2*

(SERIES I: CONSTANT WATER-CONTENT TEST)

THE CHANGE OF PWP, DEV.STRESS & M.SUCTION(KN/SQ.M)

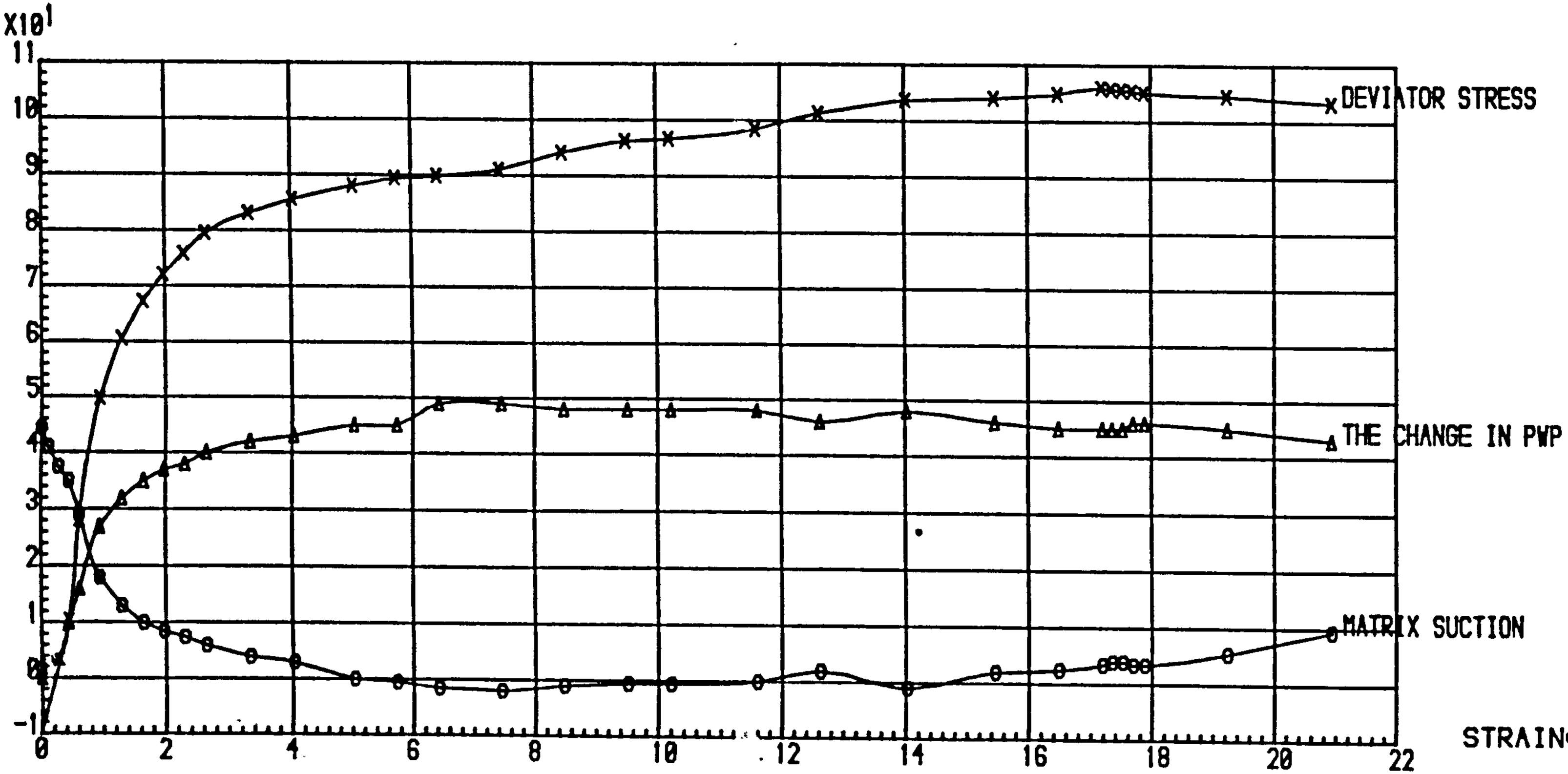

Fig.10.7: *THE DEGREE OF SATURATION(%) AGAINST STRAIN(%) DURING SHEAR*

(SERIES I: CONSTANT WATER-CONTENT TEST)

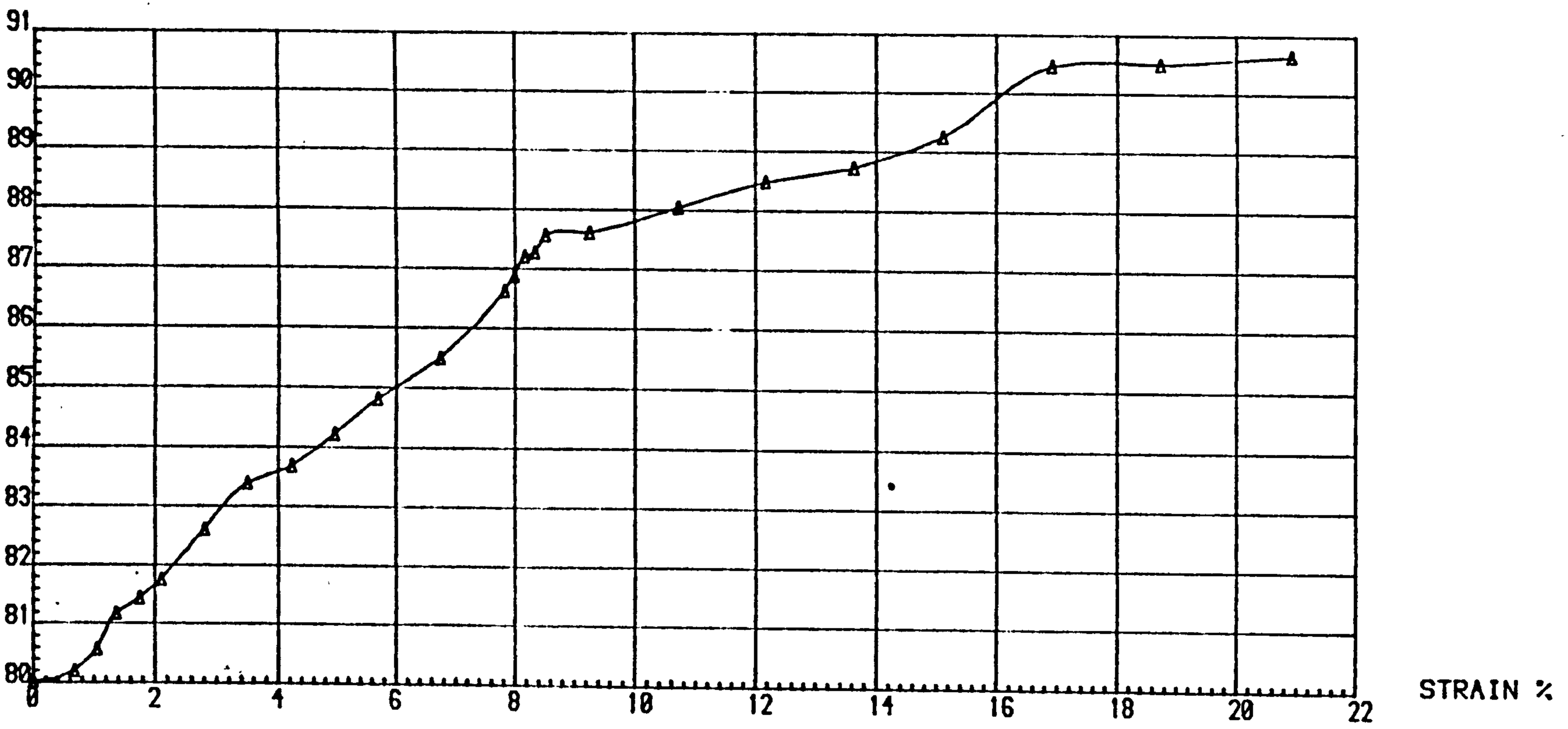

Fig.10.8 : *THE DRAINAGE OF WATER FROM SAMPLE DURING DESAT. & CONSOLID. VS. SQR(TIME)-G211U4*

(SERIES I: UNCONFINED TEST)

DRAINAGE OF WATER FROM SAMPLE(C.C.)

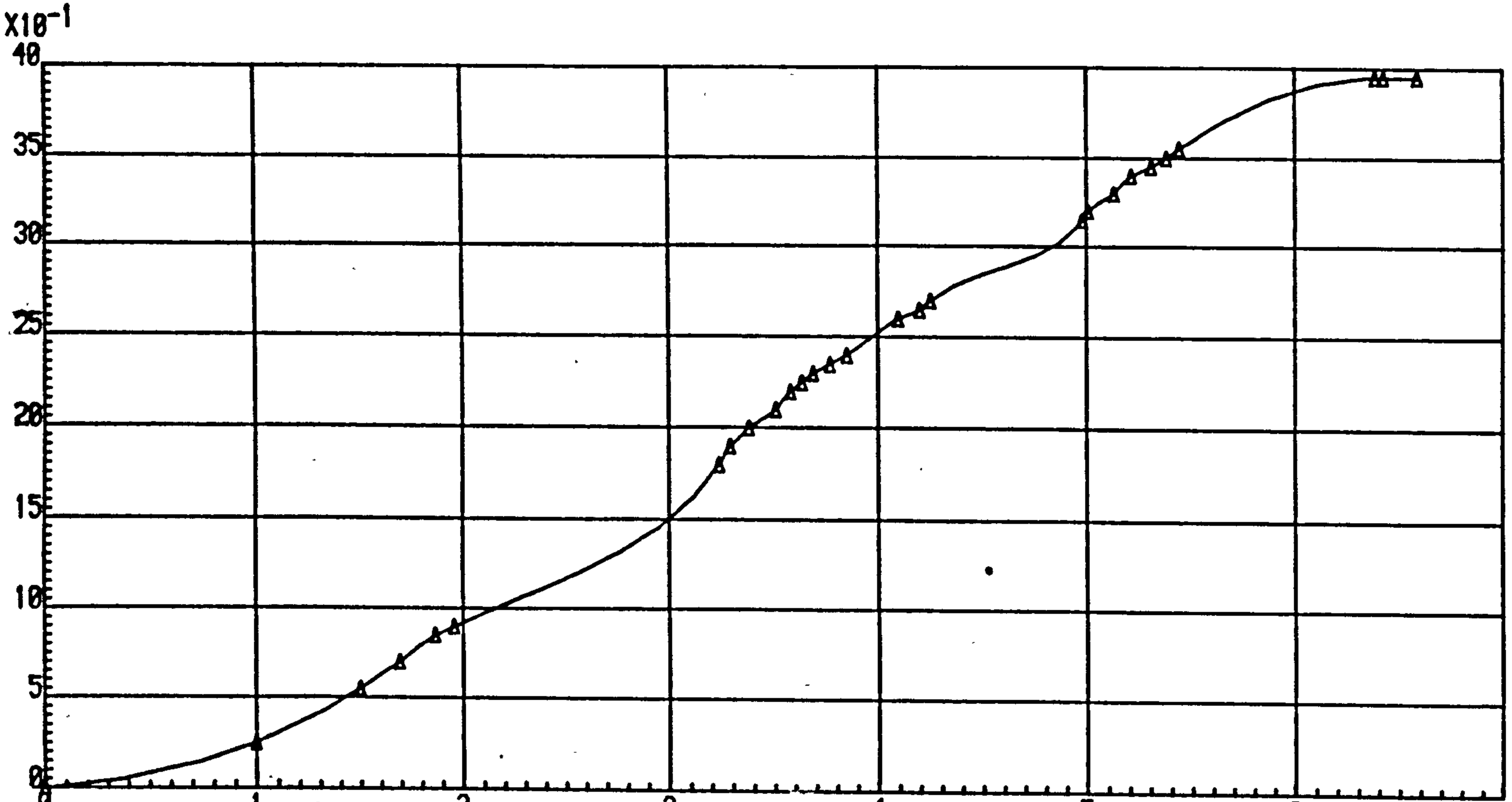

Fig.10. 9 : *THE CHANGE IN PWP, DEVIATOR STRESS & MATRIX SUCTION VS. STRAIN(%)*

(SERIES I: UNCONFINED TEST)

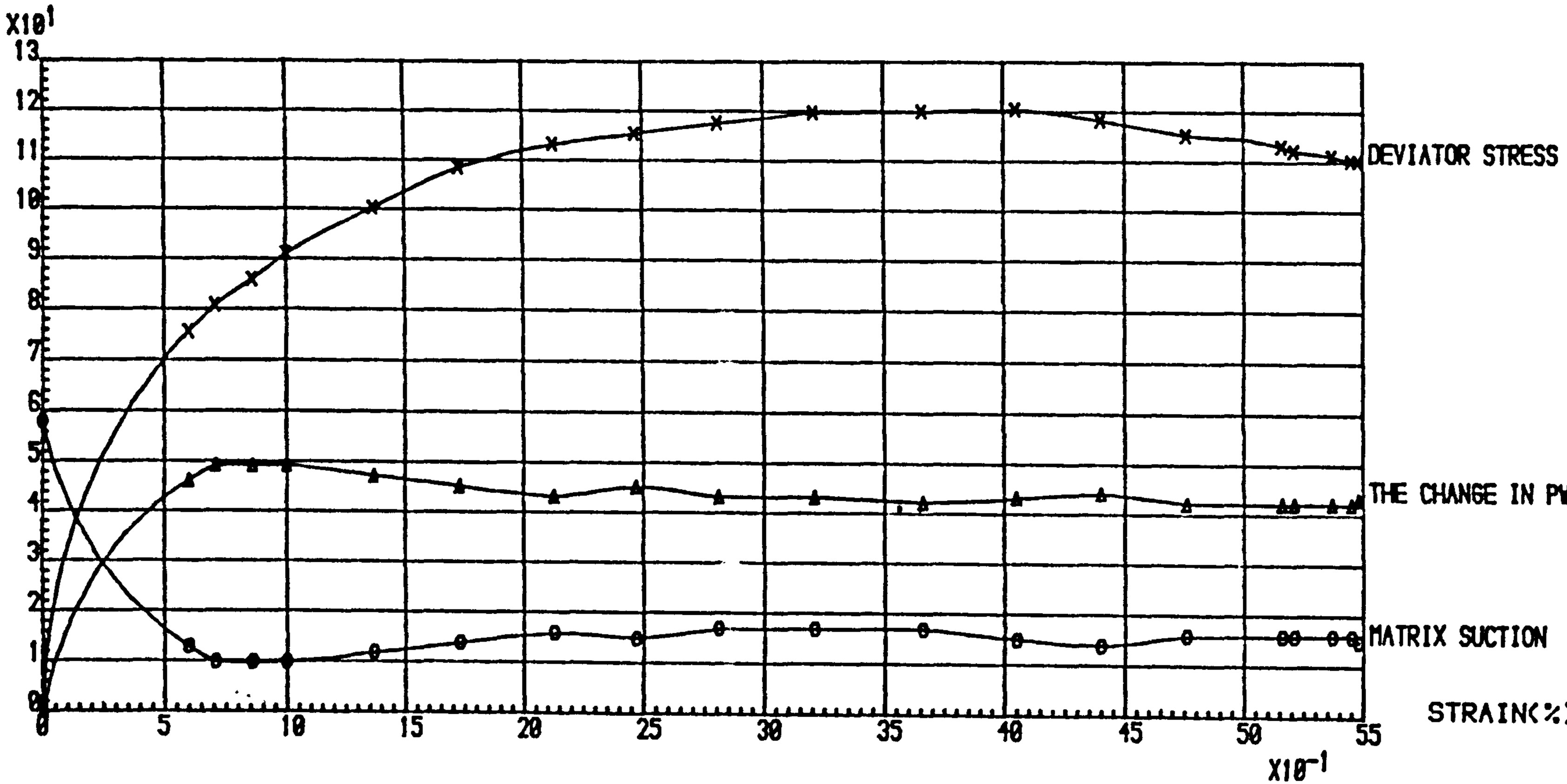

FIG.10.10: THE CHANGE OF TOTAL & WATER VOLUME DURING DESATURATION STAGE (SERIESII:DRAINED TEST)

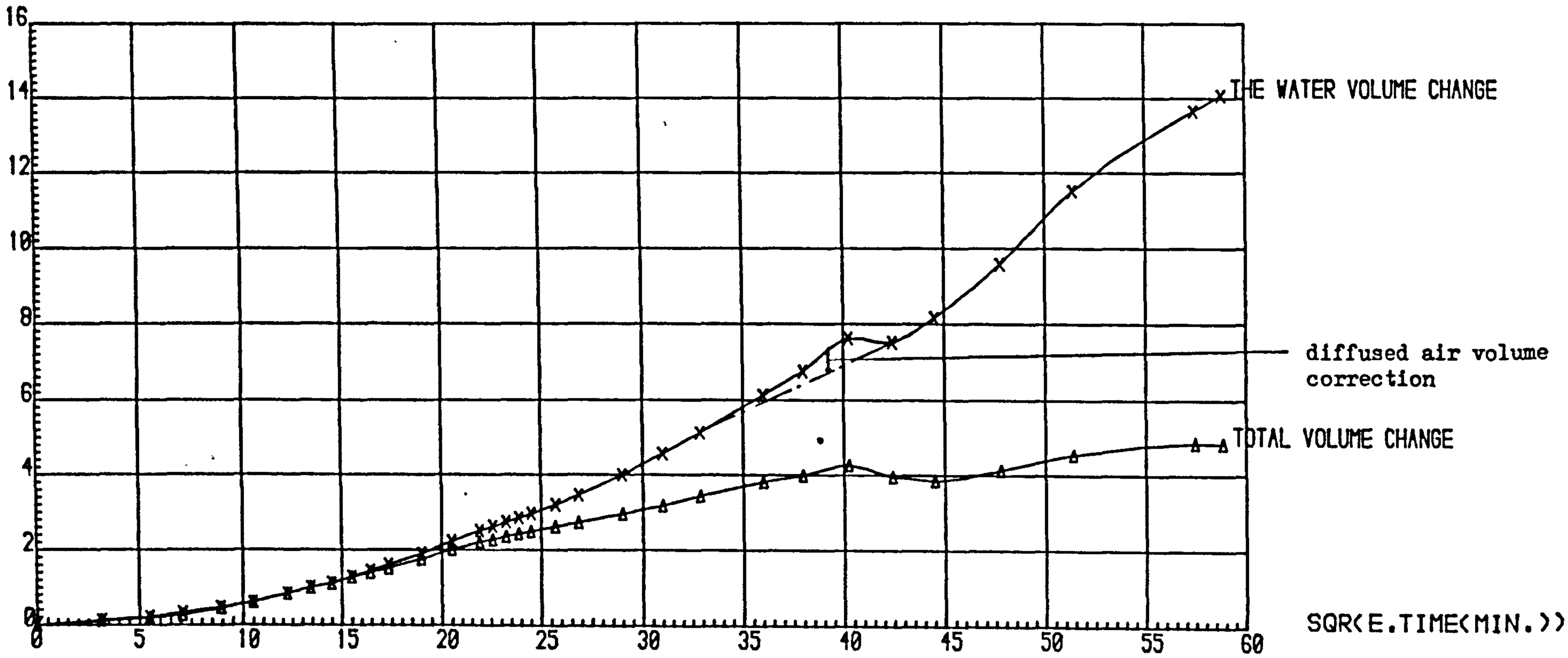

FIG.10.11: THE CHANGE OF DEVIATOR STRESS & MATRIX SUCTION VS. STRAIN (SERIES II:DRAINED TEST)

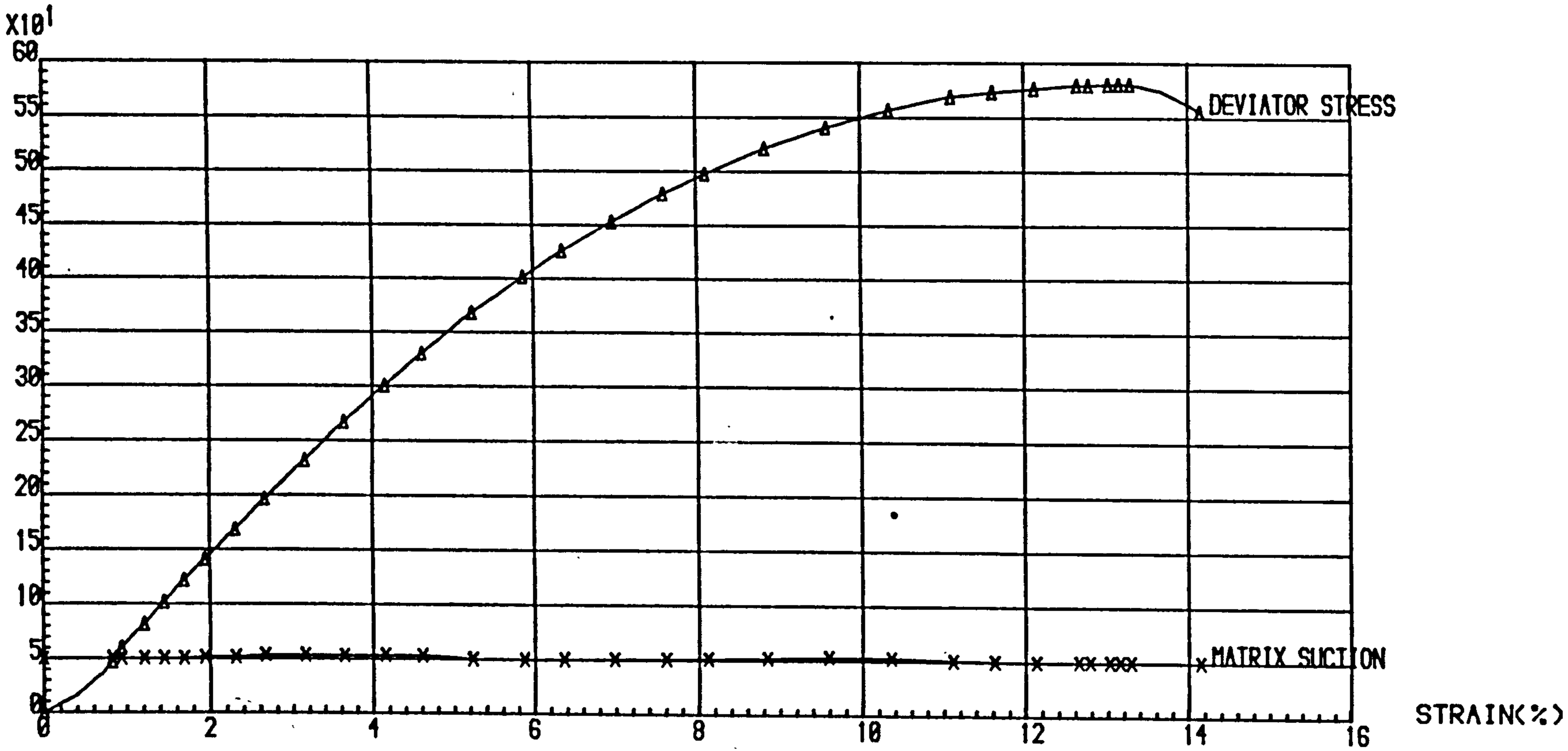

FIG.10.12: THE CHANGE OF DEGREE OF SATURATION(%) AGAINST STRAIN(%) (SERIES II:DRAINED TEST)

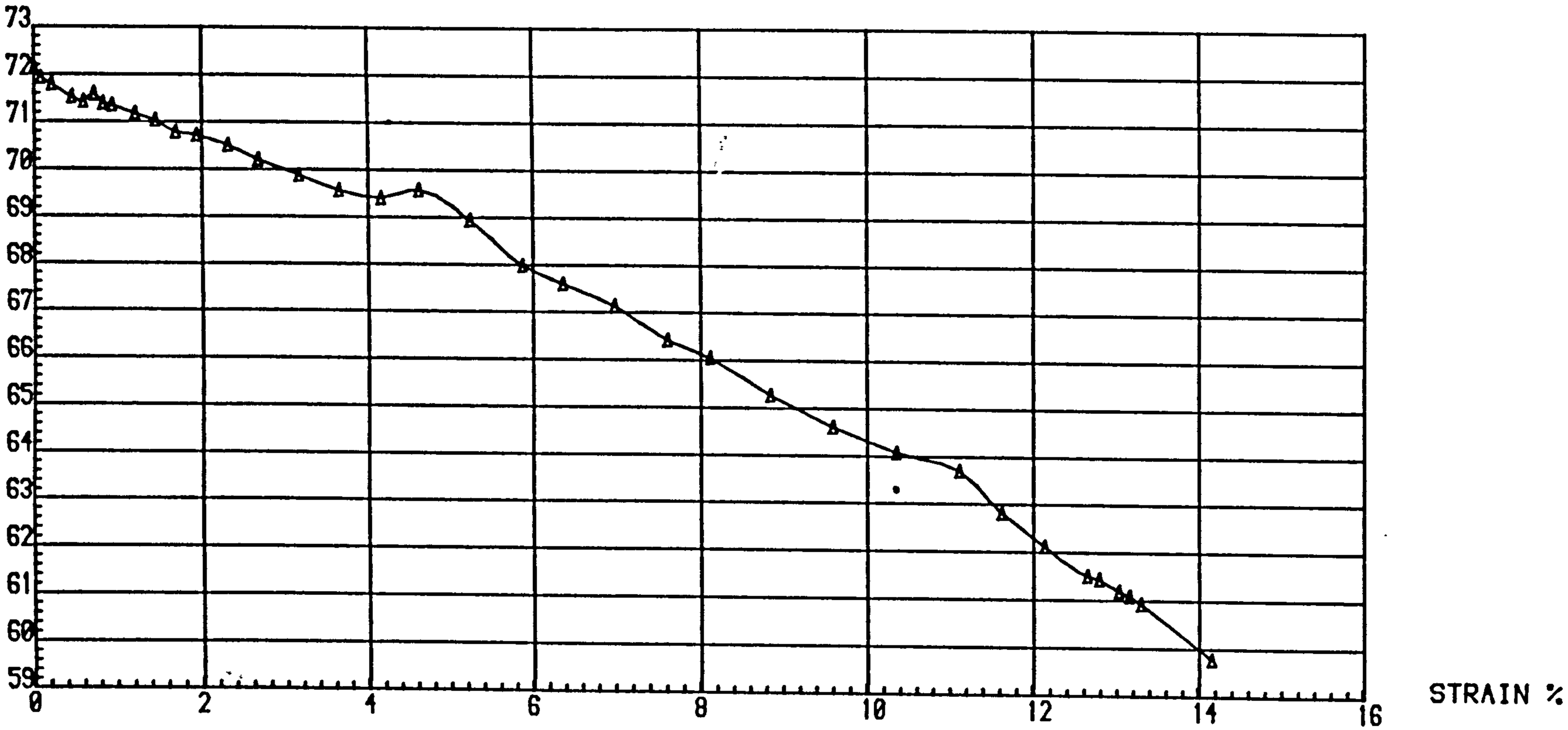

FIG.10.13: THE CHANGE OF VOID RATIO(%) AGAINST STRAIN(%)(SERIES II:DRAINED TEST)

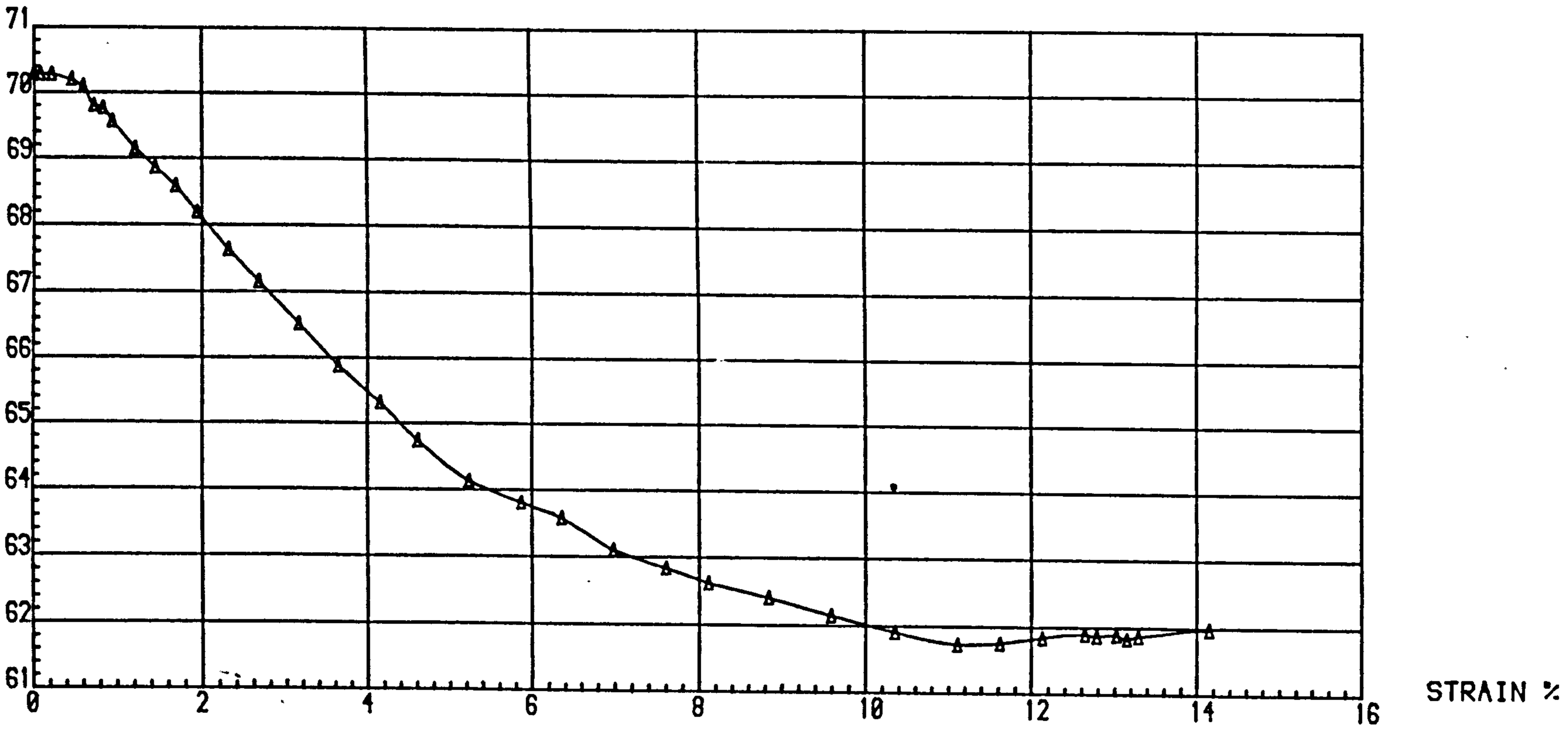

verifies that this was, in fact, the case. For the test shown, the matrix suction was maintained at approximate 200 KN/sq.m. The deviator stress did not reach a peak value, so failure was assumed at 20% strain(see section 8.6).

Figures 10.3 and 10.4 show that the degree of saturation and the void ratio decrease with strain, and therefore the total volume and the water volume continually decrease during the second stage of the test when the deviator stress is applied.

Typical Constant water-content tests are shown in Figures 10.5 to 10.7, Fig.10.5 shows the total and water volume changes during desaturation and consolidation. These are very similar to Fig.10.1, as they should be. When the deviator stress is applied, the pore water pressure increases fairly rapidly and, because the pore air pressure is maintained, the matrix suction decreases at a similar rate. Fig.10.6 illustrates these features of a constant water-content test. The change in pore water pressure reflects the change in deviator stress. Failure occurred at approximate 17% strain, after which the matrix suction increased slightly. The increase in degree of saturation during shear is shown in Fig.10.7.

During the desaturation and consolidation stage in unconfined tests, shown typically in Figs.10.8 and 10.9, the air pressure surrounding the sample forces water out of the sample through the high air entry porous stone. It is assumed that the total volume change of the sample is zero. The water volume change is shown in Fig.10.8. The variation of deviator stress, pore water pressure and matrix suction during an unconfined test is shown in Fig.10.9. The general trend of the curves is similar

to that in Fig.10:6 for a constant water-content test, but in the unconfined test, failure takes place at a much lower value of strain.

The graphs for the drained tests of series II (Fig.10.10 to 10.13) consider the same variables as the graphs for the drained tests of series I(Fig.10.1 to 10.4) and show the same trends.

10.3 Verification of Fredlund et al's theory

In order to investigate the validity of Fredlund et al's shear strength theory, the numerical method or the 2-dimensional graphical method must be used in conjunction with the 3-dimensional plot. The numerical method and the 2-dimensional graphical method indicate the correlation of the data points with respect to a straight line; they do not confirm that the 3-dimensional failure surface is planar. On the other hand, the 3-dimensional graphical method indicates the nature of the failure surface but at present, it is not possible to measure the angles subtended by the best plane(i.e. ϕ^b, ϕ°). The necessary software would have to be developed for the 3-dimensional subroutine to accomplish this task. However, using either the numerical method or the 2-dimensional graphical method in conjunction with the 3-dimensional graphical method, any warping of the surface and scatter of data can be easily investigated.

In the following sections, the information used in the discussion is contained in Table 9.1 and Appendix 8, unless otherwise indicated.

10.3.1 Previous investigations

Bishop et al(1960) their results produced a very high correlation coefficient for $\phi^{'}_{b}$, using either the 2-dimensional graphical or the numerical method. The application of the 2-dimensional graphical method is illustrated in pages A134-A137 and the results are summarised in tabular form on page A138. Eight constant water-content tests were conducted in each soil. The percentage clay fraction was 22% and 18% for the compacted shale and the compacted boulder clay respectively. The correlation coefficient for the shale (0.98) is marginally greater than that for the boulder clay (0.97).

The first set of 3-dimensional plots for the results on compacted shale show reasonable planar failure surfaces (page A139). The 3-dimensional plots for the compacted boulder clay are equally good, with no sharp peaks or troughs in any of the three different plots(page A140).

Donald(1961) carried out 42 undrained tests on remoulded London clay. The correlation coefficient for angle $\phi^{'}_{b}$ is 0.71. The soil had a clay fraction of 55%. The drained (21), constant water-content (9) and over-drained (3) test results on remoulded Braehead silt give correlation coefficients of 0.92, 0.64 and 0.99, respectively. For this soil, the clay fraction was 53%.

Ignoring the occasional sharp peak or trough, the first two 3-dimensional plots for the London clay results are good representations of planar failure surfaces(page A143). It is therefore surprising that the third plot, using the stress state variables $[(\bar{\sigma}1+\bar{\sigma}3)/2 - Uw]f$ and $[(\bar{\sigma}1+\bar{\sigma}3)/2 - Ua]f$, should be so poor. This may be due to the distribution of data when using

these stress state variables or it may be that the combination of stress state variables used in the third plot is not the most suitable choice to describe the behaviour of unsaturated samples of London clay. Presently, no attempt has been made to distinguish between these two effects.

The 3-dimensional plots for the Braehead silt constant water-content and drained tests also show reasonable planar failure surfaces, but again the third plot is the least satisfactory version(pages A144 and A145).

It was not possible to reproduce 3-dimensional plots for the over-drained test results because too few results were available (see appendix 2).

Blight(1961) performed constant water-content tests on four soils: 30 tests on Talybont clay(% clay fraction=4%); 27 on Mangla shale(% clay fraction=21%); 15 on Selset clay(% clay fraction=20%); 8 on Vaich moraine(% clay fraction=0%). As can be seen from Table 9.1, the type of failure condition applied altered the correlation coefficient for the shale from 0.92 to 0.93, for the Selset clay from 0.96 to 0.97 and for the Talybont clay from 0.61 to 0.48. The Vaich moraine results were reported with respect to only one failure condition (max. deviator stress) and yielded a correlation coefficient of 0.73.

Considering both the failure criteria used, the Talybont clay 3-dimensional plots are all very good, with only the occasional sharp peak or trough(pages A149 and A150). The actual physical representation of a plane is unaffected by the choice of failure criterion. The actual position of the plane in 3-

dimensional space, is, of course, dependent on the failure criterion used. A similar situation exists for the Mangla shale results, although in this case using the maximum deviator stress failure criterion provides a slightly better representation of a planar failure surface(pages A151-A152).

Considering the Selset clay results, it is difficult to decide which failure criterion gives a better representation of a planar surface(pages A153 and A154). Using either criterion gives a reasonable representation, which is least satisfactory in the third plot version.

The 3-dimensional plots for Vaich moraine were obtained using the maximum deviator stress failure criterion and show good representations of planar failure surfaces(page A155).

Matyas(1963) tested samples of Selset boulder clay (P.I.=18%, 8 tests) and red Sasumua clay (P.I.{ 26%, 7 tests) under constant water-content condition. The results produced a correlation coefficient for angle $\emptyset^b$ of 0.96, for both types of soils.

The two sets of 3-dimensional plots shown for Selset clay differ in one respect only; the second set contains results from tests on saturated as well as unsaturated samples(pages A157 and A158). The inclusion of the results for the saturated samples provides more data points for the 3-dimensional plots, but the points are all in the Y-Z plane (i.e. (Ua-Uw)=0). This leads to a smoothing out of the kinks on the edge of the failure plane which intersects the Y-Z plane. Each version of the 3-dimensional plot provides a better representation of a planar failure surface when the saturated results are included. This

gives support to Fredlund et al's contention that the shear strength equation for saturated soils is a special case of their more general shear strength equation for unsaturated soils.

The planar representation obtained for unsaturated samples of red Sasumua clay are not good(page A159). As explained in section 9.3.4, when the results from tests on saturated samples were included, it was not possible to obtain the first two 3-dimensional plots. However, the third plot is a good representation of a planar failure surface. Large negative values of $(\sigma 1-\sigma 3)f/2$ are shown on the Z-axis but the failure surface itself does not, in general, break the horizontal plane denoted by $(\sigma 1-\sigma 3)f/2 = 0$.

M.I.I.(1963) conducted five constant water-content tests on a mixture of Potters flint and Peerless clay which was compacted at a water content of 17.5%. The relative high value of compaction moisture content and the 20% Peerless clay in the mixture, suggests that the soil had a substantial clay fraction. The correlation coefficient for angle ϕ^b is 0.89.

The 3-dimensional plots are not good representations of planar failure surfaces(page A162). Using the C' value from tests on saturated samples, only six data points were available, which is the absolute minimum necessary for the operation of the 3-dimensional subroutine. The range of suction values was small (82 to 133 KN/m^2) and this also may have contributed to the poor planar failure surfaces.

Gulbati(1972) carried out nine drained tests and 10 constant water-content tests on samples of Delhi silt (% clay fraction=

15%). He also carried out a series of seven drained tests on samples of Dhanauri clay (% clay fraction =35%). The correlation coefficients for angle ϕ^b are: 0.72(Dhanauri,drained); 0.80(Delhi,constant water-content); 0.45(Delhi,drained). The results of Gulhati's tests are peculiar for two reasons. Firstly, the ϕ^b angles are very large and the ϕ' angles are all positive. Secondly, the corrected C' values are negative, which is not possible in practice. The values of ϕ^b and ϕ' do not compare well with those of the next investigator, Satija, who also used Dhanauri clay and obtained what appear to be more realistic values for ϕ^b and ϕ' and a positive value for corrected C'. The Gulhati values of ϕ^b and ϕ' must therefore be viewed with some doubt.

Despite the doubts cast on the results from the numerical method, the 3-dimensional plots for Dhanauri clay are reasonable representations of planar failure surfaces(page A165). The positive nature of angle ψ and therefore ϕ') is confirmed by the orientation of the surface shown in the second plot. Considering the Delhi silt, the 3-dimensional plots for both drained and constant water-content tests results are also reasonably planar(pages A166 to A169). The application of a correction to take account of the change in cross-sectional area that occurs during testing had little effect on the form of the failure surface, which is not surprising.

Satija(1978) conducted four series of tests on samples of compacted Dhanauri clay. Both constant water-content and drained tests were performed on samples at high and low as-compacted densities. The Dhanauri clay had a clay fraction of 35%. The

correlation coefficient for each of the four test series is high, ranging from 0.96 to 0.99. The 2-dimensional graphical method has also been used on these results and, with respect to the values of ϕ^b and correlation coefficient R, it shows very good agreement with the numerical method(page A172).

Satija specifically chose values of initial stress state which provided an even distribution of data points when plotted in three dimensions. However, Satija used the stress state variable ($\bar{\sigma}3$-Ua) instead of [($\bar{\sigma}1$+$\bar{\sigma}3$)/2-Ua], which was used by Fredlund et al. By using the latter version, the shear strength equation for unsaturated soil reduced to the Terzaghi expression for saturated soil. This consistency is not maintained if the Satija version is used as explained in section 5.3. The 3-dimensional plots of Satija's results show extremely good planar surfaces with very few disturbance, even when using the third combination of stress state variables(pages A173-A176).

Escario(1980) performed a number of direct shear tests on compacted samples of Madrid gray clay. The clay had a plastic index (P.I.) of 43%. The value of ϕ' varied from 19^o at a low suction value (zero) to 25^o at a high suction value(850 KN/m^2). The average value of ϕ' was 22.5^o. Only the 2-dimensional graphical method was applied to the test results and, for $\phi'=22.5^o$, the resulting value of ϕ^b is 16.1^o, with an extremely high correlation coefficient of 0.997(page A179).

Ho(1981) reported the results of an investigation into the shear strength of two unsaturated Hong Kong soils; decomposed granite and decomposed rhyolite. Both soils had a low percent

clay fraction (14%). The results of eight drained, multi-stage tests on decomposed granite and seven drained, multi-stage tests on decomposed rhyolite are reported in Table 9.1. Values of ϕ^b and ϕ' show very good agreement between the numerical method and the 2-dimensional graphical method. For each individual test, the correlation coefficient for ϕ^b is very high(0.94), whereas when all the results for each soil are used, the correlation coefficients fall to 0.51 and 0.72 for the granite and rhyolite, respectively. This reduction in correlation coefficient is explained in section 10.4.

Ignoring the sharp peaks and troughs, the 3-dimensional plots for decomposed granite are good representation of planar failure surfaces, as are the 3-dimensional plots for the decomposed rhyolite(pages A187 and A188).

10.3.2 Author's test results

The author's tests were described in full in Chapter 8. The Grangemouth clay had a fairly low clay fraction of 15%. In series I, the 10 constant water-content tests, the 12 drained tests and the seven unconfined tests give correlation coefficients for angle ϕ^b of 0.69,0.53 and 0.99, respectively. The nine drained tests conducted in series II give a correlation coefficient of 0.50. The values of corrected C', ϕ^b and ϕ' for the series II tests are extremely large(and ϕ' is also positive). This is a result of the small range of failure suction values in these tests. Referring to Table A8.2 in Appendix 8(page A195), the suction value at failure ranges from 48 KN/m^2 to 55 KN/m^2, a difference of only 7 KN/m^2. This, of

course, is a consequence of the definition of series II tests, where $(\sigma_3-Ua) > (Ua-Uw)$=constant. Time constraints in the testing programme allowed the use of only one constant value of $(Ua-Uw)$ (i.e.50 KN/m^2). Viewed in the Z-X plane (i.e. shear strength versus suction), the results would form a near vertical straight line at a suction value of approximately 50 KN/m^2. Consequently, the ϕ^b and ϕ^* angles are close to 90^o and the C′ intercept is very large and negative. In practice, it is impossible to have a negative cohesion value and for series II test results, it is invalid to use the numerical method, at least until results from tests using a greater range of suction values are available.

The 3-dimensional plots for all types of tests in series I give very good representations of planar failure surfaces(pages A191-A193). Only the third plot for the constant water-content tests shows any significant deviation from a plane(page A192). The quality of the failure surfaces may be a reflection of the systematic way in which the initial stress state variables were applied during testing, which resulted in a good distribution of data points on each of the coordinate axes. It was not possible to obtain the 3-dimensional plots for the drained tests of series II. This was again due to the small range of suction at failure; the 3-dimensional subroutine could not extrapolate from such a restricted set of data.

10.3.3 Comparison between numerical method and 2-dimensional graphical method

The most significant difference between the numerical and graphical methods is in the values of corrected C′ that they provide. Referring to Table 9.1, for the test results in which a comparison is made, the value of corrected C′ obtained using the graphical method is almost invariably greater than that obtained using the numerical method; sample No.22 of Ho(1981) is the exception. For Bishop′s results, corrected C′(graphical) = 4.5 x corrected C′(numerical) whereas in Ho′s results the difference between corrected C′(graphical) and corrected C′(numerical) ranges from x1.8 to x0.88.

Therefore, in general, the numerical method gives a more conservative value of corrected C′ than the 2-dimensional graphical method. The difference between the values of corrected C′ obtained from these two methods is entirely due to the nature of the methods themselves. The numerical method uses linear regression to obtain a best fit straight line and hence a corrected C′ intercept, whereas in the 2-dimensional graphical method the best fit straight line is drawn by hand. The corrected C′ intercept is therefore different from that obtained by linear regression.

In addition to the difference between the numerical and 2-dimensional graphical values of corrected C′, either of these corrected C′ values can differ substantially from the input C′ value obtained from tests on saturated soil samples and used in the numerical and 2-dimensional graphical methods. Referring to Table 9.1, the results of Matyas(Boulder clay), Satija and the

author's constant water-content tests are the only ones in which the input and corrected C′ values are similar. For the other test results, the input C′ is either greater or less than the corrected C′, in some cases by a substantial amount.

From a practical point of view, the choice of C′ is extremely important, especially with respect to slope stability problems. The effect of increasing the cohesion value on the factor of safety in slope stability calculations was discussed in Chapter 5, section 2. In this section, figure 5.7(page 110) shows the factor of safety increasing with increasing cohesion. Therefore, in choosing a value of C′ to be used in design calculations, the 2-dimensional graphical method should be discounted, as it provides not only the largest value of corrected C′(i.e. the least conservative) but also the least reliable value due to the nature of the method.

For a particular soil and test type, the choice then reduces to one between the numerical C′ value and the input C′ value(i.e. the value for a saturated soil). From the results shown in Table 9.1, neither of these values would give a consistently more or less safe design than the other. The choice of cohesion value would then be influenced by other considerations, e.g. the type of test used(i.e. the drainage conditions). The effect of test type on the shear strength parameters C′ and ϕ'_b will be discussed in section 10.6.

Finally, considering the angles ϕ'_b and ϕ', the 2-dimensional graphical and numerical methods gave very similar results in all cases.

10.4 Correlation coefficient and angle ϕ^b

It should be clearly understood that the ϕ^b correlation coefficient is merely an indication of how well the results compare to a straight line sloping at an angle ϕ^b to the matrix suction axis. Correlation coefficients are, of course, affected by the number of data points used. In the extreme, using only two data points leads to a correlation coefficient of one. For three data points, unless they are extremely scattered, a correlation coefficient close to unity is not difficult to obtain. This explains why the individual test results of Ho have such high correlation coefficients; only three data points were used. When all the tests are included, the number of data points increases to 24 for the decomposed granite and 21 for the decomposed rhyolite, while the correlation coefficient drops to 0.51 and 0.72, respectively. However, the idea that there is some relationship between number of tests and correlation coefficient is not sustained in practice. No sensible relationship was found for the results given in Table 9.1.

A high correlation coefficient for the numerical or 2-dimensional graphical method does not necessary indicate that the 3-dimensional surface will be planar, or very nearly so. Blight's results for Talybont clay have a correlation coefficient of 0.48(max. deviator stress failure criterion) but good 3-dimensional plots, whereas for Selset clay, the correlation coefficient is 0.96 but the 3-dimensional plots are not particularly good. Similarly, for the red Sasumua clay of Matyas, and the M.I.T. results, the correlation coefficients are high but the 3-dimensional plots do not match this indication of

good experimental results. On the other hand, the results of Satija have high correlation coefficients and good 3-dimensional plots, while the author's results for series I, constant water-content and drained tests have good 3-dimensional plots and average correlation coefficients

10.5 Effect of clay content

Ho(1981) suggested that the percentage clay fraction of samples may influence the value of $\emptyset^b$ obtained during testing. He argued that the contribution of the suction term to the shear strength of an unsaturated soil would be greater in soils with a significant clay fraction. Figure 10.14 shows a scattergram between percentage clay fraction(X-axis) and angle $\emptyset^b$ (Y-axis) for the results of Table 9.1. Where the percentage clay fraction was not available, estimated values were used based on the soil plasticity index. The statistics below the scattergram indicate that the correlation coefficient(R) is very low(0.2359) and also the significance is very low(11.81%). However, discounting the results at the remote edges of the scattergram, there is a trend shown of increasing $\emptyset^b$ with increasing clay content. It would be difficult to assess the practical significance of this trend, but it does lend support to the suggestion by Ho that the contribution of the suction term to the shear strength of an unsaturated soil would be greater in soils with a significant clay fraction.

To take account of clay mineralogy and the wider range of clay contents used by other investigators, a more relevant parameter may be the activity of the clay. The activity expresses the plasticity of the finest fraction, which is largely composed of clay minerals. Activity is a measure of the water-holding ability of the clay minerals and also suggests whether the clay is a kaolinite(low activity, <1), a montmorillonite(high activity,>4), or illite(intermediate activity,1-2). The influence of clay mineralogy and pore water composition on the angle $\emptyset^b$ is a topic for further investigation.

Fig.10.14 : MATRIX SUCTION ANGLE, ϕ^b IN DEGREES VS. CLAY FRACTION IN %

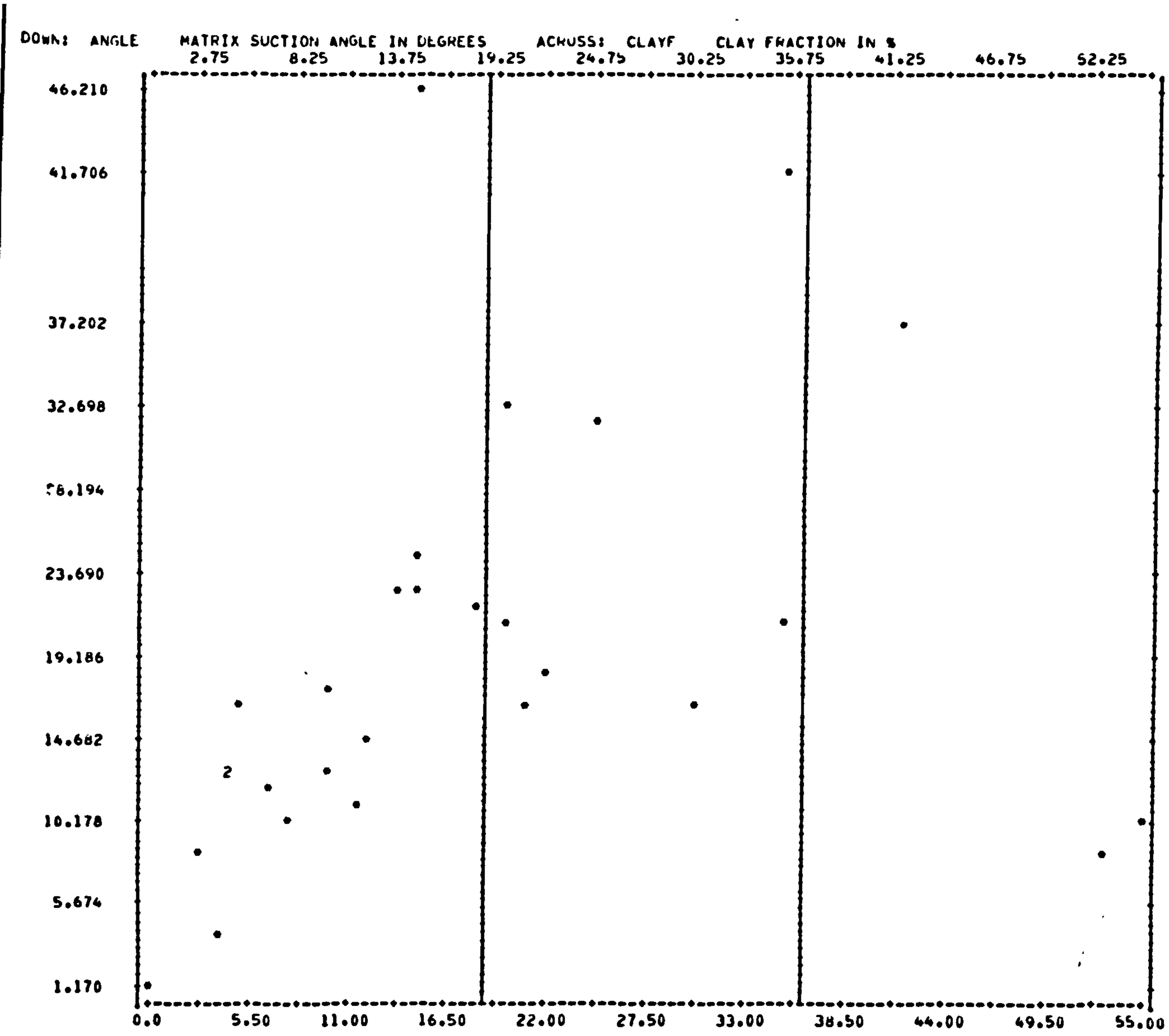

STATISTICS..

CORRELATION (R)-	.23540	R SQUARED -	.05565	SIGNIFICANCE -	.11410
STD ERR OF EST -	10.34062	INTERCEPT (A) -	15.09647	SLOPE (B) -	.17556
PLOTTED VALUES -	27	EXCLUDED VALUES-	0	MISSING VALUES -	0

10.6 Effect of test type

In Chapter 8 it was stated that, as part of the overall test programme, the effect of test type on the shear strength parameters of unsaturated soil would be investigated. The two most common tests used by the investigators reported in this thesis were the constant water-content(CW) and the drained test(D). Other test types, such as undrained and overdrained, have been used, but there is not enough data available to permit sensible comparisons between these test types and the more common CW and D tests. The author also carried out some unconfined tests.

Of the ten investigators, only four have performed different tests on the same soil. These are Donald(1961), Gulhati(1972), Satija(1978) and the author. The results supplied by Gulhati have already been discussed and queried in section 10.4 and are therefore omitted from the discussion in this section. The results of the remaining three investigators are presented in Table 10.1.

Table 10.1: Summary of unsaturated soil shear strength parameters: C', ϕ^b and ϕ°

Investigator	Soil	corrected C' KN/sq.m		ϕ^b Degrees		ϕ° Degrees	
		D	CW	D	CW	D	CW
Donald	Braehead silt	3.38	8.55	16.93	8.72	-19.55	-26.84
Satija	Dhanauri clay (low Yd)	20	12	12.77	16.00	-18.15	-14.98
	Dhanauri clay (high Yd)	35	18	16.13	21.33	-14.24	-8.67
Wong	Grange-mouth clay	18.69	6.42	5.88	22.49	-29.97	-14.87

where Yd = dry density

In addition, the shear strength parameters from the author's unconfined tests are:

corrected $C' = 14.89$ KN/sq.m ; $\phi^b = 12.05^\circ$ and $\phi^\circ = -24.99^\circ$

In the discussion which follows, the value of C' is the corrected C' obtained from the numerical method, unless otherwise indicated.

It is clear that the values of shear strength parameters C′, ϕ^b and ϕ^* depend on the type of test used, which implies that the test drainage conditions affect the final form of the shear strength equation. It was shown in Chapter 5, section 2 that the suction in an unsaturated soil increases the cohesion of an unsaturated soil. In equation 5.11, the total or apparent cohesion, C, was equal to the effective cohesion, C′, plus a term involving the suction and the angle ϕ^b, i.e.

$$C = C' + (Ua-Uw)\tan\phi^b \qquad \text{(Eqn.5.11)}$$

This is part of the overall shear strength equation for unsaturated soils(Eqn.5.7 or Eqn.9.2).

Figure 10.15 shows graphs of total cohesion, C, versus matrix suction for the test results presented in Table 10.1. Using the results of Satija and of Wong, for a particular value of matrix suction, the total cohesion is greater for the drained tests than the constant water-content tests. The results of Donald give the opposite relationship, at least initially. The relative positions of the lines shown in Fig. 10.15 will be affected by the value of C′ used. The C′ shown is the corrected C′ obtained from the numerical method. As discussed in section 10.3.3, it may be equally valid to use the input C′ on the graphs of Fig.10.15. For saturated soils, the value of the shear strength parameters C′ is dependent on the type of test used to obtain it. In unsaturated soils, this dependency is accentuated by the methods used to 'correct' the value of cohesion for a saturated soil to a value which is supposed to be appropriate to the same soil in an unsaturated condition. The assessment of

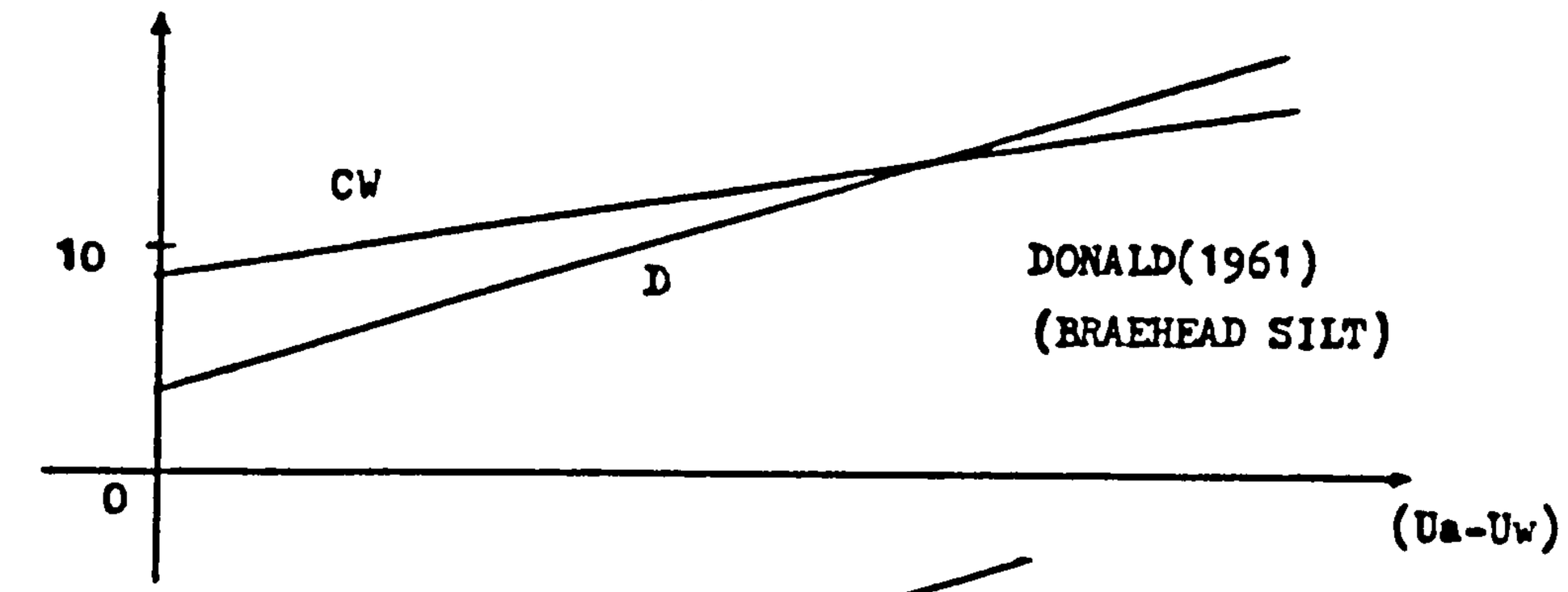

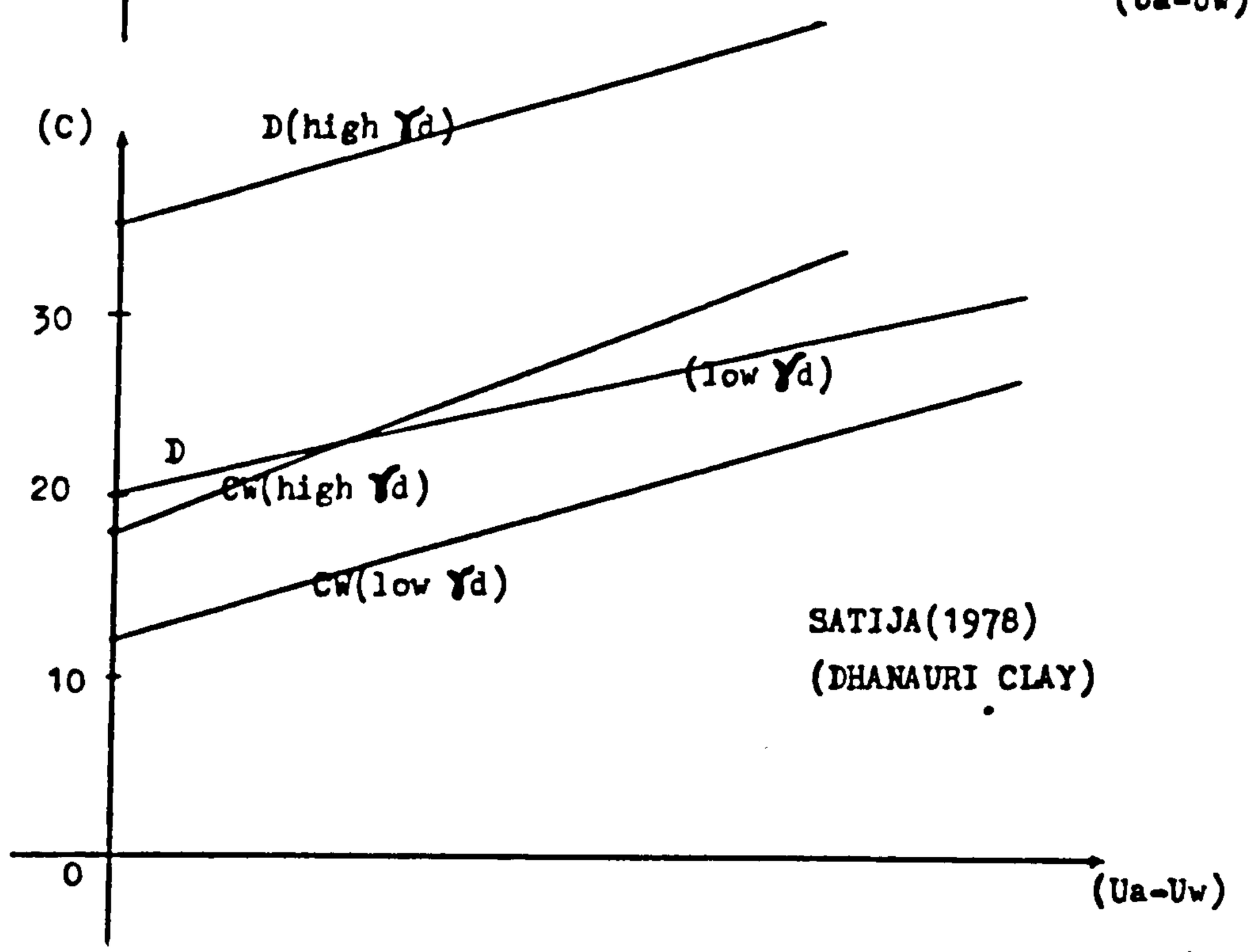

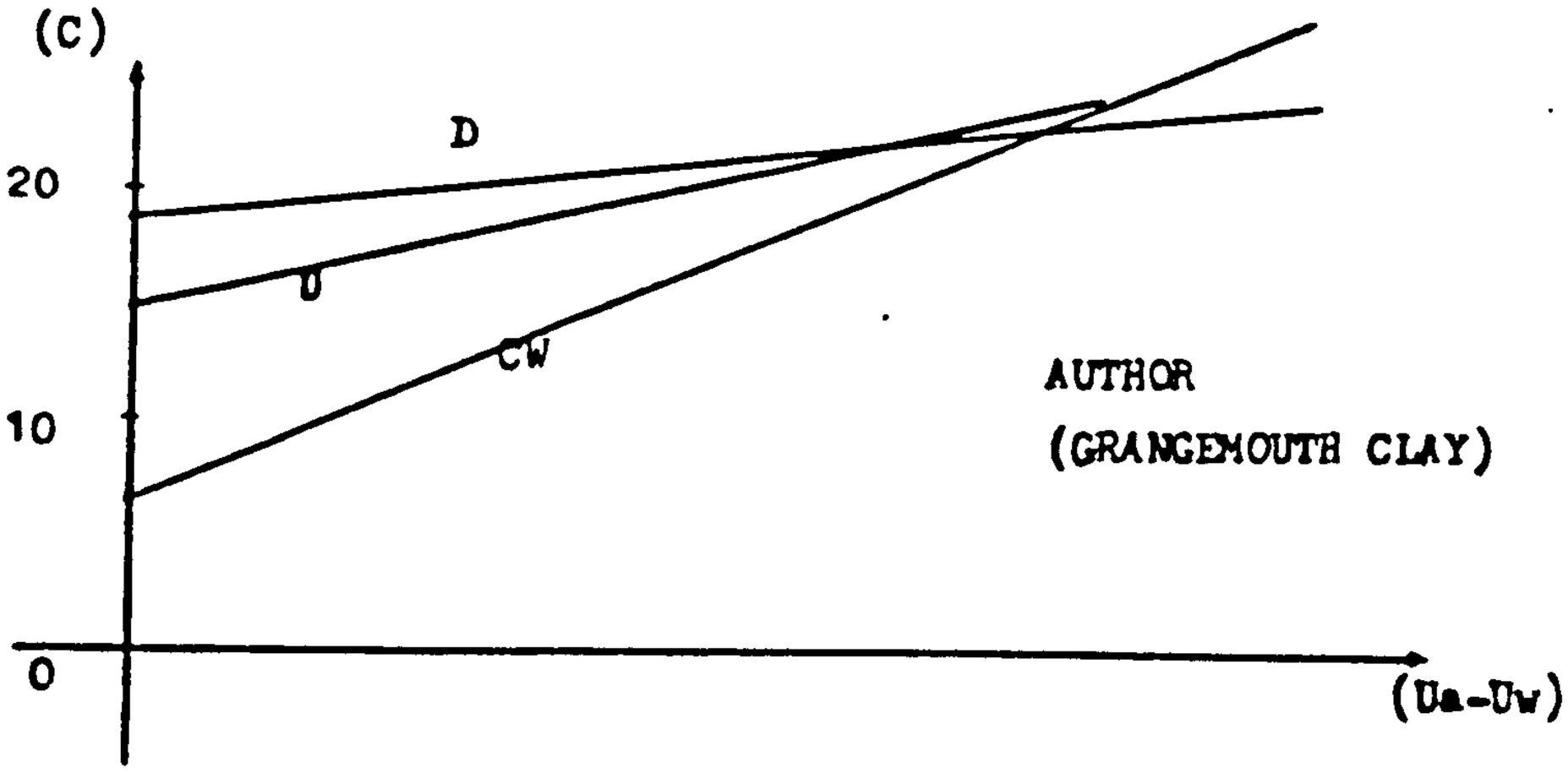

Fig.10.15 : TOTAL COHESION (C) VERSUS MATRIX SUCTION FOR THE TEST RESULTS PRESENTED IN TABLE 10.1.

which value of C′ to use is thus extremely difficult and the final choice will continue to be based largely on experience and considerations of factors of safety rather than any analytical techniques.

For the author′s tests, the difference in the shear strength parameters C′ and ϕ^b arising from different test types may be related to how the degree of saturation varied during each test. All the tests began with a desaturation and consolidation stage which resulted in an unsaturated sample. During the shearing stage in drained tests, the degree of saturation continued to decrease, whereas in a constant water-content test, the degree of saturation increased from its value at the end of the desaturation and consolidation stage. Thus, in the drained test the sample was continually drying out, but in the constant water-content test the sample was subjected to a drying process and then a wetting process. In section 10.2, Figs.10.3 and 10.12 for drained tests and fig.10.7 for constant water-content tests, illustrated the change in degree of saturation during testing. In terms of the cohesion C′ and the angle ϕ^b, the results from the unconfined tests, shown below Table 10.1, lie between the values obtained in drained and constant water-content tests. The unconfined test is a special case of the constant water-content test and the samples were also subjected to drying and wetting, but on the wetting cycle failure occurred at a much lower value of strain than the drained or constant water-content tests. The drying and wetting of soils was referred to in section 3.6 with respect to the relationship between soil suction and moisture

content. A similar hysteresis may be taking place in the samples of the drained and constant water-content tests, which affects the evaluation of the shear strength parameters C′ and $\emptyset^{b}$. This has important implications in practice, where field drainage characteristics will dictate which test results are most appropriate. For example, a desiccated soil can achieve a high value of saturation by the application of an external load which reduces the void ratio(or total volume). Full saturation by means of compression is unlikely to occur and a small suction will probably be maintained in the soil. This process can be simulated in the shearing stage of a constant water-content test and, provided the degree of saturation at the commencement of the shearing stage is similar to that in the field, the shear strength parameters obtained from a constant water-content test should be used in these circumstances. Conversely, if the degree of saturation of a soil in the field continually decreases after loading, the shear strength parameters obtained from drained tests should be used.

It is extremely important therefore to acertain how the degree of saturation of a soil is likely to vary with time and hence use a test type which simulates the field conditions as closely as possible.

CHAPTER 11 CONCLUSIONS

Chapter 11 Conclusions

11.1 Conclusions

This thesis was concerned with various aspects of the shear strength of unsaturated soils. The main objective was to demonstrate, using test results from this and other investigations, the general applicability of the shear strength equation for unsaturated soils suggested by Fredlund et al(1978). Early attempts by previous investigators to describe the behaviour of unsaturated soils used the principle of effective stress, modified to suit unsaturated soils. This line of reasoning has been superseded by an approach, developed from the principle of continuum mechanics, which describes the shear strength of unsaturated soils in terms of two independent stress state variables(Fredlund,1973). The author has based his work on this approach, and in particular investigated unverified assumptions made by Fredlund regarding a planar form of failure surface.

Apparatus was constructed to carry out triaxial tests on unsaturated samples of Grangemouth clay. The unsaturated samples were obtained from saturated samples by applying a desaturation and consolidation process. The standard triaxial set-up was modified to allow for the measurement and control of the pore air and pore water pressures during testing. Other modifications included the use of a double-walled cell, a diffused air volume indicator and an automatic volume change logging system. A series of tests was carried out specifically to establish suitable strain rates which would allow the proper dissipation

and equalization of pore pressures during testing. This resulted in a strain rate of 0.003 mm/min. being adopted for drained tests and 0.0041 mm/min. for all other test types used.

The main test programme consisted of two series, which were distinguished by the initial stress state applied to the sample. In series I, drained, constant water-content and unconfined tests were carried out. Series II consisted of drained tests only. Four truly undrained tests were also carried out.

The results of these tests and those of nine previous investigations were analysed using three methods. The first two of these, the numerical method and the 2-dimensional graphical method, are based on the theory of Fredlund et al(1978). This theory assumes that, when triaxial test results are recorded in terms of stress state variables and plotted in terms of three orthogonal axes, the resulting failure surface will be a plane. For the angle ϕ^b used in the shear strength equation, the numerical and 2-dimensional graphical methods gave very similar results. However,due to the nature of the methods, the value of cohesion, C′, that they produced varied considerably. In general, the numerical method produced a more conservative(i.e. lower) value for C′.

The value of the correlation coefficient obtained from the numerical or 2-dimensional graphical method was an indication of how well the results compared to a straight line sloping at an angle ϕ^b to the matrix suction axis. A high correlation coefficient for angle ϕ^b does not necessarily imply that the failure surface is planar. Similarly, a low correlation

coefficient does not necessarily imply that the failure surface is not planar. Therefore, neither method could be used to confirm that the failure surface was planar.

The author used a third method whereby the form of the failure surface was obtained by using a 3-dimensional graphical program called GINOPLOT. In all but a few cases, the 3-dimensional plot in verification of Fredlund assumption was essentially planar, irrespective of the combination of stress state variables used to describe it. Therefore, to verify that the shear strength equation for unsaturated soils proposed by Fredlund et al represents a planar failure surface, and to obtain the shear strength parameters for use in the equation, the numerical method and the 3-dimensional graphical method must be used together.

The test results used in this thesis were obtained from different types of tests on different types of soil under different initial conditions(degree of saturation, moisture content, initial stress states). The application of the numerical method(or 2-dimensional graphical method) and the 3-dimensional graphical method to these results has, in most cases, confirmed that the failure surface, when plotted in terms of stress state variables, is a planar surface. The general applicability of the shear strength equation proposed by Fredlund et al is therefore also confirmed.

In practical terms, the choice of parameters for use in the shear strength equation remains difficult. The effect of test type on C' and $\emptyset^b$ was clearly demonstrated, as was the additional problem of 'correcting' the C' value in the numerical

and 2-dimensional graphical methods. The nature of the variation of degree of saturation may influence the values of shear strength parameters obtained from tests and when dealing with unsaturated soil it is extremely important to assess how the degree of saturation will vary in the field and reproduce, as closely as possible the same conditions in the test set up. For a soil in which the degree of saturation decreases after loading, a drained test should be used, whereas if the degree of saturation increases, a constant water-content test should be used.

With respect to the test equipment and procedures, the following conclusions were reached:

(1) Appropriate shear strain rates must be used to ensure proper dissipation or equalization of pore pressures.

(2) The validity of the stress state variables was confirmed experimentally by using null tests.

(3) The accuracy of volume measurement can be improved by:

(i) using a diffused air volume indicator

(ii) using a double-walled cell

(iii) using a constant temperature room. If this is not possible, apply a temperature correction.

(4) The automatic volume change logging system operated satisfactorily.

DAMAGED
TEXT
IN
ORIGINAL

11.2 Suggestions for future work

The following recommendations are made for future work:

(1) Develop improvements in the 3-dimensional graphical method so that the data points can be shown and the angles subtended by the best plane representing these data points can be determined. The numerical method, used for calculating C', $\emptyset$ and $\emptyset^b$ would then be redundant.

(2) Investigate the effects of degree of saturation, dry density and structure on the shear strength of unsaturated soils, in order to identify the properties which have an overriding influence on the shear strength parameters C' and $\emptyset^b$. This would be a major investigation and would have to be undertaken in parts.

(3) Further investigation of the influence of percentage clay content on angle $\emptyset^b$ including other parameters such as activity and the chemical composition of the soil water. A scattergram of percentage clay content and angle $\emptyset^b$ showed that there was a general trend of increasing $\emptyset^b$ with increasing percentage clay content. It may be possible to develop a more practical relationship for a particular soil parameter. It may be possible to develop a more practical relationship for particular soil type.

(4) Investigate the variation of pore air and pore water pressures during isotropic compression. Initially, this will involve a thorough investigation of the test equipment and procedures, to identify the source of the problem described in section 8.1.

REFERENCES

REFERENCES

Aitchison,G.D.(1956)
'Some preliminary studies of unsaturated soils (a) The circumstances of unsaturation in soils with particular reference to the Australian environment',Proceedings of 2nd Australia-New Zealand Conference on Soil Mechanics and Foundation Engineering,pp.173-191.

Aitchison,G.D.(1960)
'Relationship of moisture stress and effective stress functions in unsaturated soils', Pore Pressure and Suction in Soils, Butterworths, London,pp.47-52.

Aitchison,G.D.(1967)
'Separate roles of site investigation, quantification of soil properties, and selection of operational environment in the determination of foundation design on expansive soils', Proceedings of the third Asian Regional Conference on Soil Mechanics and Foundation Engineering, Haifa, Israel.

Aitchison,G.D.(1969)
'Soil suction in Foundation Design', Proceedings of the Seventh International Conference on Soil Mechanics and Foundation Engineering, Volume 2, Mexico.

Aitchison,G.D. and Donald,I.B.(1956)
'Some preliminary studies of unsaturated soils (6) Effective stress in unsaturated soils', Proceedings of the 2nd Australia-New-Zealand Conference on Soil Mechanics and Foundation Engineering(Jan.,1956), Christchurch, pp.192-199.

Aitchison,G.D. and Richards,B.G.(1965)
'A broad scale study of moisture conditions in pavement subgrades throughout Australia', Moisture Equilibria and moisture change in soils beneath covered areas, Butterworths, Australia, pp.184-282.

Aitchison,G.D.,Russam,K. and Richards,B.G.(1965)
'Statement of the review panel: Engineering concepts of moisture equilibria and moisture changes in soils', Symposium on moisture equilibria and moisture changes in soils beneath covered areas, Ed. by G.D. Aitchison, Soil mechanics, section CSIRO Australia, Butterworths, Australia, pp.7-21.

Akroyd,T.N.W.(1957)
'Laboratory Testing in Soil Mechanics', Clockhouse Engineering Ltd., New Barnet.

Barden,L.B.(1965)
'Consolidation of compacted and unsaturated clays', Geotechnique, Volume 15, pp.267-286.

Barden,L., Madedor,A.O. and Sides,G.R.(1969)
'Volume change characteristics of unsaturated clay', ASCE Journal of the Soil Mechanics and Foundations Division, 95(SM1), pp.33-51.

Barden,L. and Pavlakis,G.(1971)
'Air and water permeabilities of compacted unsaturated cohesive soil', Journal of Soil Science, Volume 22, No.3, pp.302-318.

Biot,M.A.(1941)
'General theory of three-dimensional consolidation', Journal of Applied Physics, 12(2), pp.155.

Bishop,A.W.(1950)
'Summarized proceedings of a Conference on stress analysis', British Journal, Applied Physics, 1, pp.241-251.

Bishop,A.W.(1954)
'The use of pore pressure coefficients in practice', Geotechnique, Dec., 1954.

Bishop,A.W.(1955)
see Bishop,A.W.(1959).

Bishop,A.W.
Some factors controlling the pore pressures set up during the construction of earth dam', Fifth International Conference on Soil Mechanics and Foundation Engineering, Volume 2.

Bishop,A.W.(1959)
The principle of effective stress', Teknisk Ukeblad, Oslo 39(22, October), Norway, pp.859-863.

Bishop,A.W.(1973)
'The influence of an undrained change in stress on the pore pressure in porous media of low compressibility', Geotechnique, Volume 23, 1973, pp.435-442.

Bishop,A.W.,Alpan,I.,Blight,B.G. and Donald,I.B.(1960)
'Factors controlling the strength of partly saturated cohesive soils', Proceedings ASCE Research Conference on Shear Strength, June, 1960, Boulder, Colorado, pp.503-532.

Bishop,A.W. and Blight,G.E.(1963)
'Some aspects of effective stress in saturated and partly saturated soils', Geotechnique, Volume 13, No.3, Sept.,1963, pp.177-197.

Bishop,A.W. and Donald,I.B.(1961)
'The experimental study of partly saturated soils in the triaxial apparatus', Proceedings of 5th International Conference on Soil Mechanics and Foundation Engineering, Paris,Volume 1, pp.13-21.

Bishop,A.W. and Eldin,G.(1950)
'Undrained triaxial tests on saturated sands and their significance in the general theory of shear strength', Geotechnique, 2:1:13-22.

Bishop,A.W. and Gibson,R.E.(1963)
'The influence of the provisions for boundary drainage on strength and consolidation characteristics of soils measured in the triaxial apparatus', Laboratory shear testing of soils, ASTM special technical publication No.361, pp.435-458.

Bishop,A.W. and Henkel,D.J.(1957)
'The measurement of soil properties in the triaxial test', first edition, Edward Arnold (Publisher) Ltd., London, England.

Bishop,A.W. and Henkel,D.J.(1962)
The measurement of soil properties in the triaxial test', 2nd edition, Edward Arnold (Publisher) Ltd., London, England.

Blight,G.E.(1961)
'Strength and consolidation characteristics of compacted soils', Ph.D. thesis, University of London.

Blight,G.E.(1963)
'The effect of non-uniform pore pressures on laboratory measurements of the shear strength of soils', Symp. Laboratory shear testing of soils, Ottawa, ASTM, STP, pp.173-184.

Blight,G.E.(1965)
'A study of effective stresses for volume change', Symp. on moisture equilibria and moisture changes in soils beneath covered areas, ed. by G.D. Aitchison, Soil Mechanics section, CSIRO, Australia, Butterworths, Australia, pp.259-269.

Blight,G.E.(1966)
'Strength characteristics of desiccated clays', Proceedings of ASCE 92 SM6, pp.19-37.

Blight,G.E.(1967)
'Effective stress evaluation for unsaturated soils', Journal of the Soil Mechanics and Foundation Division, American Society of Civil Engineers, Volume 93, No. SM2.

Bocking,K.A. and Fredlund,D.G.(1980)
'Limitations of the axis translation technique', 4th International Conference on expansive soils, Volume 1, Donald Snethen, Editor.

Bolt,G.H. and Miller,R.D.(1958)
'Calculation of component and total potentials of water and soil', Trans. Amer. Geophys. Union, 39, pp.917-928.

Brackley,I.J.A.(1971)
'Partial collapse in unsaturated expansive clay', Proceedings 5th Regional Conference on Soil Mechanics and Foundation Engineering, South Africa, pp.23-30.

Burland,J.B.(1961)
'The concept of effective stress in partly saturated soils', M.Sc. thesis, University of the Witwatersrand, South Africa.

Burland,J.B.(1965)
'Some aspects of the mechanical behaviour of partly saturated soils', Symp. on moisture equilibria and moisture changes in soils beneath covered areas, ed. by G.D. Aitchison, Soil Mechanics section, CSIRO Australia, Butterworths, Australia, pp.270-278.

Coleman,J.D.(1962)
'Stress/strain relations for partly saturated soil', correspondence, Geotechnique, 12(4), pp.348-350.

Corey,A.T.(1954)
'The interrelation between gas and oil relative permeabilities', Producer's Monthly, pp.38-41.

Corey,A.T.(1957)
'Measurement of water and air permeability in unsaturated soil', Proceedings of the Soil Science Society of America, Volume 21, No.1, pp.7-10.

Coulomb,C.A.(1776)
'Essai sur une application des règles de maximis et minimis á quelques problèmes de statique relatifs á L'Architecture', Memorandum Academie Royale, Pres. Div. Sav., Vol.7, pp.343-382.

Crawford,C.B.(1960)
'The influence of rate of strain on effective stresses in sensitive clays', Spec. tech. Publs. Am. Soc. Test Mater.254,31.

Croney,D.(1952)
'The movement and distribution of water in soils', Geotechnique, Volume 3, pp.1-16.

Croney,D. and Coleman,J.D.(1948)
'Soil thermodynamics applied to the movement of moisture in road foundations', Proceedings 7th International Congress in Applied Mechanics 3, pp.163-177.

Croney,D. and Coleman,J.D.(1954)
'Soil structure in relation to soil suction(pF)', Journal Soil Science 5(1), pp.75-84.

Croney D. and Coleman J.D.(1960)
'Pore pressure and suction in soil', Pore Pressure and Suction in Soils (1960), Butterworths, London, pp.31-37.

Croney,D., Coleman,J.D. and Black, W.P.M.(1958)
'The movement and distribution of water in soil in relation to highway design and performance', Highway Research Board Special Report No.40, Washington,D.C..

Croney,D., Coleman,J.D. and Bridge,P.M.(1952)
'The suction of moisture held in soil and other porous materials', Road Research Technical Paper No.24, London(H.M.S. office).

Croney,D., Lewis,W.A. and Coleman,J.D.(1950)
'Calculation of the moisture distribution beneath structures', Civil Engineering (L.) 45(524):103-106.

Darley,P.(1972)
'Discussion: apparatus for measuring volume change suitable for automatic logging by G.C. Rowlands', Geotechnique, Volume 23, No.1, pp.140-141.

Donald,I.B.(1961)
'The mechanical properties of saturated and partly saturated soils with special reference to negative pore water pressures', Ph.D. thesis, University of London.

Donald,I.B.(1963)
'Effective stress parameters in unsaturated soils', Proc. 4th Australia New-Zealand Conference on Soil Mechanics and Foundation Engineering, Adelaide, pp.41-46.

Dorsey,N.E.(1940)
'Properties of ordinary water-substance', America Chemical Society, Monograph Series, Reinhold Publishing Corporation.

Durelli,A.J., Phillips,E.A. and Tsao,C.H.(1958)
'Introduction to the theoretical and experimental analysis of stress and strain', Mcgraw-Hill Book Company, Inc., pp.233-236.

Escario,V.(1980)
'Suction controlled penetration and shear tests', Proc. of the Fourth International Expansive Soil Conference, Denver, Colorado, U.S.A.,1980.

Foster,A.G.(1948)
'Pore size and pore distribution', Disc. Faraday Soc.,No.3.

Fredlund,D.G.(1973)
'Volume change behaviour of unsaturated soils', Ph.D. thesis, University of Alberta at Edmonton, Alberta, Canada in 1973.

Fredlund,D.G.(1974)
'Engineering approach to soil continua', Proceedings Volume 1, Second Symposium Application of Solid Mechanics, June,17 and 18, 1974.

Fredlund,D.G.(1975)
'A diffused air volume indicator for unsaturated soils', Canadian Geotechnical Journal Volume 12, No.4, 1975, pp.533-539.

Fredlund,D.G.(1976)
'Density and compressibility characteristics of air-water mixtures', Canadian Geotechnical Journal, Volume 13, No.4, 1976, pp. 386-396.

Fredlund,D.G.(1979)
'Appropriate concepts and technology for unsaturated soil', Canadian Geotechnical Journal Volume 16, No.1,(2/1979), pp.121-139.

Fredlund,D.G.(1980)
'The shear strength of unsaturated soils and its relationship to slope stability problems in Hong Kong', Hong Kong Engineer Volume 9, No.4, pp.37-45.

Fredlund,D.G.(1981)
'Seepage in saturated soils in ground water and seepage problems', Proceedings of 10th International Conference on Soil Mechanics and Foundation Engineering, pp. 629-641.

Fredlund,D.G. and Hasan,J.U.(1979)
'One-dimensional consolidation theory: unsaturated soils', Canadian Geotechnical Journal Volume 16, No.3, 1979, pp.521-531.

Fredlund,D.G. and Morgenstern,N.R.(1973)
'Pressure response below high air entry discs', Proceedings of the 3rd International Conference on Expansive soils, pp.97-108.

Fredlund,D.G. and Morgenstern,N.R.(1976)
'Constitutive relations for volume change in unsaturated soils', Canadian Geotechnical Journal, Volume 13, pp.261-276.

Fredlund,D.G. and Morgenstern,N.R.(1977)
'Stress state variables for unsaturated soils', ASCE Journal of the Geotechnical Engineering Division, 103(GT5), pp.447-466.

Fredlund,D.G., Morgenstern,N.R. and Widger,R.A.(1978)
'The shear strength of unsaturated soils', Canadian Geotechnical Journal, Volume 15, No.3(8/1978), pp.313-322.

Gardner,W.R.(1960)
'Soil suction and water movement', Pore Pressure and Suction in Soils, Butterworths, London, pp.137-140.

Garlanger,J.E.(1970)
'Pore pressures in partially saturated soils', Ph.D. thesis, University of Illinois at Urbana-Champaign.

Gibson,R.E. and Henkel,D.J.(1954)
'Influence of duration of tests at constant rate of strain on measured 'drained' strength', Geotechnique, 4:6-15.

Gibson,R.E. and Lumb,P.(1953)
'Numerical solution of some problems in the consolidation of clay', Journal Instn. Civ. Engrs. 1, Pt.1,182.

Green,R.B.(1951)
'Ordinary liquid water-substance, its thermodynamic property, dynamic behaviour, and tensile strength', Ph.D. thesis, Massachusetts Institute of Technology at Cambridge, Massachusetts, 1951.

Gulhati,S.K.(1972)
'Shear behaviour of compacted soils in the saturated and partially saturated states', Ph.D. thesis, Indian Inst. of Tech. Delhi.

Gulhati,S.K.(1975)
'Shear behaviour of partially saturated soils', 5th Asian Regional Conference on Soil Mechanics and Foundation Engineering, India.

Gulhati,S.K.(1978)
'Engineering properties of soils', Tata Mcgraw Hill Publishing Co. Ltd., New Delhi, 184.

Gulhati,S.K.(1980)
'Partially saturated soils selection of design parameters', Proceedings of GEOTECH-80 Conf. of Indian Geotechnical Society, Bombay, 1980, Volume 2, pp.19-24.

Gulhati,S.K. and Satija,B.S.(1981)
'Shear strength of partially saturated soils', Proc. 10th International Conference on Soil Mechanics and Foundation Engineering (1981), Stockholm, Swedwn.

Haines,W.B.(1930)
'The hysteresis effect in capillary properties and the modes of moisture distribution associated therewith', Journal Agric. Sci. 19, pp.97.

Hamilton,L.W.(1939)
'The effect of internal hydrostatic pressure on the shearing strength of soils', Proc. ASTM. Volume 39, pp.1100.

Hasan,J.U. and Fredlund,D.G.(1980)
'Pore pressure parameters for unsaturated soils', Canadian Geotechnical Journal, Volume 17, No.3, 1980, pp.395-404.

Henkel,D.J.(1959)
'The relationships between the strength, pore water pressure and volume-change characteristics of saturated clays', Geotechnique 9:119-135.

Henkel,D.J.(1960)
'The shear strength of saturated remoulded clays', Proc. research conf. on shear strength of cohesive soils, Boulder, Colorado, pp.533-554.

Hilf,J.W.(1948)
'Estimating construction pore-pressures in rolled earth dams', Proc. 2nd International Soil Mechanics, 3: 234-240.

Hilf,J.W.(1956)
'An investigation of pore water pressure in compacted cohesive soils', Technical memorandum 654, Department of the interior bureau of reclamation, Denver, Colorado, USA.

Ho,D.Y.F.(1981)
'The shear strength of unsaturated Hong Kong soils', M.Sc. thesis, University of Saskatchewan, Saskatoon, Saskachewan, Canada.

Ho,D.Y.F. and Fredlund,D.G.(1982)
'Increase in strength due to suction for two Hong Kong soils', (Engineering and construction in tropical and residual soils), Proceedings of the ASCE Geotechnical Engineering Division, Specialty Conference, Honolulu, 1982, pp.263-295.

Hvorslev,M.J.(1937)
'Ingeniorvidenskabelige skifter A No.45'

Jennings,J.E.(1957)
'Discussion on M.S. Youssef's paper', Proceedings of the 4th International Conference on Soil Mechanics and Foundation Engineering, Volume 3, pp.168.

Jennings,J.E.(1960)
'A revised effective stress law for use in the prediction of the behaviour of unsaturated soils', Pore Pressure in Soils (1960), Butterworths, London, pp.26-30.

Jennings,J.E. and Burland,J.B.(1962)
'Limitations to the use of effective stress in partly-saturated soils', Geotechnique 12, No.2, pp.125-144.

Kawakami,H and Abe,H.(1975)
'Volume change characteristics and collapse in unsaturated soils during triaxial test', 5th Asian Regional Conference on Soil Mechanics and Foundation Engineering, India.

Koning,H.L.(1963)
'Some observations on the modulus of compressibility of water', Conference on settlement and compressibility of soils, Weisbaden, West Germany, pp.33-36.

Krahn,J. and Fredlund,D.G.(1972)
'On total, matrix and osmotic suction', Soil Science 114(5), pp.339-348.

Ladd,C.C.(1960)
'Mechanics of swelling by compacted clay', Highway Research Board Bulletin No. 245, National Academy of Science-National Research Council(USA), Publication 731, pp.10-26.

Lambe,T.W.(1960a)
'A mechanistic picture of shear strength in clay', Proceedings ASCE Research Conference on shear strength of cohesive soils, Boulder, Colorado, pp.555-580.

Lambe,T.W.(1960b)
'Discussion: session 5(on 'Factors controlling the strength of partly saturated cohesive soils')', Proc. ASCE Research Conf. on shear strength of cohesive soils, Boulder, Colorado, pp. 1094-1095.

Langfelder,L.J.,Chen,C.G. and Justice,J.A.(1968)
'Air permeability of compacted cohesive soils', Journal of the Soil Mechanics and Foundation Division, Proceedings of the American Society of Civil Engineers, Vol.94, No.SM4, pp.981-1001.

Lee,K.L., Morrison,R.A. and Haley,S.C.(1969)
'A note on the pore pressure parameter B', Proceedings of the 7th International Conference on Soil Mechanics and Foundation Engineering, pp.231-238.

Lewis,W.A. and Ross,N.F.(1955)
'An investigation of the relationship between the shear strength of remoulded cohesive soil and the soil moisture suction', Road Research Laboratory Research Note RN/2389/WAL.NFR (Unpublished).

Lloret,A and Alonso,E.E.(1980)
'Consolidation of unsaturated soils including swelling and collapse behaviour', Getechnique Volume 30(1980).

Lowe,J. and Johnson,T.C.(1960)
'Use of back pressure to increase degree of saturation of triaxial test specimens', ASCE Research Conference on shear strength of cohesive soils (1960).

Lumb,P.(1966)
'The residual soils of Hong Kong', Correspondence, Geotechnique, Volume 16, No.4, pp.359-360.

Lumb,P.(1968)
'Choice of strain-rate for drained tests on unsaturated soils', Correspondence, Geotechnique, 18(4), pp.511-514.

M.I.T.(1963)
'Engineering behaviour of partially saturated soils', Phase Report No.1 to U.S. army engineers waterways experimental station, Vicksburg, Mississippi, The Soil Engineering Division, Department of Civil Engineering, M.I.T., Contract No. DA-22-079-eng-288.

Maranha das Neves,E.(1971)
'The influence of negative pore water pressures on the strength characteristics of compacted soils', Publication No.386, National Laboratory of Civil Engineering, Lisbon, Portugal.

Marshall,T.J.(1959)
'Relations between water and soil', Com. Bureau Soils Tech. Comm. No.50, C.A.B. Harpenden.

Matyas,E.L.(1963)
'Compressibility and shear strength of compacted soils', Ph.D. thesis, University of London.

Matyas,E.L.(1966)
'Air and water permeability of compacted soils', Permeability and Capillarity of soils, American Society for Testing Materials, Special Technical Publication, No.417, Philadelphia, Pa.,U.S.A..

Matyas,E.L. and Radhakrishna,H.S.(1968)
'Volume change characteristics of partially saturated soils', Geotechnique, Volume 18(4), pp.432-448.

Muir-Wood,D.(1979)
'The behaviour of partly saturated soils', University Engineering Department, Trumpington St.,Cambridge.

Newland,P.L.(1965)
'The behaviour of soils in terms of two kinds of effective stress', Proceedings of Conference on engineering effects of moisture changes in soils, Texas, A and M University, pp.78-92.

Olson,R.E. and Langfelder,L.J.(1965)
'Pore water pressures in unsaturated soils', Journal of the Soil Mechanics and Foundations Division, Proceedings of the American Society of Civil Engineers, July, 1965, pp.127-150.

Omer,B.M.A.(1978)
'A study of layered clay from Grangemouth', Ph.D. thesis, 1978, University of Glasgow.

PORE PRESSURE AND SUCTION IN SOILS (1960), BUTTERWORTHS, LONDON.

Poulos,S.J.(1964)
'Control of leakage in the triaxial test', Ph.D. thesis, Harvard University, Cambridge, Massachusetts, March, 1964.

Poulos,S.J.(1981)
'Discussion of soil testing practices', Laboratory shear strength of soil ASTM Special Technical Publication 740, pp.665-666.

Rendulic,L(1936)
'Relation between void ratio and effective principal stresses for a remoulded silty clay', Proc. 1st International Conf. on Soil Mechanics, Volume 3, pp.48-51.

Rendulic,L.(1937)
'Ein Grundgesetz der Tonmechanik und sein experimentaler Beweis', Bauingenieur, 18, pp.459-467.

Richards,B.G.(1966)
'The significance of moisture flow and equilibria in unsaturated soils in relation to the design of engineering structures built on shallow foundations in Australia. Symposium on permeability and capillarity', American Society for testing and materials, Atlantic City, N.J..

Richards,B.G.(1974)
'Behaviour of unsaturated soils', Soil Mechanics-New Horizons, Edited by I.K.Lee, Newnes-Butterworths, London, pp.112-157.

Ruddock,E.C.(1966)
'The engineering properties of residual soils', Correspondence, Geotechnique, Volume 16, No.1, pp.78-81.

Satija,B.S.(1978)
'Shear behaviour of partially saturated soils', Ph.D. thesis, Indian Inst. of Tech., Delhi.

Schofield,R.K.(1935)
'The pF of the water in soil', Trans. 3rd International Congress in Soil Science 2:37-48.

Schofield,R.K.(1960)
'Suction in swollen clays', Pore Pressure and Suction in Soils, Butterworths, London, pp.59-60 and 143-144.

Schuurman,E.(1964)
'De Compressibiliteit van een water-Lucht-mengsel en de relatie tussen de lucht-en de waterspanning', LGM-Mededelingen, 9(1), pp.1-16.

Schuurman,E.(1966)
'The compressibility of an air/water mixture and a theoretical relation between the air and water pressures', Geotechnique 16(4), pp.269-281.

Silveira,I.(1953)
'Consolidation of a cylindrical clay sample with external radial flow of water', Proc. 3rd Int. Conf. Soil Mechanics, 1:55.

Skempton,A.W.(1948)
'A study of the immediate triaxial test on cohesive soils', Proc. Second Int. Conf. Soil Mechanics, 1:192-196.

Skempton,A.W.(1954)
'The pore pressure coefficients A and B', Geotechnique 4, 4, pp.143-147.

Skempton,A.W.(1960)
'Effective stress in soils, concrete and rocks', Pore Pressure and Suction in Soils(1960), Butterworths, London, pp.4-16.

Skempton,A.W. and Bishop,A.W.(1954)
'Building materials, their elasticity and inelasticity', Soils, Chapter 10, North Holland Publication Co., Amsterdam.

Sparks,A.D.W.(1963)
'Theoretical considerations of stress equations for partly saturated soils', Proceedings 3rd Regional Conference for Africa on Soil Mechanics and Foundation Engineering, Salisbury, Southern Rhodesia, Volume 1, pp.215-218.

Sridharan,A.(1968)
'Some studies on the strength of partly-saturated clays', Dissertation Abstracts, V.29:11(B), Ph.D. thesis, Purdue University, 1968, University microfilm service, No. 69-7502, 198pp..

Taylor,D.W.(1944)
'Tenth progress report on shear research to U.S. Engineers', M.I.T. Publication.

Taylor,D.W.(1948)
'Fundamentals of soil mechanics', New York:Wiley.

Terzaghi,K.(1923)
'Die Berechnungder Durchlassigkeitsziffer des Tones aus dem Verlauf der hydrodynamischen spannungserscheinungen'('Calculation of the porosity index of clay from hydrodynamic tension conditions'), Sitzbericht (Abt.IIa) Akademie der Wissenchaften, Vienna, 132.

Terzaghi,K. and Frohlich,O.K.(1936)
'Theorie de Setzung von Tonschichten', Deuticke Verlag, Vienna.

Towner,G.D.(1961)
'Influence of soil-water suction on some mechanical properties of soils', Journal Soil Science 12:1, pp.180-187.

Wissa,A.E.Z.(1969)
'Pore pressure measurement in saturated stiff soils', Journal Soil Mechanics Foundations Division, Am. Soc. Civ. Engrs. 95, SM4, pp.1063-1073.

Wood,D.M.(1979)
'The behaviour of partly saturated soils: A review by D.M. Wood', CUED/D-SOILS/TR 69 1979, Department of Engineering, University of Cambridge, England.

Yong,R.N.(1979)
'Some aspects of soil suction, shear strength and soil stability', Proceedings of Geotechnical Engineering Seminar of the Southeast Asian Society of Soil Engineering at the Sixth Asian Regional Conf. on Soil Mech. and Found. Eng.,31th, July.

Yong,R.N., Japp,R.D. and How,G.(1971)
'Shear strength of partially saturated clays', Proc. 4th Asian Regional Conference on Soil Mechanics and Foundation Engineering, Bangkok 1, pp.183-187.

Yong,R.N. and Warkentin,B.P.(1975)
'Soil properties and behaviour', Developments in Geotechnical Engineering 5, Elsevier Scientific Publishing Company.

APPENDIX 1

AXIS-TRANSLATION TECHNIQUE

Appendix 1

Axis translation technique

A1.1 General

The axis translation technique is commonly used to measure the matrix suction of undisturbed and remoulded soil samples. This technique was developed by Hilf (1956) as a means of avoiding the cavitation problem, but it has subsequently seen limited application in triaxial shear and volume change testing of unsaturated soils. According to Hilf, the technique simply translates the origin of reference for the pore water pressure measurement from standard atmospheric condition to the final air pressure value; hence the term 'axis translation'.

A1.2 Limitations of the axis translation technique

For the axis translation technique to be valid it must be possible to increase the ambient air pressure around and within a soil sample without producing deformation. This implies that the value of stress state variables (σ - Ua) and (Ua - Uw) must be unchanged. In other words, $\Delta\sigma$, ΔUa and ΔUw must be equal. Clearly all pore-air must be interconnected to the surface of the sample for an increase in total stress (i.e. applied by increasing the air pressure around the sample) to induce an equal change in pore-air pressure throughout the sample. The experimental data presented by Hilf demonstrates the equal translation of all stress components (Fig.A1.1). Olson and Langfelder (1965) also concluded that the 'axis translation technique is valid provided all gas voids are interconnected'.

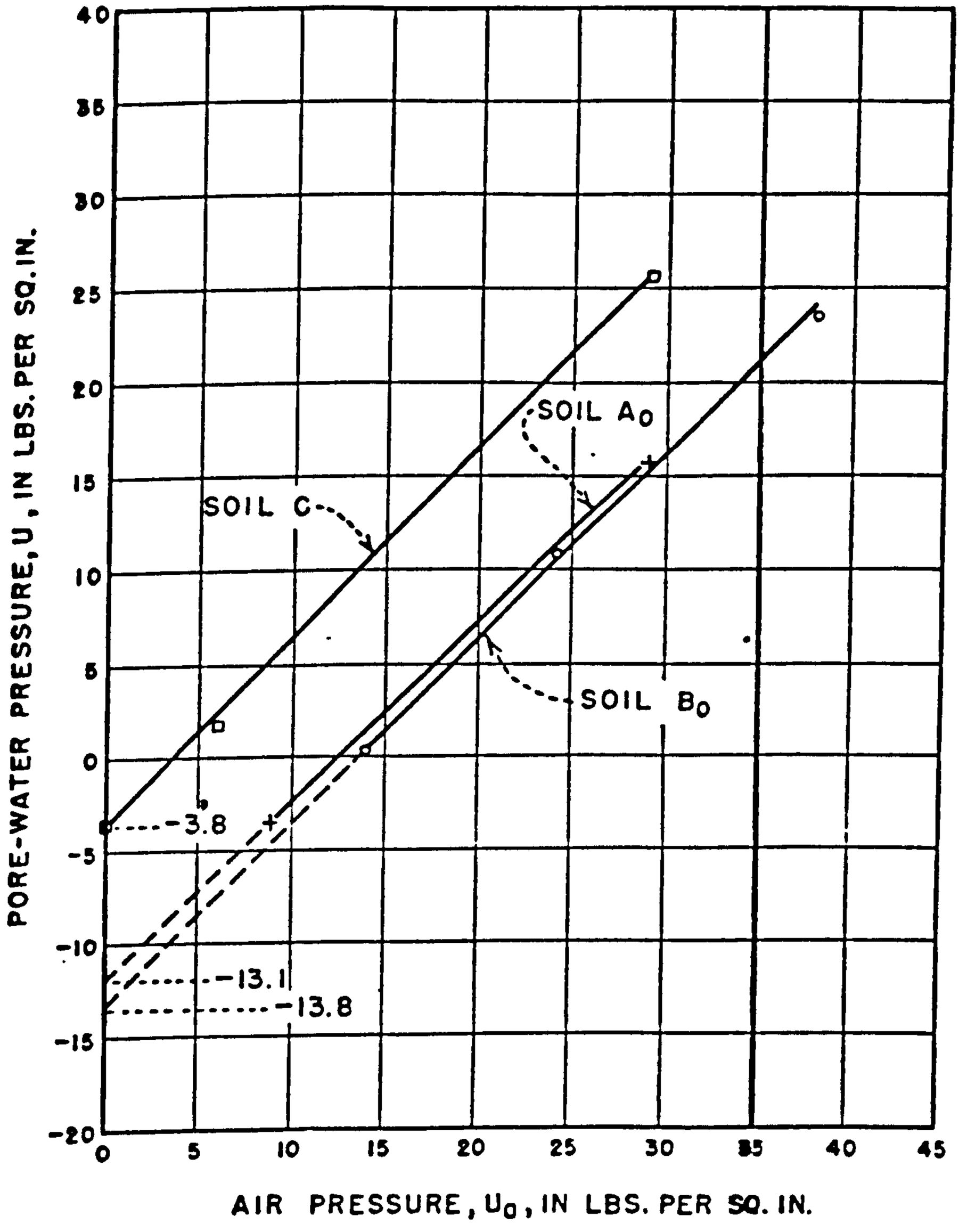

Fig. A1.1: Determination of capillary pressure by translation of the origin (Hilf, 1956).

Pore-water containing occluded (i.e. non-interconnected) air bubbles renders the pore fluid highly compressible.

Experimental evidence indicates that air does become occluded in the pore-water of a soil. Numerous researchers (Corey, 1954; Corey, 1957; Ladd, 1960; Matyas, 1966; Langfelder, Chen and Justice, 1968; Barden and Pavlakis, 1971) have shown that the air permeability of an unsaturated soil decreases to essentially zero as the degree of saturation is increased to about 85 percent. In the case of remoulded soils, this corresponds to approximately optimum water content.

Bocking and Fredlund (1980) developed two versions of a mathematical model to study the following:

(i) the effect of pressure measuring system flexibility on the results of axis translation tests. (All such devices require the flow of a small but finite amount of water out of the soil sample in order to register pressure changes. Therefore it follows that the soil sample must undergo some volume change during the test. Bishop and Henkel (1962) and Fredlund and Morgenstern (1973) showed that even slight flexibility in the pressure measuring system could greatly affect the response time).

(ii) the effect of the presence of occluded air bubbles on the measurement of suction.

(iii) possible errors in the interpretation of axis translation test results.

In version I, it was assumed that the pore air was totally

interconnected; in version II, it was assumed that the pore air was totally occluded.

The results indicated that the actual soil suction could be over-estimated if the sample contained significant amounts of occluded air. The use of the axis translation test to measure soil suction in totally interconnected pore-air soils was theoretically correct. Also, air diffusion through the high air entry disc could cause an under-estimation of the soil suction.

APPENDIX 2

THREE-DIMENSIONAL GRAPHICAL METHOD

APPENDIX 2

THREE-DIMENSIONAL GRAPHICAL METHOD

A2.1 General Strategy

GINOSURF allows a user to specify a surface as heights at a series of randomly spaced points in the (X,Y) plane. In such a case the first step is to interpolate from the random points to get heights at the nodes of a sufficiently finely spaced regular rectangular grid of points in the (X,Y) plane.

Of course, if the surface is already defined as values at the nodes of such a grid then no interpolation is necessary to obtain grid points. Again, if the surface is defined by a function which will yield the height of the surface at any given (X,Y) point, a regular grid of surface heights can be obtained directly by calling the function to evaluate the height at each node. The regular grid values obtained permit each contour to be traced simply through the specified regior, or an isometric projection to be drawn.

The strategy is illustrated by the flow diagram in figure A2.1.

A2.2 Interpolating from Random Data Points

The method GINOSURF uses to interpolate from randomly distributed points to obtain a regular grid of points is that described by Falconer (1971). Briefly, the algorithm is as follows.

To obtain the height of the surface at a given point

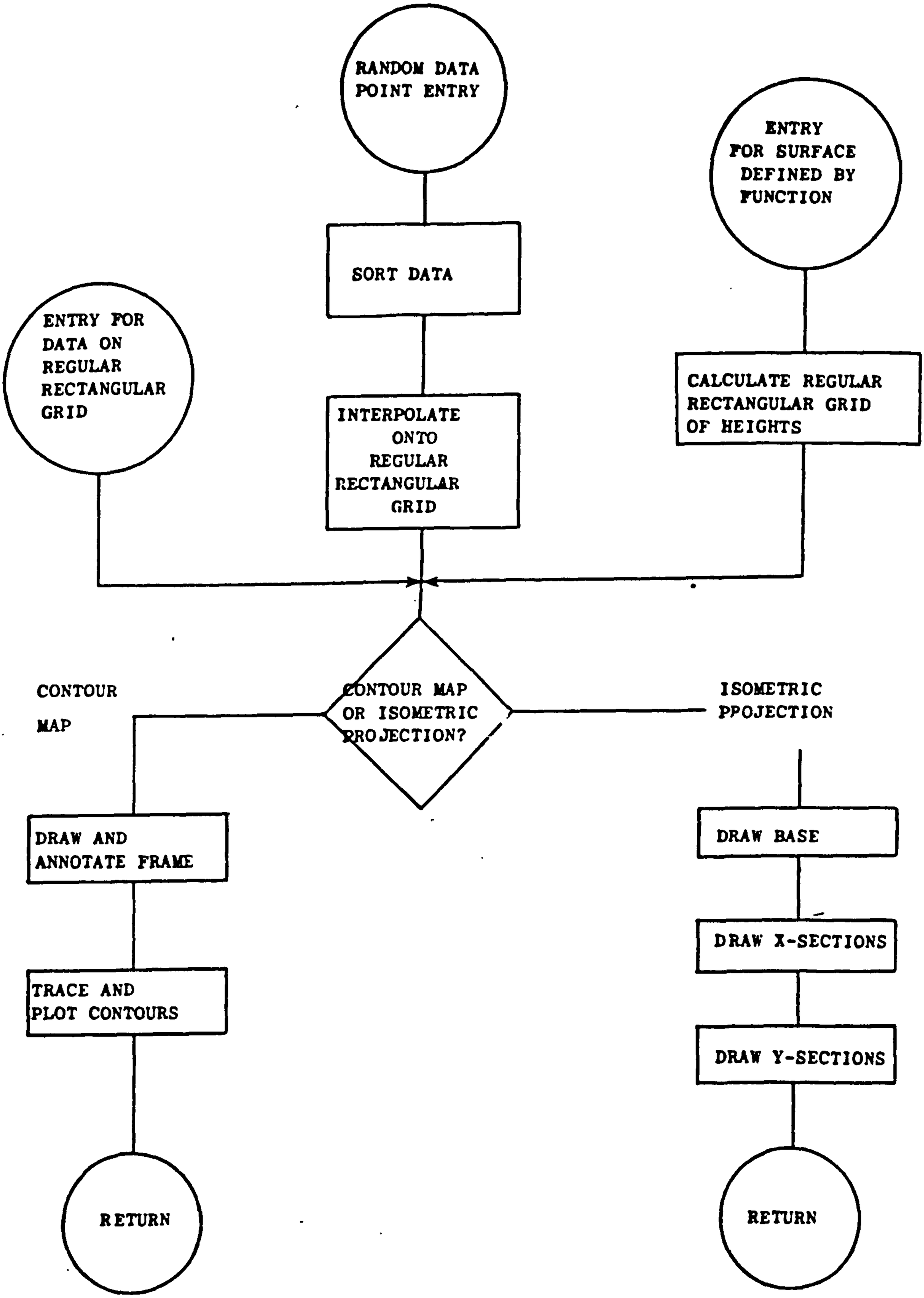

Figure 2.1 GENERAL STRATEGY OF GINOSURF

only those data points which lie within a circle of radius S centred on the given point are used. The height values of the data points used are weighted by a factor W depending on their distance from the given points:

$$W = \left(\frac{S-D}{D}\right)^2$$

where D is the distance between the data point and the given point.

The required height is then obtained by a least squares fit of a paraboloid surface to the weighted data points. Since four parameters are required to specify a paraboloid, it is essential that the circle contains at least four data points if the least squares equations are to be non-singular. Provided S is kept constant, the surface defined by this interpolating technique will be continuous and have continuous first derivatives.

The algorithm chooses S so that, on average, there will be LP data points inside the circle. At the risk of introducing discontinuities in the surface, if any circular patch contains fewer than six data points then the radius of that patch only is increased until at least six points are included. The value six has been found desirable in order to avoid singularity problems when solving the least squares equations.

LP is a parameter which can be changed by the user by calling routine CIRPTS before calling RANCON or RANGRD. Its default value is 24. A value of at least 24 should normally be used since near the corners of the data region the patches are effectively reduced to quarter circles. Values much less than

24 for LP would result in frequent changes of S and the consequent dangers of surface discontinuity. For the same reason, a higher value of LP may be desirable if the random data points have a very variable density of distribution.

However, larger values of LP will tend to have an increased smoothing effect on the surface, and will result in a longer computation time (varying linearly with LP). Of course LP must never exceed NP, the total number of data points.

A2.3 Tracing Contours Through the Regular Grid of Surface Values

In GINOSURF Mark I the regular grid of surface values is used as the basis for contour tracing. The method of contour tracing is due to Heap and Pink (1969). With a given contour level the algorithm first locates segments between adjacent grid points on the boundary of the region and along horizontal mesh lines which the contour must cross. All open contours are traced from the boundary, through each elementary mesh square until the boundary is again reached. Closed contours are then detected and similarly traced by looking for crossed segments through which no contour of the desired level has yet been traced. The method of tracing through an elementary mesh square (figure A2.2) is roughly as follows: Assume the square is entered through OA (O,A,B,C being the mesh points). Locate the point R at which OA is crossed by linear interpolation using heights of O and A. Estimate height of centre of square D as average of those of O, A, B and C. Decide whether the contour then crosses OD or AD and find the crossing

points of the diagonal by linear interpolation between O and D or A and D. Continue similarly across any further diagonals and/or sides until the point of exit from the square is determined. The technique is then repeated in the next square and so on.

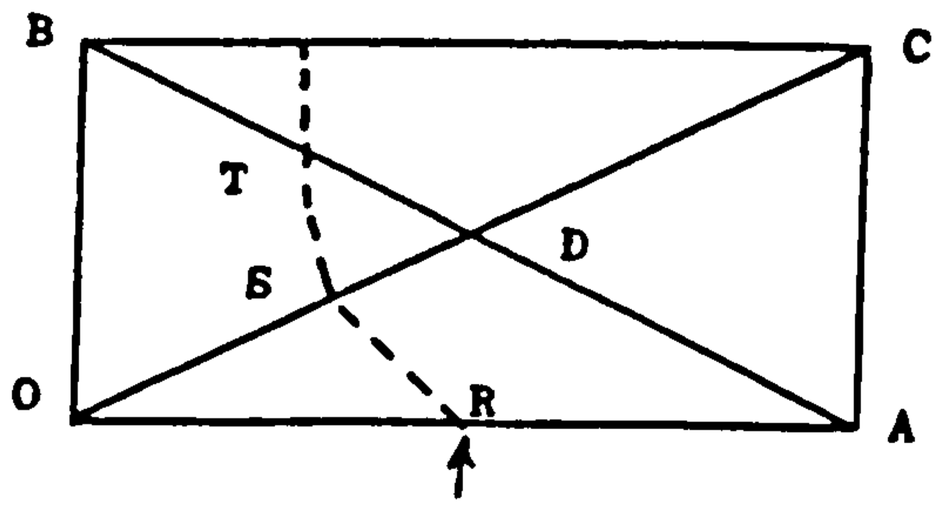

Figure A2.2

It is essential, therefore, that the regular grid spacing should be sufficiently fine for linear interpolation to be adequate and for it to be assumed that, in general, a contour will not cross a mesh line more than once between adjacent grid points.

Normally the contouring routines automatically annotate any contours produced at suitable points. The annotation can be cancelled and the type of line (continuous, broken etc) changed by calling the routine LABCON.

The smooth curves algorithnm is that of McConalogue (1970) and in any section uses only the four nearest points determined by the tracing algorithm to define the curve.

A2.4 Isometric plotting

An isometric projection of a surface is an orthogonal projection of the surface (i.e. a projection from infinity onto

a plane at right angles to the line of sight) in which the coordinate axes make equal angles of $\tan^{-1}\sqrt{2}$ with the line of sight.

If the surface happens to be two adjacent vertical faces and the top of a cube, its projection will be as figure A2.3.

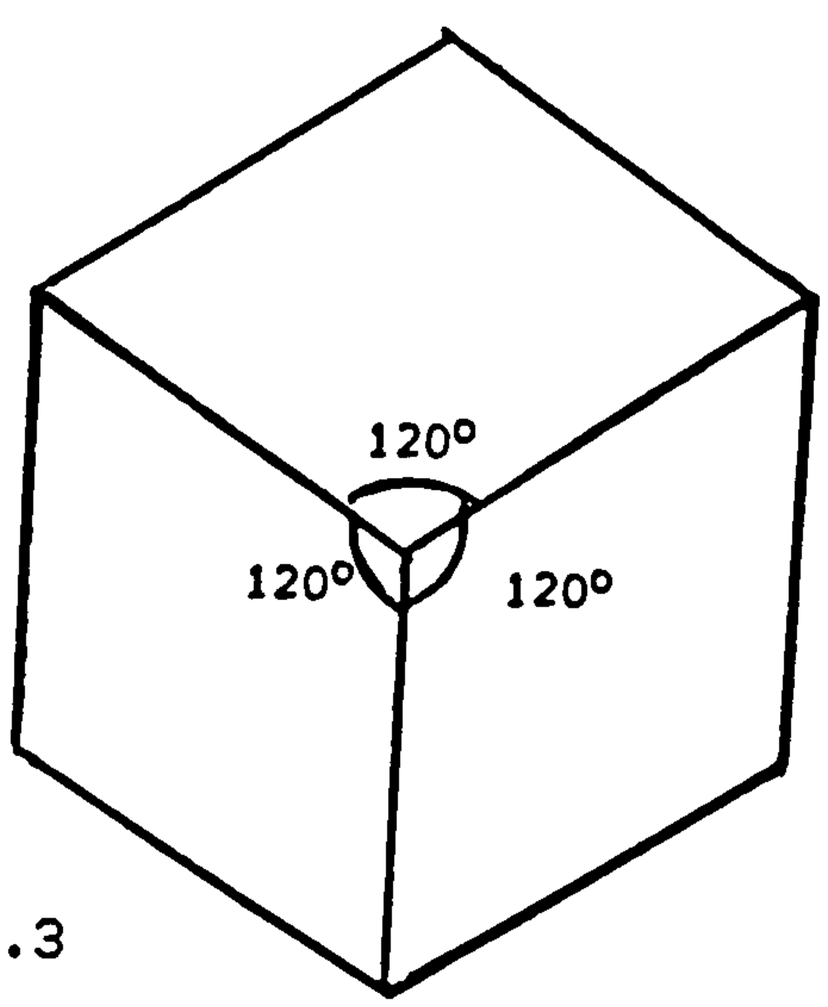

Figure A2.3

In GINOSURF the surface for isometric projection is defined by heights (Z) at the nodes of a regular rectangular grid in the X-Y plane. The algorithm of HALL (1973) is used to plot all visible points and to join adjacent visible points in both planes of constant X-value and of constant Y-value. To simplify the geometry the physical distances chosen for each X step and Y step are identical. A plane surface of constant height would thus be drawn as figure A2.4, the mesh appearing as an array of $60^{o}/120^{o}$ rhombuses.

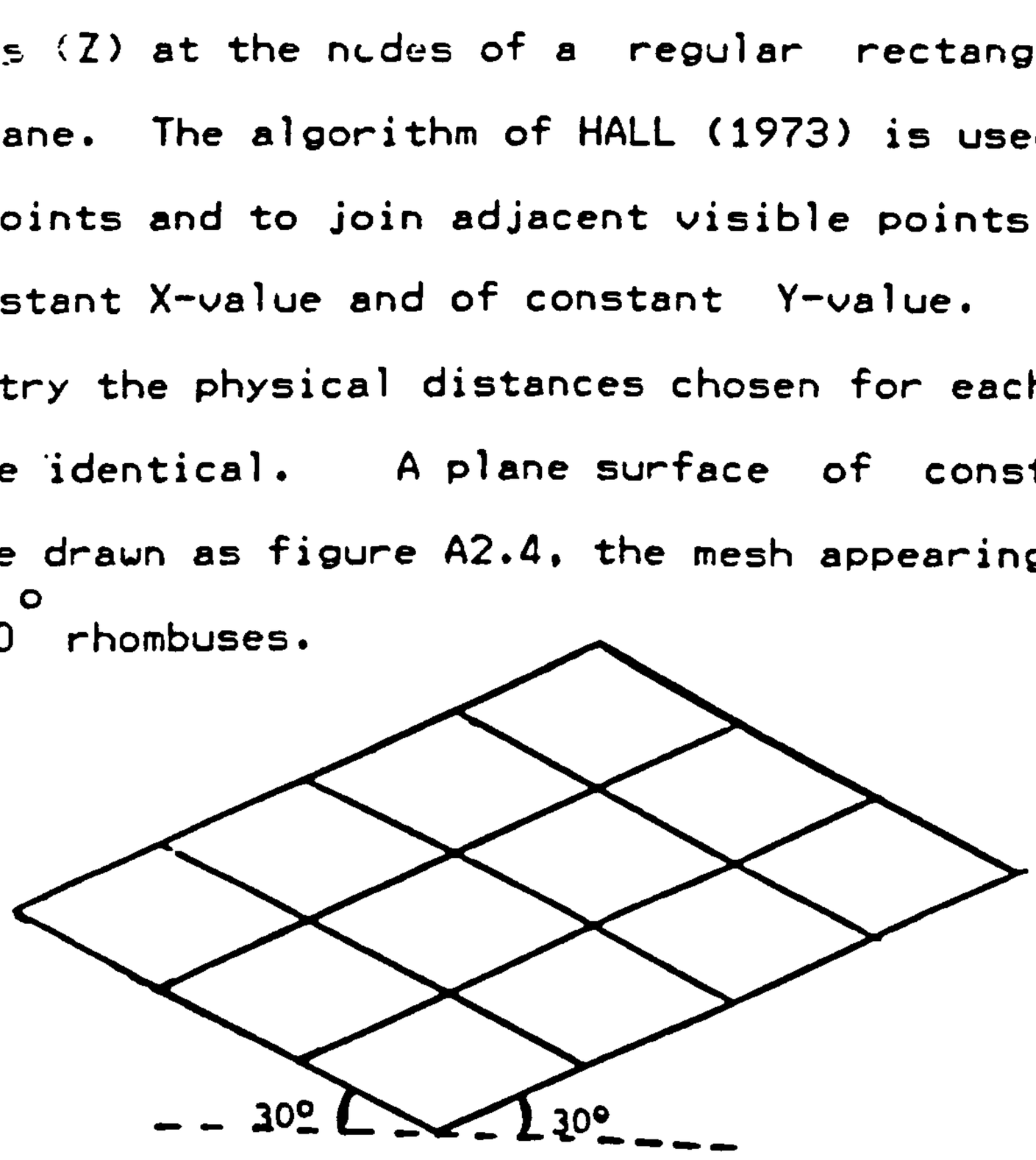

Figure A2.4

For a non-flat surface, the projections of the surface points can be obtained by measuring a vertical distance corresponding to the height above the corresponding projected mesh points.

The algorithm connects adjacent mesh points by line segments, working in slices of the surface from the front edges backwards. It keeps a record of visible points so that hidden points are not drawn, and contains a simple interpolation algorithm for drawing only the visible elements of each line segment (this can lead to slightly incomplete lines in very undulating surface areas in certain circumstances).

To give a feeling of solidity to the drawing the default option is to draw, as a base, lines corresponding to the front X- and Y- edges of the mesh at the minimum height level of the surface and to draw in verticals linking these base lines to the projections of the front-edge mesh points. (See figure A2.5). Again the default option is to put scale information on the X- and Y- base lines, and to draw height scales up from the extreme left- and right-hand ends of the base (figure A2.5).

To give the effect of altering the vertical angle of view of the surface, the user is provided with a facility for controlling the ratio of the physical scale chosen for representing the height to the scales used for representing X and Y displacements (routine HEIRAT).

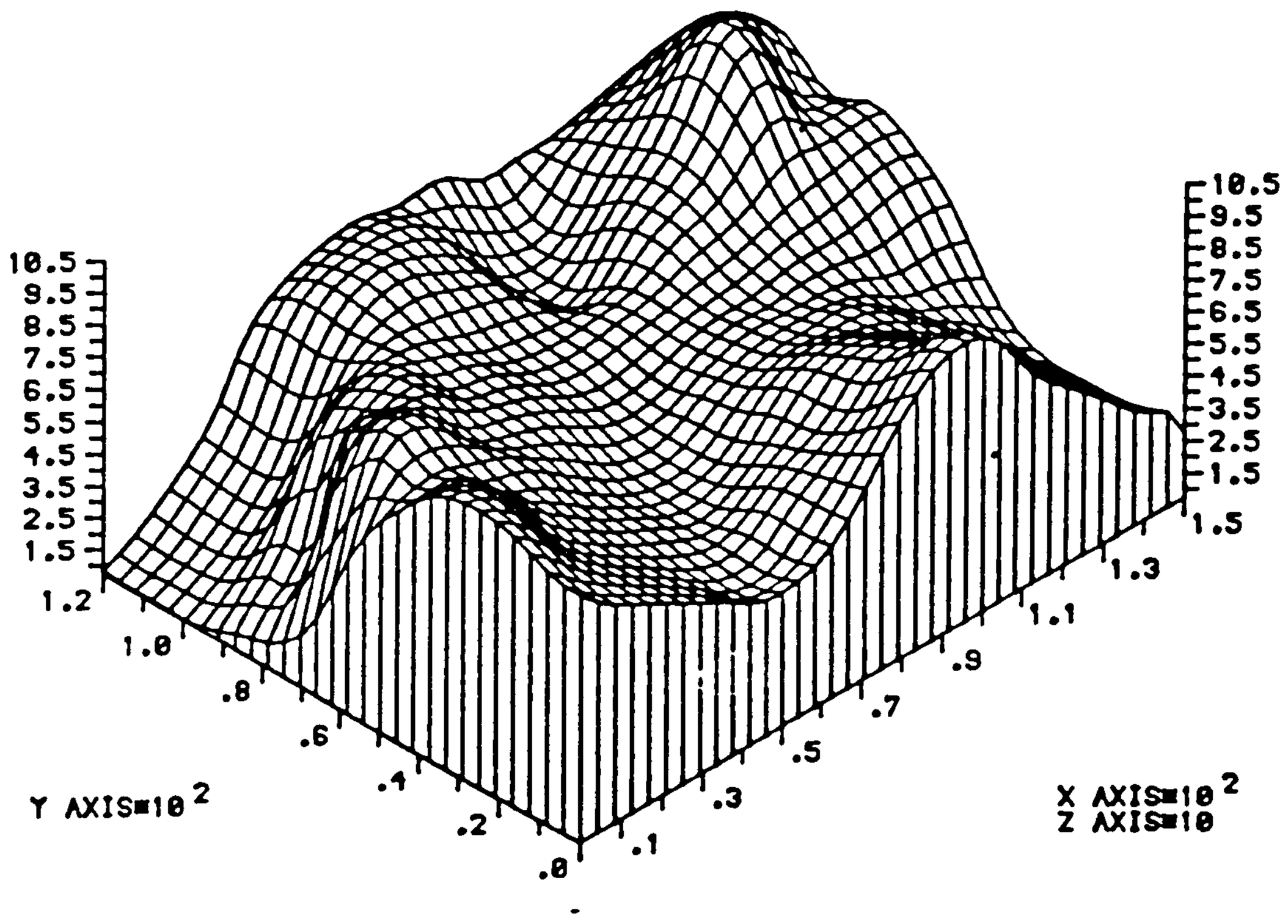
10.5
9.5
8.5
7.5
6.5
5.5
4.5
3.5
2.5
1.5
1.2
1.0
.8
.6
.4
.2
.0
Y AXIS=10 2
.1
.3
.5
.7
.9
1.1
1.3
10.5
9.5
8.5
7.5
6.5
5.5
4.5
3.5
2.5
1.5
1.5
X AXIS=10 2
Z AXIS=10

Fig. A2.5

REFERENCES

Falconer,K.J.(1971)
'A general purpose algorithm for contouring over scattered data points', National physical laboratory report NAC6, September, 1971.

Hall,C.(1973)
'An algorithm for the production of an isometric projection of a three-dimensional surface', National physical laboratory report NAC41, November, 1973.

Heap,B.R. and Pink,M.G.(1969)
'Three contouring algorithms', National physical laboratory report DNAM81, December, 1969.

McConalogue,D.J.(1970)
'A quasi-intrinsic scheme for passing a smooth curve through a discrete set of points', Computer Journal, Volume 13, No.4, November, 1970.

McConalogue,D.J.(1971)
'Algorithm 66 - An automatic French-curve procedure for use with an incremented plotter', Computer Journal, Volume 14, No.2, May, 1971.

APPENDIX 3

ANALYSIS OF THE NULL TESTS

(NO VOLUME CHANGE TESTS)

Appendix 3

Analysis of the Null tests (No volume change tests)

A3.1 Null test programme

The Null Test programme involved a series of tests on saturated samples. The programme was divided into two sections, in which the ten tests in Section I were performed by changing simultaneously the total and water pressures and measuring the overall volume change with time. These tests were performed to check the procedure and equipment for a known case, thereby establishing the degree of reliability and accuracy that could be anticipated. In the triaxial apparatus, the change in the total volume of the sample, the change in the volume of water in the sample and the change in volume of water going into or out of the triaxial cell were measured.

The six tests in Section II had an air pressure applied to the top of the saturated samples. The null tests involved changing simultaneously the total, air and water pressures by equal amounts. In this case, the air pressure reaction time was instantaneous and it was desirable to ascertain whether or not equilibrium could be maintained with an air-water interface (contractile skin) at the surface of the sample. The total and water volume changes were monitored for all tests. These tests (section II) were used to verify the proposed stress state variables.

The basic data acquired and presented for all the null tests are the total and water volume changes with respect to time. In general, these volume changes are divided by the

total volume of the sample. That is, the data is presented as a percent volume change or as a porosity change. The volume change is defined as positive (+) when the sample volume decreases or when water or air come out of the sample.

A3.2 Discussion of null tests.

Although the main purpose of the null tests was to check the reliability of the procedure and equipment used in this research, the test results can also be used to prove or disprove the validity of the proposed stress state variables.

Since the tests attempted to measure 'no volume change', the factors affecting volume change should be considered.

(i) test procedure

(ii) system leaks

(iii) compressibility corrections

(iv) air diffusion through the water

(v) secondary consolidation

(i) test procedure

For the tests in Section II, it was difficult to apply all three pressures simultaneously. This meant that volume change could occur as a result of the changes in pressure.

(ii) system leaks(see preparation of equipment in chapter 6)

(iii) compressibility corrections

Since the total volume change was measured by water passing either into or out of the cell, it was necessary to

calibrate the cell for changes in volume with cell pressure. However, it was found that for a standard perspex cell there was no simple, direct relationship between volume and pressure. Perspex suffers from large creep strain, and therefore at a particular pressure the cell volume varies with time and depends on its previous pressure history. For this reason, a double-walled cell was used in this research (see appendix 5).

Entrapped air inside the cell and between the sample and the membrane may also affect the total and water volume change measurements.

(iv) air diffusion through the water

The diffusion of air through the water phase of the sample was measured as water leaving the sample. As a result, the water volume change could be misleading. This was corrected by flushing the diffused air to the diffused air volume indicator apparatus and subtracting the volume of diffused air from the apparent water volume change.

(v) secondary consolidation

Long term volume changes are related to small amounts of secondary compression of the soil structure and compression of the pore fluid.

A3.3 Saturating laboratory samples by Back Pressure

Conventionally, complete saturation is accomplished by increasing the back pressure to an amount equal to or greater than P_{100} (back pressure to produce 100 % saturation) and

waiting until a simple pore pressure response or B-value test (Skempton, 1954) indicates that saturation has been achieved.

However, it has been observed (Lowe and Johnson,1960) that for soils known to be initially less than fully saturated, a period of time of up to several days is usually required to achieve complete saturation even with back pressures equal to or greater than P_{100}.

It can be reasoned that the time delays in bringing a soil sample to complete saturation fall into two categories: (1) The time required for water to flow into the soil and compress the air under a given back pressure increase - a permeability problem and (2) the time required for the bubbles of pore air to dissolve into the surrounding pore water after they have been compressed - a diffusion problem.

It is possible to calculate the degree of saturation which can be achieved almost immediately following application of a certain back pressure, assuming no delay due to permeability, but also assuming that none of the free air goes into solution in the pore water. From Boyle's Law it follows that the degree of saturation, S, resulting from any applied back pressure, P, is

$$S = 1 - \frac{1}{49R + \frac{1}{1 - Si}} \quad \ldots\ldots \text{(A3.1)}$$

in which $R = \frac{P}{P_{100}}$

Application of P_{100} to any soil sample will immediately produce 98% saturation or more. However, to increase S to 99% requires

twice the back pressure, and to increase, S to 99.6% requires 10 times P_{100}. Combining theoretical and experimental studies on the pore pressure response of fully and partially saturated soils led to the suggestion that for many soft and medium stiff soils it may be acceptable to use degrees of saturation of 99.5% to 99.0% rather than insisting on 100%. For stiff or very stiff soils a full 100% saturation is probably required to ensure adequate pore pressure response.

Conventionally, both the cell pressure and the back pressure are maintained at the same magnitude when using back pressure to saturate a soil sample.

A3.4 IQ IESI EQR SAIURAIIQN

2

1. Apply cell pressure of 50 kN/m
2. Apply back pressure of 50 kN/m^2

   With (A) closed and (B) open ;

   Close (B) and open (A). Allow time for equalisation (say 1 hr) and measure pore pressure.

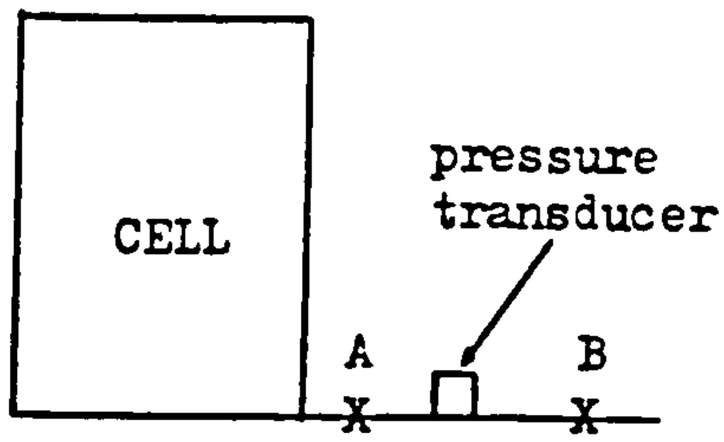

3. Increase cell pressure to 100 kN/m^2 (i.e. $\Delta P = 50$ kN/m^2) and after time for equalisation, measure pore pressure and calculate B.

$$\text{i.e. } \left(B = \frac{\text{Change in pore pressure(U)}}{\text{Change in cell pressure}} \right)$$

(Could increase cell pressure to 150 kN/m^2 to check B value)

4. If B acceptable (0.97) take cell pressure to required value.

5. If B too low set back pressure to value greater than measured pore pressure but less than cell pressure. Apply back pressure via burette to obtain volume of water entering sample. Equalise, shut valve (B), increase cell pressure. Allow time to measure B. If B still too low increase back pressure to value between pore pressure and cell pressure and repeat.

SPECIMEN SATURATION BY BACK PRESSURE

Date: 18-9-82

Soil: Grangemouth clay

1st Saturation

Pressures kPa	σ_3 20	b.p. 20	
	Initial	Final	Diff.
Time 18-9-82	11:30	13:57	
AVCL	521	497	24
VCI-1	21.95	20.95	1.00
VCI-2			
Σ Diff. Burette Reading			

5th Saturation

σ_3 200	b.p. 200	
Initial	Final	Diff.
19/9 23:10	20/9 9:50	
400	394	6
16.35	16.05	0.3

σ_3	b.p.	
Initial	Final	Diff.

2nd Saturation

Pressures kPa	σ_3 50	b.p. 50	
	Initial	Final	Diff.
Time	18/9 14:03	19/9 10:30	
AVCL	497	449	48
VCI-1 (c.c.)	20.95	18.90	2.05
VCI-2			
Σ Diff. Burette Reading			

6th Saturation

σ_3 250	b.p. 250	
Initial	Final	Diff.
20/9 9:58	20/9 13:52	
394	387	7
16.05	15.60	0.45

σ_3	b.p.	
Initial	Final	Diff.

3rd Saturation

Pressures kPa	σ_3 100	b.p. 100	
	Initial	Final	Diff.
Time 19-9-82	10:37	10:52	
AVCL	449	434	15
VCI-1 (c.c.)	18.90	18.15	0.75
VCI-2			

σ_3	b.p.	
Initial	Final	Diff.

σ_3	b.p.	
Initial	Final	Diff.

4th Saturation

Pressures kPa	σ_3 150	b.p. 150	
	Initial	Final	Diff.
Time 19-9-82	10:55	23:07	
AVCL	434	405	29
VCI-1 (c.c.)	18.15	16.70	1.45
VCI-2			

σ_3	b p.	
Initial	Final	Diff.

σ_3	b.p.	
Initial	Final	Diff.

CALCULATION OF PORE PRESSURE PARAMETER B.

Specimen/Stage		Initial	1st	2nd	3rd	4th	5th	6th			
σ_3 initial	kPa	0	21	50	102	152	202	252			
σ_3 final	kPa	102	51	102	152	202	252	302			
$\Delta\sigma_3$	kPa	102	30	52	50	50	50	50			
μ initial	kPa	-3	20	49	100	150	200	250			
μ final	kPa	80	42	93	145	199	250	300			
$\Delta\mu$	kPa	83	22	44	45	49	50	50			
$B = \frac{\Delta\mu}{\Delta\sigma_3}$		0.81	0.73	0.85	0.90	0.98	1.00	1.00			

A3.5 Test Results

The following table and figures summarizes all the null tests which have been carried out:

Null test No.	Press. change (KPa)	Elapsed time (Mins)	After press. Total (KPa)	change air (KPa)	water	Sample vol. change as a percentage *	Water vol. change as a percentage *
N1	+ 10	184	310	-	310	+ 0.74	+ 0.68
N2	+ 10	275	320	-	320	- 0.06	+ 0.06
N3	+ 10	49	330	-	330	- 0.06	0.00
N4	+ 20	763	350	-	350	0.00	+ 0.40
N5	+ 50	145	400	-	400	- 0.11	- 0.06
C1	consol.	1544	400	-	300	+ 8.99	+ 8.45
N6	+ 10	100	410	-	310	- 0.06	0.00
N7	+ 90	150	500	-	400	- 0.13	+ 0.06
N8	- 10	800	490	-	390	- 0.45	+ 0.13
N9	- 40	430	450	-	350	- 0.06	- 0.06
N10	- 100	6710	350	-	250	- 1.46	- 0.19
Desat+	300	9807	350	300	250	- 0.57	+ 5.41
N11	+ 10	1716	360	310	260	+ 0.06	+ 0.06
N12	+ 10	1156	370	320	270	- 0.38	+ 0.13
N13	+ 10	1682	380	330	280	+ 0.06	+ 0.13
N14	+ 20	4012	400	350	300	+ 0.06	+ 0.06
N15	+ 20	3085	420	370	320	- 0.57	+ 0.13
N16	- 20	1435	400	350	300	- 0.13	- 0.19

* All figures are rounded up to two decimal place.

In section I, on the first three null tests (N1 to N3), the total and water pressures were increased by 10 KPa. For null test N1, the general shape of the curves for total and water volume changes were almost identical (Fig.N1), the difference between the total and water volume changes was believed primarily related to the entrapped air inside the cell. For null tests N2 and N3 (Fig.N2 and N3), the total and water volume changes encountered were small about + 0.06% of the sample volume. For N4 and N5 null tests, the total and water pressures were increased by 20 and 50 KPa respectively. The volume changes measured were small. The funny paths happened at the beginning (Fig.N4 and N5) were thought to be associated with the changes in pressures.

After five null tests, the sample was allowed to consolidate and subjected to a different stress system. For N6 test, the total and water pressures were increased by 10 KPa. No water volume change, only a small increase (0.06%) of the total volume was noted (Fig.N6). For N7 test, an increase of 90 KPa was applied to the total and water pressures. The purpose was to examine whether the system could remain equilibrium under large stress changes. The results (Fig.N7) of volume changes were small. For null tests N8 to N10, the total and water pressures were decreased instead of increased. The volume changes were believed mainly due to the effect of hysteresis.

In section II, the saturated sample had an air pressure applied to the top of the sample through a coarse corrundum disc. The testing technique was more difficult since three pressures had to be applied simultaneously.

Three null tests (N11 to N13) were performed with an increase in total, air and water pressures of 10 KPa. For null tests N14 and N15, pressures were increased by 20 KPa. All results (Fig.N11 to N15) showed a reasonable small total and water volume changes. For null test N16, a decrease in pressures of 10 KPa was used. The volume changes measured was still small.

In general, the results are sufficiently accurate to prove that the equipment performs satisfactorily and verify the stress state variables for engineering purposes.

TRIAXIAL COMPRESSION TEST

SAMPLE DETAILS

Project Null Test

Job No. _____

Location of Project _____

Borehole No. _____ Sample No. 1

Description of Soil Grangemouth clay

Depth of Sample _____

Date of Testing 18-9-82

Tested by C.K.Wong

Sample Dimensions.

Length L_o (av.) 76.1 mm Diam. D_o (av.) 38.4 mm Area A_o (av.) 1158.12 mm^2

Volume V_o 88.13 cc

Moisture Content

	Before test			After test
Tare No.	34L	2L	56L	
Tare Wt. (g)	7.97	7.66	8.02	
Wt of tare + wet soil (g)	27.09	34.06	36.04	
Wt of tare + dry soil(g)	20.44	24.03	26.01	
Wt of water(g)	6.65	10.03	10.03	
Wt of dry soil(g)	12.47	16.37	17.99	
w%	53.33	61.27	55.75	

(av.) 56.78 %

Density

	Wt of tare (g)	Wt of tare + sample (g)	Wt of sample (g)	γ kg/m^3	γ_d kg/m^3
Before test	4.58	150.78	146.20	1658.91	
After test	4.56	138.21	133.65		

Consolidation Data

Initial Burette Reading _____ cc Final Burette Reading _____ cc

ΔV _____ cc

Length after consolidation $= L_o (1 - \frac{\Delta V}{3V}) =$ _____ mm

Area after consolidation $= A_o \frac{(1 - \frac{\Delta V}{V})}{(1 - \frac{\Delta V}{3V})} =$ _____ mm^2

NULL TEST N-1 ON SAMPLE NO.1

VOLUME CHANGE IN %

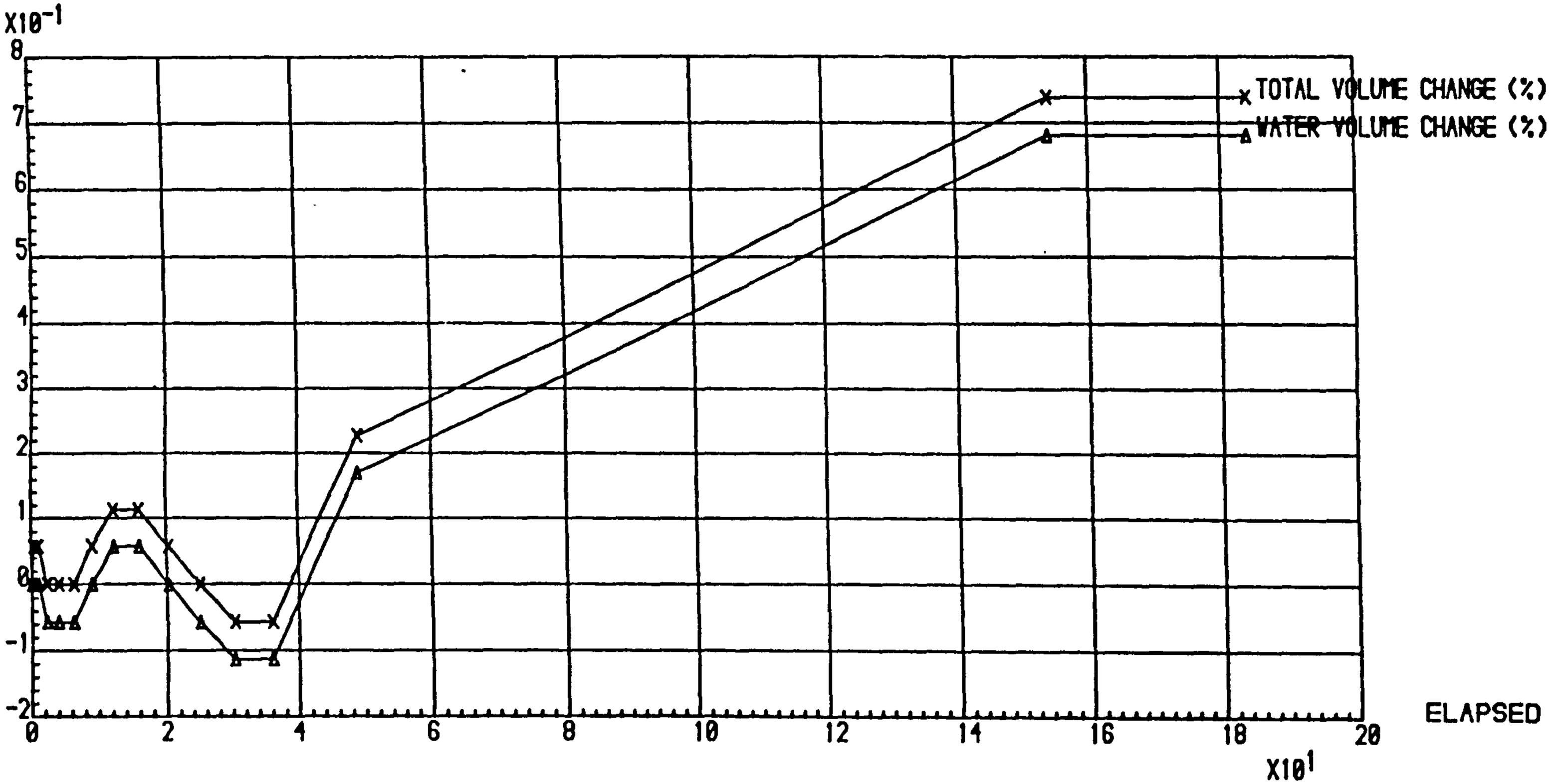

NULL TEST N-2 ON SAMPLE NO.1

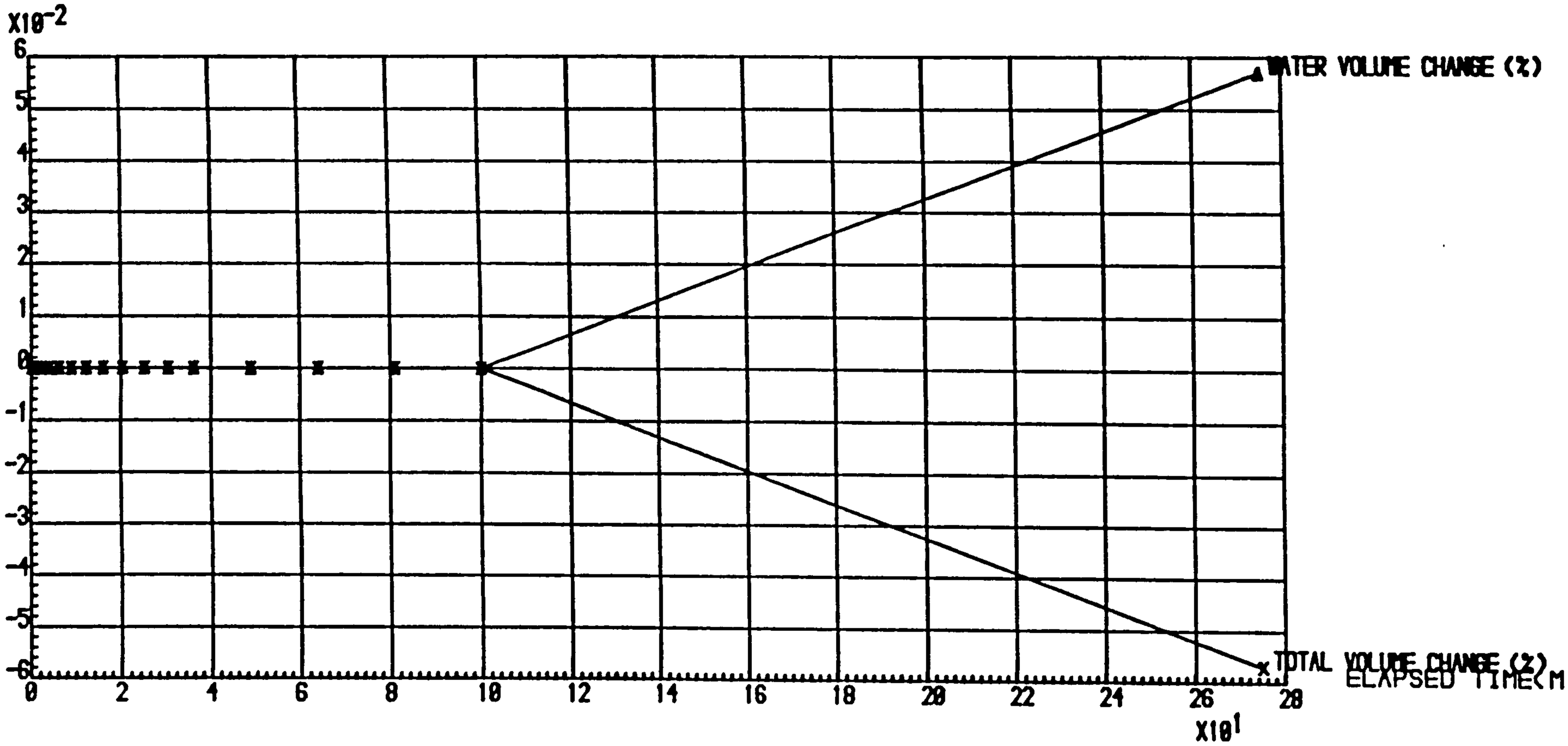

NULL TEST N-3 ON SAMPLE NO.1

VOLUME CHANGE IN %

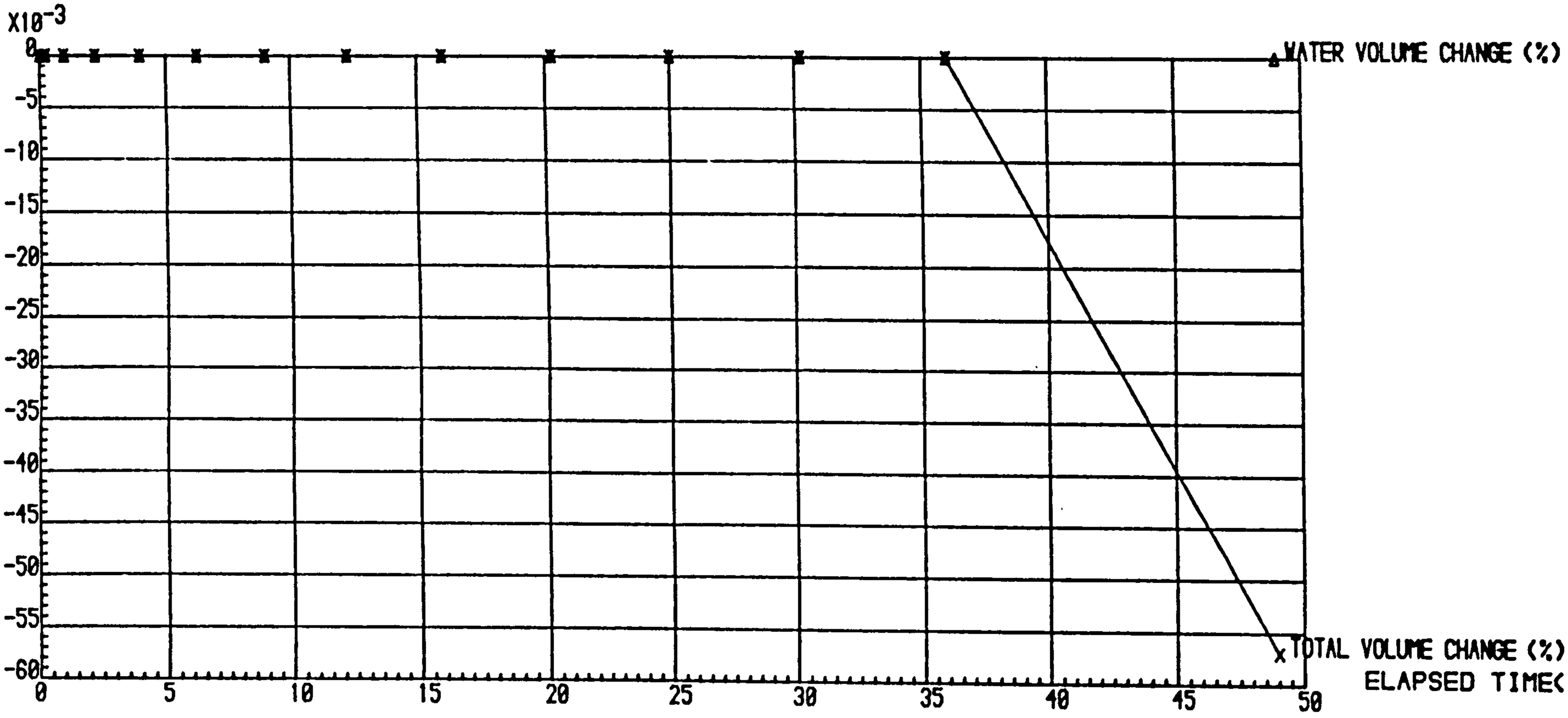

NULL TEST N-4 ON SAMPLE NO.1

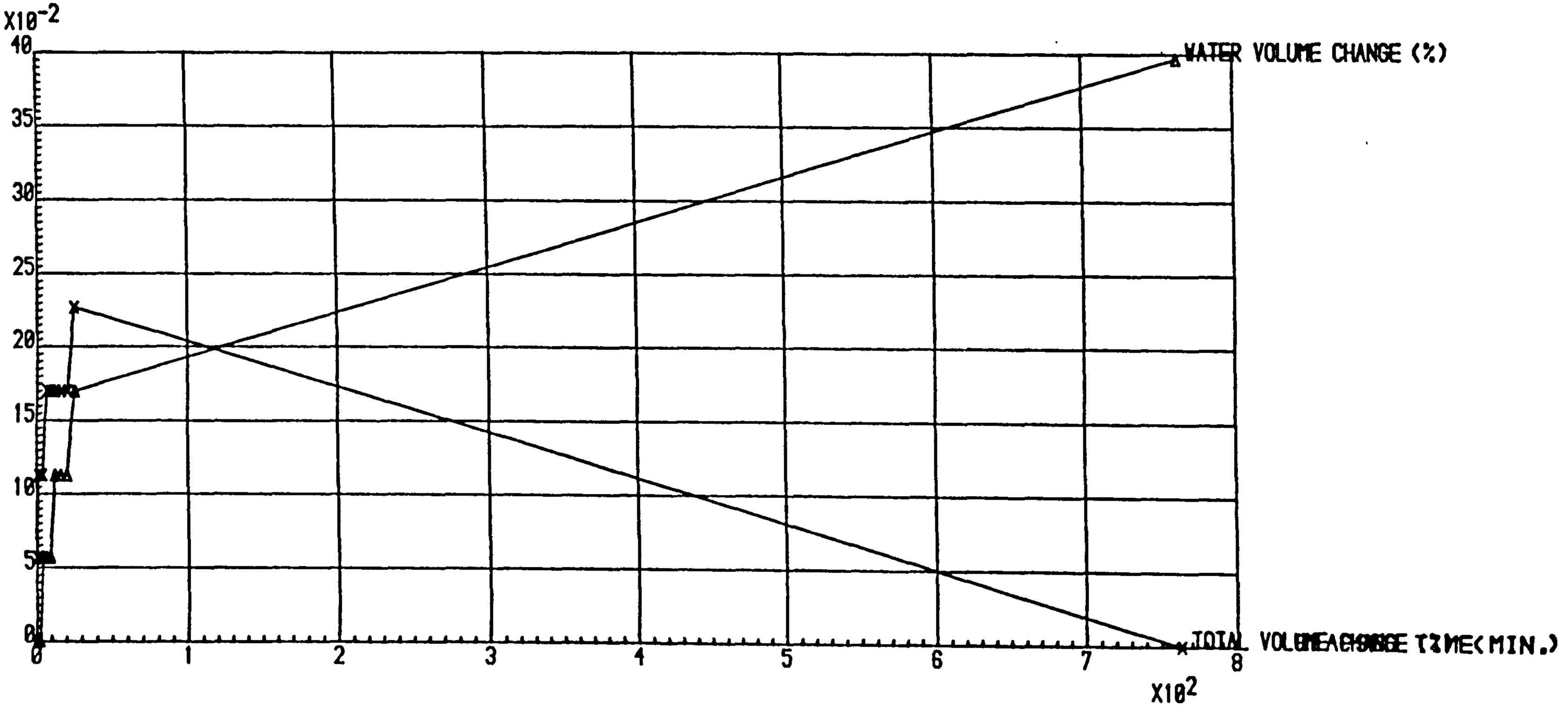

NULL TEST N-5 ON SAMPLE NO.1

VOLUME CHANGE IN %

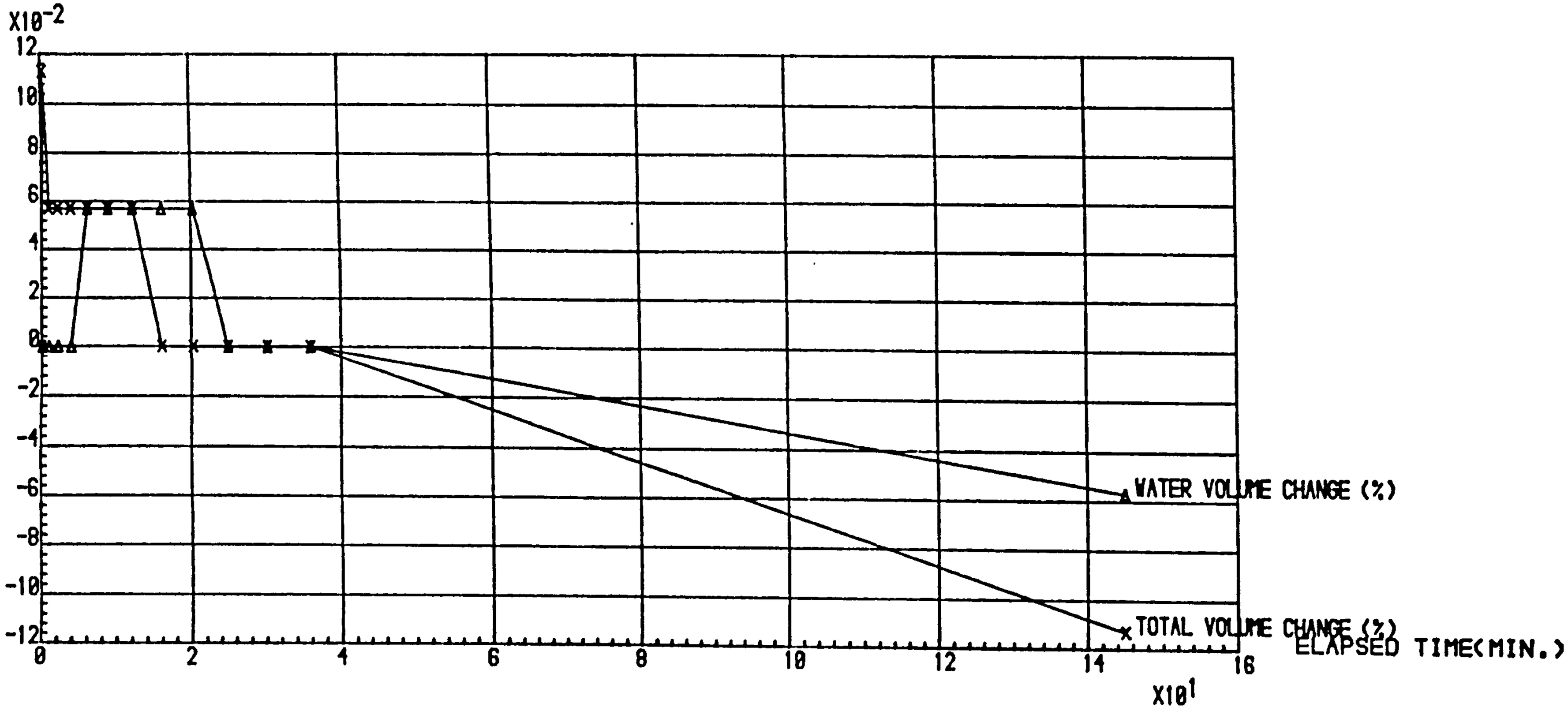

CONSOLIDATION STAGE

DRAINAGE OF WATER FROM SAMPLE(C.C.)

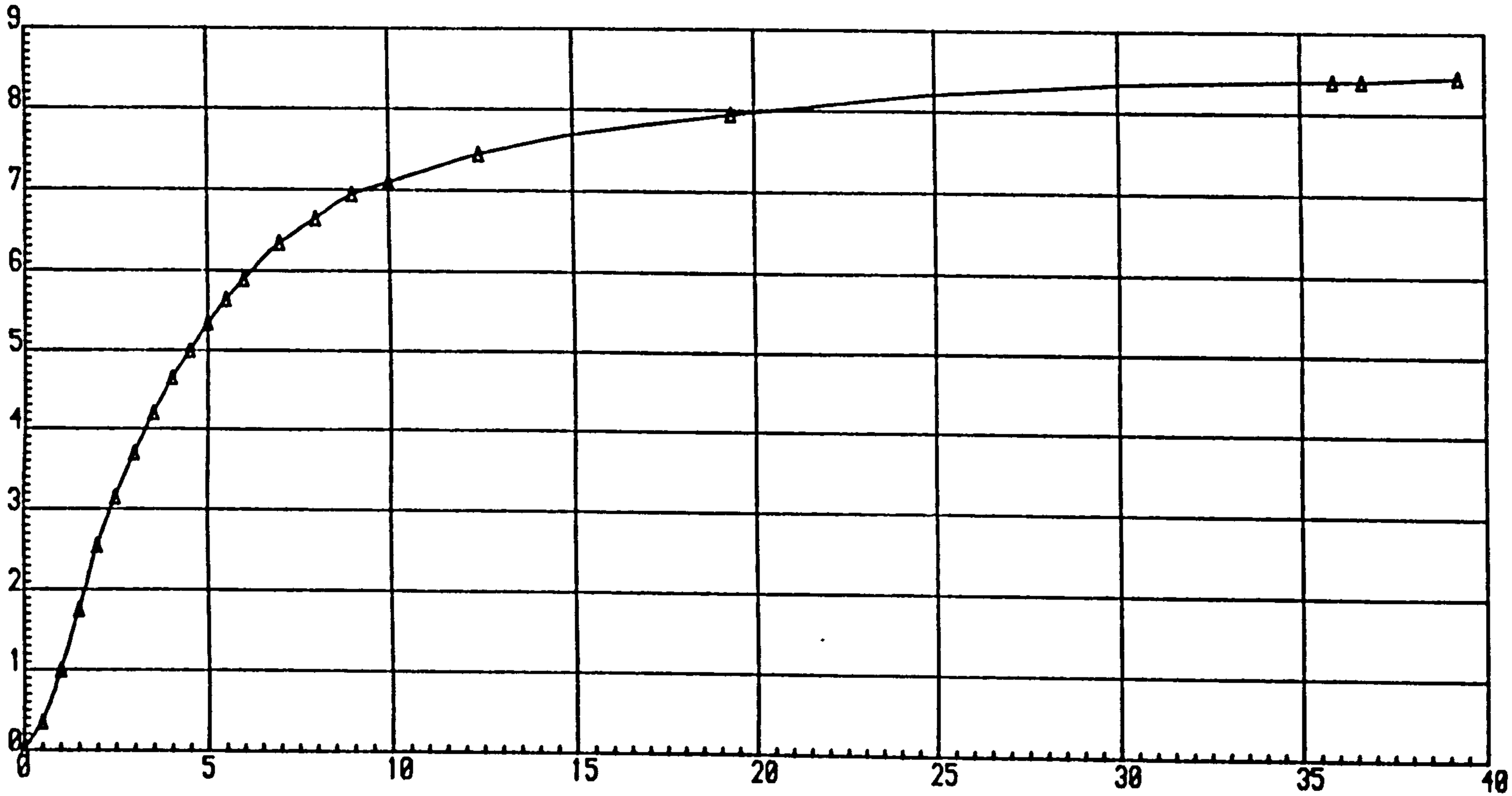

NULL TEST N-6 ON SAMPLE NO.1

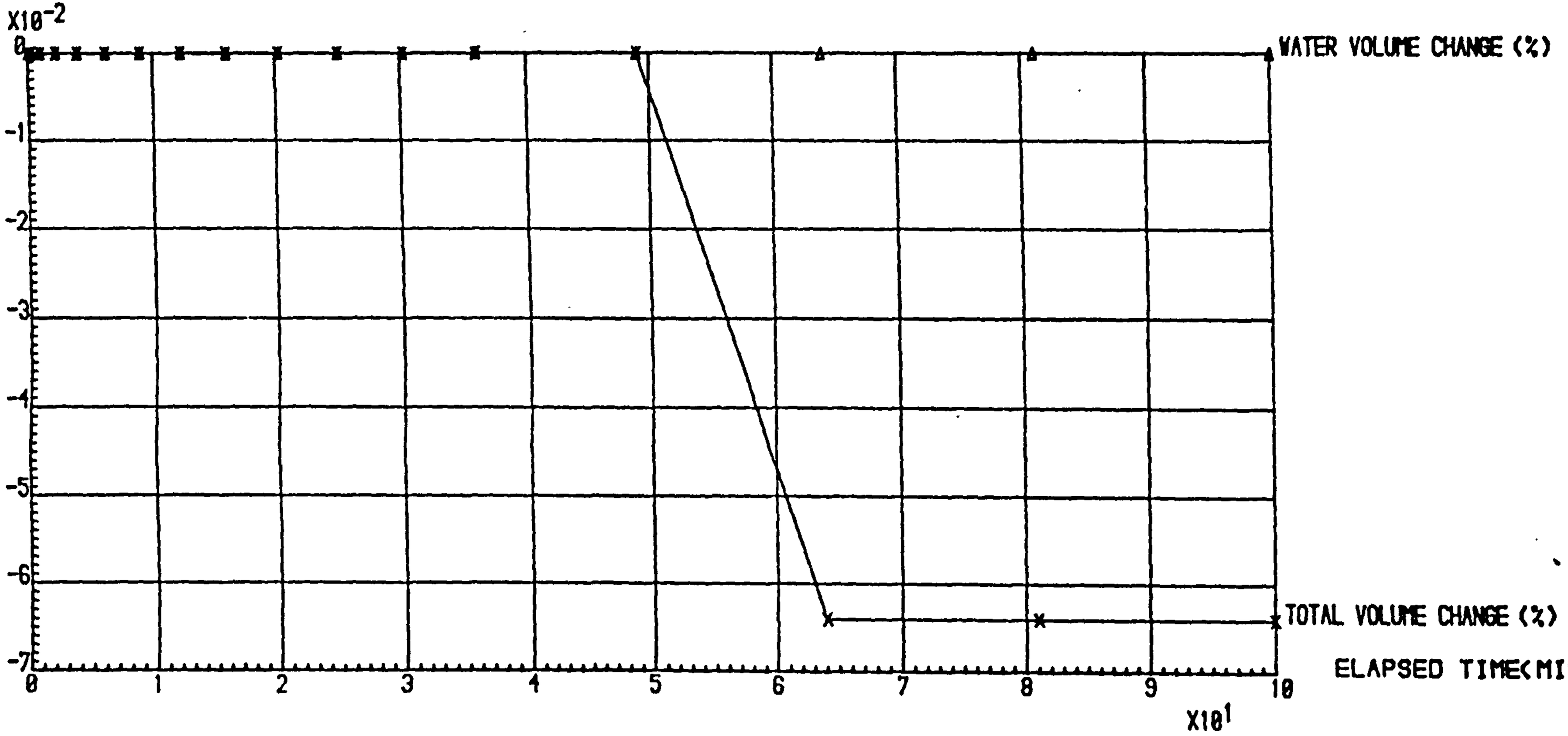

NULL TEST N-7 ON SAMPLE NO.1

VOLUME CHANGE IN %

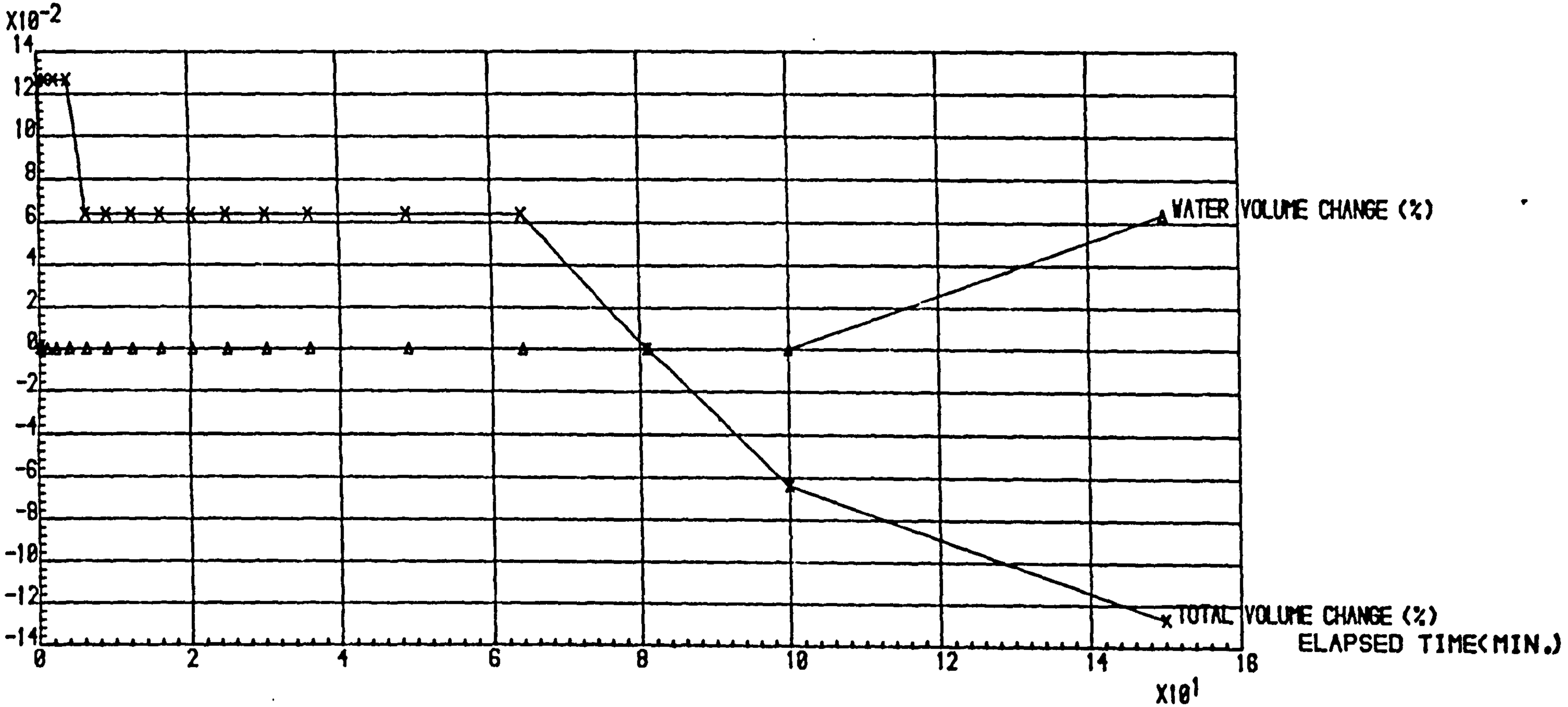

NULL TEST N-8 ON SAMPLE NO.1

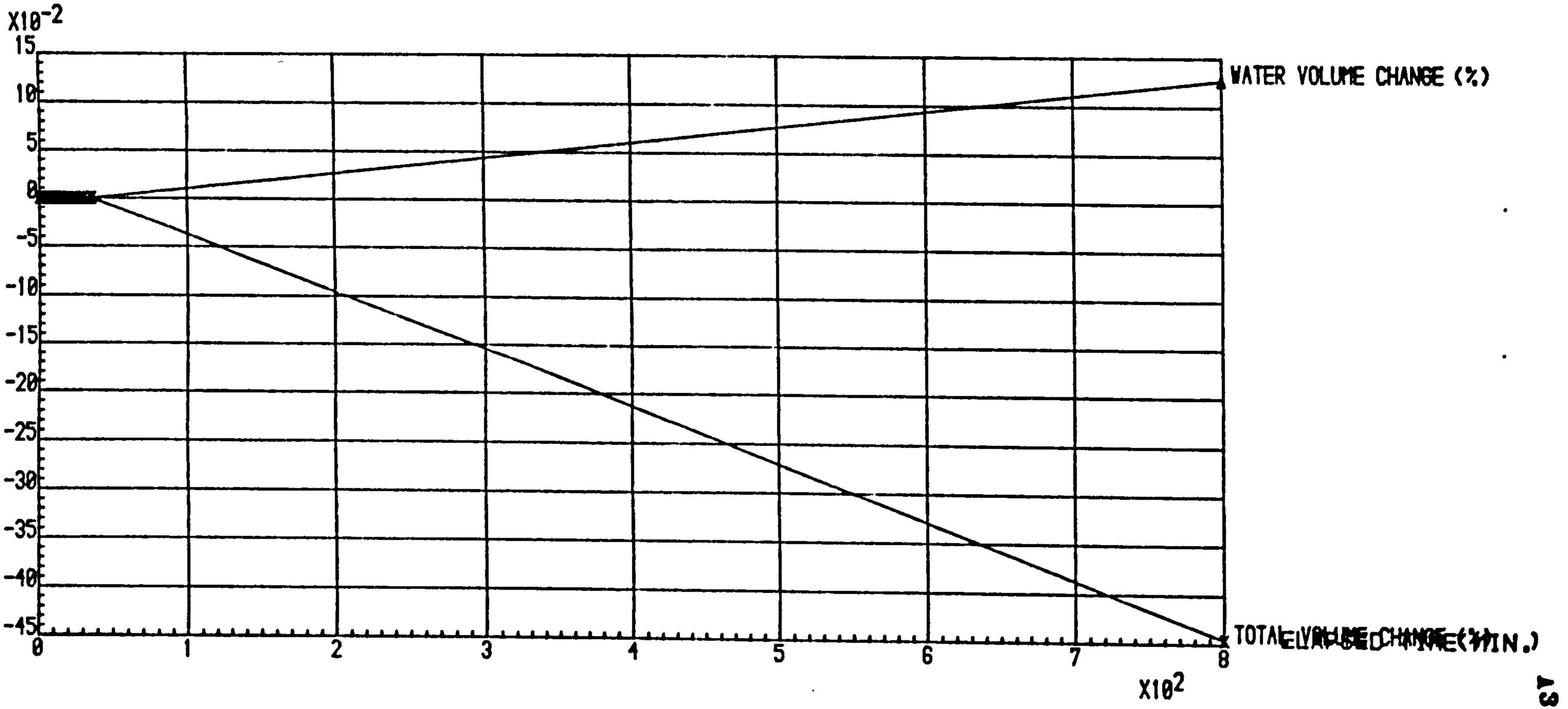

NULL TEST N-9 ON SAMPLE NO. 1

VOLUME CHANGE IN %

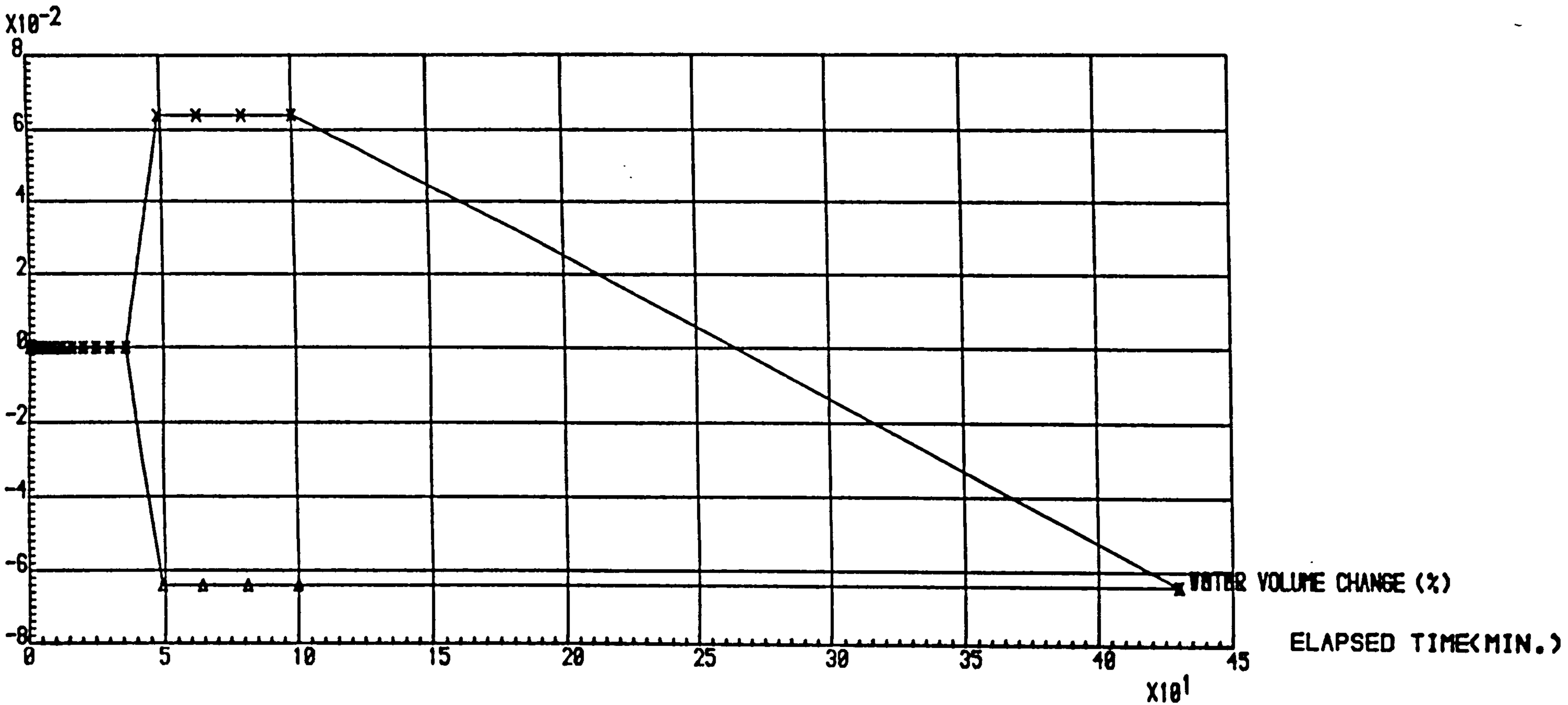

NULL TEST N-10 ON SAMPLE NO.1

VOLUME CHANGE IN %

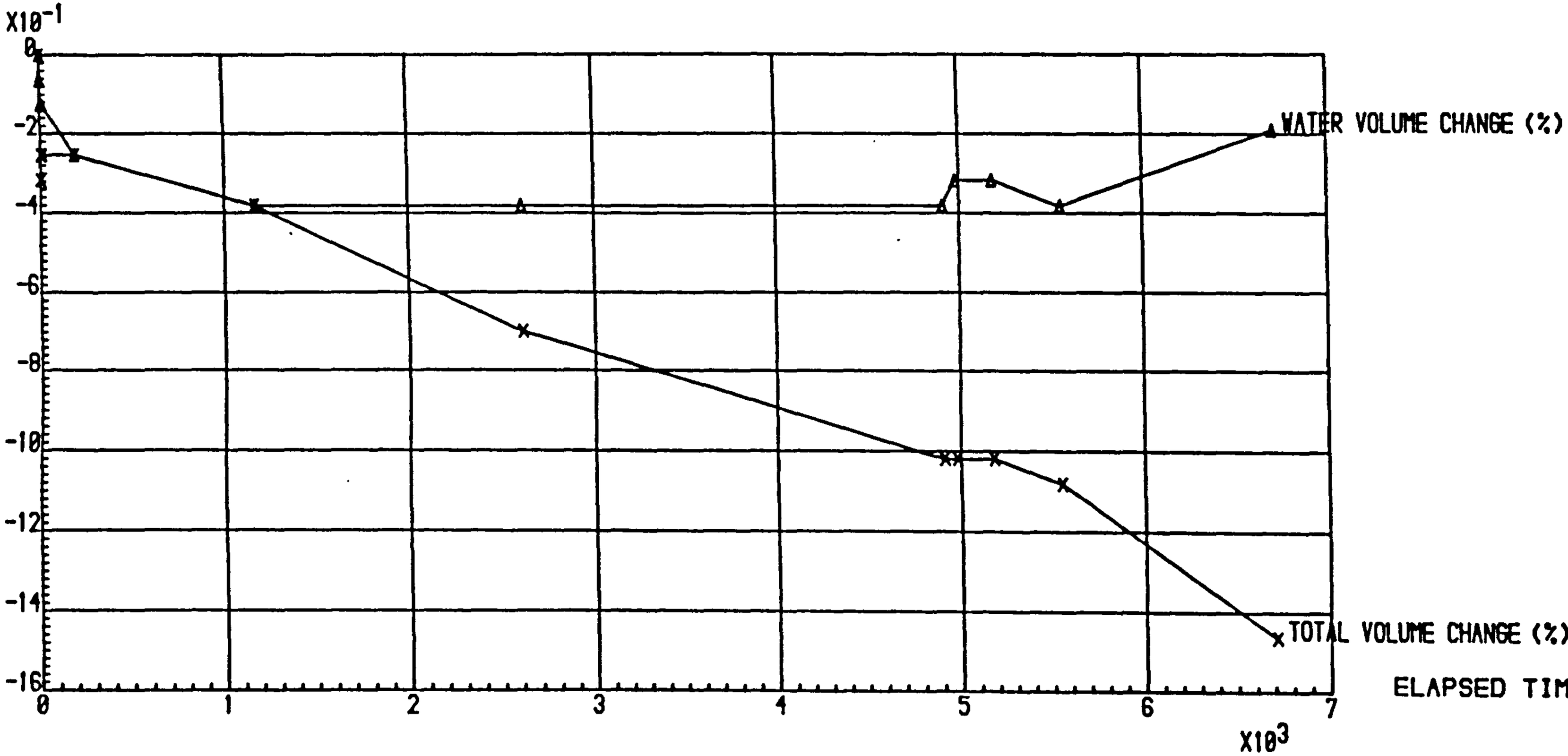

"ALLOW TO EQUILIZE" WITH APPLIED AIR PRESSURE

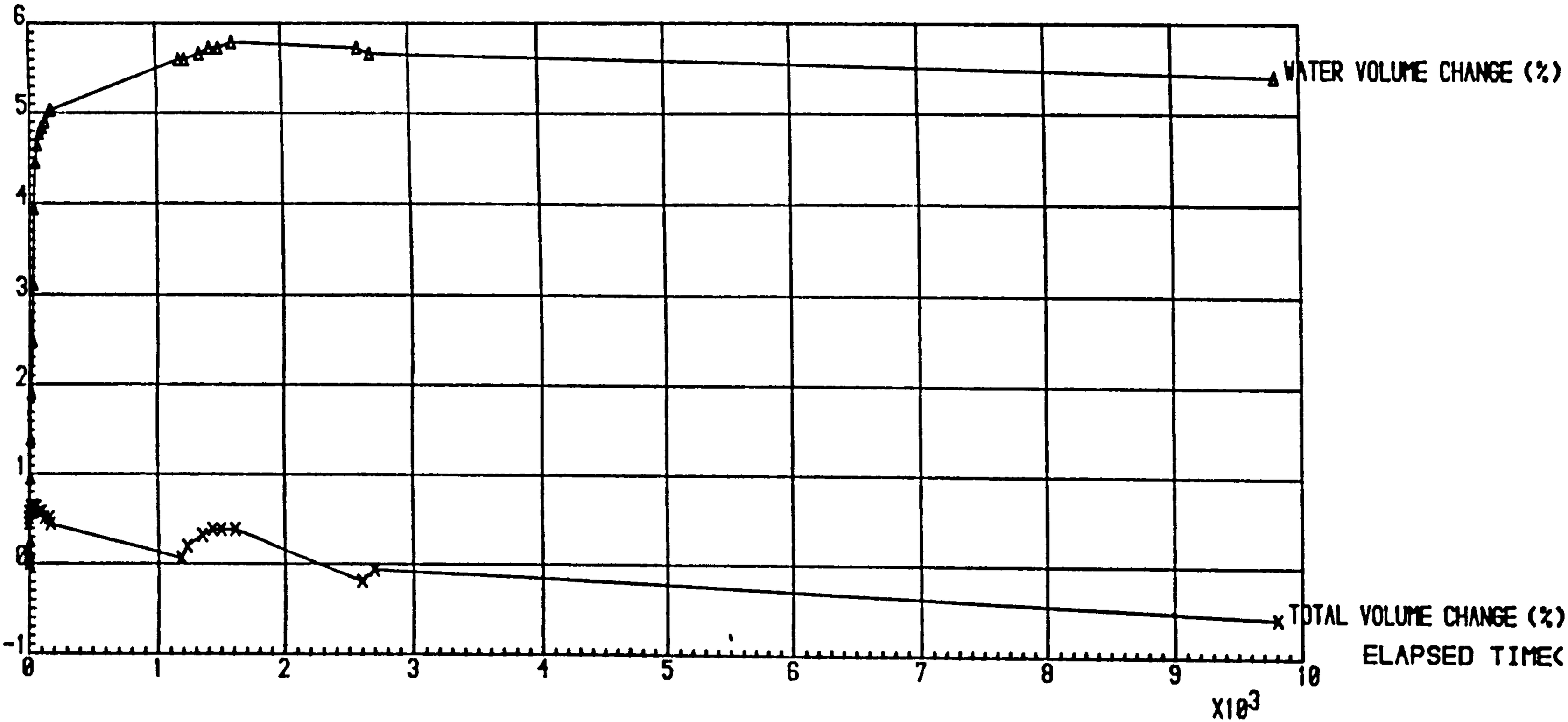

NULL TEST N-11 ON SAMPLE NO.1

VOLUME CHANGE IN %

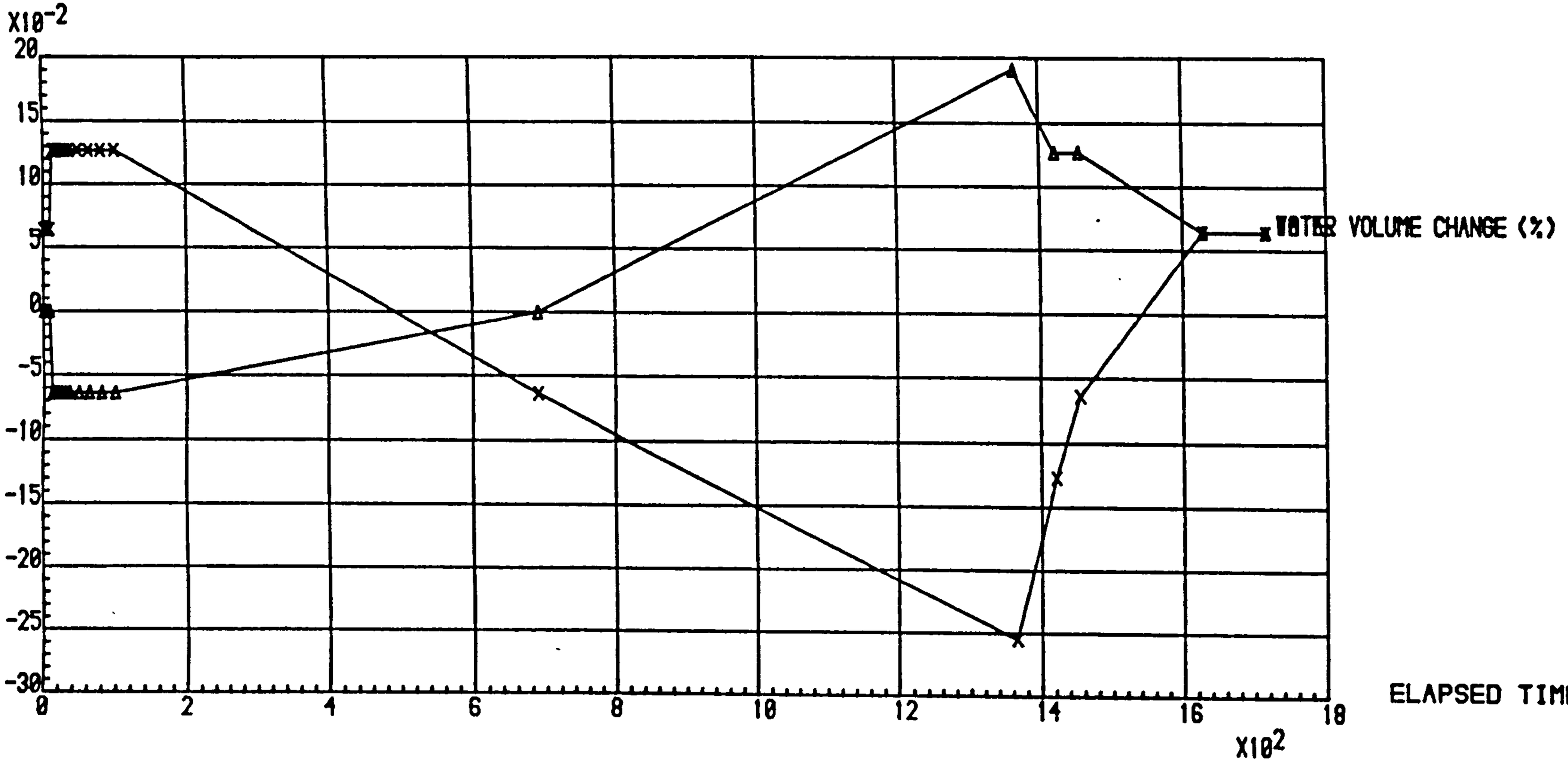

NULL TEST N-12 ON SAMPLE NO.1

VOLUME CHANGE IN %

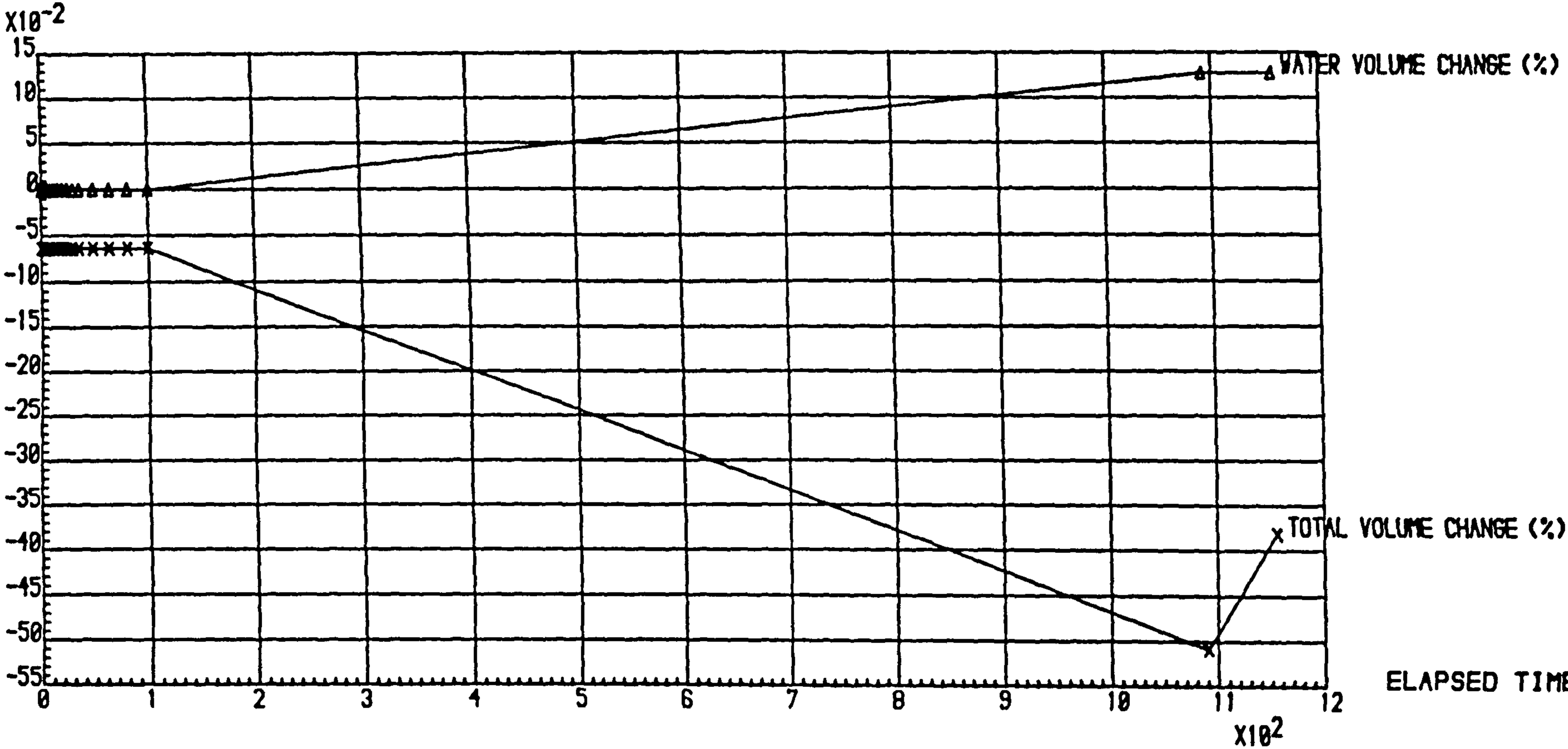

NULL TEST N-13 ON SAMPLE NO.1

VOLUME CHANGE IN %

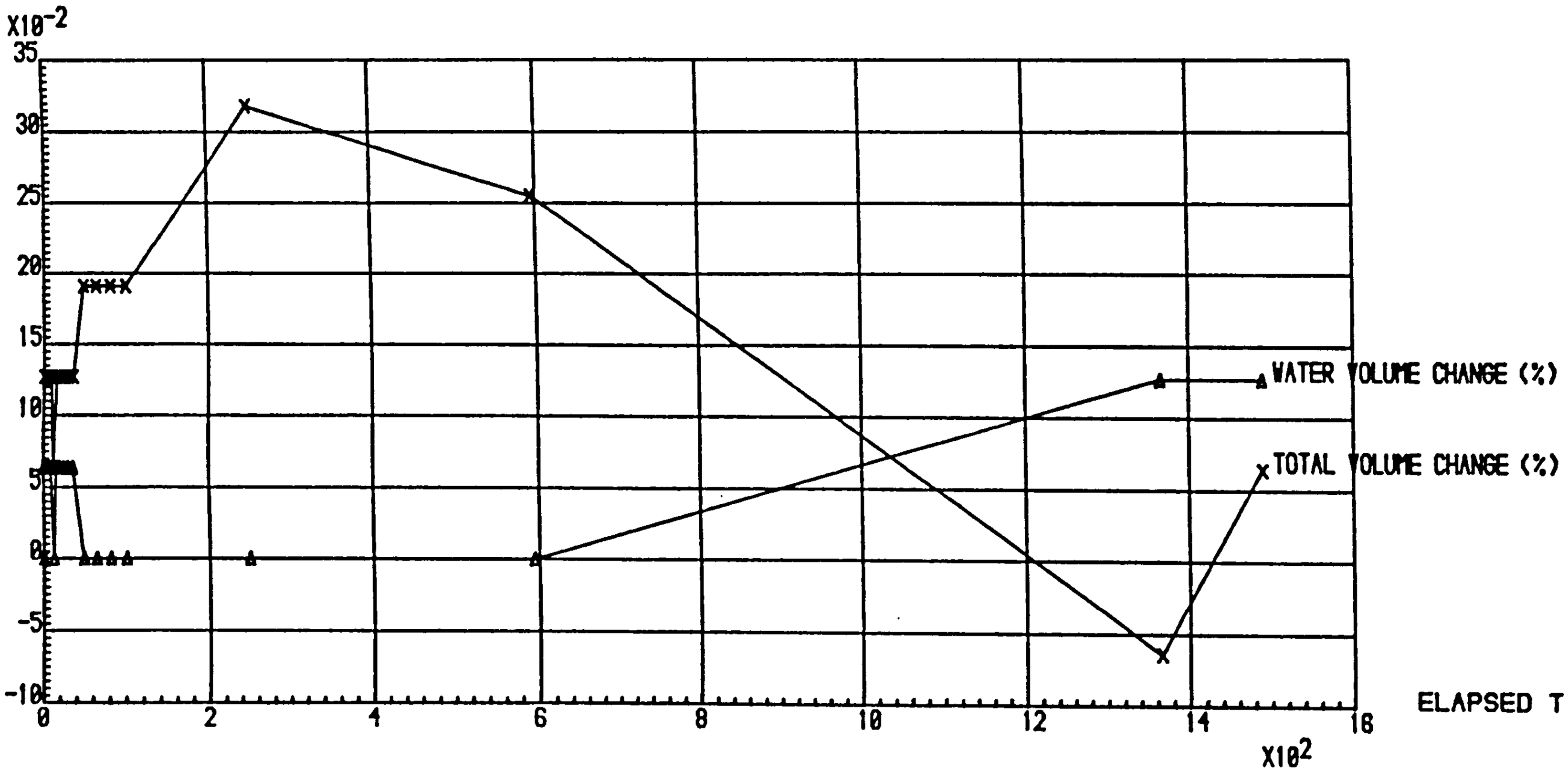

NULL TEST N-14 ON SAMPLE NO.1

VOLUME CHANGE IN %

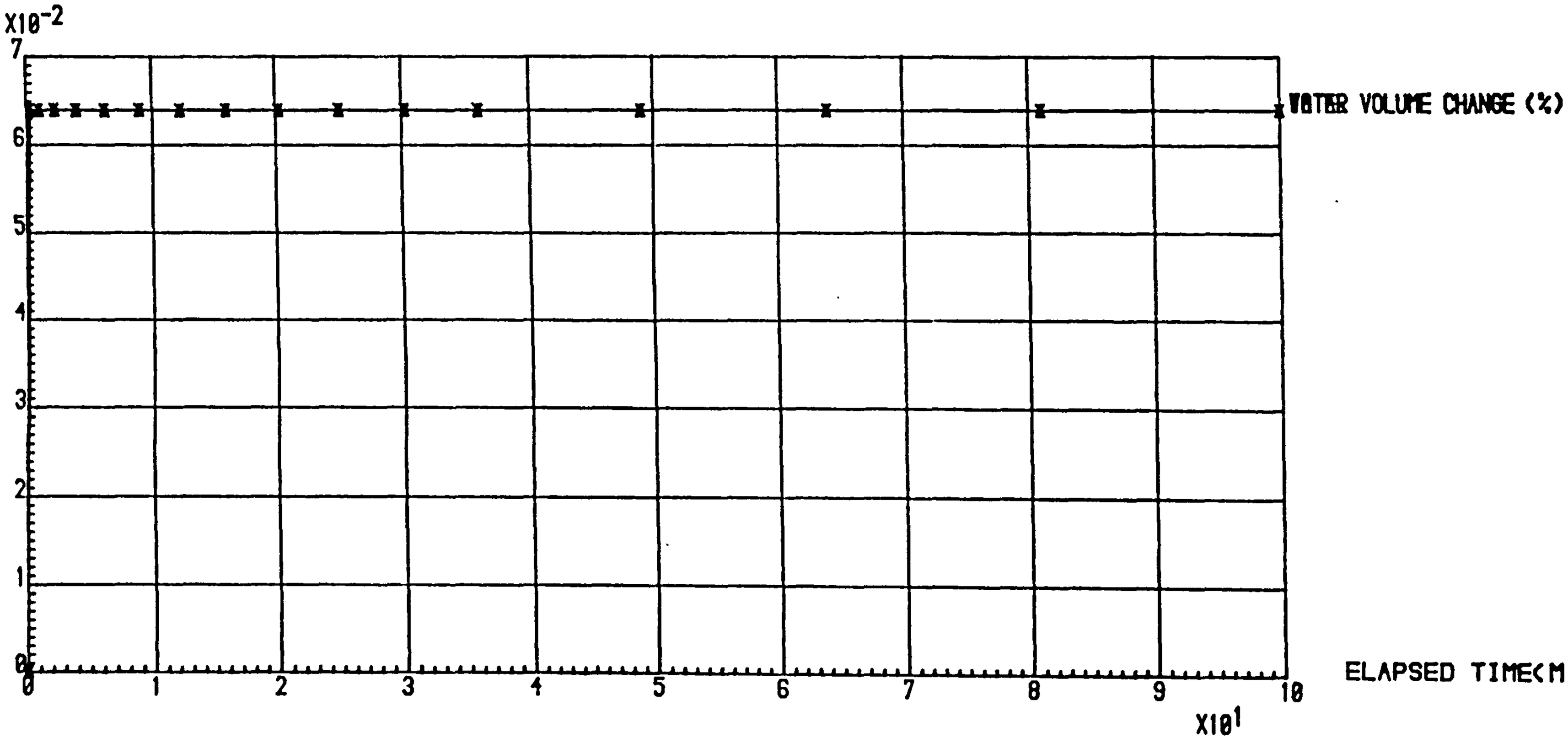

NULL TEST N-15 ON SAMPLE NO.1

VOLUME CHANGE IN %

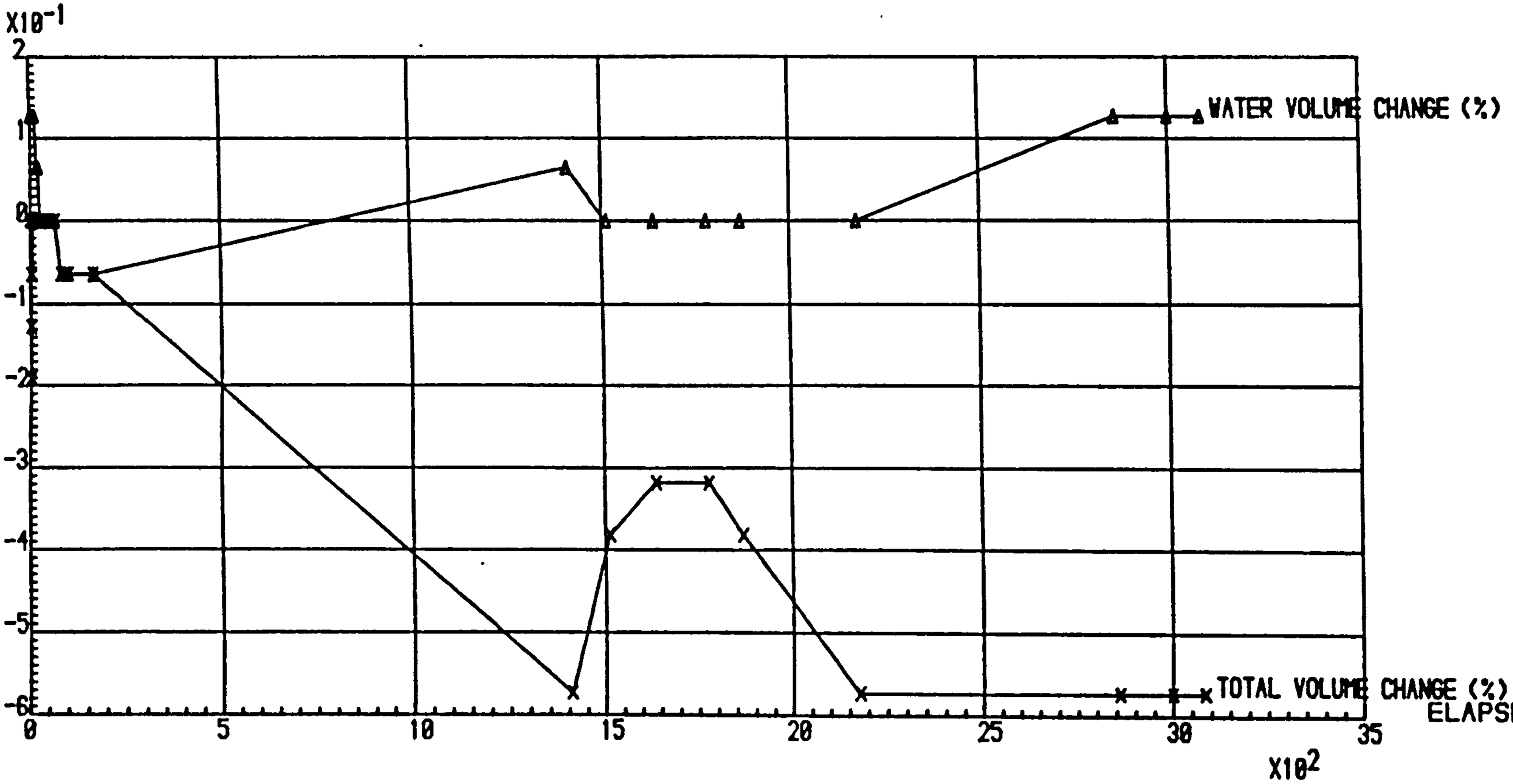

NULL TEST N-16 ON SAMPLE NO.1

VOLUME CHANGE IN %

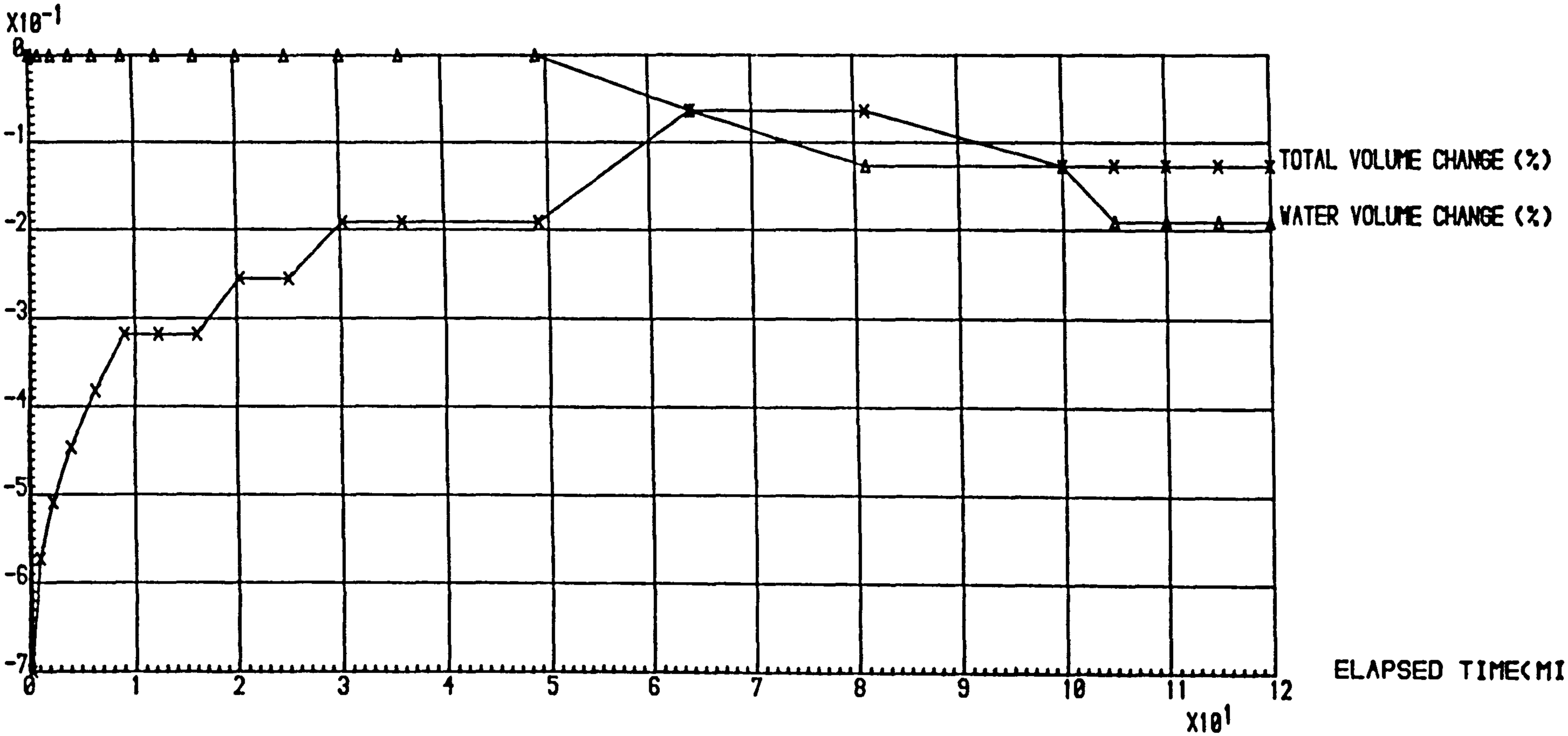

APPENDIX 4

CALIBRATIONS AND CHECKS TO ENSURE PROPER FUNCTIONING OF THE EQUIPMENT

Appendix 4

Calibrations and checks to ensure proper functioning of the equipment

A4.1 General

The equipment used in the laboratory investigations was either of a new design or had been substantially modified from existing and proven designs. This appendix explains the many calibrations and checks performed to ensure that the equipment was functioning properly. Time consuming tests were conducted to examine possible sources of error, to assess their significance and either eliminate or control them.

A4.2 Atmospheric pressure, temperature and relative humidity in the laboratory.

All equipment was in the same temperature controlled room. The atmospheric pressure, temperature and relative humidity were continuously recorded on a strip chart recorder. Figure A4.1 shows a typical atmospheric pressure,temperature and relative humidity trace for one week. The value of atmospheric pressure was used in an analysis to asses the volume of diffused air through the high air entry disc and the temperature value was used to calculate the temperature corrections for the automatic volume change logging systems. In order to estimate the diffusion rates of air and the permeabilities of water across rubber membrane and lucite, the value of relative humidity should be recorded, but no attempt was made in this research.

Fig.A4.1: Typical atmospheric pressure, temperature and relative humidity trace for one week.

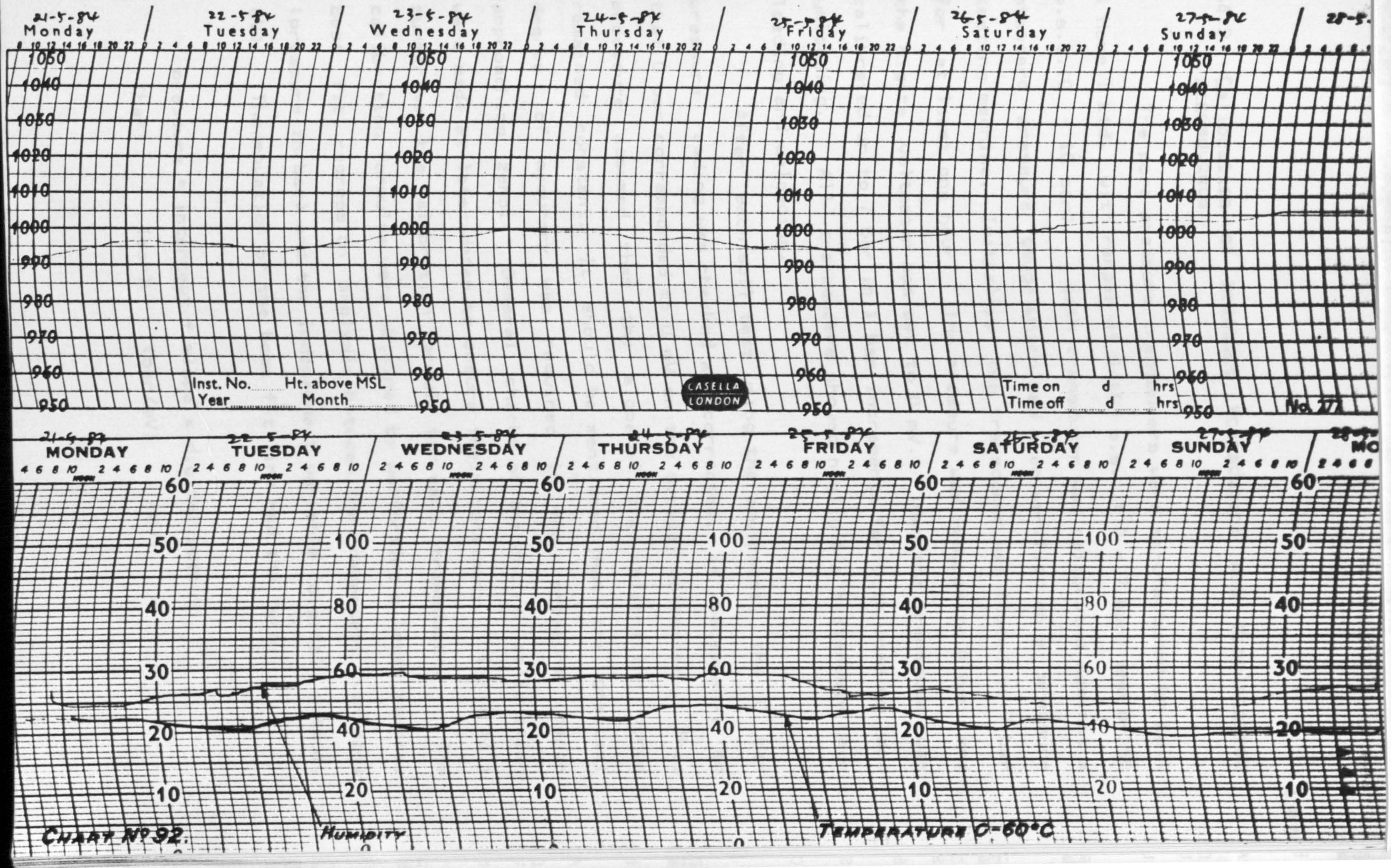

A4.3 Calibration of pressure transducers and displacement transducers

The pore pressure transducers were manufactured by Bell & Howell Ltd. with ranges of 0-100 p.s.i.(0 - 7 bar) and 0-150 p.s.i.(0 - 10 bar). Each transducer was calibrated against a standard pressure gauge which had been verified on a pressure testing machine. Initially, the transducer was loaded to 7 bar for at least one hour. The pressure was reduced to 0 bar and the digital voltmeter was set to 0 mV. Then the transducer was calibrated up to 7 bar in 1 bar increments for both loading and unloading. All transducers showed negligible hysteresis upon loading and unloading.

After each soil test using the equipment, the 0 bar pressure reading was checked and corrected, if necessary, so that 0 bar corresponded to 0 mV on the digital voltmeter. This procedure assumed that the slope of the calibration curve remained constant. It should be mentioned that the greatest degree of accuracy was required in the pressure range approaching zero. General checks of the entire calibration were made at later dates to ensure their constancy. Table A4.1 summarises the calibration formula for each transducer. The calibration formulae were obtained by performing a least square, best fit regression analysis between the dependent variable (pressure in bar) and the independent variable (digital output, mV). The equation of the best fit line had the form,

$$\underset{\text{(bar)}}{\text{pressure}} = \underset{\text{(bar)}}{\text{intercept}} + \underset{\text{(bar/mV)}}{\text{slope}} \times \underset{\text{(mV)}}{\text{digital output}}$$

Table A4.1: Summary of calibration formulae for pressure transducers

Channel No.	formula
0 (T - 1)	pressure = - 0.0066 + 0.01 * digital reading
1 (T - 1)	pressure = - 0.0029 + 0.01 * digital reading
2 (T - 1)	pressure = - 0.0033 + 0.005 * digital reading
3 (T - 1)	pressure = + 0.0278 + 0.01 * digital reading
13 (T - 2)	pressure = - 1.1964 + 1.0017 * digital reading
17 (T - 2)	pressure = - 0.0354 + 1.0041 * digital reading
18 (T - 2)	pressure = - 0.3770 + 0.9998 * digital reading

LVDTs were used to measure vertical displacements during the soil tests. The transducers were manufactured by Electro Mechanisms Ltd. (model 400D^) and had a range of 1 5/8 inches. They were calibrated against a precise micrometer (0.001 mm/division) mounted on a rigid base. The transducers showed negligible hysteresis and were essentially linear over their entire range. The calibration formulae of the LVDTs are summarised in table A4.2.

THE CALIBRATION GRAPH FOR PRESSURE TRANSDUCER:CHANNEL 0

PRESSURE IN BAR

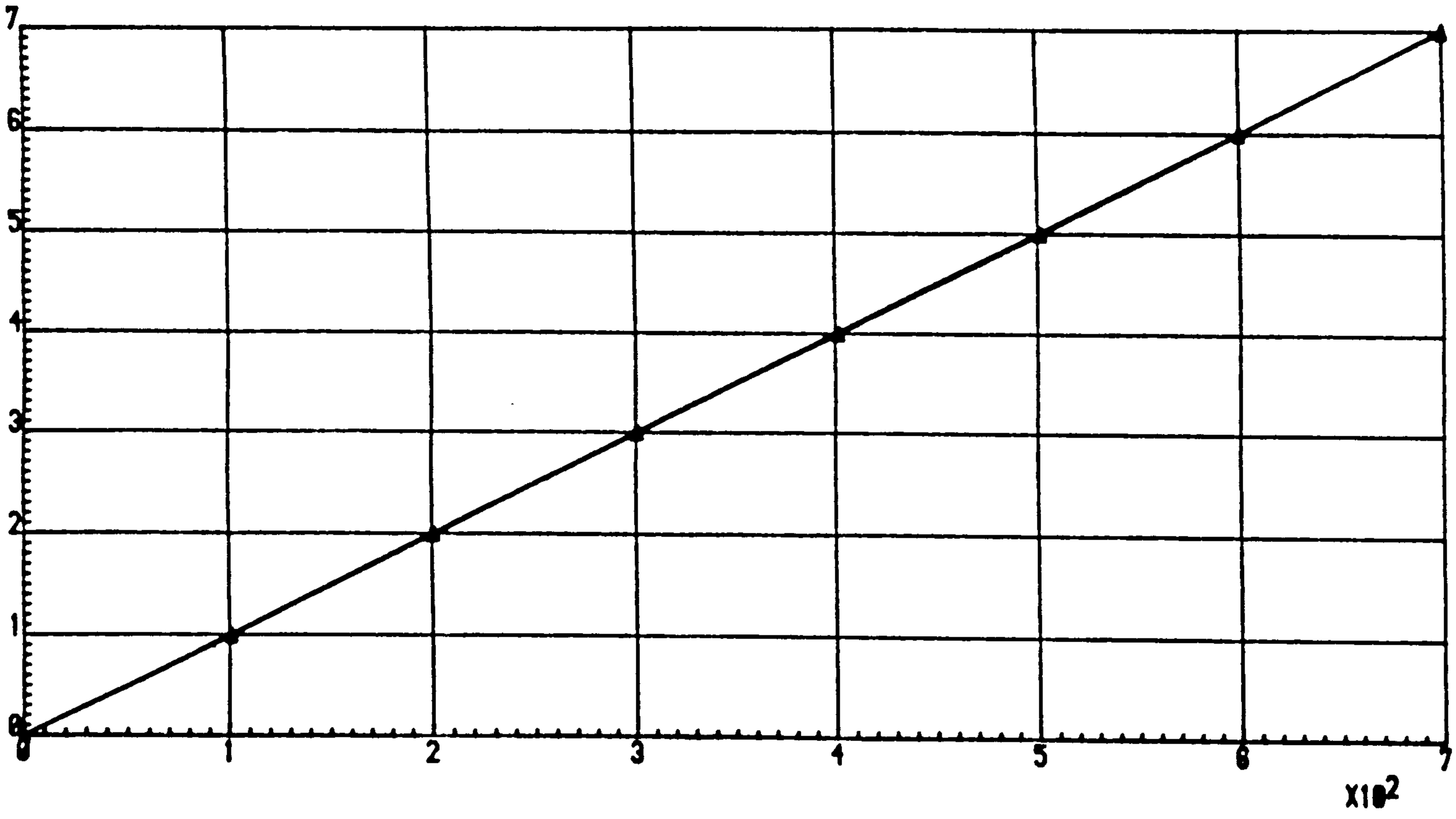

THE CALIBRATION GRAPH FOR PRESSURE TRANSDUCER:CHANNEL 1

PRESSURE IN BAR

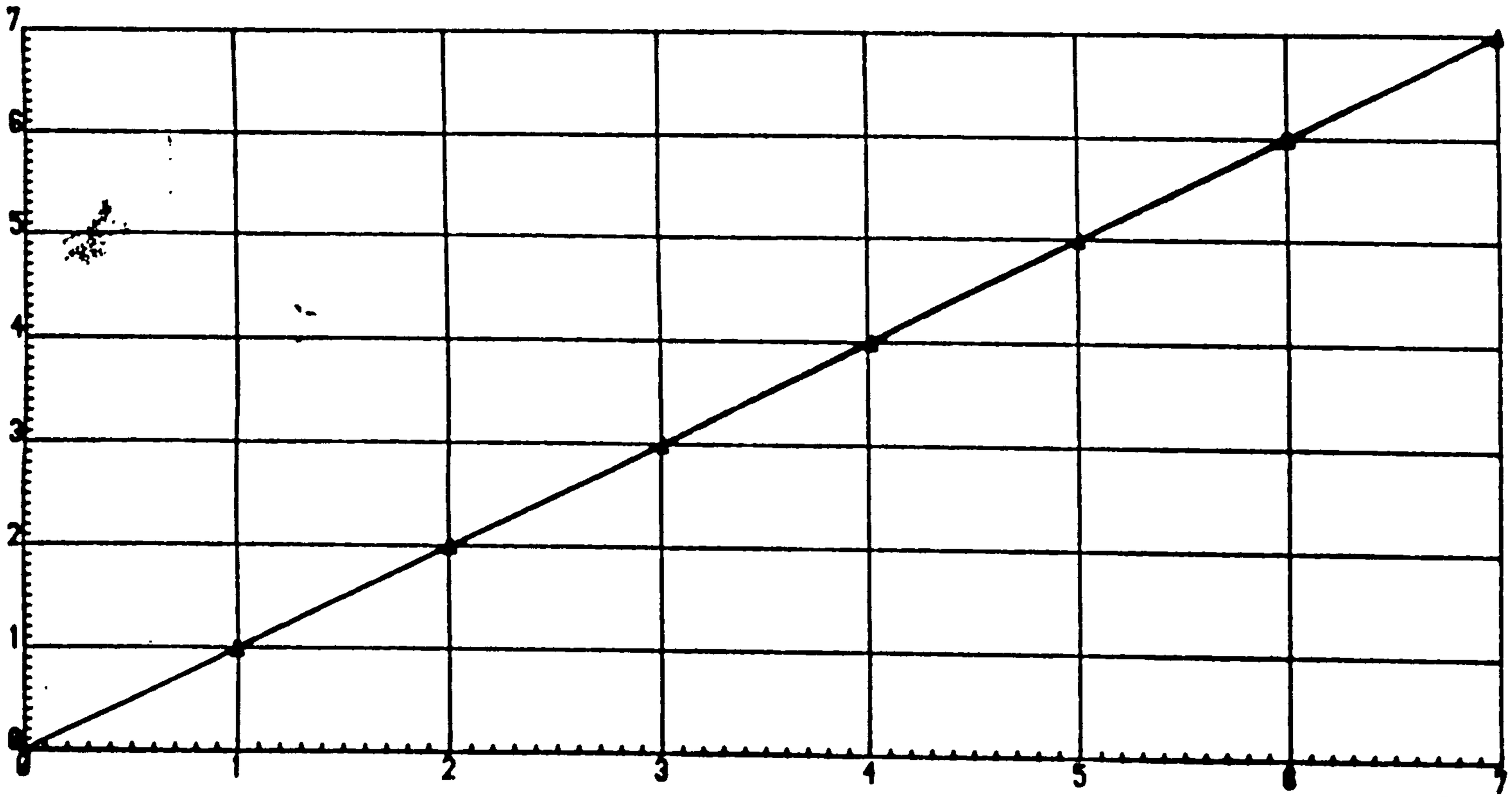

DIGITAL VOLT.READING

A18

THE CALIBRATION GRAPH FOR PRESSURE TRANSDUCER:CHANNEL 2

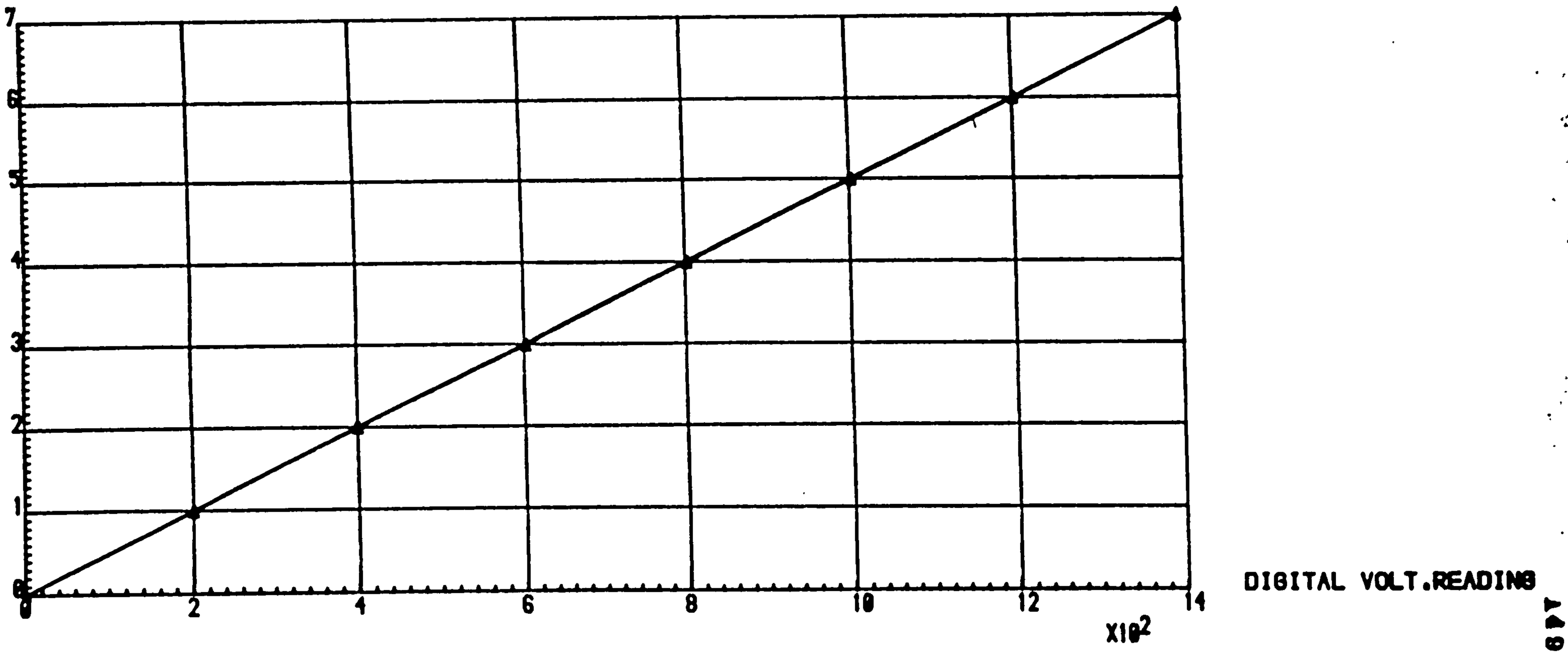

THE CALIBRATION GRAPH FOR PRESSURE TRANSDUCER:CHANNEL 3

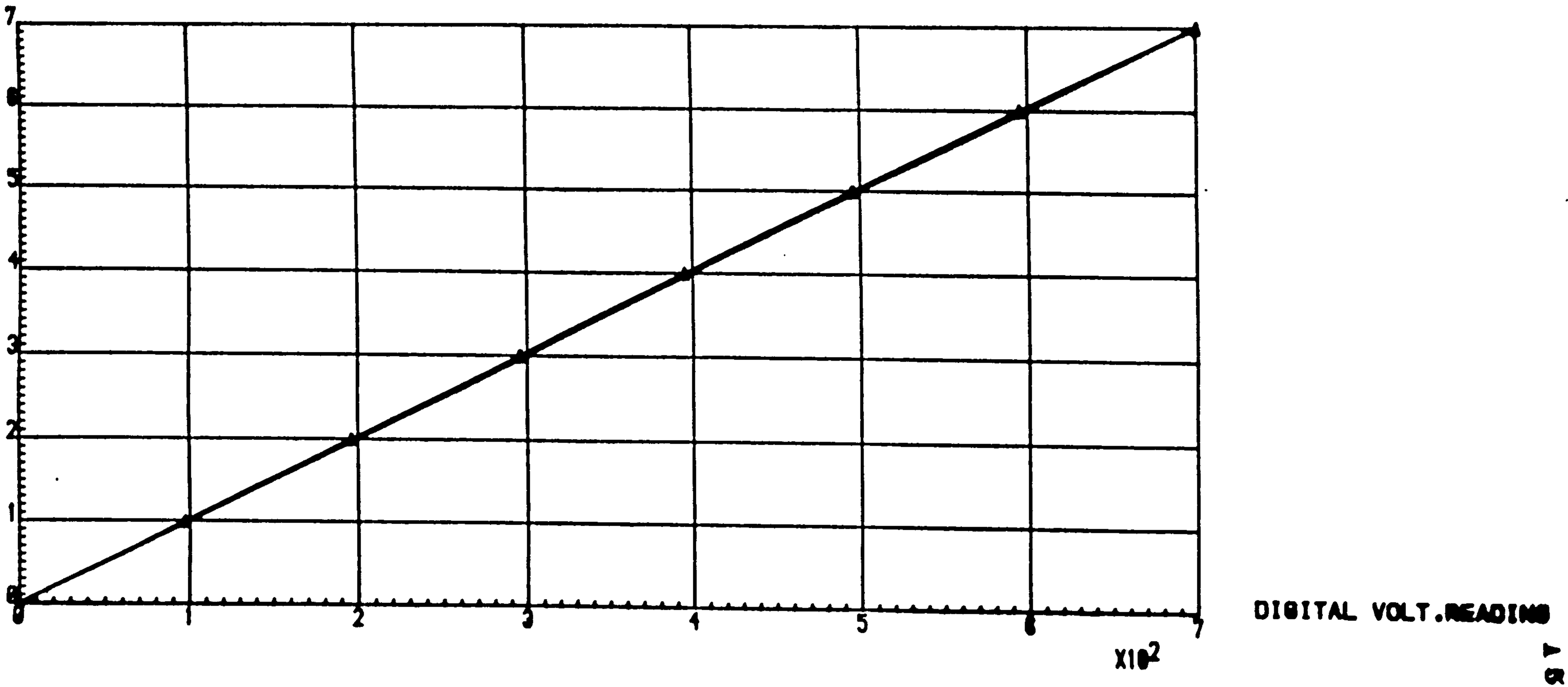

THE CALIBRATION GRAPH FOR PRESSURE TRANSDUCER:CHANNEL 13

PRESSURE IN BAR

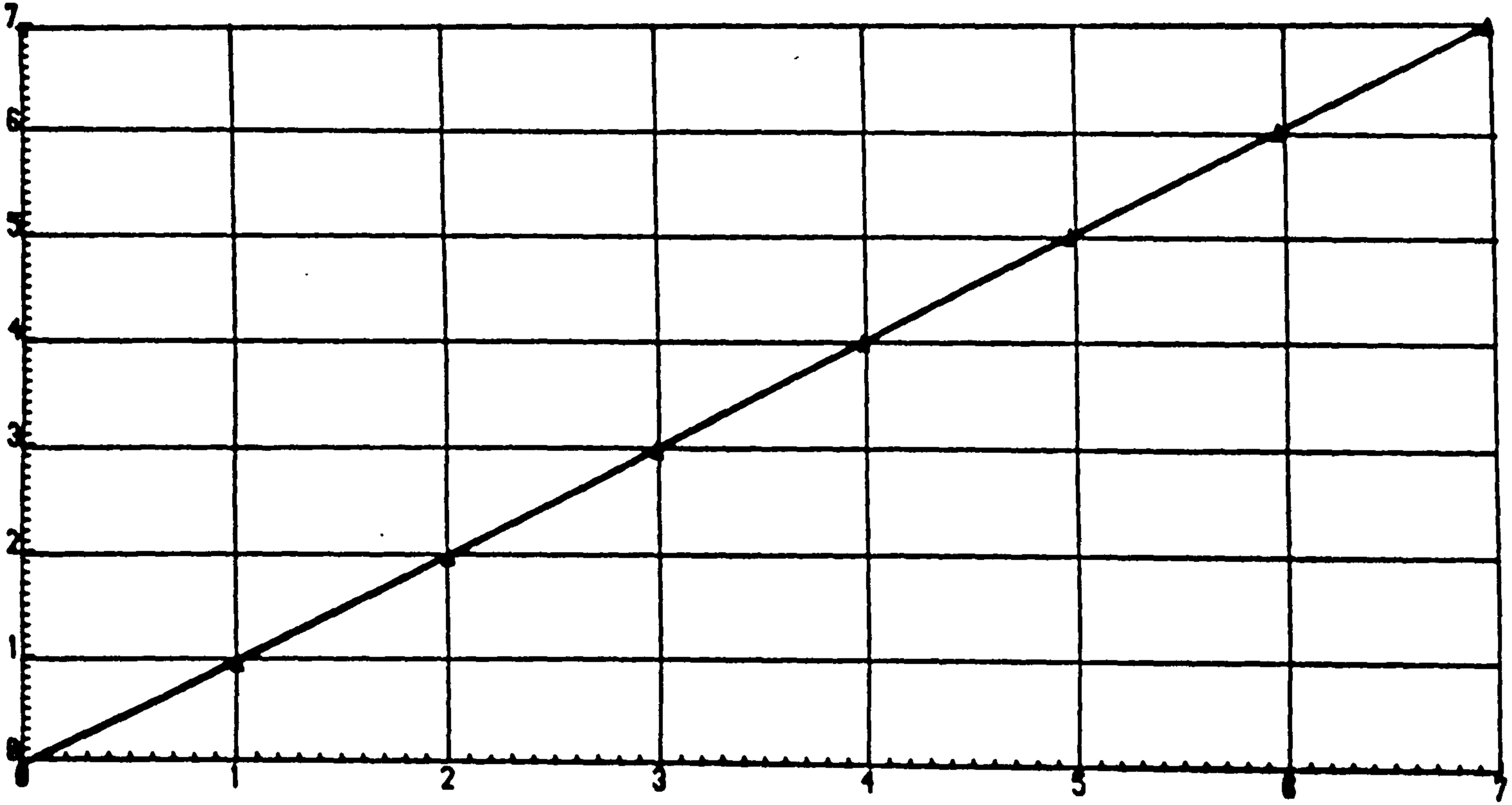

THE CALIBRATION GRAPH FOR PRESSURE TRANSDUCER:CHANNEL 17

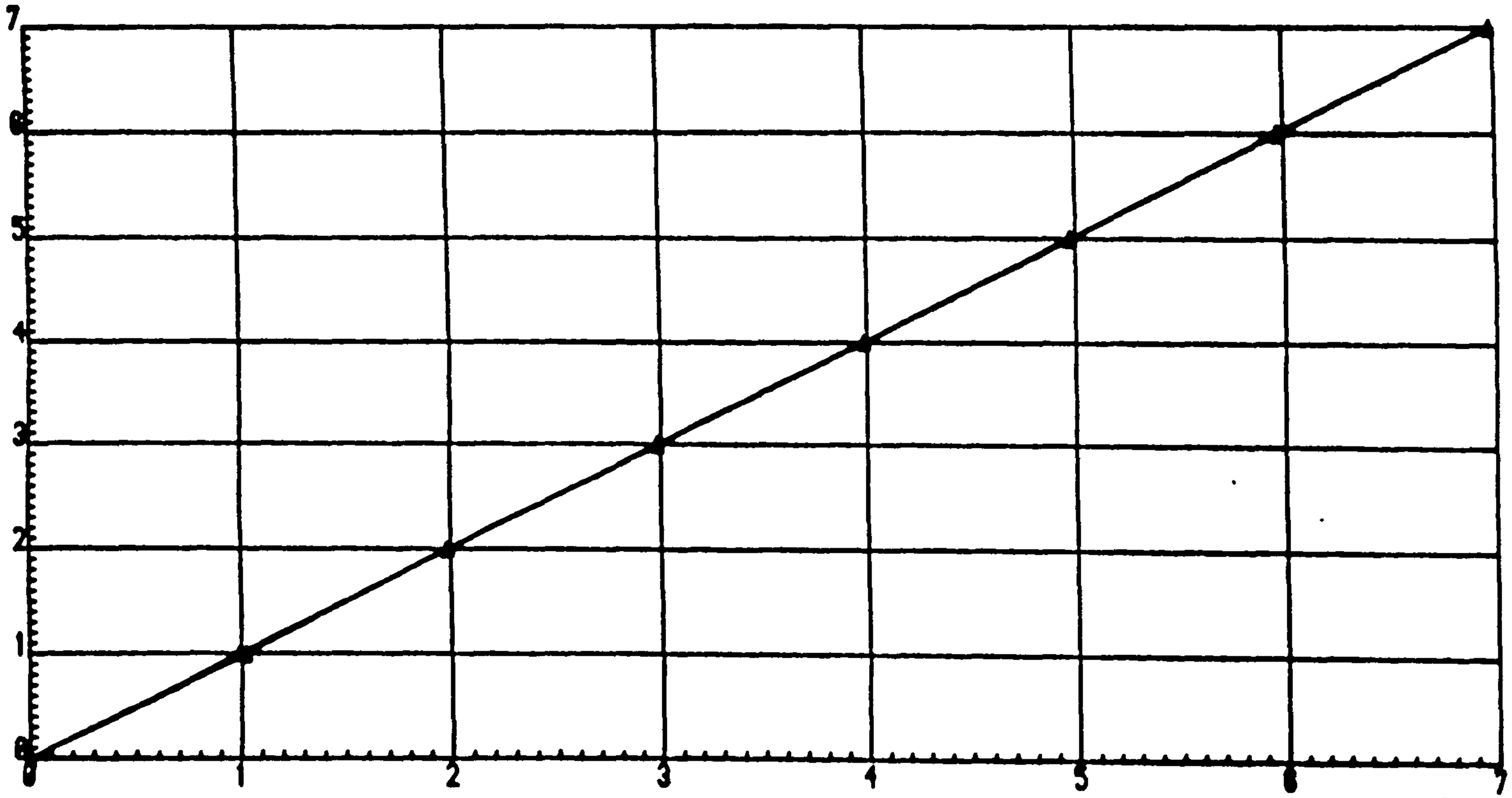

THE CALIBRATION GRAPH FOR PRESSURE TRANSDUCER:CHANNEL 18

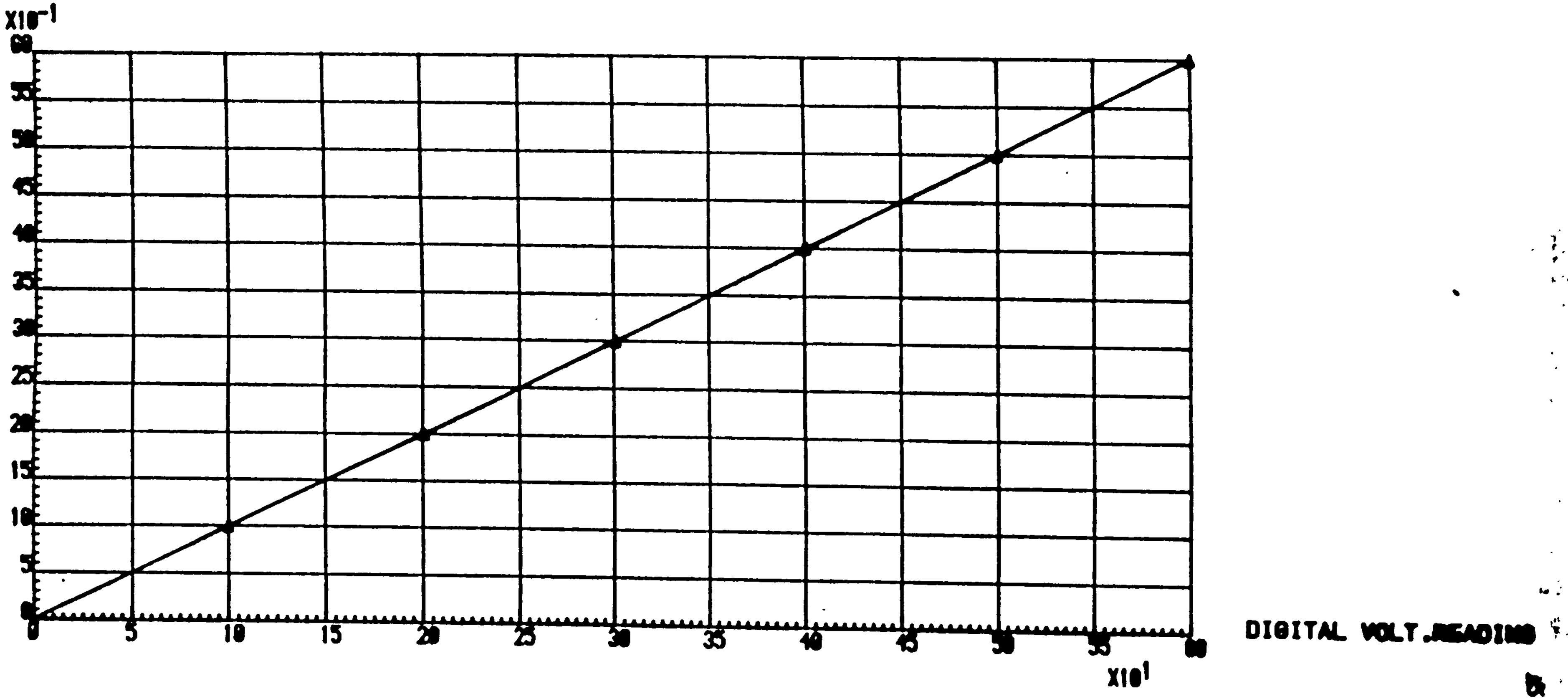

Table A4.2: Summary of calibration formulae for displacement transducers

Channel No.	formula
5 (T - 1)	displacement (mm) = 0.02 * change in digital output
6 (AVCL - 2)	displacement (mm) = 0.02 * change in digital output
7 (AVCL - 1)	displacement (mm) = 0.02 * change in digital output
15 (T - 2)	displacement (mm) = 0.02 * change in digital output

A4.4 Calibration of load cells

The load cells were calibrated using a load cell calibration press manufactured by Budenberg Gauge Co. Ltd.. It was important to ensure that the load cell being calibrated was concentric with the piston in the press.

Table A4.3 summarises the calibration formulae for the load cells.

Table A4.3: Summary of calibration formulae for load cells

Channel No.	formulae
4 (T - 1)(No. 664)	Load (kN) = 0.0136 + 0.001 * digital reading
12 (T - 2)(450 KGF/69)	Load (kN) = 0.0503 + 0.001 * digital reading

THE CALIBRATION GRAPH FOR LVDT:CHANNEL 5

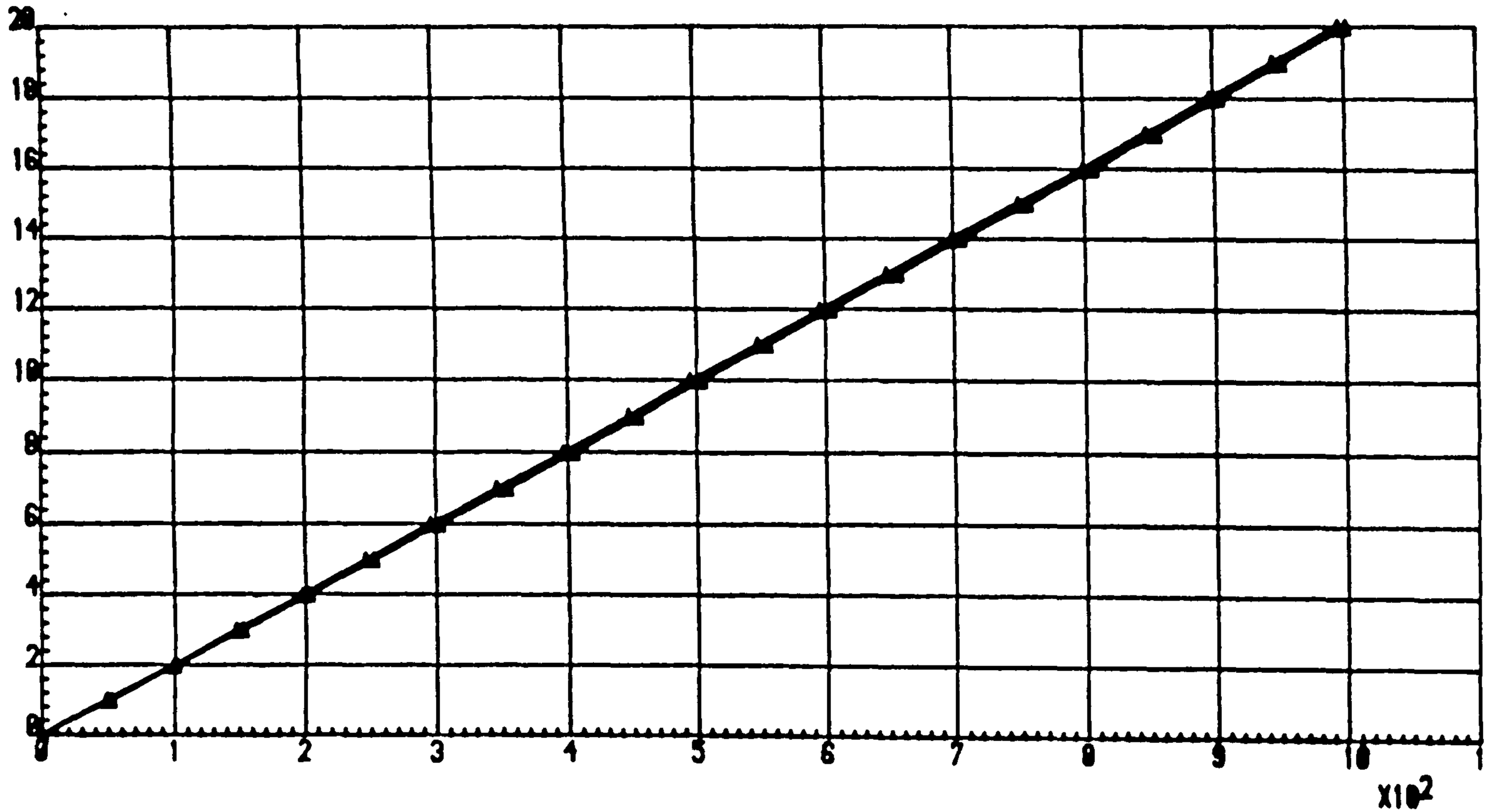

THE CALIBRATION GRAPH FOR LVDT:CHANNEL 6(AVCL-2)

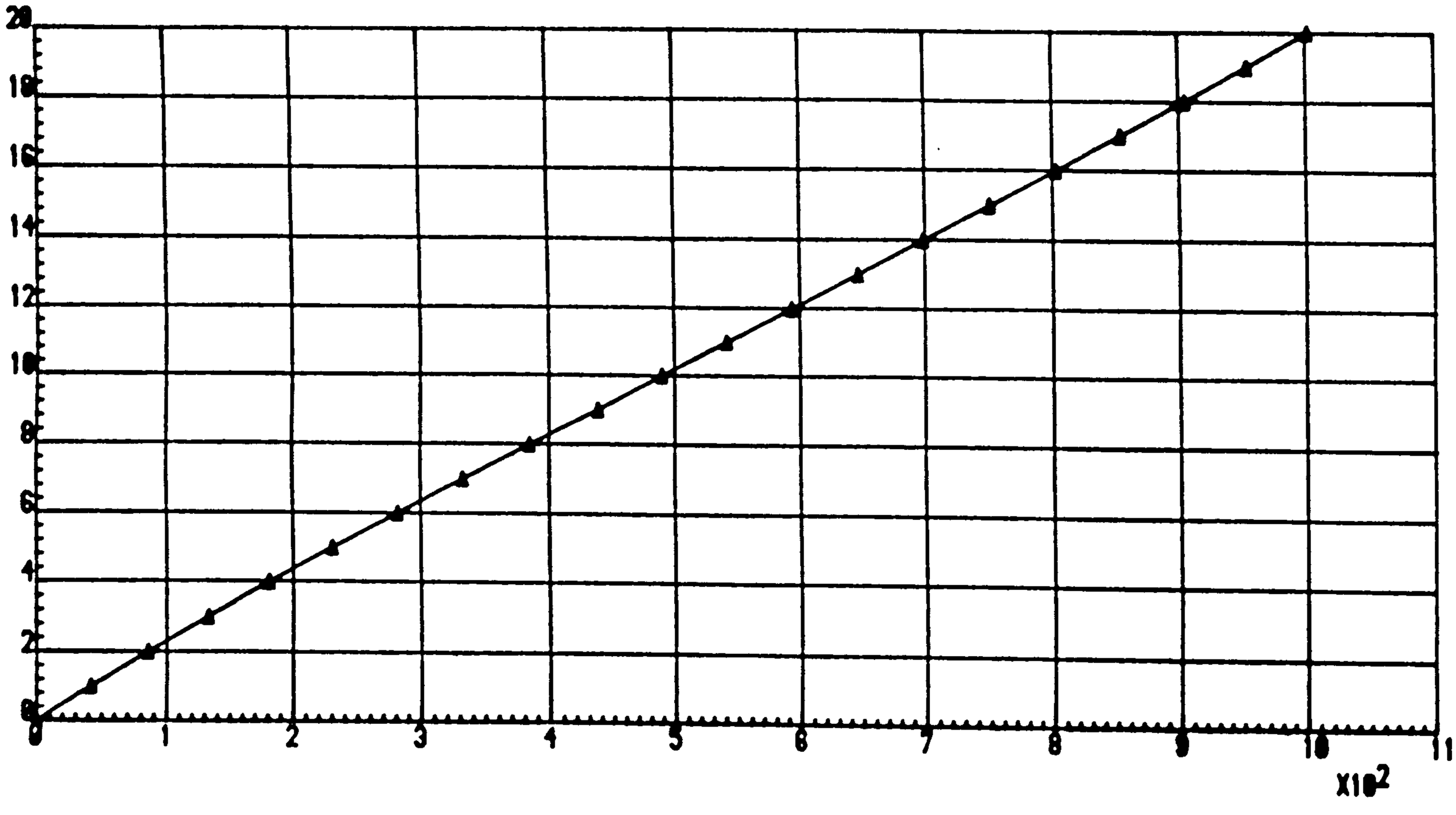

THE CALIBRATION GRAPH FOR LVDT:CHANNEL 7(AVCL-1)

DISPLACEMENT IN MM

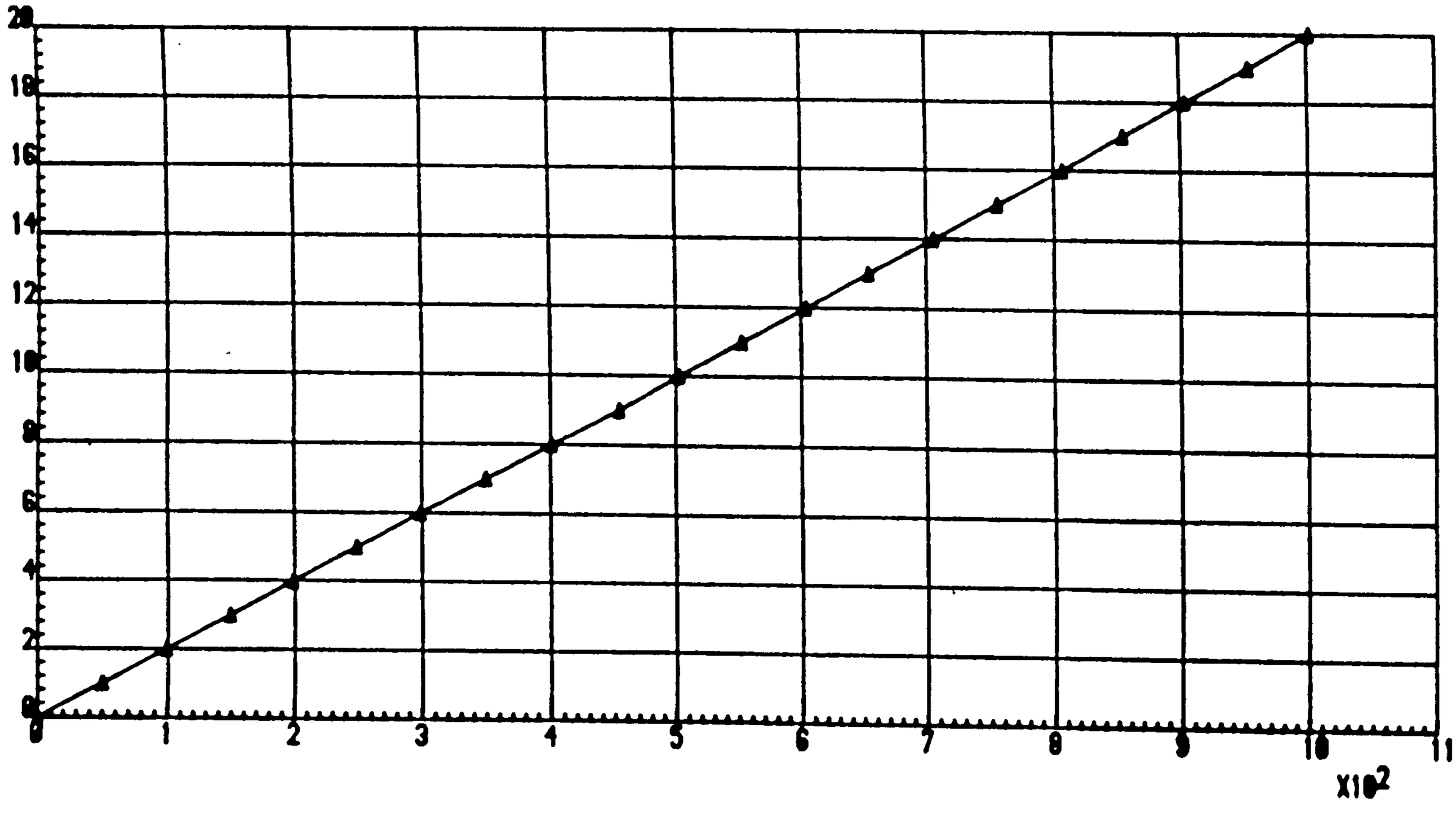

THE CALIBRATION GRAPH FOR LVDT:CHANNEL 15(T-2)

DISPLACEMENT IN MM

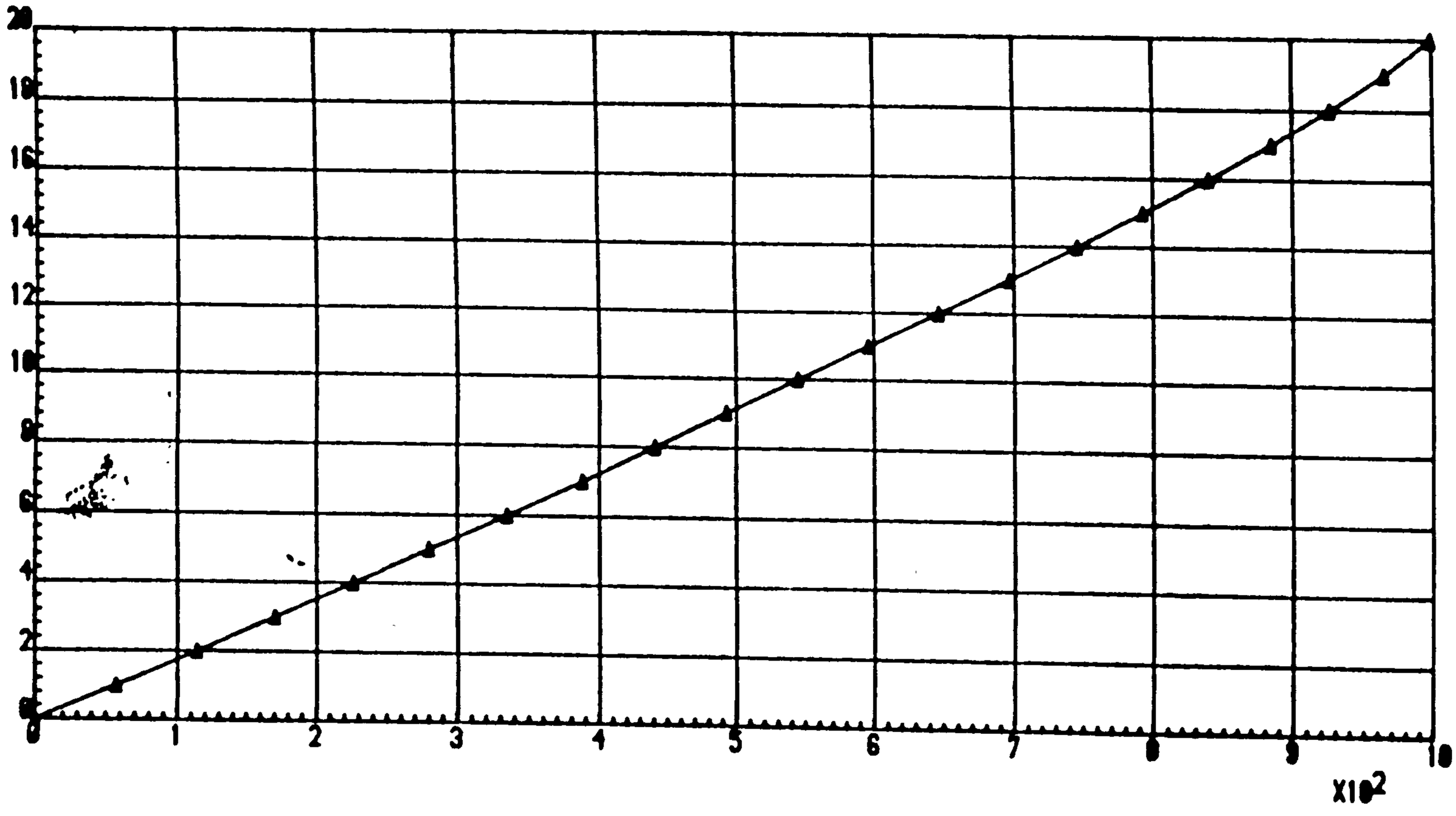

THE CALIBRATION GRAPH FOR LOAD CELL:CHANNEL 1

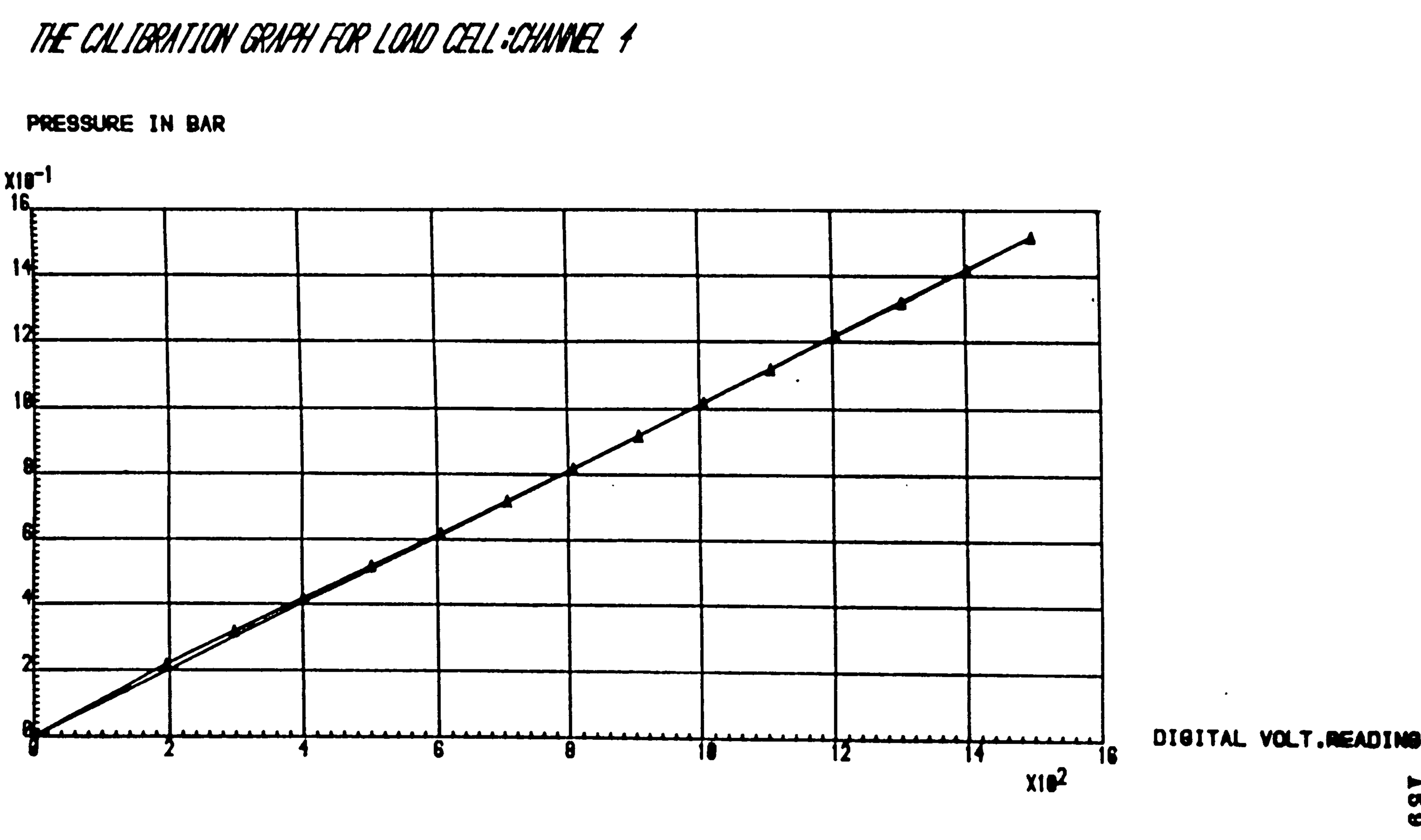

THE CALIBRATION GRAPH FOR LOAD CELL :CHANNEL 1(XT-2)

PRESSURE IN BAR

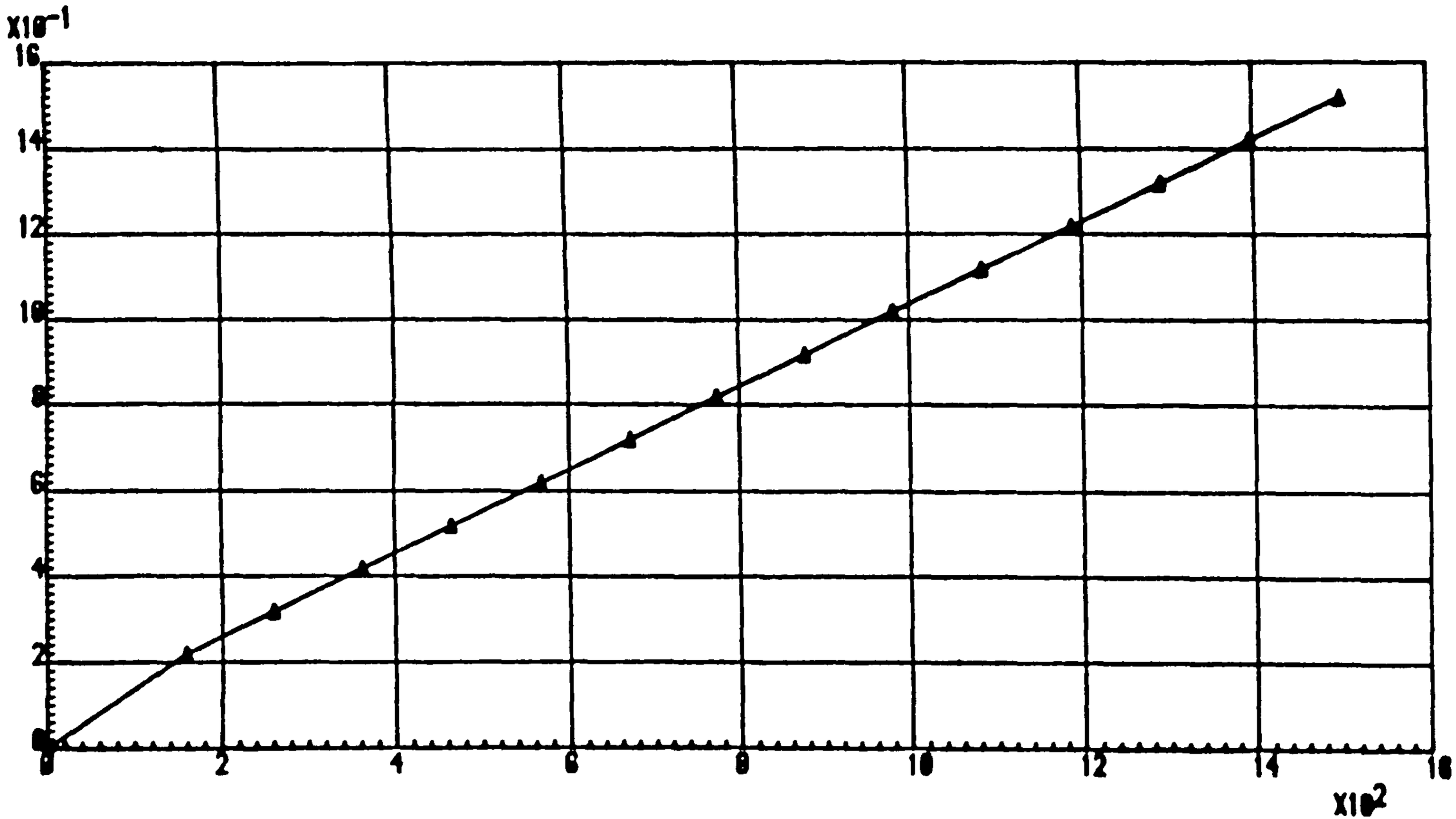

A4.5 Temperature effects on volume measurement

Rowlands (1972) described a method for automatically recording volume changes of a soil sample during a triaxial test. The method was based on the Bishop self-compensating mercury constant pressure unit and used a linear displacement transducer to measure the spring extension, which was directly proportional to the volume of fluid passing to or from the soil sample. Darley (1973) proposed a similar method which increased the sensitivity of the apparatus by using a single spring system.

The author has constructed a system based on Darley's method with only a small change in the positioning of the displacement transducer. The layout of the system is shown in Fig.A4.2. The displacement transducer has been moved from the centre of the spring to the side of pot A, thus ensuring completely frictionless movement of the inner rod of the transducer. The drainage line from the triaxial cell was connected to perspex pot A and the outlet from pot B was connected to a paraffin burette for calibration purposes. The outlet from the burette was connected to the back pressure system. Two systems were used during triaxial tests on samples of unsaturated soil; one to measure the total volume change and one to measure the water volume change. The details of the two systems are described in the following section.

Automatic volume change logger-1 (AVCL-1) was used to measure the change in pore water volume occurring during a triaxial test. The spring stiffness was 222.4 N/m and the

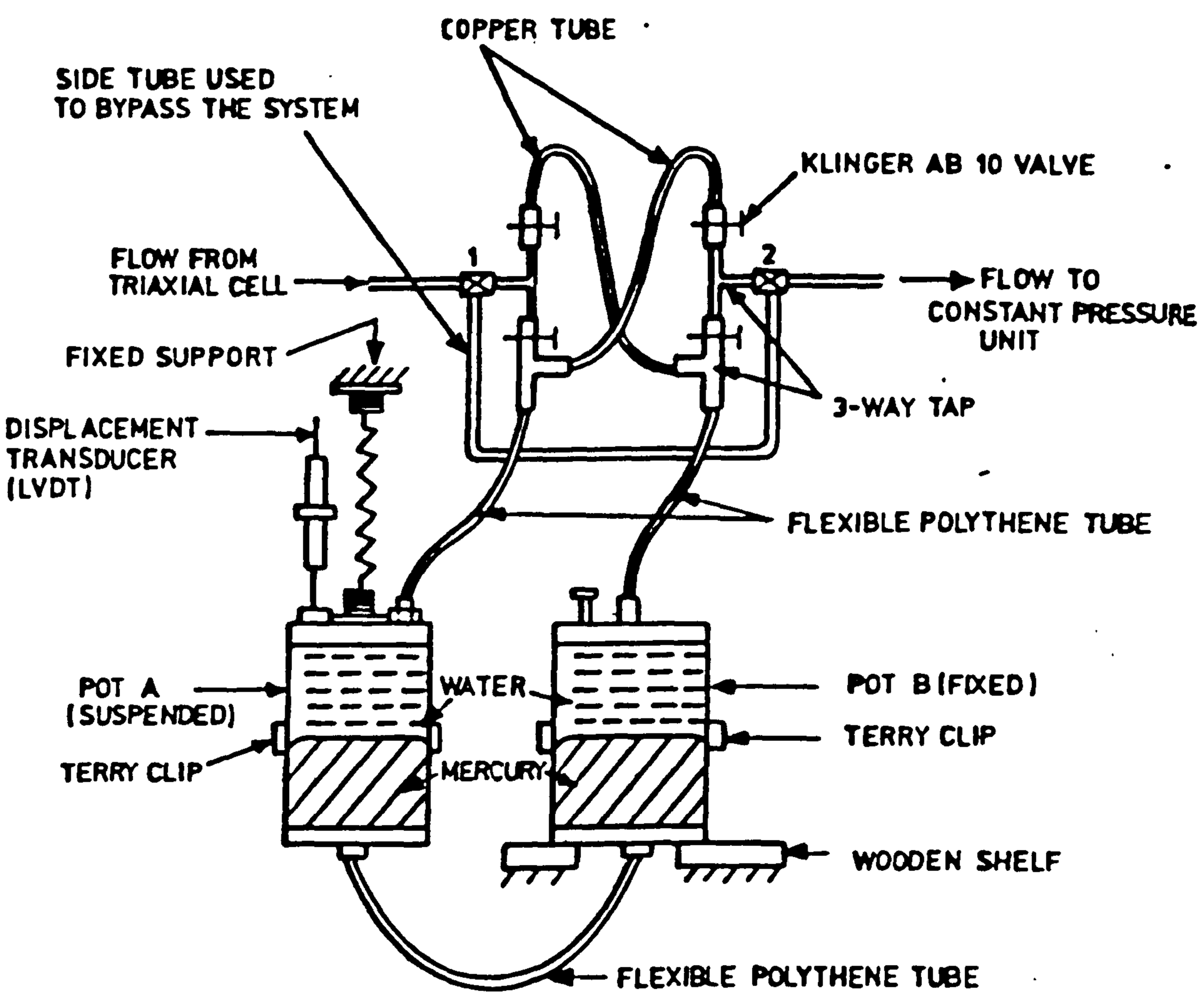

Fig. A4.2: AUTOMATIC VOLUME CHANGE APPARATUS

LOADING CONDITION: MERCURY IS TRANSFERRED FROM FIXED(RIGHT) POT TO SUSPENDED(LEFT) POT.

UNLOADING CONDITION: VICE VERSA.

internal diameter of the pots was 76.2 mm. This gave a theoretical sensitivity of 0.56 mm change in spring length per c.c. of volume change. The apparatus was calibrated against a paraffin-water volume change indicator at flow rates of 0.65 c.c./min., 0.90 c.c./min. and 5.07 c.c./min.. There was no significant change in the calibration for these values of flow, or if the direction of flow was reversed. These calibrations gave a sensitivity of 0.0377 c.c./unit readout on a digital voltmeter.

AVCL-2 was used to measure the change in total volume occurring during a triaxial test. The spring stiffness was 211.8 N/m and the internal diameter of the pots was 76.2 mm, giving a theorectical sensitivity of 0.59 mm change in spring length per c.c. of volume change. Similar calibration procedures as used on AVCL-1 confirmed the independence of flow rate and flowdirection and gave a sensitivity of 0.0366 c.c./unit readout.

A4.5.1 Effect of temperature

During calibration tests on AVCL-1 and AVCL-2, a small volume change was continually recorded when conditions should have been stable. As shown in Fig.A4.3(b), the digital voltmeter (d.v.m.) reading fluctuated up and down within a day, indicating that leakage from the system was not the problem. When the laboratory temperature was plotted alongside the voltmeter reading [Fig.A4.3(a)], it was clear that the laboratory temperature was affecting the volume change reading.

FIG.A4.3: *FLUCTUATION OF TEMP. WITH TIME:2(B)-FLUCTUATION OF D.V.M.READINGS WITH TIME*

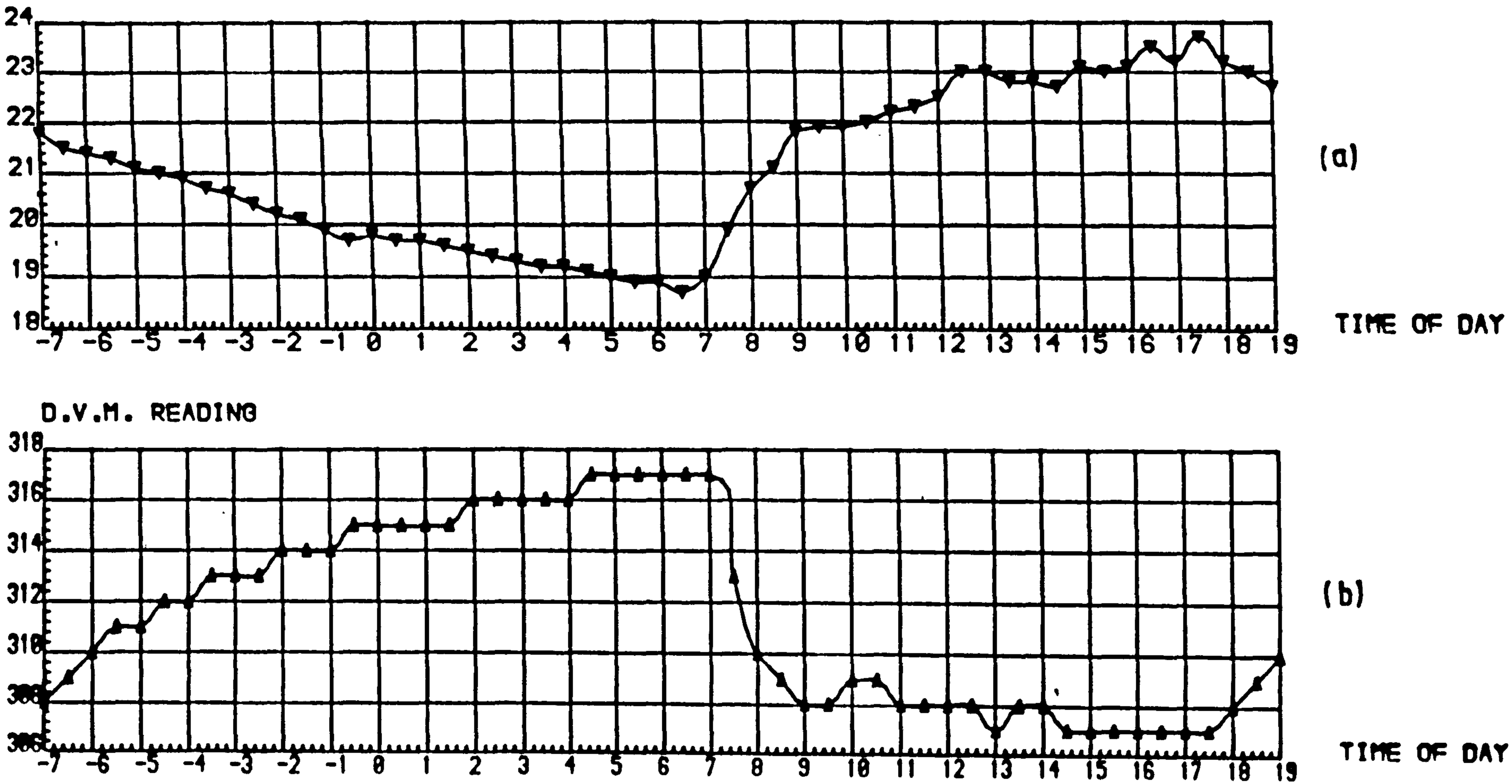

Four possible reasons for the fluctuations were identified:

1. Drift of the displacement transducer readout due to temperature variations.
2. Elongation or contraction of the spring due to temperature variations.
3. Entrapped air in the apparatus.
4. Thermal expansion of water/apparatus.

Figure A4.4 shows typical graphs of change in d.v.m. readout, (R2-R1) versus change in ambient temperature, (T2-T1) for AVCL-1 and AVCL-2. Using regression analysis the results can be represented by an equation of the form:

$$(R2 - R1) = A + B\,(T2 - T1) \quad \ldots\ldots\ldots (A4.1)$$

where A = intercept on (R2 - R1) axis

and B = slope of line

The coefficients of correlation for the results shown in Fig.A4.4(a) and (b) are 0.926 and 0.935 respectively. Equation A4.1 indicates that the value of A should be zero, but using the data illustrated in Fig.A4.4, A = 1.01; B = -2.43 for AVCL-1 and A = 0.75; B = -2.43 for AVCL-2 and the resulting equations are:

$$\text{For AVCL-1, } (R2 - R1) = 1.01 - 2.43\,(T2 - T1) \quad \ldots\ldots (A4.2(a))$$

$$\text{for AVCL-2, } (R2 - R1) = 0.75 - 2.43\,(T2 - T1) \quad \ldots\ldots (A4.2(b))$$

The high value of the correlation coefficients indicates that a close mathematical relationship exists between (R2 - R1)

FIG.A4.4: (R2-R1) VERSUS (T2-T1) FOR AVCL-1 & AVCL-2

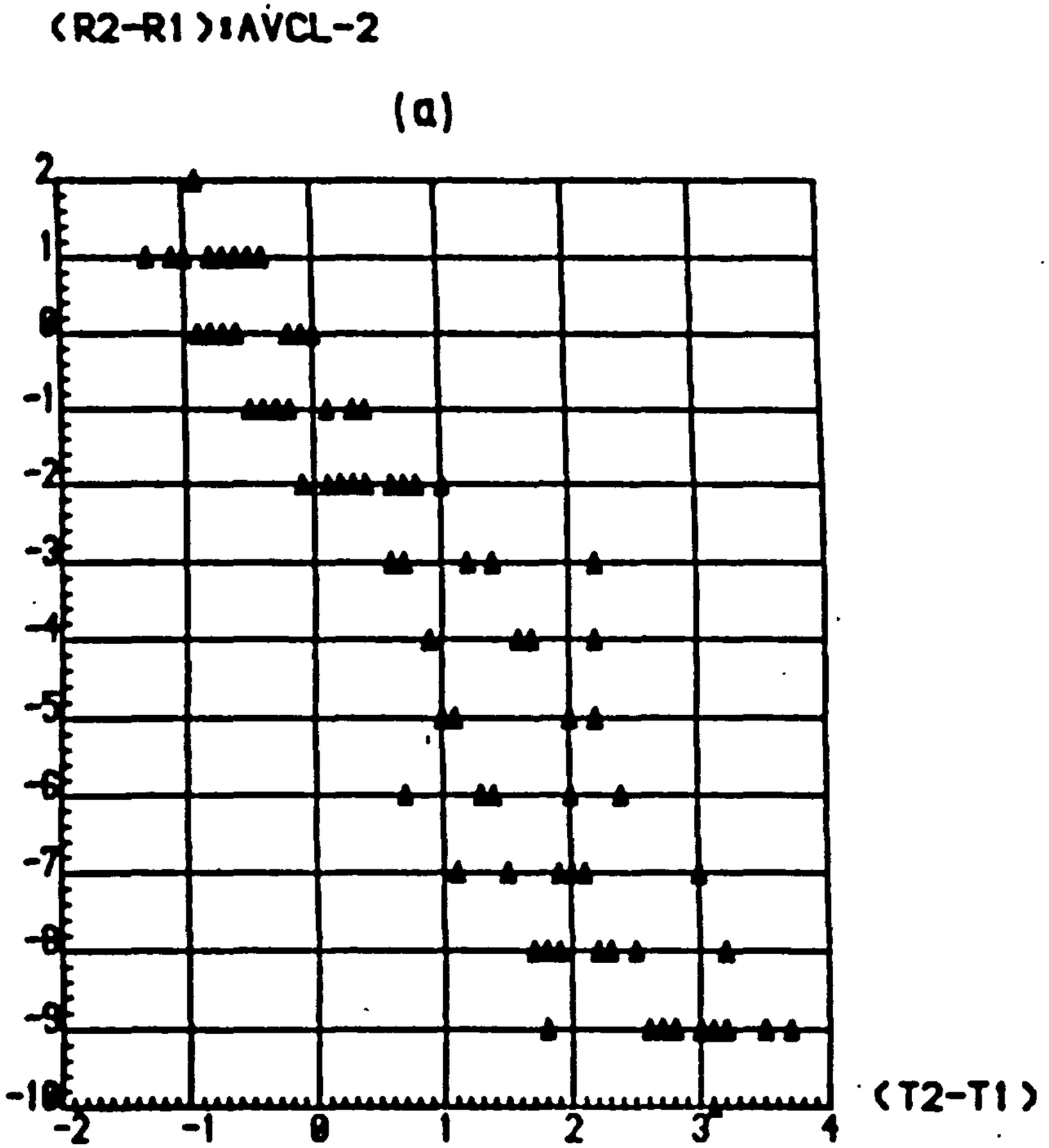

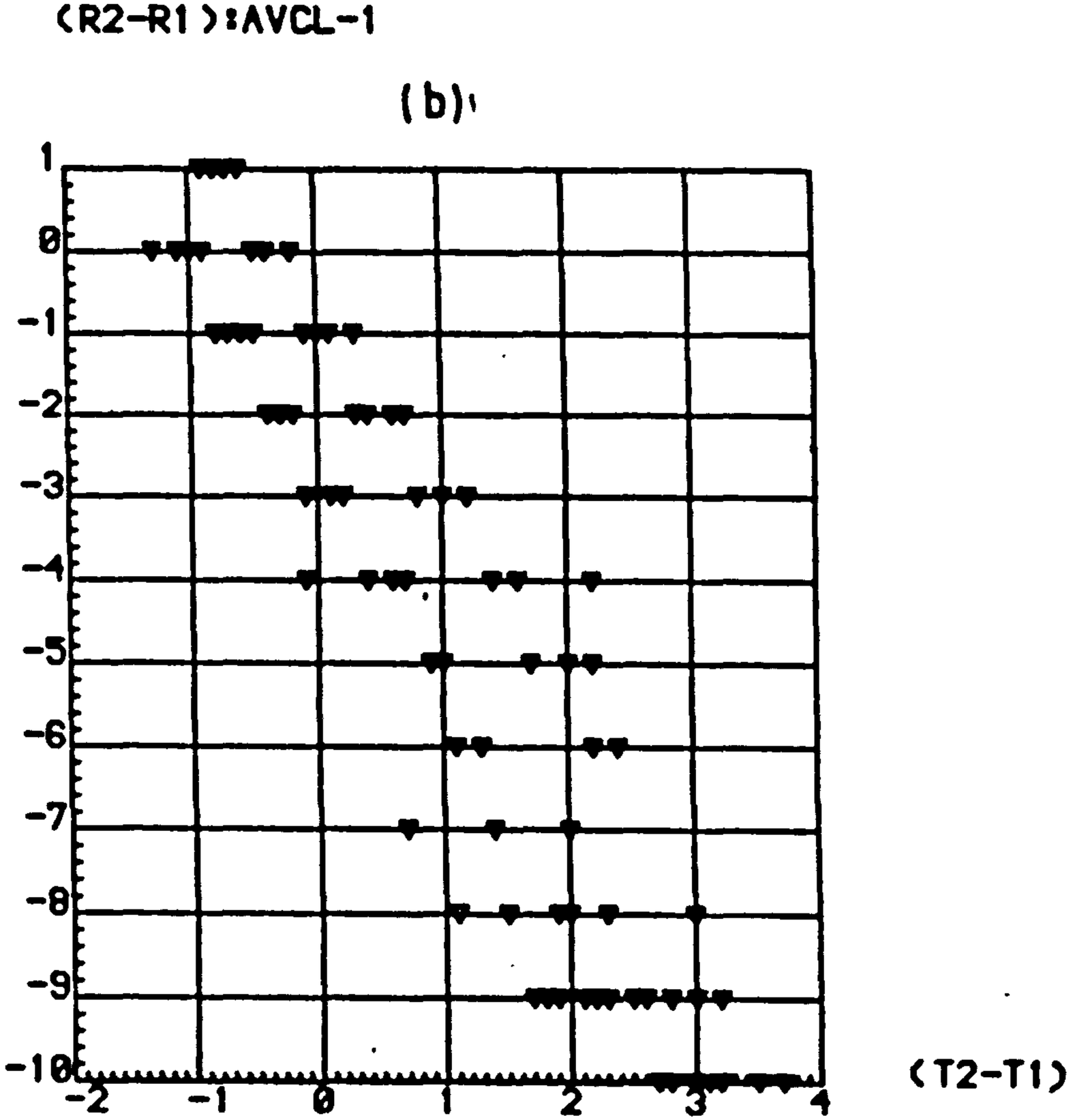

and (T2 - T1); it does not necessarily follow that a change in digital readout is caused by a change in temperature. Fig.A4.3 shows that it is not unreasonable to assumed that changes in temperature affect the readings given by AVCL-1 and AVCL-2.

Drift of displacement transducer

This was quickly eliminated as a problem by setting the transducer at a particular value and monitoring the readout over several days. It soon became obvious that, within the temperature range prevailing in the laboratory, the transducer was not sensitive to variations in temperature.

Elongation or contraction of spring

The springs used were approximately 200 mm long. Using a coefficient of linear expansion for steel of 10×10^{-6} per ^{o}C, the change in length per ^{o}C was 0.0022 mm. The maximum temperature change in the laboratory was about 5 ^{o}C, giving a maximum change in length of the spring of 0.011 mm. From the calibration of spring displacement (measured by displacement transducer) versus volume change (measured by a burette), 0.011 mm corresponded to a volume change of 0.0196 c.c. or a d.v.m. change of only 1 unit, which was a negligible variation in reading.

Entrapped air

In any air/water system, it is extremely difficult to flush out all the free air volume present in the system.

Despite thorough flushing of AVCL-1 and AVCL-2, it is probable that a small volume of air remained trapped in the

apparatus. In addition, although de-aired water was used throughout the apparatus, it is again probable that the water contained in AVCL-1 and AVCL-2 had some dissolved air present. The presence of these small amounts of free air and dissolved air will not make a significant contribution to the overall temperature effect.

Thermal expansion of water/apparatus

The total volume of water in each of the two measuring systems was approximately 750 c.c. (including the triaxial cell, tubing, etc.). Taking the coefficient of volumetric expansion of water as 2.1×10^{-4} per ^{o}C and a typical temperature difference during testing as $5\ ^{o}$C, then the change in volume due to temperature is 0.79 c.c.. This compares with a value of 0.42 c.c. found by using equation A4.2(b) with the same temperature difference and incorporating the sensitivity of AVCL-2 (0.0366 c.c./unit readout). The difference between these two values is caused by the thermal expansion of the apparatus, which would certainly restrict the volume change caused by the thermal expansion of the water. The magnitude of this reduction would be difficult to calculate accurately, as it would involve the calculation of the thermal expansion of all the components containing water.

The maximum total volume change in any of the tests completed to date was not greater than 5 c.c.. Using equation A4.2(b), the volume change due to a temperature difference of $5\ ^{o}$C was 0.42 c.c., which represents nearly 10 % of the measured

value and the percentage would increase for smaller values of the total volume change.

The most accurate measurement of volume change is obtained under constant temperature conditions. If this is not possible, the effect of temperature change on the whole measuring system, including entrapped air, triaxial cell, tubing, etc. can be taken into account by using equations similar to those presented for the automatic volume change measuring system.

REFERENCES

Darley,P.(1973)
'Discussion: 'Apparatus for Measuring Volume Change Suitable for Automatic Logging' by Rowlands,G.O.', Geotechnique Volume 23, No.1, pp.140-141, March, 1973.

Dorsey,N.E.(1940)
'Properties of Ordinary Water-Substance', American Chemical Society, Monograph Series, Reinhold Publishing Corporation, 1940.

Rowlands,G.O.(1972)
'Apparatus for Measuring Volume Change Suitable for Automatic Logging', Geotechnique Volume 22, No.3, pp.525-526, September, 1972.

APPENDIX 5

ERRORS IN THE ACTUAL MEASUREMENT OF TOTAL VOLUME CHANGE OF SOIL SAMPLE USING A DOUBLE-WALLED CELL TECHNIQUE

Appendix 5

Errors in the actual measurement of total volume change of soil sample using a double-walled cell technique

The following factors may lead to errors, and are discussed below.

(a) Differential pressure build up between two circuits

(b) The solubility of air in water

(c) Volume change due to the compression of water in the system

(d) Linear change in dimension of perspex under all round pressure

(e) Entrapped air in the cell

(f) Leakage from inner cell to outer cell

(a) Differential pressure build up between two circuits

To test the hypothesis, a differential pressure was established between the inner and outer cells, which allowed the inner cell to expand slightly before steady state conditions were achieved. Then the inner circuit was sealed off at the lower pressure before the next increment was applied to the external circuit. In this way the inner cell could not develop pressure faster than the outer circuit. However, no significant difference in the size of the calibration correction was observed.

The author has used the same pressure gauge for measuring the pressures in both circuits in an attempt to eliminate this problem.

(b) The solubility of air in water

It should be noted that, although the weight of a gas is proportional to the pressure(Henry's law), the volume occupied by a gas is inversely proportional to the pressure (i.e.Gas law). In other words, the volume of a gas decreases with increasing pressure, just as rapidly as the solubility increases. Therefore, the volume of gas dissolved in a given volume of liquid is independent of pressure.

This can be proven as follows:

From Gas law, $Uao.Vdo = Wdo.R.T. \ldots\ldots (1)$

and $Ua.Vd = Wd.R.T. \ldots\ldots (2)$

where Uao,Ua are initial and final pressure(absolute) in KN/sq.m

Wdo,Wd are initial and final weight of dissolved gas in Mg

R is universal molar gas constant(8313.5 KN/Mg/^{o}K)

and T is temperature (^{o}K)

In addition, Henry's Law states that

$$\frac{Wdo}{Wd} = \frac{Uao}{Ua} \quad \ldots\ldots\ldots (3)$$

From (1) $$Vdo = \frac{Wdo.R.T}{Uao}$$

Substituting (3) into (2), we have

$$Vd = \frac{Wd.R.T.}{Ua} = \left[\frac{Ua.Wdo}{Uao}\right]\left[\frac{R.T}{Ua}\right]$$

Therefore, $$Vd = \frac{Wdo.\ R.T}{Uao} = Vdo$$

Since the volume of dissolved air remains constant, it is

also possible to combine the free and dissolved air, and apply Boyle's Law to the entire volume. To separate the air into its dissolved and free phases at any point, the volume of dissolved air can be subtracted from the total volume of air. This is the procedure used by Hilf (1956) ,Bishop (1957) and Fredlund(1976). Therefore, the solubility of air in water does affect the total volume change at the beginning of pressure applied, but not when the water is saturated with air.

(c) Volume change due to the compression of water in the system

The volume change can be calculated from the compressibility of water (3.4×10^{-6} c.c./c.c./p.s.i) and the volume of water in the inner circuit.

Details of inner cell: Height = 22 cm

Internal diameter = 9 cm

External diameter = 10.2 cm

Wall thickness = 0.6 cm

$$\text{Volume inside the inner cell} = \frac{\pi * 9^2 * 22}{4} = 1400 \text{c.c.(approx.)}$$

Volume occupied by load cell and pedestal = 250 c.c.(approx.)

Actual volume of water inside inner cell

= 1400 - 250

= 1150c.c.

(It should be noted that when there is a sample in the cell, the volume of water present is reduced and the calibration correction would have to be adjusted accordingly)

Taking the compressibility of water as 3.4×10^{-6} c.c.

-5
/c.c./psi(i.e.4.93x10 c.c./c.c./bar) and the volume of water as 1150 c.c., then at 7 bar pressure there should be a volume change of the order of 0.4 c.c.. This is considerably smaller than the measured mean value of cell volume change (3.38 c.c.).

(d) Linear change in dimension of 'Perspex' under a uniform pressure on inner and outer surfaces.

From the 'Introduction to the Theoretical and Experimental Analysis of stress and strain' by Durelli, Phillips and Tsao (1958). The radial displacement, Ur:

$$Ur = \frac{1}{E} (\nu - 1)\, p.r$$

where E = Young's modulus = $2.75 * 10^{6}$ KN/sq.m

ν = Poisson's ratio = 0.38

p = applied pressure

and r = internal radius

As the cell pressure is increased, the inner cell will thus grow smaller, although there is no pressure difference across its surface.

At 7 bar: $Ur = \frac{1}{2.75*10^{6}}(0.38 - 1) * 700 * 4.5$ cm

$= -0.00071$ cm

Therefore, r = 4.49929 cm

$$V = \frac{\pi * 9^{2}}{4} * 22 - \pi(4.49929)^{2} * 22 = 0.4416 \text{ c.c.}$$

This largely cancelled out the volume change due to compression of water in the inner cell(i.e.0.4c.c.from (c)).

(e) Entrapped air in the cell

If the volume change is due to air in the cell assuming constant temperature conditions, the volume change should obey Boyle's Law.

Let initial total air volume be V1

and V1 = V1′ + hVw

Final total air volume be V2

and V2 = V2′ + hVw

where V1′ and V2′ are free air volume

hVw = volume of dissolved air = constant(from (b))

Therefore, V2 - V1 = V2′ - V1′

From Boyle's law: P1*V1′ = P2*V2′ = K

$$\text{i.e. } V1 - V2 = V1' \left(\frac{P2-P1}{P2}\right)$$

Taking the initial absolute pressure to be mean atmospheric (1.01 bar), then at any cell pressure,

$$\text{Cell volume change} = \frac{\text{Cell Pressure}}{\text{Cel pressure} + 1.01} * (\text{Initial volume of air in the cell})$$

If the cell volume change is due to air, then if the calibration results are plotted in accordance with this equation, they should give a straight line graph. Fig.A5.1 shows that the curves are straight at the initial portion and then start to curve up. It indicates that the error due to entrapped air is significant.

FIG: A5.1:

THE CHANGE IN VOLUME C.C. VS. CELL PRESSURE/(CELL PRESSURE + 1.01)

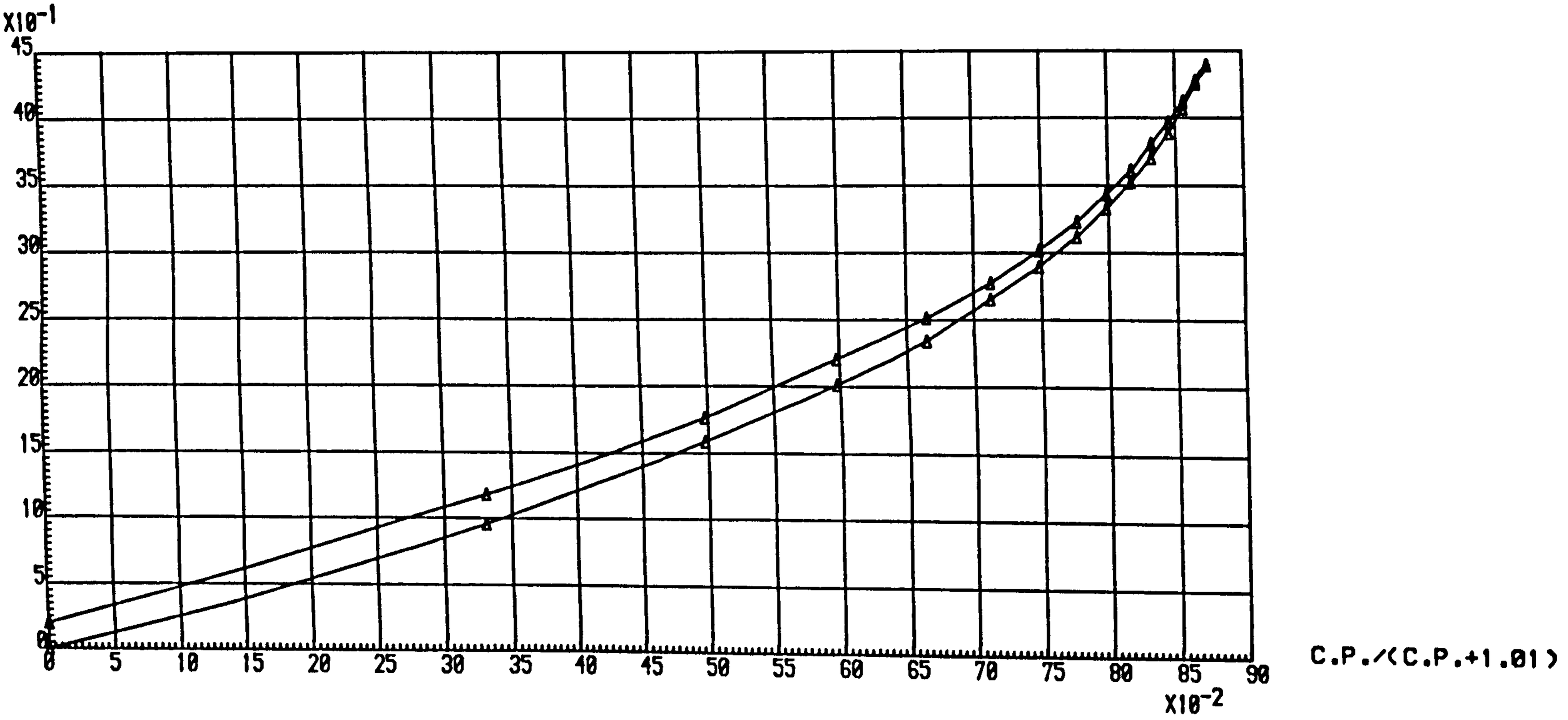

(f) Leakage from inner cell to outer cell

This was checked by applying an air pressure in the inner cell (before the outer cell was installed). By means of this, any leakage from the inner cell could be easily detected and stopped.

As a conclusion, the errors in the actual measurement of the total volume change of soil sample are mainly due to the entrapped air inside the cell.

In general, the double-walled cell modification of the triaxial system for measuring volume change of soil samples is an improvement on the existing single-walled (see figure A5.2 and A5.3), as it:

(1) reduces the variability of the calibration correction and thus increases confidence in the measurement of sample volume change.

(2) It saves time in making the calibrations and helps to take account of creep effects.

FIG. A5.2:

THE CALIBRATION GRAPH FOR VOLUME CHANGE OF SINGLE-WALLED CELL DUE TO PRESSURE CHANGE

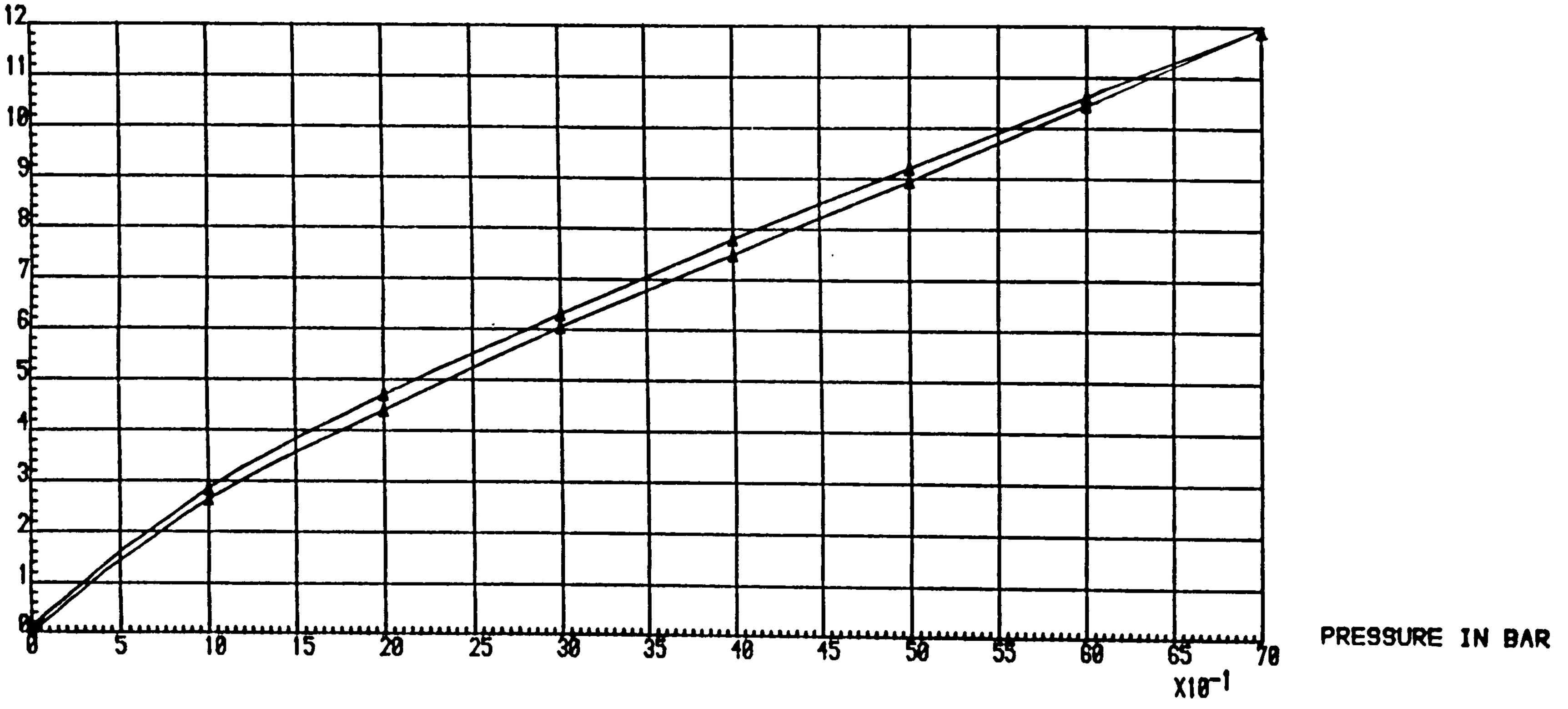

FIG. A5.3:
THE CALIBRATION GRAPH FOR VOLUME CHANGE OF DOUBLE-WALLED CELL DUE TO PRESSURE CHANGE

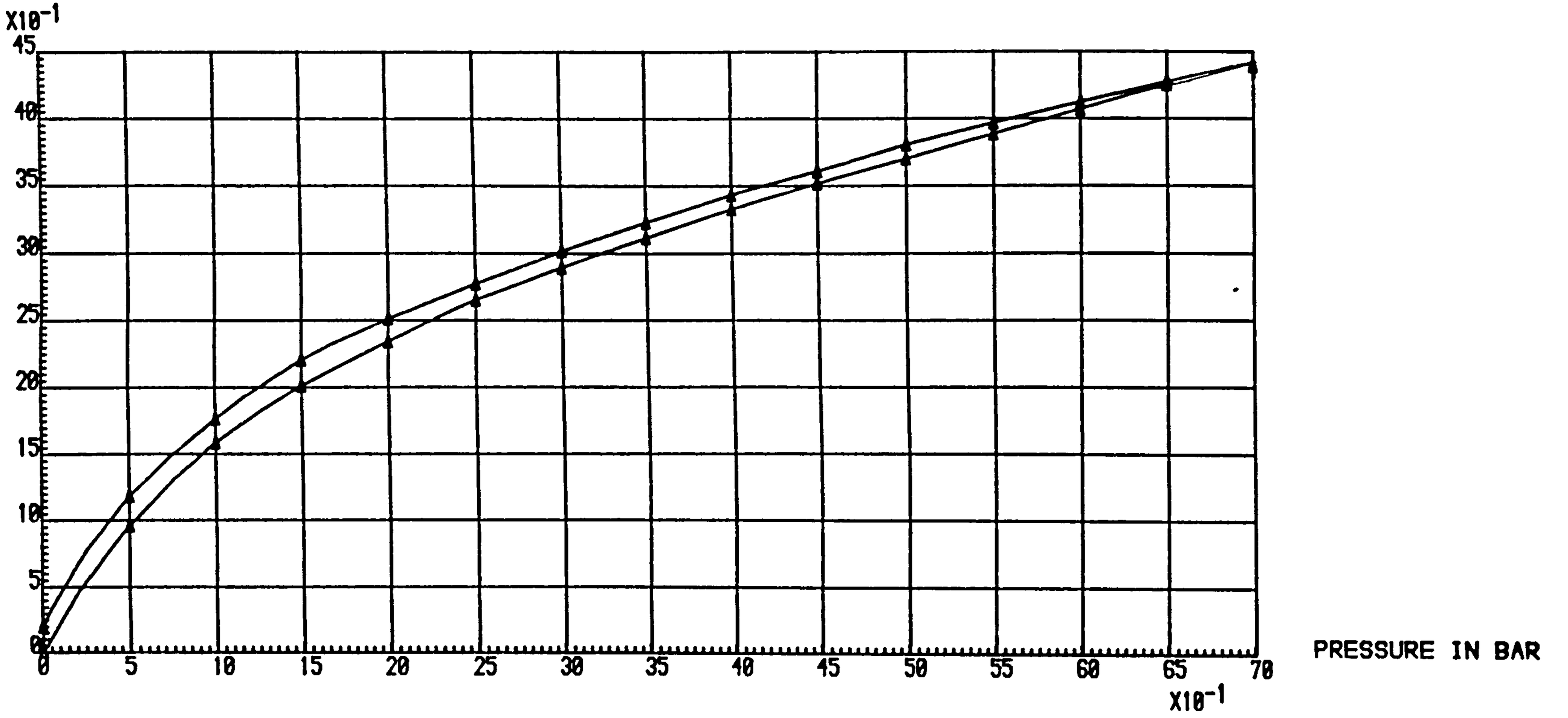

APPENDIX 6

A DIFFUSED AIR VOLUME INDICATOR FOR UNSATURATED SOILS

Appendix 6

A6.1 A diffused air volume indicator for unsaturated soils

The diffusion of air through saturated high air entry discs presents a serious problem in the testing of unsaturated soils. When determining either the strength (drained) or volume change characteristics of unsaturated soils, a technique must be available to measure the amount of diffused air in order that the appropriate corrections can be applied to the volume-weight relationships.

Unsaturated soils contain a relatively small amount of water and require lengthy periods of time for testing. In order to obtain accurate measurements of the water in the soil at any time, it is necessary to measure the amount of air that diffuses through the high air entry disc and apply a correction to the measured water volume change.

Undrained strength or volume change tests on unsaturated soils are performed with the water phase controlled as a closed system. As air diffuses through the high air entry disc, it comes out of solution in the compartment below the disc (Fig.A6.1). Therefore, the water is forced upward through the disc, back into the soil. Slowly the measured pressure changes from the original water pressure to the applied air pressure. In other words, the difference between the air and water pressures should tend towards a constant value but instead it continuously decreases. The reason for this is at present unknown.

Drained strength and volume change tests can be

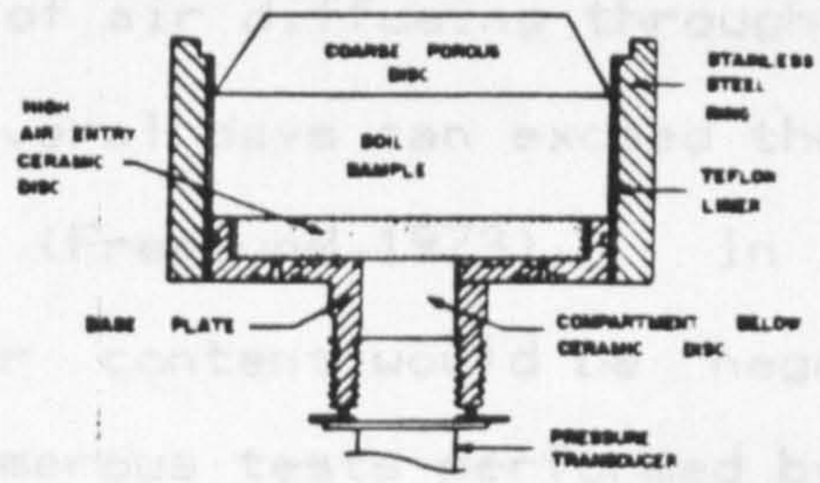

(A) ASSEMBLY SHOWING THE COMPARTMENT BELOW THE CERAMIC DISC

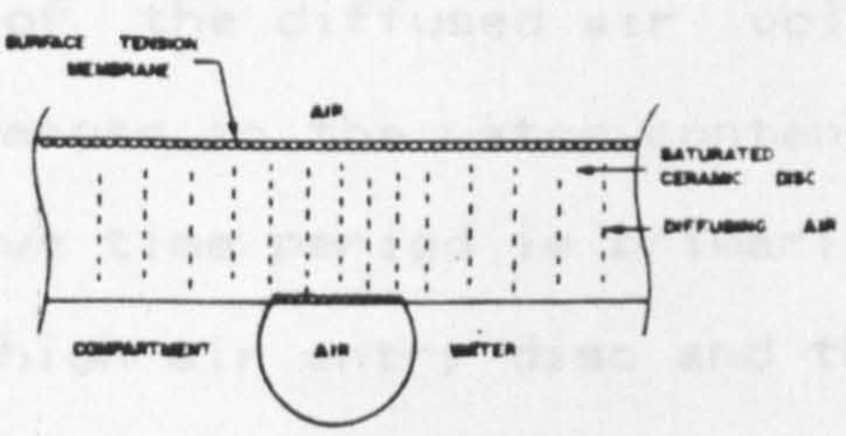

(B) AIR DIFFUSION THROUGH SATURATED CERAMIC DISC

Fig.A6.1: Removal of water by air diffusion from below the ceramic disc.

performed by controlling the air and water pressures. In this case, the water volume change measured is a combination of the flow of water to and from the sample plus the flow of diffused air through the water in the high air entry disc. In order to assess accurately the water volume change only, it is necessary to measure the diffused air volume and subtract it from the measured volume change.

The amount of air diffusing through a high entry disc over a period of several days can exceed the total volume of water in the sample (Fredlund,1973). In other words, the computed final water content would be negative. Based on observations from numerous tests performed by Fredlund, (1975), it appears that any drained test lasting in excess of 1 day should take account of the diffused air volume, if it is desirous to monitor changes in the water content or degree of saturation. The above time period is primarily dependent on the thickness of the high air entry disc and the magnitude of the matrix suction. Initially, attempts were made to predict theorectically the diffused air volume, but there appear to be many factors affecting the rate of diffusion, rendering a strictly theoretical approach unreliable.

The diffused air volume indicator described by Fredlund(1975) is relatively simple to build and can be operated under a back pressure of up to 70 p.s.i.(or 4 82 kN/m^2) applied to the water phase(see Fig.A6.2). The following description of a diffused air volume indicator is based on that given in Fredlund's paper and used by the author.

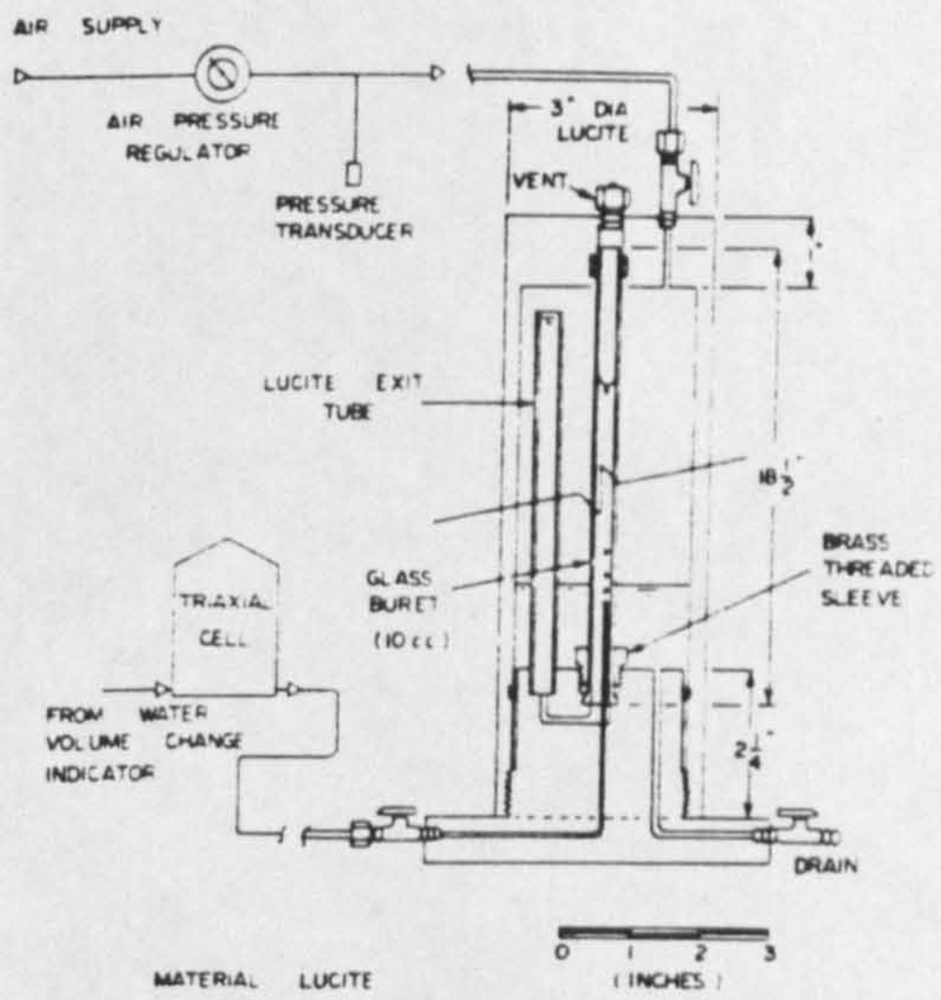

Fig.A6.2: Diffused air volume indicator (after Fredlund,1975).

A6.2 Description of the Diffused Air Volume Indicator

Basically, the diffused air volume indicator consisted of a standard 10 cc graduated burette that was inverted and placed inside a 3 in. (7.6 cm) diameter lucite cylinder (Fig.A6.2). The valve at the end of the burette was removed. Two rolling O-rings were placed around the top of the burette to form a seal with the lucite. A vent on the top could be opened when filling the burette and remained closed when the indicator was in operation. The seal at the base of the burette consisted of a threaded brass sleeve tightened down against an O-ring. The brass sleeve was machined with a hexagonal top and an inside diameter slightly larger than the burette. The lower part of the brass sleeve was threaded into the lucite block at the base. The exit tube maintained a constant pressure head on the air in the burette.

By momentarily creating a pressure gradient of 1 to 10 p.s.i. (6.9 to 69 kN/m^2) across the base plate (i.e. below the high air entry disc in the triaxial or oedometer apparatus), air bubbles were flushed out and their volume measured by displacement of the water in the burette. The pressure inside the lucite cylinder could be controlled by an air pressure regulator, at a value that maintained the desired gradient across the base plate. For example, if the water pressure below the high air entry was controlled at 30 p.s.i. (207 kN/m^2), the lucite cylinder was pressurized to approximately 25 p.s.i. (172 kN/m^2). The volume of diffused air was recorded in either of two ways:

(i) The initial burette reading was taken after the diffused air indicator chamber was pressurized (e.g. to 25 p.s.i.) (172 kN/m^2). The base plate was flushed out and the final burette reading was recorded. The indicator chamber pressure was measured on a pressure transducer to the nearest 1/100th of a p.s.i..

(ii) The initial burette reading was taken when the diffused air indicator chamber was at atmospheric pressure. The chamber was then pressurized (e.g. to 25 p.s.i. or 172 kN/m^2) and the air flushed from the base plate. The chamber was depressurized and the final burette reading was recorded. It is possible to take into account slight fluctuations in atmospheric pressure if a barometer is located in the laboratory.

In either of the above cases, the volume occupied by the diffused air at the base of the ceramic disc was computed by applying Boyle's law to the measured volume of diffused air (Fredlund 1973). Both of the above procedures produced satisfactory results: however, the second procedure was generally used by the author. Applying the first of the above procedures, the drop in pressure from the base plate to the indicator was small and the amount of air that came out of solution due to this pressure drop was negligible. Even when the second procedure was used, the amount of air immediately coming out of solution was negligible.

Provided the temperature of the diffused air volume indicator and the base plate of the triaxial or oedometer apparatus were the same, there was no need to apply a

temperature correction. All tests on the indicator were performed in a temperature-controlled laboratory.

When the burette in the diffused air volume indicator became empty, the vent at the top was opened and the burette was filled with water. Initially there was some difficulty in getting the bubbles of diffused air to move up freely in the burette. This problem was overcome by filling the burette with a commerical cleaner which had a low surface tension. The diffused air volume indicator has been used with triaxial test apparatus. Figure A6.2 shows how the indicator was used in conjunction with a modified triaxial cell. It should be noted that the water volume change indicator was bypassed when the diffused air was flushed from the base plate.

A6.3 Computation Procedure

The accuracy of the diffused air volume indicator could be readily checked by allowing the diffusion of air through a saturated ceramic disc and monitoring the volume change on a water volume change indicator. By turning off the water volume change indicator and flushing the base plate, the volume of diffused air could be measured directly. The two results should be essentially the same if the diffused air volume indicator is performed satisfactorily.

The diffused air can always be visualized as a fictitious volume of water flowing out of the sample. The water volume change indicator has recorded it as such and therefore the correction for diffused air must always be subtracted from

recorded water flow.

The determination of the correction for the diffused air depends on a precise evaluation of the pressure in the diffused air volume indicator as well as the base plate. The pressure on the diffused air in the indicator is equal to the applied backpressure plus the head difference between the exit tube and the air-water interface in the burette. The pressure in the base plate was measured by a pressure transducer mounted in the base plate. Figure A6.3 shows the detailed calculation of the air pressure and volume. The volume of diffused air is reduced to an equivalent volume in the base of the cell by means of Boyle's law.

$$Vd = \frac{\Delta V1 \cdot U1}{Ub}$$

where Vd = volume of diffused air, $\Delta V1$ = difference between the initial and final readings on the diffused air volume indicator, U1 = absolute pressure in the indicator, and Ub = absolute pressure in the base plate of the apparatus.

The base plate generally needs to be flushed about once each day. Corrections to intermediate water volume change readings can be made on the basis of a linear interpolation with respect to time.

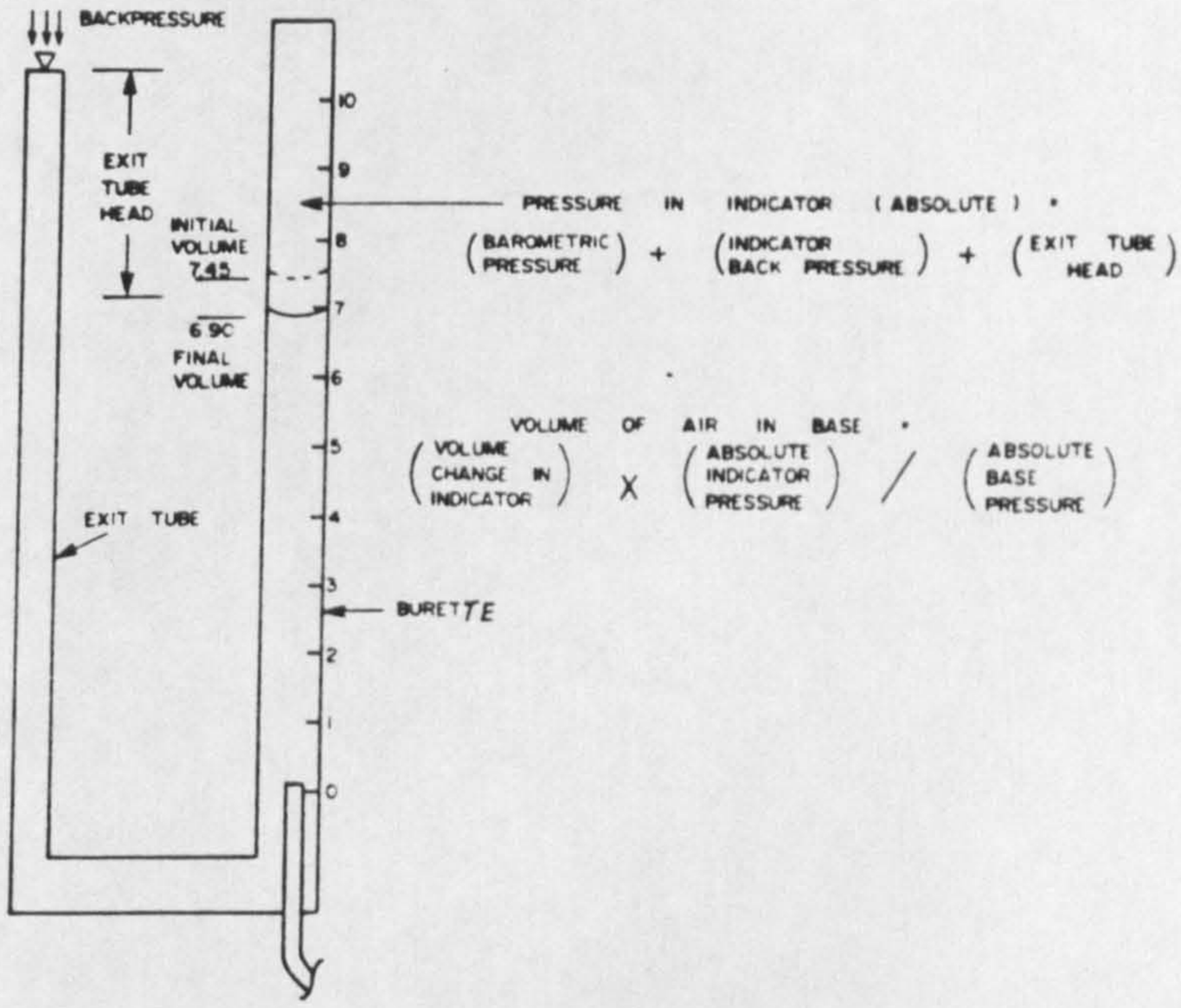

Fig.A6.3: Computations for the diffused air volume correction under isothermal conditions.

A6.4 Computation for the diffused air volume correction
(Refer to Fig.A6.4)

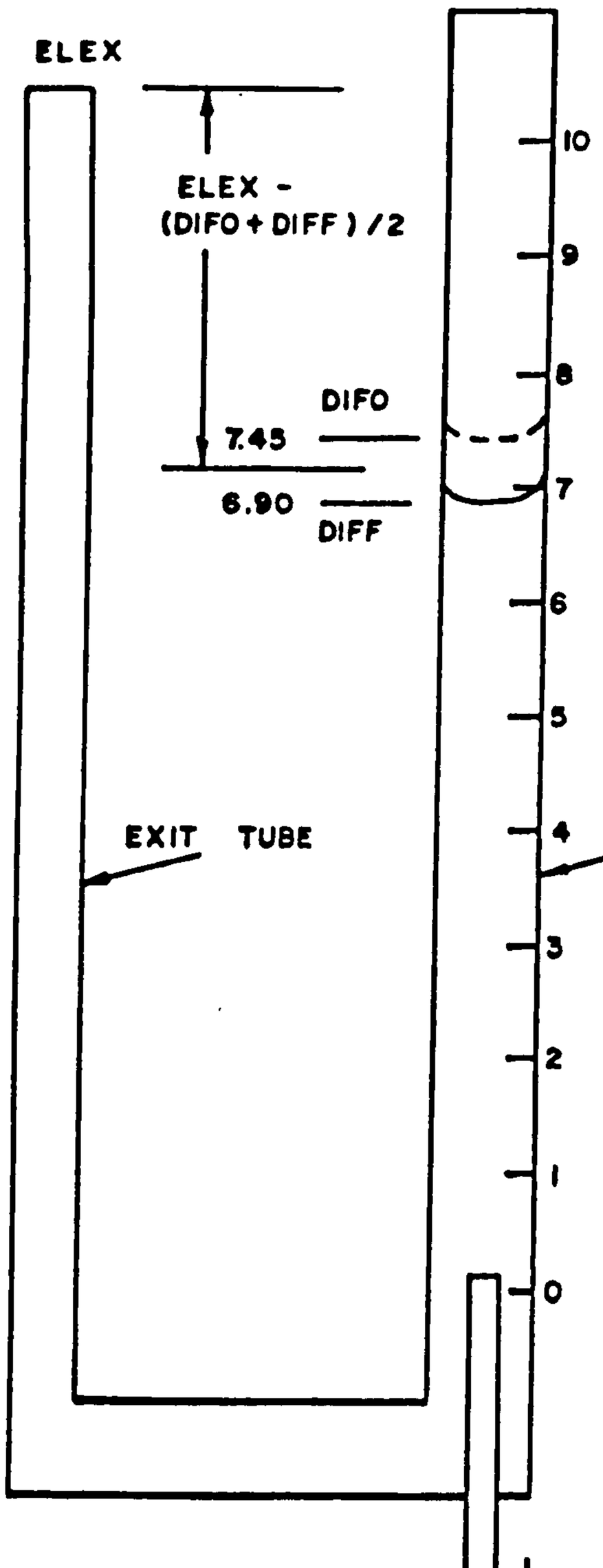

Calib = 1.4 cm/c.c.

Assume 1 Atmospheric Pressure

= 1.01325 bar

= 1.01 bar(approx.)

Air back pressure to indicator

ATM = DIFPR + 1.01 bar

where DIFPR = air back pressure(gauge)

Head on air in tube in cm of water

$$EXHEAD = \left[ELEX - \frac{(DIFO + DIFF)}{2}\right] * CALIB \quad cm$$

$$= \left[17 - \frac{(DIFO + DIFF)}{2}\right] * 1.4 \quad cm$$

The Air Volume Change in Indicator

ADIF = DIFO - DIFF c.c.

The Corresponding Change in the base of the Cel

$$ADIFF = \frac{(ADIF) * (EXHEAD * CONVER + ATM}{PORE + 1.01}$$

where CONVER = 0.001 bar/cm of Water

and PORE = back water pressure

$$ADIFF = \frac{(ADIF) * (EXHEAD * 0.001 + ATM}{(PORE + 1.01)}$$

Fig.A6.4: Computation for the diffused air volume correction.

A6.5 To test the proper functioning of the diffused air volume indicator

Three different tests were performed on the modified triaxial cell using an applied air pressure equal to 5 bar and a back water pressure equal to 3 bar. The following calculations and figures showed the measured diffusion of air through a saturated, ceramic disc with an air entry value of approximately 3 bar.

(1) Date : 27/8/82 Time (Starting) : 17 : 24 p.m.

From AVCL : change in digital voltmeter
= 526 - 103
= 423

From calibration curve, volume change = 16 c.c.

From DAVI : volume change = 16.40 c.c.
under air back pressure 2.5 bar

Calculation: ATM = 2.5 + 1.01 = 3.51 bar
take atm. pressure = 1.01 bar

$$EXHEAD = [17 - \frac{(24.20 + 7.80)}{2}] * 1.4$$

$$= 1.4 \text{ cm}$$

PORE = 3 bar ADIF = 24.20 - 7.80 = 16.40

$$ADIFF = \frac{16.40 * (1.4 * 0.001 + 3.51)}{(3 + 1.01)}$$

$$= 14.36 \text{ c.c.}$$

(2) Date : 28/8/82 Starting time: 11:03 a.m.

From AVCL: change in digital voltmeter = 464 - 245 = 219

From calibration curve, volume change = 8.6 c.c.

From DAVI: Volume change = 24.60 - 14.90 = 9.7 c.c.

under air back pressure 2.5 bar

Calculation: ATM = 2.5 + 1.01 = 3.51 bar

EXHEAD = (17 - 19.75) x 1.4 = - 3.85 cm

ADIF = 9.70

$$ADIFF = \frac{9.70 * (3.51 - 3.85 * 0.001)}{4.01}$$

= 8.48 c.c.

(3) Date: 28/8/82 Starting time: 13 :18 p.m.

From AVCL: change in digital voltmeter

= 509 - (- 72)

= 581

From calibration curve, volume change = 22.40 c.c.

From DAVI: volume change = 25.60 c.c.

under air back pressure 2.5 bar

Calculation: ATM = 2.5 + 1.01 = 3.51 bar

$$EXHEAD = [17 - \frac{(24.60 - 1.00)}{2}] * 1.4$$

= 7.28 cm

PORE = 3 bar ADIF = 24.60 - (-1.00) = 25.60 c.c.

$$ADIFF = \frac{25.60 * (7.28 * 0.001 + 3.51)}{4.01}$$

= 22.45 c.c.

Both the automatic water volume change logging system and the diffused air volume indicator registered essentially the same volumes of diffused air, therefore, the diffused air volume indicator functioned satisfactorily.

DIFFUSION OF AIR THROUGH SATURATED CERAMIC DISC(TEST NO. 1)

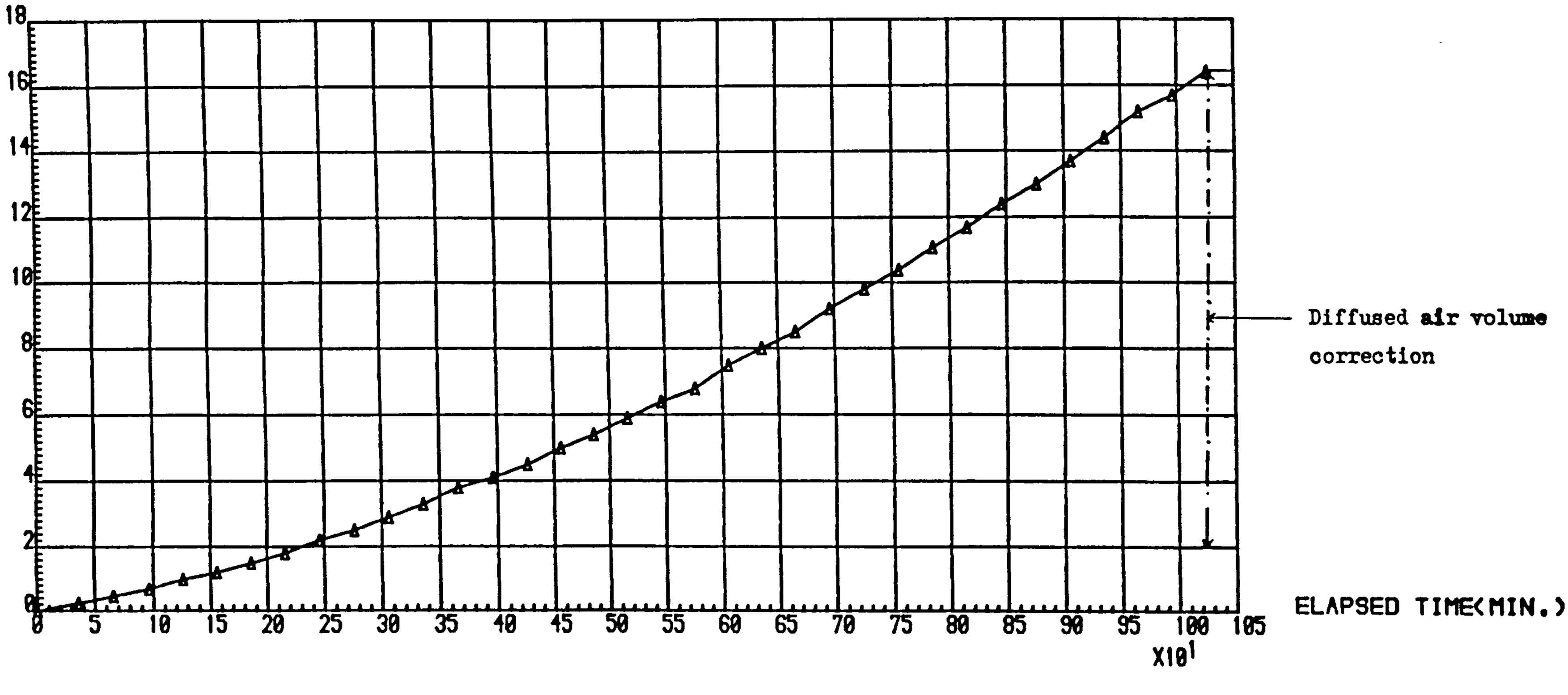

DIFFUSION OF AIR THROUGH SATURATED CERAMIC DISC (TEST NO.2)

VOLUME CHANGE IN C.C.

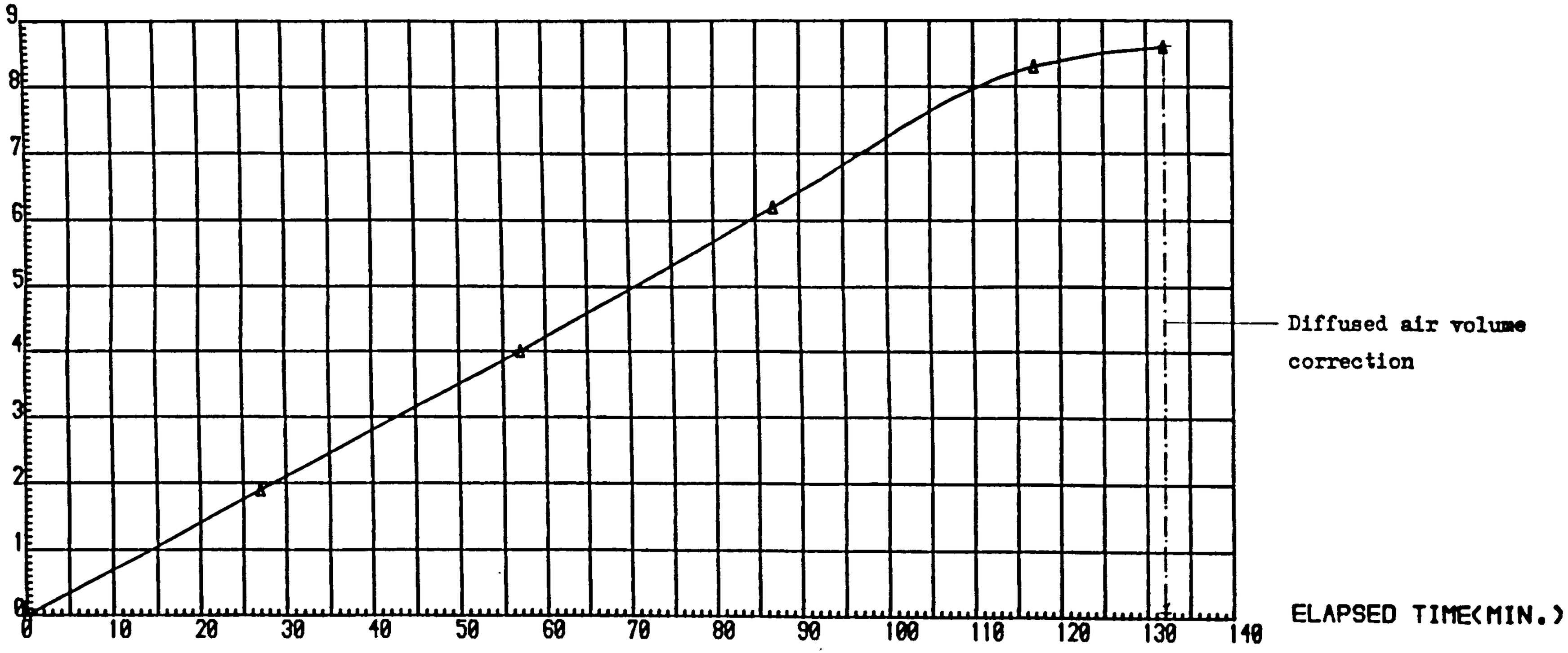

DIFFUSION OF AIR THROUGH SATURATED CERAMIC DISC (TEST NO.3)

VOLUME CHANGE IN C.C.

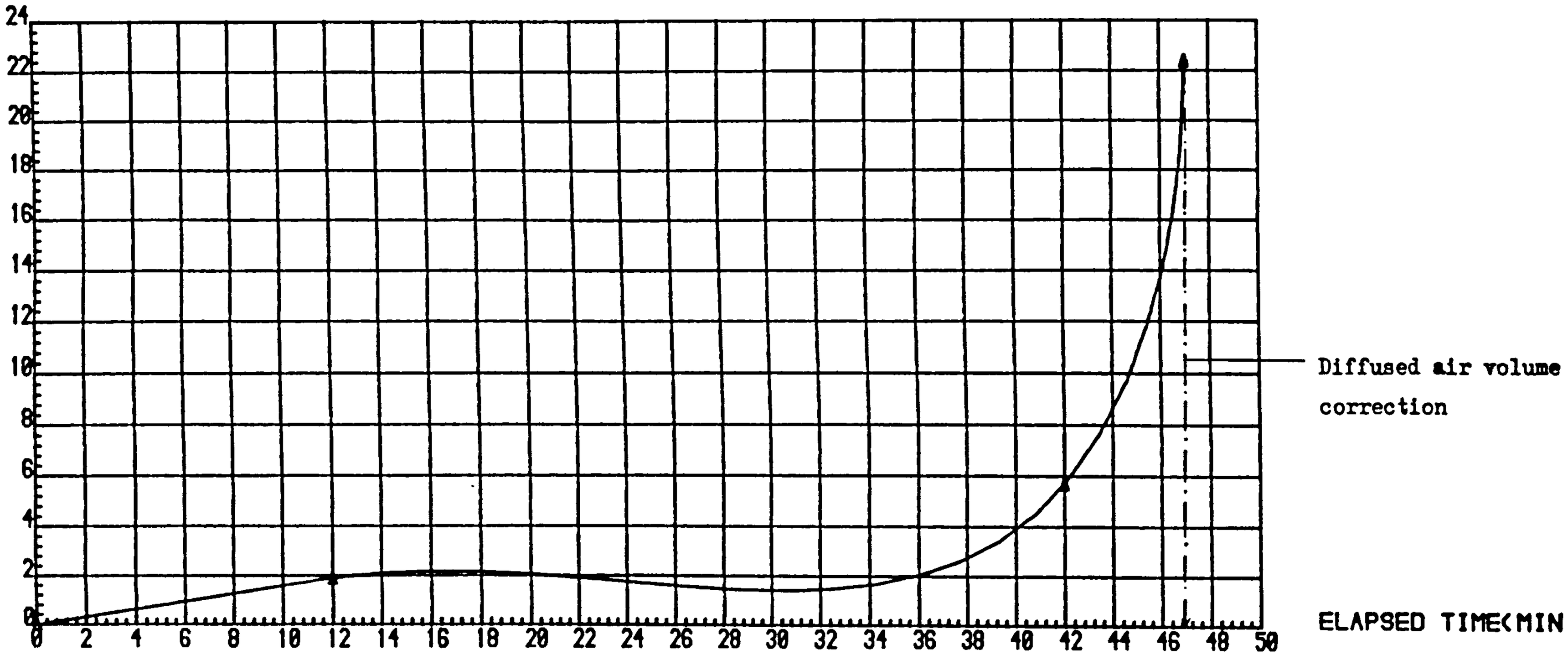

APPENDIX 7

POROUS CERAMIC FOR SOIL RESEARCH WORK

Appendix 7

POROUS CERAMICS FOR SOIL RESEARCH WORK

A7.1 Properties of high air entry ceramic discs

The high air entry discs on which the soil samples are placed act as a semi-permeable membrane to separate the air and water pressures. The ceramic disc must have an air entry value in excess of the maximum differential air-water pressure. At the same time, it is desirable to have the largest possible pore size in the disc to obtain rapid equilization and to prevent impeded drainage.

The different types of porous ceramics are designated by their bubbling pressure or air entry value, measured in bars of pressure. All types have considerable mechanical strength and may be shaped by conventional grinding and machining techniques.

In the soils research field the unit of pressure, the bar, has come into general use and has also been selected as the standard unit for the expression of soil suction. The bar is an international unit of pressure in the metric system. According to definition 1 bar equals 10^6 dynes/cm^2. This is the equivalent of 0.987 atmospheres, 14.5 psi or 750 mm of mercury. It is also equivalent to 1020 cm, or 401.6 in., or 33.5 ft. of water.

The bubbling pressure or, as it is also termed, the air entry value, for a porous ceramic plate is the pressure required to force air through the plate after the plate has been

thoroughly wetted with water. It is defined by the capillary model equation

$$(Ua - Uw)_{max} = \frac{2Ts}{r}$$

where Ts = surface tension of water with respect to air

= (72 dynes/cm)

r = radius of the largest pore

The smaller the pores in the plate, the higher this pressure will be. The relationship between pore size and bubbling pressure is defined by the equation D = 30 Ts/P where D is the pore diameter measured in microns, P is the bubbling pressure measured in millimeters of mercury, and Ts is the surface tension of water measured in dynes/cm. Using this formula, a porous ceramic plate that has a bubbling pressure of 1 bar or 14.5 psi or 750 mm of mercury, would have a pore diameter of 2.9 microns.

For soil moisture extraction work it is essential that the porous ceramic plates are used at pressures below the bubbling pressure of the plate. Manufacturer's designation of, for example, a 1 bar ceramic means that the bubbling pressure is in excess of 1 bar, or in excess of 14.5 psi, and that the plate is suitable for use in the range of 0 to 1 bar of soil suction. Similarly a 15 bar ceramic has a bubbling pressure in excess of 15 bars or 218 psi and is suitable for use in the range of 0 to 15 bars of soil suction.

The pore diameter in the 15 bar ceramic is, of course, much smaller than in the 1 bar ceramic. Consequently, for plates of equal thickness the flow of water through the 15 bar

ceramic is much slower than through the 1 bar ceramic for any given pressure differential across the plate. In studies involving moisture equilibrium, such as between a soil sample in contact with the porous plate and an applied gas pressure, the time required to reach equilibrium is dependent on the permeability of the porous plate. In order to obtain equilibrium in the shortest possible time, it is desirable to use a porous plate with the largest pore size possible that will still have a bubbling pressure higher than the maximum equilibrium pressure to be used.

The coefficient of permeability of the ceramic disc mounted in the base plate can be readily measured by placing water above the disc, increasing the chamber pressure and measuring the flow in the water volume change indicator. For the ceramic discs used in this research, numerous permeability tests were performed and the results are summarized in Table A7.1.

In general, the permeability decreases as the pressure difference across the ceramic disc increases (Fig. A7.1).

Minute cracks in the discs caused an increase in the coefficient of permeability. However, the increase in permeability was generally small while the decrease in the air entry value was substantial.

FIG.A7.1:VARIATION OF PERMEABILITY OF CERAMIC DISC W.R.T. WATER WITH DIFFERENT PRESSURE GRADIENTS

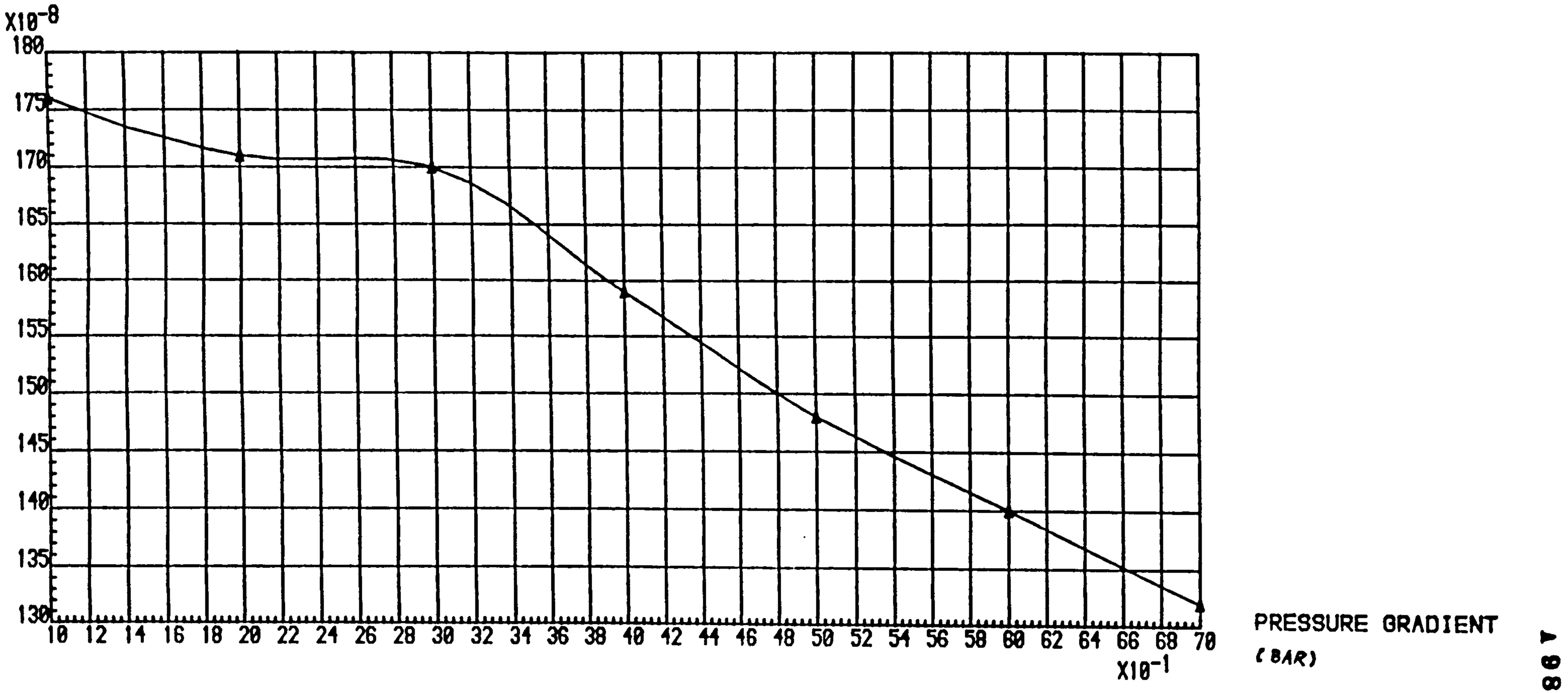

Table 7.1

Disc No.	Pressures applied (bar)	Permeability (cm/sec)	Av. flow (cc/min)	No. of tests
1	c.p.=1 bar ; b.p.=0 bar	1.76×10^{-6}	0.875	2
	c.p.=2 bar ; b.p.=0 bar	1.71×10^{-6}	1.705	2
	c.p.=3 bar ; b.p.=0 bar	1.70×10^{-6}	2.54	1
	c.p.=4 bar ; b.p.=0 bar	1.59×10^{-6}	3.17	1
	c.p.=5 bar ; b.p.=0 bar	1.48×10^{-6}	3.68	1
	c.p.=6 bar ; b.p.=0 bar	1.40×10^{-6}	4.18	1
	c.p.=7 bar ; b.p.=0 bar	1.32×10^{-6}	4.60	1
2	c.p.=2 bar ; b.p.= 1 bar	1.87×10^{-6}	0.93	1
3	c.p.=2 bar ; b.p.= 1 bar	1.63×10^{-6}	0.815	2
4	c.p.=2 bar ; b.p.= 1 bar	2.81×10^{-6}	0.14	2
5	c.p.=2 bar ; b.p.= 1 bar	2.00×10^{-6}	0.995	2
	c.p.=3 bar ; b.p.= 1 bar	1.92×10^{-6}	1.913	1
	c.p.=4 bar ; b.p.= 1 bar	1.97×10^{-6}	2.95	1
	c.p.=5 bar ; b.p.= 1 bar	1.96×10^{-6}	3.91	1

Disc No.	bubbling pressure (i.e. air entry value) (bar)
1	$\leqslant$ 2.95
2	$\leqslant$ 3.03
3	$\leqslant$ 3.10
4	$\leqslant$ 3.20
5	$\leqslant$ 3.10

A7.2 Types of porous ceramic used in this research

The high air entry discs 5 bar and 15 bar used in this thesis were manufactured by Soilmoisture Equipment Corporation, Santa Barbara, California*. The manufacturer's disc properties are given in Table A7.2.

Table A7.2

Soilmoisture's properties on high air entry disc

air entry value (bar)	porosity (%)	permeability (cm/sec)	Bubbling pressure(bar)
5	34	*1.21×10^{-7}	> 5.51
		**1.33×10^{-8}	
15	32	*2.59×10^{-9}	> 15.17
		**5.47×10^{-9}	

* given by manufacturer

** measured by the author

The weight and volumes of high air entry discs were measured. The results were summarized in Table A7.3.

(*Soilmoisture equipment Corporation, P.O. Box 30025, Santa Barbara, California 93105 or 801 SO. Kellogg Ave. Coleta, CA.93117)

Table A7.3

Weight-volume relationships of two ceramic discs

air entry value (bar)	diameter (cm)	thickness (cm)	density (air dried) (g/c.c.)	pore size (approx) (microns)
5	3.02	0.642	1.820	0.5
15	3.01	0.649	1.715	0.16

The density of the 5 bar disc was unexpectedly greater than that of the 15 bar disc. However, Soilmoisture Co. reported that 1 bar discs can be purchased that have a low flow rate and a porosity of 25 percent, or a high flow with a porosity of 42 percent. It appears that the sintering process is controlled to produce the desired air entry value rather than have the porosity controlling the air entry value.

The average coefficient of permeability of the 5 bar disc was 1.33×10^{-8} cm per second and 5.47×10^{-9} cm per second for the 15 bar disc. These values compare closely with the manufacturer's results.

APPENDIX 8

COMPUTATIONS,DATA REDUCTION AND RESULTS

Appendix 8 Computational Data Reduction and Results

A8.1 Data reduction

A8.1.1 General

A considerable amount of data is accummulated when testing unsaturated soils. This data is most efficiently analysed by using simple computer programs.

This section presents the computer programs written to analyse the data from the triaxial tests. A program was developed for each particular type of test and all the programs were written in commodore BASIC.

The tests were carried out on two triaxial setups which differed only in the type of volume change indicators used. Setup 1 used an automatic volume change logging system, whereas setup 2 used paraffin-water volume change indicators. This was taken into account in the programming.

A8.1.2 Commodore BASIC source statement listings

The following pages present the BASIC source statement listings for triaxial apparatus 1 and 2 respectively. Each program is self-explanatory with an appropriate heading and description of variable names.

DESATURATION AND CONSOLIDATION PROCESS

```
100 INPUT"OUTPUT DEVICE? 3 FOR SCREEN,4 FOR PRINTER";F
110 AC=0
120 DEF FNA(X)=SGN(X)*INT(ABS(X)*1E2+0.5)/1E2
130 INPUT"INITIAL LENGTH OF SAMPLE BEFORE CONSOLIDATION MM";L0
140 INPUT"INITIAL DIAMETER OF SAMPLE BEFORE CONSOLIDATION MM";D0
150 A0=π*D0*D0/4
160 V0=L0*A0*1E-3
170 OPENF,F
180 PRINT#F,"*****************************************************"
190 PRINT#F,"* THIS IS THE STAGE OF CONSOLIDATION & DESATURATION *"
200 PRINT#F,"*****************************************************"
210 PRINT#F," "
220 PRINT#F,"INITIAL LENGTH OF SAMPLE  BEFORE CONSOLIDATION IS";L0;"MM"
230 PRINT#F,"INITIAL DIAMETER OF SAMPLE BEFORE CONSOLIDATION IS";D0;"MM"
240 PRINT#F,"INITIAL AREA OF SAMPLE BEFORE CONSOLIDATION IS";FNA(A0);"MM↑2"
250 PRINT#F,"INITIAL VOLUME BEFORE CONSOLIDATION=";FNA(V0);"CC"
260 CLOSEF
270 INPUT"INITIAL WEIGHT OF SAMPLE(GRAMS)";W0
280 INPUT"INITIAL MOISTURE OF SAMPLE %";W
290 MS=W0/(1+0.01*W):VS=MS/2.75:WW=W0-MS
300 VV=V0-VS:E0=VV/VS*100
310 S0=W*2.75/E0*100
320 OPENF,F
330 PRINT#F,"WEIGHT OF SOLIDS=";FNA(MS);"GRAMS"
340 PRINT#F,"VOLUME OF SOLIDS=";FNA(VS);"CC"
350 PRINT#F,"INITIAL VOLUME OF VOIDS=";FNA(VV);"CC"
360 PRINT#F,"INITIAL VOLUME OF WATER IN SAMPLE";FNA(WW)
370 PRINT#F,"INITIAL MOISTURE CONTENT=";FNA(W);"%"
380 PRINT#F,"INITIAL VOID RATIO=";FNA(E0);"%"
390 PRINT#F,"INITIAL DEGREE OF SATURATION=";FNA(S0);"%"
400 PRINT#F," "
410 PRINT#F,"*************************************************************"
420 PRINT#F,"*** +VE VOLUME CHANGE VALUE MEANS SAMPLE VOLUME DECREASES ***"
430 PRINT#F,"*************************************************************"
440 PRINT#F," "
450 Z$="*****************************************************************"
460 A$="   E.T. SQR(E.T.)      VT      VW      VA      SR      E       W     D.A."
470 B$="(MIN.) SQR(MIN.)   (C.C.) (C.C.) (C.C.)  (%)     (%)     (%)  (C.C.)
480 PRINT#F,Z$
490 PRINT#F,A$
500 PRINT#F,B$
```

```
510 PRINT#F,Z$
520 CLOSEF
530 INPUT"CORRECTION FOR AIR TRAPPED % SAMPLE & MEMBRANE & CELL IN C.C.";T
540 INPUT"HOUR AT START IS";H1
550 INPUT"MIN. AT START IS";M1
560 REM DOUBLE-WALL CELL WITH GLASS-FIBRE WAS USED
570 INPUT"VOLUME CHANGE OF CELL DUE TO APPLIED PRESSURE C.C.";M
580 INPUT"TEMPERATURE AT START IS";T1
590 INPUT"AVCL-1 READING AT START IS";A1
600 INPUT"AVCL-2 READING AT START IS";A2
610 REM DAY STARTED=0  DAY ONE=1
620 REM DAY TWO=2  DAY THREE=3  ETC.
630 INPUT"DAY NOW";D2
640 INPUT"HOUR NOW";H2
650 INPUT"MIN. NOW";M2
660 ET=(24*60-(H1*60+M1))+((D2-1)*24*60)+(H2*60+M2)
670 IF D2=0 THEN ET=(H2*60+M2)-(H1*60+M1)
680 EQ=SQR(ET)
690 INPUT"TEMPERATURE NOW IS";T2
700 INPUT"AVCL-1 READING NOW";A3
710 INPUT"AVCL-2 READING NOW";A4
715 REM TAKING THE EFFECT OF TEMP. INTO ACCOUNT
720 A5=A3+1.01-2.43*(T2-T1)
725 IF T2=T1 THEN A5=A3
730 A6=A4+0.75-2.43*(T2-T1)
735 IF T2=T1 THEN A6=A4
740 INPUT"IS THERE ANY DIFFUSED AIR VOLUME CORRECTION 1=YES,0=NO";K
750 IF K=1 GOTO910
760 VT=(A6-A2)*0.0366-M-T
770 VW=(A5-A1)*0.0377-AC
780 VA=FNA(VT)-F' 'VW)
790 L1=L0*(1-VT/(3*V0))
800 AI=A0*(1-VT/V0)/(1-VT/(3*V0))
810 V1=AI*L1*1E-3
820 E9=(V1-VS)/VS*100:S9=(W0-MS-VW)/(V1-VS)*100
830 W9=E9*S9*0.01/2.75
840 OPENF,F,2
850 OPENF+1,F,1
860 C$="999999   999.99   S99.99 S99.99 S99.99 999.99 999.99 999.99  99.99
870 PRINT#F,C$
880 PRINT#F+1,ET,FNA(EQ),FNA(VT),FNA(VW),VA,FNA(S9),FNA(E9),FNA(W9),FNA(AC)
890 CLOSEF:CLOSEF+1
900 GOTO630
910 INPUT"INITIAL WATER LEVEL OF BURETTE IN DAVI CC";F1
920 INPUT"FINAL WATER LEVEL OF BURETTE IN DAVI CC";F2
930 INPUT"ATM. PRESSURE IS (BAR)";AM
940 INPUT"AIR BACKPRESSURE TO DAVI (BAR)";AB
950 INPUT"POREWATER PRESSURE READING";WR
960 WP=-0.0029+0.01*WR
970 IF WR=0 THEN WP=0
980 AT=(AB+AM)
990 EX=(17-(F1+F2)/2)*1.4
1000 AD=F1-F2
1010 AC=(AD*(EX*0.001+AT))/(WP/100+AM)+AC
1020 GOTO760
```

DRAINED TEST(TRIAXIAL CELL-1)

```
100 INPUT"OUTPUT DEVICE? 3 FOR SCREEN,4 FOR PRINTER";J
110 DEF FNA(X)=SGN(X)*INT(ABS(X)*1E2+0.5)/1E2
120 DEF FNB(Y)=SGN(Y)*INT(ABS(Y)*1E4+0.5)/1E4
130 INPUT"INITIAL LENGTH OF SAMPLE BEFORE CONSOLIDATION MM";L0
140 INPUT"INITIAL DIAMETER OF SAMPLE BEFORE CONSOLIDATION MM";D0
150 A0=π*D0*D0/4
160 V0=L0*A0*1E-3
170 OPENJ,J
180 PRINT#J,"*****************************"
190 PRINT#J,"*     TRIAXIAL CELL NO.1    *"
200 PRINT#J,"*****************************"
210 PRINT#J," "
220 PRINT#J,"INITIAL AREA BEFORE CONSOLIDATION=";FNA(A0);"MM12"
230 PRINT#J,"INITIAL VOLUME BEFORE CONSOLIDATION=";FNA(V0);"CC"
240 PRINT#J," ":CLOSEJ
250 INPUT"INITIAL WEIGHT OF SAMPLE(GRAMS)";W0
260 INPUT"INITIAL MOISTURE CONTENT %";W
270 MS=W0/(1+0.01*W):VS=MS/2.75
280 VV=V0-VS:E0=VV/VS*100
290 S0=W*2.75/E0*100
300 OPENJ,J
310 PRINT#J,"*************************************"
320 PRINT#J,"WEIGHT OF SOLIDS=";FNA(MS);"GRAMS"
330 PRINT#J,"VOLUME OF SOLIDS=";F   VS);"CC"
340 PRINT#J,"VOLUME OF VOIDS=";FNA(VV);"CC"
350 PRINT#J,"INITIAL MOISTURE CONTENT":FNA(W);"%"
360 PRINT#J,"INITIAL VOID RATIO=";FNA(E0);"%"
370 PRINT#J,"INITIAL DEGREE OF SATURATION=";FNA(S0);"%"
380 PRINT#J," ":CLOSEJ
390 INPUT"CHANGE IN TOTAL VOLUME CC IN CONSOLIDATION STAGE";M
400 INPUT"CHANGE IN WATER VOLUME CC IN CONSOLIDATION STAGE";F
410 L1=L0*(1-M/(3*V0))
420 A1=A0*(1-M/V0)/(1-M/(3*V0))
430 V1=A1*L1*1E-3
440 E9=(V1-VS)/VS*100:S9=(W0-MS-F)/(V1-VS)*100
450 W9=E9*S9*0.01/2.75
460 OPENJ,J
470 PRINT#J,"*****************************************"
480 PRINT#J,"LENGTH OF SAMPLE AFTER CONSOLIDATION=";FNA(L1);"MM"
490 PRINT#J,"AREA OF SAMPLE AFTER CONSOLIDATION=";FNA(A1);"MM12"
500 PRINT#J,"VOLUME OF SAMPLE AFTER CONSOLIDATION";FNA(V1);"CC"
510 PRINT#J,"MOISTURE CONTENT AFTER CONSOLIDATION";FNA(W9);"%"
520 PRINT#J,"VOID RATIO AFTER CONSOLIDATION";FNA(E9);"%"
530 PRINT#J,"DEGREE OF SATURATION AFTER CONSOLIDATION";FNA(S9);"%"
540 PRINT#J,"*****************************************"
550 PRINT#J," ":CLOSEJ
```

```
560 AC=0
570 REM ENTER DAY AS FOLLOWS:
580 REM DAY STARTED=0  DAY ONE=1
590 REM DAY TWO=2  ETC.
600 INPUT"HOUR AT START IS";H1
610 INPUT"MIN. AT START IS";M1
620 INPUT"STRAIN CORRECT ZERO";Z0
630 INPUT"INITIAL TEMPERATURE";T7
640 INPUT"INITIAL AVCL-1 READING";R1
650 INPUT"INITIAL AVCL-2 READING";R2
660 OPENJ,J
670 PRINT#J,"CORRECTION FOR STRENGTH OF  1:R.MEMBRANE,2:DRAINS,3:HG LAYER"
680 PRINT#J,"X=19 KN/MT2  FOR 1,2 & 3"
690 PRINT#J,"X=14 KN/MT2 FOR 1 & 2"
700 CLOSEJ
710 INPUT"STRENGTH CORRECTION VALUE X";X
720 REM DRAW THE TABLE
730 OPENJ,J
740 PRINT#J," "
750 PRINT#J,"**************************************************************"
760 PRINT#J," +VE VOLUME CHANGE VALUE MEANS A DECREASE IN SAMPLE VOLUME "
770 PRINT#J,"**************************************************************"
780 PRINT#J," "
790 Z$="**************************************************************
*"
800 A$="  E.T.    STR.     VT      VW      VA      SR      E      W      D.S.    M.S.
810 B$="(MINS.)  (%)     (%)     (%)     (%)     (%)     (%)    (%)  KN/MT2 KN/MT2
820 PRINT#J,Z$
830 PRINT#J,A$
840 PRINT#J,B$
850 PRINT#J,Z$
860 CLOSEJ
870 INPUT"DAY NOW";D2
880 INPUT"HOUR NOW";H2
890 INPUT"MIN. NOW";M2
900 REM CALCULATE THE ELAPSED TIME
910 ET=(24*60-(H1*60+M1))+((D2-1)*24*60)+(H2*60+M2)
920 IF D2=0 THEN ET=(H2*60+M2)-(H1*60+M1)
930 INPUT"TEMPERATURE NOW";T8
940 INPUT"STRAIN LVDT READING";S1
950 INPUT"LOAD CELL READING";S2
960 INPUT"CELL PRESSURE READING";CR
970 INPUT"POREAIR PRESSURE READING";AR
980 INPUT"POREWATER PRESSURE READING";WR
990 INPUT"AVCL-1 READING";R3
1000 INPUT"AVCL-2 READING";R4
1010 REM TAKING THE EFFECT OF TEMP. INTO ACCOUNT
1020 R5=R3-(1.01-2.43*(T8-T7))
1030 IF (T8-T7)=0 THEN R5=R3
1040 R6=R4-(0.75-2.43*(T8-T7))
1050 IF (T8-T7)=0 THEN R6=R4
1060 CL=ABS(S1-Z0)*0.02
1070 U=CL/L1:UU=100*U
1080 CP=(0.0278+0.0100*CR)*100
1090 IFCR=0 THEN CP=0
1100 AP=(-0.0033+0.0050*AR)*100
```

```
1110 IFAR=0 THEN AP=0
1120 WP=(-0.0029+0.0100*WR)*100
1130 IFWR=0 THEN WP=0
1140 INPUT"IS THERE ANY DIFFUSED AIR VOLUME CORRECTION 1=YES,0=NO";K
1150 IFK=1 GOTO1380
1160 REM SUBTRACT DIFFUSED AIR VOLUME FROM WATER VOLUME CHANGE
1170 VW=(R5-R1)*0.0377-AC
1180 VT=(R6-R2)*0.0366+((1.5912)*3.1416/4)*(CL/10)
1190 REM VT HAS INCLUDED THE VOLUME CHANGE DUE TO LOADING RAM PENETRATION
1200 SV=(MS*WS/100-VW)/(V1-VT-VS)*100
1210 EV=(V1-VT-VS)/VS*100
1220 WV=SV*EV*0.01/2.75
1230 VA=FNA(VT)-FNA(VW)
1240 Z1=(1-VT/V1)/(1-U)
1250 A2=Z1*A1
1260 DZ=(0.0136+0.001*S2)/(A2*1E-6)-X
1270 IF DZ<0 OR CL=0 THEN DZ=0
1280 VP=VT/V1*100
1290 V5=VW/V1*100
1300 V6=FNA(VP)-FNA(V5)
1310 OPENJ,J,2
1320 OPENJ+1,J,1
1330 C$="999999  99.99 S99.99 S99.99 S99.99 999.99 999.99 99.99 9999.99 999.99
1340 PRINT#J,C$
1350 PRINT#J+1,ET,UU,FNA(VP),FNA(V5),V6,SV,EV,WV,DZ,(AP-WP)
1360 CLOSEJ:CLOSEJ+1
1370 GOTO870
1380 INPUT"INITIAL WATER LEVEL OF BURETTE IN D   CC";F1
1390 INPUT"FINAL WATER LEVEL OF BURETTE IN DAVI  CC";F2
1400 INPUT"ATM. PRESSURE IS BAR";AM
1410 INPUT"AIR BACKPRESSURE TO DAVI  BAR";AB
1420 AT=(AB+AM)
1430 EX=(17-(F1+F2)/2)*1.4
1440 AD=F1-F2
1450 AC=(AD*(EX*0.001+AT))/(WP/100+AM)+AC
1460 OPENJ,J
1470 PRINT#J,"**********************************"
1480 PRINT#J,"DIFFUSED AIR VOLUME CORRECTION IS";FNA(AC);"CC"
1490 PRINT#J,"**********************************"
1500 CLOSEJ
1510 GOTO1170
```

CONSTANT WATER-CONTENT TEST(TRIAXIAL CELL-1)

```
100 INPUT"OUTPUT DEVICE? 3 FOR SCREEN,4 FOR PRINTER";F
110 DEF FNA(X)=SGN(X)*INT(ABS(X)*1E2+0.5)/1E2
120 INPUT"INITIAL LENGTH OF SAMPLE BEFORE CONSOLIDATION MM";L0
130 INPUT"INITIAL DIAMETER OF SAMPLE BEFORE CONSOLIDATION MM";D0
140 A0=π*D0*D0/4
150 V0=L0*A0*1E-3
160 OPENF,F
170 PRINT#F,"**********************************"
180 PRINT#F,"***  C-CW TEST(TRIAXIAL CELL-1) ***
190 PRINT#F,"**********************************"
200 PRINT#F," "
210 PRINT#F,"INITIAL AREA BEFORE CONSOLIDATION=";FNA(A0);"MM↑2"
220 PRINT#F,"INITIAL VOLUME BEFORE CONSOLIDATION=";FNA(V0);"CC"
230 CLOSEF
240 INPUT"INITIAL WEIGHT OF SAMPLE(GRAMS)";W0
250 INPUT"INITIAL MOISTURE CONTENT %";W
260 MS=W0/(1+0.01*W):VS=MS/2.75
270 VV=V0-VS:E0=VV/VS*100
280 S0=W*2.75/E0*100
290 OPENF,F
300 PRINT#F,"**********************************"
310 PRINT#F,"WEIGHT OF SOLIDS=";FNA(MS);"GRAMS"
320 PRINT#F,"VOLUME OF SOLIDS=";FNA(VS);"CC"
330 PRI   ,"VOLUME OF VOIDS=";FNA(VV);"CC"
340 PRINT#F,"INITIAL MOISTURE CONTENT";FNA(W);"%"
350 PRINT#F,"INITIAL VOID RATIO=";FNA(E0);"%"
360 PRINT#F,"INITIAL DEGREE OF SATURATION=";FNA(S0);"%"
370 CLOSEF
380 INPUT"CHANGE IN TOTAL VOLUME CC IN CONSOLIDATION STAGE";M
390 INPUT"CHANGE IN WATER VOLUME CC IN CONSOLIDATION STAGE";G
400 L1=L0*(1-M/(3*V0))
410 A1=A0*(1-M/V0)/(1-M/(3*V0))
420 V1=A1*L1*1E-3
430 E9=(V1-VS)/VS*100:S9=(W0-MS-G)/(V1-VS)*100
440 W9=E9*S9*0.01/2.75
450 OPENF,F
460 PRINT#F,"**********************************"
470 PRINT#F,"LENGTH OF SAMPLE AFTER CONSOLIDATION=";FNA(L1);"MM"
480 PRINT#F,"AREA OF SAMPLE AFTER CONSOLIDATION=";FNA(A1);"MM↑2"
490 PRINT#F,"VOLUME OF SAMPLE AFTER CONSOLIDATION";FNA(V1);"CC"
500 PRINT#F,"MOISTURE CONTENT AFTER CONSOLIDATION";FNA(W9);"%"
510 PRINT#F,"VOID RATIO AFTER CONSOLIDATION";FNA(E9);"%"
520 PRINT#F,"DEGREE OF SATURATION AFTER CONSOLIDATION";FNA(S9);"%"
530 PRINT#F,"**********************************"
540 PRINT#F," "
550 PRINT#F,"**********************************"
```

```
560 PRINT#F,"*** +VE VOLUME CHANGE VALUE MEANS SAMPLE VOLUME DECREASES ***"
570 PRINT#F,"*****************************************************************"
580 PRINT#F," "
590 CLOSEF
600 REM ENTER DAY AS FOLLOWS:
610 REM DAY STARTED=0  DAY ONE=1
620 REM DAY TWO=2  ETC.
630 INPUT"HOUR AT START IS";H1
640 INPUT"MIN. AT START IS";M1
645 INPUT"INITIAL TEMPERATURE";T7
650 INPUT"STRAIN CORRECT ZERO";Z0
660 INPUT"INITIAL AVCL-2 READING";R2
670 INPUT"INITIAL POREWATER PRESSURE READING";O1
680 OPENF,F,
690 PRINT#F,"CORRECTION FOR STRENGTH OF 1:R.MEMBRANE,2:DRAINS,3:HG LAYER"
700 PRINT#F,"X=19 KN/M12 FOR 1,2 & 3"
710 PRINT#F,"X=14 KN/M12 FOR 1 & 2"
720 CLOSEF
730 INPUT"STRENGTH CORRECTION VALUE X";X
740 O2=(-0.0029+0.01*O1)*100
750 IFO1=0 THEN O2=0
760 REM DRAW THE TABLE
770 OPENF,F
780 Z$="*****************************************************************"
790 A$="  E.T.    STR.     VT       SR       E        DU       PW       BA     D.S.    M.S.
800 B$="(MINS.)  (%)      (%)      (%)      (%)    KN/M12     (W)      (W)  KN/M^2 KN/M^2
810 PRINT#F,Z$
820 PRINT#F,A$
830 PRINT#F,B$
840 PRINT#F,Z$
850 CLOSEF
860 INPUT"DAY NOW";D2
870 INPUT"HOUR NOW";H2
880 INPUT"MIN. NOW";M2
890 REM CALCULATE THE ELAPSED TIME
900 ET=(24*60-(H1*60+M1))+((D2-1)*24*60)+(H2*60+M2)
910 IF D2=0 THEN ET=(H2*60+M2)-(H1*60+M1)
915 INPUT"TEMPERATURE NOW";T8
920 INPUT"STRAIN LVDT READING";S1
930 INPUT"LOAD CELL READING";S2
940 INPUT"CELL PRESSURE READING";CR
950 INPUT"POREAIR PRESSURE READING";AR
960 INPUT"POREWATER PRESSURE READING";WR
970 INPUT"AVCL-2 READING";R4
972 REM TAKING ACCOUNT TEMP. EFFECT ON AVCL READINGS
974 R6=R4-(0.75-2.43*(T8-T7))
976 IF (T8-T7)=0 THEN R6=R4
980 CL=ABS(S1-Z0)*0.02
990 U=CL/L1:UU=100*U
1000 CP=(0.0278+0.0100*CR)*100
```

```
1010 IFCR=0 THEN CP=0
1020 AP=(-0.0033+0.0050*AR)*100
1030 IFAR=0 THEN AP=0
1040 WP=(-0.0029+0.0100*WR)*100
1050 IFWR=0 THEN WP=0
1060 T1=(R6-R2)*0.0366
1070 REM VT HAS INCLUDED THE VOLUME CHANGE DUE TO LOADING RAM PENETRATION
1080 VT=((1.5912)*π/4)*(CL/10)+T1
1090 DU=WP-02
1100 SV=(MS*W9/100)/(V1-VT-VS)*100
1110 EV=(V1-VT-VS)/VS*100
1120 Z1=(1-VT/V1)/(1-U)
1130 A2=Z1*A1
1140 DZ=(0.0136+0.001*S2)/(A2*1E-6)-X
1150 IF DZ<0 OR CL=0 THEN DZ=0
1160 VP=VT/V1*100
1170 IF DZ<=0 THEN BA=0:GOTO1190
1180 BA=DU/DZ
1190 RW=DZ/(CP-WP)
1200 OPENF,F,2
1210 OPENF+1,F,1
1220 C$="999999  99.99 999.99 999.99 999.99 999.99 999.99 999.99 999.999999.99
1230 PRINT#F,C$
1240 PRINT#F+1,ET,UU,FNA(VP),FNA(SV),FNA(EV),FNA(DU),RW,BA,DZ,(AP-WP)
1250 CLOSEF:CLOSEF+1
1260 GOTO860
```

TRULY UNDRAINED TEST(TRIAXIAL CELL-1)

```
100 Q=1
110 INPUT"OUTPUT DEVICE? 3 FOR SCREEN,4 FOR PRINTER";F
120 DEF FNA(X)=SGN(X)*INT(ABS(X)*1E2+0.5)/1E2
130 INPUT"INITIAL LENGTH OF SAMPLE BEFORE CONSOLIDATION MM";L0
140 INPUT"INITIAL DIAMETER OF SAMPLE BEFORE CONSOLIDATION MM";D0
150 A0=π*D0*D0/4
160 V0=L0*A0*1E-3
170 OPENF,F
180 PRINT#F,"*********************************"
190 PRINT#F,"***  TU   TEST(TRIAXIAL CELL-1) ***
200 PRINT#F,"*********************************
210 PRINT#F," "
220 PRINT#F,"INITIAL AREA BEFORE CONSOLIDATION=";FNA(A0);"MM↑2"
230 PRINT#F,"INITIAL VOLUME BEFORE CONSOLIDATION=";FNA(V0);"CC"
240 CLOSEF
250 INPUT"INITIAL WEIGHT OF SAMPLE(GRAMS)";W0
260 INPUT"INITIAL MOISTURE CONTENT %";W
270 MS=W0/(1+0.01*W):VS=MS/2.75
280 VV=V0-VS:E0=VV/VS*100
290 S0=W*2.75/E0*100
300 J0 = MS/V0*1000
310 OPENF,F
320 PRINT#F,"*********************  **********************"
330 PRINT#F,"WEIGHT OF SOLIDS=";FNA(MS);"GRAMS"
340 PRINT#F,"VOLUME OF SOLIDS=";FNA(VS);"CC"
350 PRINT#F,"VOLUME OF VOIDS=";FNA(VV);"CC"
360 PRINT#F,"INITIAL MOISTURE CONTENT";FNA(W);"%"
370 PRINT#F,"INITIAL VOID RATIO=";FNA(E0);"%"
380 PRINT#F,"INITIAL DEGREE OF SATURATION=";FNA(S0);"%"
390 PRINT#F,"INITIAL DRY DENSITY = ";FNA(J0);"KG/CU.M"
400 CLOSEF
410 INPUT"CHANGE IN TOTAL VOLUME CC IN CONSOLIDATION STAGE";M
420 INPUT"CHANGE IN WATER VOLUME CC IN CONSOLIDATION STAGE";G
430 L1=L0*(1-M/(3*V0))
440 A1=A0*(1-M/V0)/(1-M/(3*V0))
450 V1=A1*L1*1E-3
460 E9=(V1-VS)/VS*100:S9=(W0-MS-G)/(V1-VS)*100
470 W9=E9*S9*0.01/2.75
480 J1 = MS/V1*1000
490 OPENF,F
500 PRINT#F,"*************************************************"
510 PRINT#F,"LENGTH OF SAMPLE AFTER CONSOLIDATION=";FNA(L1);"MM"
520 PRINT#F,"AREA OF SAMPLE AFTER CONSOLIDATION=";FNA(A1);"MM↑2"
530 PRINT#F,"VOLUME OF SAMPLE AFTER CONSOLIDATION";FNA(V1);"CC"
540 PRINT#F,"MOISTURE CONTENT AFTER CONSOLIDATION";FNA(W9);"%"
550 PRINT#F,"VOID RATIO AFTER CONSOLIDATION";FNA(E9);"%"
560 PRINT#F,"DEGREE OF SATURATION AFTER CONSOLIDATION";FNA(S9);"%"
570 PRINT#F,"DRY DENSITY AFTER CONSOLIDATION =";FNA(J1);"KG/CU.M"
580 PRINT#F,"*************************************************"
590 PRINT#F," "
600 PRINT#F,"*****************************************************************"
```

```
610 PRINT#F,"*** +VE VOLUME CHANGE VALUE MEANS SAMPLE VOLUME DECREASES ***"
620 PRINT#F,"*****************************************************"
630 PRINT#F," "
640 CLOSEF
650 REM DRAW THE TABLE
660 OPENF,F
670 Z$="**********************************************************************
680 A$="  E.T.     UAC      UA       SR       E       C.P.     BA       BW     M.S.
690 B$="(MINS.) KN/M12  KN/M12    (%)      (%)    KN/M12                      KN/M12
700 PRINT#F,Z$
710 PRINT#F,A$
720 PRINT#F,B$
730 PRINT#F,Z$
740 CLOSEF
750 REM ENTER DAY AS FOLLOWS:
760 REM DAY STARTED=0  DAY ONE=1
770 REM DAY TWO=2  ETC.
780 INPUT"HOUR AT START IS";H1
790 INPUT"MIN. AT START IS";M1
800 INPUT"INITIAL TEMPERATURE";T7
810 INPUT"INITIAL AVCL-2 READING";R2
820 INPUT"INITIAL POREWATER PRESSURE READING";01
830 INPUT"INITIAL PORE-AIR PRESSURE READING";I0
840 INPUT"INITIAL CELL PRESSURE READING";C1
850 C9=(0.0278+0.01*C1)*100
860 IF C1=0 THEN C9=0
870 INPUT"DAY NOW";D2
880 INPUT"HOUR NOW";H2
890 INPUT"MIN. NOW";M2
900 REM CALCULATE THE ELAPSED TIME
910 ET=(24*60-(H1*60+M1))+((D2-1)*24*60)+(H2*60+M2)
920 IF D2=0 THEN ET=(H2*60+M2)-(H1*60+M1)
930 INPUT"TEMPERATURE NOW";T8
940 INPUT"POREWATER PRESSURE READING";WR
950 INPUT"POREAIR PRESSURE READING";AR
960 INPUT"CELL PRESSURE READING";CR
970 INPUT"AVCL-2 READING";R4
980 REM TAKING ACCOUNT TEMP. EFFECT ON AVCL READINGS
990 R6=R4-(0.75-2.43*(T8-T7))
1000 IF (T8-T7)=0 THEN R6=R4
```

```
1010 PA = (-0.0033+0.005*AR)*100
1020 PW = (-0.0029+0.01*WR)*100
1030 CS=(0.0278+0.01*CR)*100
1040 IF CR=0 THEN CS=0
1050 CP=CS-C9
1060 IF 0=0 GOTO 1110
1070 OPENF,F:PRINT#F," "
1080 PRINT#F,"INITIAL CELL PRESSURE";FNA(C9);"KN/MT2"
1090 PRINT#F,"INCREASE IN CELL PRESSURE";FNA(CP);"KN/MT2"
1100 PRINT#F," ":CLOSEF
1110 AP=(-0.0033+0.0050*(AR-I0))*100
1120 WP=(-0.0029+0.0100*(WR-01))*100
1130 VT=(R6-R2)*0.0366
1140 SV=(MS*W9/100)/(V1-VT-VS)*100
1150 EV=(V1-VT-VS)/VS*100
1160 VP=VT/V1
1170 REM (PA+101) IN ABSOLUTE PRESSURE UNIT
1180 P1 = ((-0.0033+0.005*I0)*100+101)*VP
1190 REM P2 = VOLUME OF WATER
1200 P2 = S9*E9*VS/V1/10000
1210 P3 = 1-VS/V1-P2+0.02*P2-VP
1220 P4 = P1/P3+(-0.0033+0.005*I0)*100
1230 BA = AP/CP
1240 BW = WP/CP
1250 RW = PA-PW
1260 OPENF,F,2
1270 OPENF+1,F,1
1280 C$="999999 9999.99 9999.99 999.99 999.99 999.99 S99.99 S99.99 S999.99"
1290 PRINT#F,C$
1300 PRINT#F+1,ET,FNA(P4),FNA(PA),FNA(SV),FNA(EV),FNA(CS),FNA(BA),FNA(BW),RW
1310 CLOSEF:CLOSEF+1
1320 INPUT"IS CELL PRESSURE INCREASED,1 FOR YES,0 FOR NO";Q
1330 IF Q = 1 THEN V1 = V1 - VT: GOTO 780
1340 GOTO870
```

UNCONFINED TEST(TRIAXIAL CELL-2)

```
100 REM TRIAXIAL CELL-2
110 REM TEST:DESATURATED WITH ELEVATED AIR PRESSURE,THEN SHEAR UNDER CW
120 INPUT"OUTPUT DEVICE? 3 FOR SCREEN,4 FOR PRINTER";F
130 DEF FNA(X)=SGN(X)*INT(ABS(X)*1E2+0.5)/1E2
140 INPUT"INITIAL LENGTH OF SAMPLE BEFORE CONSOLIDATION MM";L0
150 INPUT"INITIAL DIAMETER OF SAMPLE BEFORE CONSOLIDATION MM";D0
160 A0=π*D0*D0/4
170 V0=L0*A0*1E-3
180 OPENF,F
190 PRINT#F,"*****************************"
200 PRINT#F,"*** CU-CW TEST(TRIAXIAL CELL-2) ***"
210 PRINT#F,"*****************************":PRINT#F," "
220 PRINT#F,"INITIAL AREA BEFORE CONSOLIDATION=";FNA(A0);"MM†2"
230 PRINT#F,"INITIAL VOLUME BEFORE CONSOLIDATION=";FNA(V0);"CC"
240 CLOSEF
250 INPUT"INITIAL WEIGHT OF SAMPLE(GRAMS)";W0
260 INPUT"INITIAL MOISTURE CONTENT %";W
270 MS=W0/(1+0.01*W):VS=MS/2.75
280 VV=V0-VS:E0=VV/VS*100
290 S0=W*2.75/E0*100
300 OPENF,F
310 PRINT#F,"***********************************"
320 PRINT#F,"WEIGHT OF SOLIDS=";FNA(MS);"GRAMS"
330 PRINT#F,"VOLUME OF SOLIDS=";FNA(VS);"CC"
340 PRINT#F,"VOLUME OF VOIDS=";FNA(VV);"CC"
350 PRINT#F,"INITIAL MOISTURE CONTENT";FNA(W);"%"
360 PRINT#F,"INITIAL VOID RATIO=";FNA(E0);"%"
370 PRINT#F,"INITIAL DEGREE OF SATURATION=";FNA(S0);"%"
380 CLOSEF
390 REM ASSUME NO CHANGE IN TOTAL VOLUME DURING DRAINAGE UNDER CONT.SUCTION
400 INPUT"CHANGE IN WATER VOLUME CC IN CONSOLIDATION STAGE";H
410 S9=(W0-MS-H)/(V0-VS)*100
420 W9=E0*S9*0.01/2.75
430 OPENF,F
440 PRINT#F,"***********************************************"
450 PRINT#F,"MOISTURE CONTENT AFTER CONSOLIDATION";FNA(W9);"%"
460 PRINT#F,"DEGREE OF SATURATION AFTER CONSOLIDATION";FNA(S9);"%"
470 PRINT#F,"***********************************************"
480 CLOSEF
490 REM ENTER DAY AS FOLLOWS:
500 REM DAY STARTED=0  DAY ONE=1
```

```
510 REM DAY TWO=2  ETC.
520 INPUT"HOUR AT START IS";H1
530 INPUT"MIN. AT START IS";M1
540 INPUT"STRAIN CORRECT ZERO";Z0
550 INPUT"INITIAL POREWATER PRESSURE READING";O1
560 O2=-0.0354+1.0041*O1
570 IF O1=0 THEN O2=0
580 REM DRAW THE TABLE
590 OPENF,F
600 Z$="**********************************************************************
*"
610 A$="  E.T.    STR.     CL      Z1     AP       WP       RW     DU      D.S.    M.S.
620 B$="(MINS.)  (%)      MM           KN/MT2 KN/MT2     (W) KN/MT2  KN/MT2 KN/MT2
630 PRINT#F,Z$
640 PRINT#F,A$
650 PRINT#F,B$
660 PRINT#F,Z$
670 CLOSEF
680 INPUT"DAY NOW";D2
690 INPUT"HOUR NOW";H2
700 INPUT"MIN. NOW";M2
710 REM CALCULATE THE ELAPSED TIME
720 ET=(24*60-(H1*60+M1))+((D2-1)*24*60)+(H2*60+M2)
730 IF D2=0 THEN ET=(H2*60+M2)-(H1*60+M1)
740 INPUT"STRAIN LVDT READING";S1
750 INPUT"LOAD CELL READING";S2
760 INPUT"CELL-AIR PRESSURE READING";AP
770 INPUT"POREWATER PRESSURE READING";WR
780 CL=ABS(S1-Z0)*0.02
800 U=CL/L0:UU=100*U
810 AP=-0.377+0.9998*AR
820 IFAR=0 THEN AP=0
830 WP=-0.0354+1.0041*WR
840 IFWR=0 THEN WP=0
850 Z1=1/(1-U)
860 A2=Z1*A0
870 DU=WP-O2
880 DZ=(0.0503+0.001*S2)/(A2*1E-6)
890 IF S2=0 THEN DZ=0
900 RW=DZ/(AP-WP)
910 OPENF,F,2
920 OPENF+1,F,1
930 C$="999999  99.99 999.99 999.99 999.99 999.99 999.99 9999.99 999.999999.99
940 PRINT#F,C$
950 PRINT#F+1,ET,UU,CL,Z1,FNA(AP),FNA(WP),FNA(RW),FNA(DU),FNA(DZ),FNA(AP-WP)
960 CLOSEF:CLOSEF+1
970 GOTO630
```

CONSTANT WATER-CONTENT TEST(TRIAXIAL CELL-2)

```
100 INPUT"OUTPUT DEVICE? 3 FOR SCREEN,4 FOR PRINTER";F
110 DEF FNA(X)=SGN(X)*INT(ABS(X)*1E2+0.5)/1E2
120 INPUT"INITIAL LENGTH OF SAMPLE BEFORE CONSOLIDATION MM";L0
130 INPUT"INITIAL DIAMETER OF SAMPLE BEFORE CONSOLIDATION MM";D0
140 A0=π*D0*D0/4
150 V0=L0*A0*1E-3
160 OPENF,F
170 PRINT#F,"*********************************"
180 PRINT#F,"***  C-CW TEST(TRIAXIAL CELL-2) ***
190 PRINT#F,"*********************************
200 PRINT#F," "
210 PRINT#F,"INITIAL AREA BEFORE CONSOLIDATION=";FNA(A0);"MM↑2"
220 PRINT#F,"INITIAL VOLUME BEFORE CONSOLIDATION=";FNA(V0);"CC"
230 CLOSEF
240 INPUT"INITIAL WEIGHT OF SAMPLE(GRAMS)";W0
250 INPUT"INITIAL MOISTURE CONTENT %";W
260 MS=W0/(1+0.01*W):VS=MS/2.75
270 VV=V0-VS:E0=VV/VS*100
280 S0=W*2.75/E0*100
290 OPENF,F
300 PRINT#F,"*************************************"
310 PRINT#F,"WEIGHT OF SOLIDS=";FNA(MS);"GRAMS"
320 PRINT#F,"VOLUME OF SOLIDS=";FNA(VS);"CC"
330 PRINT#F,"VOLUME OF VOIDS=";FNA(VV);"CC"
340 PRINT#F,"INITIAL MOISTURE CONTENT";FNA(W);"%"
350 PRINT#F,"INITIAL VOID RATIO=";FNA(E0);"%"
360 PRINT#F,"INITIAL DEGREE OF SATURATION=";FNA(S0);"%"
370 CLOSEF
380 INPUT"CHANGE IN TOTAL VOLUME CC IN CONSOLIDATION STAGE";M
390 INPUT"CHANGE IN WATER VOLUME CC IN CONSOLIDATION STAGE";G
400 L1=L0*(1-M/(3*V0))
410 A1=A0*(1-M/V0)/(1-M/(3*V0))
420 V1=A1*L1*1E-3
430 E9=(V1-VS)/VS*100:S9=(W0-MS-G)/(V1-VS)*100
440 W9=E9*S9*0.01/2.75
450 OPENF,F
460 PRINT#F,"*************************************"
470 PRINT#F,"LENGTH OF SAMPLE AFTER CONSOLIDATION=";FNA(L1);"MM"
480 PRINT#F,"AREA OF SAMPLE AFTER CONSOLIDATION=";FNA(A1);"MM↑2"
490 PRINT#F,"VOLUME OF SAMPLE AFTER CONSOLIDATION";FNA(V1);"CC"
500 PRINT#F,"MOISTURE CONTENT AFTER CONSOLIDATION";FNA(W9);"%"
```

```
510 PRINT#F,"VOID RATIO AFTER CONSOLIDATION";FNA(ES);"%"
520 PRINT#F,"DEGREE OF SATURATION AFTER CONSOLIDATION";FNA(SS);"%"
530 PRINT#F,"**************************************************"
540 PRINT#F," "
550 PRINT#F,"**************************************************"
560 PRINT#F,"*** +VE VOLUME CHANGE VALUE MEANS SAMPLE VOLUME DECREASES ***"
570 PRINT#F,"**************************************************"
580 PRINT#F," "
590 CLOSEF
600 REM ENTER DAY AS FOLLOWS:
610 REM DAY STARTED=0  DAY ONE=1
620 REM DAY TWO=2  ETC.
630 INPUT"HOUR AT START IS";H1
640 INPUT"MIN. AT START IS";M1
650 INPUT"STRAIN CORRECT ZERO";Z0
660 INPUT"INITIAL VCI-2 READING";R2
670 INPUT"INITIAL POREWATER PRESSURE READING";O1
680 OPENF,F
690 PRINT#F,"CORRECTION FOR STRENGTH OF 1:P.MEMBRANE,2:DRAINS,3:HG LAYER"
700 PRINT#F,"X=19 KN/M12 FOR 1,2 & 3"
710 PRINT#F,"X=14 KN/M12 FOR 1 & 2"
720 CLOSEF
730 INPUT"STRENGTH CORRECTION VALUE X";X
740 O2=-0.0354+1.0041*O1
750 IFO1=0 THEN O2=0
760 REM DRAW THE TABLE
770 OPENF,F
780 Z$="**********************************************************************"
790 A$="  E.T.    STR.     VT       SR       E        DU       RW       BA     D.S.    M.S."
800 B$="(MINS.)  (%)      (%)      (%)      (%)    KN/M12    (W)      (W)  KN/M12 KN/M12
810 PRINT#F,Z$
820 PRINT#F,A$
830 PRINT#F,B$
840 PRINT#F,Z$
850 CLOSEF
860 INPUT"DAY NOW";D2
870 INPUT"HOUR NOW";H2
880 INPUT"MIN. NOW";M2
890 REM CALCULATE THE ELAPSED TIME
900 ET=(24*60-(H1*60+M1))+((D2-1)*24*60)+(H2*60+M2)
910 IF D2=0 THEN ET=(H2*60+M2)-(H1*60+M1)
920 INPUT"STRAIN LVDT READING";S1
930 INPUT"LOAD CELL READING";S2
940 INPUT"CELL PRESSURE READING";CR
950 INPUT"POREAIR PRESSURE READING";AR
960 INPUT"POREWATER PRESSURE READING";WR
970 INPUT"VCI-2 READING";R4
980 CL=ABS(S1-Z0)*0.02
990 U=CL/L1:UU=100*U
1000 CP=-1.1964+1.0017*CR
```

```
1010 IFCR=0 THEN CP=0
1020 AP=-0.3770+0.9998*AR
1030 IFAR=0 THEN AP=0
1040 WP=-0.0354+1.0041*WP
1050 IFWR=0 THEN WP=0
1060 T1=R4-R2
1070 REM VT HAS INCLUDED THE VOLUME CHANGE DUE TO LOADING RAM PENETRATION
1080 VT=((1.5912)*π/4)*(CL/10)+T1
1090 DU=WP-OZ
1100 SV=(MS*W9/100)/(V1-VT-VS)*100
1110 EV=(V1-VT-VS)/VS*100
1120 Z1=(1-VT/V1)/(1-U)
1130 A2=Z1*A1
1140 DZ=(0.0503+0.001*S2)/(A2*1E-6)-%
1150 IF DZ<0 THEN DZ=0
1160 VP=VT/V1*100
1170 IF DZ=0 THEN BA=0:GOTO1190
1180 BA=DU/DZ
1190 RW=DZ/(CP-WP)
1200 OPENF,F,2
1210 OPENF+1,F,1
1220 C$="999999  99.99 999.99 999.99 999.99 999.99 999.99 999.99 999.99999.99
1230 PRINT#F,C$
1240 PRINT#F+1,ET,UU,FNA(VP),FNA(SV),FNA(EV),FNA(DU),RW,BA,DZ,(AP-WP)
1250 CLOSEF:CLOSEF+1
1260 GOTO860
```

DRAINED TEST(TRIAXIAL TEST)

```
100 INPUT"OUTPUT DEVICE ? 3 FOR SCREEN,4 FOR PRINTER";J
110 DEF FNA(X)=SGN(X)*INT(ABS(X)*1E2+0.5)/1E2
120 DEF FNB(Y)=SGN(Y)*INT(ABS(Y)*1E4+0.5)/1E4
130 INPUT"INITIAL LENGTH OF SAMPLE BEFORE CONSOLIDATION MM";L0
140 INPUT"INITIAL DIAMETER OF SAMPLE BEFORE CONSOLIDATION MM";D0
150 A0=π*D0*D0/4
160 V0=L0*A0*1E-3
170 OPENJ,J
180 PRINT#J,"**************************"
190 PRINT#J,"*  TRIAXIAL CELL NO.2    *"
200 PRINT#J,"**************************"
210 PRINT#J," "
220 PRINT#J,"INITIAL AREA BEFORE CONSOLIDATION=";FNA(A0);"MM^2"
230 PRINT#J,"INITIAL VOLUME BEFORE CONSOLIDATION=";FNA(V0);"CC"
240 PRINT#J," ":CLOSEJ
250 INPUT"INITIAL WEIGHT OF SAMPLE(GRAMS)";W0
260 INPUT"INITIAL MOISTURE CONTENT %";W
270 MS=W0/(1+0.01*W):VS=MS/2.75
280 VV=V0-VS:E0=VV/VS*100
290 S0=W*2.75/E0*100
300 OPENJ,J
310 PRINT#J,"**************************************"
320 PRINT#J,"WEIGHT OF SOLIDS=";FNA(MS);"GRAMS"
330 PRINT#J,"VOLUME OF SOLIDS=";FNA(VS);"CC"
340 PRINT#J,"VOLUME OF VOIDS=";FNA(VV);"CC"
350 PRINT#J,"INITIAL MOISTURE CONTENT";FNA(W);"%"
360 PRINT#J,"INITIAL VOID RATIO=";FNA(E0);"%"
370 PRINT#J,"INITIAL DEGREE OF SATURATION=";FNA(S0);"%"
380 PRINT#J," ":CLOSEJ
390 INPUT"CHANGE IN TOTAL VOLUME CC IN CONSOLIDATION STAGE";M
400 INPUT"CHANGE IN WATER VOLUME CC IN CONSOLIDATION STAGE";F
410 L1=L0*(1-M/(3*V0))
420 A1=A0*(1-M/V0)/(1-M/(3*V0))
430 V1=A1*L1*1E-3
440 E9=(V1-VS)/VS*100:S9=(W0-MS-F)/(V1-VS)*100
450 W9=E9*S9*0.01/2.75
460 OPENJ,J
470 PRINT#J,"**************************************"
480 PRINT#J,"LENGTH OF SAMPLE AFTER CONSOLIDATION=";FNA(L1);"MM"
490 PRINT#J,"AREA OF SAMPLE AFTER CONSOLIDATION=";FNA(A1);"MM^2"
500 PRINT#J,"VOLUME OF SAMPLE AFTER CONSOLIDATION";FNA(V1);"CC"
```

```
510 PRINT#J,"MOISTURE CONTENT AFTER CONSOLIDATION";FNA(W9);"%"
520 PRINT#J,"VOID RATIO AFTER CONSOLIDATION";FNA(E9);"%"
530 PRINT#J,"DEGREE OF SATURATION AFTER CONSOLIDATION";FNA(S9);"%"
540 PRINT#J,"**************************************************"
550 PRINT#J," ":CLOSEJ
560 REM ENTER DAY AS FOLLOWS:
570 REM DAY STARTED=0  DAY ONE=1
580 REM DAY TWO=2  ETC.
590 INPUT"HOUR AT START IS";H1
600 INPUT"MIN. AT START IS";M1
610 INPUT"STRAIN CORRECT ZERO";Z0
620 INPUT"INITIAL VCL-1 READING";R1
630 INPUT"INITIAL VCL-2 READING";R2
640 OPENJ,J
650 PRINT#J,"CORRECTION FOR STRENGTH OF 1:R.MEMBRANE,2:DRAINS,3:HD LAYER"
660 PRINT#J,"X=19 KN/M12 FOR 1,2 & 3"
670 PRINT#J,"X=14 KN/M12 FOR 1 & 2"
680 CLOSEJ
690 INPUT"STRENGTH CORRECTION VALUE X";X
700 REM DRAW THE TABLE
710 OPENJ,J
720 PRINT#J," "
730 PRINT#J,"**************************************************"
740 PRINT#J," +VE VOLUME CHANGE VALUE MEANS A DECREASE IN SAMPLE VOLUME "
750 PRINT#J,"**************************************************"
760 PRINT#J," "
770 Z$="**************************************************":
780 A$="  E.T.    STR.      VW      VA      SR      E      W      D.S.    M.S.
790 B$="(MINS.)  (%)     (%)     (%)     (%)     (%)    (%)    (%)  KN/M12 KN/M12
800 PRINT#J,Z$
810 PRINT#J,A$
820 PRINT#J,B$
830 PRINT#J,Z$
840 CLOSEJ
850 INPUT"DAY NOW";D2
860 INPUT"HOUR NOW";H2
870 INPUT"MIN. NOW";M2
880 REM CALCULATE THE ELAPSED TIME
890 ET=(24*60-(H1*60+M1))+((D2-1)*24*60)+(H2*60+M2)
900 IF D2=0 THEN ET=(H2*60+M2)-(H1*60+M1)
910 INPUT"STRAIN LVDT READING";S1
920 INPUT"LOAD CELL READING";S2
930 INPUT"CELL PRESSURE READING";CR
940 INPUT"POREAIR PRESSURE READING";AR
950 INPUT"POREWATER PRESSURE READING";WR
960 INPUT"VCL-1 READING";R3
970 INPUT"VCL-2 READING";R4
980 CL=ABS(S1-Z0)*0.02
1000 U=CL/L1:UU=100*U
```

```
1010 CP=-1.1964+1.0017*CR
1020 IFCR=0 THEN CP=0
1030 AP=-0.3770+0.9998*AR
1040 IFAR=0 THEN AP=0
1050 WP=-0.0354+1.0041*WR
1060 IFWR=0 THEN WP=0
1070 VW=R3-R1
1080 VT=(R4-R2)+((1.5912)*3.1416/4)*(CL/10)
1090 REM VT HAS INCLUDED THE VOLUME CHANGE DUE TO LOADING RAM PENETRATION
1100 SV=(MS*WS/100-VW)/(V1-VT-VS)*100
1110 EV=(V1-VT-VS)/VS*100
1120 WV=SV*EV*0.01/2.75
1130 VA=FNA(VT)-FNA(VW)
1140 Z1=(1-VT/V1)/(1-U)
1150 A2=Z1*A1
1160 DZ=(0.0503+0.001*S2)/(A2*1E-6)-X
1170 IFDZ<0 OR CL=0 THEN DZ=0
1180 VP=VT/V1*100
1190 V5=VW/V1*100
1200 V6=FNA(VP)-FNA(V5)
1210 OPENJ,J,2
1220 OPENJ+1,J,1
1230 C$="999999 99.99 999.99 999.99 999.99 999.99 999.99 99.99 9999.99 999.99"
1240 PRINT#J,C$
1250 PRINT#J+1,ET,UU,FNA(VP),FNA(V5),V6,SV,EV,WV,DZ,(AP-WP)
1260 CLOSEJ:CLOSEJ+1
1270 GOTO850
```

A8.1.3 Description of output

Typical printouts are shown on the following pages. The variables used in the printouts are listed below:

E.T. = elapsed time in minutes
SQR(E.T.) = square root of elapsed time
VT = total volume change in c.c. or percentage
VW = water volume change in c.c. or percentage
VA = air volume change in c.c. or percentage
SR = degree of saturation in percentage
E = void ratio in percentage
W = moisture content in percentage
D.A. = diffused air correction in c.c.
STR. = axial strain in percentage
D.S. = deviator stress in KN/sq.m
M.S. = matrix suction in KN/sq.m

Finally, the stress state variables associated with the failure condition are calculated. These are :

$[1/2(\bar{\sigma}1+\bar{\sigma}3)-Ua]f$; $[1/2(\bar{\sigma}1+\bar{\sigma}3)-Uw]f$; $(Ua-Uw)f$; $1/2(\bar{\sigma}1-\bar{\sigma}3)f$

where $\bar{\sigma}1$ = axial stress in KN/sq.m
$\bar{\sigma}3$ = equal all-round pressure in KN/sq.m
Ua = pore air pressure in KN/sq.m
Uw = pore water pressure in KN/sq.m
$(\bar{\sigma}1-\bar{\sigma}3)$ = deviator stress in KN/sq.m

The subscript f represents the stresses corresponding to failure. In Chapter 9, these stress state variables are used to plot three-dimensional failure surfaces.

****
* THIS IS THE STAGE OF CONSOLIDATION & DESATURATION *
****

INITIAL LENGTH OF SAMPLE BEFORE CONSOLIDATION IS 75.7 MM
INITIAL DIAMETER OF SAMPLE BEFORE CONSOLIDATION IS 38.1 MM
INITIAL AREA OF SAMPLE BEFORE CONSOLIDATION IS 1140.09 MM12
INITIAL VOLUME BEFORE CONSOLIDATION= 86.3 CC
WEIGHT OF SOLIDS= 133.13 GRAMS
VOLUME OF SOLIDS= 48.41 CC
INITIAL VOLUME OF VOIDS= 37.89 CC
INITIAL VOLUME OF WATER IN SAMPLE 37.84
INITIAL MOISTURE CONTENT= 28.42 %
INITIAL VOID RATIO= 78.27 %
INITIAL DEGREE OF SATURATION= 99.85 %

****
*** +VE VOLUME CHANGE VALUE MEANS SAMPLE VOLUME DECREASES ***
****

E.T. (MIN.)	SQR(E.T.) SQR(MIN.)	VT (C.C.)	VW (C.C.)	VA (C.C.)	SR (%)	E (%)	W (%)	D.A. (C.C.)
0	.00	+ .00	+ .00	+ .00	99.85	78.27	28.42	.00
1	1.00	+ .00	+ .00	+ .00	99.85	78.27	28.42	.00
4	2.00	+ .00	+ .00	+ .00	99.85	78.27	28.42	.00
9	3.00	+ .04	+ .04	+ .00	99.85	78.20	28.39	.00
16	4.00	+ .05	+ .10	- .05	99.72	78.18	28.35	.00
36	6.00	+ .04	+ .16	- .12	99.52	78.19	28.30	.00
64	8.00	+ .07	+ .31	- .24	99.22	78.12	28.19	.00
75	8.66	+ .12	+ .40	- .28	99.12	78.02	28.12	.00
99	9.95	+ .12	+ .51	- .39	98.82	78.02	28.04	.00
120	10.95	+ .12	+ .62	- .50	98.52	78.02	27.95	.00
133	11.53	+ .16	+ .66	- .50	98.51	77.95	27.92	.00
188	13.71	+ .22	+ .99	- .77	97.81	77.82	27.68	.00
221	14.87	+ .26	+ 1.19	- .93	97.40	77.72	27.53	.00
1072	32.74	+ .70	+ 5.22	- 4.52	87.70	76.82	24.50	.00
1151	33.93	+ .71	+ 5.61	- 4.90	86.69	76.80	24.21	.00
1173	34.25	+ .69	+ 5.70	- 5.01	86.39	76.84	24.14	.00
2350	48.48	+ 1.25	+11.33	-10.08	72.35	75.68	19.91	.00
2835	53.24	+ 1.39	+13.32	-11.93	67.17	75.40	18.42	.00
3658	60.48	+ .85	+13.97	-13.12	64.43	76.51	17.93	.00
3744	61.19	+ 1.21	+14.68	-13.47	63.13	75.77	17.39	.00
3860	62.13	+ 1.39	+14.94	-13.55	62.73	75.40	17.20	.00
3929	62.68	+ 1.19	+14.65	-13.46	63.16	75.82	17.41	.00
3998	63.15	+ 1.19	+14.73	-13.54	62.95	75.82	17.36	.00
4100	64.03	+ 1.15	+14.77	-13.62	62.79	75.90	17.33	.00
4163	64.52	+ 1.10	+14.83	-13.73	62.53	75.99	17.28	.00
4335	65.84	+ 1.26	+15.14	-13.88	61.95	75.67	17.05	.00
4448	66.69	+ 1.34	+15.34	-14.00	61.55	75.50	16.90	.00
4559	67.52	+ 1.40	+15.48	-14.08	61.27	75.37	16.79	.00
5150	71.76	+ 1.13	+15.47	-14.34	60.86	75.93	16.80	.00
5256	72.50	+ 1.23	+15.68	-14.45	60.44	75.73	16.64	.00
5256	72.50	+ 1.23	+15.68	-14.45	60.44	75.73	16.64	.00
5280	72.66	+ 1.22	+15.71	-14.49	60.34	75.74	16.62	.00

```
**************************
*     TRIAXIAL CELL NO.1   *
**************************
INITIAL AREA BEFORE CONSOLIDATION= 1140.09 MM12
INITIAL VOLUME BEFORE CONSOLIDATION= 86.3 CC

*************************************
WEIGHT OF SOLIDS= 133.13 GRAMS
VOLUME OF SOLIDS= 48.41 CC
VOLUME OF VOIDS= 37.89 CC
INITIAL MOISTURE CONTENT 28.42 %
INITIAL VOID RATIO= 78.27 %
INITIAL DEGREE OF SATURATION= 99.85 %

*****************************************************
LENGTH OF SAMPLE AFTER CONSOLIDATION= 75.34 MM
AREA OF SAMPLE AFTER CONSOLIDATION= 1129.3 MM12
VOLUME OF SAMPLE AFTER CONSOLIDATION 85.08 CC
MOISTURE CONTENT AFTER CONSOLIDATION 16.62 %
VOID RATIO AFTER CONSOLIDATION 75.75 %
DEGREE OF SATURATION AFTER CONSOLIDATION 60.34 %
*****************************************************

CORRECTION FOR STRENGTH OF 1:R.MEMBRANE,2:DRAINS,3:HG LAYER
X=19 KN/M12  FOR 1,2 & 3
X=14 KN/M12 FOR 1 & 2

*****************************************************************
 +VE VOLUME CHANGE VALUE MEANS A DECREASE IN SAMPLE VOLUME
*****************************************************************
```

E.T. (MINS.)	STR. (%)		VT (%)		VW (%)		VA (%)	SR (%)	E (%)	W (%)	D.S. KN/M12	M.S. KN/M12
0	.00	+	.00	+	.00	+	.00	60.33	75.75	16.61	.00	54.96
35	.02	+	.05	+	.04	+	.01	60.29	75.66	16.59	1.58	54.96
42	.05	+	.05	+	.04	+	.01	60.30	75.65	16.59	3.35	54.46
62	.10	+	.00	+	.05	-	.05	60.20	75.75	16.58	7.75	54.46
217	.71	+	.20	+	.24	-	.04	60.05	75.39	16.46	104.57	54.46
260	.87	+	.27	+	.29	-	.02	60.04	75.27	16.43	137.03	54.46
285	.95	+	.33	+	.33	+	.00	60.02	75.17	16.40	151.07	54.46
641	2.33	+	1.29	+	1.07	+	.22	59.63	73.48	15.93	343.97	55.96
1301	4.96	+	2.72	+	2.29	+	.43	58.72	70.96	15.15	633.60	53.46
1336	5.12	+	2.74	+	2.41	+	.33	58.44	70.93	15.07	646.47	53.46
1376	5.28	+	2.80	+	2.45	+	.35	58.45	70.82	15.05	661.30	53.46
1411	5.41	+	2.87	+	2.54	+	.33	58.32	70.71	14.99	673.75	53.46
1461	5.62	+	2.94	+	2.62	+	.32	58.23	70.58	14.94	690.78	53.46
1481	5.70	+	2.95	+	2.66	+	.29	58.14	70.56	14.92	698.03	53.46
1503	5.81	+	3.01	+	2.70	+	.31	58.12	70.45	14.89	705.42	54.46
1581	6.10	+	3.10	+	2.78	+	.32	58.05	70.30	14.84	731.27	54.46
1653	6.39	+	3.19	+	2.91	+	.28	57.85	70.14	14.75	753.64	54.46
1728	6.71	+	3.29	+	3.00	+	.29	57.77	69.96	14.70	776.59	54.46
1758	6.82	+	3.32	+	3.06	+	.26	57.68	69.91	14.66	785.31	54.46
1925	7.51	+	3.50	+	3.34	+	.16	57.23	69.60	14.48	830.92	54.46
1973	7.69	+	3.54	+	3.39	+	.15	57.15	69.52	14.45	844.01	54.46
2128	8.33	+	3.69	+	3.61	+	.08	56.82	69.26	14.31	881.53	56.46
2742	10.83	+	4.14	+	4.21	-	.06	55.94	68.47	13.92	991.42	53.96
2769	10.93	+	4.05	+	4.18	-	.12	55.90	68.62	13.94	994.25	54.46
2835	11.22	+	4.09	+	4.25	-	.16	55.76	68.55	13.90	1001.19	54.46
2914	11.54	+	4.10	+	4.38	-	.28	55.45	68.55	13.82	1011.45	54.46
2940	11.65	+	4.10	+	4.41	-	.31	55.37	68.53	13.80	1015.20	54.46
3019	11.99	+	4.12	+	4.45	-	.33	55.28	68.50	13.77	1023.56	53.96
3080	12.23	+	4.13	+	4.55	-	.41	55.04	68.49	13.71	1029.76	53.96
3136	12.47	+	4.17	+	4.65	-	.48	54.85	68.41	13.64	1034.65	53.96
3163	12.58	+	4.15	+	4.65	-	.50	54.81	68.46	13.64	1037.15	53.96
3190	12.68	+	4.14	+	4.66	-	.51	54.78	68.46	13.63	1039.07	53.96
3329	13.27	+	4.10	+	4.73	-	.63	54.54	68.54	13.59	1049.15	53.96
3372	13.45	+	4.16	+	4.81	-	.64	54.43	68.43	13.54	1053.98	54.96
3608	14.44	+	4.17	+	5.03	-	.86	53.86	68.42	13.40	1067.99	55.96
4172	16.74	+	4.20	+	5.36	-	1.16	53.07	68.36	13.19	1083.78	52.46
4191	16.82	+	4.16	+	5.44	-	1.28	52.82	68.43	13.14	1083.05	52.96
4216	16.93	+	4.14	+	5.48	-	1.34	52.67	68.48	13.11	1082.13	52.96
4256	17.12	+	4.20	+	5.56	-	1.36	52.56	68.36	13.06	1083.46	52.46
4293	17.25	+	4.13	+	5.55	-	1.42	52.49	68.49	13.07	1082.41	52.46
4318	17.36	+	4.10	+	5.55	-	1.45	52.46	68.53	13.07	1081.49	52.46
4340	17.46	+	4.08	+	5.59	-	1.51	52.31	68.58	13.04	1081.33	52.46
4376	17.59	+	4.08	+	5.66	-	1.58	52.14	68.57	13.00	1081.86	52.46
4397	17.70	+	4.09	+	5.65	-	1.56	52.18	68.56	13.01	1082.06	52.46
4436	17.86	+	4.05	+	5.71	-	1.66	51.96	68.62	12.96	1081.05	52.96
4462	17.97	+	4.06	+	5.70	-	1.64	52.00	68.61	12.97	1080.48	53.46
4498	18.13	+	4.05	+	5.75	-	1.70	51.87	68.64	12.94	1079.70	53.46
4518	18.20	+	4.02	+	5.75	-	1.73	51.83	68.69	12.94	1079.06	53.46
4535	18.26	+	4.03	+	5.79	-	1.76	51.73	68.67	12.91	1079.97	53.46
4565	18.39	+	4.01	+	5.79	-	1.78	51.70	68.70	12.91	1079.51	52.96
4608	18.55	+	4.03	+	5.84	-	1.81	51.62	68.66	12.89	1078.41	52.96
4637	18.68	+	4.03	+	5.85	-	1.82	51.59	68.67	12.88	1078.02	53.46
4664	18.79	+	4.03	+	5.88	-	1.85	51.51	68.66	12.86	1078.19	53.46
4777	19.27	+	3.96	+	5.94	-	1.98	51.26	68.79	12.82	1073.16	53.46
4794	19.32	+	3.98	+	5.95	-	1.97	51.26	68.75	12.81	1072.67	53.96
4820	19.43	+	4.00	+	5.99	-	1.99	51.17	68.72	12.78	1072.19	54.46
4874	19.66	+	3.94	+	6.03	-	2.09	51.01	68.81	12.76	1069.11	54.46
5017	20.25	+	3.95	+	6.11	-	2.16	50.82	68.80	12.71	1062.80	55.46
5819	23.54	+	3.87	+	6.58	-	2.71	49.51	68.94	12.41	1018.90	54.46

A8.1.4 Computations

(1) Strain is calculated, using the strain LVDT readings, as follows:

$$\varepsilon = \frac{\Delta l}{lo}$$

where Δl = change in axial length
lo = initial length of the specimen
ε = axial strain

(2) The volume changes during desaturation and consolidation (ΔVc) and during shear (ΔVs) together with the axial strain (ε), are used to calculate the length and cross-sectional area of the sample during shear.

The formulae used in this respect are (Akroyd,1957):

(i) For the length after desaturation and consolidation:

$$Lc = Lo\left(1 - \frac{\Delta Vc}{3Vo}\right)$$

(ii) For the area after desaturation and consolidation:

$$Ac = Ao \frac{\left(1 - \frac{\Delta Vc}{Vo}\right)}{\left(1 - \frac{\Delta Vc}{3Vo}\right)}$$

(iii) For the area during shear:

$$As = Ac \frac{\left(1 - \frac{\Delta Vs}{Vc}\right)}{(1 - \varepsilon)}$$

where Lo,Ao = initial length and cross-sectional area of sample
Vo = initial volume of sample
Lc,Ac = length and cross-sectional area of sample after desaturation and consolidation

Vc = volume of sample after desaturation and consolidation
As = cross-sectional area of sample during shear
ΔVc = change in volume of sample during desaturation and consolidation
ΔVs = change in volume of sample from the moment at which shear begins
and ε = the measured axial strain from the same moment as above

The first and second equations consider the influence of the volume change as a result of the triaxial consolidation, whereas the third equation takes into account both the volume change during shear and the applied axial strain. In all cases, the approximation is made that the sample remains cylindrical.

(3) Deviator stress at any strain is calculated from

$$(\sigma_1 - \sigma_3) = \frac{P}{As}$$

where P = deviator load

For other soil properties, the calculations are set out in each individual computer program described in the data reduction section.

A8.2 Program for numerical method --- "ANGLE"

THE DETERMINATION OF SUCTION ANGLE

```
100 DIM S(100),Y(100)
110 I=1:SX=0:SY=0:XY=0:XX=0:YY=0
120 INPUT"OUTPUT DEVICE? 3 FOR SCREEN,4 FOR PRINTER";F
130 DEF FNA(X)=SGN(X)*INT(ABS(X)*1E2+0.5)/1E2
140 INPUT"COHESION,C' IN KN/M12";CI
150 INPUT"ANGLE OF INTERNAL FRICTION IN DEGREES";FI
160 INPUT"(MEAN STRESS - PAP) IN KN/M12 IS";M
170 IF M = 1E6 GOTO 310
180 INPUT"(DEVIATOR STRESS AT FAILURE)/2 IN KN/M12 IS";P
190 INPUT"MATRIX SUCTION AT FAILURE IN KN/M12 IS";S(I)
200 FO=FI/57.29578
210 D=CI*COS(FO)
220 FA=FO
230 QA=ATN(SIN(FA))
240 TP=TAN(QA)*M+D
250 TD=P-TP
260 Y(I)=TD*(COS(QA))
270 SX=SX+S(I):SY=SY+Y(I)
280 XY=XY+S(I)*Y(I):XX=XX+S(I)*S(I):YY=YY+Y(I)*Y(I)
290 I=I+1
300 GOTO 160
310 NN=I-1
320 MX=SX/NN:MY=SY/NN
330 B1=(NN*XY-SX*SY)/(NN*XX-SX*SX)
340 B0=MY-B1*MX
350 R1=NN*XY-SX*SY:R2=SQR((NN*XX-SX*SX)*(NN*YY-SY*SY))
360 R=R1/R2
370 AU=ATN(B1)
380 FB=ATN(TAN(AU)/COS(QA)/COS(FA))
390 FT=ATN(TAN(FB)-TAN(FO))
400 FT=FT*57.29578
410 FA=FA*57.29578
420 FB=FB*57.29578
430 OPENF,F
440 PRINT#F,"**********************************************************************"
450 PRINT#F," "
460 PRINT#F,"INPUT COHESION,C' IN KN/M12 IS";FNA(CI)
470 PRINT#F," "
480 PRINT#F,"INPUT ANGLE OF INTERNAL FRICTION IN DEGREES,0' IS";FNA(FI)
490 PRINT#F," "
500 PRINT#F,"**********************************************************************"
510 PRINT#F," "
520 PRINT#F,"SUCTION ANGLE IN DEGREES (UA) IS";FNA(FB)
530 PRINT#F," "
540 PRINT#F,"SUCTION ANGLE IN DEGREES (UW) IS";FNA(FT)
550 PRINT#F," "
560 PRINT#F,"CORRECTED COHESION,C' IN KN/M12 IS";FNA(B0+CI)
570 PRINT#F," "
580 PRINT#F,"CORRELATION FACTOR FOR SUCTION ANGLE(UA),R IS";FNA(R)
590 PRINT#F," "
600 CLOSEF
```

Description of variable names for the computer program---"ANGLE"

VARIABLE NAME	DESCRIPTION
CI	C'
FI	ϕ'
M	$((\sigma 1+\sigma 3)/2-Ua)$
P	$(\sigma 1-\sigma 3)/2$
S(I)	(Ua-Uw)
D	d'
QA	μ'
AU	αa
FB	ϕ^b
FT	ϕ''
R	correlation coefficient

```
C
C*************************************************************************
C
C     GRAPHICAL REPRESENTATION OF THE SHEAR STRENGTH DATA FOR           *
C
C                        UNSATURATED SOIL                               *
C
C*************************************************************************
C
C      THIS IS "SHEARLIB.SHEARIH" DATA=DATALIB OR DLIB SERIES           *
C
C*************************************************************************
C
      REAL X(100),XX(100),Y(100),Z(100),AZ(100,100),W(10000)
      INTEGER ITITLE(30)
      DATA NMAX/100/
      READ(8,100)(ITITLE(I),I=1,30)
  100 FORMAT(30A4)
      READ(8,*) X(1),XX(1),Y(1),Z(1)
      XMAX=X(1)
      XMIN=X(1)
      XXMAX=XX(1)
      XXMIN=XX(1)
      YMAX=Y(1)
      YMIN=Y(1)
      ZMAX=Z(1)
      ZMIN=Z(1)
      I=2
   10 READ(8,*,END=20) X(I),XX(I),Y(I),Z(I)
      XMAX=MAX(X(I),XMAX)
      XMIN=MIN(X(I),XMIN)
      XXMAX=MAX(XX(I),XXMAX)
      XXMIN=MIN(XX(I),XXMIN)
      YMAX=MAX(Y(I),YMAX)
      YMIN=MIN(Y(I),YMIN)
      ZMAX=MAX(Z(I),ZMAX)
      ZMIN=MIN(Z(I),ZMIN)
      I=I+1
      IF (I.LE.NMAX) GOTO 10
      PRINT 600
  600 FORMAT('*** TOO MANY LINES OF DATA ***')
   20 N=I-1
      CALL HP747
      CALL WINDOW(3)
      CALL TITLE(4,30,ITITLE)
      CALL RANGRD(N,Y,X,Z,N,YMIN,YMAX,N,XMIN,XMAX,AZ,2*N*N+4*N,W)
      CALL ISOPRJ(N,0.,YMAX,N,0.,XMAX,AZ,0,2*N*N+4*N,W)
      CALL MOVTO2(25.,45.)
      CALL CHAHOL('((P1+P3)/2-U*LA)F*.')
      CALL MOVTO2(160.,45.)
      CALL CHAHOL('(U*LA-*UU*LW)F*.')
      CALL MOVTO2(10.,150.)
      CALL CHAHOL('(P1-P3)*LF/2*.')
      CALL MOVTO2(195.,150.)
      CALL CHAHOL('(P1-P3)*LF/2*.')
      CALL DEVEND
      WRITE(6,*)N,XMIN,XMAX,XXMIN,XXMAX,YMIN,YMAX,ZMIN,ZMAX
      STOP
      END
```

```
C
C*************************************************************************
C
C    GRAPHICAL REPRESENTATION OF THE SHEAR STRENGTH DATA FOR            *
C
C                        UNSATURATED SOIL                               *
C
C*************************************************************************
C
C     THIS IS "SHEARLIB.SHEAR2H" DATA=DATALIB OR DLIB                   *
C
C*************************************************************************
C
      REAL X(100),XX(100),Y(100),Z(100),AZ(100,100),W(10000)
      INTEGER ITITLE(30)
      DATA NMAX/100/
      READ(8,100)(ITITLE(I),I=1,30)
  100 FORMAT(30A4)
      READ(8,*) X(1),XX(1),Y(1),Z(1)
      XMAX=X(1)
      XMIN=X(1)
      XXMAX=XX(1)
      XXMIN=XX(1)
      YMAX=Y(1)
      YMIN=Y(1)
      ZMAX=Z(1)
      ZMIN=Z(1)
      I=2
   10 READ(8,*,END=20) X(I),XX(I),Y(I),Z(I)
      XMAX=MAX(X(I),XMAX)
      XMIN=MIN(X(I),XMIN)
      XXMAX=MAX(XX(I),XXMAX)
      XXMIN=MIN(XX(I),XXMIN)
      YMAX=MAX(Y(I),YMAX)
      YMIN=MIN(Y(I),YMIN)
      ZMAX=MAX(Z(I),ZMAX)
      ZMIN=MIN(Z(I),ZMIN)
      I=I+1
      IF (I.LE.NMAX) GOTO 10
      PRINT 600
  600 FORMAT('*** TOO MANY LINES OF DATA ***')
   20 N=I-1
      CALL HP747
      CALL WINDOW(3)
      CALL TITLE(4,30,ITITLE)
      CALL RANGRD(N,Y,XX,Z,N,YMIN,YMAX,N,XXMIN,XXMAX,AZ,2*N*N+4*N,W)
      CALL ISOPRJ(N,0.,YMAX,N,0.,XXMAX,AZ,0,2*N*N+4*N,W)
      CALL MOVTO2(25.,45.)
      CALL CHAHOL('((P1+P3)/2-U*LW)F*.')
      CALL MOVTO2(160.,45.)
      CALL CHAHOL('(U*LA-*UU*LW)F*.')
      CALL MOVTO2(10.,150.)
      CALL CHAHOL('(P1-P3)*LF/2*.')
      CALL MOVTO2(195.,150.)
      CALL CHAHOL('(P1-P3)*LF/2*.')
      CALL DEVEND
      WRITE(6,*)N,XMIN,XMAX,XXMIN,XXMAX,YMIN,YMAX,ZMIN,ZMAX
      STOP
      END
```

```
C
C*************************************************************************
C
C     GRAPHICAL REPRESENTATION OF THE SHEAR STRENGTH DATA FOR           *
C
C                          UNSATURATED SOIL                             *
C
C*************************************************************************
C
C    THIS IS PROGRAM "SHEARLIB.SHEAR3H" DATA=DATALIB.S-SERIES
C
C*************************************************************************
C
      REAL X(100),XX(100),Y(100),Z(100),AZ(100,100),W(10000)
      INTEGER ITITLE(30)
      DATA NMAX/100/
      READ(8,100)(ITITLE(I),I=1,30)
  100 FORMAT(30A4)
      READ(8,*) X(1),XX(1),Y(1),Z(1)
      XMAX=X(1)
      XMIN=X(1)
      XXMAX=XX(1)
      XXMIN=XX(1)
      YMAX=Y(1)
      YMIN=Y(1)
      ZMAX=Z(1)
      ZMIN=Z(1)
      I=2
   10 READ(8,*,END=20) X(I),XX(I),Y(I),Z(I)
      XMAX=MAX(X(I),XMAX)
      XMIN=MIN(X(I),XMIN)
      XXMAX=MAX(XX(I),XXMAX)
      XXMIN=MIN(XX(I),XXMIN)
      YMAX=MAX(Y(I),YMAX)
      YMIN=MIN(Y(I),YMIN)
      ZMAX=MAX(Z(I),ZMAX)
      ZMIN=MIN(Z(I),ZMIN)
      I=I+1
      IF (I.LE.NMAX) GOTO 10
      PRINT 600
  600 FORMAT('*** TOO MANY LINES OF DATA ***')
   20 N=I-1
      CALL HP747
      CALL TITLE(4,30,ITITLE)
      CALL RANGRD(N,X,XX,Z,N,XMIN,XMAX,N,XXMIN,XXMAX,AZ,2*N*N+4*N,W)
      CALL ISOPRJ(N,0.,XMAX,N,0.,XXMAX,AZ,0,2*N*N+4*N,W)
      CALL MOVTO2(25.,45.)
      CALL CHAHOL('((P1+P3)/2-U*LW)F*.')
      CALL MOVTO2(160.,45.)
      CALL CHAHOL('((P1+P3)/2-U*LA)F*.')
      CALL MOVTO2(10.,150.)
      CALL CHAHOL('(P1-P3)*LF/2*.')
      CALL MOVTO2(195.,150.)
      CALL CHAHOL('(P1-P3)*LF/2*.')
      CALL DEVEND
      WRITF(6,*)N,XMIN,XMAX,XXMIN,XXMAX,YMIN,YMAX,ZMIN,ZMAX
      STOP
      END
```

A8.4 Results

A8.4.1 Bisbee et al(1960)

(i) Numerical method

Compacted shale(results from tests on unsaturated soil specimens only)

```
**************************************************
 INPUT COHESION C´ IN KN/SQ.M IS 15.8

 INPUT ANGLE OF INTERNAL FRICTION IN DEGREES,Ø´ IS 24.8
**************************************************
                                   b
 SUCTION ANGLE IN DEGREES,Ø  IS 18.61

 SUCTION ANGLE IN DEGREES,Ø° IS -7.15

 CORRECTED COHESION,C´ IN KN/SQ.M IS 4.99
                                                  b
 CORRELATION FACTOR FOR SUCTION ANGLE(Ø ), R IS 0.98
**************************************************
```

Compacted Boulder clay

```
**************************************************
 INPUT COHESION,C´ IN KN/SQ.M IS 9.6

 INPUT ANGLE OF INTERNAL FRICTION IN DEGREES,Ø´ IS 27.3
**************************************************
                                   b
 SUCTION ANGLE IN DEGREES,Ø  IS 22.19

 SUCTION ANGLE IN DEGREES,Ø° IS -6.18

 CORRECTED COHESION,C´ IN KN/SQ.M IS 3.29
                                   b
 CORRELATION FACTOR FOR SUCTION ANGLE(Ø ),R IS 0.97
**************************************************
```

(ii) 2-dimensional graphical method

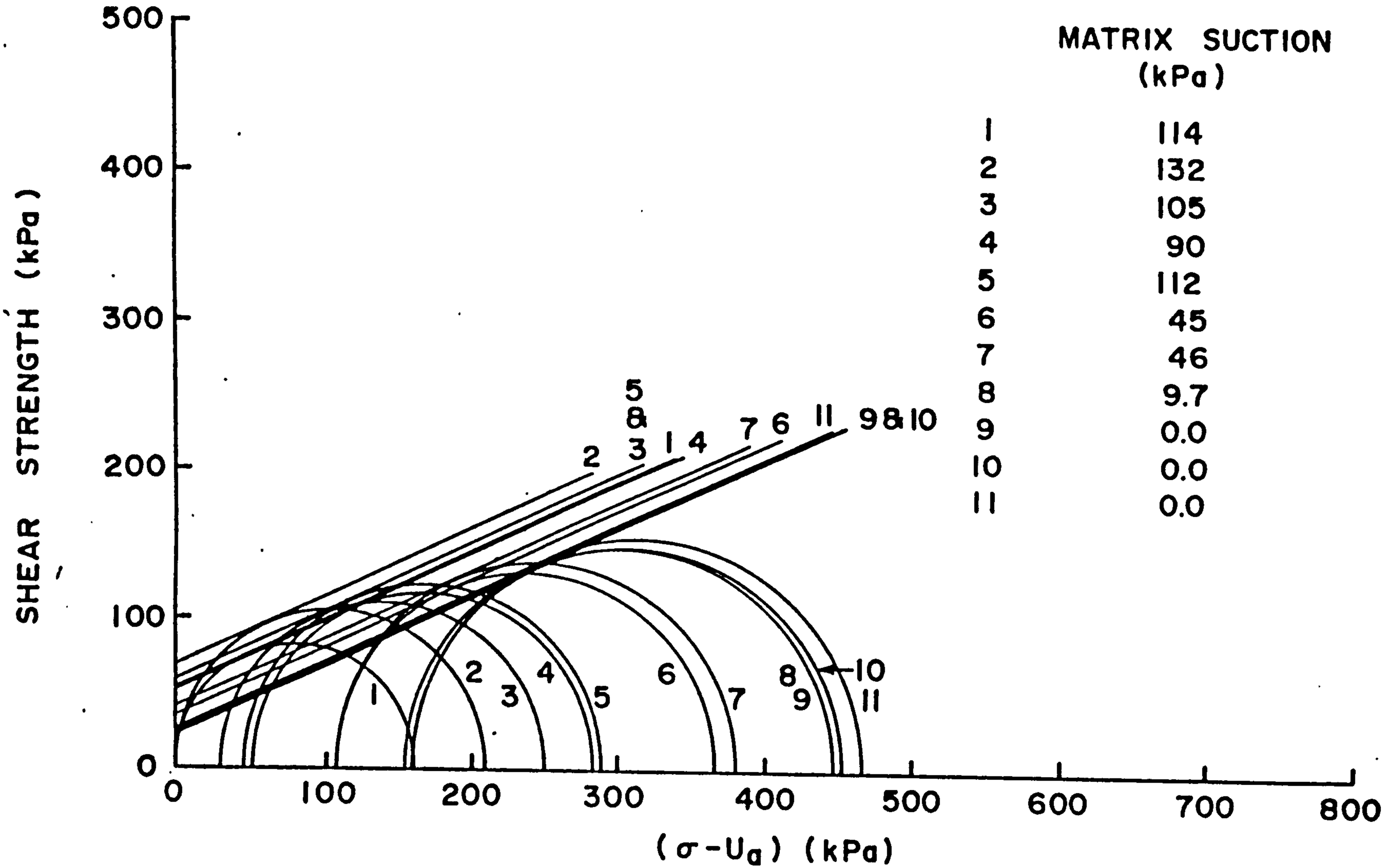

Fig.A8.1: Mohr-Coulomb failure circles for compacted shale (after Bishop et al, 1960).

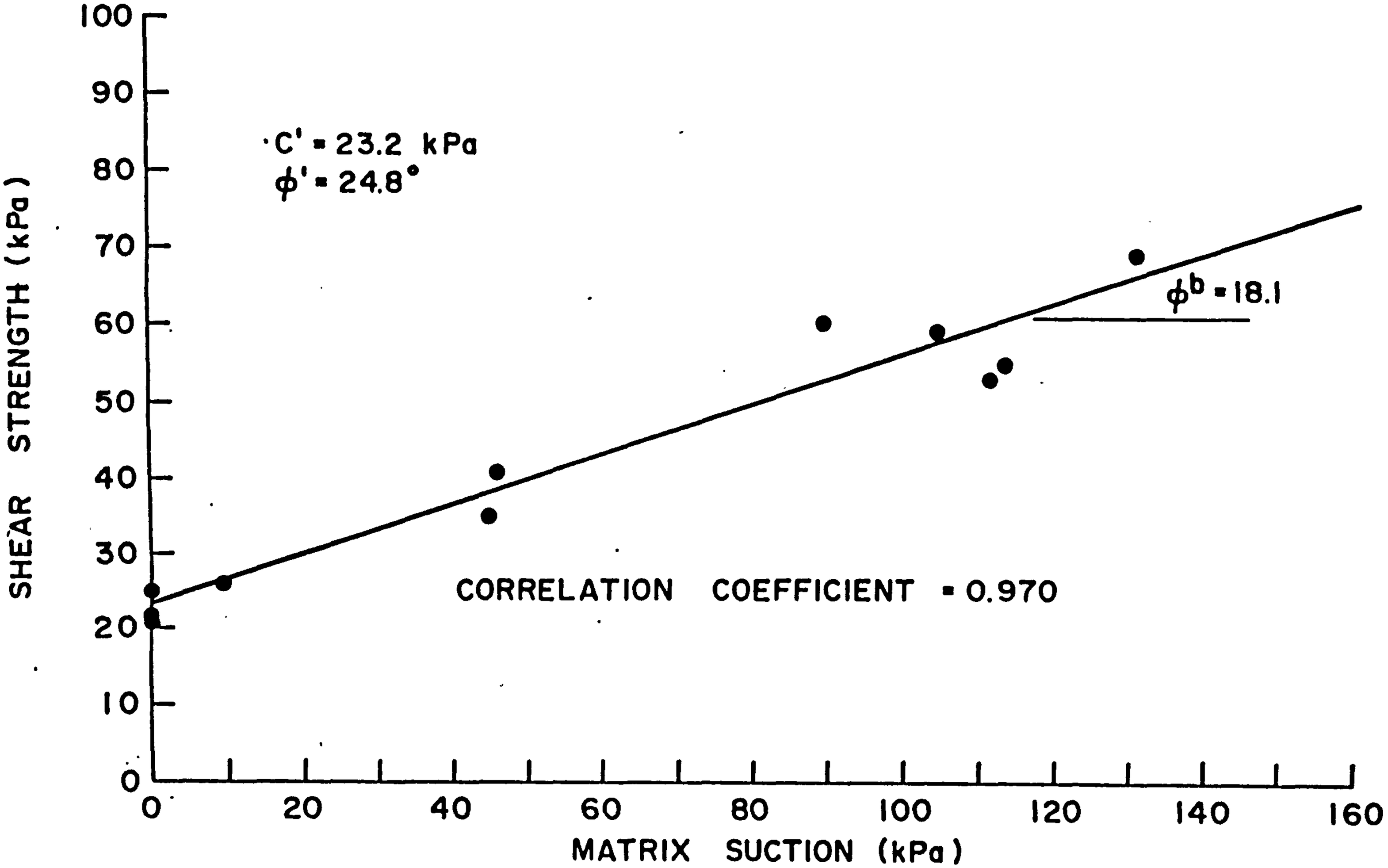

Fig.A8.2: Shear strength versus matrix suction for compacted shale (after Bishop et al, 1960).

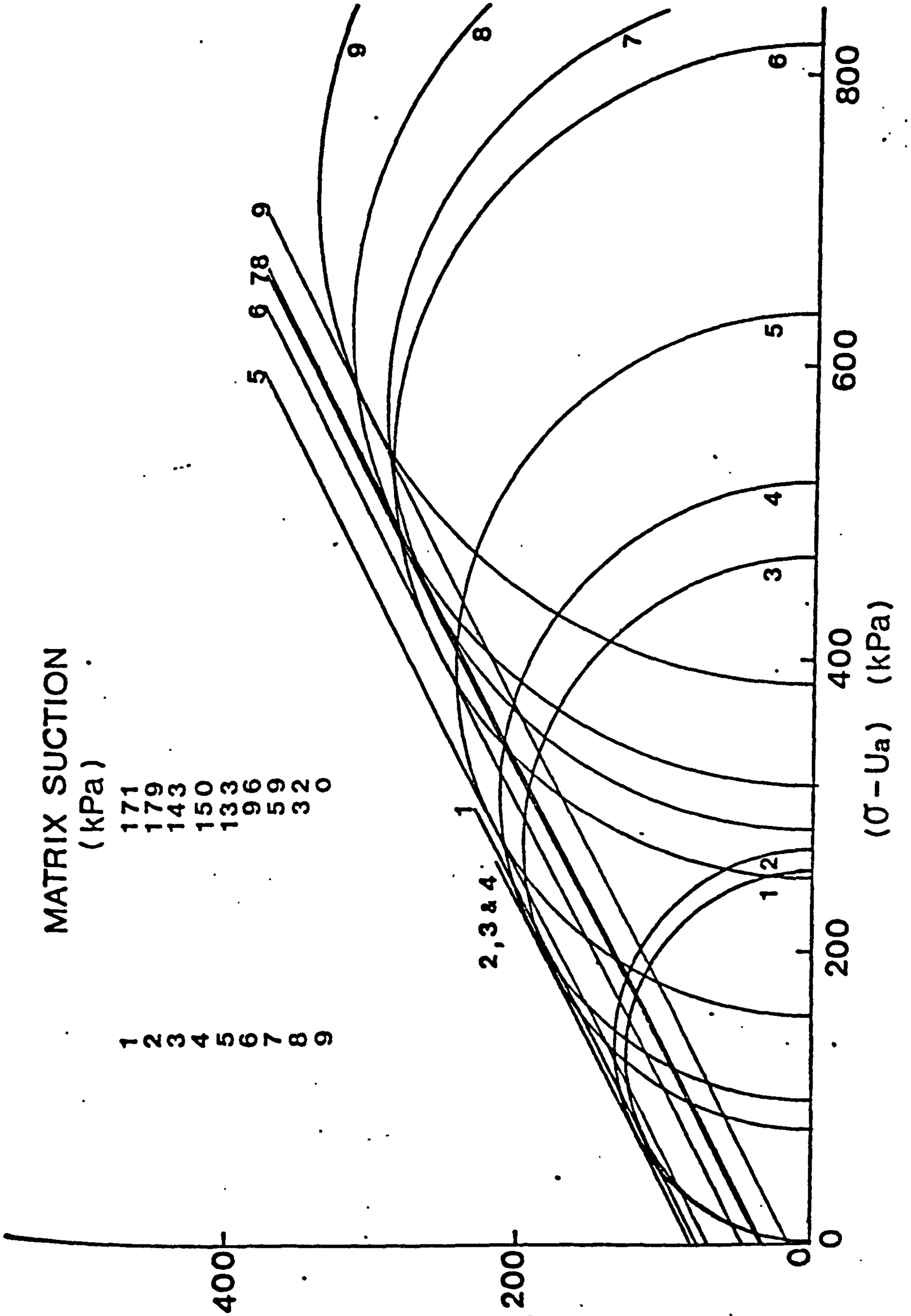

Fig.A8.3: Mohr failure circles for Boulder clay (after Bishop et al, 1960).

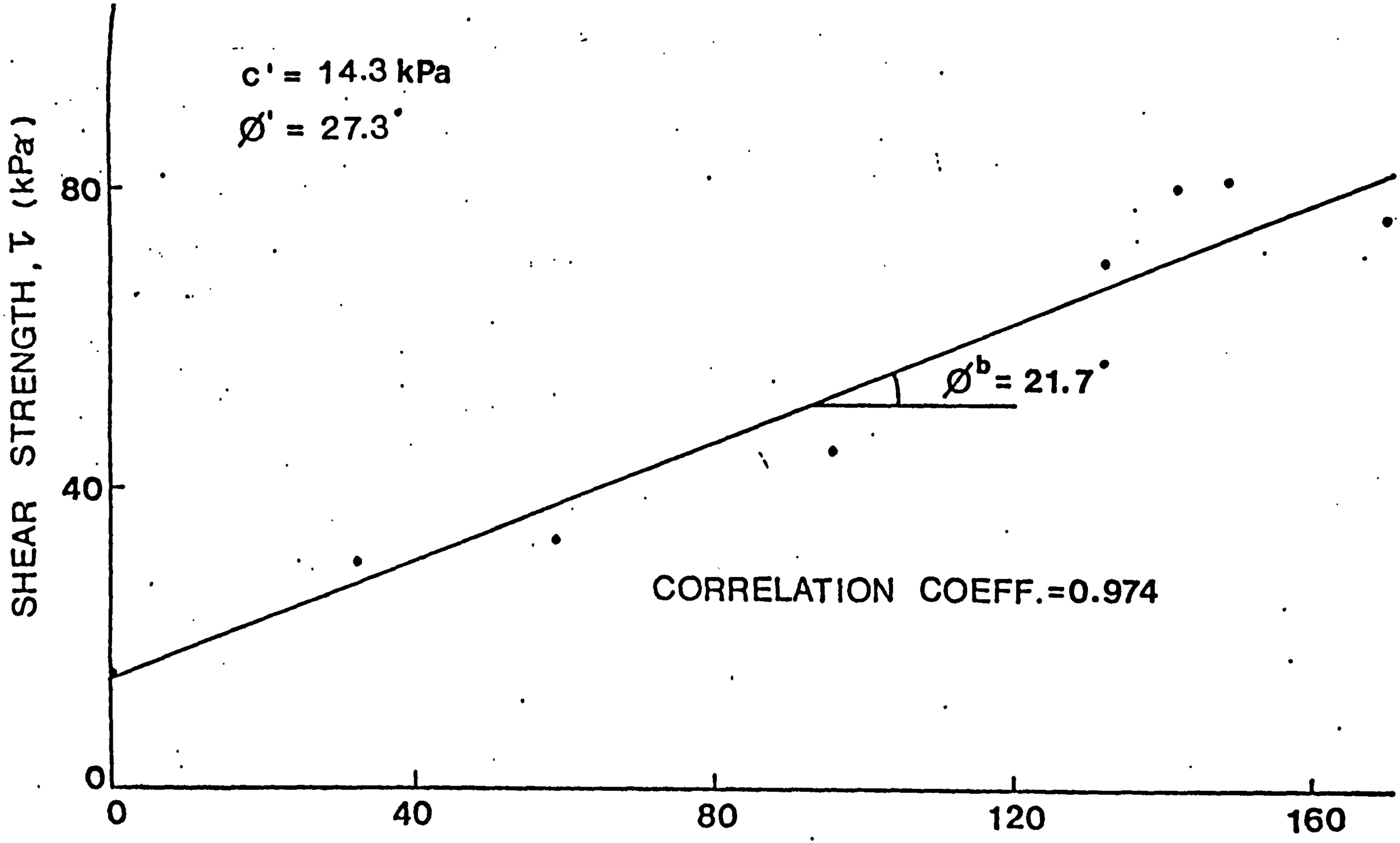

Fig.A8.4: Shear strength versus matrix suction for Boulder clay (after Bishop et al, 1960).

Data analysed by 2-dimensional graphical method :

Soil Type	INPUT c'(kPa)	ϕ'	ϕ^b	Correlation*
Compacted Shale w = 18.6%	15.8	24.8	18.1	0.970
Boulder Clay w = 11.6%	9.6	27.3	21.7	0.974

* Correlation coefficient is for the computation of ϕ^b

(iii) 3-dimensional graphical method

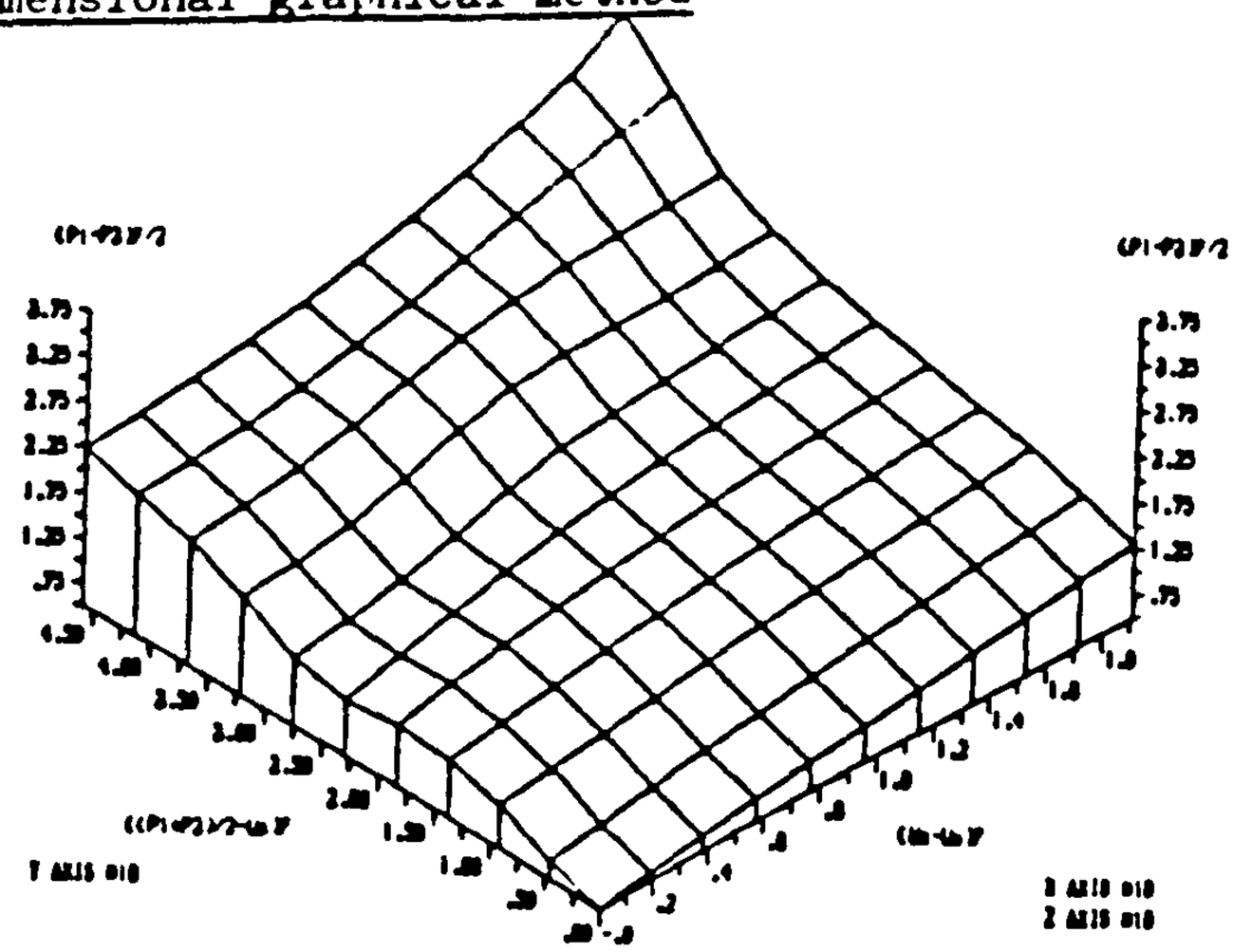

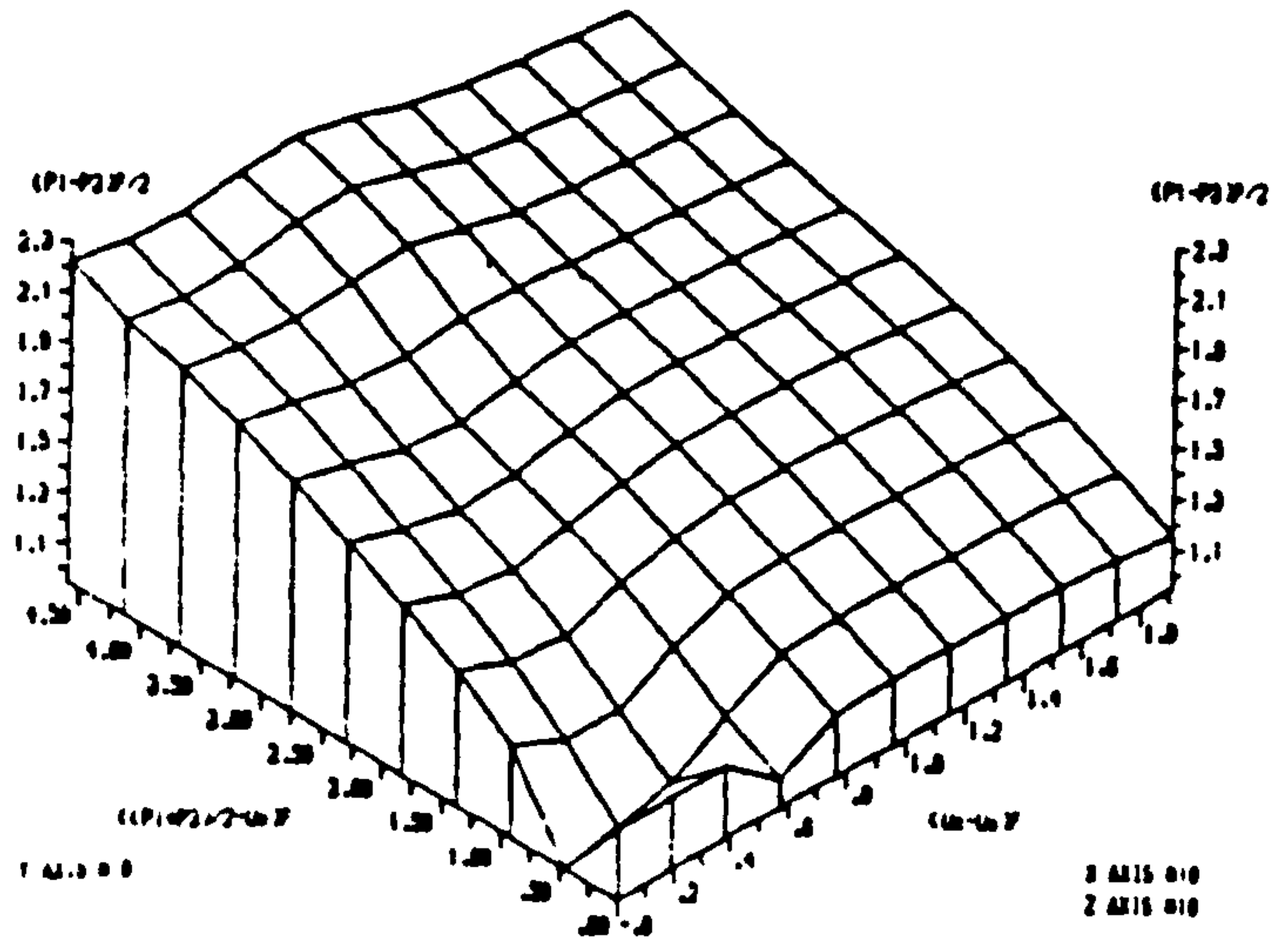

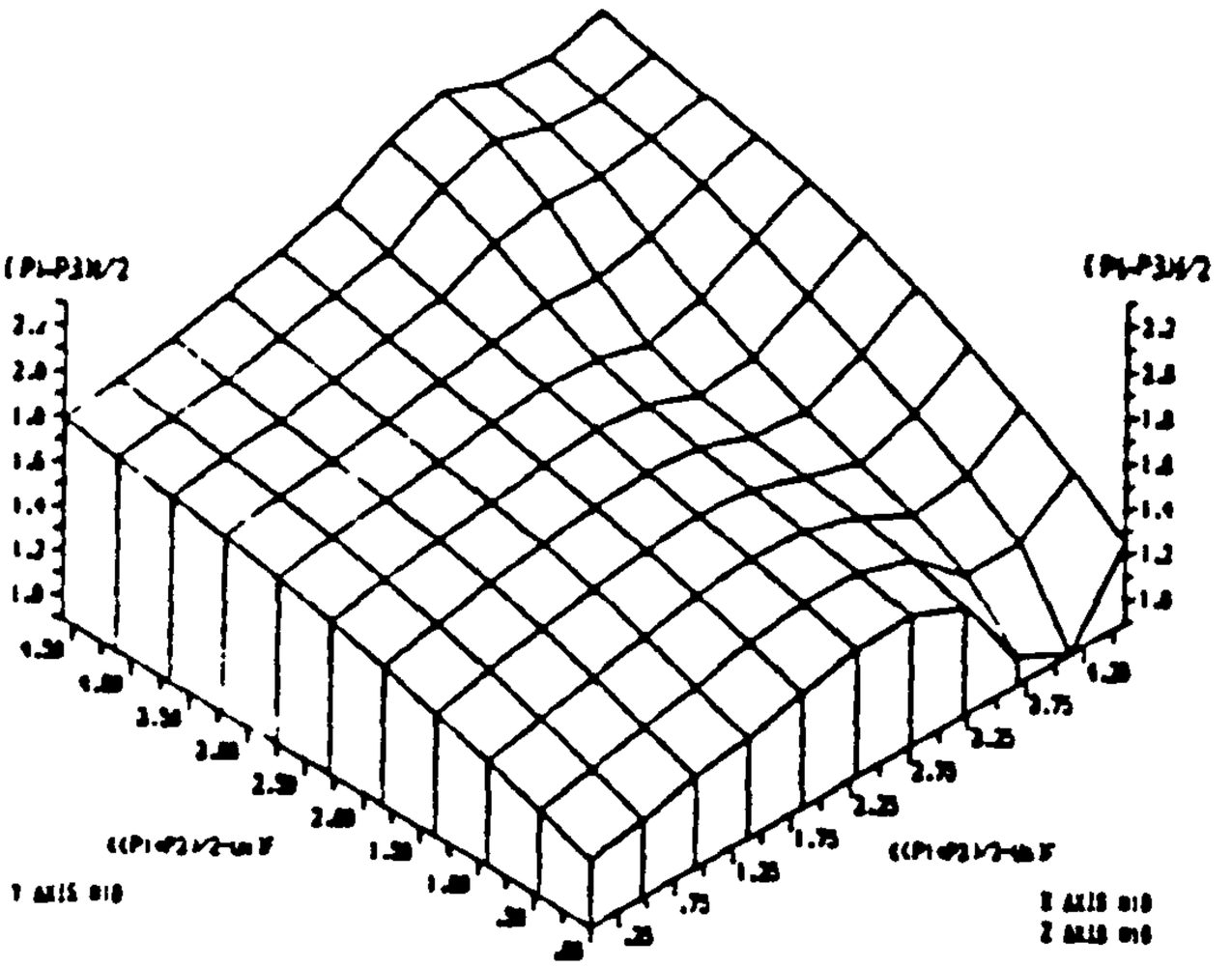

*UNITS IN KN/SQ.M

SHEAR STRENGTH DATA FOR COMPACTED SHALE (BISHOP ET AL,1960)

(DATA FROM FREDLUND,1978).

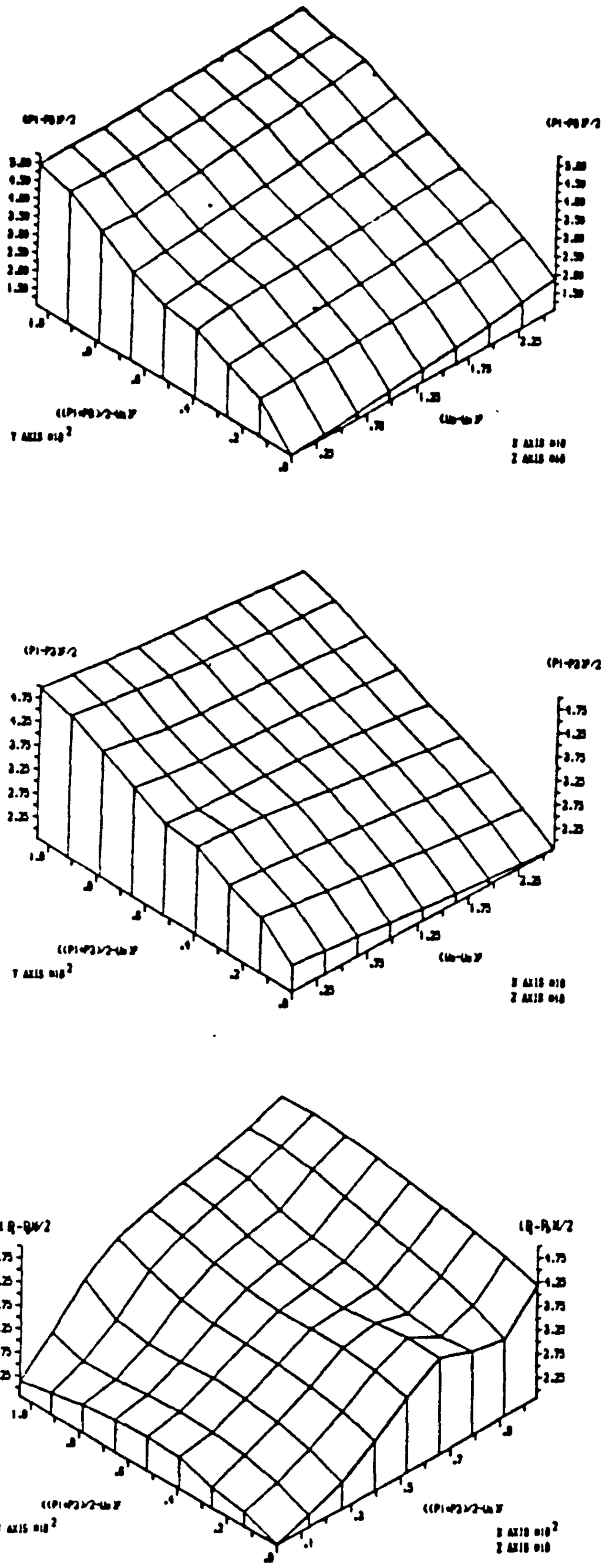

(UNITS IN KN/SQ.M)

SHEAR STRENGTH DATA FOR COMPACTED BOULDER CLAY(BISHOP ET AL,1960)

(DATA FROM FREDLUND,1978).

A8.4.2 Donald(1961)

(i) Numerical method

Remoulded London clay (Undrained tests)

```
**************************************************************
 INPUT COHESION,C' IN P.S.I. IS 0

 INPUT ANGLE OF INTERNAL FRICTION IN DEGREES,Ø' IS 20.3
**************************************************************
                              b
 SUCTION ANGLE IN DEGREES,Ø   IS 10.44

 SUCTION ANGLE IN DEGREES,Ø' IS -10.52

 CORRECTED COHESION,C' IN P.S.I. IS 2.37
                                          b
 CORRELATION FACTOR FOR SUCTION ANGLE(Ø ),R IS 0.71
**************************************************************
```

Braehead silt (Constant water-content tests)

```
**************************************************************
 INPUT COHESION,C' IN P.S.I. IS 0

 INPUT ANGLE OF INTERNAL FRICTION IN DEGREES,Ø' IS 33.4
**************************************************************
                              b
 SUCTION ANGLE IN DEGREES,Ø   IS 8.72

 SUCTION ANGLE IN DEGREES,Ø' IS -26.84

 CORRECTED COHESION,C' IN P.S.I. IS 1.24
                                          b
 CORRELATION FACTOR FOR SUCTION ANGLE(Ø ),R IS 0.64
**************************************************************
```

Braebead silt (drained tests)

```
**************************************************************
 INPUT COHESION,C' IN P.S.I. IS 0

 INPUT ANGLE OF INTERNAL FRICTION IN DEGREES,Ø' IS 33.4
**************************************************************
                                   b
 SUCTION ANGLE IN DEGREES,Ø   IS 16.93

  SUCTION ANGLE IN DEGREES,Ø° IS -19.55

  CORRECTED COHESION,C' IN P.S.I. IS 0.49
                                                  b
  CORRELATION FACTOR FOR SUCTION ANGLE(Ø ),R IS 0.92
**************************************************************
```

Braehead silt (over-drained tests)

```
**************************************************************
 INPUT COHESION,C' IN P.S.I. IS 0

 INPUT ANGLE OF INTERNAL FRICTION IN DEGREES,Ø' IS 33.4
**************************************************************
                                   b
 SUCTION ANGLE IN DEGREES,Ø   IS 18.58

 SUCTION ANGLE IN DEGREES,Ø° IS -17.92

 CORRECTED COHESION,C' IN P.S.I. IS 0.64
                                                 b
 CORRELATION FACTOR FOR SUCTION ANGLE(Ø ),R IS 0.99
**************************************************************
```

(iii) 3-dimensional graphical method

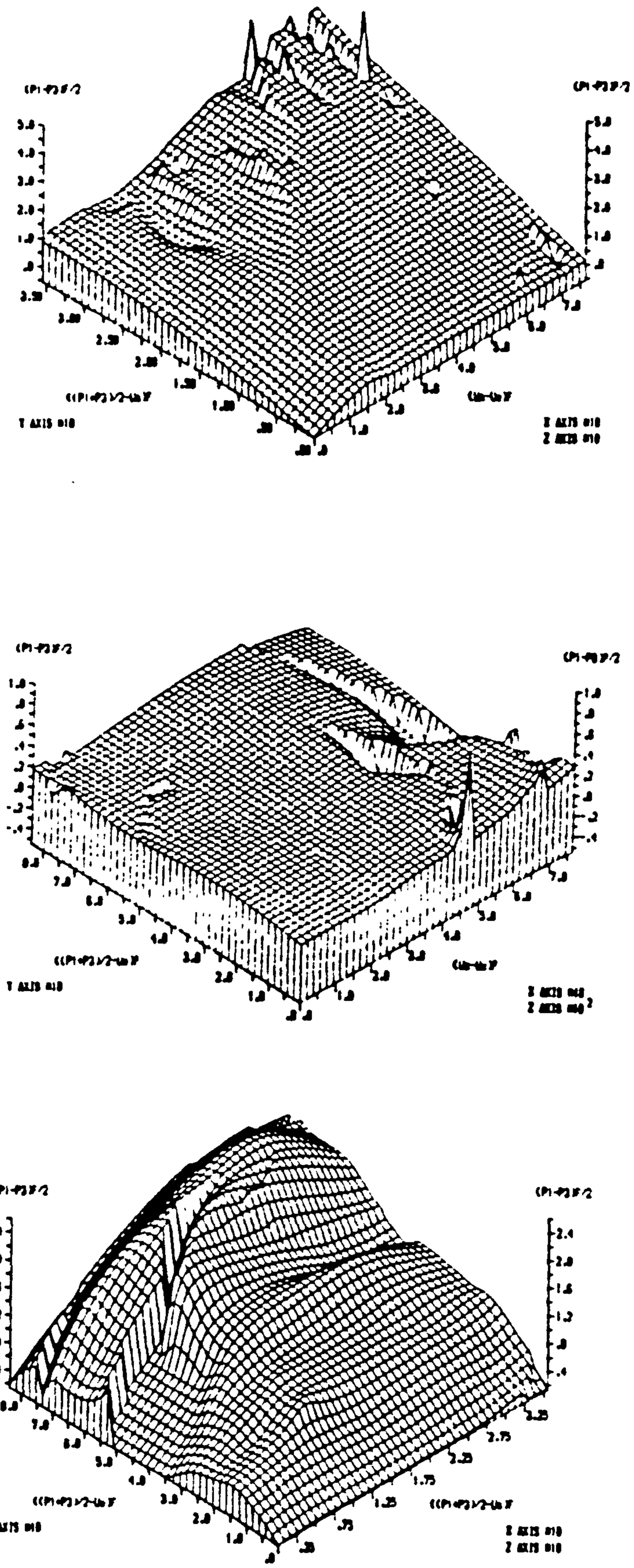

(UNITS IN POUNDS PER SQ. INCHES)

THE SHEAR STRENGTH DATA FOR LONDON CLAY(I.B.DONALD,1961,.

(UNDRAINED TESTS)

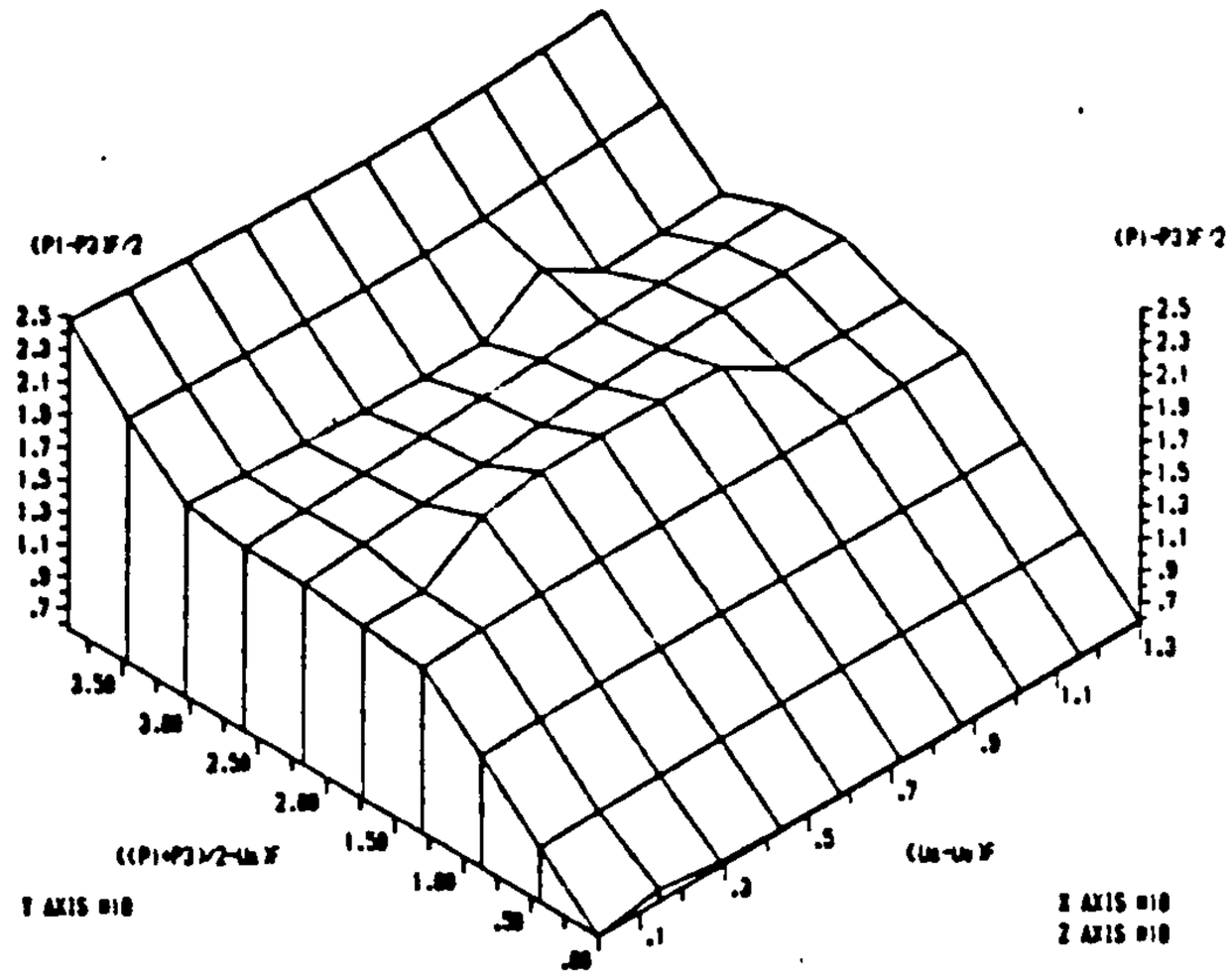

THE SHEAR STRENGTH DATA FOR BAREHEAD SILT FROM CU TESTS (I.B.DONALD,1961)

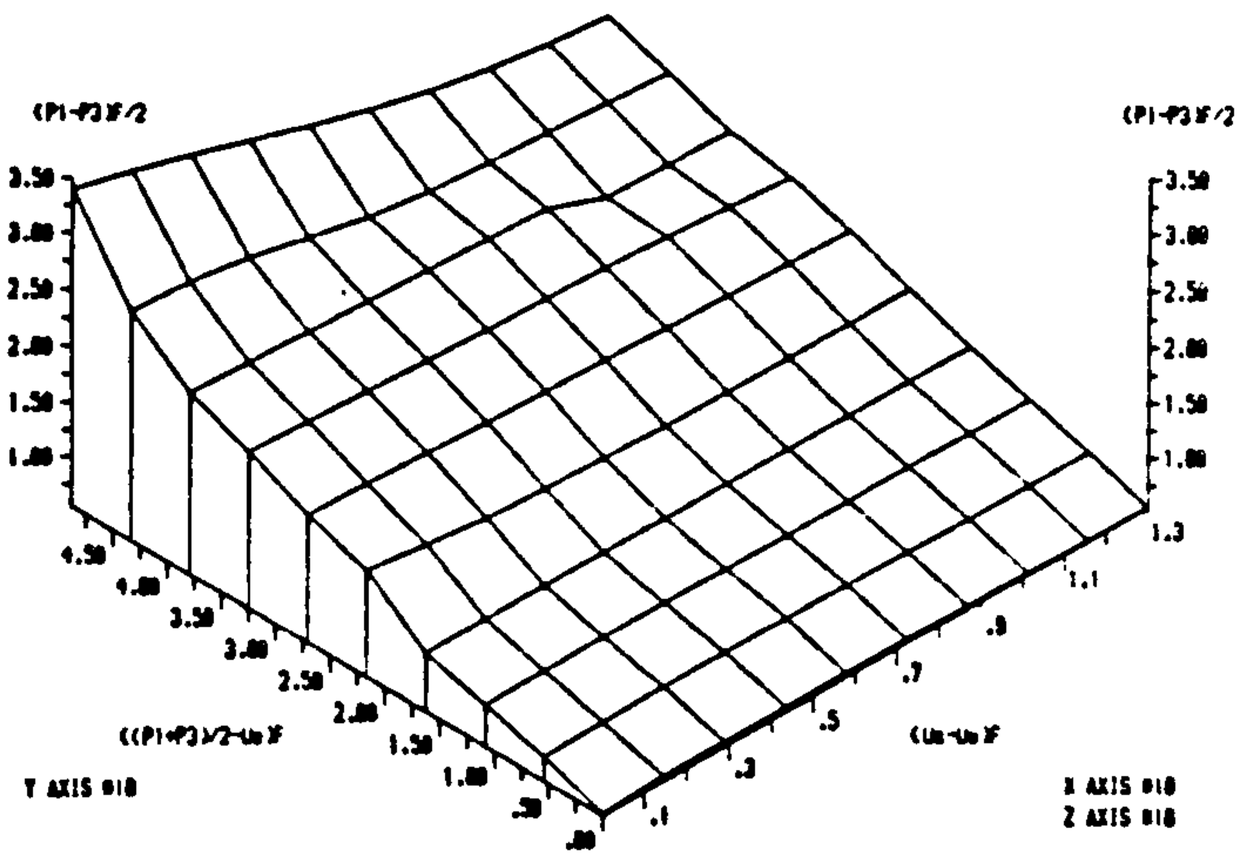

THE SHEAR STRENGTH DATA FOR BAREHEAD SILT FROM CU TESTS (I.B.DONALD,1961)

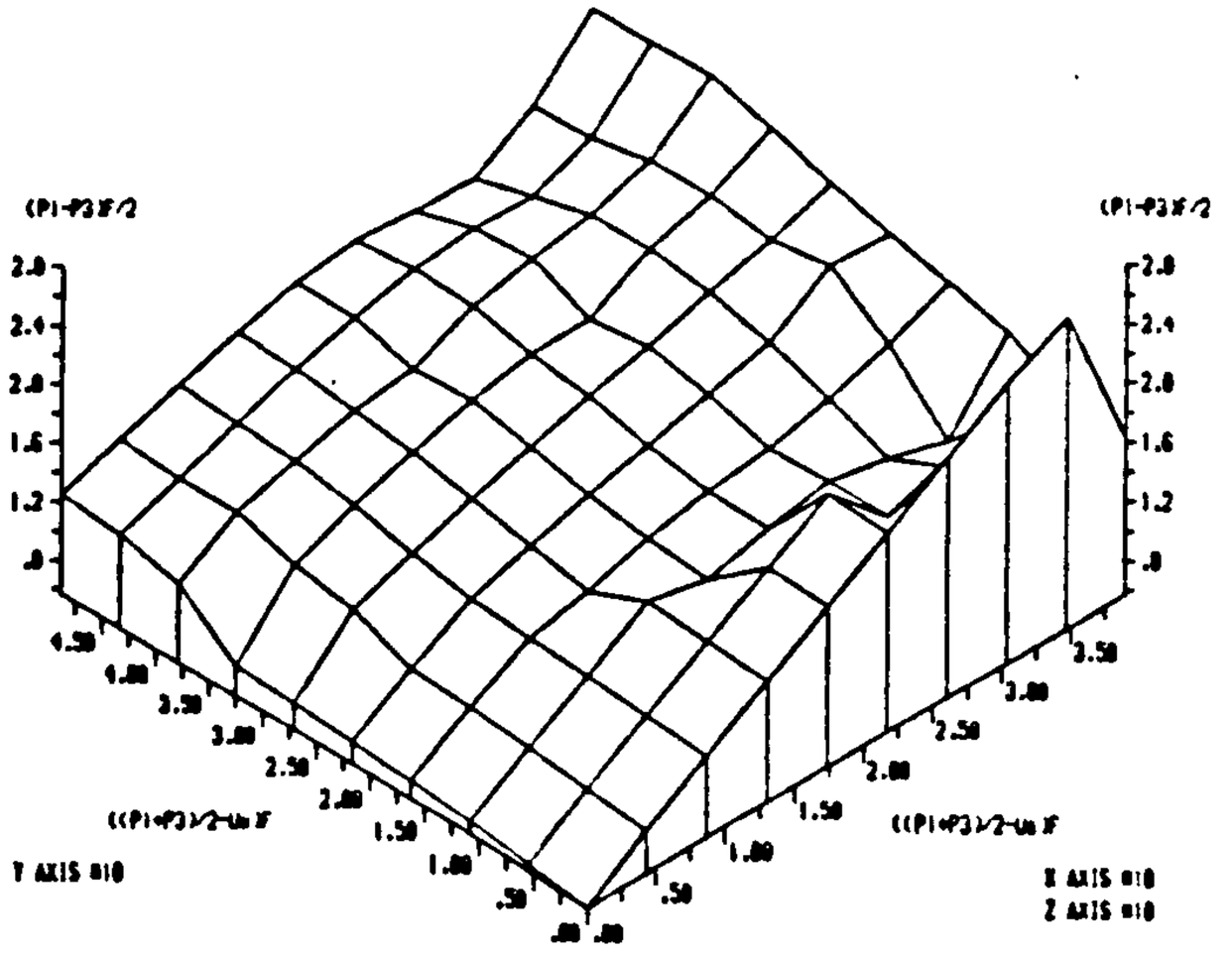

THE SHEAR STRENGTH DATA FOR BAREHEAD SILT FROM CU TESTS (I.B.DONALD,1961)

(UNITS IN POUNDS PER SQ. INCHES)

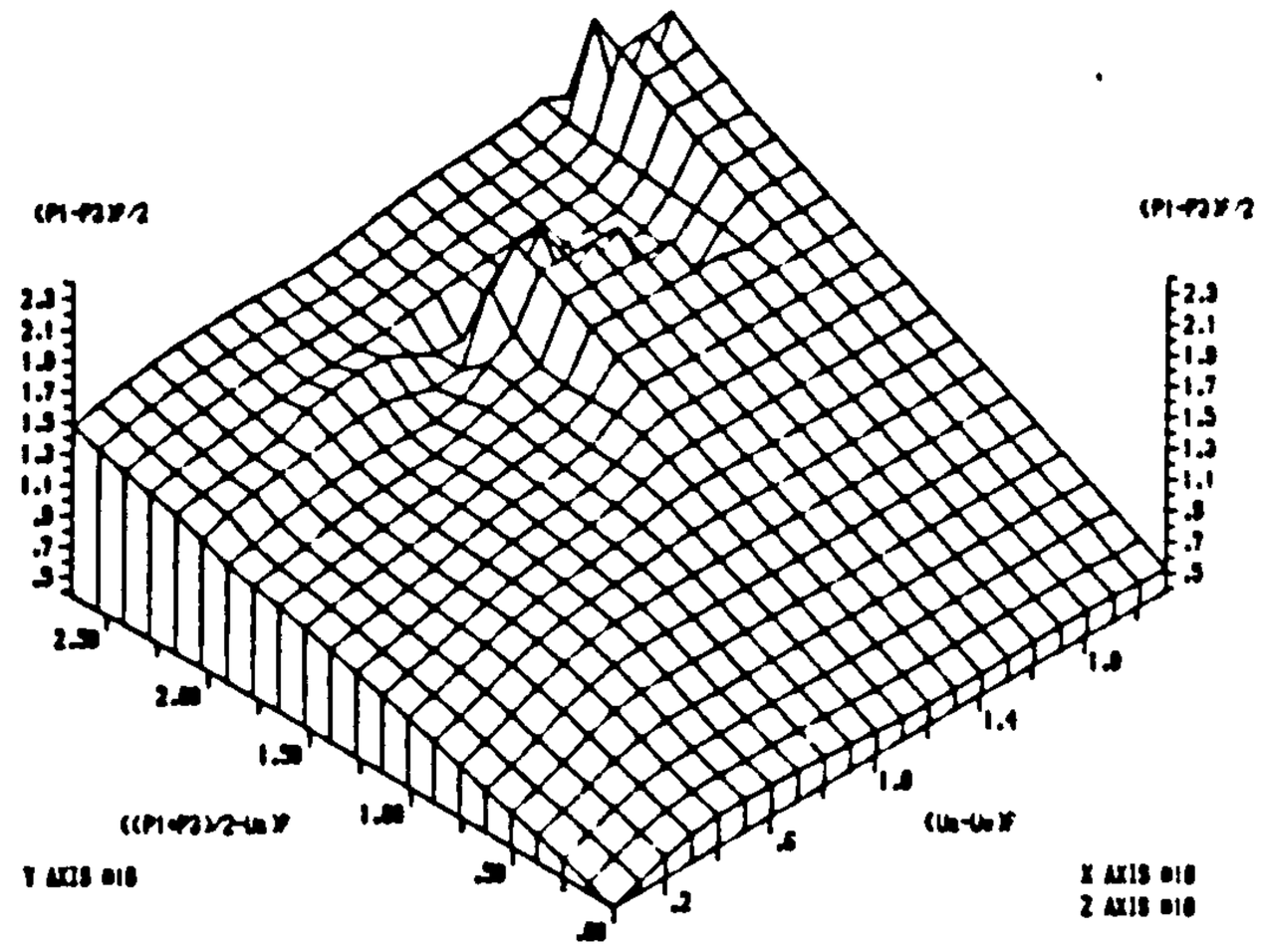

THE SHEAR STRENGTH DATA FOR BAREHEAD SILT FROM DRAINED TESTS (I.B.DONALD,1981)

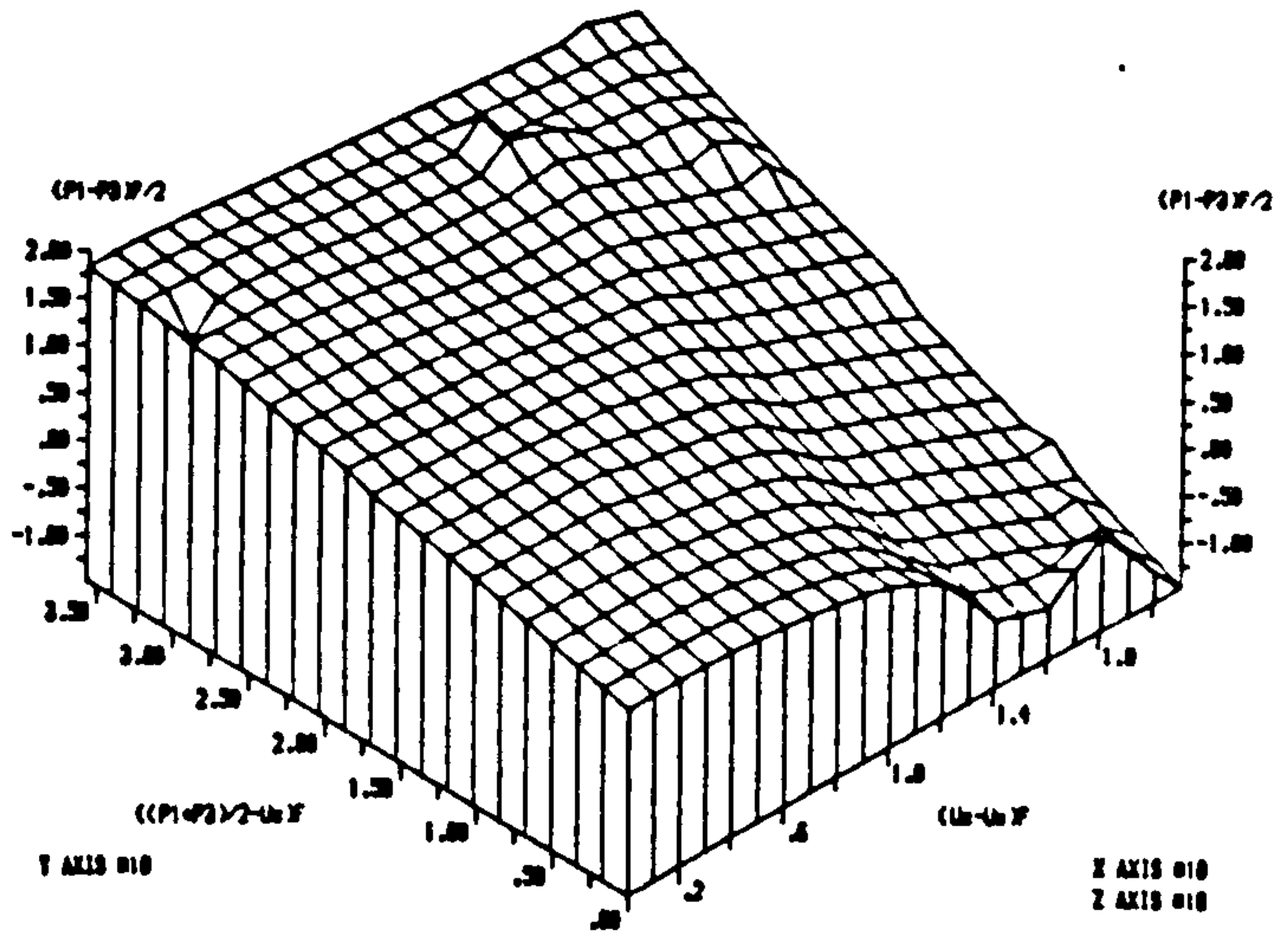

THE SHEAR STRENGTH DATA FOR BAREHEAD SILT FROM DRAINED TESTS (I.B.DONALD,1981)

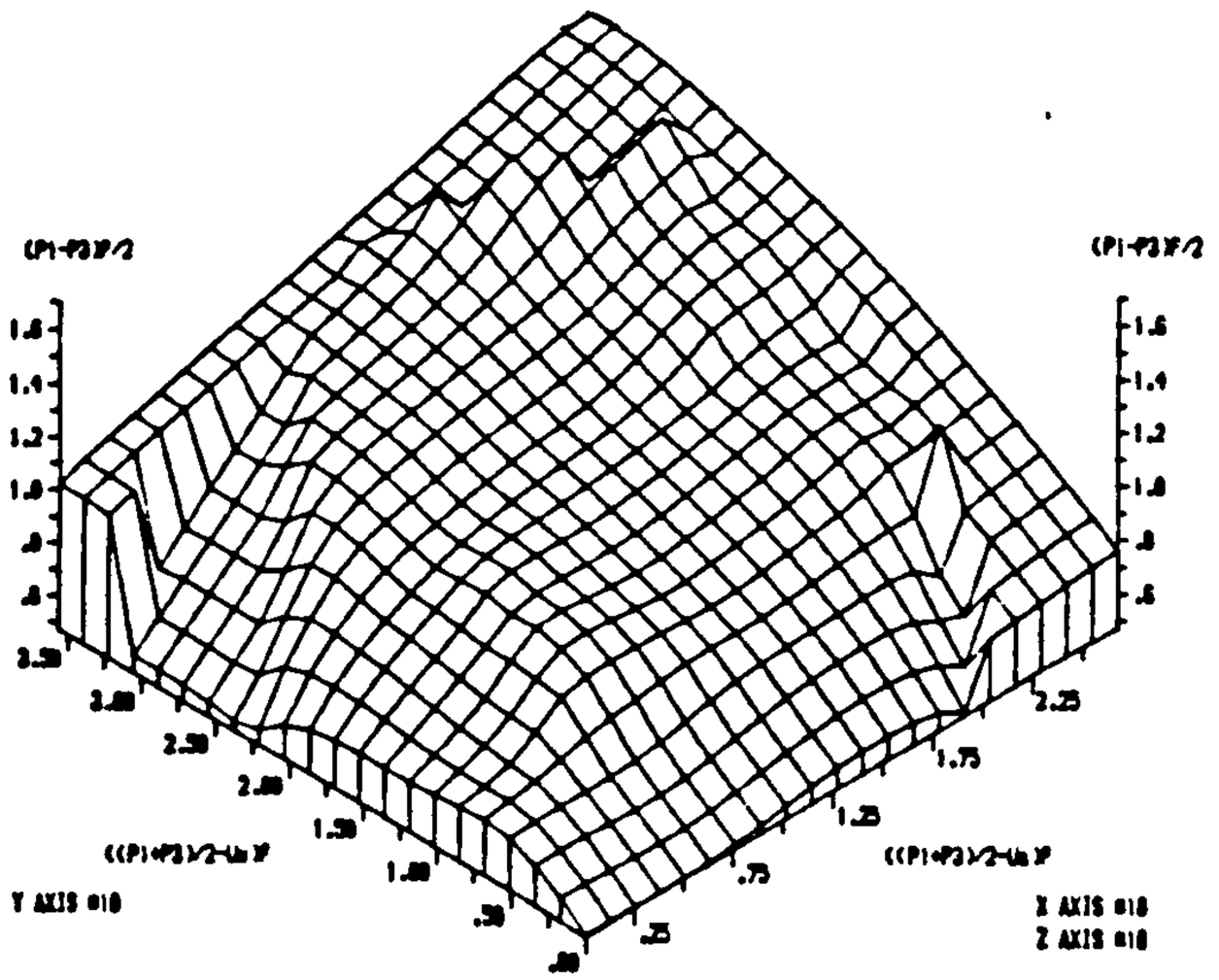

THE SHEAR STRENGTH DATA FOR BAREHEAD SILT FROM DRAINED TESTS (I.B.DONALD,1981)

(UNITS IN POUNDS PER SQ. INCHES)

A8.4.3 Blight(1961)

The following summarises all the results of tests on saturated compacted soils and partly saturated compacted soils by Blight(1961).

(i) Numerical method

Ialybont clay (maximum stress ratio)

```
**************************************************************
 INPUT COHESION,C´ IN P.S.I. IS 0

 INPUT ANGLE OF INTERNAL FRICTION IN DEGREES,Ø´ IS 36.3
**************************************************************
                                  b
 SUCTION ANGLE IN DEGREES,Ø   IS 5.98

 SUCTION ANGLE IN DEGREES,Ø° IS -32.2

 CORRECTED COHESION,C´ IN P.S.I. IS 2.12
                                          b
 CORRELATION FACTOR FOR SUCTION ANGLE(Ø ),R IS 0.61
**************************************************************
```

Ialybont clay(maximum deviator stress)

```
**************************************************************
 INPUT COHESION,C´ IN P.S.I. IS 0

 INPUT ANGLE OF INTERNAL FRICTION IN DEGREES,Ø´ IS 36.3
**************************************************************
                                  b
 SUCTION ANGLE IN DEGREES,Ø   IS 4.23

 SUCTION ANGLE IN DEGREES,Ø° IS -33.45

 CORRECTED COHESION,C´ IN P.S.I. IS 2.95
                                          b
 CORRELATION FACTOR FOR SUCTION ANGLE(Ø ),R IS 0.48
**************************************************************
```

Mangla sbale(maximum stress ratio)

```
**************************************************************************
 INPUT COHESION,C´ IN P.S.I. IS 1.5

 INPUT ANGLE OF INTERNAL FRICTION IN DEGREES,Ø´ IS 24.1
**************************************************************************
                                    b
 SUCTION ANGLE IN DEGREES,Ø  IS 14.89

 SUCTION ANGLE IN DEGREES,Ø° IS -10.28

 CORRECTED COHESION,C´ IN P.S.I. IS 3.07
                                                  b
 CORRELATION FACTOR FOR SUCTION ANGLE(Ø ),R IS 0.92
**************************************************************************
```

Mangla sbale(maximum deviator stress)

```
**************************************************************************
 INPUT COHESION,C´ IN P.S.I. IS 1.5

 INPUT ANGLE OF INTERNAL FRICTION IN DEGREES,Ø´ IS 24.1
**************************************************************************
                                    b
 SUCTION ANGLE IN DEGREES,Ø  IS 16.27

 SUCTION ANGLE IN DEGREES,Ø° IS -8.84

 CORRECTED COHESION,C´ IN P.S.I. IS 2.44
                                                  b
 CORRELATION FACTOR FOR SUCTION ANGLE(Ø ),R IS 0.93
**************************************************************************
```

Selset clay(maximum stress ratio)

****

INPUT COHESION,C′ IN P.S.I. IS 0

INPUT ANGLE OF INTERNAL FRICTION IN DEGREES,Ø′ IS 26.4

****

$\emptyset_b$ SUCTION ANGLE IN DEGREES, IS 20.54

SUCTION ANGLE IN DEGREES,Ø* IS -6.94

CORRECTED COHESION,C′ IN P.S.I. IS 1.49

$\emptyset_b$ CORRELATION FACTOR FOR SUCTION ANGLE( ),R IS 0.96

****

Selset clay(maximum deviator stress)

****

INPUT COHESION,C′ IN P.S.I. IS 0

INPUT ANGLE OF INTERNAL FRICTION IN DEGREES,Ø′ IS 26.4

****

$\emptyset_b$ SUCTION ANGLE IN DEGREES, IS 21.15

SUCTION ANGLE IN DEGREES,Ø* IS -6.25

CORRECTED COHESION,C′ IN P.S.I. IS 0.74

$\emptyset_b$ CORRELATION FACTOR FOR SUCTION ANGLE( ),R IS 0.97

****

Vaich moraine(constant water-content tests)(Max. deviator stress)

****

INPUT COHESION,C′ IN P.S.I. IS 0

INPUT ANGLE OF INTERNAL FRICTION IN DEGREES,Ø′ IS 38

****

$\emptyset_b$ SUCTION ANGLE IN DEGREES, IS 1.17

SUCTION ANGLE IN DEGREES,Ø* IS -37.26

CORRECTED COHESION,C′ IN P.S.I. IS 1.33

$\emptyset_b$ CORRELATION FACTOR FOR SUCTION ANGLE( ),R IS 0.73

****

(iii) 3-dimensional graphical method

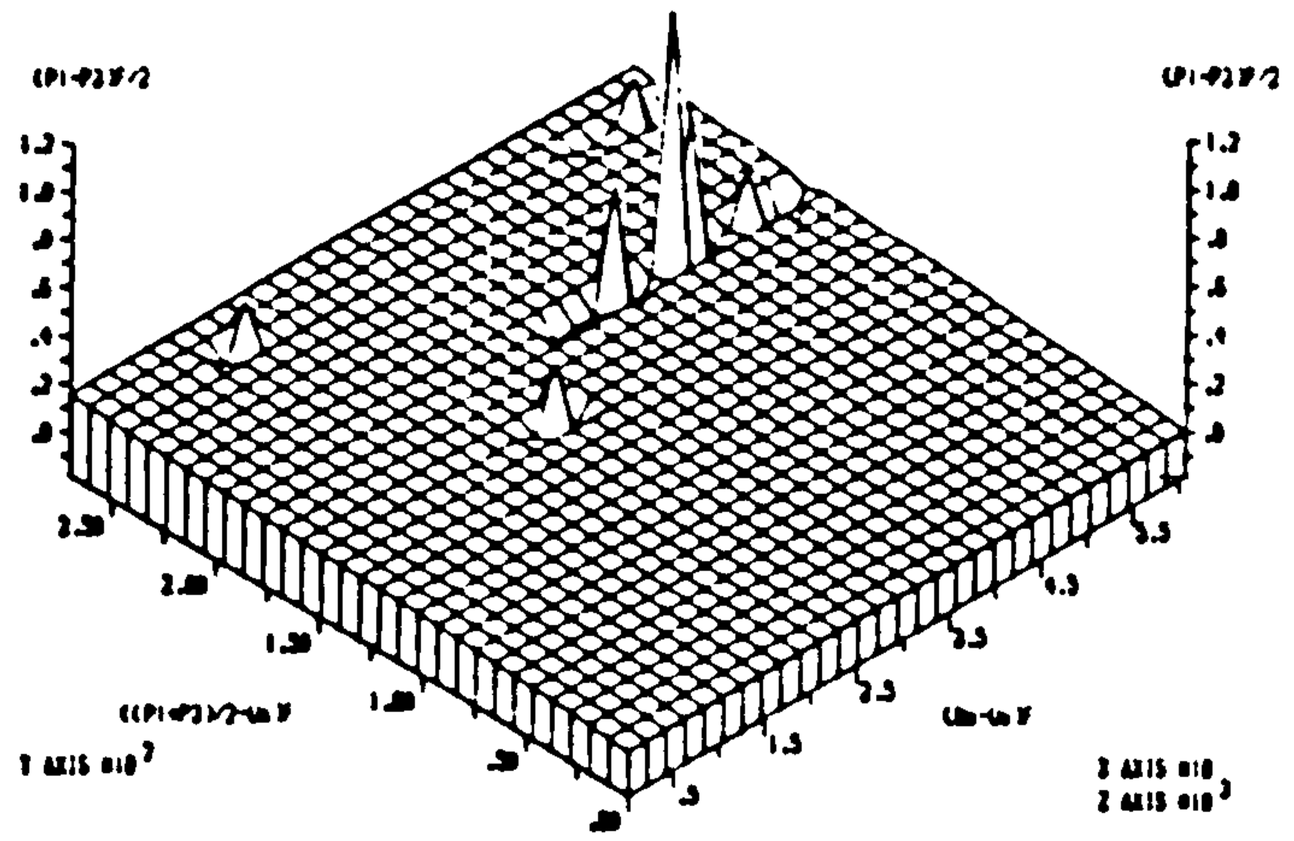

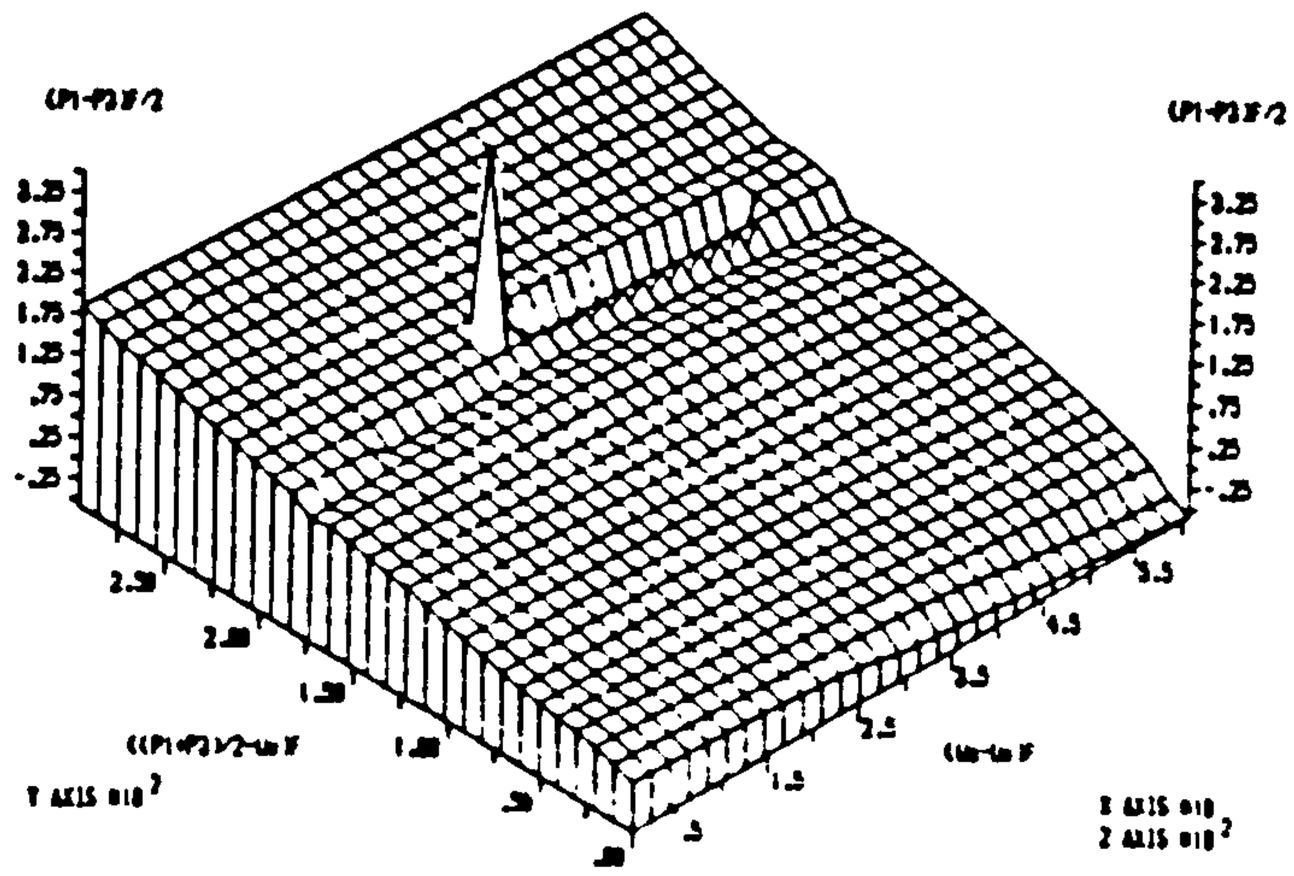

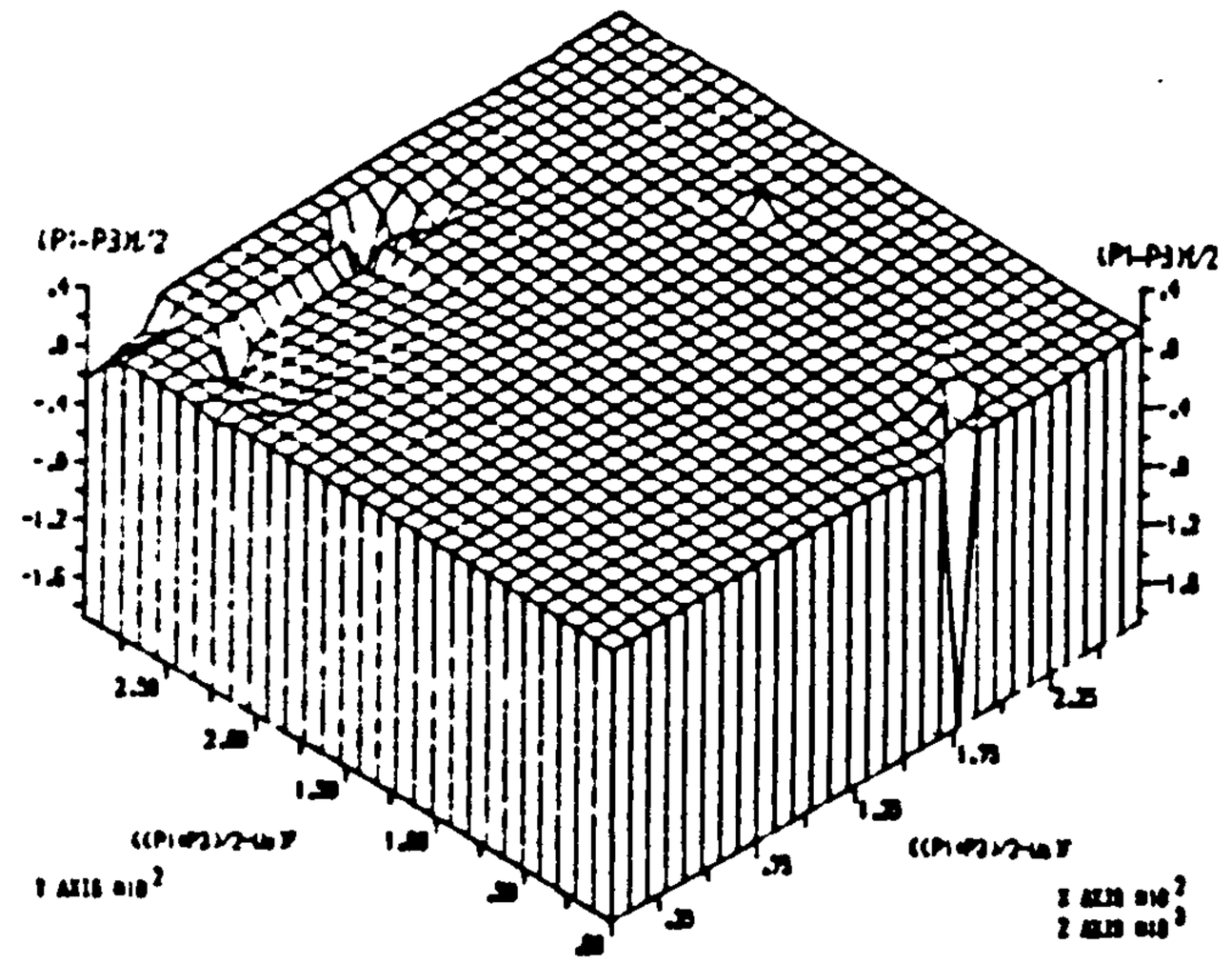

(UNITS IN POUNDS PER SQ. INCHES)
SHEAR STRENGTH DATA FOR TALYBONT CLAY UNDER CW CONDITION
(BLIGHT,1961)(FAILURE CRITERION: MAX. STRESS RATIO
i.e. $(\sigma_1-\sigma_3)/(\sigma_3-u_w)$.)

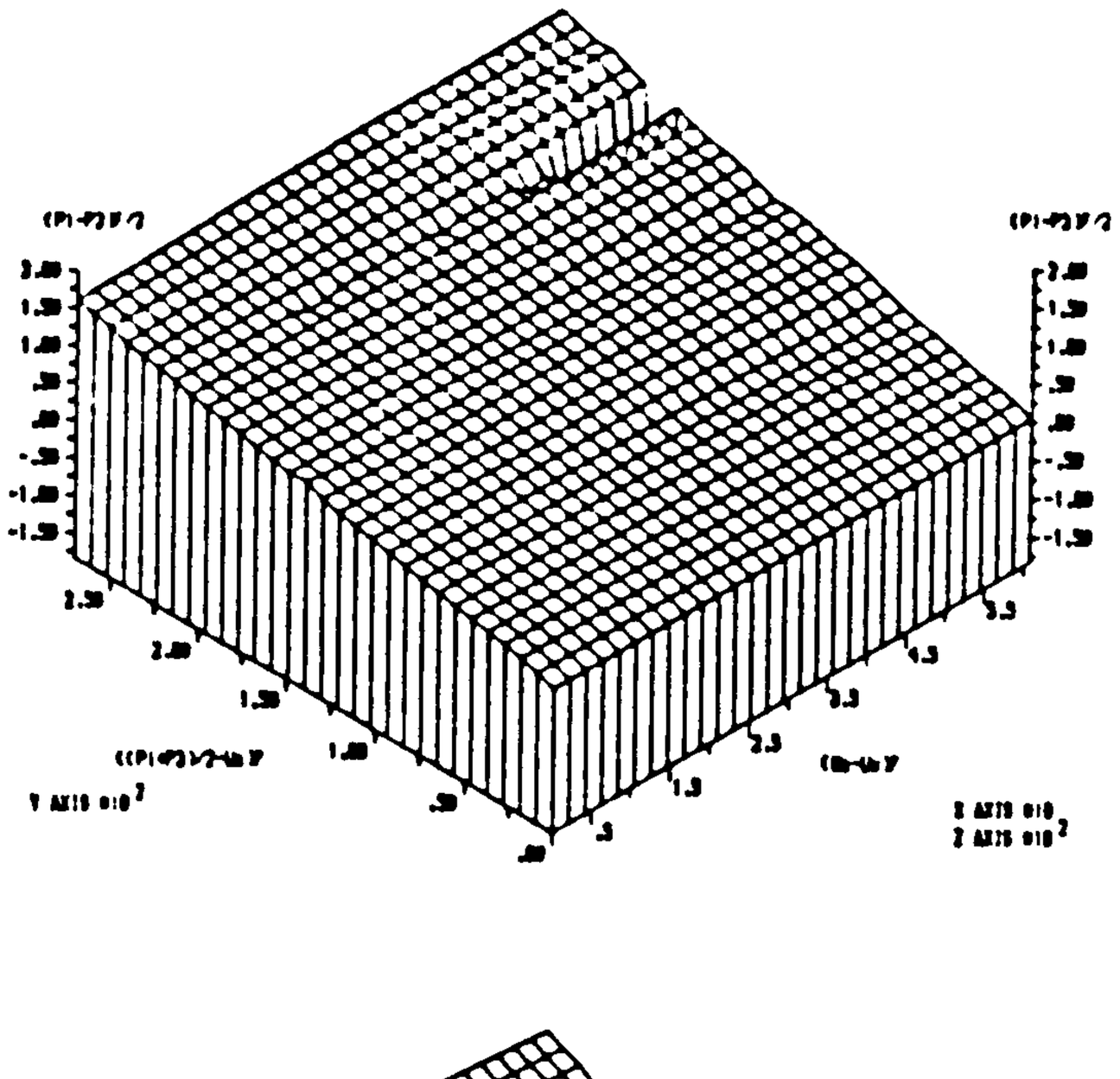

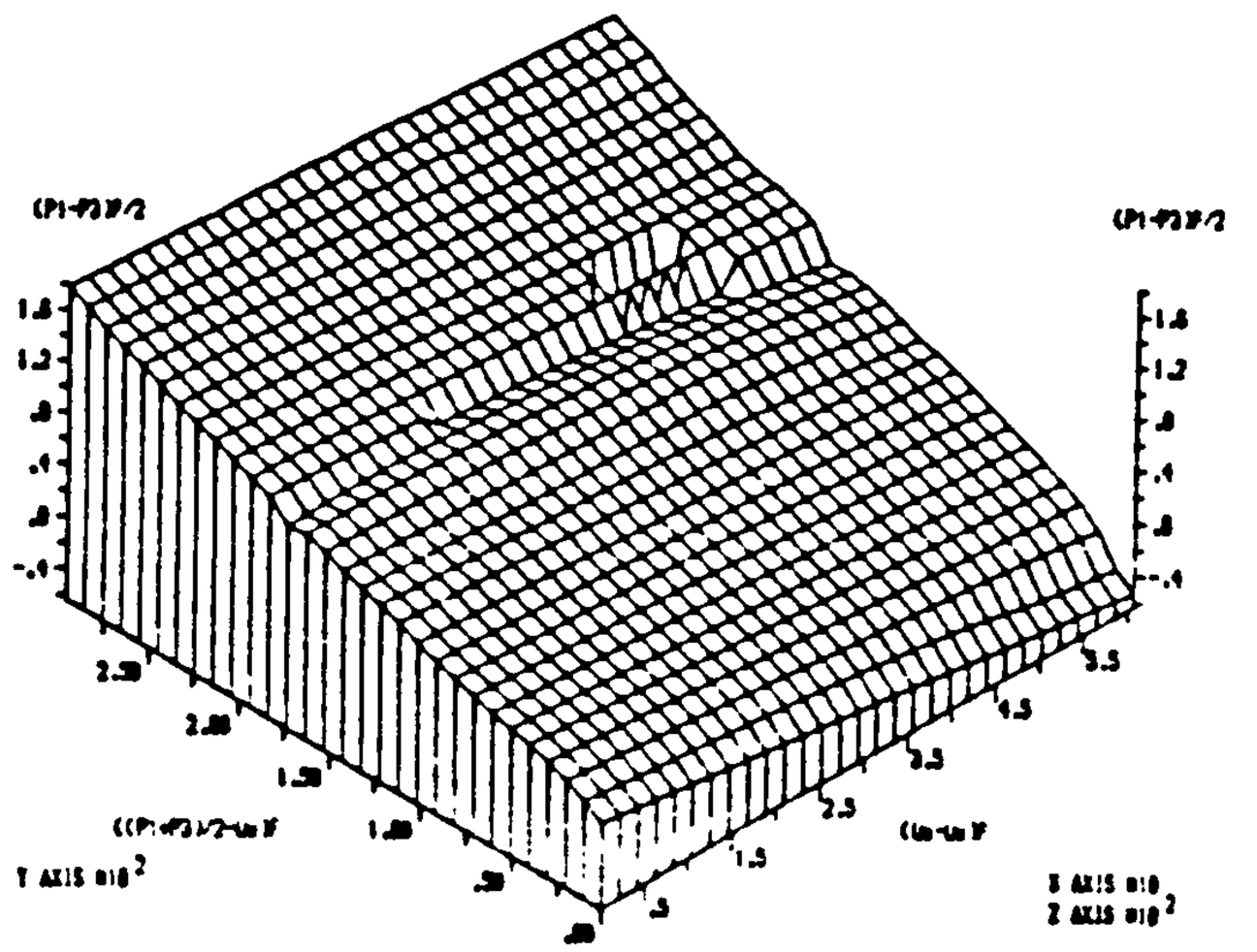

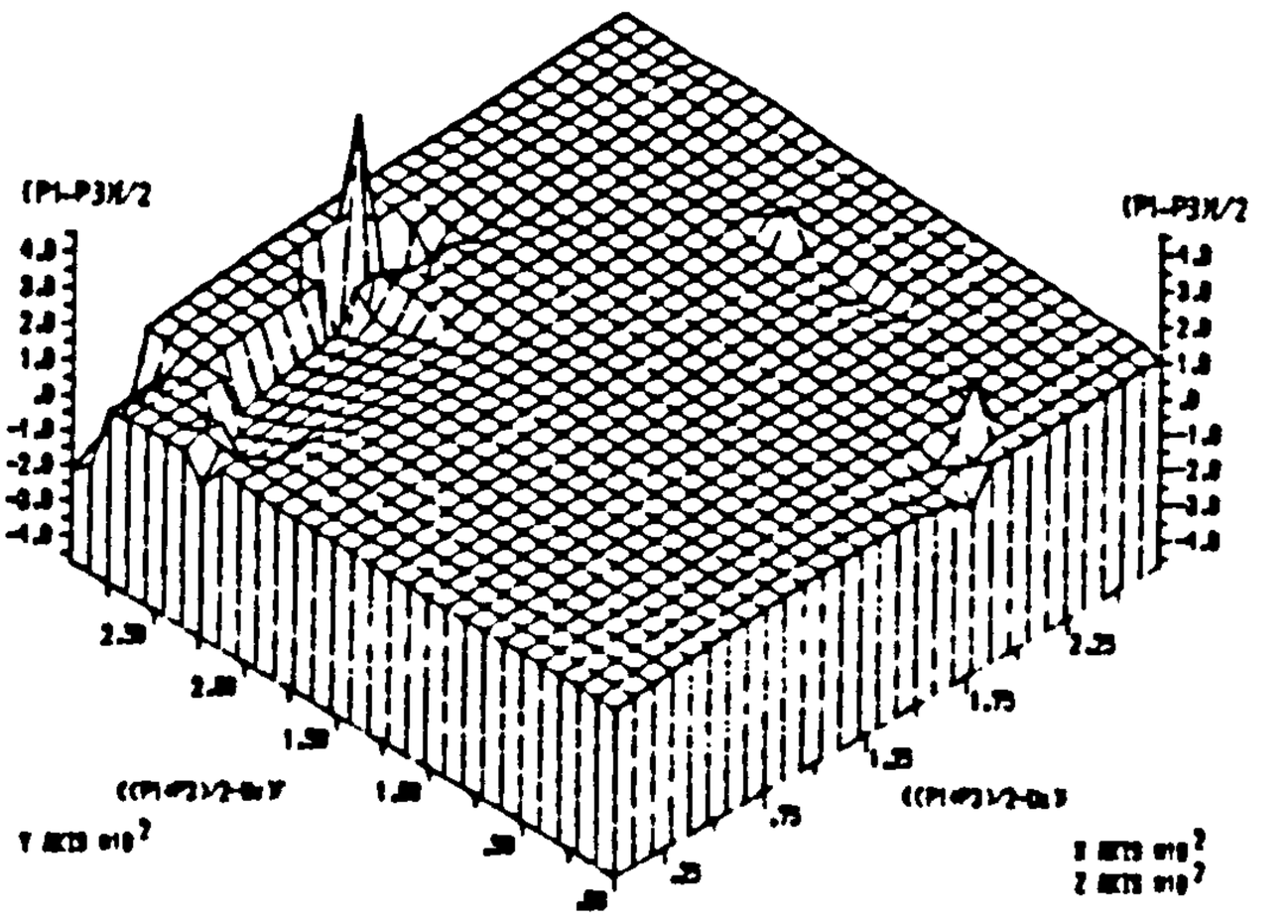

(UNITS IN POUNDS PER SQ. INCHES)

SHEAR STRENGTH DATA FOR TALYBONT CLAY UNDER CW CONDITION

(BLIGHT, 1961) (FAILURE CRITERION: MAX. DEVIATOR STRESS

i.e. $(\sigma_1 - \sigma_3)$).

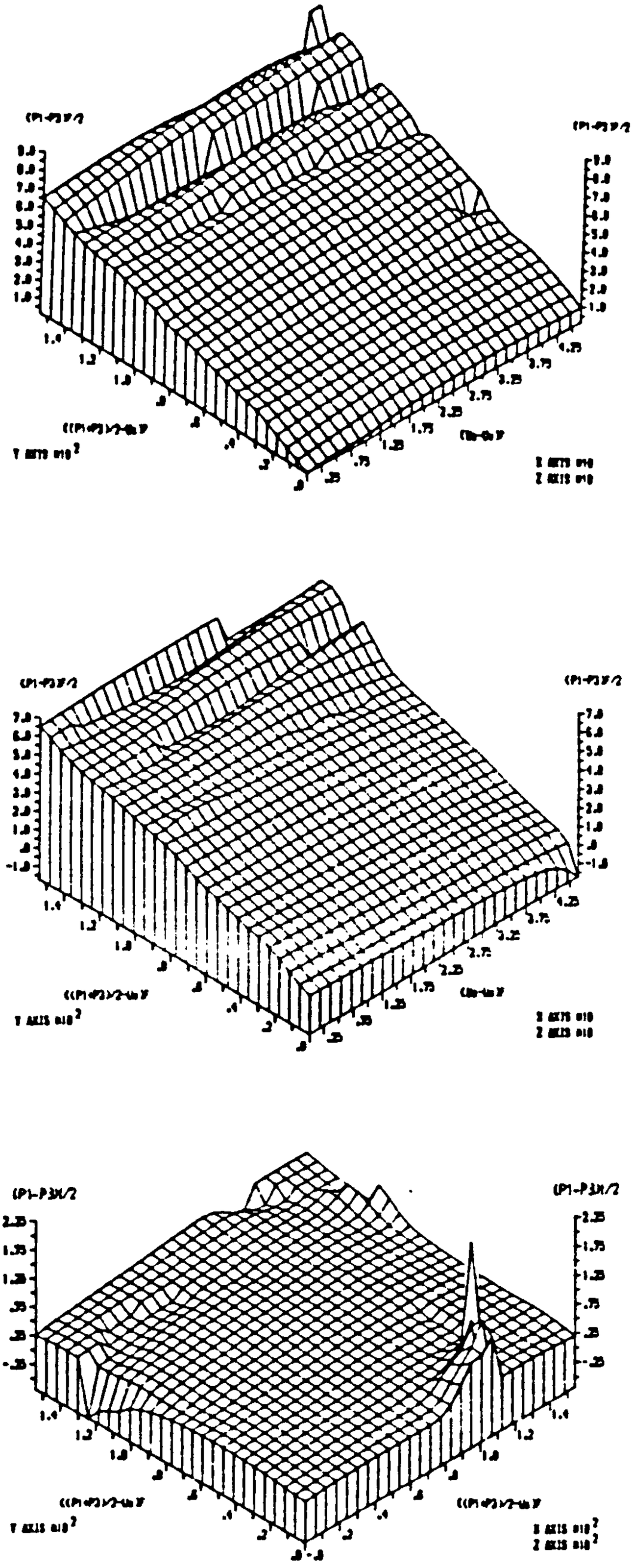

(UNITS IN POUNDS PER SQ. INCHES)
SHEAR STRENGTH DATA FOR MANGLA SHALE UNDER CW CONDITION

(BLIGHT,1961)(FAILULE CRITERION: MAX. STRESS RATIO

i.e. $(\sigma 1-\sigma 3)/(\sigma 3-Uw)$).

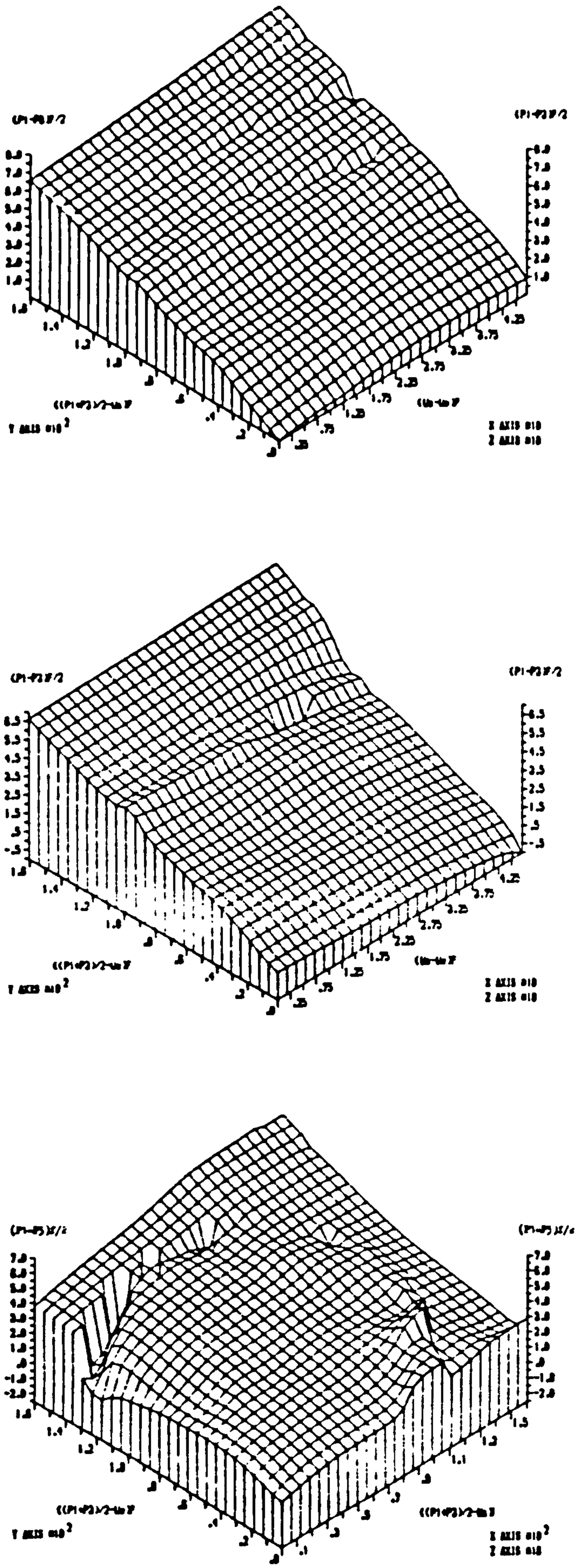

(UNITS IN POUNDS PER SQ. INCHES)

SHEAR STRENGTH DATA FOR MANGLA SEALE UNDER CW CONDITION

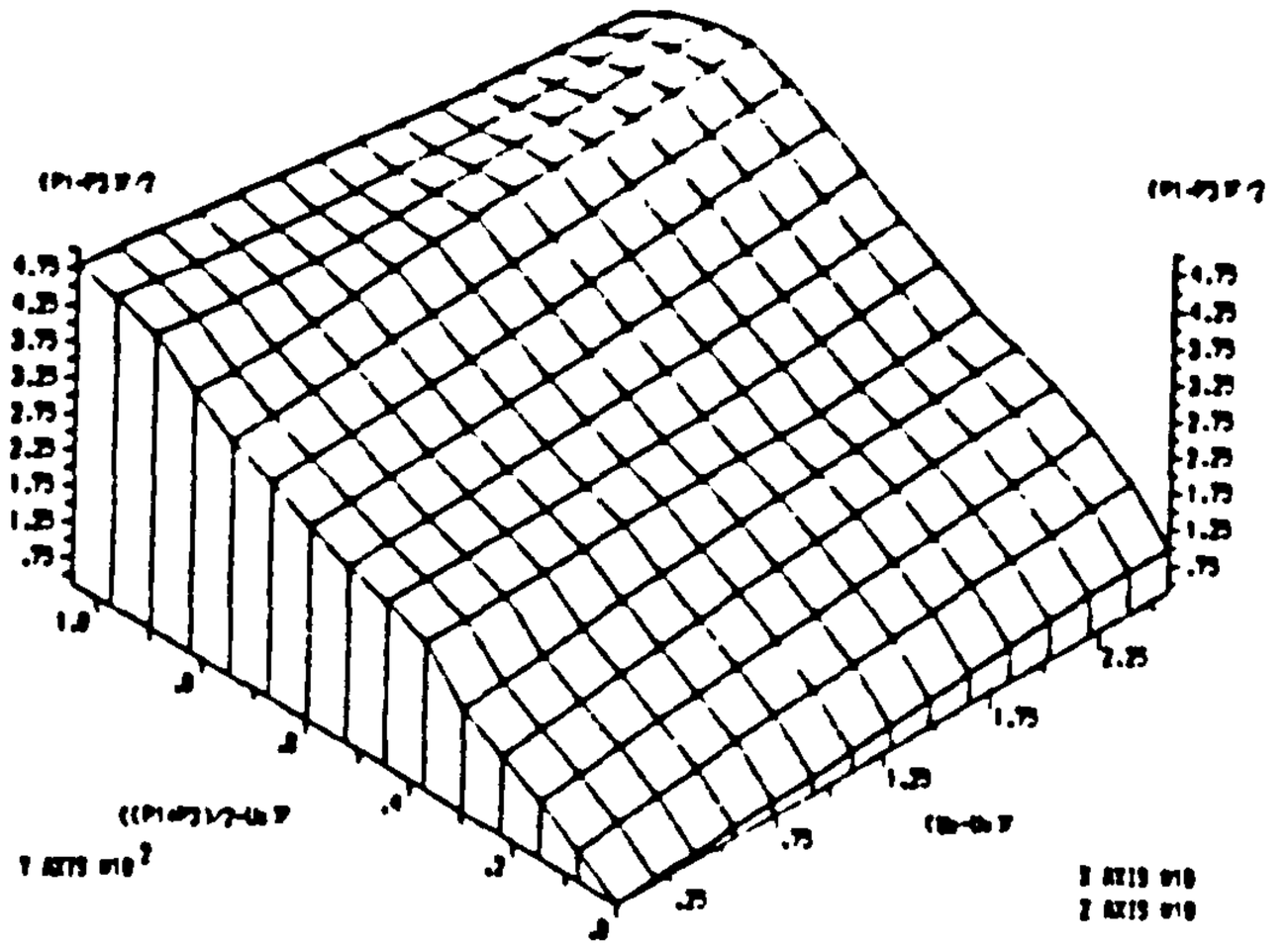

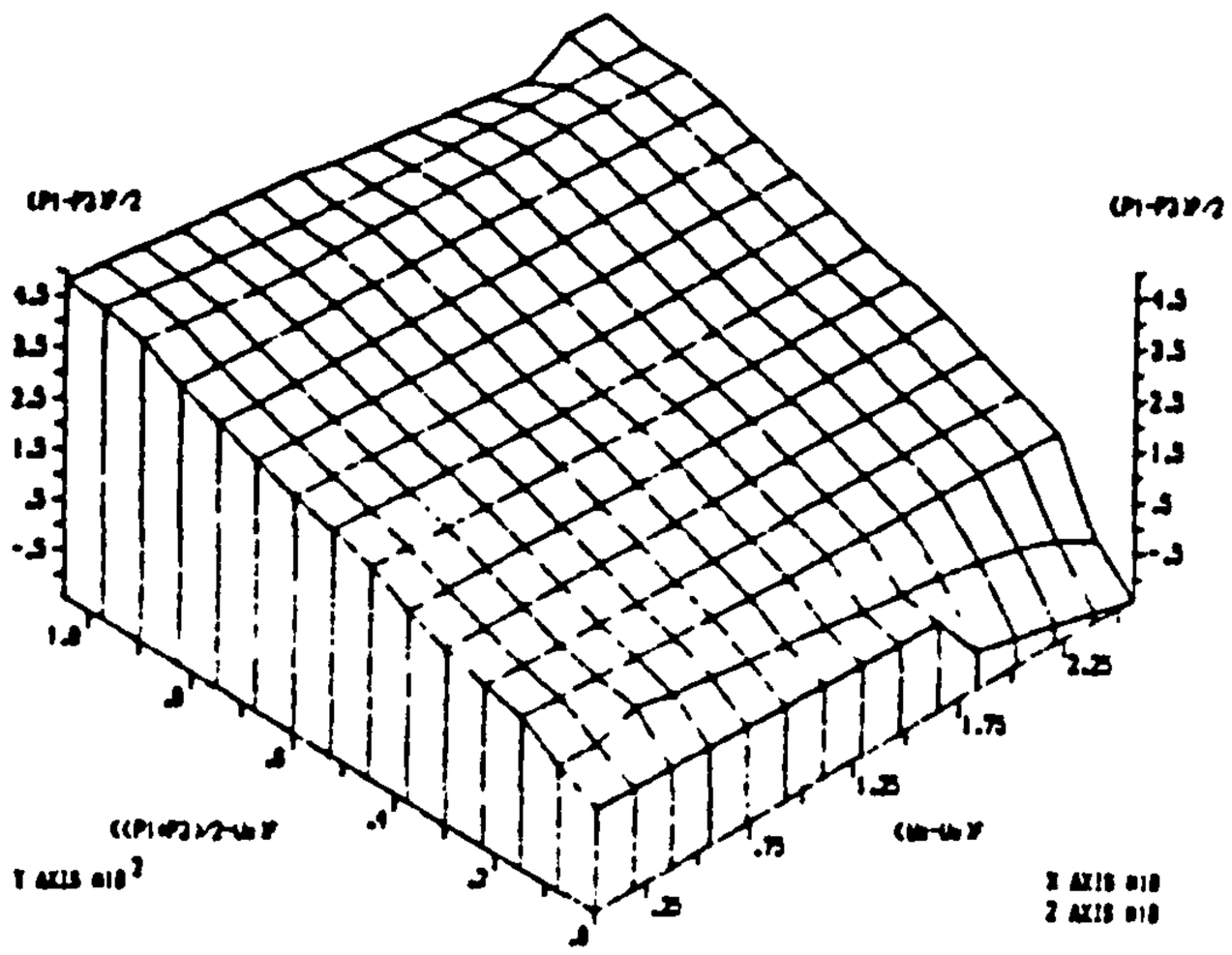

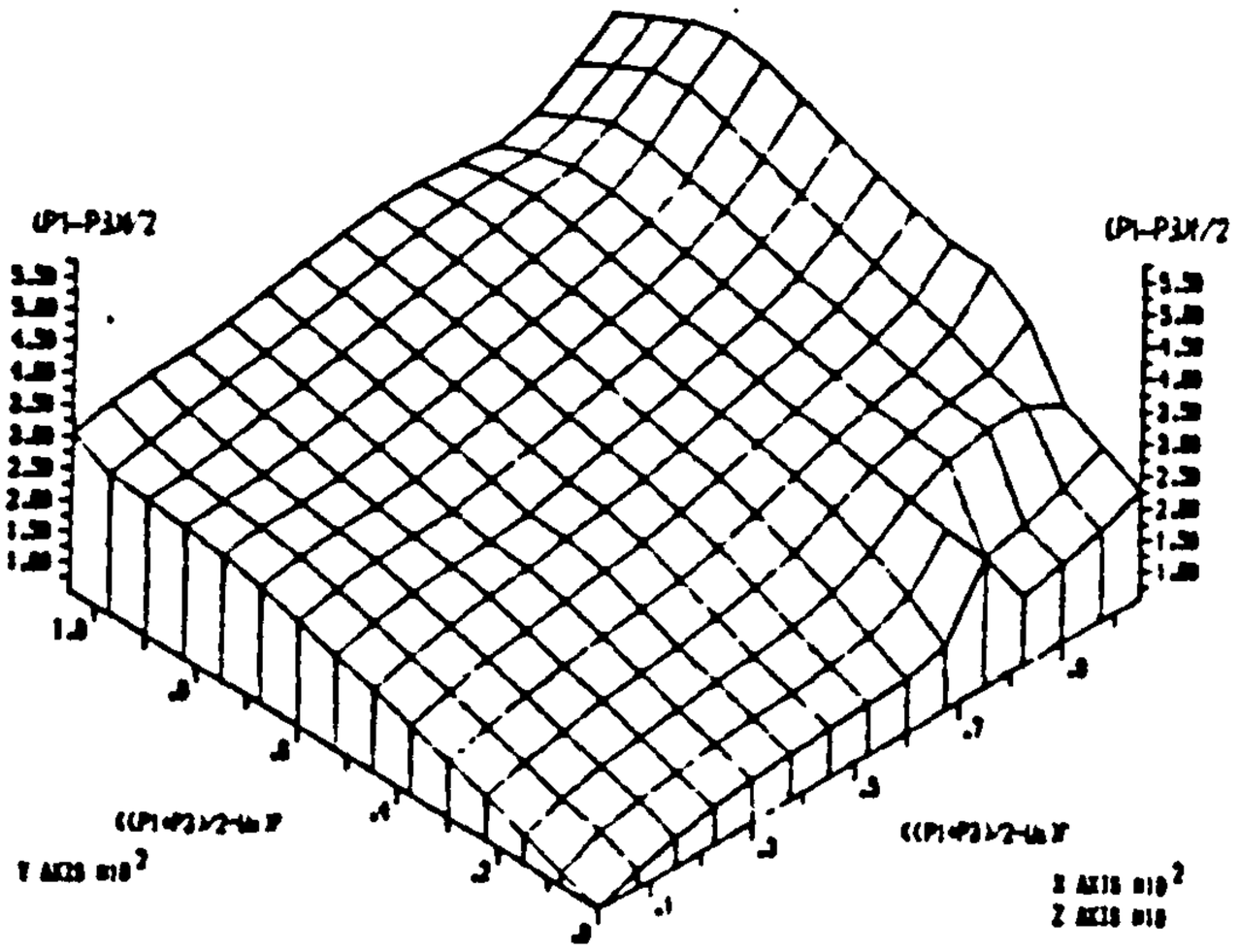

(UNITS IN POUNDS PER SQ. INCHES)
SHEAR STRENGTH DATA FOR SELSET CLAY UNDER CW CONDITION
(BLIGHT,1961)(FAILURE CRITERION: MAX. STRESS RATIO
i.e. $(\sigma 1-\sigma 3)/(\sigma 3-Uw)$).

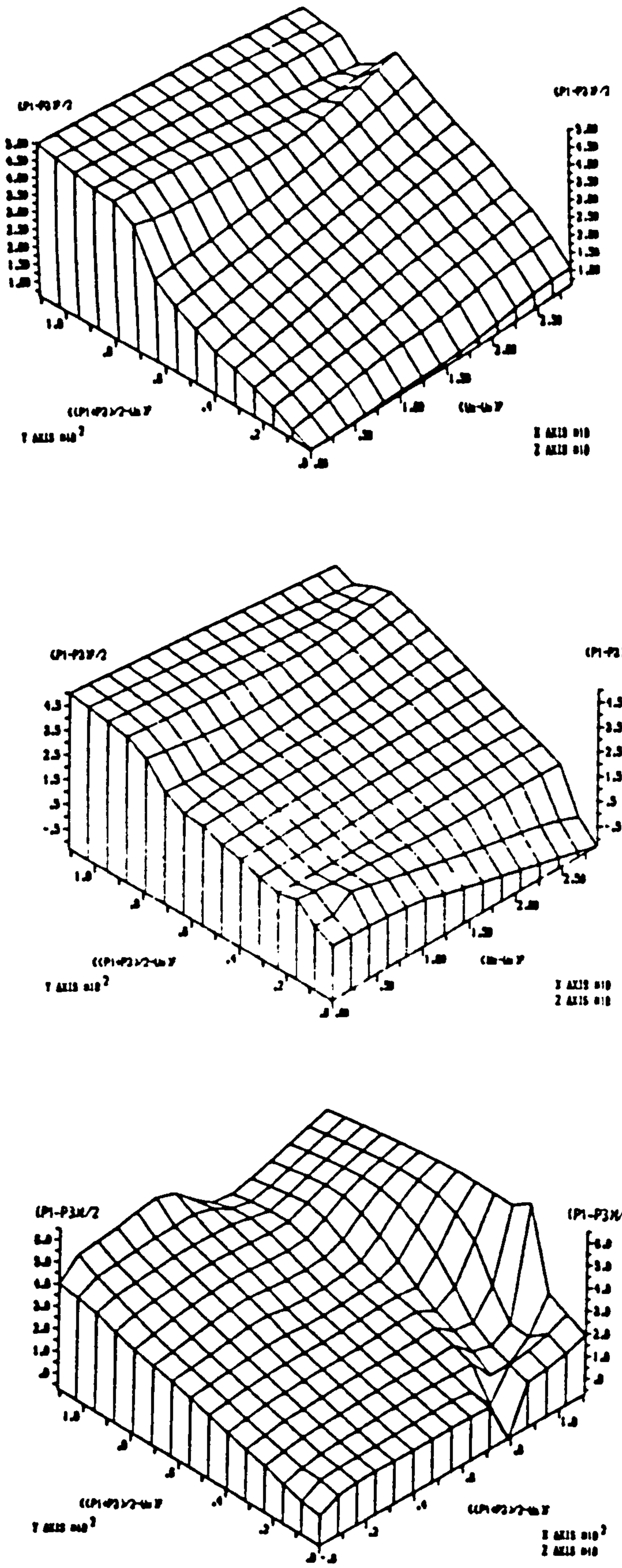

(UNITS IN POUNDS PER SQ. INCHES)
SHEAR STRENGTH DATA FOR SELSET CLAY UNDER CW CONDITION
(BLIGHT,1961)(FAILURE CRITERION: MAX. DEVIATOR STRESS
i.e. ($\sigma_1-\sigma_3$)).

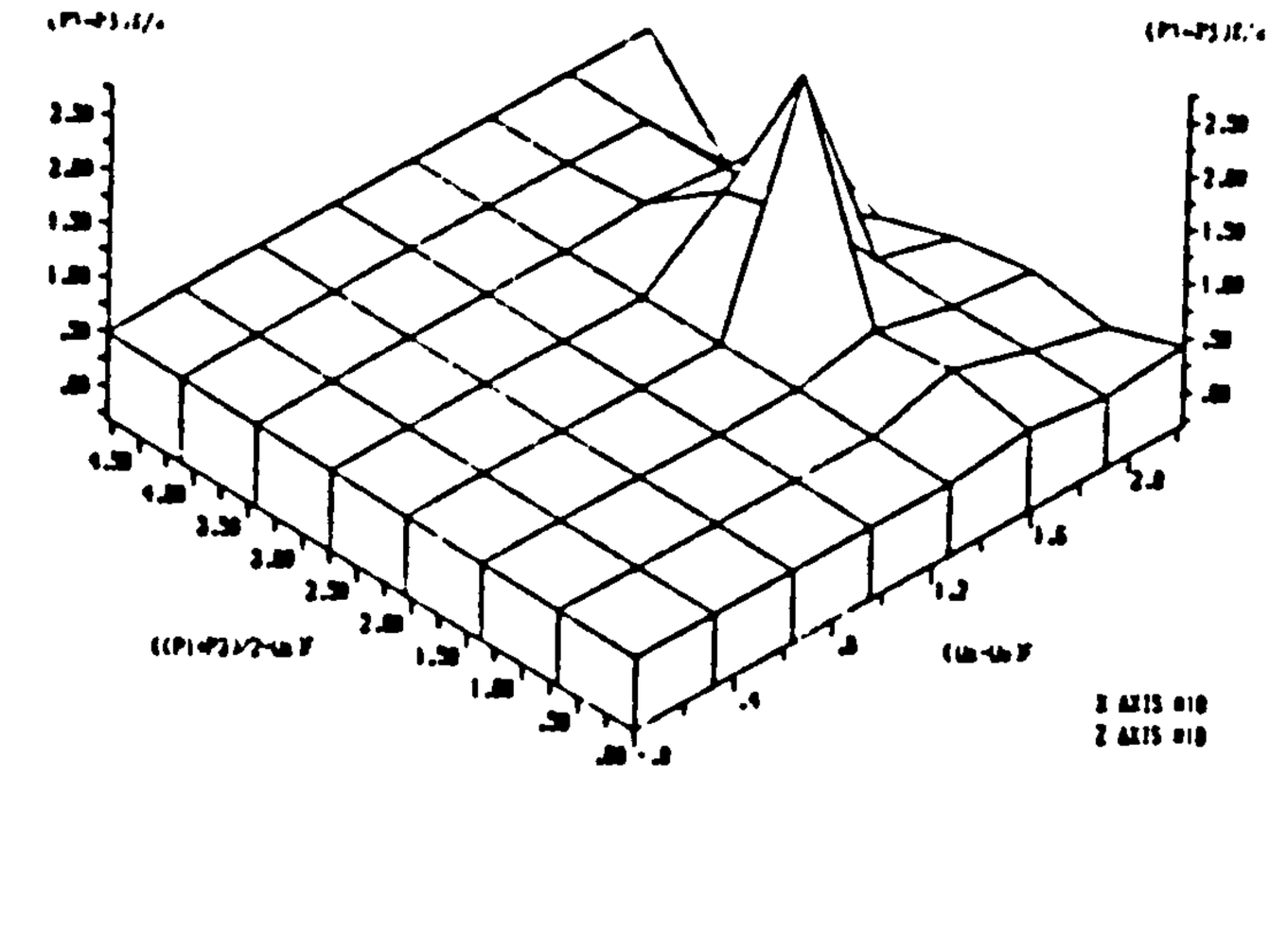

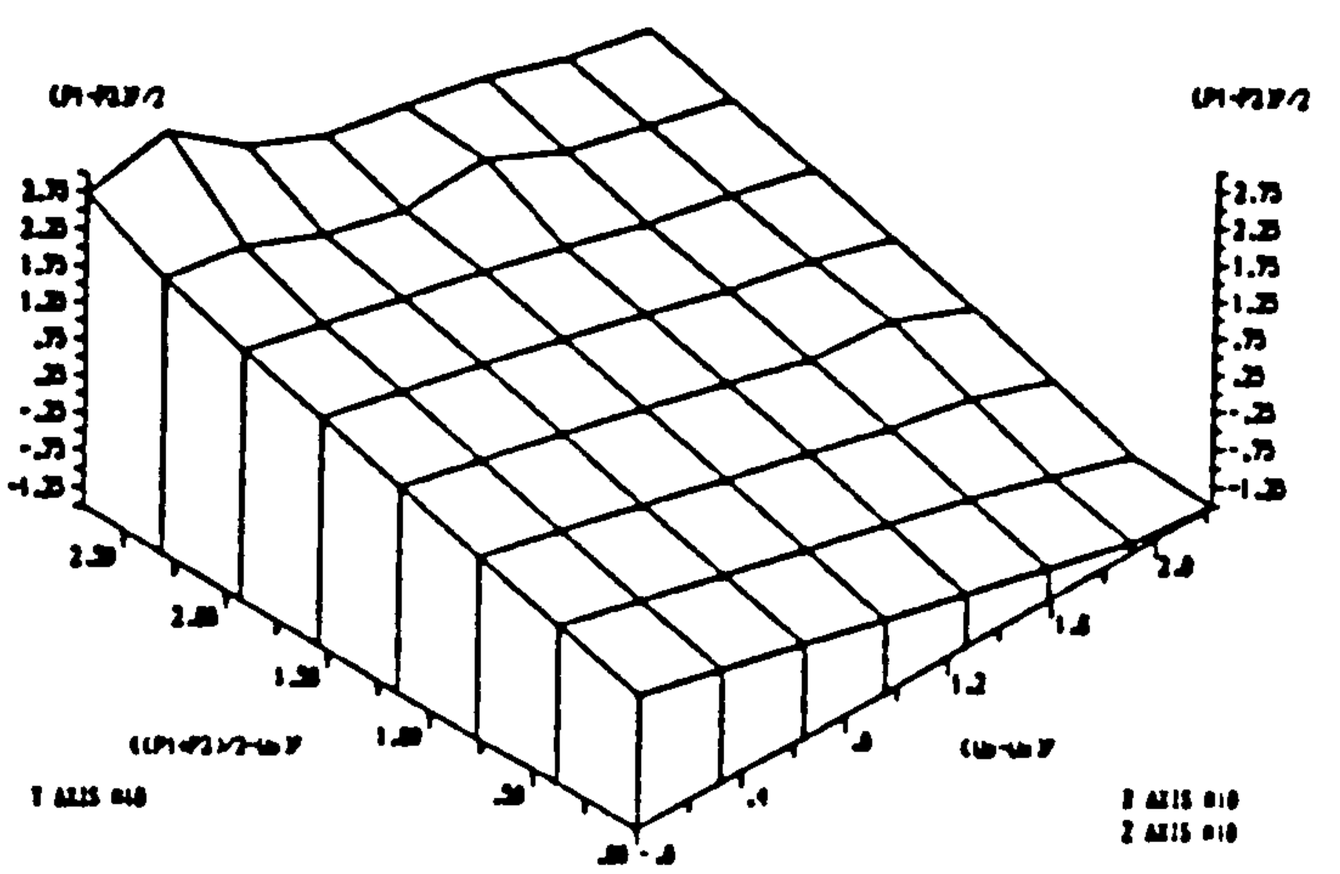

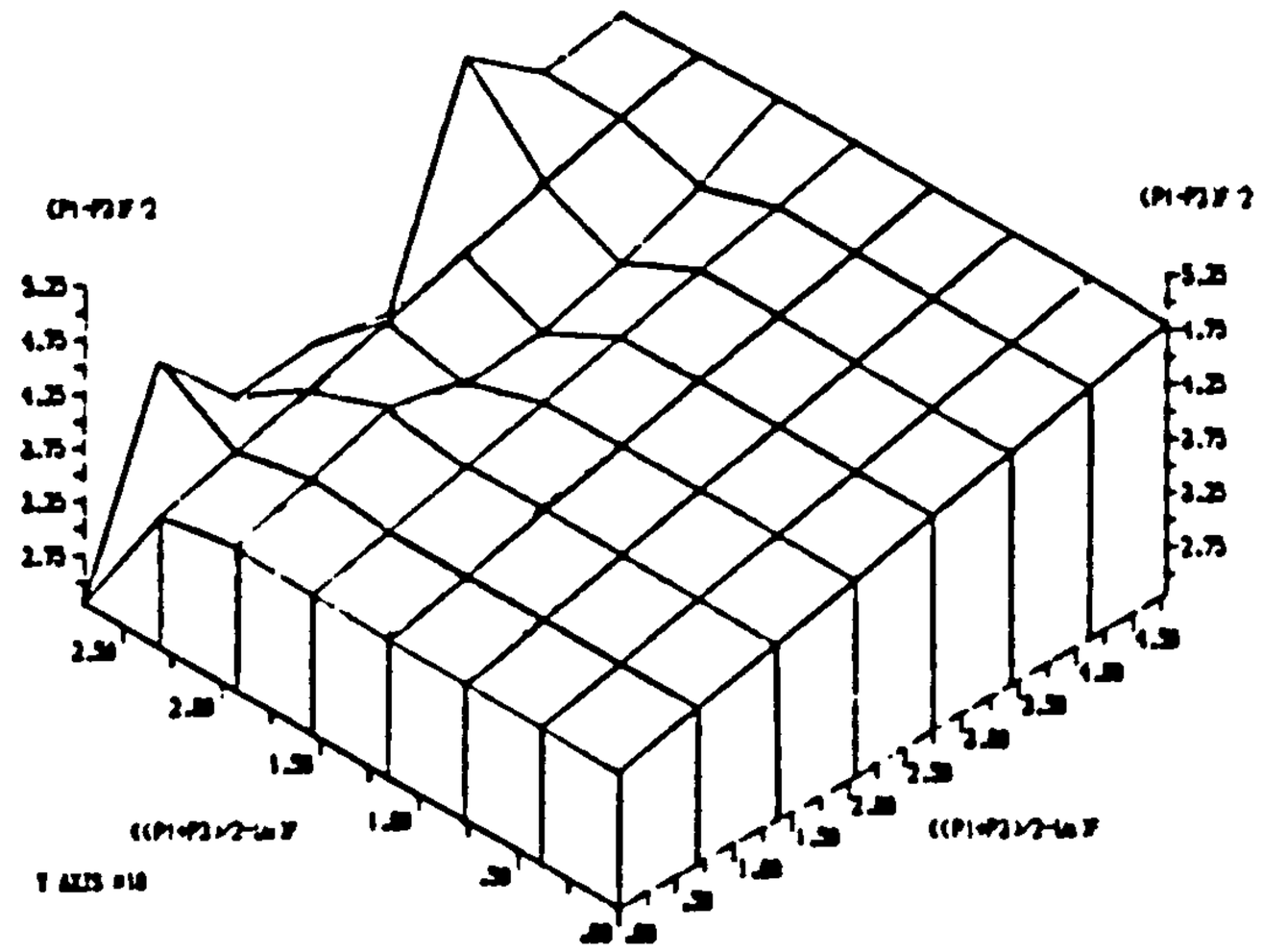

(UNITS IN POUNDS PER SQ. INCHES)
SHEAR STRENGTH DATA FOR VAICH MORAINE UNDER CW CONDITION

(BLIGHT,1961).

A8.4.4 Matyas(1963)

(i) Numerical method

Selset Boulder clay(tests on unsaturated soil specimens)

```
**************************************************
 INPUT COHESION,C´ IN P.S.I. IS 1.3

 INPUT ANGLE OF INTERNAL FRICTION IN DEGREES,Ø´ IS 24.7
**************************************************
                                   b
 SUCTION ANGLE IN DEGREES,Ø   IS 24.22

 SUCTION ANGLE IN DEGREES,Ø° IS -0.57

 CORRECTED COHESION,C´ IN P.S.I. IS 1.02
                                        b
 CORRELATION FACTOR FOR SUCTION ANGLE(Ø ),R IS 0.96
**************************************************
```

Red Sasumua clay(tests on unsaturated soil specimens)

```
**************************************************
 INPUT COHESION,C´ IN P.S.I. IS 3.6

 INPUT ANGLE OF INTERNAL FRICTION IN DEGREES,Ø´ IS 34
**************************************************
                                   b
 SUCTION ANGLE IN DEGREES,Ø   IS 31.94

 SUCTION ANGLE IN DEGREES,Ø° IS -2.92

 CORRECTED COHESION,C´ IN P.S.I. IS 0.79
                                        b
 CORRELATION FACTOR FOR SUCTION ANGLE(Ø ),R IS 0.96
**************************************************
```

(iii) 3-dimensional graphical method

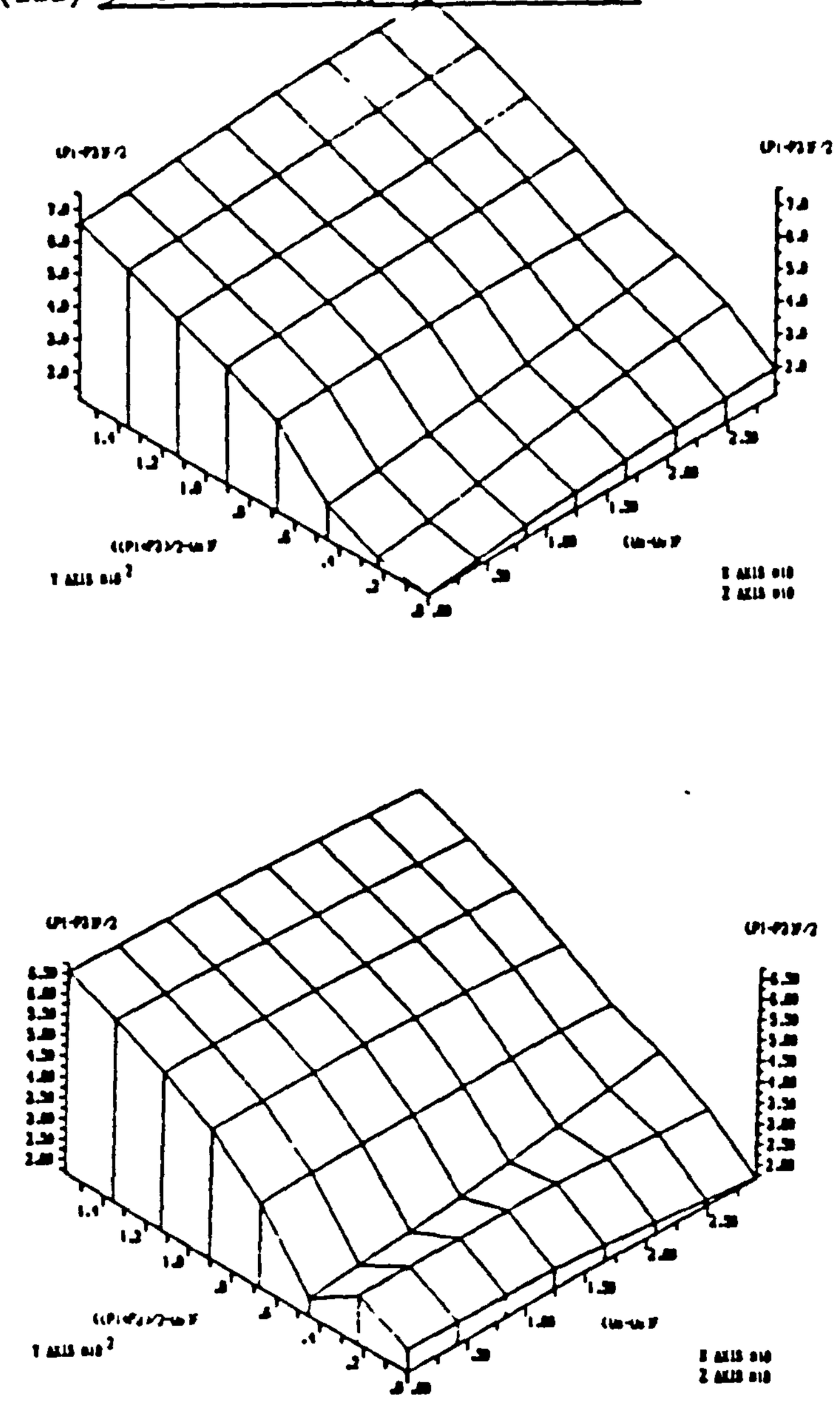

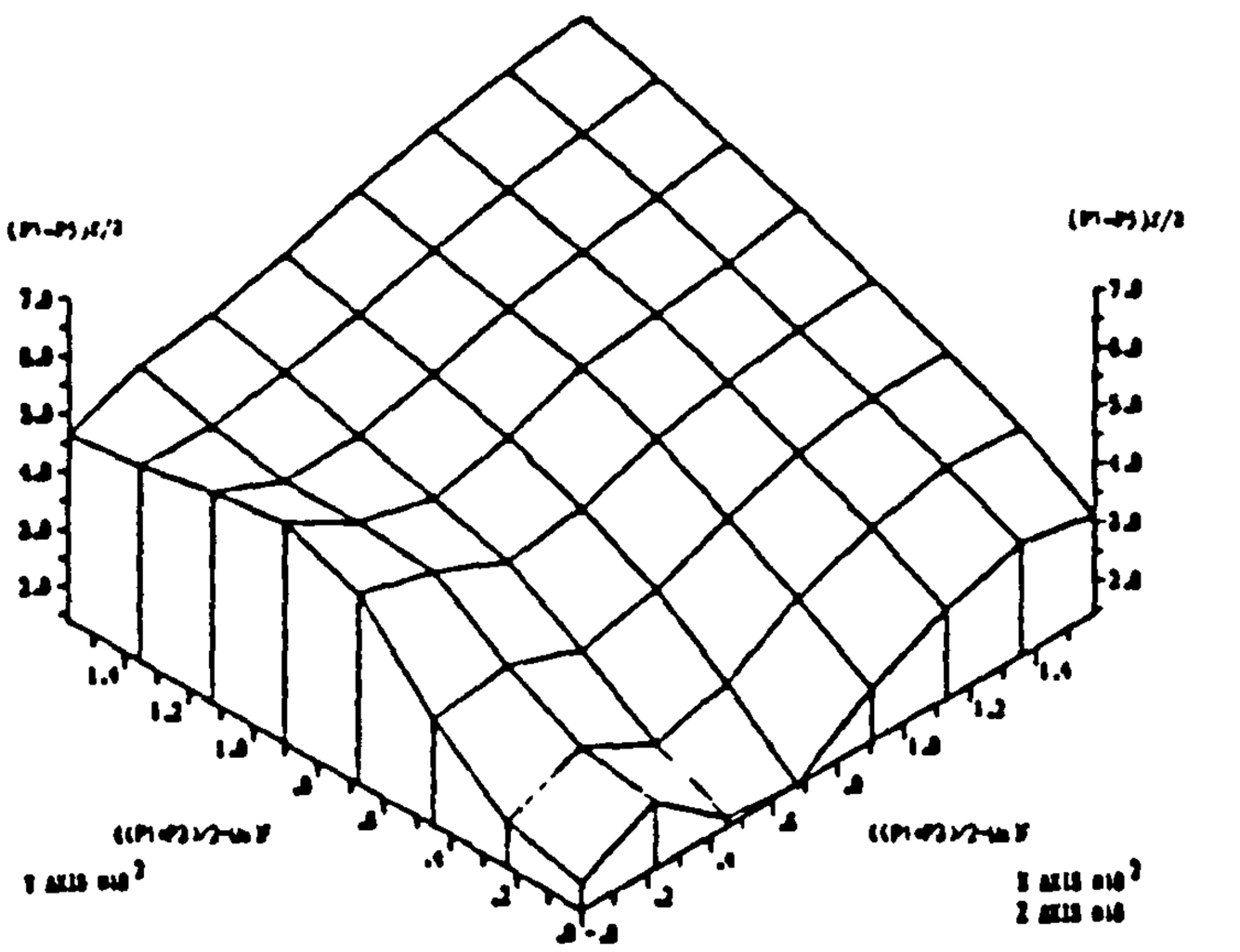

(UNITS IN POUNDS PER SQ. INCHES)
THE SHEAR STRENGTH DATA FOR SELSET BOULDER CLAY

(MATYAS,1963)(UNSATURATED SOILS ONLY).

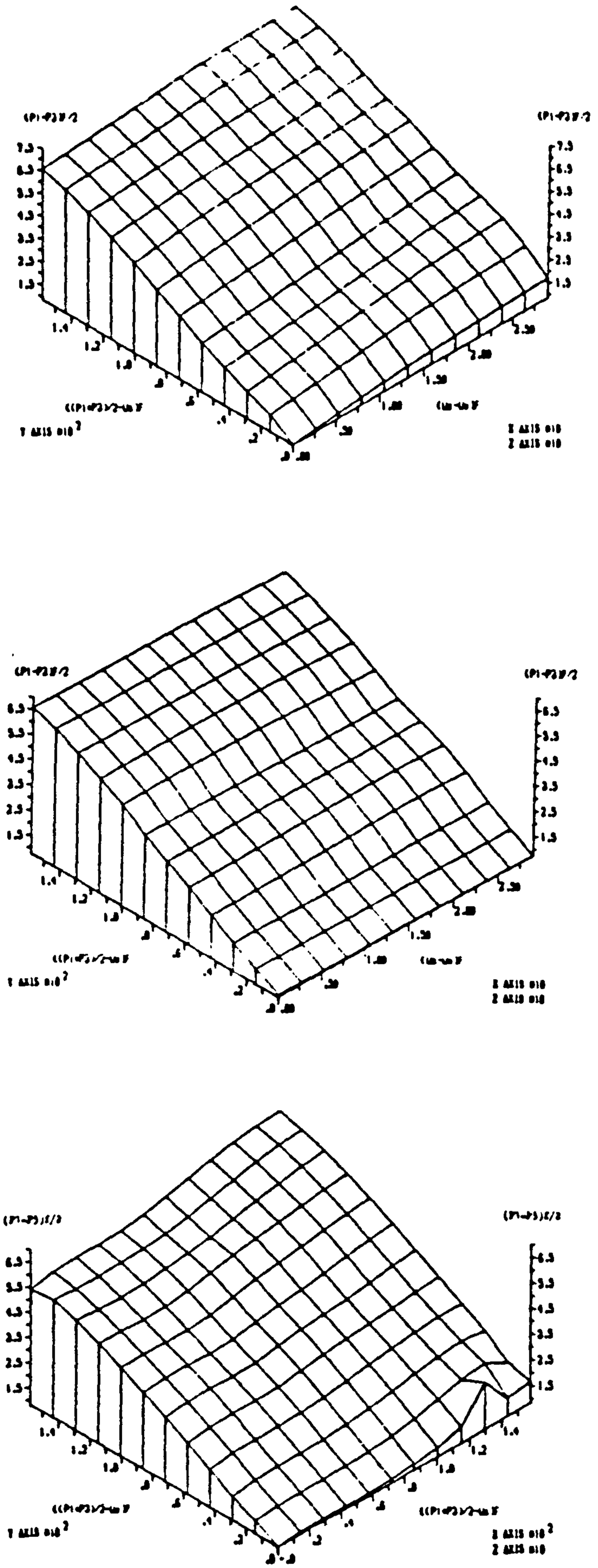

(UNITS IN POUNDS PER SQ. INCHES)
THE SHEAR STRENGTH DATA FOR SELSET BOULDER CLAY
(KATYAS,1963)(UNSATURATED & SATURATED SOILS).

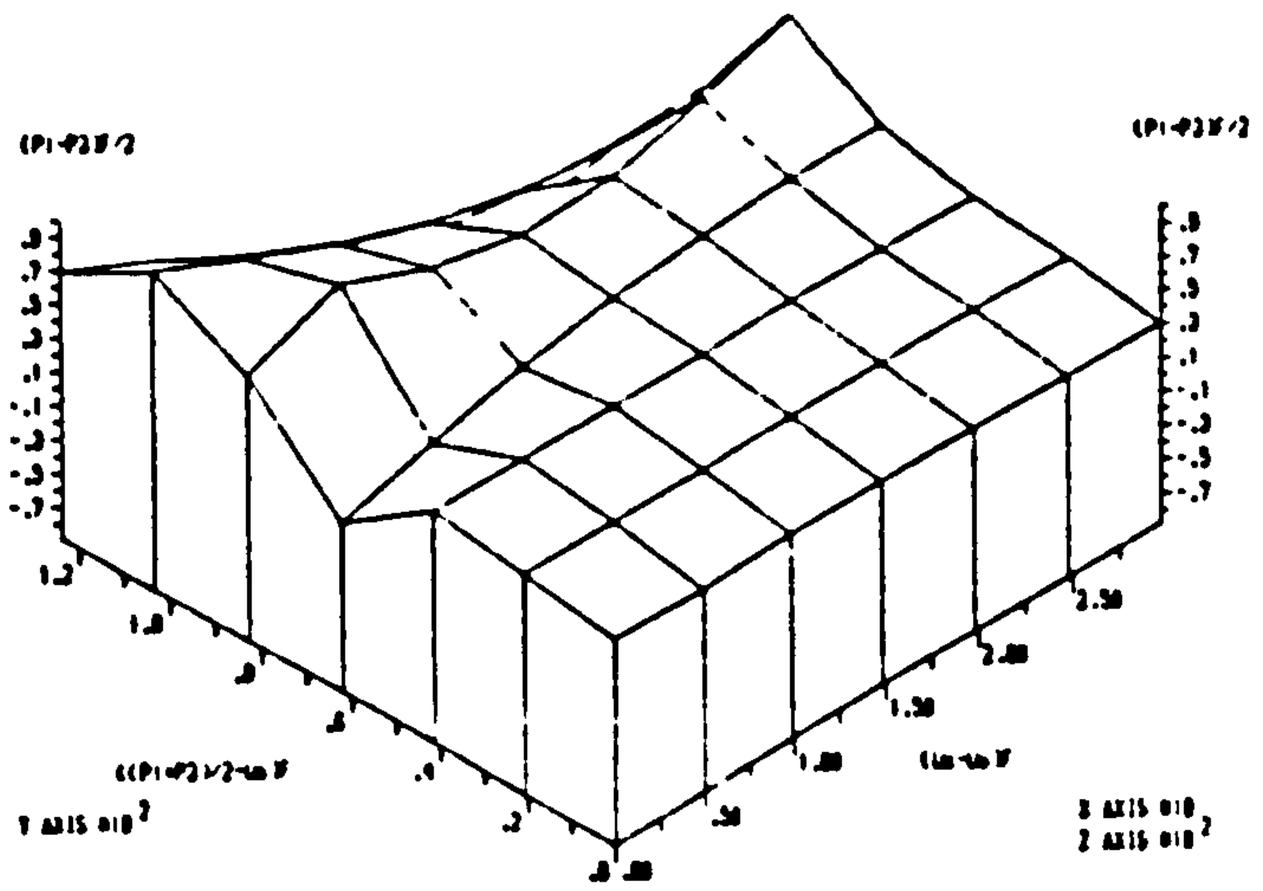

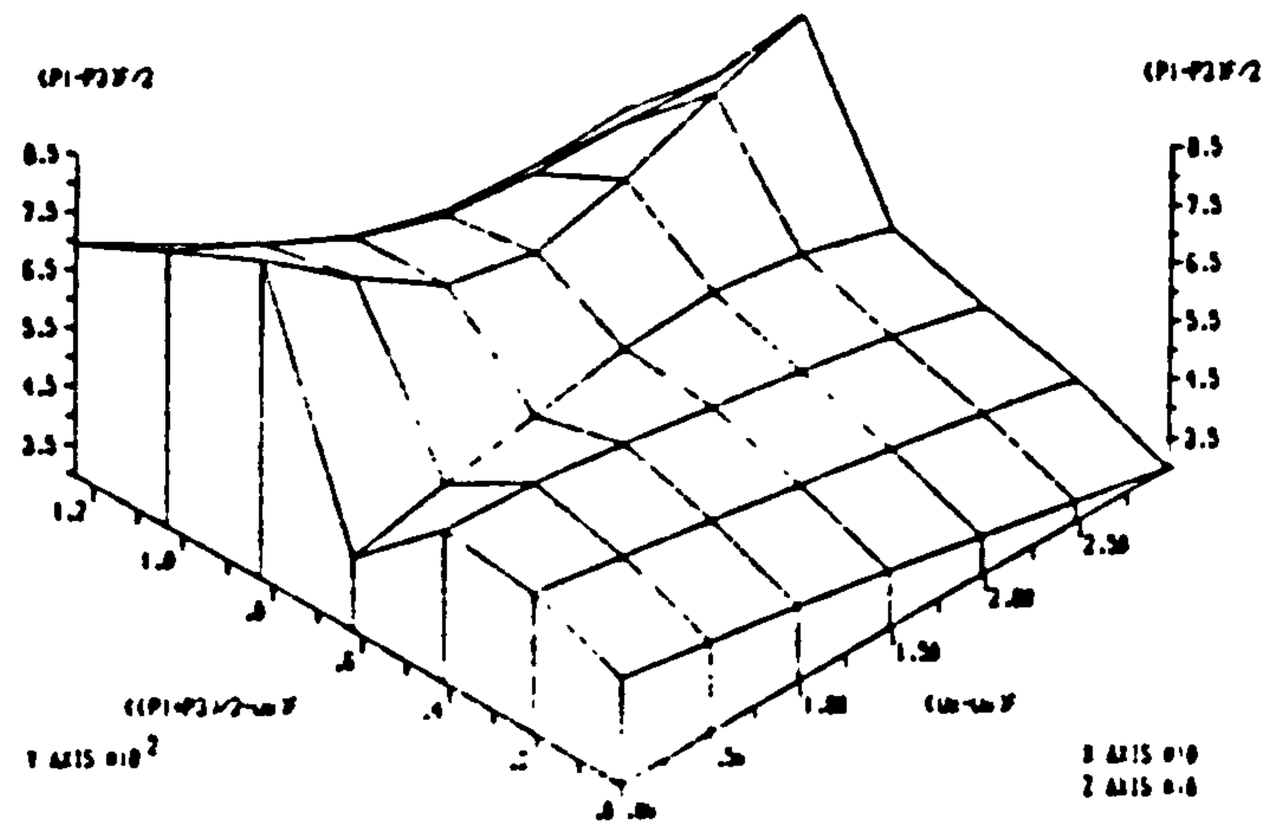

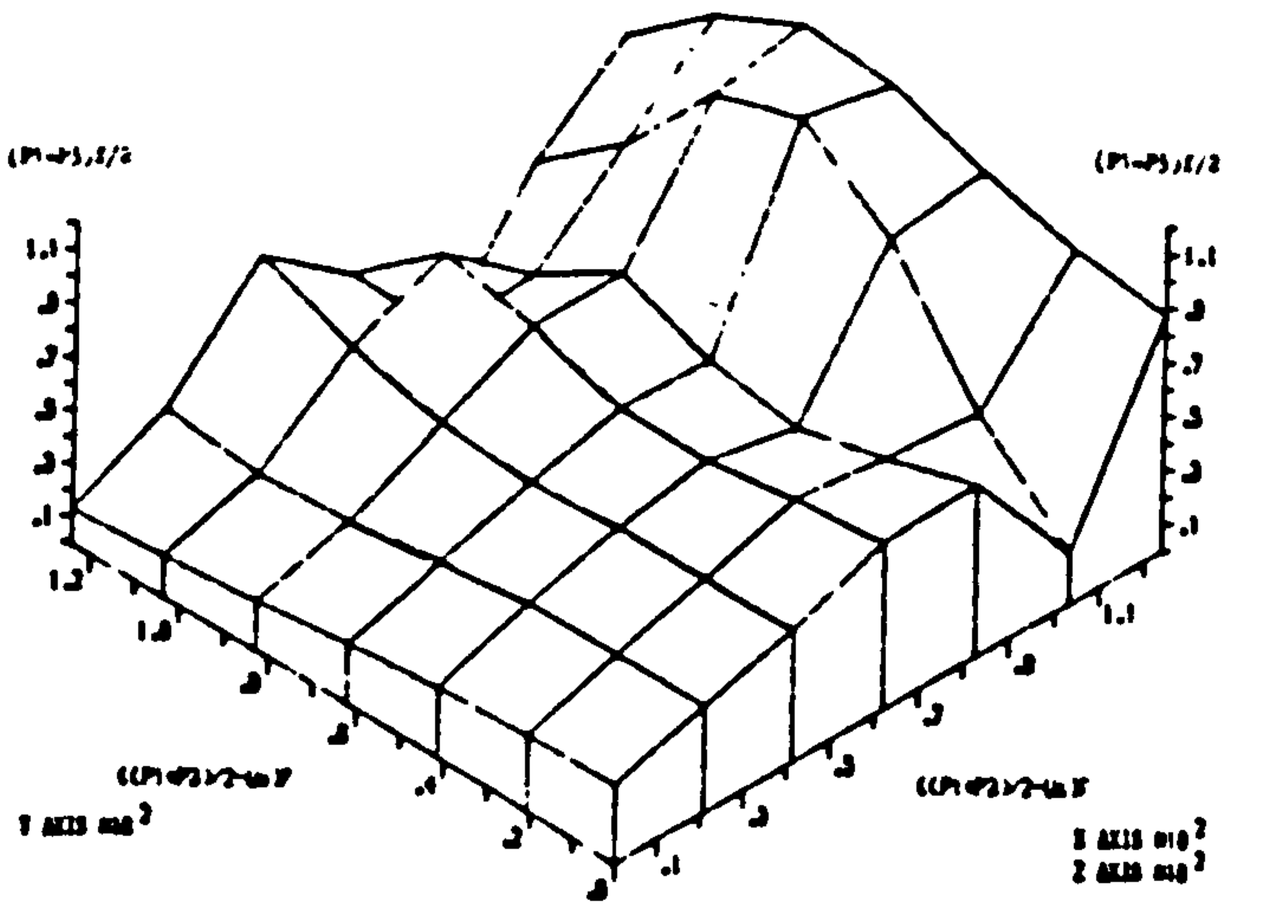

(UNITS IN POUNDS PER SQ. INCHES)
THE SHEAR STRENGTH DATA FOR RED SASUMUA CLAY
(MATYAS, 1963) (UNSATURATED SOILS ONLY).

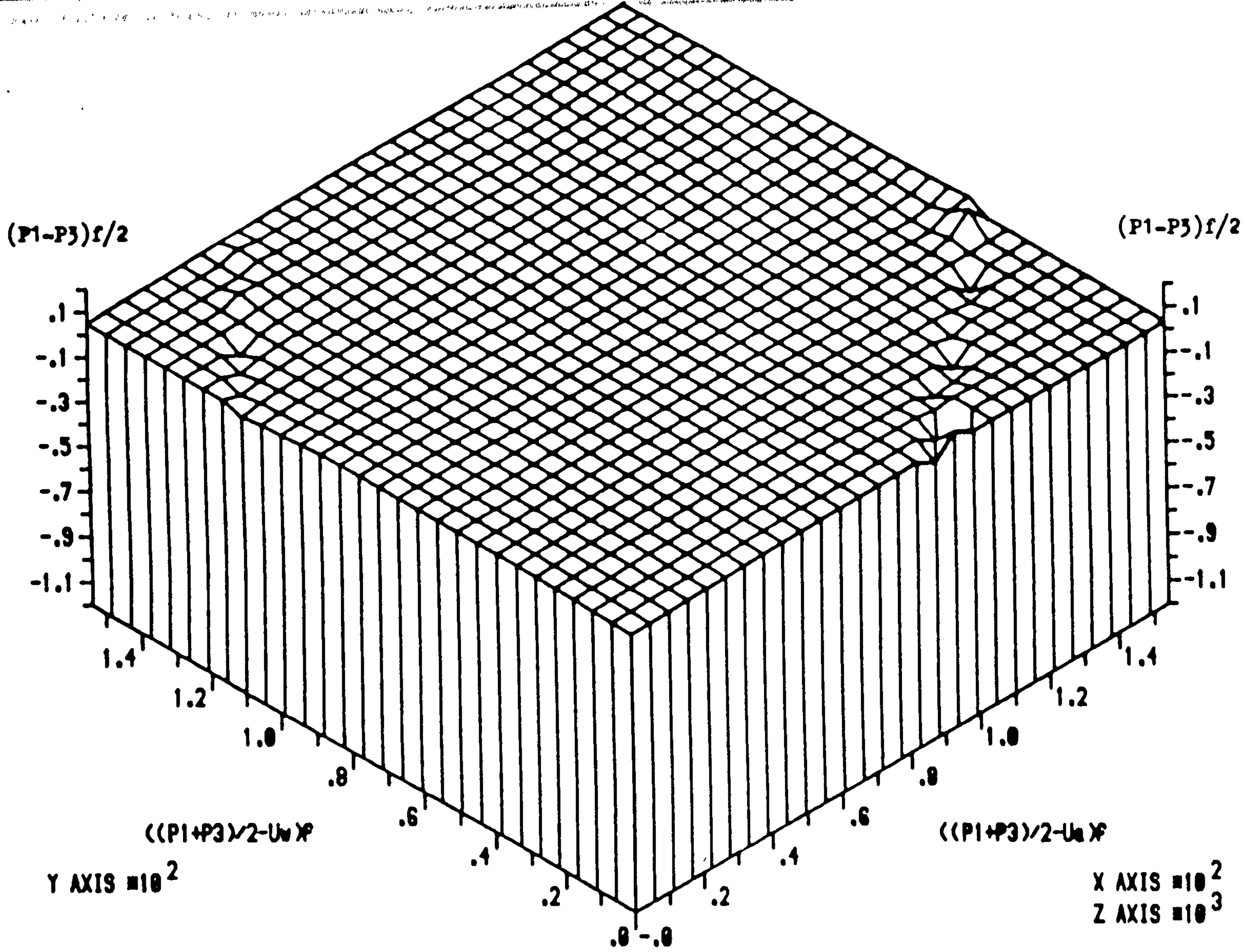

THE SHEAR STRENGTH DATA FOR RED SASUMUA CLAY (MATYAS, 1963) (UNSATURATED & SATURATED SOILS FOR THIRD PLOT ONLY).

(UNITS IN POUNDS PER SQ. INCHES)

A8.4.5 M.I.I.(1963)

(i) Numerical method

Potters flint and Peerless clay(tests on unsaturated soils)

```
**************************************************************
 INPUT COHESION,C' IN KG/SQ.CM IS 0

 INPUT ANGLE OF INTERNAL FRICTION IN DEGREES,Ø' IS 35.6
**************************************************************
                                  b
 SUCTION ANGLE IN DEGREES,Ø   IS 32.49

 SUCTION ANGLE IN DEGREES,Ø° IS -4.5

 CORRECTED COHESION,C' IN KG/SQ.CM IS 0.13
                                                  b
 CORRELATION FACTOR FOR SUCTION ANGLE(Ø ),R IS 0.89
**************************************************************
```

(iii) 3-dimensional graphical method

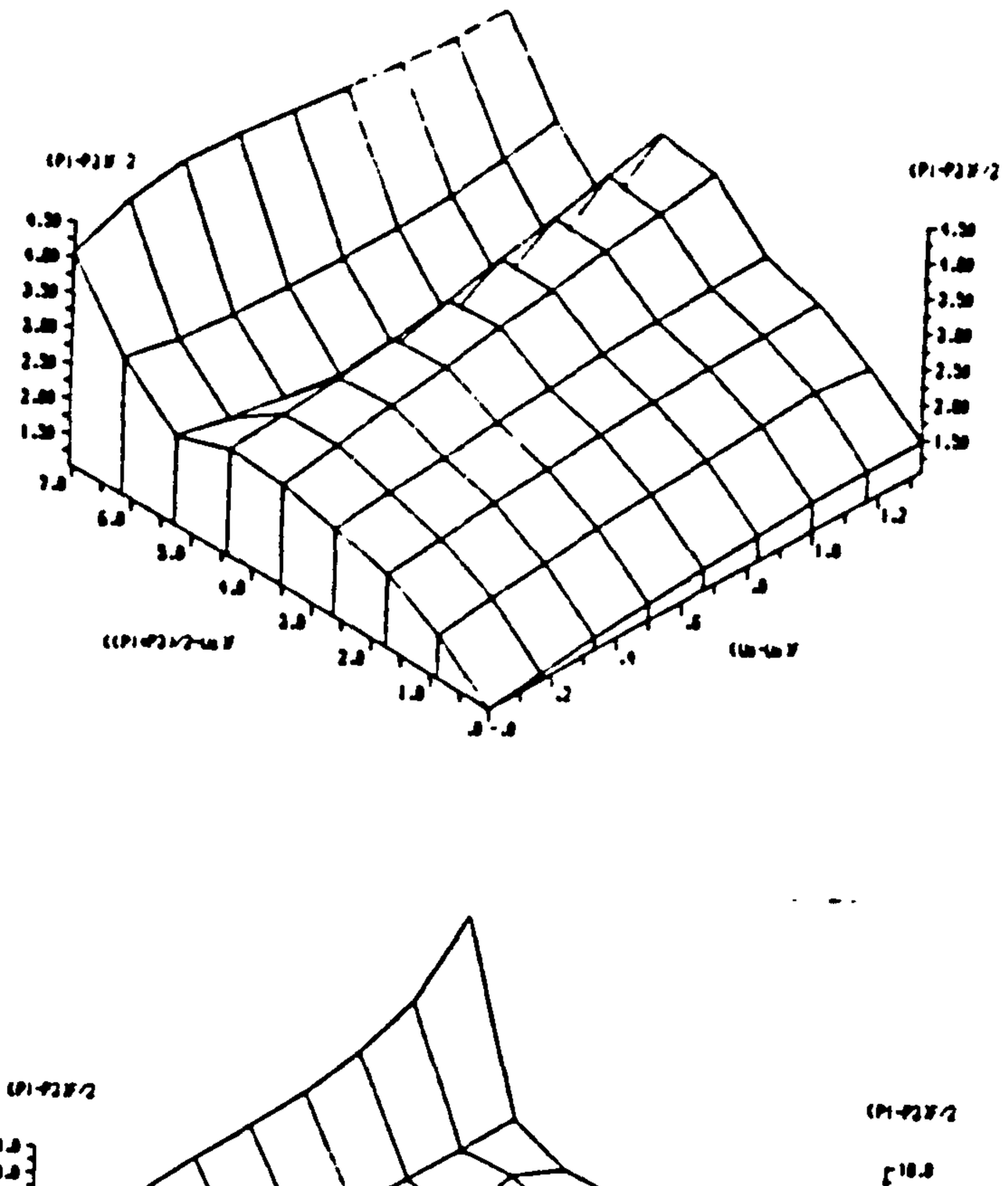

(UNITS IN KG/SQ.CM)

SHEAR STRENGTH DATA FOR POTTERS FLINT AND PEERLESS CLAY (M.I.T.,1963) (DATA FROM FREDLUND,1978).

A8.4.6 Gulbati(1972)

(i) Numerical method

Dhanauri clay(tests on unsaturated soil specimens only)

(Drained tests)

```
**************************************************************
 INPUT COHESION,C´ IN KG/SQ.CM IS 0.11

 INPUT ANGLE OF INTERNAL FRICTION IN DEGREES,Ø´ IS 29.1
**************************************************************
                                   b
 SUCTION ANGLE IN DEGREES,Ø   IS 41.99

 SUCTION ANGLE IN DEGREES,Ø° IS 18.95

 CORRECTED COHESION,C´ IN KG/SQ.CM IS -0.34
                                                  b
 CORRELATION FACTOR FOR SUCTION ANGLE(Ø ),R IS 0.72
**************************************************************
```

Delbi silt(tests on unsaturated soil specimens only)

(drained tests)

```
**************************************************************
 INPUT COHESION,C' IN KG/SQ.CM IS 0

 INPUT ANGLE OF INTERNAL FRICTION IN DEGREES,Ø' IS 38.4
**************************************************************
                                                    b
 SUCTION ANGLE IN DEGREES,Ø  IS 46.21

 SUCTION ANGLE IN DEGREES,Ø° IS 14.07

 CORRECTED COHESION,C' IN KG/SQ.CM IS 0.06
                                                    b
 CORRELATION FACTOR FOR SUCTION ANGLE(Ø ),R IS 0.45
**************************************************************
```

Delbi silt(tests on unsaturated soil specimens only)

(constant water-content tests)

```
**************************************************************
 INPUT COHESION,C' IN KG/SQ.CM IS 0

 INPUT ANGLE OF INTERNAL FRICTION IN DEGREES,Ø' IS 38.4
**************************************************************
                                    b
 SUCTION ANGLE IN DEGREES,Ø  IS 47.98

 SUCTION ANGLE IN DEGREES,Ø° IS 17.61

 CORRECTED COHESION,C' IN KG/SQ.CM IS -0.19
                                                    b
 CORRELATION FACTOR FOR SUCTION ANGLE(Ø ),R IS 0.80
**************************************************************
```

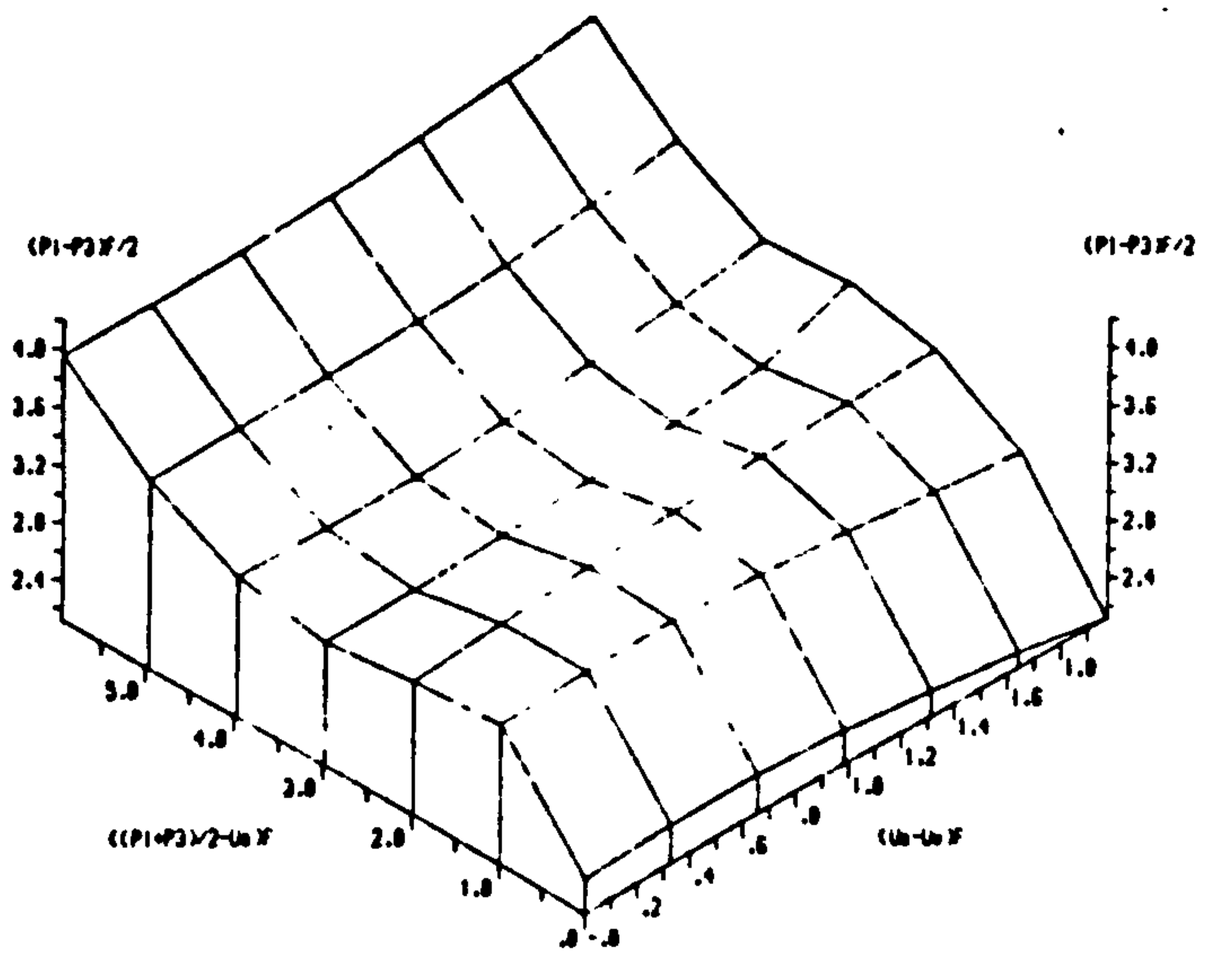

DATA FOR D TESTS CONDUCTED ON "AS-COMPACTED" SAMPLES OF DHANAURI CLAY(BALWATI,72)

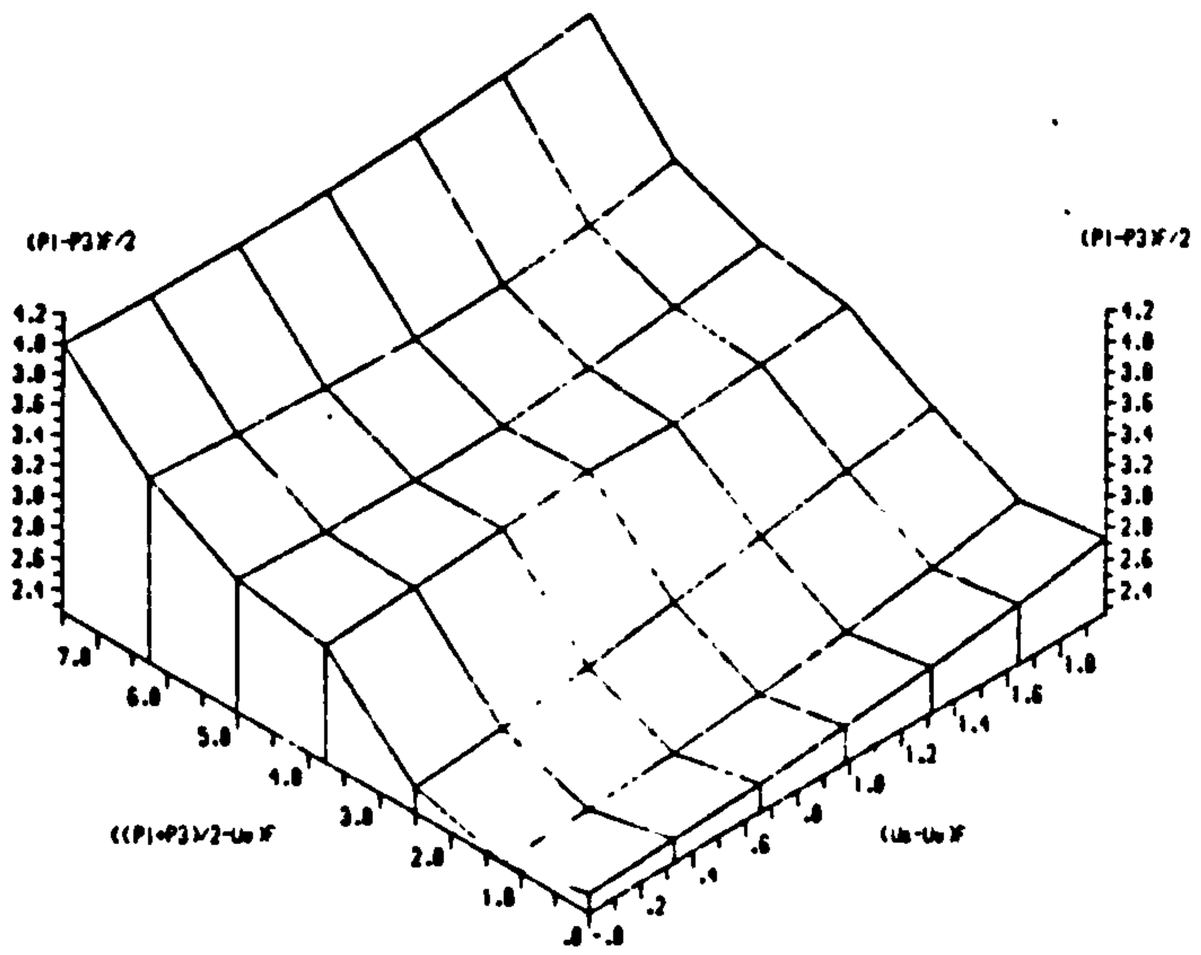

DATA FOR D TESTS CONDUCTED ON "AS-COMPACTED" SAMPLES OF DHANAURI CLAY(BALWATI,72)

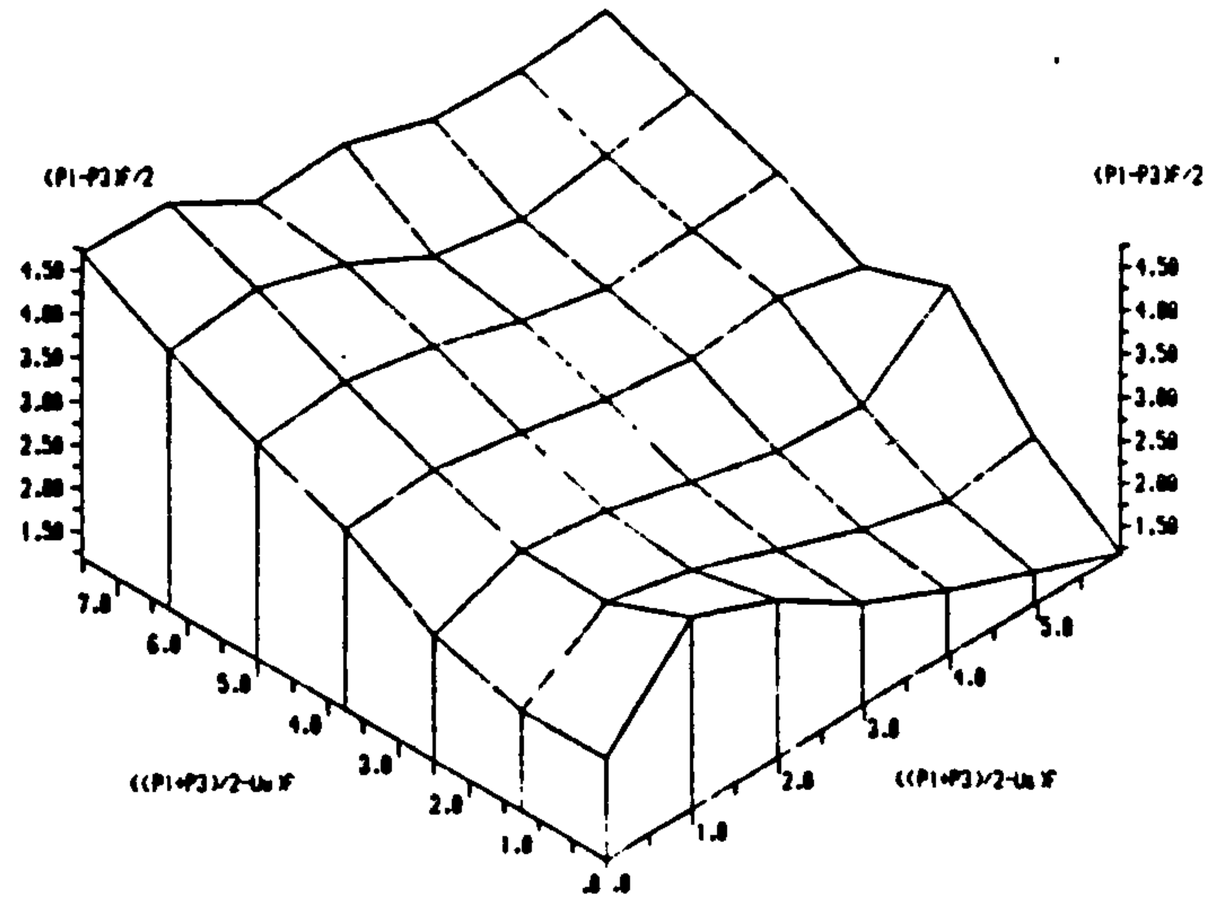

DATA FOR D TESTS CONDUCTED ON "AS-COMPACTED" SAMPLES OF DHANAURI CLAY(BALWATI,72)

(UNITS IN KG/SQ.CM)

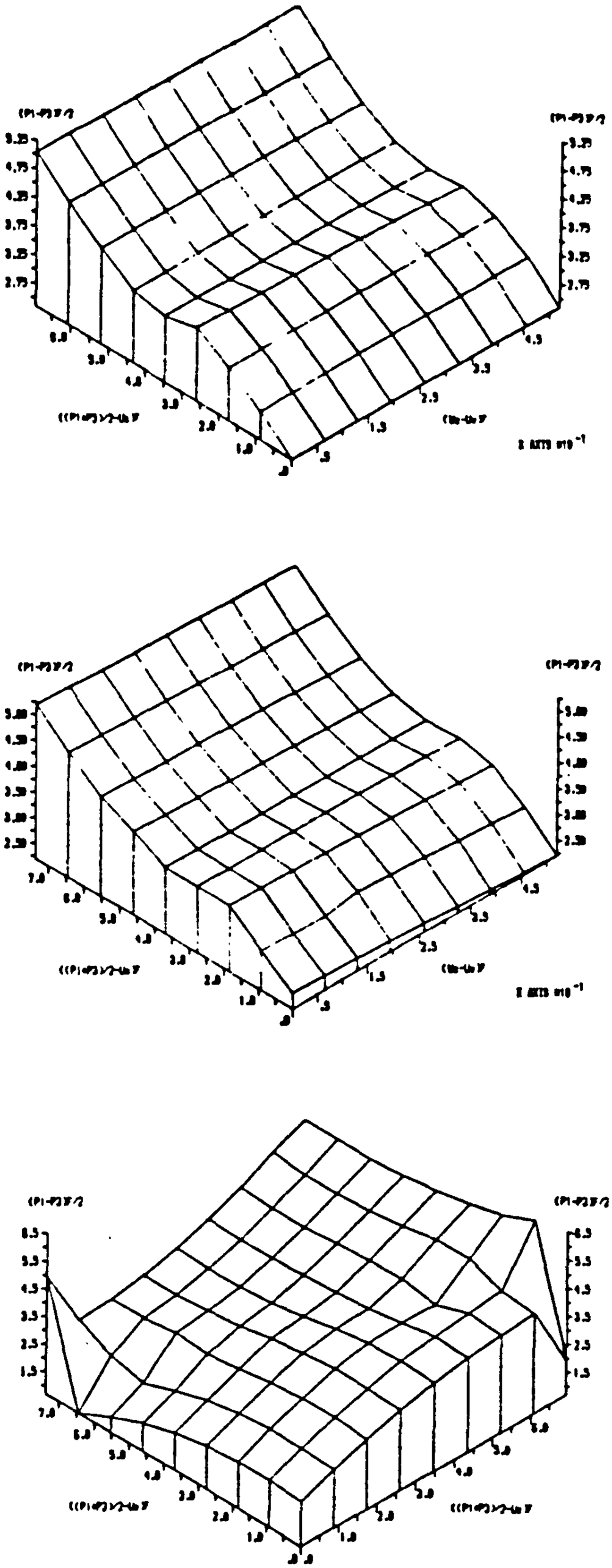

(UNITS IN KG/SQ. CM)
DATA FOR 'D TESTS CONDUCTED ON "AS-COMPACTED" SAMPLES OF DELHI SILT(GUWAHATI,1972).

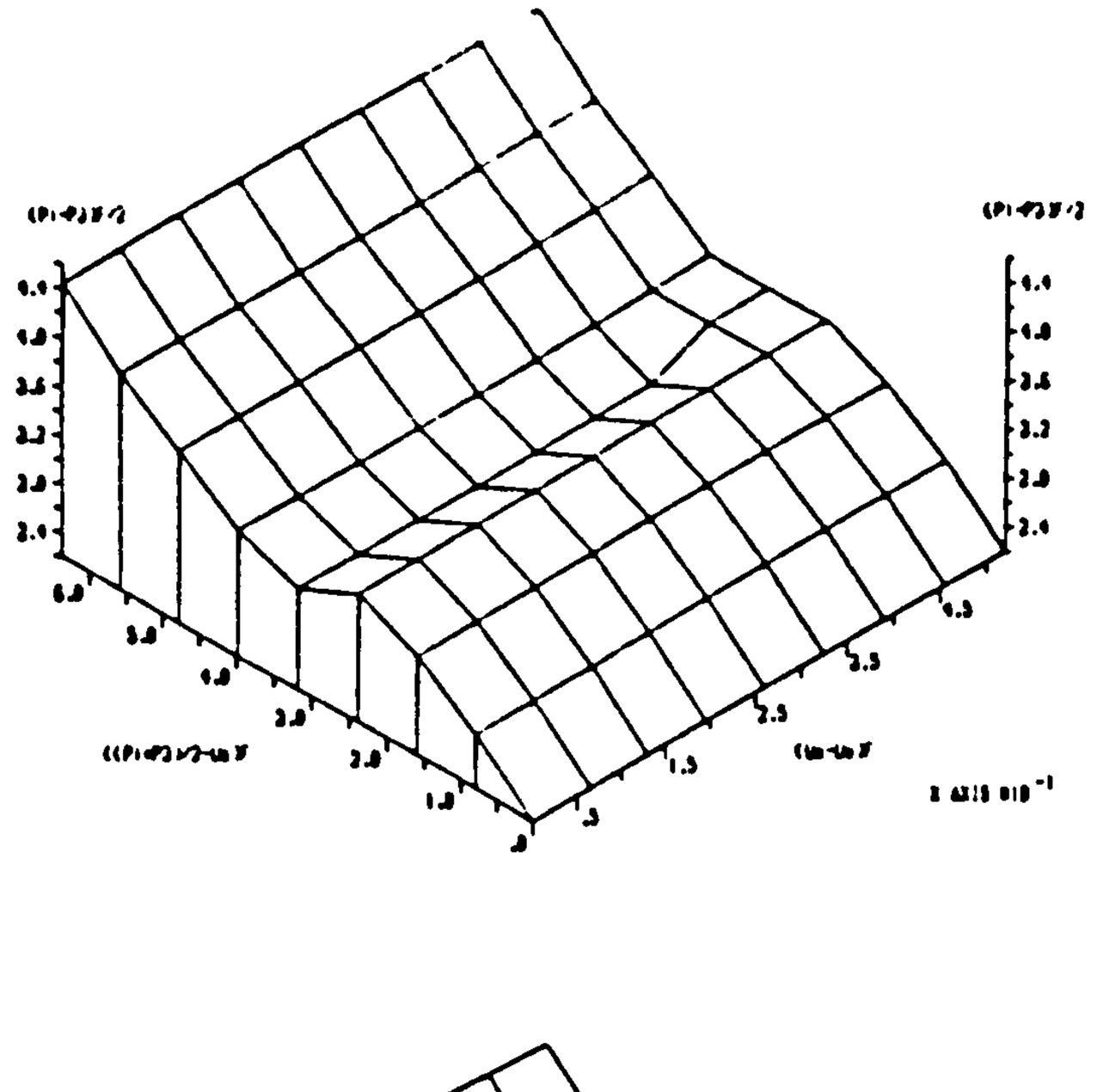

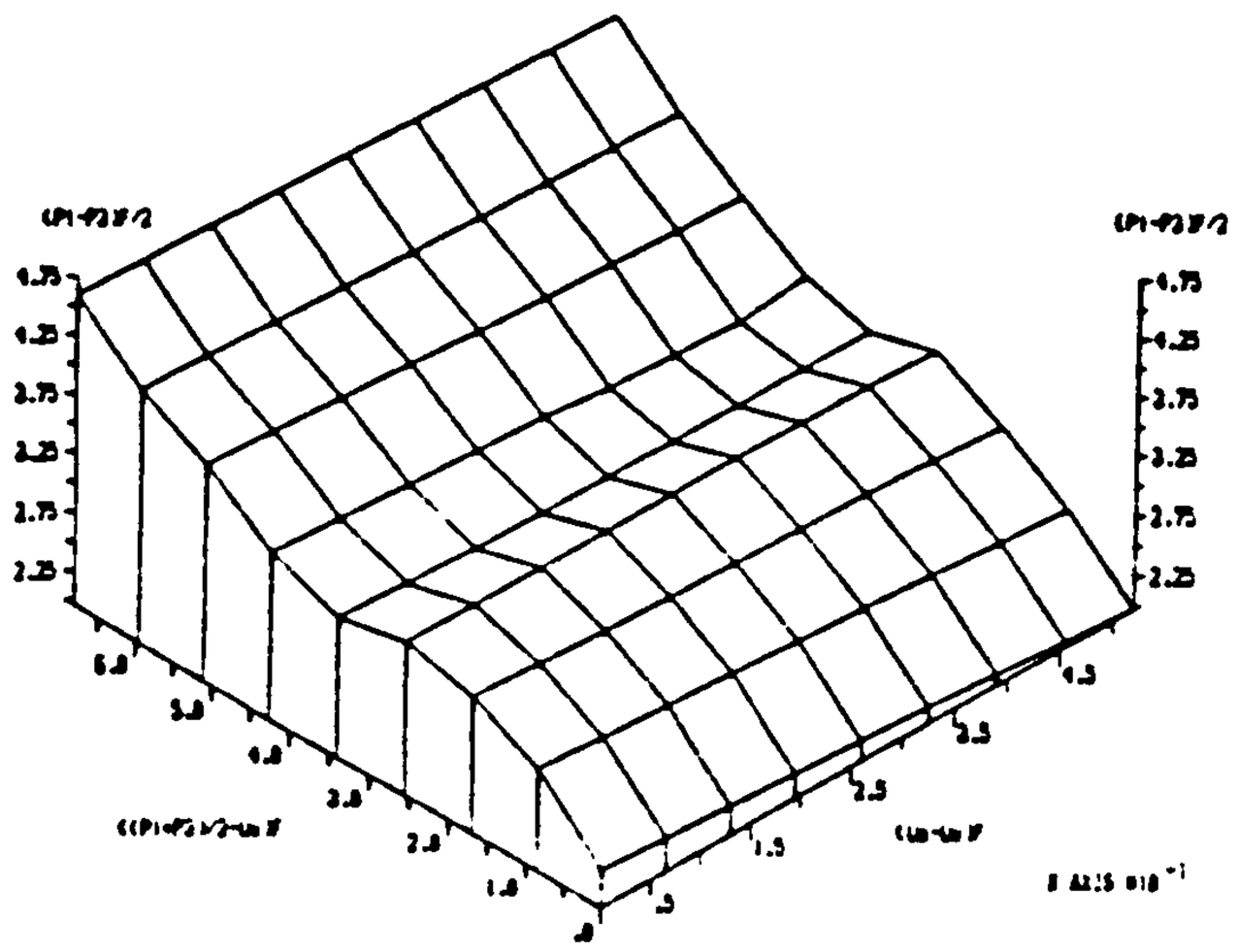

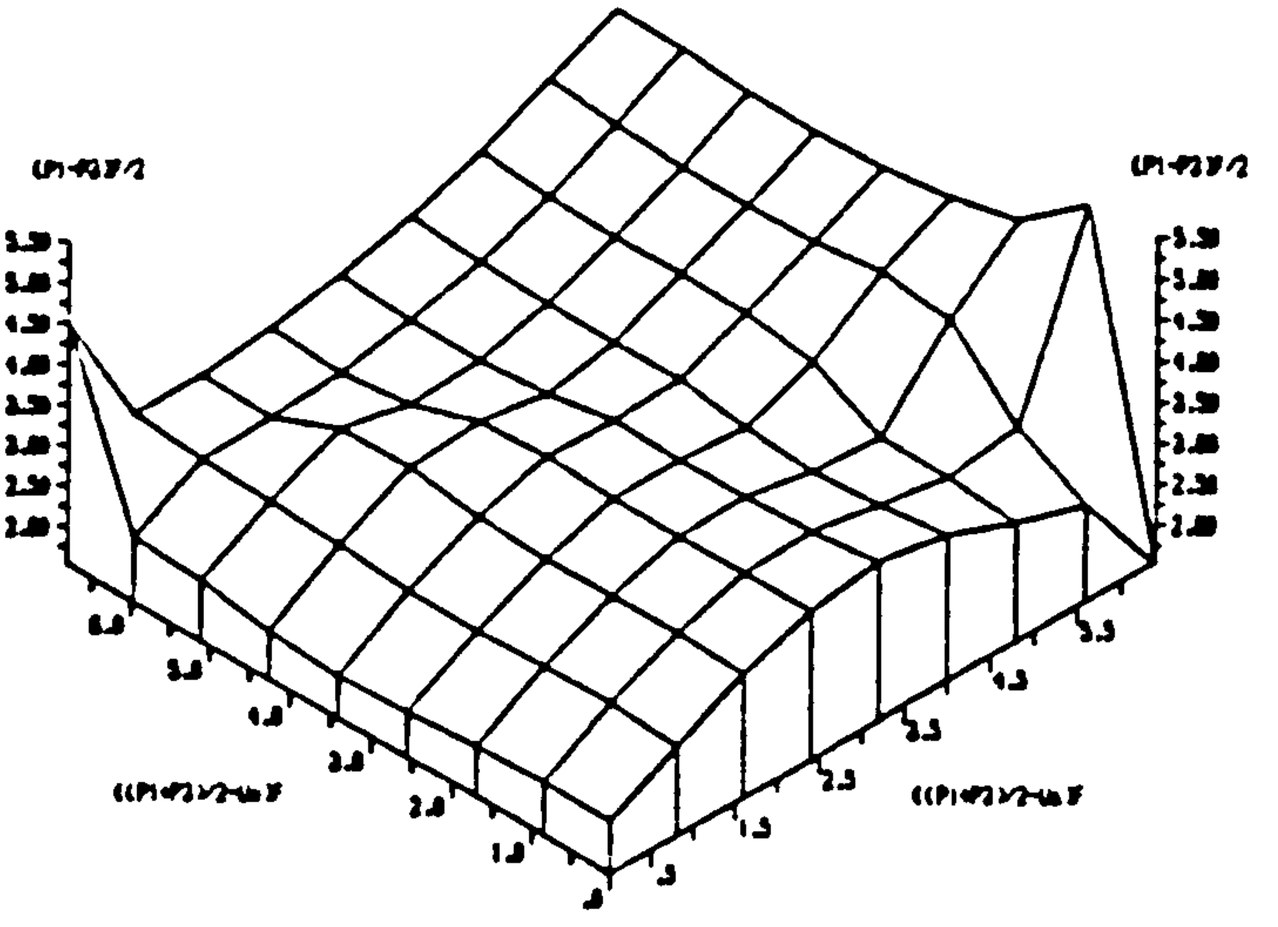

(UNITS IN KG/SQ.CM)
DATA FOR D TESTS CONDUCTED ON "AS-COMPACTED" SAMPLES OF DELHI SILT(GULHATI,1972) (CORRECTION).

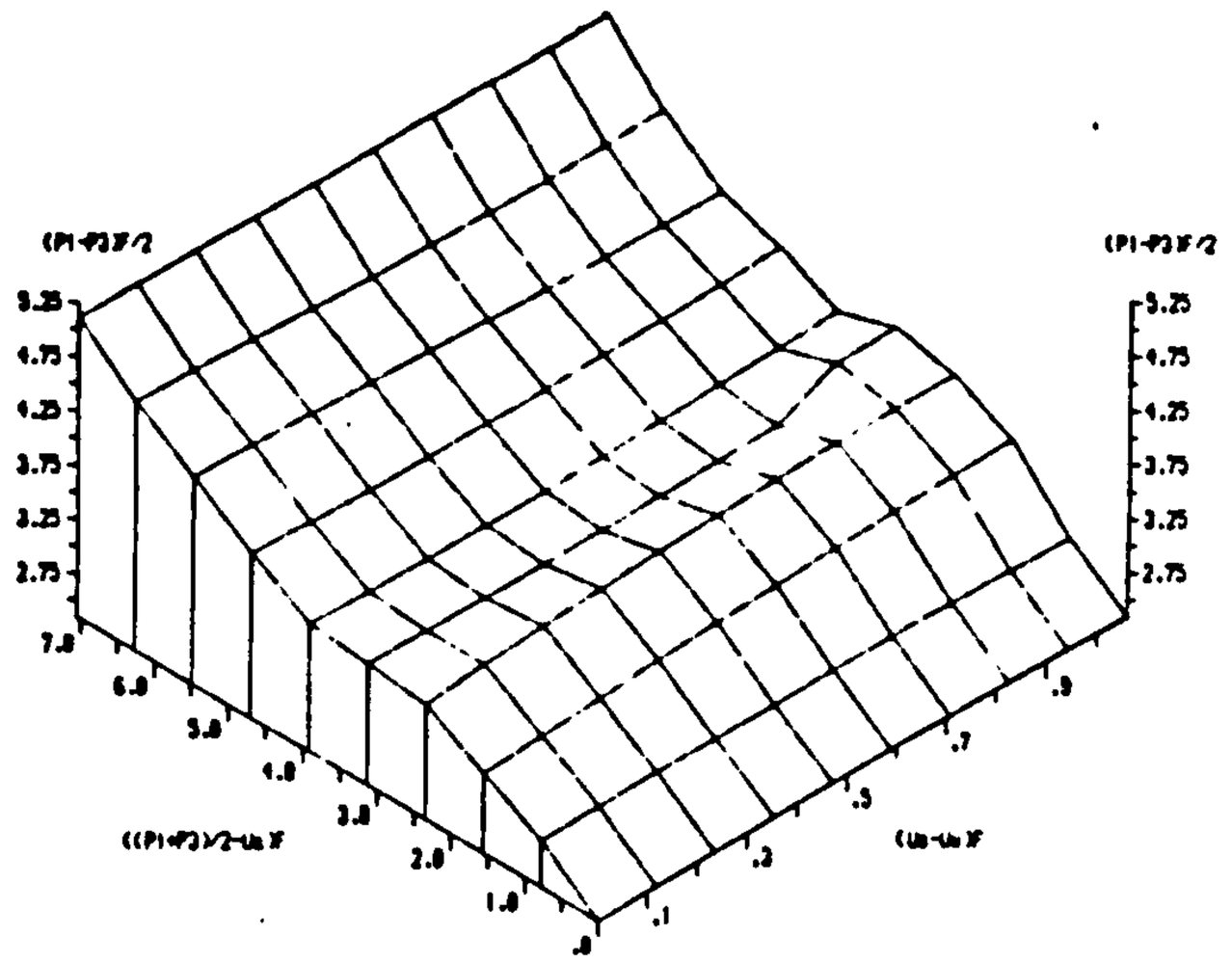

DATA FOR CU TESTS CONDUCTED ON "AS-COMPACTED" SAMPLES OF DELHI SILTS (BALHATI,72)

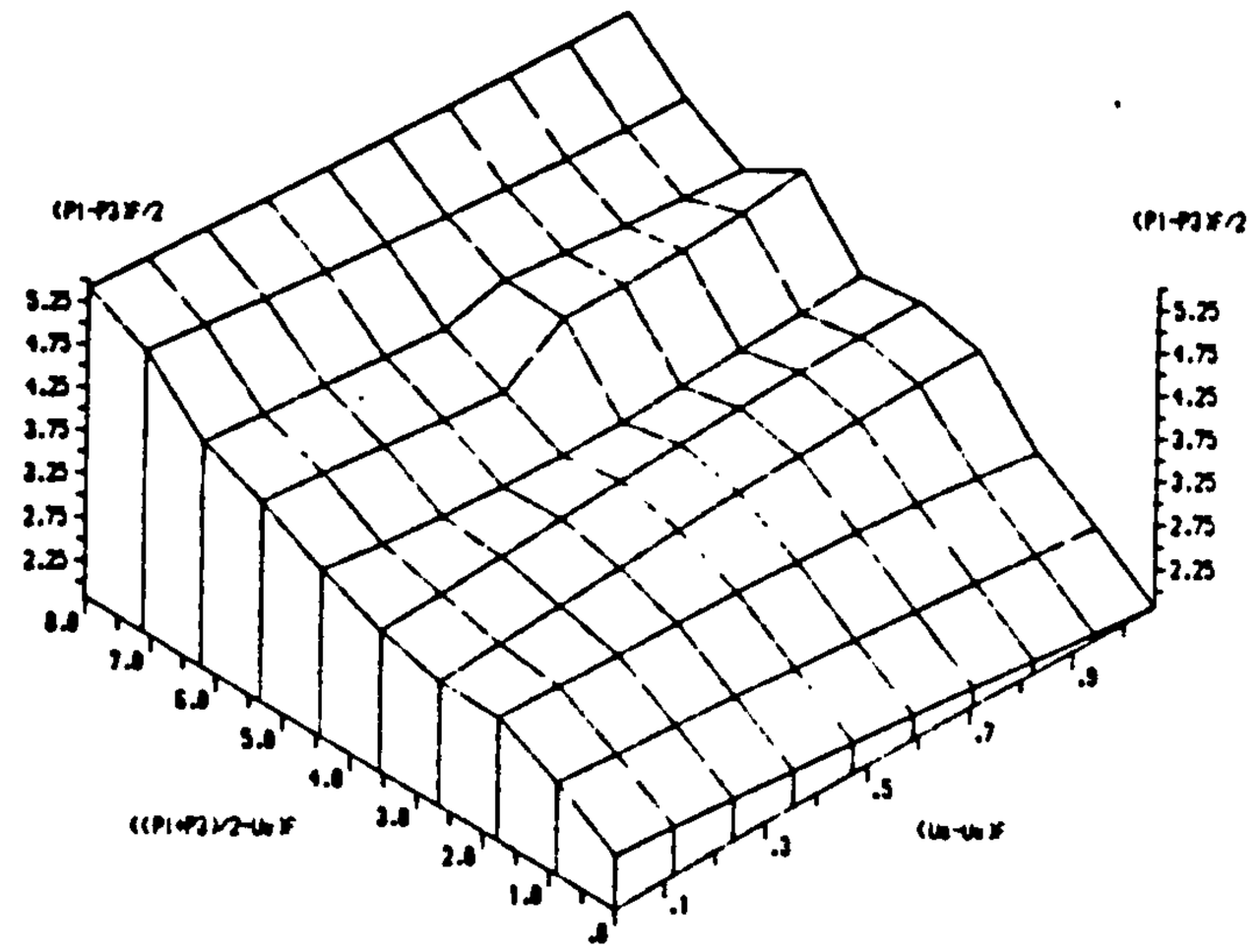

DATA FOR CU TESTS CONDUCTED ON "AS-COMPACTED" SAMPLES OF DELHI SILTS (BALHATI,72)

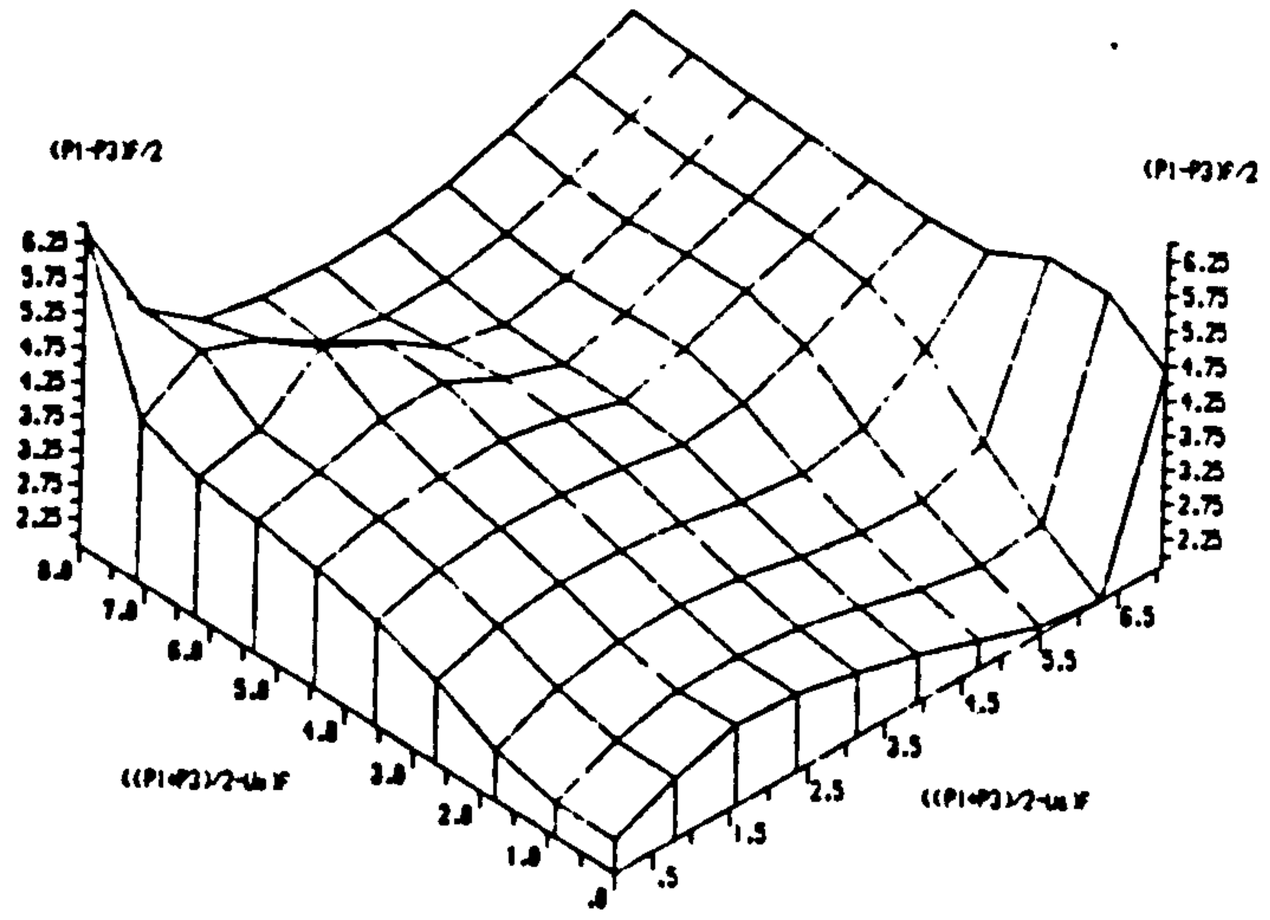

DATA FOR CU TESTS CONDUCTED ON "AS-COMPACTED" SAMPLES OF DELHI SILTS (BALHATI,72)

(UNITS IN KG/SQ.CM)

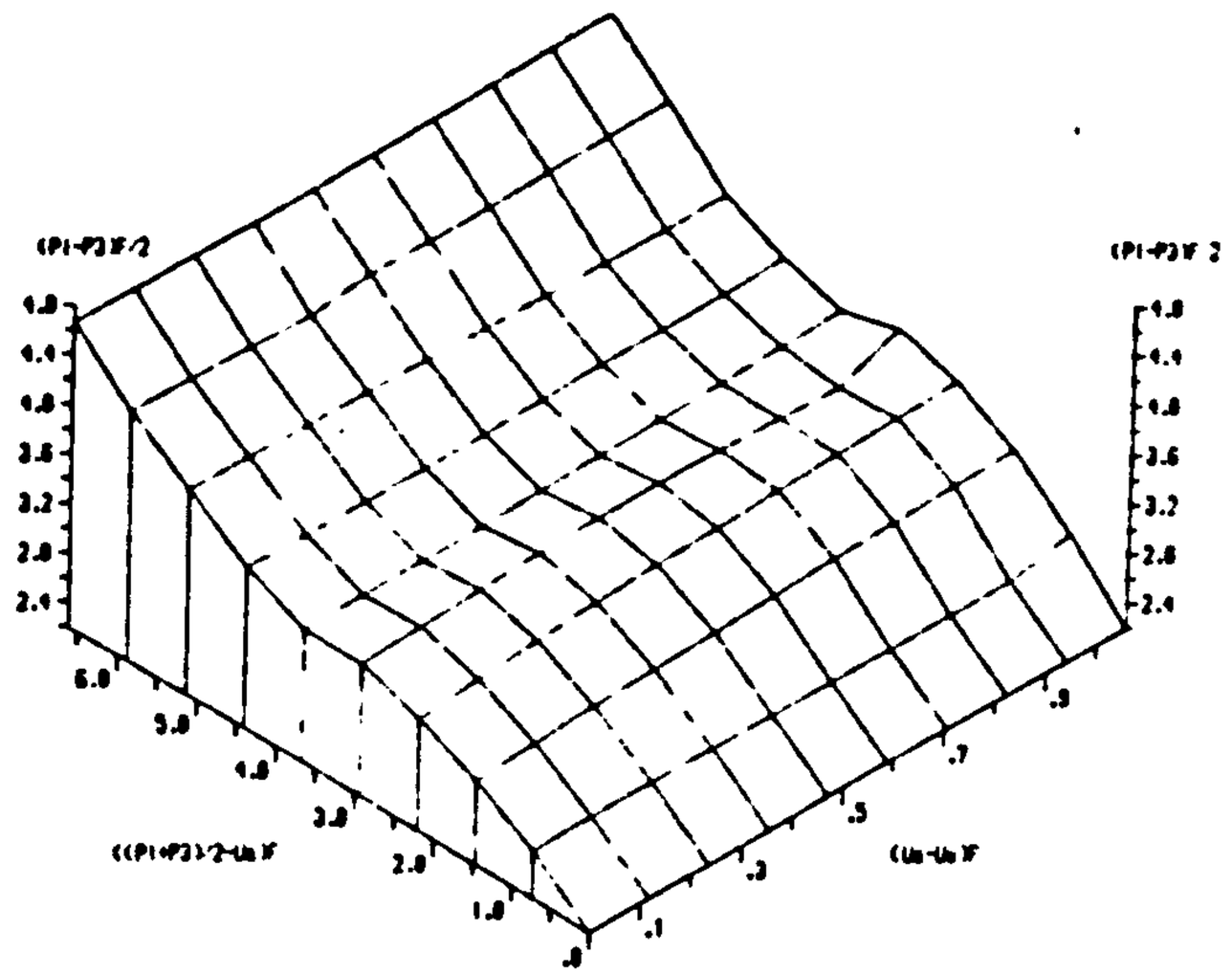

DATA FOR CU TESTS CONDUCTED ON "AS COMPACTED" SAMPLES OF DELHI SILT (BULHATI,72%CORRECTION)

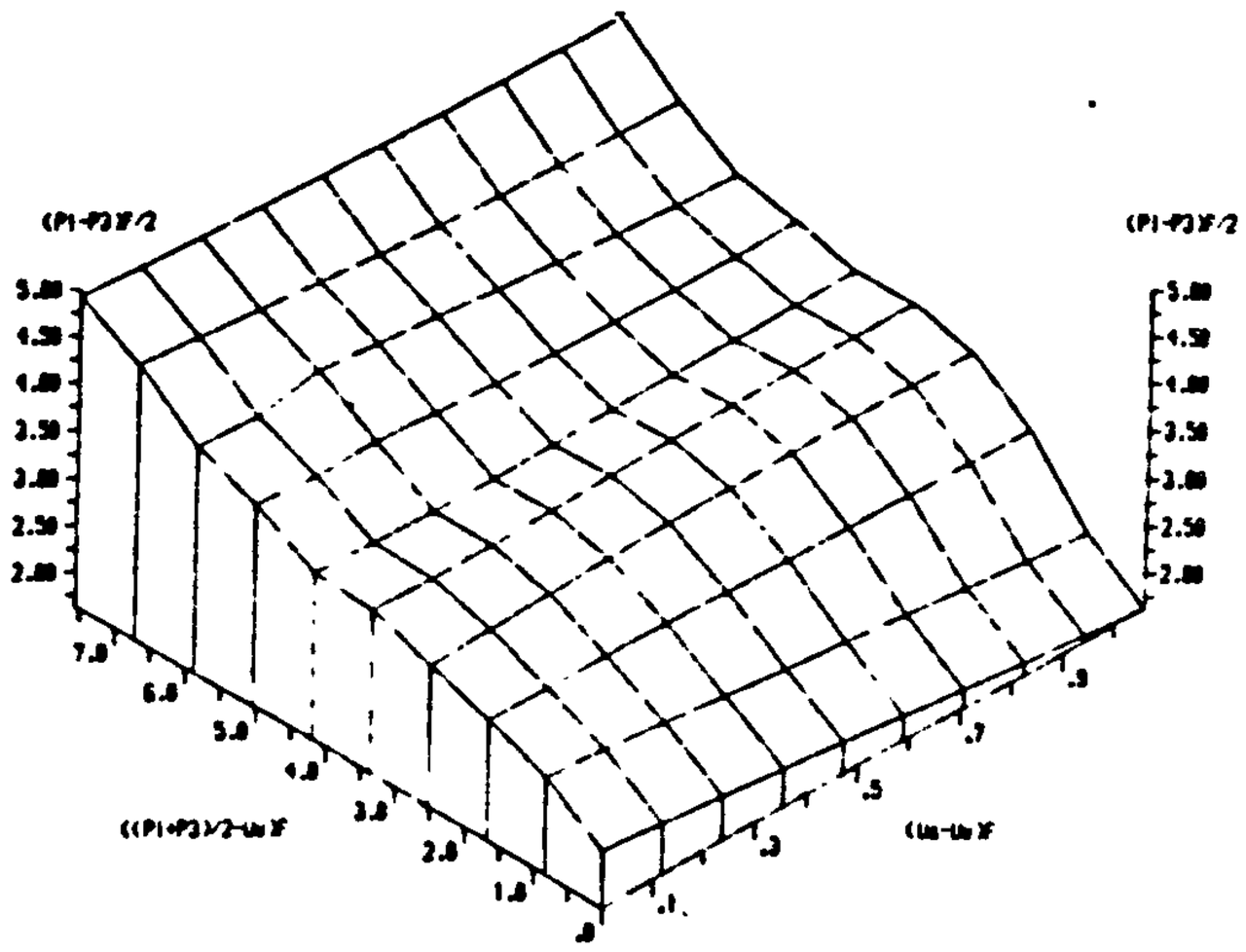

DATA FOR CU TESTS CONDUCTED ON "AS COMPACTED" SAMPLES OF DELHI SILT (BULHATI,72%CORRECTION)

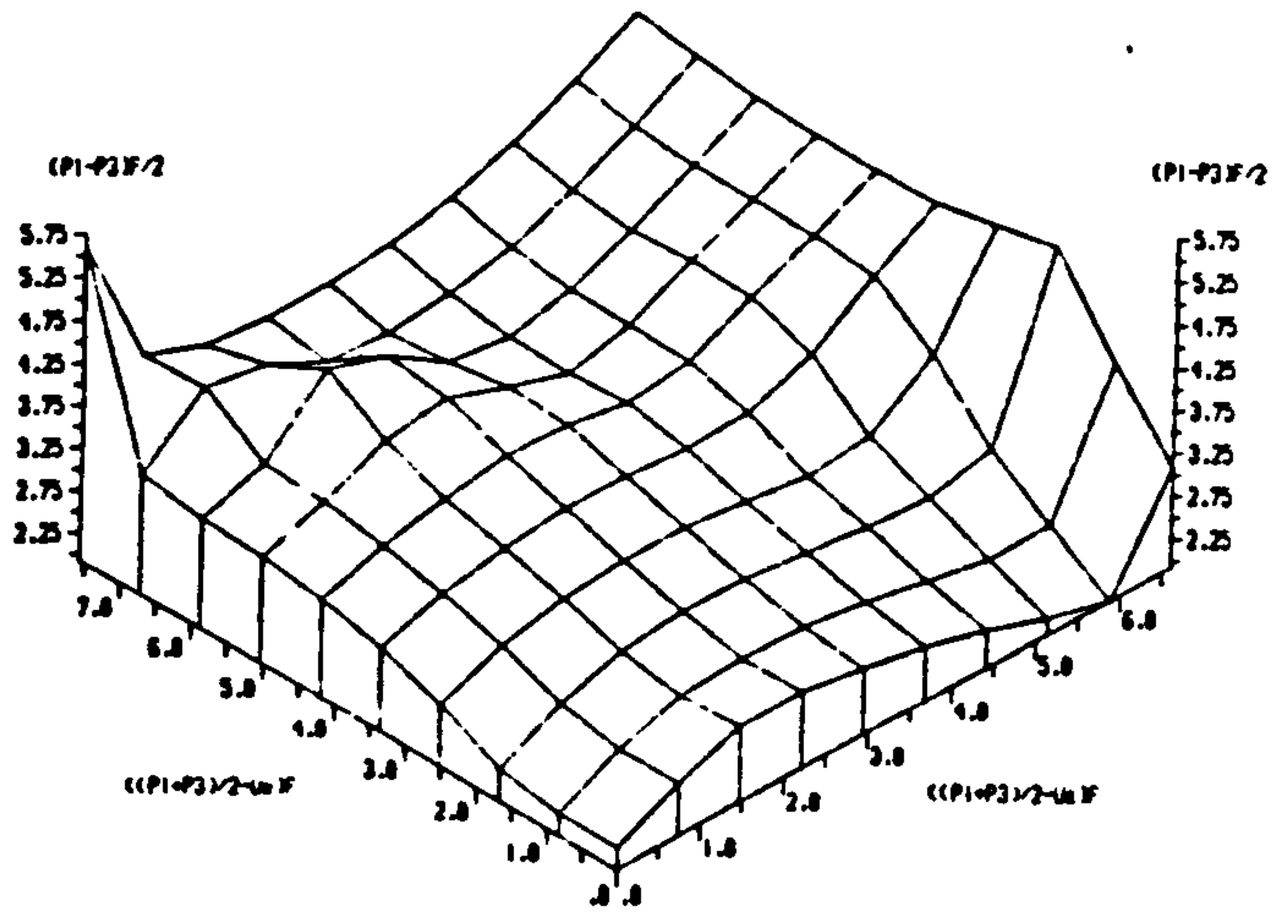

DATA FOR CU TESTS CONDUCTED ON "AS COMPACTED" SAMPLES OF DELHI SILT (BULHATI,72%CORRECTION)

(UNITS IN KG/SQ.CM)

A8.4.7 Satija(1978)

(i) Numerical method

(CD test, γd = 14.5 KN/cu.m, w = 22.2%)

```
**********************************************************************
 INPUT COHESION,C' IN KG/SQ.CM IS 0.20

 INPUT ANGLE OF INTERNAL FRICTION IN DEGREES,ø' IS 29
**********************************************************************
                                    b
 SUCTION ANGLE IN DEGREES,ø  IS 12.77

 SUCTION ANGLE IN DEGREES,ø° IS -18.15

 CORRECTED COHESION,C' IN KG/SQ.CM IS 0.20
                                                    b
 CORRELATION FACTOR FOR SUCTION ANGLE(ø ),R IS 0.96
**********************************************************************
```

(CW test, γd = 14.5 KN/ cu.m, w = 22.2%)

```
**********************************************************************
 INPUT COHESION,C' IN KG/SQ.CM IS 0.11

 INPUT ANGLE OF INTERNAL FRICTION IN DEGREES,ø' IS 29
**********************************************************************
                                    b
 SUCTION ANGLE IN DEGREES,ø  IS 16

 SUCTION ANGLE IN DEGREES,ø° IS -14.98

 CORRECTED COHESION,C' IN KG/SQ.CM IS 0.12
                                                    b
 CORRELATION FACTOR FOR SUCTION ANGLE(ø ),R IS 0.98
**********************************************************************
```

(CW test, γ_d = 15.5 KN/cu. m, ω = 22.2%)

```
**************************************************************
 INPUT COHESION,C' IN KG/SQ.CM IS 0.16

 INPUT ANGLE OF INTERNAL FRICTION IN DEGREES,Ø' IS 28.5
**************************************************************
                                    b
 SUCTION ANGLE IN DEGREES,Ø  IS 21.33

 SUCTION ANGLE IN DEGREES,Ø° IS -8.67

 CORRECTED COHESION,C' IN KG/SQ.CM IS 0.18
                                                  b
 CORRELATION FACTOR FOR SUCTION ANGLE(Ø ),R IS 0.99
**************************************************************
```

(CD test, γ_d = 15.5 KN/cu. m, ω = 22.2%)

```
**************************************************************
 INPUT COHESION,C' IN KG/SQ.CM IS 0.37

 INPUT ANGLE OF INTERNAL FRICTION IN DEGREES,Ø' IS 28.5
**************************************************************
                                    b
 SUCTION ANGLE IN DEGREES,Ø  IS 16.13

 SUCTION ANGLE IN DEGREES,Ø° IS -14.24

 CORRECTED COHESION,C' IN KG/SQ.CM IS 0.35
                                                  b
 CORRELATION FACTOR FOR SUCTION ANGLE(Ø ),R IS 0.98
**************************************************************
```

(ii) 2-dimensional graphical method

Qhanauri clay

Soil type	INPUT C′ KG/SQ.CM	ø′	$ø^b$	* Correlation coefficient
CD test				
$Yd=14.5\ KN/m^3$	0.20	29.0^o	12.6^o	0.96
w=22.2%				
CW test				
$Yd=14.5\ KN/m^3$	0.11	29.0^o	16.5^o	0.97
w=22.2%				
CW test				
$Yd=15.5\ KN/m^3$	0.16	28.5^o	22.6^o	0.99
w=22.2%				
CD test				
$Yd=15.5\ KN/m^3$	0.37	28.5^o	16.2^o	0.97
w=22.2%				

*Refers to the best-fit line for $ø^b$

(iii) 3-dimensional graphical method

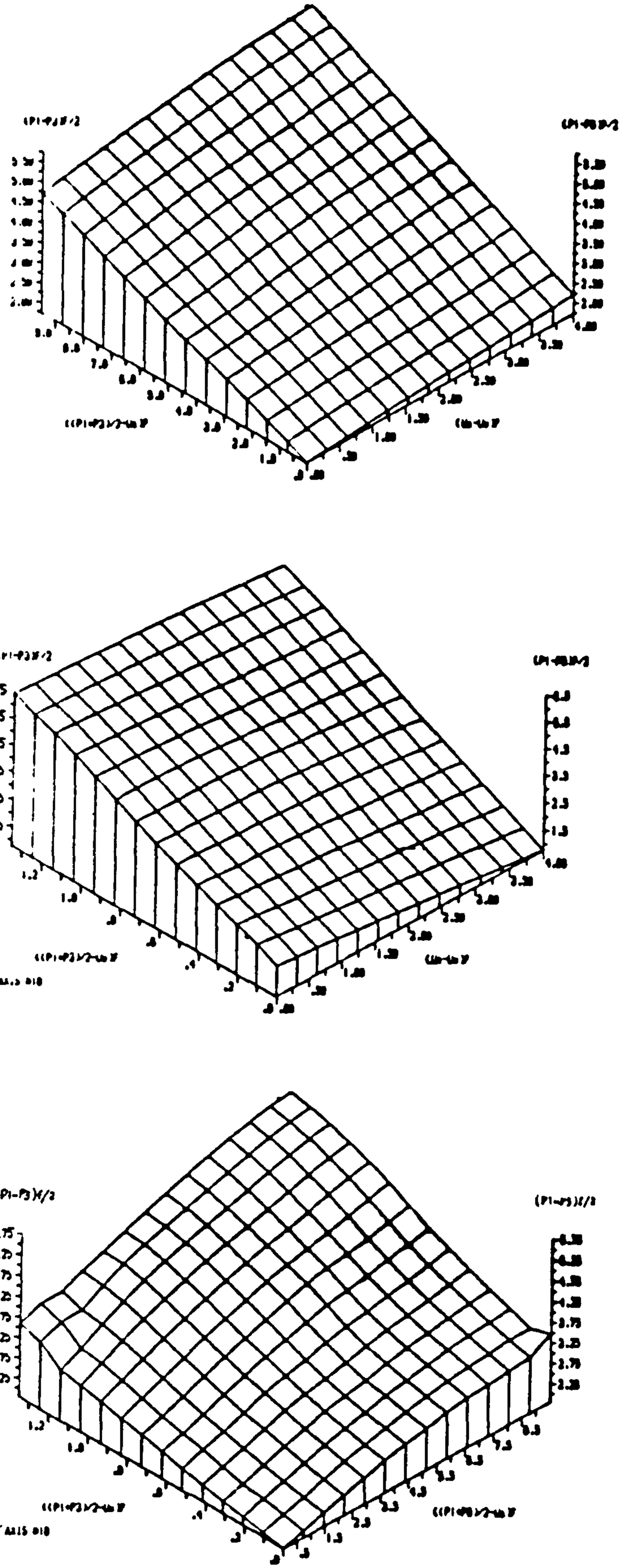

(UNITS IN KG/SQ.CM)

SHEAR STRENGTH DATA FOR LOW AS-COMPACTED DENSITY DHANAURI CLAY UNDER D CONDITION(SATIJA,1978).

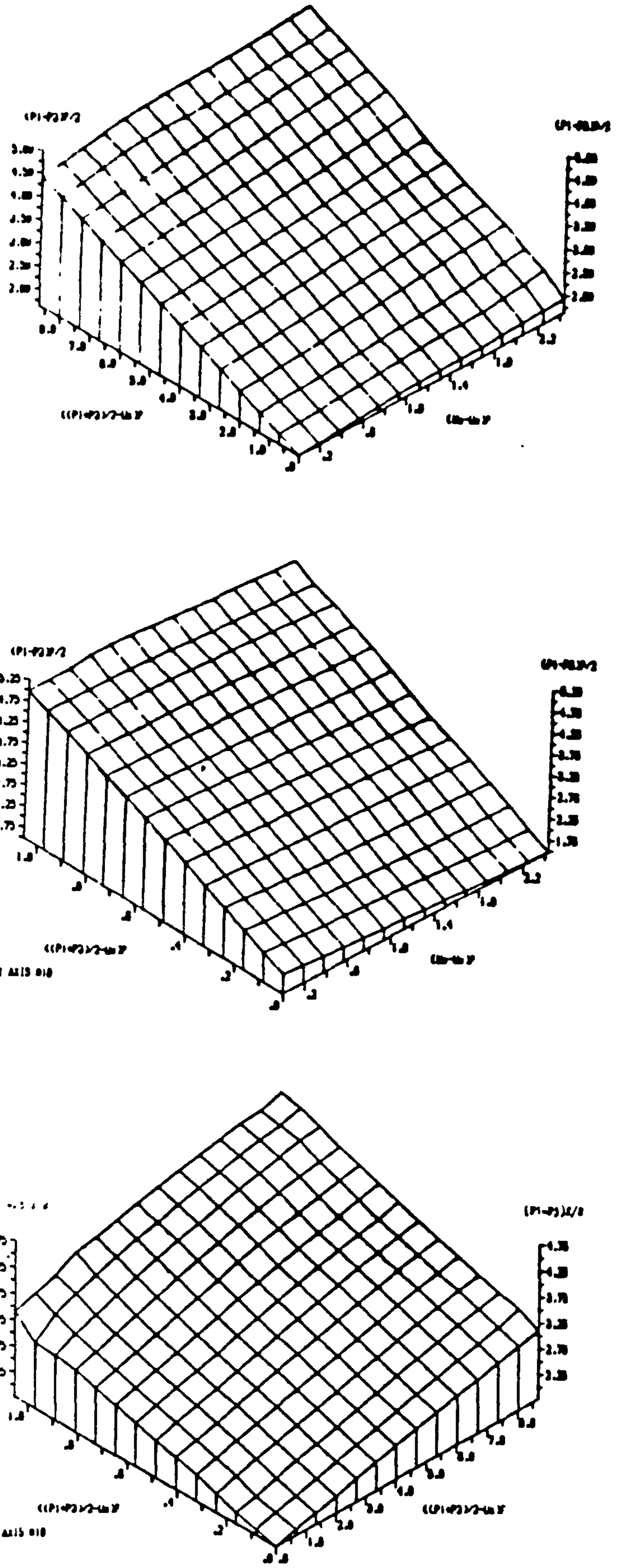

(UNITS IN KG/SQ.CM)

SHEAR STRENGTH DATA FOR LOW AS-COMPACTED DENSITY DHANAURI CLAY UNDER CW CONDITION(SATIJA,1978).

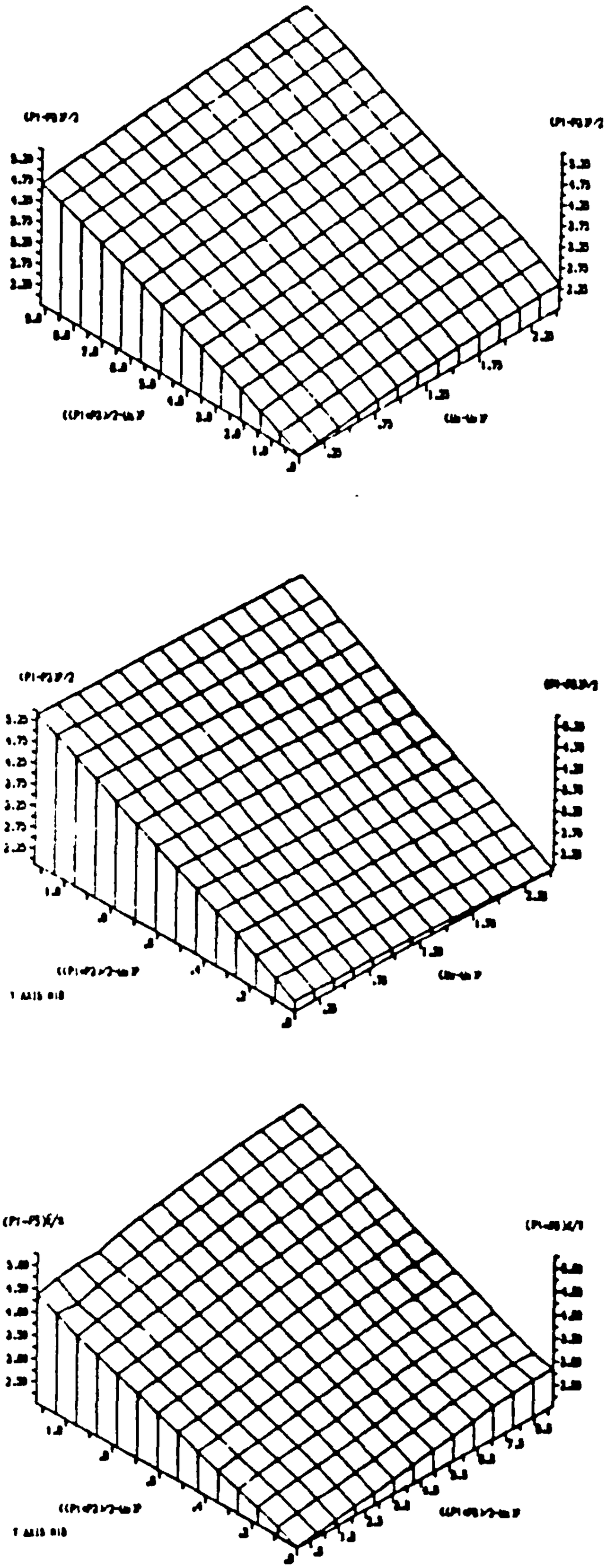

(UNITS IN KG/SQ.CM)
SHEAR STRENGTH DATA FOR HIGH AS-COMPACTED DENSITY DHANAURI CLAY UNDER CW CONDITION(SATIJA,1978).

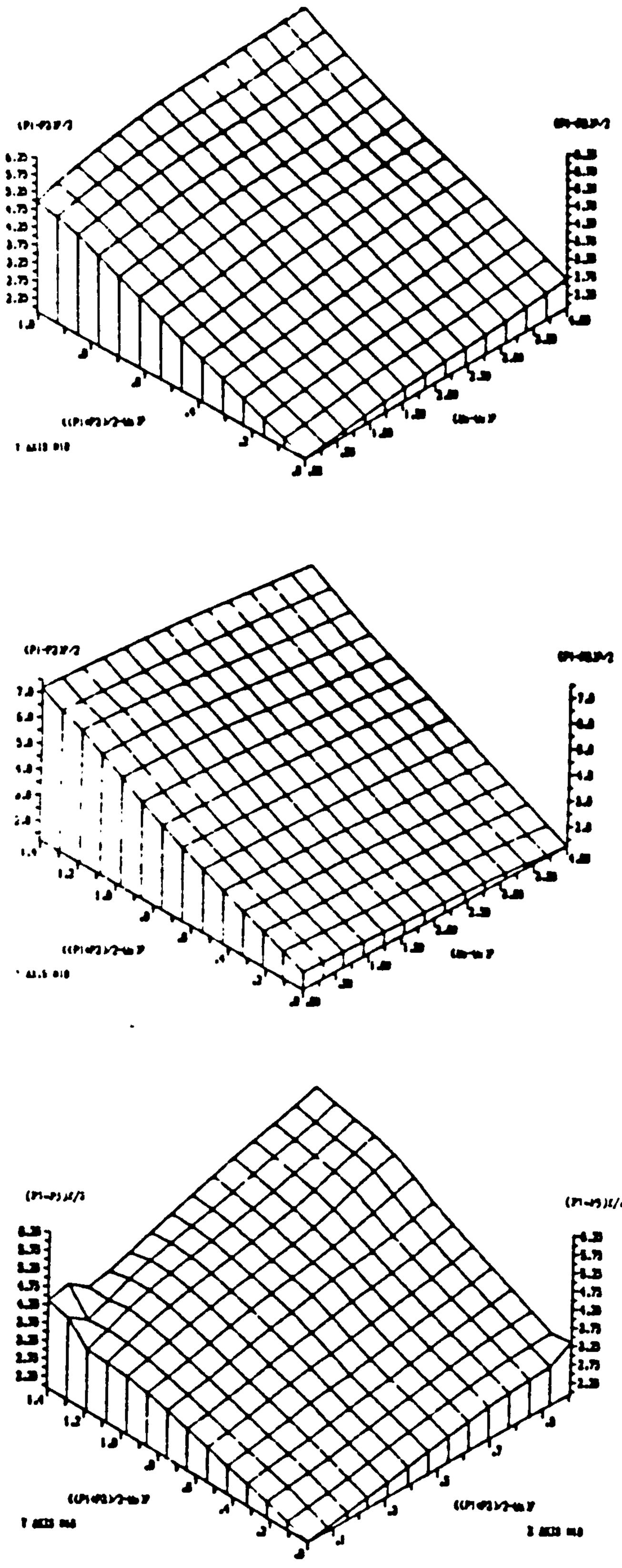

(UNITS IN KG/SQ.CM)

SHEAR STRENGTH DATA FOR HIGH AS-COMPACTED DENSITY DHANAURI CLAY UNDER D CONDITION(SATIJA,1978).

A8.4.8 Escario(1980)

Figure A8.5 shows the failure surfaces for various suction values. The failure conditions show a $\emptyset'$ varying from 19^{o} at low suction to 25^{o} at high suctions and an average of 22.5^{o}. Figure A8.6 shows the matrix suction versus shear strength for the Madrid Gray clay. The $\emptyset^{b}$ value is 16.1^{o} when 22.5^{o} is used for $\emptyset'$ in the analysis.

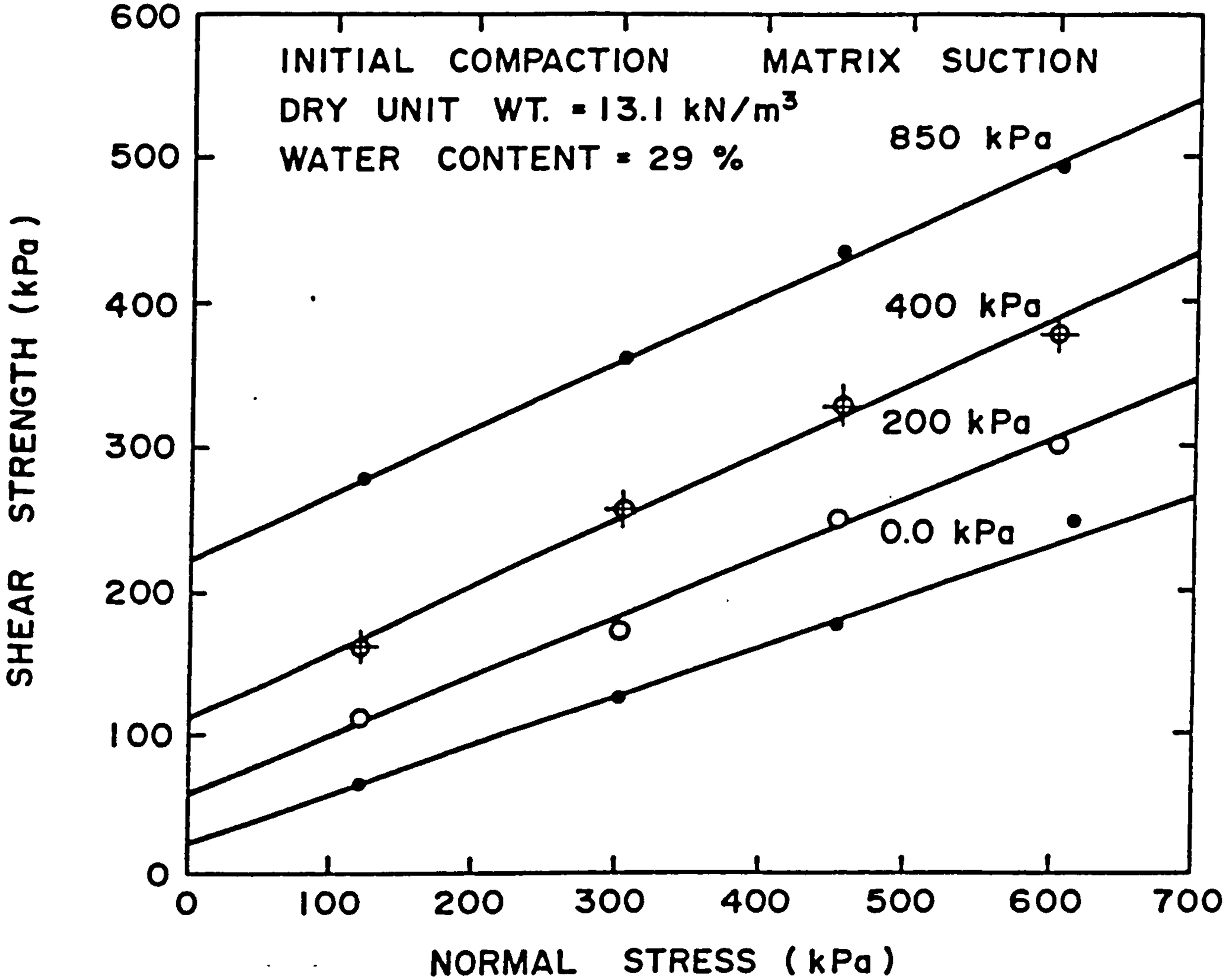

Fig.A8.5: Shear strength of Madrid gray clay at various suction levels (after Escario, 1980).

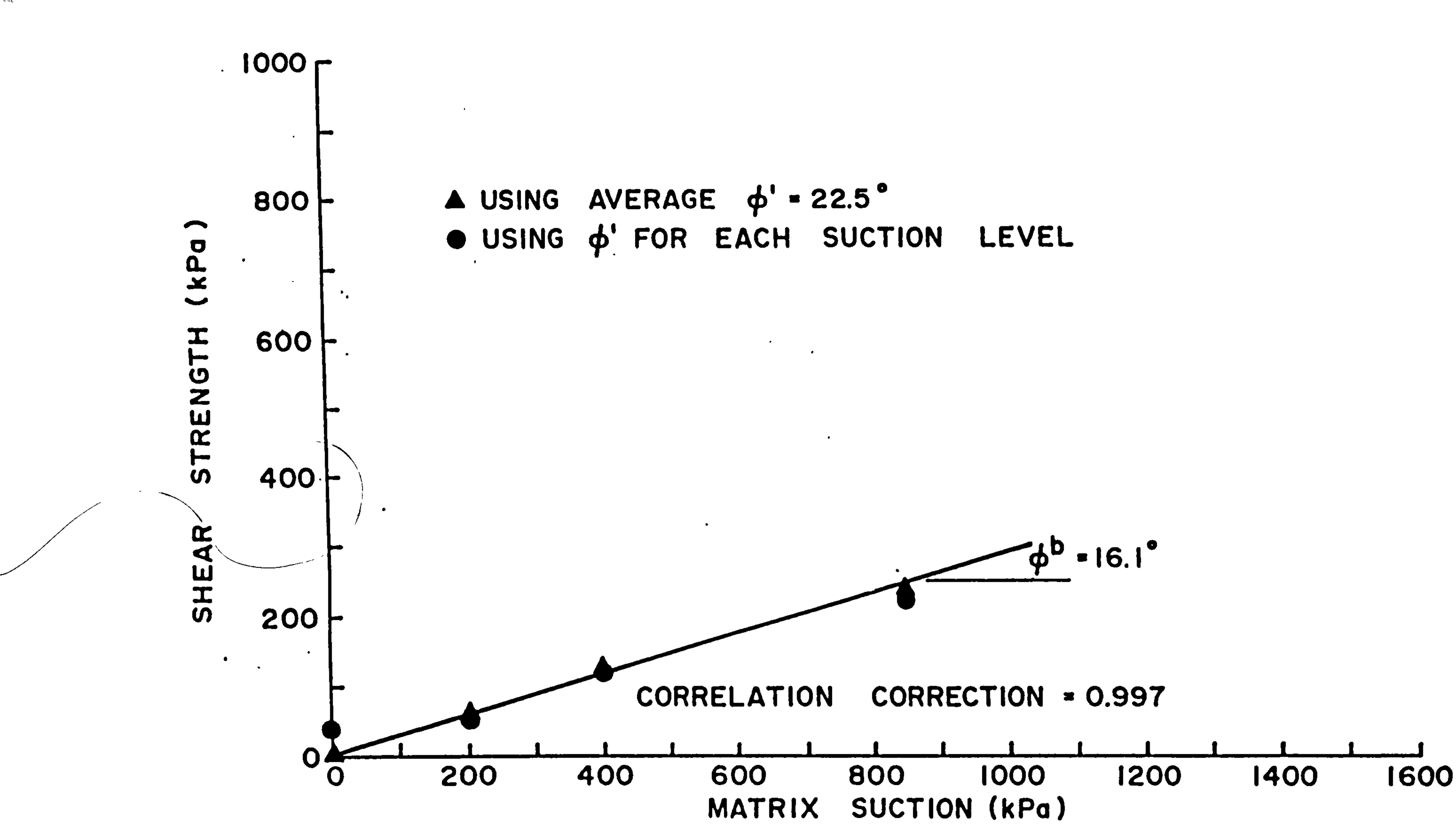

Fig.A8.6: Shear strength versus matrix suction for Madrid gray clay (after Escario, 1980).

A8.4.9 Ho(1981)

(i) Numerical method

Decomposed granite (sample No.5)

```
**************************************************************
 INPUT COHESION,C' IN KN/SQ.M IS 28.9

 INPUT ANGLE OF INTERNAL FRICTION IN DEGREES,Ø' IS 33.4
**************************************************************
                                    b
 SUCTION ANGLE IN DEGREES,Ø  IS 12.59

 SUCTION ANGLE IN DEGREES,Ø° IS -23.56

 CORRECTED COHESION,C' IN KN/SQ.M IS 24.4
                                                  b
 CORRELATION FACTOR FOR SUCTION ANGLE(Ø ),R IS 0.99
**************************************************************
```

Decomposed granite (sample No.6)

```
**************************************************************
 INPUT COHESION,C' IN KN/SQ.M IS 28.9

 INPUT ANGLE OF INTERNAL FRICTION IN DEGREES,Ø' IS 33.4
**************************************************************
                                    b
 SUCTION ANGLE IN DEGREES,Ø  IS 36.77

 SUCTION ANGLE IN DEGREES,Ø° IS 5.03

 CORRECTED COHESION,C' IN KN/SQ.M IS 20.46
                                                  b
 CORRELATION FACTOR FOR SUCTION ANGLE(Ø ),R IS 0.95
**************************************************************
```

Decomposed granite (sample No.8)

```
**************************************************************
 INPUT COHESION,C´ IN KN/SQ.M IS 28.9

 INPUT ANGLE OF INTERNAL FRICTION IN DEGREES,Ø´ IS 33.4
**************************************************************
                                  b
 SUCTION ANGLE IN DEGREES,Ø   IS 15.77

 SUCTION ANGLE IN DEGREES,Ø' IS -20.65

 CORRECTED COHESION,C´ IN KN/SQ.M IS 78.33
                                      b
 CORRELATION FACTOR FOR SUCTION ANGLE(Ø ),R IS 1
**************************************************************
```

Decomposed granite (sample No.10)

```
**************************************************************
 INPUT COHESION,C´ IN KN/SQ.M IS 28.9

 INPUT ANGLE OF INTERNAL FRICTION IN DEGREES,Ø´ IS 33.4
**************************************************************
                                 b
 SUCTION ANGLE IN DEGREES,Ø   IS 15.37

 SUCTION ANGLE IN DEGREES,Ø' IS -20.03

 CORRECTED COHESION,C´ IN KN/SQ.M IS 30.89
                                     b
 CORRELATION FACTOR FOR SUCTION ANGLE(Ø ),R IS 0.99
**************************************************************
```

Decomposed granite (sample No.20)

```
**************************************************************
 INPUT COHESION,C' IN KN/SQ.M IS 28.9

 INPUT ANGLE OF INTERNAL FRICTION IN DEGREES,Ø' IS 33.4
**************************************************************
                                    b
 SUCTION ANGLE IN DEGREES,Ø   IS 12.74

 SUCTION ANGLE IN DEGREES,Ø° IS -23.43

 CORRECTED COHESION,C' IN KN/SQ.M IS 43.63
                                                  b
 CORRELATION FACTOR FOR SUCTION ANGLE(Ø ),R IS 0.98
**************************************************************
```

Decomposed granite (sample No.21)

```
**************************************************************
 INPUT COHESION,C' IN KN/SQ.M IS 28.9

 INPUT ANGLE OF INTERNAL FRICTION IN DEGREES,Ø' IS 33.4
**************************************************************
                                    b
 SUCTION ANGLE IN DEGREES,Ø   IS 12.74

 SUCTION ANGLE IN DEGREES,Ø° IS -23.42

 CORRECTED COHESION,C' IN KN/SQ.M IS 43.8
                                                  b
 CORRELATION FACTOR FOR SUCTION ANGLE(Ø ),R IS 0.99
**************************************************************
```

Decomposed granite (sample No.22)

****
INPUT COHESION,C′ IN KN/SQ.M IS 28.9

INPUT ANGLE OF INTERNAL FRICTION IN DEGREES,Ø′ IS 33.4
****

SUCTION ANGLE IN DEGREES,$Ø_b$ IS 22.45

SUCTION ANGLE IN DEGREES,Ø° IS -13.83

CORRECTED COHESION,C′ IN KN/SQ.M IS 22.05

CORRELATION FACTOR FOR SUCTION ANGLE($Ø_b$),R IS 1
****

Decomposed granite (sample No.23)

****
INPUT COHESION,C′ IN KN/SQ.M IS 28.9

INPUT ANGLE OF INTERNAL FRICTION IN DEGREES,Ø′ IS 33.4
****

SUCTION ANGLE IN DEGREES,$Ø_b$ IS 7.98

SUCTION ANGLE IN DEGREES,Ø° IS -27.44

CORRECTED COHESION,C′ IN KN/SQ.M IS 108.07

CORRELATION FACTOR FOR SUCTION ANGLE($Ø_b$),R IS 0.99
****

Decomposed rhyolite(sample No.11A)

****
INPUT COHESION,C′ IN KN/SQ.M IS 7.35

INPUT ANGLE OF INTERNAL FRICTION IN DEGREES,Ø′ IS 35.3
****

SUCTION ANGLE IN DEGREES,$Ø_b$ IS 11.65

SUCTION ANGLE IN DEGREES,Ø° IS -26.65

CORRECTED COHESION,C′ IN KN/SQ.M IS 21.5

CORRELATION FACTOR FOR SUCTION ANGLE($Ø_b$),R IS 1
****

Decomposed rhyolite(sample No.11B)

****
INPUT COHESION,C´ IN KN/SQ.M IS 7.35

INPUT ANGLE OF INTERNAL FRICTION IN DEGREES,Ø´ IS 35.3
****

SUCTION ANGLE IN DEGREES,$Ø^{b}$ IS 9.88

SUCTION ANGLE IN DEGREES,Ø° IS -28.1

CORRECTED COHESION,C´ IN KN/SQ.M IS 46.82

CORRELATION FACTOR FOR SUCTION ANGLE($Ø^{b}$),R IS 0.96
****

Decomposed rhyolite(sample No.11C)

****
INPUT COHESION,C´ IN KN/SQ.M IS 7.35

INPUT ANGLE OF INTERNAL FRICTION IN DEGREES,Ø´ IS 35.3
****

SUCTION ANGLE IN DEGREES,$Ø^{b}$ IS 14.84

SUCTION ANGLE IN DEGREES,Ø° IS -23.9

CORRECTED COHESION,C´ IN KN/SQ.M IS 28.37

CORRELATION FACTOR FOR SUCTION ANGLE($Ø^{b}$),R IS 0.99
****

Decomposed rhyolite(sample No.11D)

****
INPUT COHESION,C´ IN KN/SQ.M IS 7.35

INPUT ANGLE OF INTERNAL FRICTION IN DEGREES,Ø´ IS 35.3
****

SUCTION ANGLE IN DEGREES,$Ø^{b}$ IS 16.41

SUCTION ANGLE IN DEGREES,Ø° IS -22.47

CORRECTED COHESION,C´ IN KN/SQ.M IS 38.47

CORRELATION FACTOR FOR SUCTION ANGLE($Ø^{b}$),R IS 1
****

Decomposed rhyolite(sample No.12)

```
**************************************************************
 INPUT COHESION,C' IN KN/SQ.M IS 7.35

 INPUT ANGLE OF INTERNAL FRICTION IN DEGREES,Ø' IS 35.3
**************************************************************
                                   b
 SUCTION ANGLE IN DEGREES,Ø  IS 13.02

 SUCTION ANGLE IN DEGREES,Ø' IS -25.49

 CORRECTED COHESION,C' IN KN/SQ.M IS 9.63
                                    b
 CORRELATION FACTOR FOR SUCTION ANGLE(Ø ),R IS 0.96
**************************************************************
```

Decomposed rhyolite(sample No.14)

```
**************************************************************
 INPUT COHESION,C' IN KN/SQ.M IS 7.35

 INPUT ANGLE OF INTERNAL FRICTION IN DEGREES,Ø' IS 35.3
**************************************************************
                                   b
 SUCTION ANGLE IN DEGREES,Ø  IS 11.4

 SUCTION ANGLE IN DEGREES,Ø' IS -26.86

 CORRECTED COHESION,C' IN KN/SQ.M IS 14.81
                                    b
 CORRELATION FACTOR FOR SUCTION ANGLE(Ø ),R IS 0.95
**************************************************************
```

Decomposed rhyolite(sample No.15)

```
**************************************************************
 INPUT COHESION,C' IN KN/SQ.M IS 7.35

 INPUT ANGLE OF INTERNAL FRICTION IN DEGREES,Ø' IS 35.3
**************************************************************
                                   b
 SUCTION ANGLE IN DEGREES,Ø  IS 17.72

 SUCTION ANGLE IN DEGREES,Ø' IS -21.24

 CORRECTED COHESION,C' IN KN/SQ.M IS 10.45
                                    b
 CORRELATION FACTOR FOR SUCTION ANGLE(Ø ),R IS 0.94
**************************************************************
```

Decomposed granite(including all results)

```
**************************************************************
 INPUT COHESION,C´ IN KN/SQ.M IS 28.9

 INPUT ANGLE OF INTERNAL FRICTION IN DEGREES,Ø´ IS 33.4
**************************************************************
                                  b
 SUCTION ANGLE IN DEGREES,Ø   IS 12.67

 SUCTION ANGLE IN DEGREES,Ø° IS -23.49

 CORRECTED COHESION,C´ IN KN/SQ.M IS 55.15
                                                  b
 CORRELATION FACTOR FOR SUCTION ANGLE(Ø ),R IS 0.51
**************************************************************
```

Decomposed rhyolite(including all results)

```
**************************************************************
 INPUT COHESION,C´ IN KN/SQ.M IS 7.35

 INPUT ANGLE OF INTERNAL FRICTION IN DEGREES,Ø´ IS 35.3
**************************************************************
                                  b
 SUCTION ANGLE IN DEGREES,Ø   IS 13.59

 SUCTION ANGLE IN DEGREES,Ø° IS -25

 CORRECTED COHESION,C´ IN KN/SQ.M IS 24.29
                                                  b
 CORRELATION FACTOR FOR SUCTION ANGLE(Ø ),R IS 0.72
**************************************************************
```

(iii) 3-dimensional graphical method

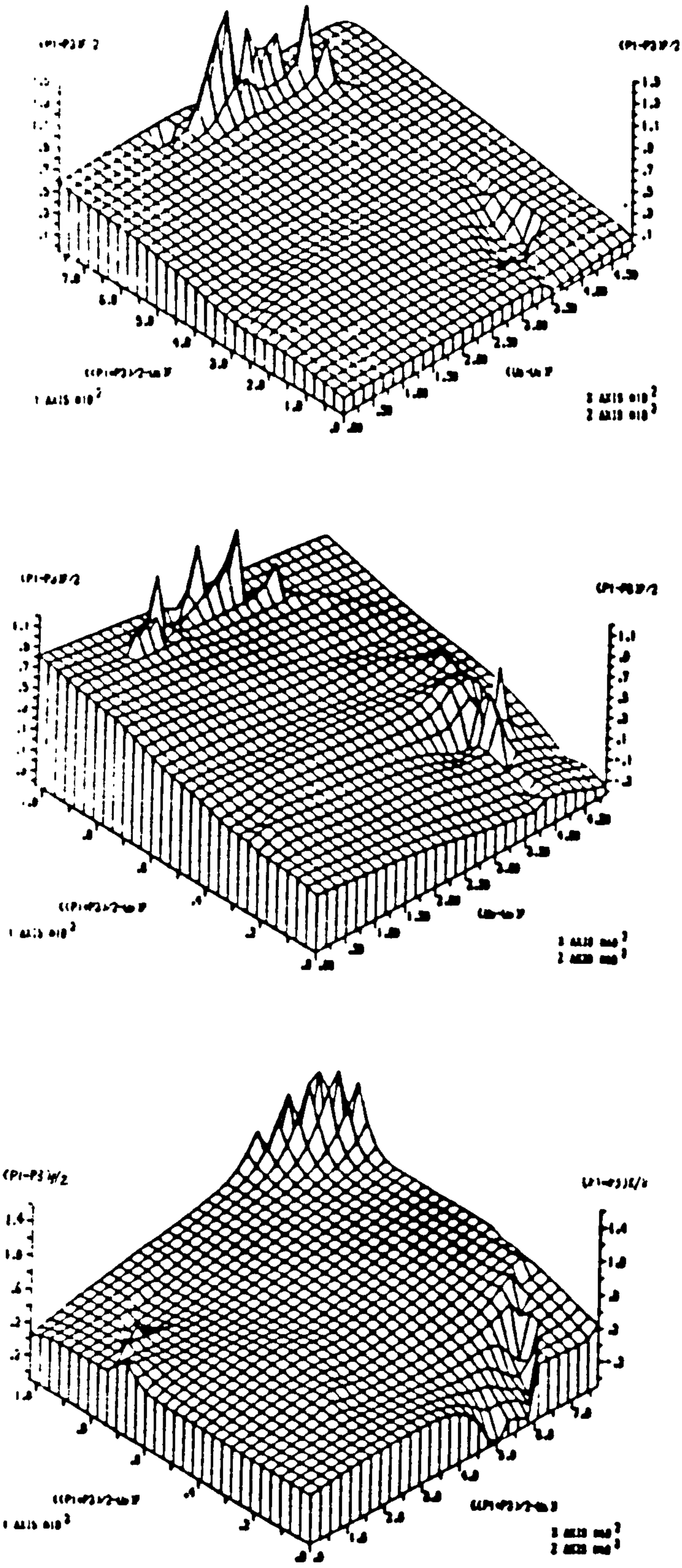

(UNITS IN KN/SQ.M)

SHEAR STRENGTH DATA OF DECOMPOSED GRANITE SAMPLES

(HO , 1981).

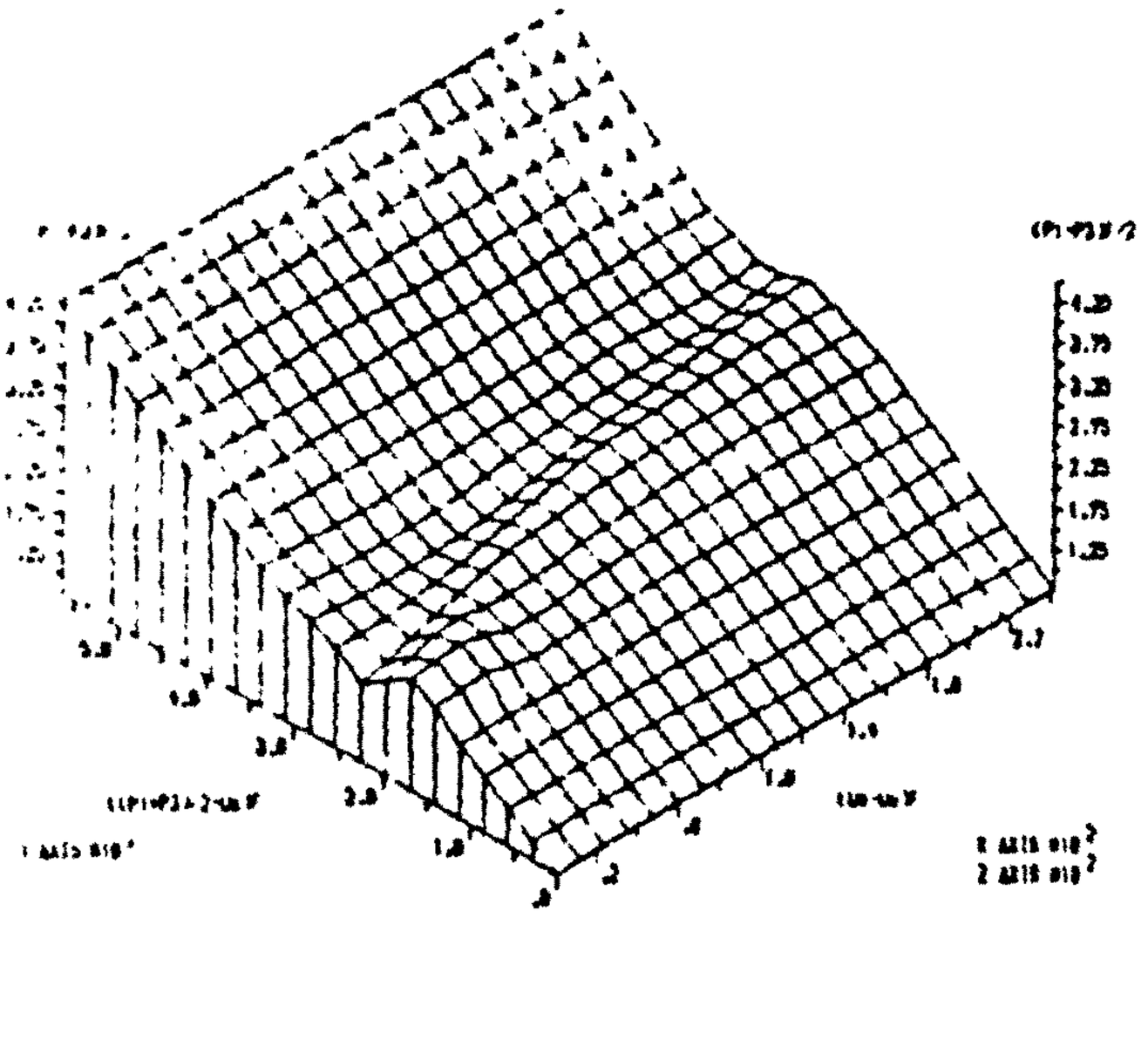

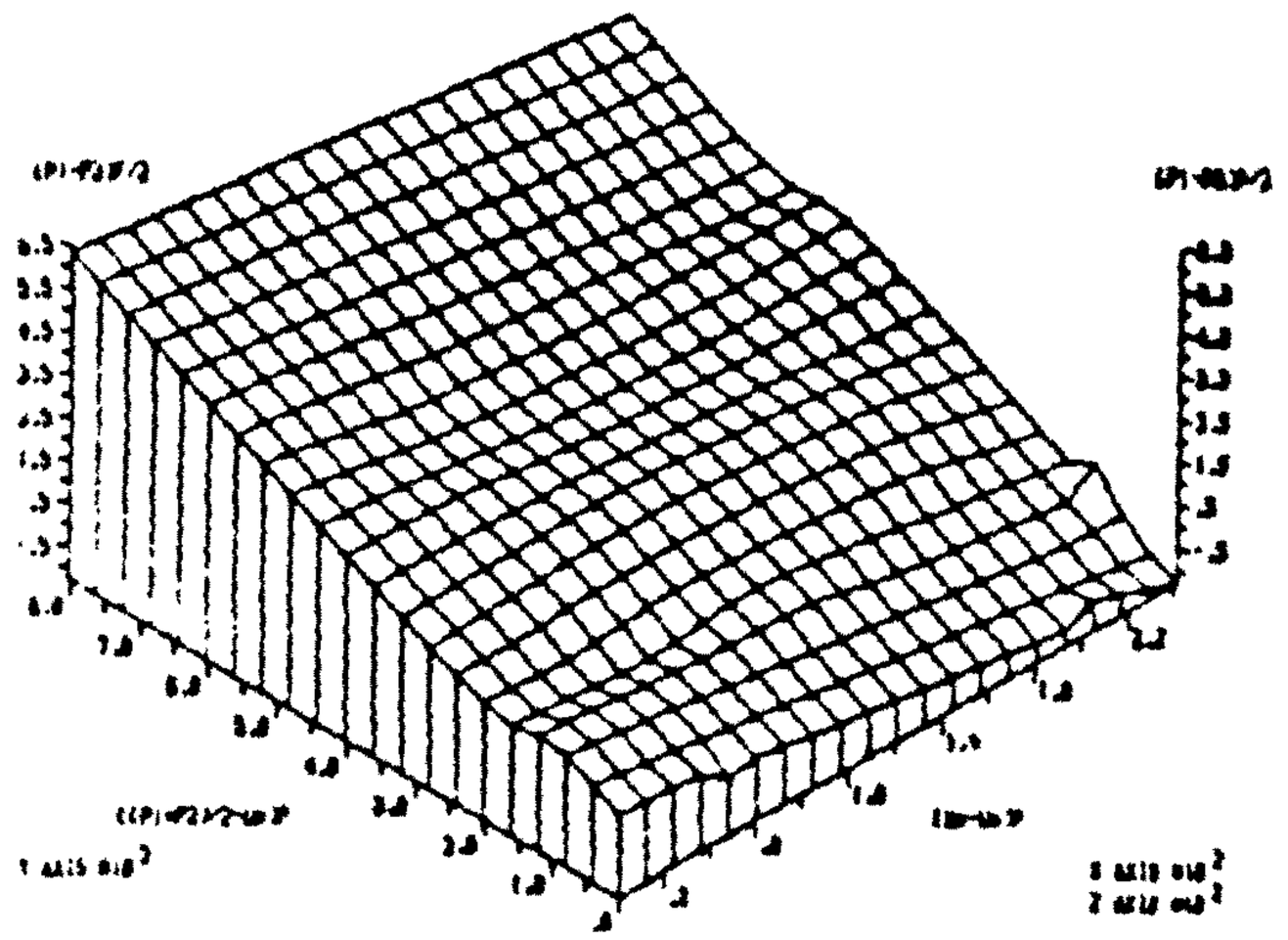

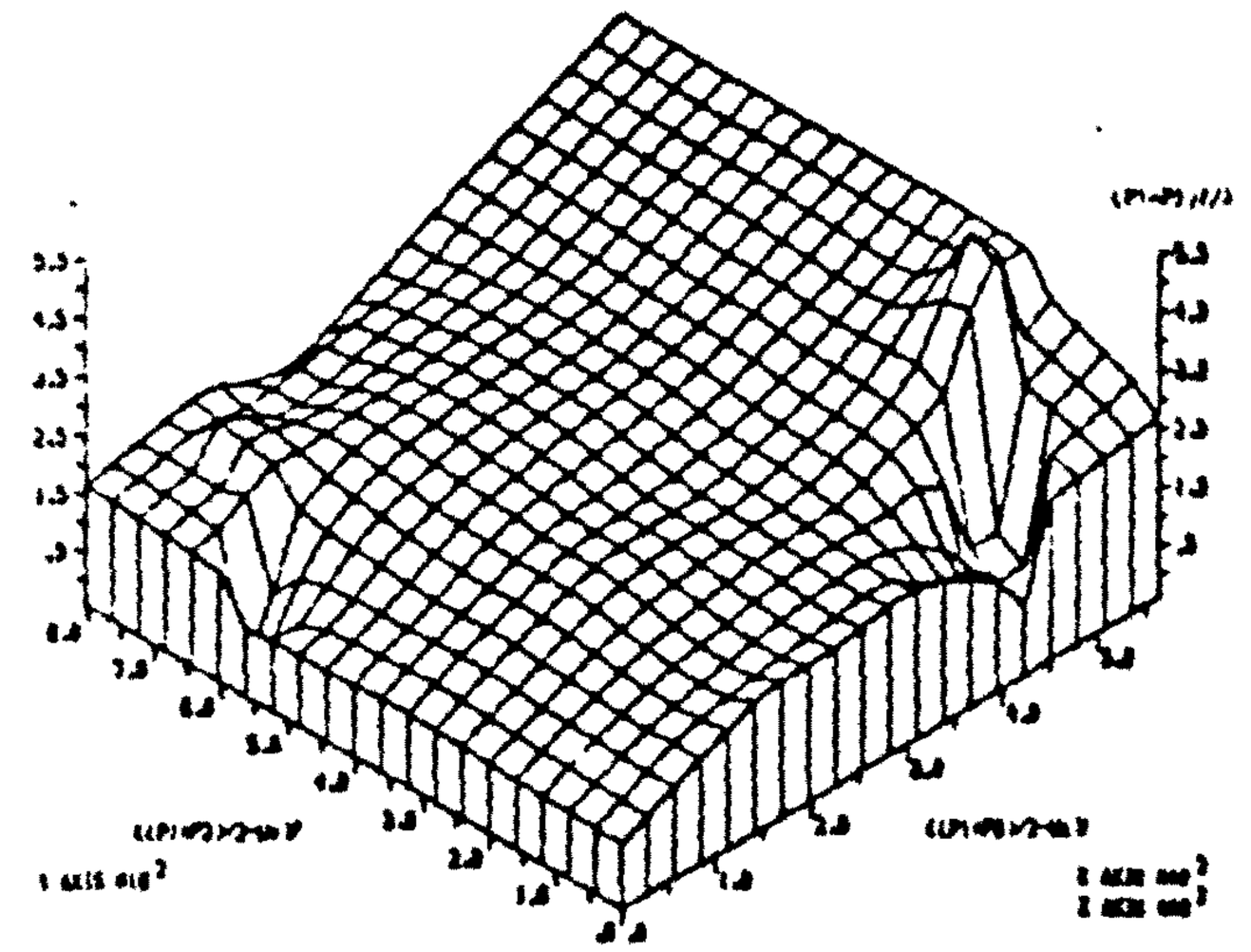

(UNITS IN KN/SQ.M)
SHEAR STRENGTH DATA OF DECOMPOSED RHYOLITE

(HO, 1981).

A8.4.10 Author's results

Series I: Constant water-content tests

```
**********************************************************************
 INPUT COHESION,C' IN KN/SQ.M IS 6.7

 INPUT ANGLE OF INTERNAL FRICTION IN DEGREES,Ø' IS 34.2
**********************************************************************
                                   b
 SUCTION ANGLE IN DEGREES,Ø  IS 22.49

 SUCTION ANGLE IN DEGREES,Ø° IS -14.87

  CORRECTED COHESION,C' IN KN/SQ.M IS 6.42
                                        b
  CORRELATION FACTOR FOR SUCTION ANGLE(Ø ),R IS 0.69
**********************************************************************
```

Series I: Drained tests

```
**********************************************************************
 INPUT COHESION,C' IN KN/SQ.M IS 6.7

 INPUT ANGLE OF INTERNAL FRICTION IN DEGREES,Ø' IS 34.2
**********************************************************************
                                   b
 SUCTION ANGLE IN DEGREES,Ø  IS 5.88

  SUCTION ANGLE IN DEGREES,Ø° IS -29.97

  CORRECTED COHESION,C' IN KN/SQ.M IS 18.69
                                        b
  CORRELATION FACTOR FOR SUCTION ANGLE(Ø ),R IS 0.53
**********************************************************************
```

Series I: Unconfined tests

```
**********************************************************************
 INPUT COHESION,C' IN KN/SQ.M IS 6.7

 INPUT ANGLE OF INTERNAL FRICTION IN DEGREES,Ø' IS 34.2
**********************************************************************
                                   b
 SUCTION ANGLE IN DEGREES,Ø  IS 12.05

 SUCTION ANGLE IN DEGREES,Ø° IS -24.99

 CORRECTED COHESION,C' IN KN/SQ.M IS 14.89
                                        b
 CORRELATION FACTOR FOR SUCTION ANGLE(Ø ),R IS 0.99
**********************************************************************
```

Series II: Drained tests

****
INPUT COHESION,C´ IN KN/SQ.M IS 6.7

INPUT ANGLE OF INTERNAL FRICTION IN DEGREES,Ø´ IS 34.2
****

SUCTION ANGLE IN DEGREES,$Ø^{b}$ IS 86.16

SUCTION ANGLE IN DEGREES,Ø° IS 85.97

CORRECTED COHESION,C´ IN KN/SQ.M IS -545.05

CORRELATION FACTOR FOR SUCTION ANGLE($Ø^{b}$),R IS 0.50
****

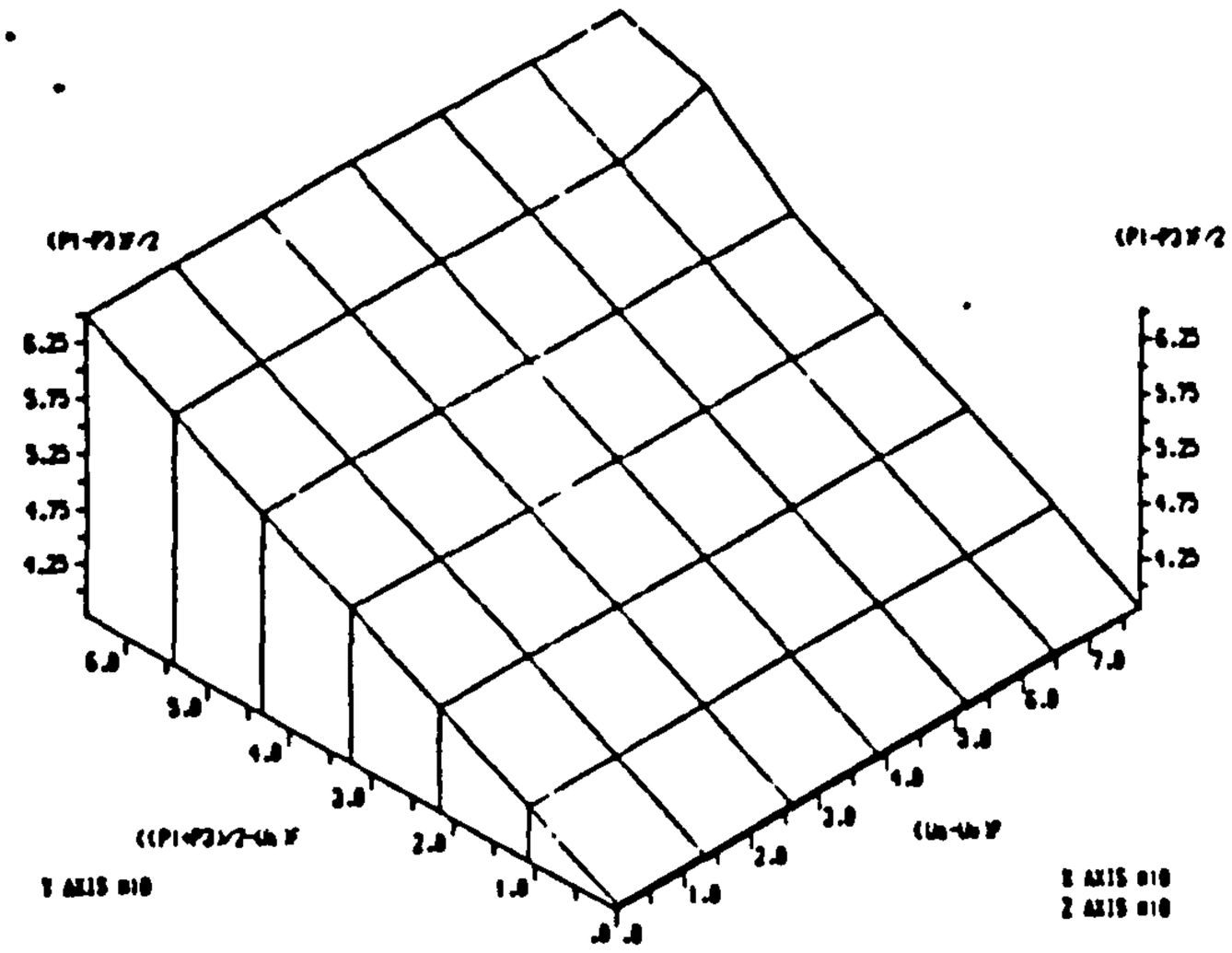

THE SHEAR STRENGTH DATA FOR BRANDESBURTON CLAY UNDER UNCONFINED CONDITION SERIES 1)

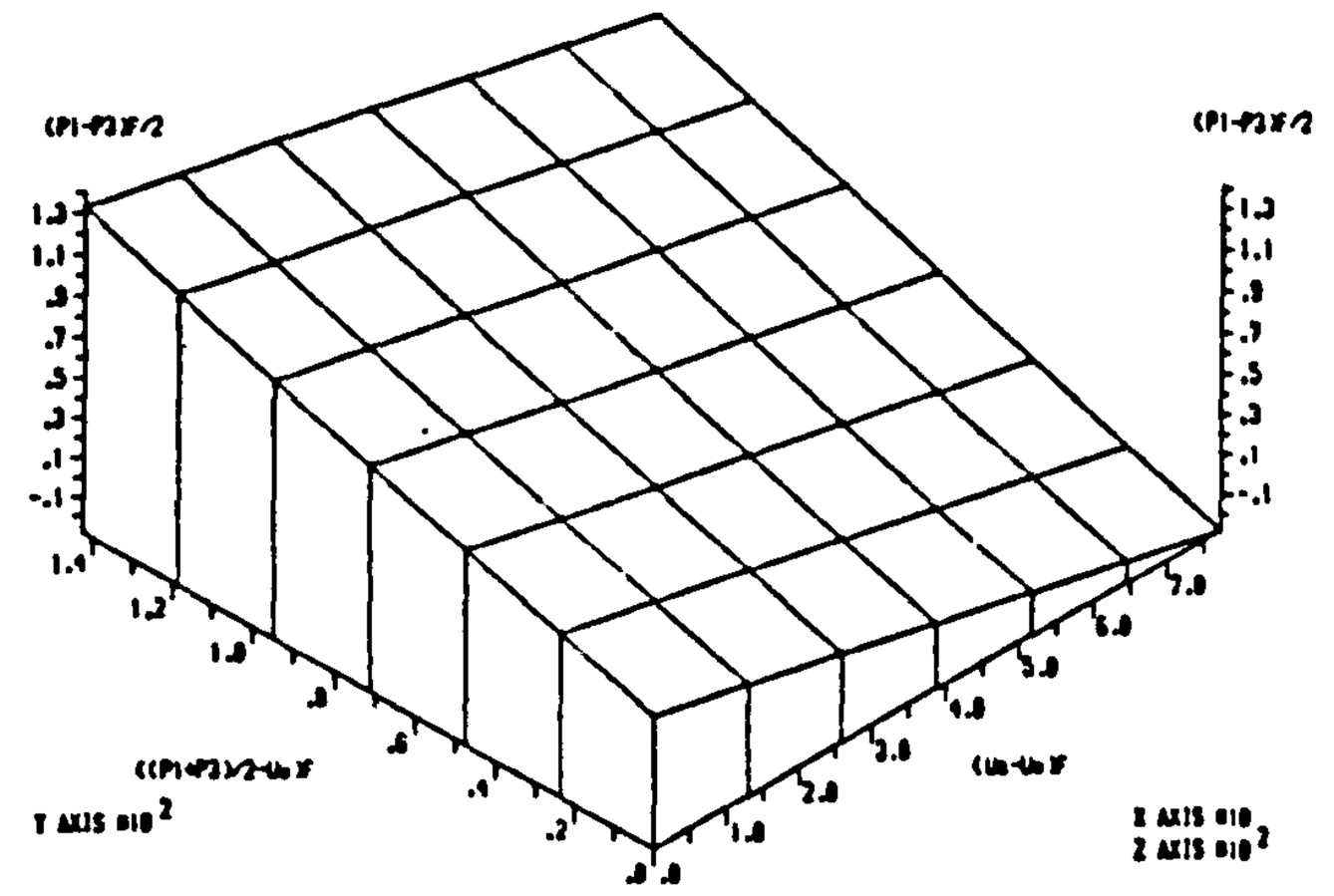

THE SHEAR STRENGTH DATA FOR BRANDESBURTON CLAY UNDER UNCONFINED CONDITION SERIES 1)

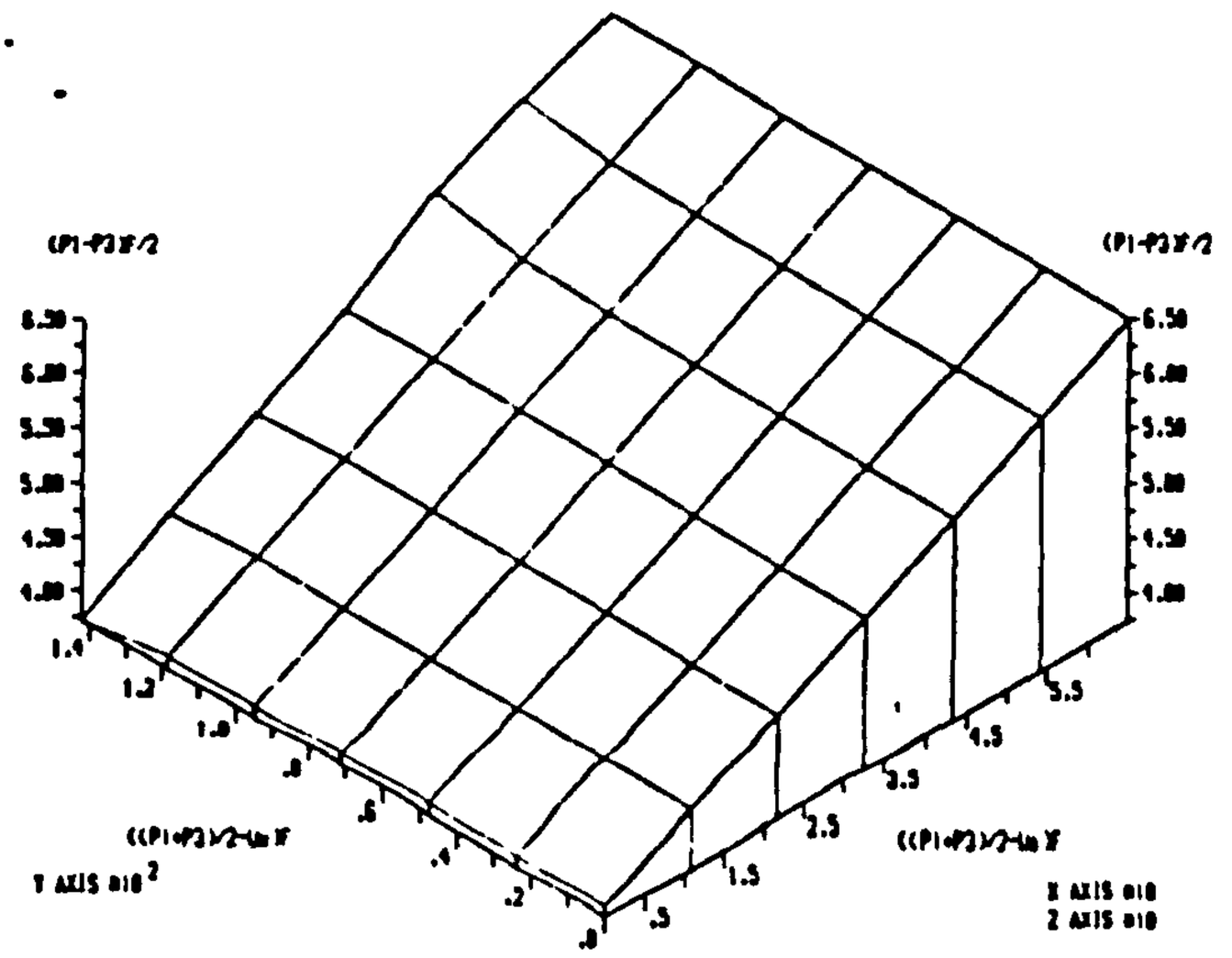

THE SHEAR STRENGTH DATA FOR BRANDESBURTON CLAY UNDER UNCONFINED CONDITION SERIES 1)

(UNITS IN KN/SQ.M)

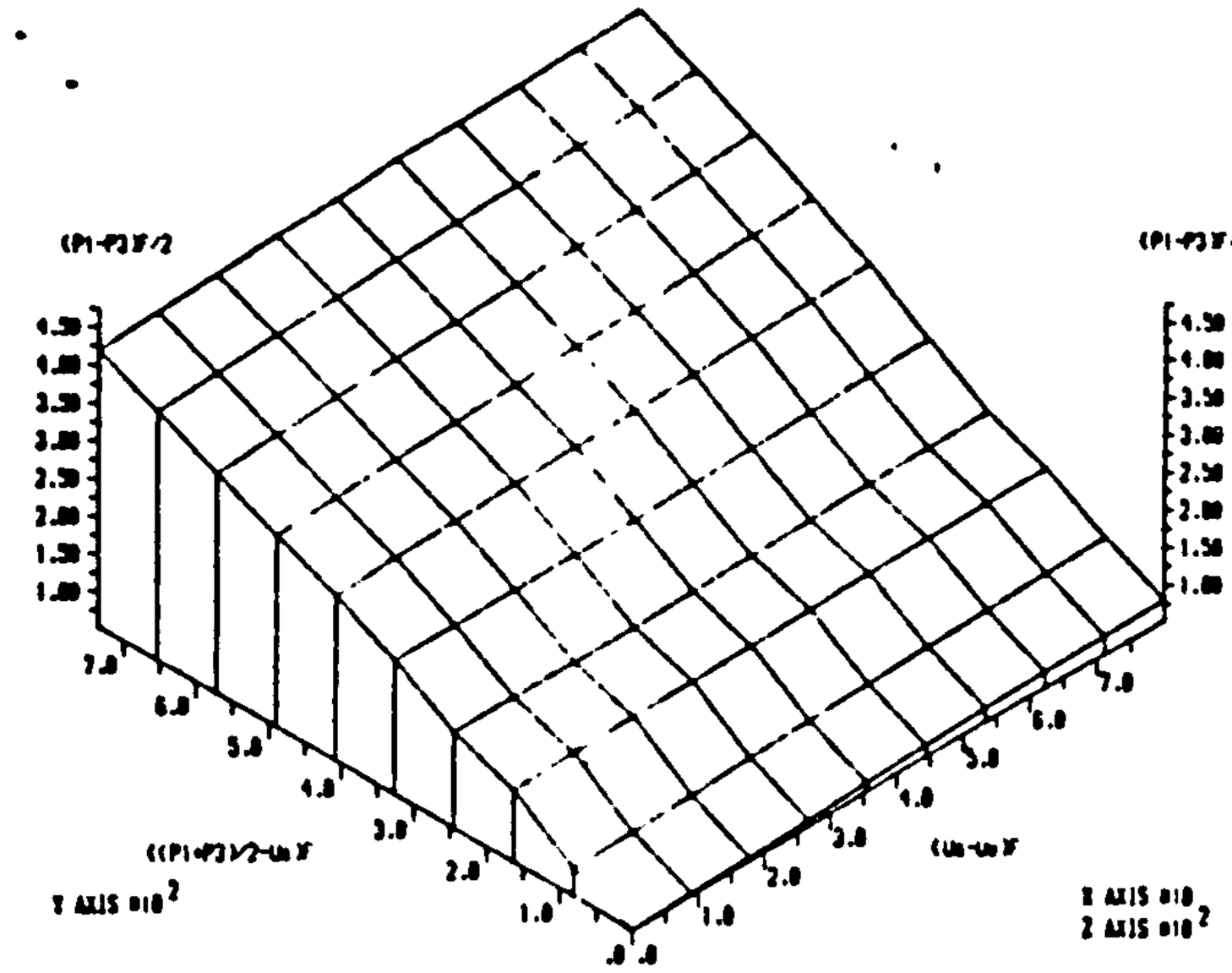

THE SHEAR STRENGTH DATA FOR BRANDEFOUTH CLAY UNDER CU CONDITION SERIES 1)

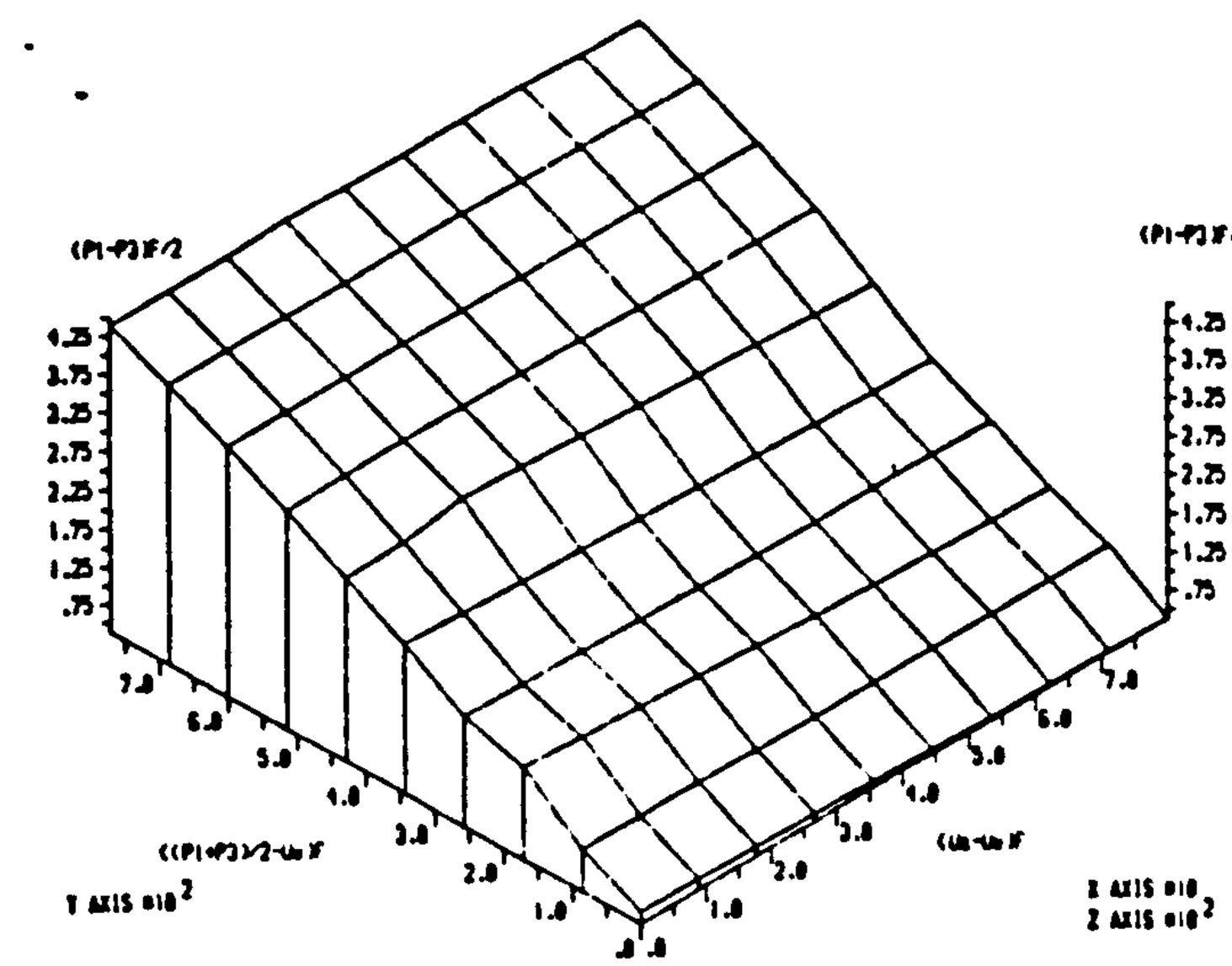

THE SHEAR STRENGTH DATA FOR BRANDEFOUTH CLAY UNDER CU CONDITION SERIES 1)

THE SHEAR STRENGTH DATA FOR BRANDEFOUTH CLAY UNDER CU CONDITION SERIES 1)

(UNITS IN KN/SQ.M)

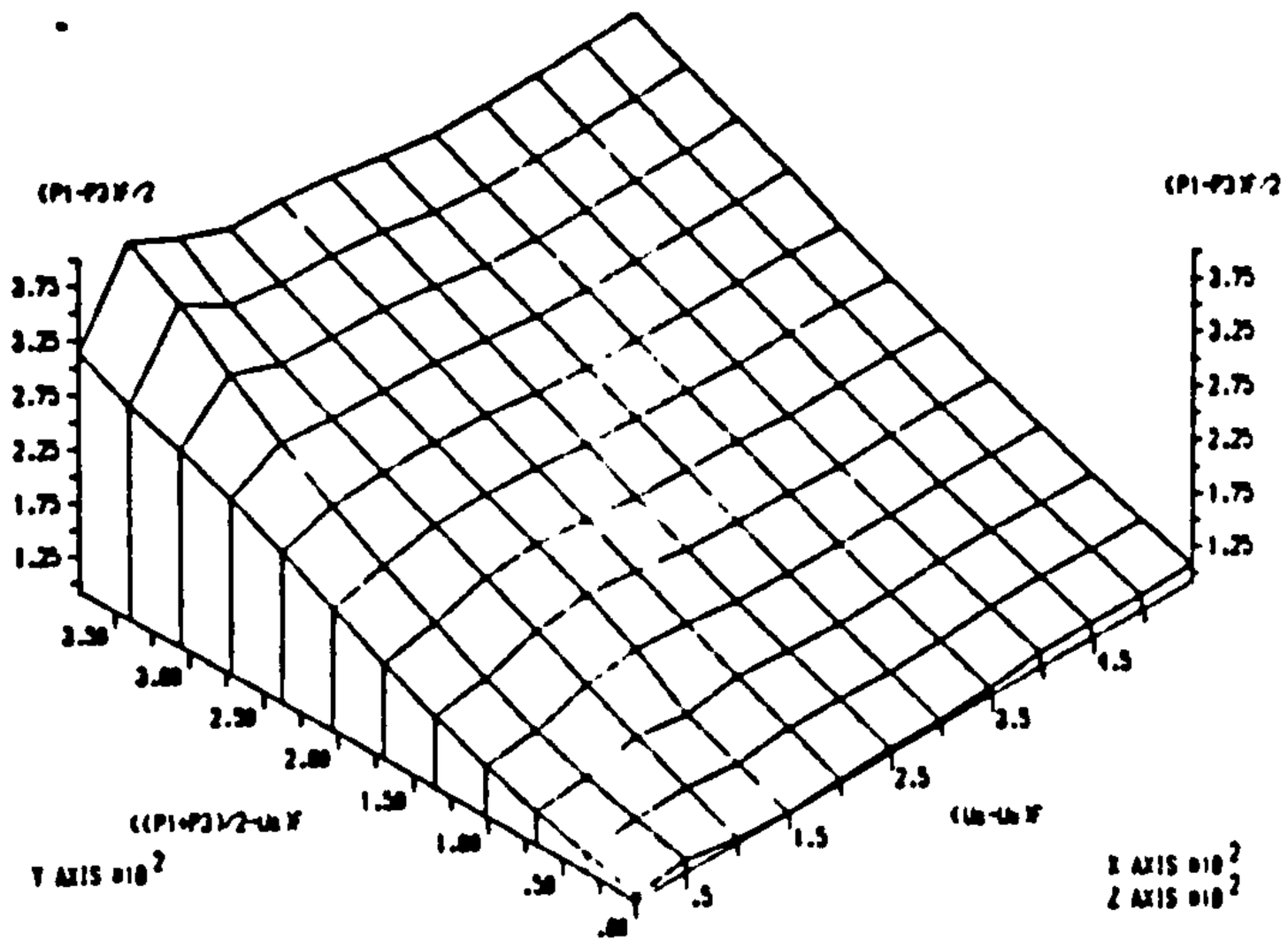

THE SHEAR STRENGTH DATA FOR BRANDEFOUTH CLAY UNDER DRAINED CONDITION SERIES 1)

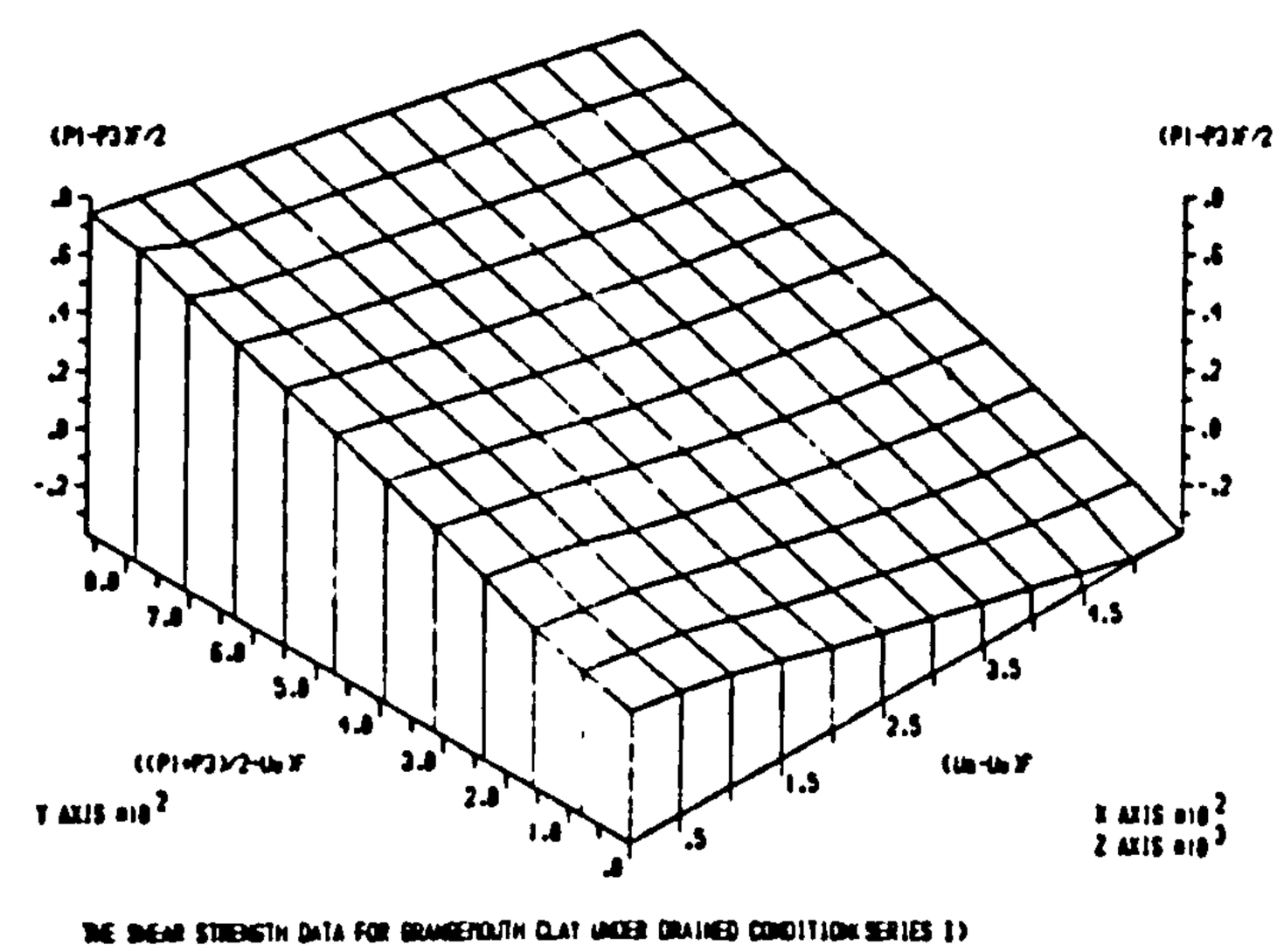

THE SHEAR STRENGTH DATA FOR BRANDEFOUTH CLAY UNDER DRAINED CONDITION SERIES 1)

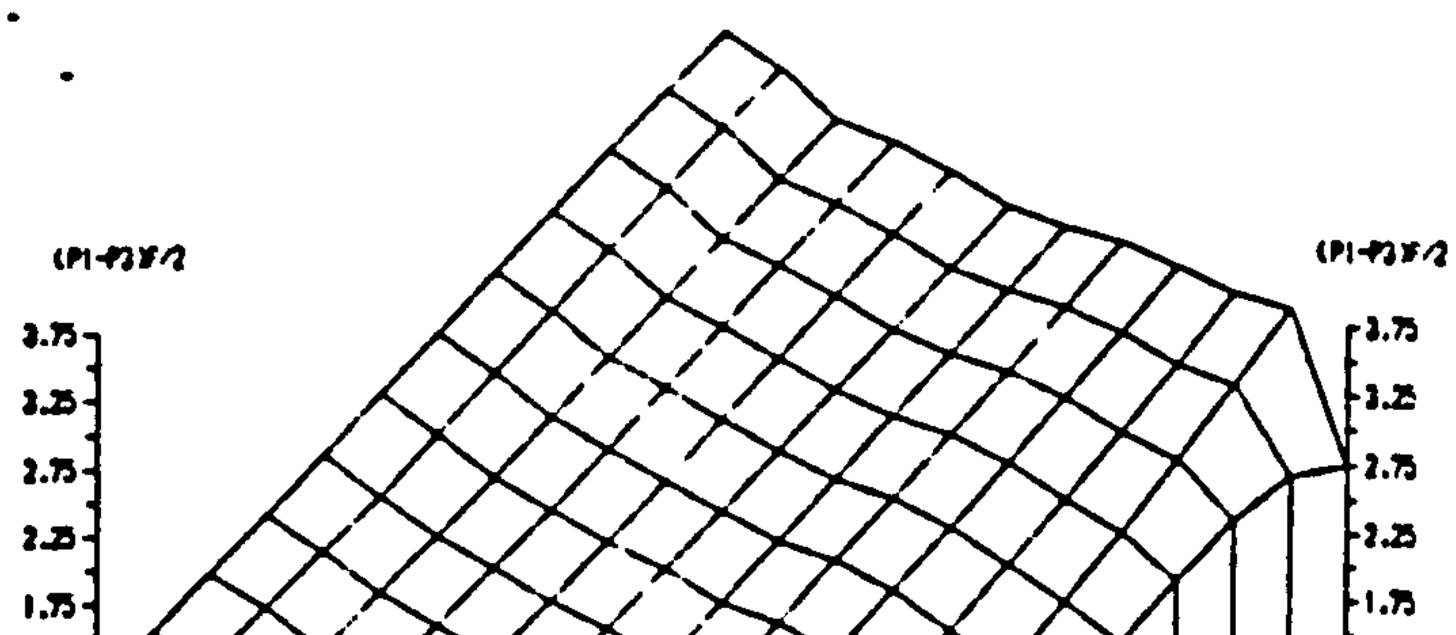

THE SHEAR STRENGTH DATA FOR BRANDEFOUTH CLAY UNDER DRAINED CONDITION SERIES 1)

(UNITS IN KN/SQ.M)

TABLE : A8.1 STRESS CONDITIONS AT FAILURE - SERIES I

(a) Constant water-content tests

Test No.	Initial Stress State	σ3 (KPa)	Ua (KPa)	Uw (KPa)	σ_1 peak (KPa)	$[(\frac{\sigma_1+\sigma_3}{2})-Ua]_f$ (KPa)	$[(\frac{\sigma_1+\sigma_3}{2})-Uw]_f$ (KPa)	$(Ua-Uw)_f$ (KPa)	$(\frac{\sigma_1-\sigma_3}{2})_f$ (KPa)	Initial soil properties γd (kg/m³)	W (%)	Sr (%)	Comments
1	2	194.78	153.17	149.72	300.7	94.57	98.02	3.45	52.96	1867	19.68	80.23	Desaturated
2	4	294.78	251.67	228.71	434.4	112.92	135.88	22.96	69.81	2146	15.04	79.31	consolidated
3	6	390.78	352.67	292.71	595.6	140.52	200.48	59.96	102.41	2292	13.73	80.02	constant
4	6a	397.78	251.67	217.71	877.16	385.80	419.76	33.90	239.69	1757	16.24	61.67	water-
5	8	491.78	447.17	384.71	706.72	152.08	214.54	62.46	107.47	2304	10.84	61.49	content
6	8a	503.78	355.67	308.72	1031.24	411.84	458.79	46.95	263.73	1854	12.40	48.21	tests
7	10	590.78	552.67	526.71	721.86	103.65	129.61	25.96	65.54	2072	14.02	62.68	
8	10a	603.78	453.67	414.72	1129.76	413.10	452.05	38.95	262.99	2025	8.7	38.47	
9	11a	650.78	352.17	315.71	1524.28	735.36	771.82	36.46	436.75	1798	15.37	60.14	
10	12	692.78	644.67	564.72	929.92	166.68	246.63	79.95	118.57	1989	15.89	66.31	
(b)	Drained tests												
11	1	143.78	99.67	42.71	337.15	140.80	197.76	56.96	96.69	1698	23.67	92.35	Desaturated
12	2	197.14	144.59	49.17	431.62	169.79	265.21	95.42	117.24	1738	19.75	77.91	consolidated
13	3	248.78	202.67	44.71	520.07	181.76	339.72	157.96	135.65	1672	19.58	66.88	drained
14	4	298.31	247.57	51.18	576.50	189.84	386.23	196.39	139.10	1801	17.86	70.66	tests
15	4	289.78	249.67	42.71	609.56	200.00	406.96	206.96	159.89	2103	13.72	67.87	
16	5	345.78	300.67	44.71	590.32	167.38	423.34	255.96	122.27	1688	18.77	66.30	
17	6	395.48	346.55	43.14	673.33	187.86	491.27	303.41	138.93	1685	20.30	75.87	
18	7	446.78	399.67	48.71	806.60	227.02	577.98	350.96	179.91	2111	16.58	81.88	
19	8	496.65	446.53	46.15	824.99	214.29	614.67	400.38	164.17	2203	12.62	67.64	
20	9	541.78	503.17	45.71	792.98	164.21	621.67	457.46	125.60	2148	15.33	78.90	
21	10	598.82	549.51	59.21	1247.44	373.62	863.92	490.30	324.31	2131	13.97	66.03	
22	11	646.90	599.50	53.18	949.04	198.47	744.79	546.32	151.07	2167	12.30	59.49	
(c)	Unconfined tests												
23	2	149.59	149.59	139.53	226.21	38.31	48.37	10.06	38.31	1339	34.64	90.46	Desaturated
24	4	247.57	247.57	230.91	326.71	39.57	56.24	16.67	39.57	1324	35.73	91.29	Consolidated
25	6	348.55	348.55	331.32	430.05	40.75	57.99	17.24	40.75	1335	34.07	88.37	unconfined
26	8	449.53	449.53	418.67	543.81	47.14	78.00	30.86	47.14	1397	28.70	81.52	tests
27	10	552.51	552.51	527.12	639.57	43.53	68.93	25.40	43.53	1353	32.47	86.46	
28	11	598.50	598.50	521.09	728.27	64.89	142.30	77.14	64.89	1654	21.54	80.58	
29	12	651.49	651.49	622.51	747.15	47.83	76.82	28.99	47.83	1345	32.24	84.94	

TABLE : A8.2 STRESS CONDITIONS AT FAILURE - SERIES II

• Drained tests

Test No.	Initial Stress State	σ_3 (KPa)	Ua (KPa)	Uw (KPa)	σ_1 peak (KPa)	$[(\frac{\sigma_1+\sigma_3}{2})-Ua]_f$ (KPa)	$[(\frac{\sigma_1+\sigma_3}{2})-Uw]_f$ (KPa)	$(Ua-Uw)_f$ (KPa)	$(\frac{\sigma_1-\sigma_3}{2})_f$ (KPa)	Initial soil properties γ_d	W (%)	Sr (%)	Comments
30	14	200.78	104.67	49.71	567.06	279.25	334.21	54.96	183.14	1612	24.08	84.91	Desaturated-
31	15	249.78	97.67	46.71	769.17	411.81	462.77	50.96	259.70	1651	22.11	79.30	consolidated
32	16	304.78	103.67	53.71	885.32	491.38	541.34	49.96	290.27	1762	18.44	72.14	drained
33	18	398.78	103.17	52.21	1298.46	745.45	796.41	50.96	449.84	1656	21.68	79.44	tests
34	19	450.57	104.60	53.18	1517.01	879.19	930.61	51.42	533.22	1702	20.53	77.83	
35	20	490.78	100.17	47.71	1574.56	932.50	984.96	52.46	541.89	1723	16.62	60.34	
36	21	550.74	99.60	51.18	1766.81	1059.18	1107.60	48.42	608.04	1692	20.65	79.12	
37	22	597.82	100.60	50.17	1472.94	934.78	985.21	50.43	437.56	1676	26.30	93.77	
38	23	642.78	95.67	47.71	1615.30	1033.37	1081.33	47.96	486.26	1721	25.17	92.51	

A8.4.5 M.I.I.(1963)

(i) Numerical method

Potters flint and Peerless clay(tests on unsaturated soils)

```
*************************************************************
 INPUT COHESION,C' IN KG/SQ.CM IS 0

 INPUT ANGLE OF INTERNAL FRICTION IN DEGREES,Ø' IS 35.6
*************************************************************
                                  b
 SUCTION ANGLE IN DEGREES,Ø   IS 32.49

 SUCTION ANGLE IN DEGREES,Ø' IS -4.5

 CORRECTED COHESION,C' IN KG/SQ.CM IS 0.13
                                                  b
 CORRELATION FACTOR FOR SUCTION ANGLE(Ø ),R IS 0.89
*************************************************************
```